@RevFCAUNCuyo

CONTINUOUS PUBLICATION

REV FCA UNCuyo

Volume 58 Issue 1
January-June 2026
ISSN on line 1853 8665
Mendoza | Argentina



Dear Academic Community,

We are pleased to welcome you to the first issue of the year 2026 of the Revista de la Facultad de Ciencias Agrarias. This is no ordinary year in our history: *we are celebrating our 77th anniversary*. To honor this legacy, we are leading the continuous improvement and constant updating of the journal, inaugurating this cycle with key transformations.

Continuous Publication

Starting this year, the Journal will publish its articles under the *continuous publication model*, making papers immediately available and citable. This long-awaited innovation responds to the immediacy that characterizes the contemporary world and an increasingly globalized scenario.

Reducing editorial turnaround times has become essential to communicate science more rapidly, streamline peer feedback, and increase the visibility of our authors.

Editorial Policies for Changing Times

Likewise, since 2025, we have been driving a profound update and strengthening of our editorial policies. In this regard, we have worked intensively on *regulating the use of Artificial Intelligence* within the editorial workflow, ensuring transparency and ethics in each of its phases.

The Journal is part of an editorial and academic ecosystem that promotes the permanent circulation of scientific knowledge. We assume with the utmost responsibility the challenges of a dynamic and constantly transforming geopolitical context, actively contributing to the economic, social, and cultural development of our societies.

Editorial Team and Editor-in-Chief
Revista de la Facultad de Ciencias Agrarias UNCuyo

Reviewers 1-2026

Adriana Abril
CONICET

Federico Agrain
IADIZA

Juan E. Barranco Florido
UAMéxico

Carlos Barrantes Mora
GWDG-Alemania

Roberto Benech Arnold
UBA

Jorge Bonilla
INA

María Inés Catalano
UNNOBA

Liliana Cichón
INTA

Joaquín Cochero
ILPLA-CONICET

Leonardo Coll
INTA

Victoria Coll Araoz
UNTucumán

Daniela Cónsoli
UNCuyo

V. Fabiana Consolo
CONICET

Roberto Javier Crespo
CONICET

Claudivan Feitosa de Lacerda
UFederal de Ceará-Brasil

Leticia Andrea Fernández
UNSur

María Elena Fernández Long
UBA

Paula Ferrere
INTA

Georgina Frossasco
INTA

Carina Gallo
INTA

Lucrecia Gieco
INTA

Karina Grunberg
INTA

Marcos G. Guidoli
CONICET

Andrea Izquierdo
UNCórdoba

Martha Helena Jahuira Arias
INIA-Perú

María Jaureguiberry
CONICET

Carolina Kozub
CONICET

Ulises Aranda Lara
INIFAP

Víctor Mario Lipinski
UNCuyo

Ana Adela Llames
UNRío Cuarto

Marcelo Lovisolo
UNacional de Lomas de Zamora

Erica Luft Albarracín
PROIMI

Leandro Martin
UNCuyo

Mariana Martinelli
INTA

Carlos Alberto Martínez Huaman
Ude São Paulo-Brasil

Roxana B. Medina
CERELA

Pablo Meglioli
UNCuyo

Marcos Montoya
INTA

Raúl Mora Yela
INIAP-Ecuador

Ana María Murgida
UBA

María Magdalena Ordóñez-Reséndez
UNAM México

Mario Orozco
INIFAP

Paula Pedrozo
UNLP

Laura Pérez Ventura
DGIrrigación-Mendoza

Alejandra Picallo
UBA

Mariana Reginato
UNRío Cuarto

Margarita Rocca
CEPAVE

María Gladis Rosero Alpala
AGROSAVIA

Miguel Ángel Salas Marina
UNICACH-México

Gustavo Scaglia
UNSan Juan

Alejandro Schor
UBA

Ana Clara Scorsetti
UNLa Plata

Guillermo Hernán Sguazza
UNLa Plata

Celice Silva
UNEMAT-Brasil

Huseyin Tayyar Guldal
Ankara University-Turquía

Andrea Toledo
UNLa Plata

Alejandro Tonolli
UNCuyo

Laura Varone
FUEDEI-Argentina

Rafael F. Vega-Pozuelo
UNCórdoba

Gabriela Verdugo
UCV-Chile

Eduardo G. Virla
UNTucumán

Hasan Yilmaz
Isparta Üniversitesi-Turquía

Revista de la Facultad de Ciencias Agrarias
Universidad Nacional de Cuyo

Volume 58 (1) | Janury-June 2026

Index | Índice

Ecophysiology and crop management | Ecofisiología y manejo de cultivo

Ammonium Sulfate Improves Nutrient Status and Photosynthetic Activity in Sorghum (*Sorghum bicolor* L.) Grown in Alkaline-Saline-Sodic Soils **e9114**
El sulfato de amonio mejora la absorción de nutrientes y la eficiencia fotosintética del *Sorghum bicolor* L. cultivado en suelos alcalinos-salinos-sódicos
María Belén Ciacci, Rodrigo Ezequiel Domínguez, Silvia Del Carmen Imhoff, Dolores Ángela Bustos, Fernando Salvagiotti, Dario Fernando Luna

Growth and Foliar Alkaloid Content of *Clitoria ternateaunder* Different Irrigation Frequencies **e8603**
Desarrollo y contenido foliar de alcaloides de la conchita azul (*Clitoria ternatea*) con diferentes frecuencias de riego
Tatiana Gavilanez-Buñay, Juan Pio Salazar-Arias, Jorge Luis Ramirez de la Rivera

Yield and Development of Winter and Spring Rapeseed (*Brassica napus* L.) at Different Sowing Dates in Temperate Environments **e7865**
Desarrollo y rendimiento de colza (*Brassica napus* L.) invernal y primaveral ante distintas fechas de siembra en ambientes templados
Miguel Pereyra Iraola, Mateo Zubiri, José Luis Bodega, María Luján Nagore, Gastón Darwich, Roberto Dionisio Martínez

Physiological and Biochemical Responses of *Neltuma ruscifolia* under Na_2SO_4 Stress **e7759**
Respuestas fisiológicas y bioquímicas de *Neltuma ruscifolia* bajo estrés con Na_2SO_4
Diego Ariel Meloni, José Aliçandro Bezerra da Silva, María Judith Ochoa, Julia Andrea Lescano

Calcium Chloride as a Regulator of Floral Stem Bending in Cut-Flower Gerbera (*Gerbera jamesonii* L.) **e9111**
Cloruro de calcio como regulador de la curvatura del tallo floral en gerberas de corte (*Gerbera jamesonii* L.)
Analia Verónica Puerta, Carlos Alberto Bouzo, Gunther Mantilla

Natural resources and environment | Recursos naturales y ambiente

Effects of Climate Change on Nine Rainfed *Zea mays* Races in Chiapas, Mexico **e8062**
Efectos del cambio climático sobre nueve razas de temporal de *Zea mays* en Chiapas, México
Alejandro Vázquez Moreno, Tamara Mila Rioja Paradela, Arturo Carrillo Reyes, Carolina Orantes García, Eduardo Espinoza Medinilla

Radial Growth Dynamics and Drought Resilience in *Pinus pinea* L. Plantations from Central-Western Argentina: Implications for Forestry Development **e8876**
Dinámica del crecimiento radial y resiliencia a la sequía de *Pinus pinea* L. en plantaciones del centro-oeste argentino: implicancias forestales
Sergio Piraino, Luciano Diaz Dentoni, Fidel Alejandro Roig

Climatic Normals in Chacras de Coria. Evolution of Air Temperature for the 1959-2020 Period **e8658**
Normales climáticas de Chacras de Coria. La evolución de la temperatura del aire para el período 1959-2020
Carlos Alejandro Flores, Adriana Inés Caretta, Nora Beatriz Martinengo

Predictive Modeling of Effective Electrical Conductivity for Irrigation Water in Mendoza, Argentina **e9281**
Modelo predictivo de conductividad eléctrica efectiva para aguas de riego en Mendoza, Argentina
Daniela Virginia Cónsoli, María Flavia Filippini

Translocation and Experimental Adaptation of *Distichia muscoides* Cushions in a Wetland Impacted by Acid Rock Drainage, Ancash, Peru **e7623**
Translocación y adaptación experimental de cojines de *Distichia muscoides* en un bofedal impactado con drenaje ácido de roca, Áncash, Perú
Maria Cristina Otoya Fernández, Yeidy Montano, Marilín Sánchez-Purihuamán, Pedro M. Tapia, Junior Caro-Castro, Carmen Carreño-Farfán

Statistical Optimization of Seed Coating in Arid-Zone Grass Species Used as Cover Crops in Woody Agroecosystems e8966
Optimización estadística del recubrimiento de semillas en gramíneas de zonas áridas para cultivos de cobertura en agroecosistemas leñosos
Carola Meglioli, Benjamín Kuchen, Leandro Ormeño, Fabio Vazquez, Carlos Alberto Parera

Impact of Fire on the Genetic Variability of a Natural Population of *Stylosanthes hippocampoides* (Fabaceae) in Corrientes, Argentina e8610
Efecto de los incendios sobre la variabilidad genética de una población natural de *Stylosanthes hippocampoides* (Fabaceae) en Corrientes, Argentina
Julieta Berenice Arcangeli, Graciela Inés Lavia, María Celeste Silvestri

Integrating Professional and Crowdsourced Data to Address Biodiversity Knowledge Gaps in Under-Sampled Semi-Arid Wetlands e9216
Integración de datos profesionales y colaborativos para abordar vacíos de conocimiento sobre biodiversidad en humedales semiáridos
Solana Tabeni, Joaquin Asad, Ever Tallei, Benjamin Bender, Bertilde Rossi

ECONOMY AND AGRICULTURAL POLITICS | ECONOMÍA Y POLÍTICA AGRARIA

Social Welfare Effects of Water Security Improvements in Arid Regions: The Case of Mendoza, Argentina e8916
Efectos sobre el bienestar social de mejoras en la seguridad hídrica en regiones áridas: el caso de Mendoza, Argentina
Verónica Inés Farreras González, Carolina Lauro, Laura Abraham, Pablo Federico Salvador

Determinants of Agricultural Land Prices in the Mendoza River Basin: A Spatial Hedonic Analysis with Emphasis on Irrigation Water e9331
Determinantes del precio de la tierra agrícola en la Cuenca del Río Mendoza: un análisis hedónico espacial con énfasis en el agua de riego
Vanina Fabiana Ciardullo, Alejandro Juan Gennari, María Eugenia Martinez Fagliano, Patricia Lilian Winter, Juan Matías Elissonde

Farmers' Fertilizer Use Behaviour: Evidence from Western Part of Türkiye e7534
Análisis de los factores que afectan al comportamiento de los agricultores frente al uso de fertilizantes: datos de la parte occidental de Turquía
Murside Cagla Ormeci Kart, Kenan Ciftci, Sule Isin

PLANT PROTECTION | PROTECCIÓN VEGETAL

First Record of Potential Vectors (Hemiptera: Auchenorrhyncha) of *Xylella fastidiosa* in Olive Groves from Argentina e8960
Primer registro de potenciales vectores (Hemiptera: Auchenorrhyncha) de *Xylella fastidiosa* en olivares de Argentina
Bárbara S. Defea, Angelo Mazzaglia, Susana L. Paradell, Gabriela Lucero, Álvaro Foieri, Pablo Pizzuolo, Oscar Peñaloza, Eduardo G. Virla, Stefano Speranza

First Record of *Spintherophyta aurichalcea* (Germar, 1824) (Coleoptera: Chrysomelidae) Damaging *Ilex paraguariensis* (St. Hil.) Crops in Argentina e8447
Primer registro de *Spintherophyta aurichalcea* (Germar, 1824) (Coleoptera: Chrysomelidae) dañando cultivos de *Ilex paraguariensis* (St. Hil.) en Argentina
Maria Elena Schapovaloff, Abel Nicolás Scherf, Marcos Rubén Costa, Maria Cecilia Gramajo, Diana Virginia Ohashi, Daniela Sofia Ayala

Critical Point Analysis for Sustainable Management of *Cydia pomonella* (Lepidoptera: Tortricidae) in Smallholder Walnut Farms of Catamarca, Argentina e8595
Análisis de puntos críticos en la sustentabilidad del manejo de *Cydia pomonella* (Lepidoptera: Tortricidae) en pequeñas producciones nogaleras de Catamarca, Argentina
María José Cavallo, María Cecilia Castilla, Lucas Ariel Barros, Oscar Eduardo Romero, Braian Vladimir Sosa, Martin Sebastian Espinosa, Patricia Alejandra Diez

Biofungicide Formulation Based on *Bacillus velezensis* EM-A8 for Control of Maize Foliar Diseases e7859
Formulación de biofungicida a base de *Bacillus velezensis* EM-A8 para el control de enfermedades foliares en maíz
Melina Sartori, Daiana García, María Fiamma Grossi Vanacore, Aluminé Fessia, Andrea Nesci

Seed Physiological Quality and Selectivity of Pre-Emergence Herbicides in Soybean (*Glycine max* L.) e8217
Calidad fisiológica de las semillas y selectividad de herbicidas pre-emergentes en el cultivo de soja (*Glycine max* L.)
Alessandro Guerra da Silva, João Victor dos Santos Caldas, Sérgio de Oliveira Procópio, Guilherme Braga Pereira Braz, Itamar Rosa Teixeira, Camila Jorge Bernabé Ferreira, Matheus de Freitas Souza, Ricardo Scheffer de Andrade Silva

Epiphytic Microorganisms Associated with Banana Phyllosphere with Potential Antagonism to Black Sigatoka (*Pseudocercospora fijiensis*) in Los Ríos, Ecuador e8117
Identificación de microorganismos epífitos asociados a la filósfera de banano con potencial antagonismo a Sigatoka Negra (*Pseudocercospora fijiensis*) en la provincia de Los Ríos, Ecuador
Solanyi Marley Tigselema Zambrano, Aracelly Mabel Villalba Puga, Jim Raphael Ochoa Ramos, Galo Efraín Lara Hidalgo, Diana Aracelly López

Monitoring of the Community of Scandent Weeds in Yerba Mate (*Ilex paraguariensis* A. St. Hil., Aquifoliaceae) Cultivated in North-Eastern Argentina e8737
Monitoreo de la comunidad de malezas trepadoras en cultivo de yerba mate (*Ilex paraguariensis* A. St. Hil., Aquifoliaceae) en el nordeste de Argentina
Claudio Marcos Dávalos, Rafael Augusto Lovato Echeverría, Laura Itatí Giménez, María Gabriela López

Mortality of the Toad Grasshopper (*Bufonacris claraziana* Saussure) Caused by *Beauveria bassiana* (Balsamo) Vullemin (Hypocreales: Clavicipitaceae) by Two Inoculation Methods under Field-Cage Conditions e8152
Evaluación de la mortalidad causada por *Beauveria bassiana* (Balsamo) Vullemin (Hypocreales: Clavicipitaceae) contra la tucura sapo comparando dos procedimientos de inoculación en condiciones de jaulas en el campo
Yanina Mariottini, Sebastián Alberto Pelizza, Lucas Emanuel Castelli, Franco Armento, Carlos Ernesto Lange

PRODUCTION AND ANIMAL HEALTH | PRODUCCIÓN Y SANIDAD ANIMAL

Beef Quality of Braford Young Intact Males and Steers Grazing Pastures and Supplemented with Energy-Protein Sources During Growing and Fattening e7843
Calidad de la carne de machos enteros jóvenes y novillos Braford en sistema pastoril suplementados con fuentes de energía y proteína durante el crecimiento y engorde
María José Fernández Salom, Natalia Verónica Taboada, Olegario Hernández, Diego Bottegal, Sandra Luz Martinez, María Zimerman

***Enterococcus gallinarum* CRL 1826 as a Probiotic for Ranaculture: *in vitro* Safety, Technological, and Physiological Properties** e8155
Enterococcus gallinarum CRL 1826 como probiótico para ranicultura: seguridad *in vitro*, propiedades tecnológicas y fisiológicas
María Andreína Acevedo, María Claudia Otero, María Constanza Lizárraga, Cesar Emmnuel Ale, Ricardo Javier Llanos, María Elena Nader-Macías, Sergio Pasteris

Net Protein Requirements for Maintenance and Weight gain in Male Guinea Pigs (*Cavia porcellus*) of the Peru Breed e8113
Requerimientos de proteína neta para mantenimiento y ganancia de peso en cuyes machos (*Cavia porcellus*) de la raza Perú
William Armando Tapie Canacuan, Sandra Lucia Posada-Ochoa, Jaime Ricardo Rosero-Noguera

Synergistic Action of the Essential Oils of *Elionorus muticus* and *Lippia junelliana* Against the Causative Agent of Chalkbrood in Bees (*Ascosphaera apis*) e8484
Acción sinérgica de los aceites esenciales de *Elionorus muticus* y *Lippia junelliana* sobre el agente causal de la cría yesificada en abejas (*Ascosphaera apis*)
Maricel Vega, Maria Laura Susevich, María Inés Troncozo, Francisco Jose Reynaldi, Graciela Noemi Albo

Transition Management and Dairy Cow Performance: Insights from Dairy Farms in Argentina e8540
Manejo de la Transición y Desempeño de las Vacas Lecheras: Perspectivas de Establecimientos en Argentina
María Paula Turiello, Claudina Vissio

Longevity of Purebred and Triple-Cross Dairy Cows in Entre Rios, Argentina e8367
Longevidad de vacas lecheras razas puras y triples cruzas en un establecimiento de Entre Ríos, Argentina
Roberto Cheij, María Gabriela Molina, María Laura Fischman, Walter Mancuso, Pablo Roberto Marini

Agroindustrial technologies | Tecnologías agroindustriales

Valorization of Regional Crude Glycerol. Culture Media Optimization for Batch Docosahexaenoic Acid (DHA) Production with *Aurantiochytrium* sp. e7577
Valorización de glicerol crudo regional. Optimización de medios de cultivo para la producción batch de ácido docosahexaenoico (DHA) con *Aurantiochytrium* sp.
Esteban Andrés Sanchez, Debora Laura Manuale, Pablo Antonio Torresi, Vanina Elizabet Marquez, Francisco Collombati, Alejandro José Beccaria, Juan Carlos Yori

Optimization of Antioxidant Extraction from *Mutisia friesiana*, Native Plant of the Quebrada and Puna Regions of Argentina e8725
Optimización de la extracción de antioxidantes de *Mutisia friesiana*, una planta nativa de las regiones de Quebrada y Puna de Argentina
Mónica Daniela Godoy, Norma Beatriz Farfán, Diego Cristos, Gabriela Grigioni

Physicochemical Properties, Bioactive Compounds, and Antioxidant Activity of Andean Fruits: Optimization of Extraction by Response Surface Methodology e9133
Propiedades fisicoquímicas, compuestos bioactivos y actividad antioxidante de frutas andinas: optimización de la extracción mediante metodología de superficie de respuesta
Vicente Amirpasha Tirado-Kulieva, Jimy Oblitas, Noemí León-Roque, Wilson Castro

Ammonium Sulfate Improves Nutrient Status and Photosynthetic Activity in Sorghum (*Sorghum bicolor* L.) Grown in Alkaline-Saline-Sodic Soils

El sulfato de amonio mejora la absorción de nutrientes y la eficiencia fotosintética del *Sorghum bicolor* L. cultivado en suelos alcalinos-salinos-sódicos

María Belén Ciacci [1], Rodrigo Ezequiel Domínguez [1], Silvia Del Carmen Imhoff [3], Dolores Ángela Bustos [1], Fernando Salvagiotti [2, 4], Dario Fernando Luna [1*]

Originales: *Recepción:* 17/07/2025- *Aceptación:* 22/12/2025

ABSTRACT

This study investigated whether fertilization with urea or ammonium sulfate could mitigate the growth limitations of sorghum imposed by alkaline-saline-sodic (ASS) soils. We hypothesized that the application of these nitrogen sources would improve the plant's mineral status and photosynthetic activity. Experiments were conducted using three sorghum hybrids under both field and greenhouse conditions, comparing ASS soil to a non-ASS control. The treatments included fertilization with ammonium sulfate, urea, and a non-fertilized control. At the end of both experiments, soil and plant samples were analyzed to assess soil pH, nutrient content, and chlorophyll fluorescence. Our results demonstrate that ammonium sulfate, but not urea, significantly improved plant mineral status by inducing acidification in the ASS soil. This improved status led to increased photosynthetic rates and biomass production compared to unfertilized controls. These findings position ammonium sulfate as an effective tool for improving sorghum growth and productivity in challenging marginal soils.

Keywords
Sorghum bicolor • alkaline-saline-sodic soils (ASS) • ammonium sulfate (AS) fertilization • urea (U) • plant mineral nutrition • photosynthesis

https://doi.org/10.48162/rev.39.212

1 Instituto de Fisiología y Recursos Genéticos Vegetales (IFRGV). Centro de Investigaciones Agropecuarias (CIAP). Instituto Nacional de Tecnología Agropecuaria (INTA). Unidad de Estudios Agropecuarios (UDEA-CONICET). Av. 11 de Septiembre 4755. X5020ICA. Córdoba. Argentina. * luna.fernando@inta.gob.ar
2 Grupo de Manejo de cultivo suelo y agua. Estación Experimental Agropecuaria Oliveros. Instituto Nacional de Tecnología Agropecuaria (INTA). Ruta Nacional 11 km 353. (C2206) Oliveros. Santa Fe. Argentina.
3 ICiAgro Litoral (CONICET-UNL). Kreder 2805. Esperanza. Santa Fe.
4 Consejo Nacional de Investigaciones Científicas y Técnicas (CONICET). Argentina.

Licenses Creative Commons
Attribution - Non Commercial - Share Alike

Resumen

El objetivo de este estudio fue determinar si la fertilización con urea o sulfato de amonio logra mitigar las restricciones en el crecimiento del sorgo impuestas por suelos salino-sódicos alcalinos (SSA), mejorando el estado mineral de la planta y, en consecuencia, su actividad fotosintética. Para ello, se llevaron a cabo ensayos de campo y de invernadero, usando tres híbridos de sorgo en dos tipos de suelo: uno control y otro SSA. Los tratamientos incluyeron fertilización con sulfato de amonio y urea, además de un tratamiento sin fertilizar, empleado como control. Se recolectaron muestras de suelo y planta al final de cada experimento para evaluar el pH del suelo, el contenido de nutrientes y la fluorescencia de la clorofila. Nuestros resultados demuestran que, a diferencia de la urea, la aplicación de sulfato de amonio mejoró significativamente el estado mineral de la planta en respuesta a la acidificación del suelo SSA. Además, la aplicación de sulfato de amonio aumentó las tasas fotosintéticas y la producción de biomasa en comparación con las no fertilizadas. Estos hallazgos posicionan al sulfato de amonio como una herramienta agronómica eficaz para mejorar el crecimiento del cultivo de sorgo en suelos marginales.

Palabras clave

Sorghum bicolor • salino-sódicos alcalinos (SSA) • fertilización con sulfato de amonio (SA) • urea (U) • nutrición mineral de las plantas • fotosíntesis

Introduction

Alkaline saline-sodic soils (ASS) negatively impact crop growth and productivity due to the combined effect of salinity, sodicity, and alkalinity. These soils are characterized by an electrical conductivity (EC) exceeding 4 dS m^{-1} (units used throughout the manuscript, ~40 mM NaCl), a sodium adsorption ratio (SAR) greater than 13 meq L^{-1}, an exchangeable sodium percentage (ESP) over 15%, and a pH ranging from 8.5 to 10. High sodium ion (Na^+) concentrations degrade soil structure by promoting clay dispersion, thereby reducing structural stability and water infiltration rates in these soils (Rengasamy, 2010). Furthermore, the high pH associated with alkalinity severely limits plant growth and nutrient uptake of essential elements, including nitrogen (N), phosphorus (P), potassium (K), calcium (Ca), magnesium (Mg), iron (Fe), and zinc (Zn) (Marschner & Rengel, 2012; Sparks, 2003). However, this method is often costly, requires the application of substantial amounts of gypsum, and its effectiveness depends on high infiltration capacity and the presence of adequate drainage systems (González *et al.*, 2019). In addition to chemical amendments, biological processes occurring in the rhizosphere also contribute to nutrient cycling and overall soil functioning. Microorganisms associated with crop rhizospheres may play a relevant role in nutrient transformations and plant–soil interactions under agricultural conditions (Tupa-Andrade *et al.*, 2025). Conversely, nitrogen fertilizers are widely used to meet crop N requirements. Among N sources, ammonium sulfate (AS) offers potential agronomic advantages over urea (U) in alkali saline-sodic soil environments (Chien *et al.*, 2011). The main difference lies in the ability of AS to promote soil acidification. Specifically, through the nitrification process, AS theoretically generates twice the soil acidity per unit of applied N compared with urea (Adams, 1984; Pierre, 1928).

Sorghum (*Sorghum bicolor* (L.) Moench) has emerged as a highly relevant forage crop, particularly for marginal lands in regions like Córdoba, due to its inherent stress-tolerance mechanisms. Its adaptive traits include the capacity for osmotic adjustment, selective ion uptake, and a deep root system. These characteristics enable it to maintain productivity under water and saline stress, positioning it as a strategic resource for livestock systems in ASS-affected areas, where climate variability and soil degradation limit agricultural options (Giorda & Ortiz, 2012; RAGT Semillas, 2025). In these environments, salinity and alkalinity often impair photosynthetic efficiency by restricting CO_2 diffusion through the stomata and mesophyll, or by directly altering the photosynthetic metabolism (Chaves *et al.*, 2009). These changes can induce secondary damage, such as oxidative stress, which negatively affects the structure and function of photosystem II (PSII) components (Flexas *et al.*, 2004; Lawlor

& Cornic, 2002). One of the most widely used techniques for assessing the structural and functional status of PSII is chlorophyll fluorescence kinetics, specifically OJIP analysis. This mathematical model provides critical information on the redox state of the PSII electron transport chain components, and the magnitude of OJIP parameters response is linked to the salinity and alkalinity stress tolerance of the evaluated plant hybrids (Kalaji *et al.*, 2018; Stirbet & Govindjee, 2011). Based on the evidence that AS is a superior acidifying agent and that nutrient deficiency and photosynthetic damage are significant ASS constraints, we propose the following hypotheses: (1) AS is a more effective N fertilization strategy than urea for improving the nutritional status of sorghum plants in ASS soils, due to its superior soil acidification capacity and resultant enhancement of nutrient availability; and (2) Fertilizing sorghum grown in ASS soil with either AS or U will reduce damage to PSII electron transport chain components, as evaluated by OJIP analysis, with AS providing better protection due to improved plant nutritional status. Hence, this study aimed to: (i) evaluate whether ammonium sulfate or urea application can mitigate the nutrient deficiencies caused by ASS soils in sorghum hybrids under both field and greenhouse conditions; and (ii) determine the effects of AS and urea application in ASS soils on PSII activity of sorghum hybrids with different salinity-alkalinity tolerance, using OJIP analysis.

Materials and Methods

Study Site and Soil Characterization

The experiments were conducted in Villa Fontana, Córdoba, Argentina (30°52'26.9" S, 63°05'29.4" W, and 107 m above sea level). Two distinct soil types were utilized, sourced from fields situated 5 km apart: a control soil (slightly acidic) and a saline-sodic-alkaline (ASS) soil. Both soils shared a loamy-clayey texture. For the field experiment, the control soil exhibited a pH of 6.32, an electrical conductivity (EC) of 0.52 dS m^{-1}, an organic matter content of 1.5%, a total carbon content of 1.01%, a total N content of 0.10%, available P content of 16.8 mg kg^{-1}, and exchangeable Ca content of 10.24, Mg 2.37, K 1.54, Na 0.22 cmol(+) kg^{-1}. The ASS soil, conversely, had a pH of 8.27, electrical conductivity of 8.84 dS m^{-1}, an ESP of 28.8%, organic matter of 1.1%, total carbon of 0.64%, total N of 0.06%, available P of 6.8 mg kg^{-1}, Ca 11.92, Mg 3.48, K 1.41, Na 6.76 cmol(+) kg^{-1}. For the greenhouse experiment, the control and ASS soils had a pH values of 6.3 and 9.7, an electrical conductivities of 0.5 and 6.2 dS m^{-1}, a cation exchange capacity of 1.4% and 31.8%, organic matter of 1.89% and 1.37%, total carbon of 1.10% and 0.79%, total N 0.109% and 0.084%, available P 11.3 and 16.9 mg kg^{-1}, Ca 6.5 and 7.5, Mg 3.5 and 1.5, K 1.8 and 2.7, Na 0.2 and 5.4 cmol(+) kg^{-1}, respectively. Detailed soil properties for both experiments are provided in Supplementary Tables S1 and S2.

Experimental Design and Treatments

The field experiment was conducted during the 2018/2019 growing season using a split-plot design with five replicates (blocks). The main plots consisted of the two soil types -a control and ASS- while subplots were created from the factorial combinations of three sorghum hybrids and three fertilizer treatments, totaling 90 subplots (2 soil types × 3 hybrids × 3 fertilizer treatments × 5 blocks). The three evaluated sorghum hybrids were INTA Peman Silero (SIP), Argensor 155 DP (155), and Argensil 163 D (163). The three fertilizer treatments included Ammonium sulfate (AS), Urea (U), and a non-fertilized control (Non-fert). Fertilizers were applied at a rate of 120 kg N ha^{-1}, divided equally into two applications: 50% at planting and 50% at the V5 growth stage. Each plot measured 1.26 × 6.0 m, with three rows separated by 0.42 m, and had a final density of 15 plants m^{-2}. Standard agronomic practices, including weed control and irrigation, were maintained. The greenhouse experiment was conducted during 2020/2021 using a completely randomized factorial design with five replicates per treatment (n = 5), resulting in 90 pots (2 soil types × 3 hybrids × 3 fertilizer treatments × 5 replicates). Plants were cultivated in 3-L pots under controlled conditions with an average temperature of 28°C and photosynthetically active radiation (PAR) of 1500 µmol m^{-2} s^{-1}. Plants were watered three times a week to maintain field capacity at 0.30 cm^3 water content.

Sampling Protocol

Plants were harvested 60 days after emergence (DAE) in the field experiment and 35 DAE in the greenhouse trial. The shorter period in the greenhouse was due to the spatial constraints of pot cultivation, which limit root development and overall plant growth compared with field conditions. The same sampling protocol was used in both experiments, where five plants were collected per treatment combination (n = 5). In the field experiment, samples were collected from the central row of each subplot across all five replicate blocks (total N = 90). The greenhouse experiment maintained an equivalent total sample size (N = 90). For the aerial plant sampling, shoots were harvested by cutting at 0.5 cm above the soil surface. Leaf samples used for nutrient analyses were collected from the same plants used for biomass determination. Soil samples for pH analysis were collected from each subplot at harvest. Subsamples of 1.0 g of soil were collected at a depth of 20 cm in the field and at 15 cm in 18 cm-high pots. Soil pH was determined at the base of each plant, along the sowing line, at a depth of 0-2 cm. Measurements were performed in a 1:2.5 soil: water suspension after 30 minutes of equilibration using a calibrated pH meter.

Measurements

Soil pH was measured at harvest in both experiments using the procedure described in the sampling protocol. For plant dry weight determination, harvested shoots were dried in a ventilated oven at 60°C until constant weight was reached, and aerial dry matter was determined for each sampled plant. Nutrient analysis was performed on specific leaf tissues to assess nutrient status due to different nutrient mobility accurately: younger leaves (apical) typically show higher concentrations of mobile nutrients (Ca, Mg, K), while older leaves (basal) better reflect the plant's N and P status. These nutrients were also evaluated in the greenhouse plants using the same protocol as in the field experiment. Total N was determined by the Kjeldahl method, P by the colorimetric method using nitrovanadate-molybdate reagent, K was quantified by flame spectrophotometry, and Ca and Mg by atomic absorption spectrometry. This differential sampling reflected nutrient mobility: For the Photosystem II (PSII) component analysis, the chlorophyll-a fluorescence transient (ChlF) rate was measured on the newest fully expanded leaf at harvest (60 DAE in the field and 35 DAE in the greenhouse), using a Pocket-PEA fluorometer (Plant Efficiency Analyzer, Hansatech Instruments Ltd., King's Lynn, Norfolk, UK). Before the ChlF measurements, the leaves were dark-adapted for at least 30 minutes using specific leaf clips to ensure complete oxidation of the reaction centers (RCs). An actinic 1-second light pulse of 3500 µmol photons m^{-2} s^{-1} was applied to reach maximum fluorescence emission (Fm or P step) at approximately 300 ms. The minimum fluorescence (Fo O step) was recorded at ~50 ms, and the intermediate steps, called J and I, were recorded at 2 ms and 30 ms, respectively. The OJIP parameters were calculated using Pocket-PEA manufacturing software (Strasser *et al.*,2004; Supplementary Table 3).

Statistical Analysis

Statistical comparisons were performed to evaluate differences among hybrids (genotypic variation), fertilizer treatments (AS and U), soil conditions (ASS *vs.* control), and their interactions. Soil pH, plant biomass, foliar nutrient concentrations, and PSII chlorophyll fluorescence data were analyzed in R (v3.6.2) using RStudio (v1.3.959) and the *tidyverse* package (v1.3.0). Data normality was assessed through the Shapiro-Wilk test and visual inspection of Q-Q plots. As the assumptions of normality were not met in most cases, even after applying logarithmic, square-root, and Box-Cox transformations, non-parametric tests were employed. The Kruskal-Wallis test was used to evaluate overall group differences, and the pairwise Wilcoxon rank-sum test was subsequently applied for post-hoc comparisons when significant effects were detected ($p < 0.05$).

In this study, the chlorophyll fluorescence parameters derived from the OJIP test were not normalized using a standard procedure. Instead, data normalization was achieved by expressing the values relative to the corresponding control soil condition, a common approach to account for potential differences across hybrids and fertilizer treatments. Specifically, for each hybrid and fertilizer treatment combination, the mean value obtained under ASS soil conditions ($\bar{x}_{ASS,\ hybrid\ i,\ tratment\ j}$) was divided by the corresponding mean value measured in the

control soil for the same hybrid × fertilizer combination ($\bar{x}_{Control,\ hybrid\ i,\ tratment\ j}$). This calculation yielded a dimensionless ratio that expresses the relative performance of plants grown in ASS soil compared with their counterparts under non-stress conditions (Equation 1).

$$Relative\ value\ _{(parameter)} = \frac{\bar{x}_{ASS,hybrid\ i,tratment\ j}}{\bar{x}_{Control,hybrid\ i,tratment\ j}} \quad (1)$$

Where $\bar{x}$ represents the average of the valuated parameter for each sorghum hybrid (i) and N treatment (j).

Results

Soil pH and Plant Dry Weight

Soil pH

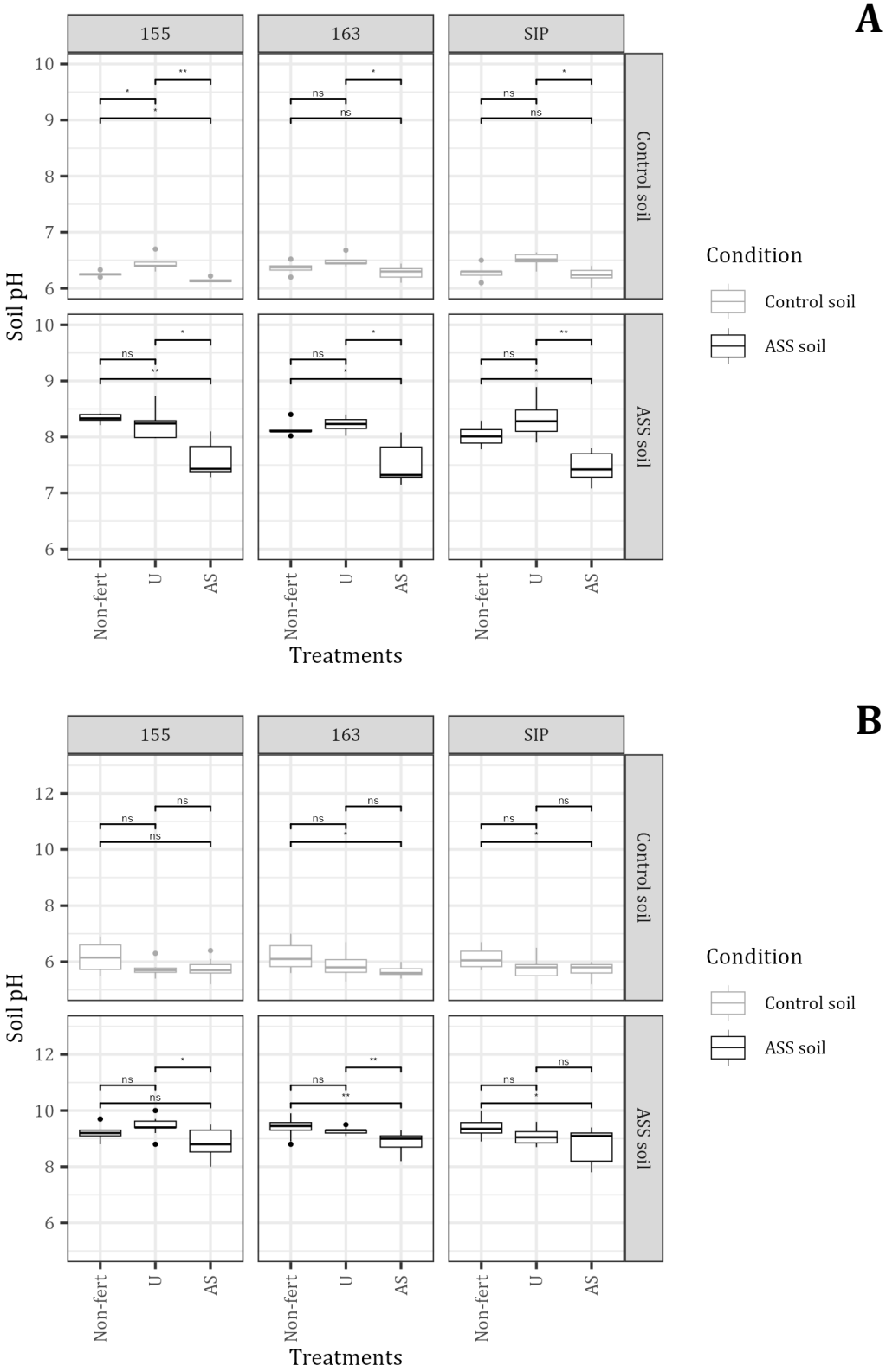
The two experiments demonstrated a consistent pattern regarding the effect of N source on soil pH across the two soil types. In the field experiment, the pH of the control soil (initially slightly acidic) remained stable, showing no significant differences across all sorghum hybrids and fertilizer treatments, with values ranging narrowly from 6.26 to 6.36 (figure 1A, page 6). In sharp contrast, ASS soil exhibited marked pH responses to fertilization. The AS application significantly reduced soil pH across all hybrids, from 8.16 (Non-fert) to 7.53, representing an approximately 0.6-unit decrease. Urea application did not affect ASS soil pH relative to the unfertilized control. However, the magnitude of AS-induced acidification varied among hybrids: in hybrid 155, all N treatments differed significantly from one another; while in hybrids 163 and SIP, AS achieved substantially lower pH values than both U and Non-fert treatments, which themselves did not statistically differ.

Similar patterns were observed in the greenhouse experiment (figure 1B, page 6). The pH in the control soil remained stable across all hybrids and treatments. In ASS soil, AS application led to a more pronounced reduction, dropping substantially from 9.54 (Non-fert) to 8.52, an approximate 1-unit decrease. Consistent with the field trial, the U application showed no significant acidifying effect compared to the unfertilized control, with both treatments maintaining high pH levels around 9.5 in the ASS soil.

Plant Dry Weight

ASS soils negatively affected sorghum growth in both field and greenhouse experiments. In the field experiment, the impact of N fertilization on biomass production in the ASS soil varied depending on the N source, hybrid, and soil type. In hybrid 155, which was identified as the most sensitive, AS treatment yielded significantly lower biomass than the U treatment under ASS conditions (62% less than the control soil), and both treatments produced biomass significantly lower than the Non-fert treatment (figure 2A, page 7). In contrast, in the more tolerant hybrids (163 and SIP), AS treatment significantly improved sorghum growth in ASS soils relative to both U and Non-fert treatments, achieving dry weight levels comparable to those observed in control soils. In these tolerant hybrids, AS treatment significantly increased biomass compared to both U and Non-fert treatments in ASS soil. Conversely, the U application did not produce significant changes in dry weight relative to non-fertilized controls in either ASS soil or control soil.

In the greenhouse experiment, fertilization treatments in the control soil produced no significant differences in dry weight across hybrids or N sources (figure 2B, page 7). However, in ASS soil, AS significantly increased dry weight compared to both U and Non-fert treatments, with improvements ranging from 2- to 5-fold depending on the hybrid. Consistent with field observations, U fertilization showed no significant effect on plant dry weight compared to Non-fert controls in ASS soil.

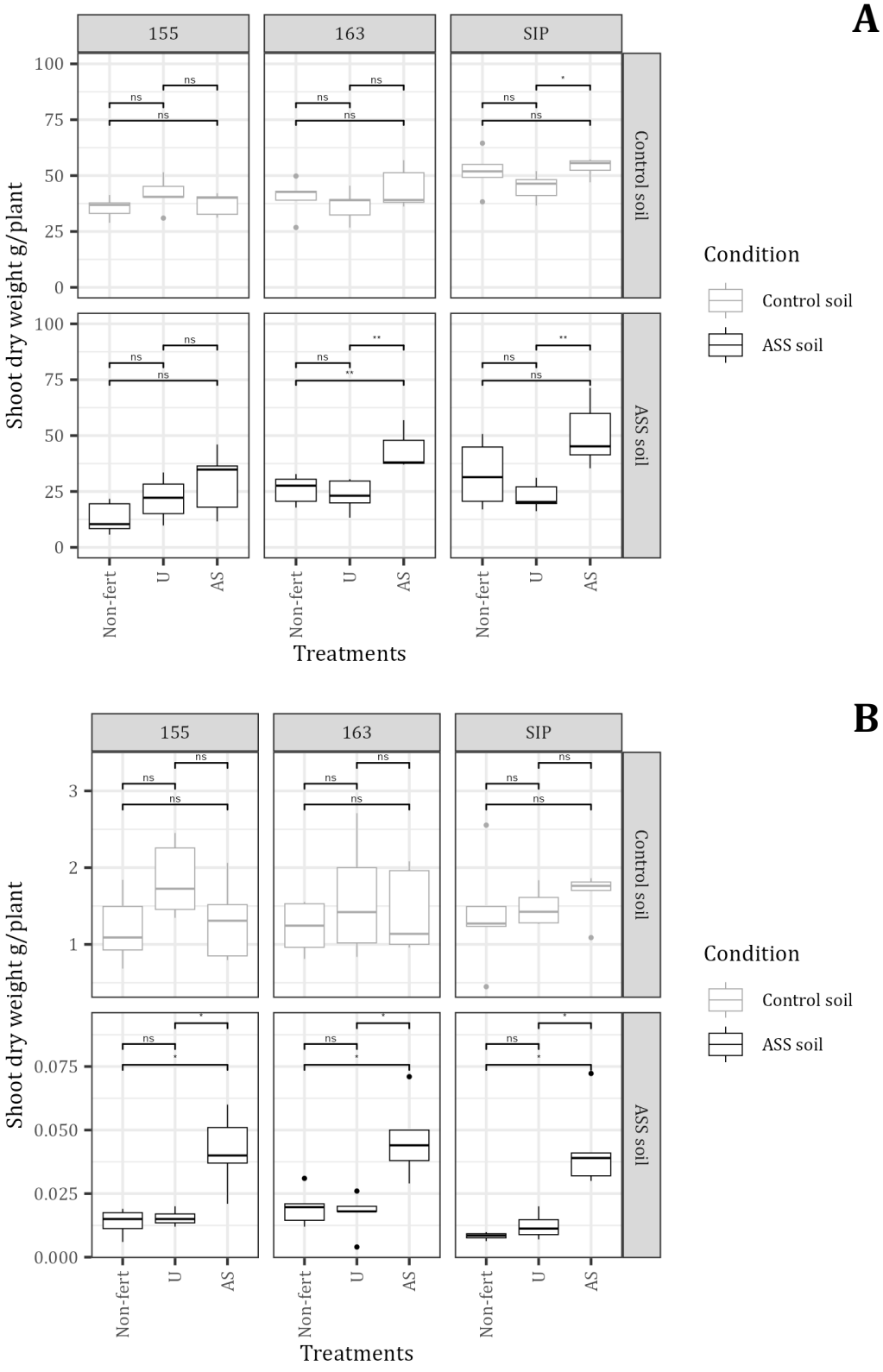


Data represent mean ± standard error (n = 5). Asterisks indicate significant differences between treatments within each hybrid-soil combination: ns = $p > 0.05$, * = $p \leq 0.05$, ** = $p \leq 0.01$, *** = $p \leq 0.001$. Black dots represent outliers.

Los datos representan medias ± error estándar (n = 5). Los asteriscos indican diferencias significativas entre tratamientos dentro de cada combinación híbrido-suelo: ns = $p > 0,05$, * = $p \leq 0,05$, ** = $p \leq 0,01$, *** = $p \leq 0,001$. Los puntos negros representan valores atípicos.

Figure 1. Soil pH in control and alkaline-saline-sodic (ASS) soils under a) field and b) greenhouse conditions for three sorghum hybrids (155, 163, SIP) fertilized with ammonium sulfate (AS), urea (U), or unfertilized (Non-fert), with $n = 5$.

Figura 1. pH del suelo en suelos control y alcalino-salino-sódicos (ASS) bajo condiciones de a) campo y b) invernadero para tres híbridos de sorgo (155, 163, SIP) fertilizados con sulfato de amonio (AS), urea (U) o sin fertilizar (Non-fert).



Asterisks indicate significant differences between treatments within each hybrid-soil combination: ns = $p > 0.05$, * = $p \leq 0.05$, ** = $p \leq 0.01$, *** = $p \leq 0.001$. Black dots represent outliers. Data represent mean ± standard error (n = 5).

Los asteriscos indican diferencias significativas entre tratamientos dentro de cada combinación híbrido-suelo: ns = $p > 0,05$, * = $p \leq 0,05$, ** = $p \leq 0,01$, *** = $p \leq 0,001$. Los puntos negros representan valores atípicos. Los datos representan medias ± error estándar (n = 5).

Figure 2. Fertilization effect (AS, U, Non-fert) on plant dry weight of three sorghum hybrids (155, 163, SIP) in control and ASS soils under a) field and b) greenhouse conditions.

Figure 2. Efecto de la fertilización (AS, U, sin fertilizar) sobre el peso seco de tres híbridos de sorgo (155, 163, SIP) en suelos testigo y ASS, bajo condiciones de a) campo y b) invernadero.

Leaf Nutrient Concentration

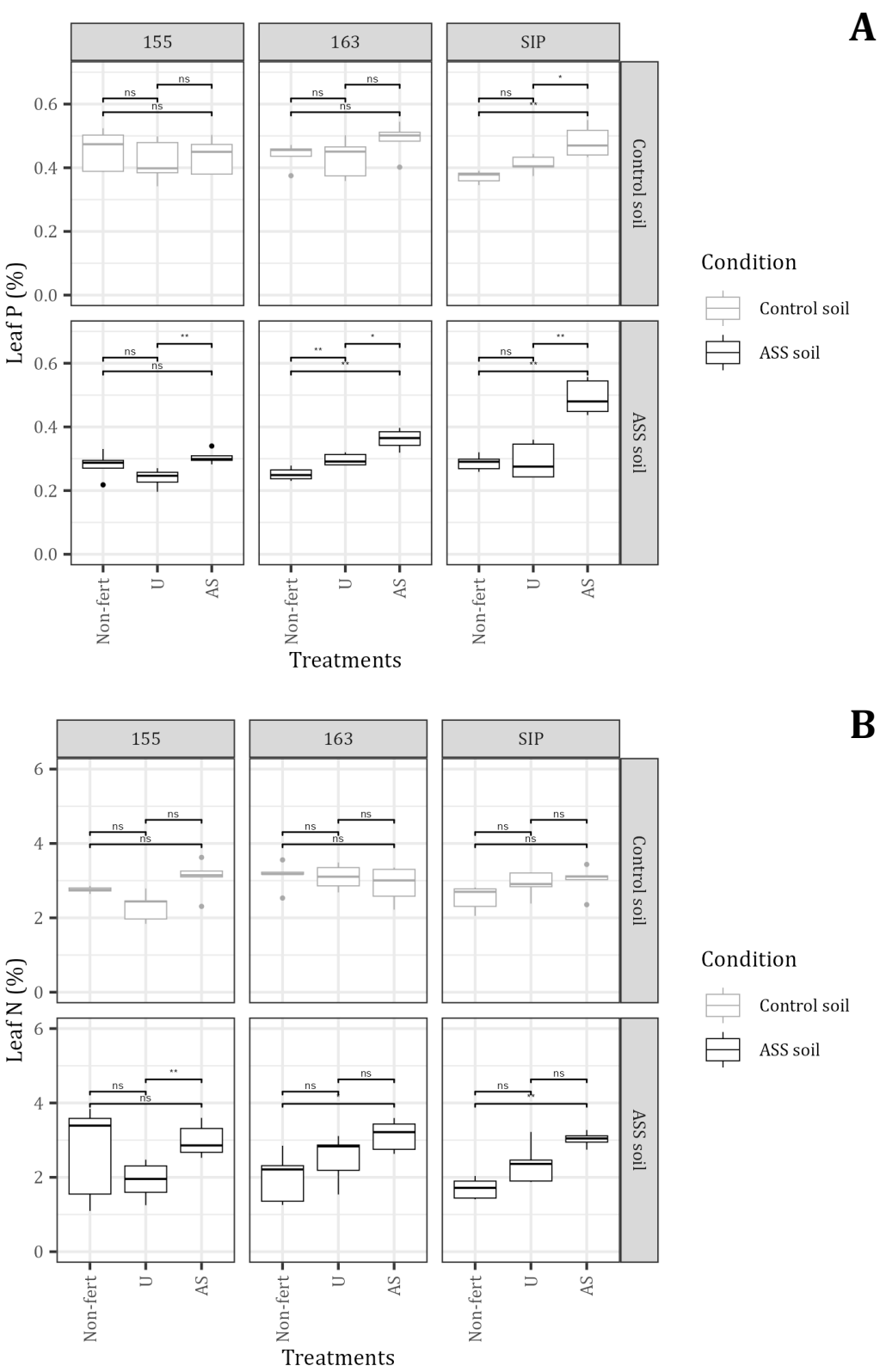
Field Experiment Nutrient Status

Sorghum plants grown in the control soil exhibited a 55% higher concentration of foliar P than those grown in unfertilized ASS soil. The most significant beneficial effect of AS fertilization in ASS soils was observed in the hybrid SIP, which showed P concentrations comparable to those of plants grown in the control soil and fertilized with AS in ASS soils (0.48% and 0.49%, respectively). In contrast, the lowest foliar P concentrations were recorded in plants grown in unfertilized control soils (0.37%) and in U-fertilized ASS soils (0.30%). For N concentration, significant differences were detected between soil conditions (C, $p \leq 0.05$) and fertilizer treatments (T, $p \leq 0.05$), with a significant C×T interaction ($p \leq 0.05$). This indicates that the effect of fertilization depends on the soil condition.

In the control soil, neither AS nor U fertilization significantly affected leaf N concentration in any of the hybrids. In contrast, in ASS soil, AS fertilization resulted in foliar N concentrations that differed substantially from U and Non-fert. In hybrids 163 and SIP, the values were 56.5% and 78% higher, respectively; while in 155, fertilization with AS did not differ significantly from the Non-Fert treatment. Across soil conditions, U-fertilization had no significant impact on N concentration in any of the hybrids. Regarding Ca concentration, significant differences were observed among hybrids, soil conditions, fertilizer treatments, and the hybrid-by-condition (H x C) interaction ($p \leq 0.05$). Generally, Ca concentration was significantly higher in the control soil across all treatments, except for the AS treatment in ASS soil, which had a Ca concentration similar to that of the control soil. In ASS soil, the highest values were observed for SIP and 163 hybrids (0.88% and 0.81%, respectively; (figure 3, page 9-10). Finally, significant differences in K concentration were found among hybrids ($p \leq 0.05$), conditions ($p \leq 0.05$), treatments ($p \leq 0.05$), and the hybrid-by-treatment (H×T) interaction ($p \leq 0.05$). The lowest K concentration was found in hybrids 155 and SIP, grown in ASS soil under the Non-fert and U treatments (~1.15%). In comparison, the highest K values were consistently recorded in plants fertilized with AS, regardless of soil type and hybrid (>1.8%).

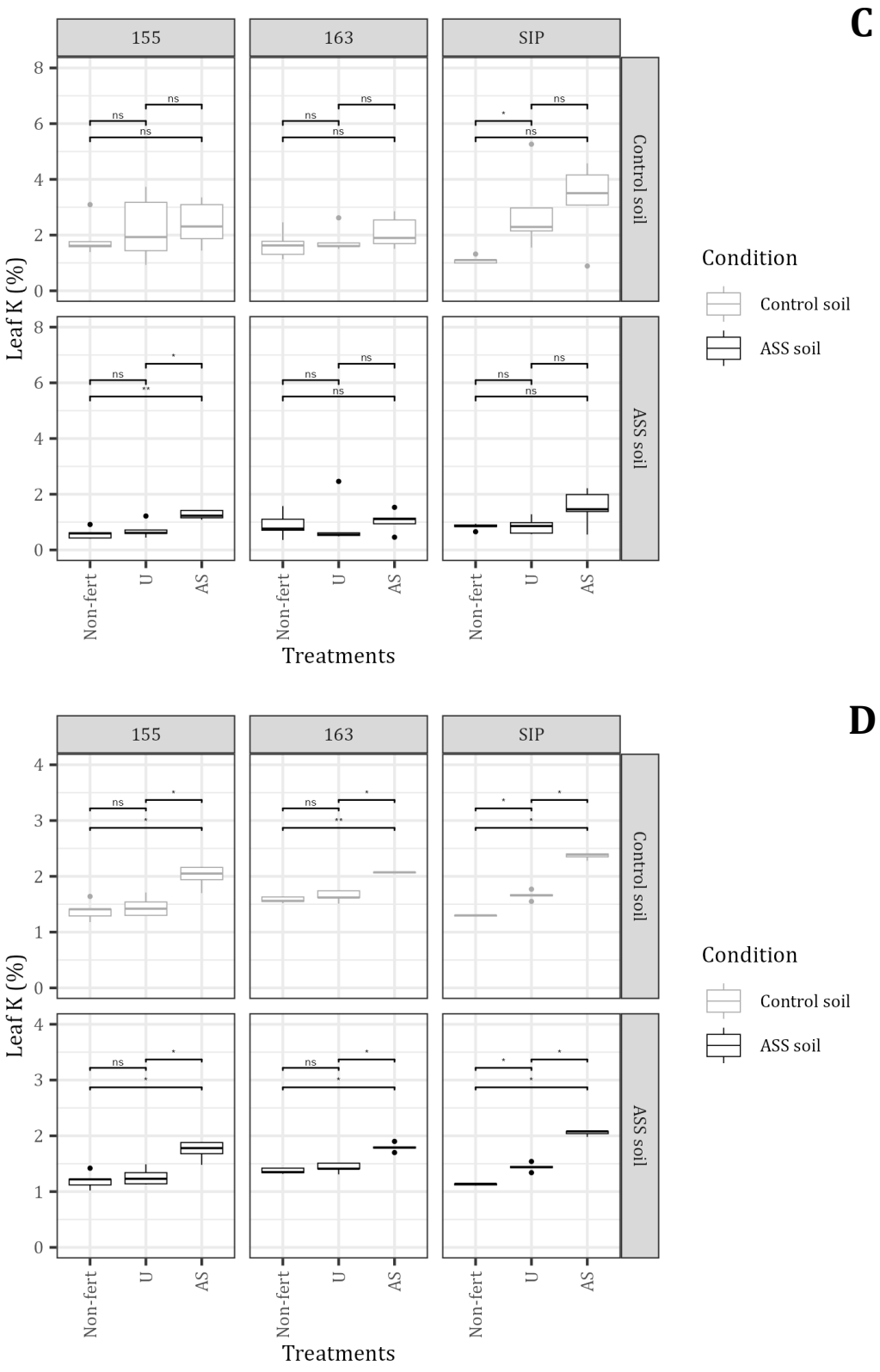
Greenhouse Experiment Nutrient Status

In the greenhouse trial, significant differences in sorghum leaf Ca concentration were observed between conditions (C, $p \leq 0.05$), treatments (T) ($p \leq 0.05$), and C×T interaction ($p \leq 0.05$) (figure 4, page 11-12). Specifically, plants in unfertilized ASS had a 62.3% lower Ca concentration than those in the control soil. Furthermore, AS treatment resulted in a Ca concentration that differed significantly from both the U and Non-fert treatments in ASS soil. For Mg concentration, significant differences were found between conditions ($p \leq 0.05$) and treatments ($p \leq 0.05$). Plants grown in unfertilized ASS soil had a significantly lower Mg concentration than those in the control soil. The AS treatment resulted in Mg concentration that differed considerably from the U and non-fertilized treatments, with the most notable difference observed in the SIP hybrid, which showed a 147% increase compared to the unfertilized ASS treatment. Finally, for K concentration, significant differences were observed only between conditions ($p \leq 0.05$). The effect of ASS on K concentration differed between greenhouse and field conditions. While the AS treatment resulted in higher K concentrations than the U and non-fertilized treatments, these differences were less pronounced than those observed in the field. No significant differences in K concentration were found among the three hybrids (figure 4, page 11-12).



Concentrations were determined in sorghum leaves:a) P, b)N, c)Ca, and d) K . The P, N, and K were analyzed in basal leaves, and Ca in apical leaves, at 60 DAE. Asterisks indicate significant differences between treatments within each hybrid-soil combination: ns = p> 0.05, * = p≤ 0.05, ** = p≤ 0.01, *** = p≤ 0.001.The black dots represent outliers.

Se determinaron las concentraciones en las hojas de sorgo: a) P, b) N, c) Ca y d) K. El P, el N y el K se analizaron en las hojas basales, y el Ca en las hojas apicales, a los 60 días después de la siembra (DAE). Los asteriscos indican diferencias significativas entre los tratamientos dentro de cada combinación de híbrido y suelo: ns = p > 0,05, * = p ≤ 0,05, ** = p ≤ 0,01, *** = p ≤ 0,001. Los puntos negros representan valores atípicos.

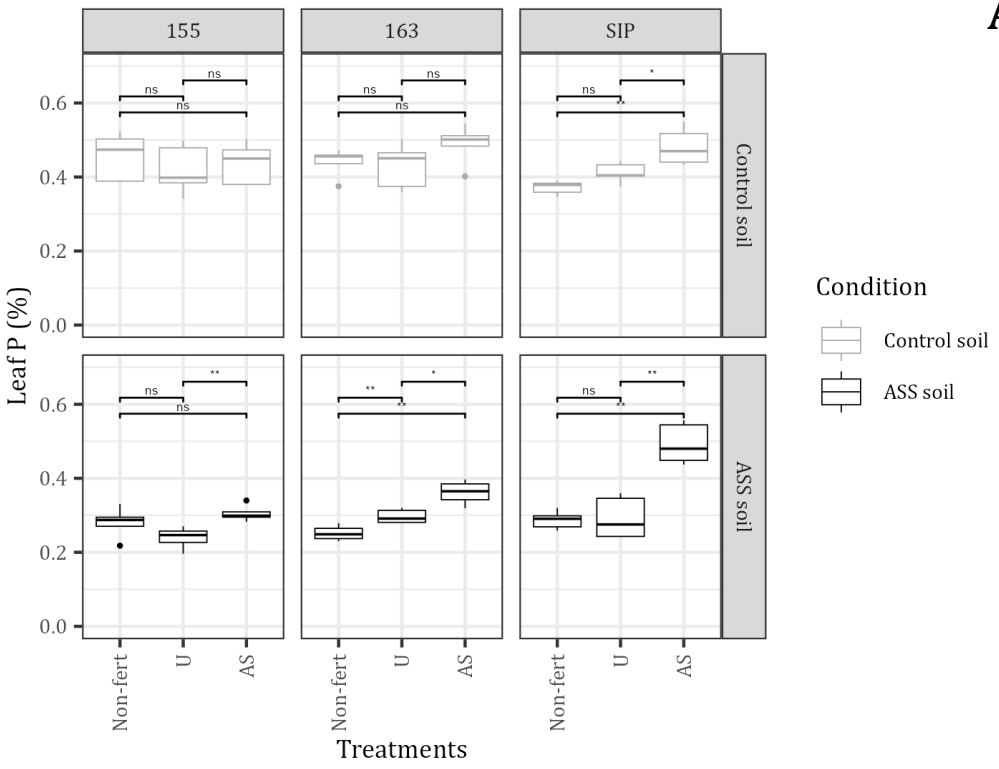


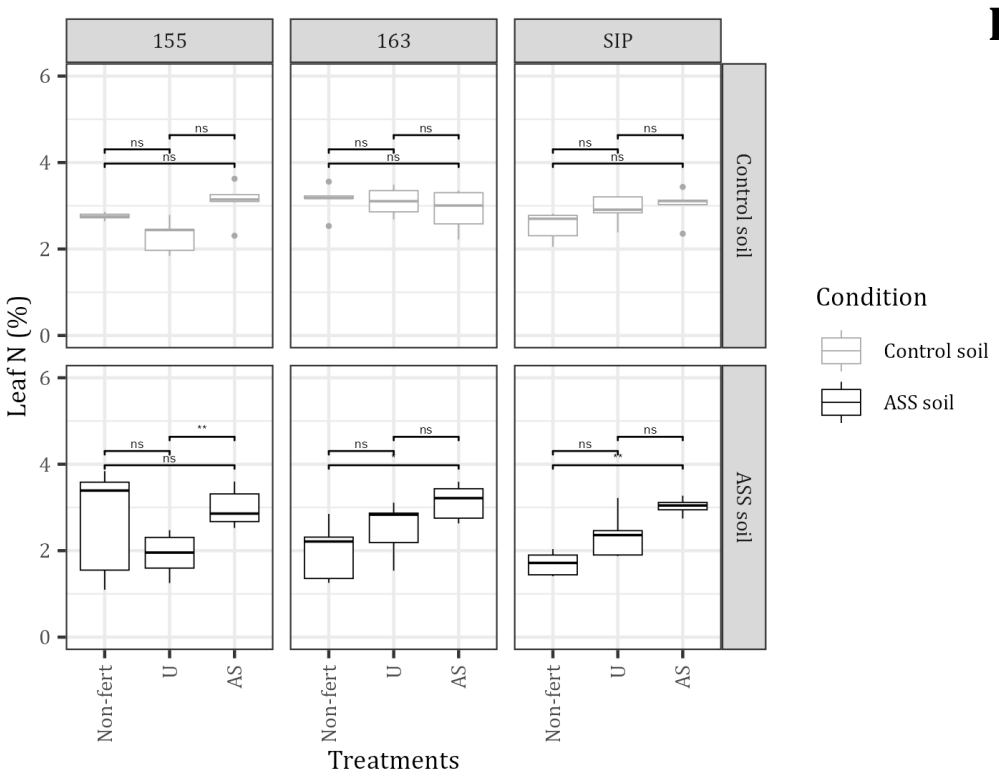
Concentrations were determined in sorghum leaves:a) P, b)N, c)Ca, and d) K . The P, N, and K were analyzed in basal leaves, and Ca in apical leaves, at 60 DAE. Asterisks indicate significant differences between treatments within each hybrid-soil combination: ns = p> 0.05, * = p≤ 0.05, ** = p≤ 0.01, *** = p≤ 0.001.The black dots represent outliers.

Se determinaron las concentraciones en las hojas de sorgo: a) P, b) N, c) Ca y d) K. El P, el N y el K se analizaron en las hojas basales, y el Ca en las hojas apicales, a los 60 días después de la siembra (DAE). Los asteriscos indican diferencias significativas entre los tratamientos dentro de cada combinación de híbrido y suelo: ns = p > 0,05, * = p ≤ 0,05, ** = p ≤ 0,01, *** = p ≤ 0,001. Los puntos negros representan valores atípicos.

Figure 3. Mineral composition (%) of sorghum leaves (Hybrids 155, SIP, and 163) under field experimental conditions, with treatments (Non-fertilized, Urea, and Ammonium Sulfate.

Figura 3. Composición mineral (%) de las hojas de sorgo (híbridos 155, SIP y 163) en condiciones experimentales de campo, con tratamientos (sin fertilizar, urea y sulfato de amonio).





Treatments were Non-fertilized (C), Urea (U), and Ammonium Sulfate (AS).

Asterisks indicate significant differences between treatments within each hybrid-soil combination: ns = $p > 0.05$, * = $p \leq 0.05$, ** = $p \leq 0.01$, *** = $p \leq 0.001$. Black dots represent outliers.

Los tratamientos fueron sin fertilizar (C), urea (U) y sulfato de amonio (AS). Los asteriscos indican diferencias significativas entre tratamientos dentro de cada combinación híbrido-suelo: ns = $p > 0,05$, * = $p \leq 0,05$, ** = $p \leq 0,01$, *** = $p \leq 0,001$. Los puntos negros representan valores atípicos.

Treatments were Non-fertilized (C), Urea (U), and Ammonium Sulfate (AS).

Asterisks indicate significant differences between treatments within each hybrid-soil combination: ns = $p > 0.05$, * = $p \leq 0.05$, ** = $p \leq 0.01$, *** = $p \leq 0.001$. Black dots represent outliers.

Los tratamientos fueron sin fertilizar (C), urea (U) y sulfato de amonio (AS). Los asteriscos indican diferencias significativas entre tratamientos dentro de cada combinación híbrido-suelo: ns = $p > 0,05$, * = $p \leq 0,05$, ** = $p \leq 0,01$, *** = $p \leq 0,001$. Los puntos negros representan valores atípicos.

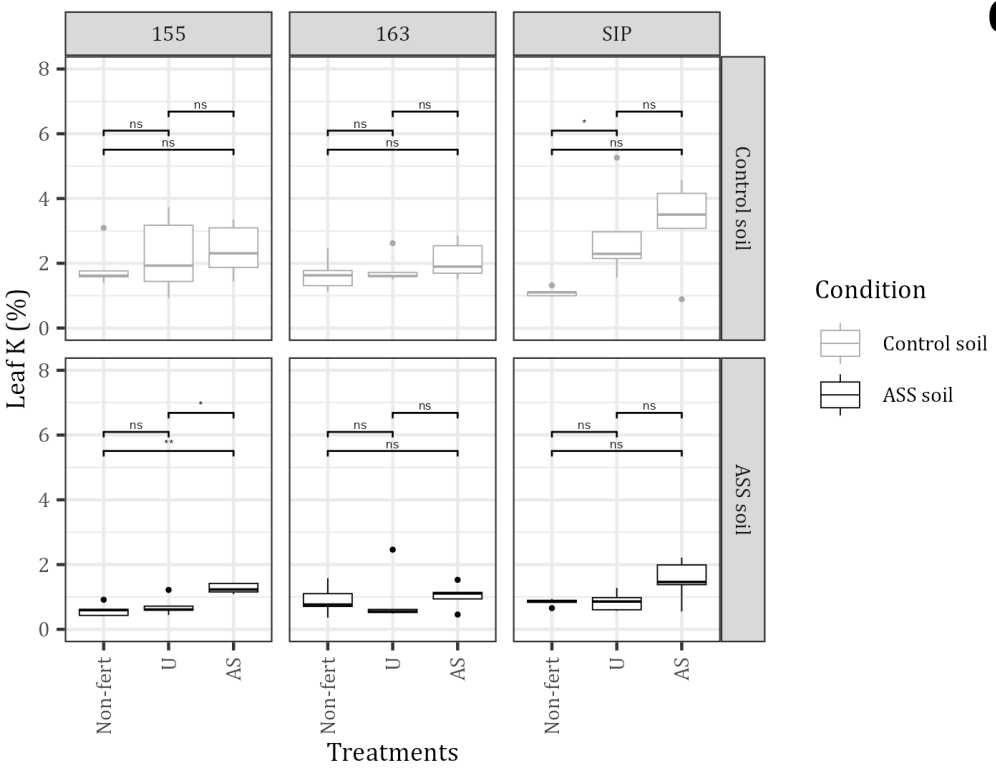


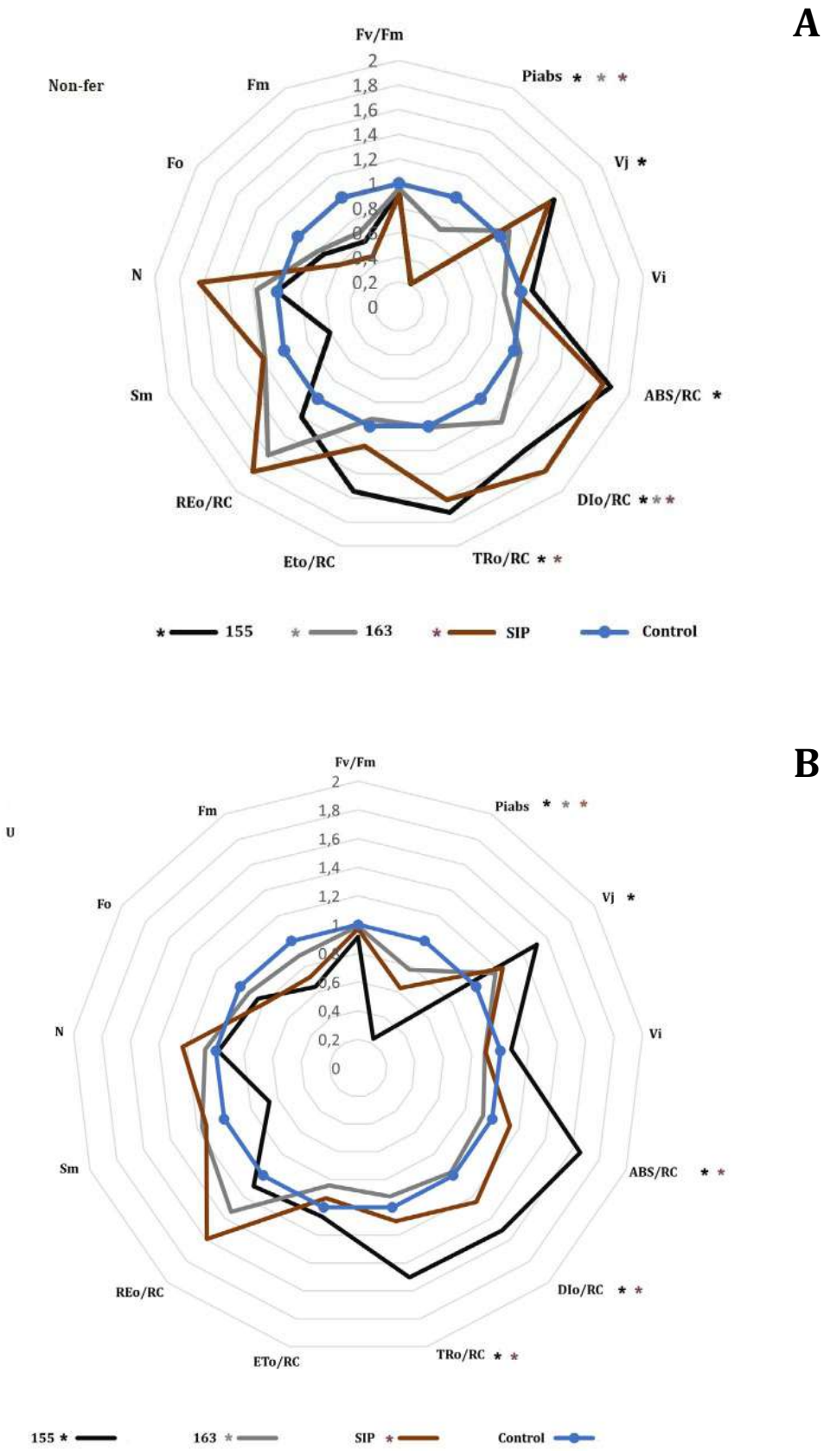
Figure 4. Mineral composition (%) of sorghum leaves from hybrids 155, SIP, and 163 grown under greenhouse conditions in control and ASS soils: a) Ca, b) Mg, and c) K.

Figura 4. Composición mineral (%) de las hojas de sorgo de los híbridos 155, SIP y 163 cultivados en condiciones de invernadero en suelos de control y ASS: a) Ca, b) Mg y c) K.

Photosystem II component (PSII)

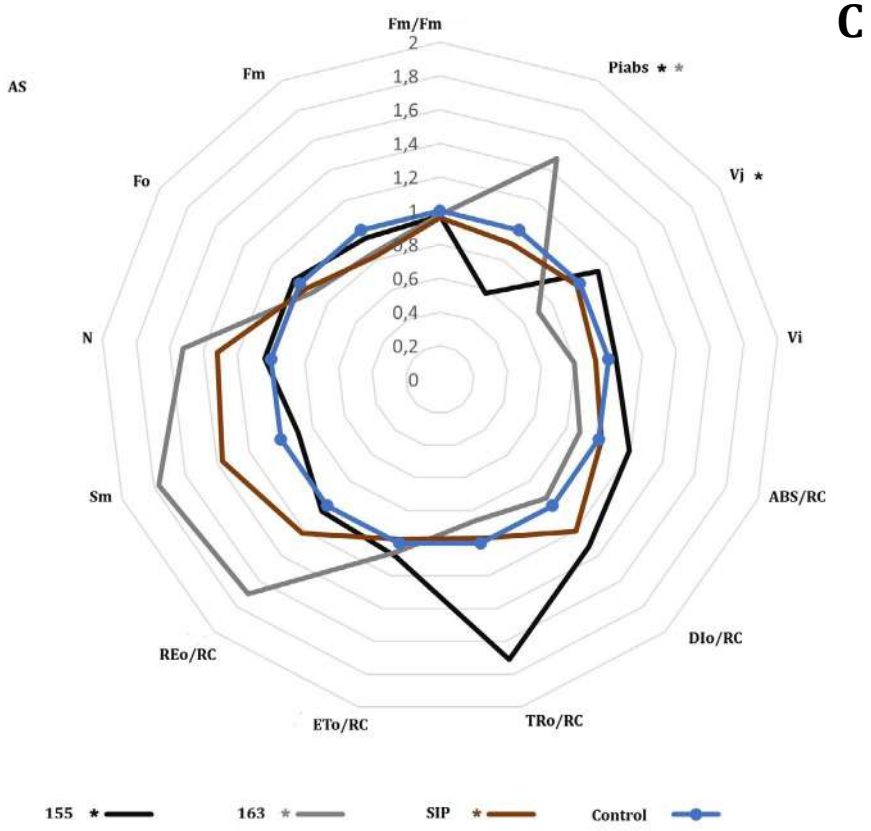
Chlorophyll fluorescence parameters were significantly affected by ASS soil at 60 DAE in the field, with responses varying with hybrid tolerance and treatment relative to plants grown in control soil (figure 5, page 13-15). Hybrid 155 was the most sensitive. PIabs decreased by 80% under both Non-fert ($p = 0.0008$) and U ($p = 0.001$) treatments, and by 43% with AS ($p = 0.0004$) (figures 5A-C, page 13-15). The Fo and Fm were not statistically significant; as a result, Fv/Fm remained unchanged. In hybrid 155, ABS/RC, TRo/RC, and DIo/RC increased by 83.7% ($p = 0.0012$), 71.7% ($p = 0.001$), and 54.9% ($p = 0.0012$), respectively, under the Non-fert treatment. In U-treated plants, increases of 65% ($p = 0.0012$), 50% ($p = 0.001$), and 51% ($p = 0.0011$) were observed. In contrast, the changes observed under AS treatment were smaller and not statistically significant (20%, 71%, and 32%, respectively). In addition, Vj increased by 52.9% ($p = 0.0043$) under Non-fert and by 51.4% ($p = 0.0012$) with U, while only a 12% increase was detected with AS ($p = 0.0018$).In hybrid SIP, PIabs decreased by 79.8% ($p = 0.0008$) under Non-fert, and by 31.8% ($p = 0.0011$) with U. ABS/RC, DIo/RC, and TRo/RC increased by 77.1% ($p = 0.0005$), 78.6% ($p = 0.0004$), and 61.3% ($p = 0.0006$), respectively, in the Non-fert treatment compared to the control. These increases were slightly reduced with U, while AS showed no significant effect. In hybrid 163, the impact of ASS soil was milder. PIabs decreased by 29% ($p = 0.0001$) under Non-fert and by 27% ($p = 0.0001$) with U, whereas AS significantly improved PIabs by 47%, indicating a mitigating effect. Under greenhouse conditions, fluorescence alterations were more pronounced (figures 5D-F, page 13-15), especially in hybrid 155. DIo/RC increased by 586% in Non-fert 155, 421% in SIP, and 181% in 163 ($p = 0.01$ in all cases). The U treatment induced 317% increases in 155 ($p = 0.0004$) and 476.2% in SIP ($p = 0.0009$). The AS application reduces DIo/RC to 92.7% in hybrids 155 and 163, and to 167% in SIP. In Non-fert plants, PIabs dropped sharply by 86%

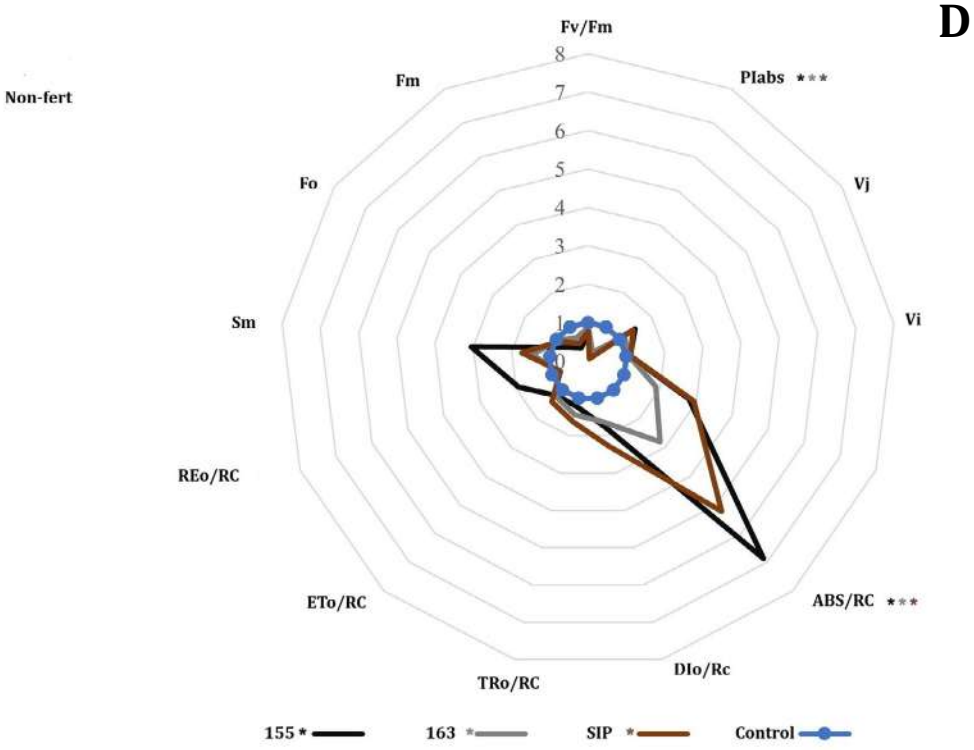
(p = 0.0004) in hybrid 155, 73.8% (p = 0.0001) in 163, and 92.9% (p = 0.0005) in SIP. The U treatment did not prevent PIabs decreases. However, AS significantly reduced PIabs losses to 62.4% in 155, 65.6% in 163, and 75% in SIP.



Data show fertilization effects (A-C: field; D-F: greenhouse). Values are normalized to the control soil mean for each genotype (blue line). Measurements were performed on fully expanded leaves at 60 DAE in the field and 35 DAE in the greenhouse. Group differences were evaluated using the Kruskal-Wallis test, followed by pairwise Wilcoxon tests when significant effects (*) were detected ($p < 0.05$).

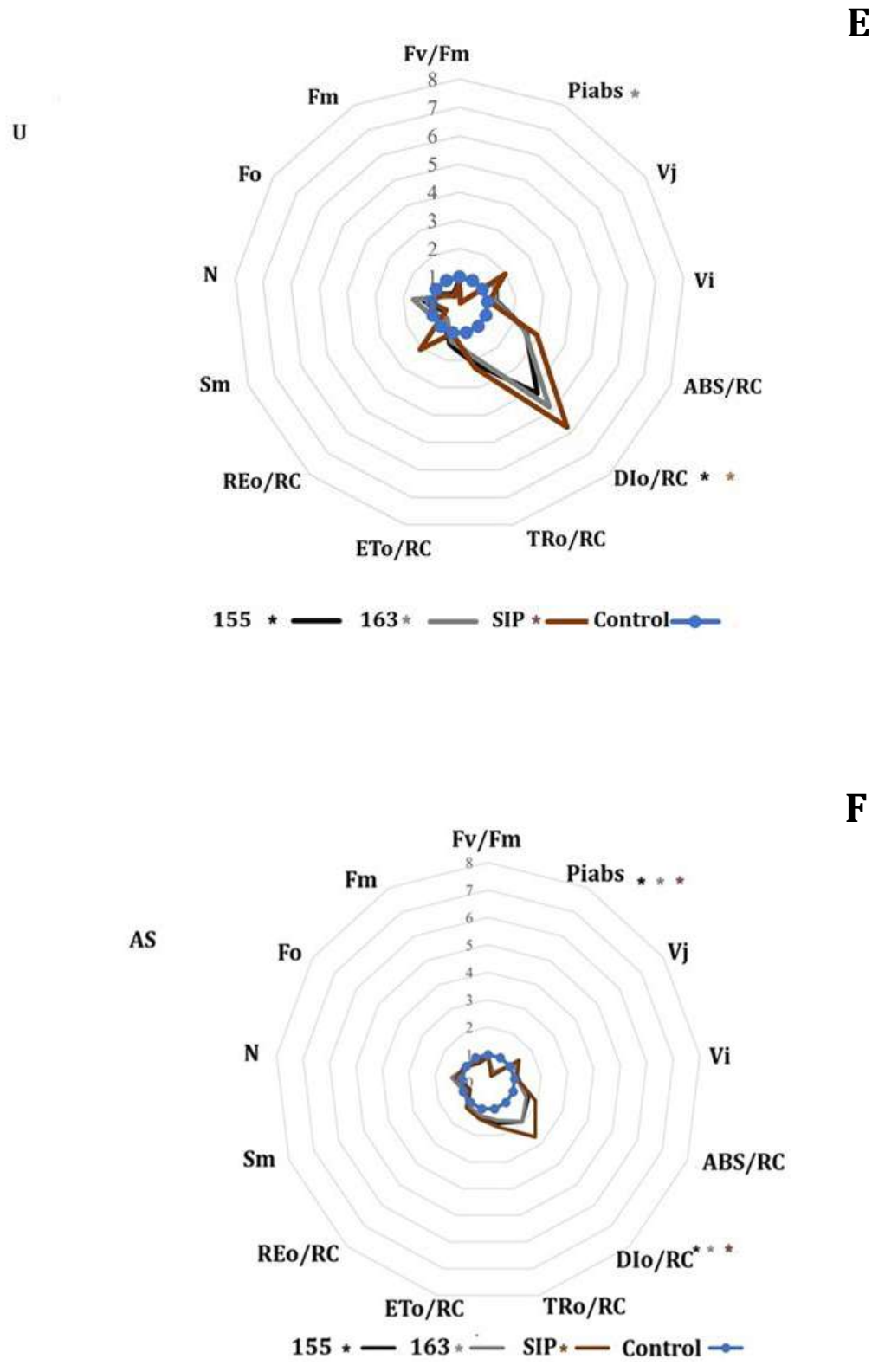
Los datos muestran los efectos de la fertilización (A-C: campo; D-F: invernadero). Los valores están normalizados respecto a la media del suelo control de cada genotipo (línea azul). Las mediciones se realizaron en hojas completamente expandidas a los 60 DAE en campo y a los 35 DAE en invernadero. Las diferencias entre grupos se evaluaron mediante la prueba de Kruskal-Wallis, seguida de pruebas pareadas de Wilcoxon cuando se detectaron efectos significativos (*) ($p < 0,05$).





Data show fertilization effects (A-C: field; D-F: greenhouse). Values are normalized to the control soil mean for each genotype (blue line). Measurements were performed on fully expanded leaves at 60 DAE in the field and 35 DAE in the greenhouse. Group differences were evaluated using the Kruskal-Wallis test, followed by pairwise Wilcoxon tests when significant effects (*) were detected ($p < 0.05$).

Los datos muestran los efectos de la fertilización (A-C: campo; D-F: invernadero). Los valores están normalizados respecto a la media del suelo control de cada genotipo (línea azul). Las mediciones se realizaron en hojas completamente expandidas a los 60 DAE en campo y a los 35 DAE en invernadero. Las diferencias entre grupos se evaluaron mediante la prueba de Kruskal-Wallis, seguida de pruebas pareadas de Wilcoxon cuando se detectaron efectos significativos (*) ($p < 0,05$).



Data show fertilization effects (A-C: field; D-F: greenhouse). Values are normalized to the control soil mean for each genotype (blue line). Measurements were performed on fully expanded leaves at 60 DAE in the field and 35 DAE in the greenhouse. Group differences were evaluated using the Kruskal-Wallis test, followed by pairwise Wilcoxon tests when significant effects (*) were detected ($p < 0.05$).

Los datos muestran los efectos de la fertilización (A-C: campo; D-F: invernadero). Los valores están normalizados respecto a la media del suelo control de cada genotipo (línea azul). Las mediciones se realizaron en hojas completamente expandidas a los 60 DAE en campo y a los 35 DAE en invernadero. Las diferencias entre grupos se evaluaron mediante la prueba de Kruskal-Wallis, seguida de pruebas pareadas de Wilcoxon cuando se detectaron efectos significativos (*) ($p < 0,05$).

Figure 5. Radar plots of chlorophyll fluorescence (OJIP test) in sorghum hybrids (155: black, 163: light gray, SIP: brown) grown in ASS soil.

Figura 5. Gráficos de radar de fluorescencia de clorofila (test OJIP) de híbridos de sorgo (155: negro, 163: gris claro, SIP: marrón) cultivados en suelo ASS.

Discussion

Soil Acidification and its Effect on Nutrient Availability

The AS application reduced ASS soil pH in both the field and greenhouse experiments (figures 1A and 1B, page 6), effectively enhancing macronutrient availability as confirmed by leaf analysis (figure 3, page 9-10 and figure 4, page 11-12). Unlike the U, AS improved nutrient uptake, although physiological responses varied with hybrid tolerance. These results align with Fageria *et al.* (2010), who observed similar beneficial effects with split AS applications. In the greenhouse experiment, the application of AS significantly reduced soil pH in the ASS soil. However, the reduction was almost half that observed in the field experiment, probably because in pots the roots grow less and, consequently, soil acidification is less. Regardless of the experimental conditions, U fertilization did not significantly change soil pH in either control or ASS soils. Upon dissolution in water, urea undergoes urease-catalyzed hydrolysis to form ammonium and bicarbonate ions, initially increasing soil pH near the application zone. Subsequently, as nitrification proceeds, the pH in the retention zone gradually decreases. In this study, soil pH was measured 30 days after fertilization in field and greenhouse experiments. Given this relatively short time interval between fertilizer application and pH measurement, the nitrification process may not have fully progressed, limiting the extent of observed pH changes (Kissel *et al.*, 2008). These results largely supported our first hypothesis, that the application of AS significantly reduced soil pH in both field and greenhouse experiments, particularly in ASS soil. This reduction in pH was associated with increased nutrient availability, as indicated by higher nutrient concentrations in the sorghum leaves. However, the magnitude of the pH reduction was greater in the field compared to the greenhouse, likely due to differences in root system development, soil volume, and soil buffering capacity. Although U did not significantly affect soil pH, it is important to note that nitrification can reduce soil pH over time. The relatively short duration of the greenhouse experiment may have limited the extent of pH changes observed with U fertilization.

Nitrogen Dynamics and Uptake in ASS Soils

High soil pH generally restricts the availability of essential macro- and microelements for crop growth, particularly N, P, K, Mg, Ca, Fe, and Zn, which is consistent with our findings. In this study, we confirmed that the application of AS was superior to U in enhancing sorghum nutrient absorption in most of the tested hybrids (figures 3, page 9-10 and figure 4, page 11-12). The greater acidifying effect of AS is the primary explanation for this (Jacoby *et al.*, 2017). The initial N content in the ASS soil was lower (0.06%) than in the control soil, probably due to the low organic matter content (1.1% vs 1.7%) (Supplementary Table 1).

Sorghum plants grown in the AAS soil showed significantly lower N concentration in their leaves, especially in the SIP hybrid (figure 3, page 9-10). This was expected due to the inhibition of N mineralization and soil enzymatic activities, which are essential for organic matter decomposition, by both high salinity and alkalinity. It is also likely that the lower N content in the leaves of U-fertilized sorghum plants compared to those fertilized with AS could be associated with the inactivation of urease enzymes, either by excess carbonate/bicarbonate, and/or high electrical conductivity (EC) (Sharma *et al.*, 2023). Optimal nitrification occurs at pH 8.5. Therefore, a reduction in soil pH, as occurred in the AS treatment, may have helped maintain the NO_3^-/NH_4^+ balance, which is advantageous for sorghum growth. In addition, the increased availability of NH_4^+ (Bernardo *et al.*, 1984) may have increased plant tolerance to high soil EC by improving their Na/K homeostasis in ASS soil (de Souza Miranda *et al.*, 2016).

Phosphorus Availability and Uptake Mechanisms

In general, the three sorghum hybrids grown in the ASS soil field showed lower P concentrations in their leaves (figure 3, page 9-10). The solubility of P decreases as soil pH increases above ~6.5, either due to adsorption on $CaCO_3$ surfaces or precipitation as a function of soil P content. Our study revealed that fertilization with AS more efficiently solubilized and mobilized P than U, as sorghum plants grown in ASS soil showed P values like those of plants grown in control soil (Clark & Baligar, 2000) (figure 3, page 9-10). This

finding is consistent with those sudies showing that lowering soil pH by 1.6 units through ammonium fertilization improves P mobilization in ryegrass seedlings (Gahoonia *et al.*, 1992). Similarly, Blair *et al.* (1970) demonstrated that pH changes at the soil-root interface caused by AS fertilization in alkaline soil altered the $H_2PO_4^-/HPO_4^{2-}$ ratio on the root surface in maize, increasing the abundance of the $H_2PO_4^-$ form and consequently improving P uptake by the roots.

Secondary Macronutrients: Calcium, Magnesium, and Potassium Dynamics

Ca availability is reduced under salinity and even more so in alkaline-saline-sodic (ASS) soils, where excess Na can hinder Ca uptake. Our results confirm the negative impact of ASS soil on foliar Ca in sorghum and the partial effectiveness of AS and U in improving its solubilization (Hadi & Karimi, 2012; Saqib *et al.*, 2020; figure 3, page 9-10 and figure 4, page 11-12). Mg concentration was also significantly lower in plants grown in ASS soil (Ranaweera & De Silva, 2021). AS improved Mg uptake under greenhouse conditions (figure 4, page 11-12), but overall, greenhouse plants absorbed less Mg than field-grown ones. This may be related to the developmental stage, the higher pH in greenhouse ASS soil (9.7), or antagonism with Ca and K (Bontpart *et al.*, 2024; Cavalcante *et al.*, 2018; Jacoby *et al.*, 2017). Sorghum plants grown in ASS soil, both in the field and greenhouses, showed lower K absorption compared to those grown in control soil (figure 3, page 9-10 and figure 4, page 11-12). Saline-alkaline soils, such as ASS, have high concentrations of Ca^{2+} and Mg^{2+}, which limit K^+ uptake by competing for absorption sites on root surfaces. Consequently, sorghum plants in the ASS soil may have experienced K deficiency even though chemical analyses of this soil showed sufficient K for sorghum growth (Supplementary Table 2). Additionally, a possible antagonistic effect between K and Na may have occurred due to the high K concentration in the studied soil. Finally, lower water uptake and, consequently, lower K^+ uptake may have resulted in a lower K^+ concentration in sorghum leaves in ASS soil (Wakeel, 2013). On the other hand, both U and AS fertilization favored the solubilization, mobilization, and absorption of K^+ by sorghum plants in the ASS soil (figure 3, page 9-10 and figure 4, page 11-12). This response could be governed by pH, as decreasing it allows H^+ to exert stronger competition with exchangeable K^+ at soil exchange sites, thereby shifting it towards the soil solution (Naeem *et al.*, 2023).

Photosynthetic Responses and Photosystem II Functionality

Our data revealed that one of the main limitations for sorghum plants grown in ASS soils was low nitrogen availability, although both soils, ASS and control, initially had equivalent N percentages (figure 3, page 9-10 and figure 4, page 11-12). The condition of the ASS soil significantly affected chlorophyll concentration in sorghum leaves in both the field and the greenhouse. This suggests that low N uptake from plants grown in ASS soils reduced chlorophyll biosynthesis in sorghum leaves. Consequently, the ASS condition affected the operation of the components of the PSII electron transport chain. Due to the low N level in the leaves, reduced synthesis of key photosynthetic enzymes, particularly Rubisco, may have led to an imbalance between PSII light absorption and electron transport in the Calvin cycle.

The extent to which these physiological variables were affected varied with the hybrid's tolerance to ASS stress. The differences between hybrids can be attributed to their ability to maintain their photosynthetic structure under such conditions, thereby enabling them to regulate the electron transport system. (Liu *et al.*, 2024; Sui *et al.*, 2015; Suzuki *et al.*, 2023).

The superior effectiveness of AS over U in overcoming the restrictions imposed by the ASS soil was also evidenced by the higher chlorophyll concentration in the leaves, which was associated with increased N uptake. This response appears to depend on sorghum's genetic background with respect to N use efficiency, given the discrepancy in N concentration among these hybrids. For example, ASS soil condition affected most of the PSII components of the most sensitive sorghum hybrid (155), such as the photosynthetic index PI (Alkhader *et al.*, 2019) (also known as the vitality index), which expresses the three main functional steps of PSII photosynthetic activity. However, the values of PI_{abs} in the AS treatment were like those of the control in the SIP hybrid or even higher than those of the control in the hybrid 163. (Strasser *et al.*, 2004). The ASS-sensitive hybrid (155) and, to a lesser degree, the moderately tolerant SIP, exhibited significant alterations in the

PSII antenna (ABS/RC), indicating loss of LHC integrity and changes in the chlorophyll a/b ratio, which were associated with increased Reactive Oxygen Species (ROS) generation, lipid peroxidation, and chlorophyll degradation (Bordenave *et al.*, 2019). AS fertilization alleviated these effects, preserving PSII, PSI, and cytochrome b6/f activity and maintaining electron transport within the thylakoids, as evidenced by increased Vj fluorescence and more efficient QA reduction (Kalaji *et al.*, 2018; Sachdev *et al.*, 2021; Zhang *et al.*, 2018). Compared to U fertilization, AS proved more effective in the tolerant hybrids (SIP and 163) by acidifying the rhizosphere, enhancing N, P, and Fe availability, and sustaining higher photosynthetic efficiency. These findings support our second hypothesis that AS fertilization reduces damage to PSII electron transport chain components in sorghum grown in ASS soil, with AS providing superior protection due to improved plant nutritional status. Overall, these results underscore the substantial potential of AS fertilization to optimize sorghum performance in saline-alkaline environments.

Conclusion

This study demonstrates that alkaline-saline-sodic (ASS) soils in the semi-arid region of Córdoba, Argentina, severely constrain sorghum growth by reducing biomass accumulation and impairing photosynthetic efficiency. Among the evaluated treatments, ammonium sulfate (AS) fertilization proved the most effective strategy at mitigating these effects by acidifying soil and improving nutrient availability. The AS application significantly lowered soil pH under both field and greenhouse conditions and increased foliar P content. Hybrids SIP and 163 exhibited greater physiological and agronomic resilience under ASS stress, showing improved Photosystem II performance and higher foliar nutrient content with AS fertilization, whereas hybrid 155 was comparatively more sensitive. These findings highlight the importance of combining stress-tolerant genotypes with appropriate N sources to sustain productivity in degraded soils. Replacing conventional urea with split applications of AS at approximately 120 kg N ha^{-1} is recommended for ASS soils, as this practice restores sorghum yield potential and enhances forage nutritional quality by increasing N and P content. Overall, this research provides science-based, locally adapted management strategies to optimize sorghum performance and promote resilient, sustainable production systems in semi-arid regions affected by alkaline-saline-sodic conditions.

Supplementary Material

https://drive.google.com/file/d/11htDuZXPbt9TSFc0g_jkY7wtjwsBS0cq/view?usp=drive_link

References

Adams, F. (1984). Crop response to lime in the southern United States. In F. Adams (Ed.). *Soil acidity and liming, 12,* 211-265. American Society of Agronomy. https://doi.org/10.2134/agronmonogr12.2ed.c5

Alkhader, A. M., Qaryouti, M. M., & Okasheh, T. Y. M. (2019). Effect of nitrogen on yield, quality, and irrigation water use efficiency of drip fertigated grafted watermelon (*Citrullus lanatus*) grown on a calcareous soil. *Journal of Plant Nutrition, 42*(1), 1-12. https://doi.org/10.1080/01904167.2019.1568464

Bernardo, L. M., Clark, R. B., & Maranville, J. W. (1984). Nitrate/ammonium ratio effects on mineral element uptake by sorghum. *Journal of Plant Nutrition*, *7*(10), 1401-1414. https://doi.org/10.1080/01904168409363290

Blair, G. J., Miller, M. H., & Mitchell, W. A. (1970). Nitrate and ammonium as sources of nitrogen for corn and their influence on the uptake of other ions. *Agronomy Journal*, *62*(4), 530-532. https://doi.org/10.2134/agronj1970.00021962006200040031x

Bontpart, T., Weiss, A., Vile, D., Gérard, F., Lacombe, B., Reichheld, J. P., & Mari, S. (2024). Growing on calcareous soils and facing climate change. *Trends in Plant Science*. https://doi.org/10.1016/j.tplants.2024.03.013

Bordenave, C. D., Rocco, R., Maiale, S. J., Campestre, M. P., Ruiz, O. A., Rodríguez, A. A., & Menéndez, A. B. (2019). Chlorophyll a fluorescence analysis reveals divergent photosystem II responses to saline, alkaline, and saline-alkaline stresses in the two *Lotus japonicus* model ecotypes MG20 and Gifu-129. *Acta Physiologiae Plantarum, 41*(9), 167. https://doi.org/10.1007/s11738-019-2956-0

Cavalcante, T. J., Castoldi, G., Rodrigues, C. R., Nogueira, M. M., & Albert, A. M. (2018). Marcha de absorção de macro- e micronutrientes na biomassa de sorgo. *Pesquisa Agropecuária Tropical*, *48*(4), 364-373. https://doi.org/10.1590/1983-40632018v4851874

Chaves, M. M., Flexas, J., & Pinheiro, C. (2009). Photosynthesis under drought and salt stress: regulation mechanisms from whole plant to cell. *Annals of Botany*, *103*(4), 551-560. https://doi.org/10.1093/aob/mcn125

Chien, S. H., Gearhart, M. M., & Villagarcía, S. (2011). Comparison of ammonium sulfate with other nitrogen and sulfur fertilizers in increasing crop production and minimizing environmental impact: A review. *Soil Science, 176*(7), 327-335. https://doi.org/10.1097/SS.0b013e31821f0816

Clark, R. B., & Baligar, V. C. (2000). Acidic and alkaline soil constraints on plant mineral nutrition. *Plant-Environment Interactions*, 133–177.

De Souza Miranda, R., Gomes-Filho, E., Prisco, J. T., & Alvarez-Pizarro, J. C. (2016). Ammonium improves tolerance to salinity stress in *Sorghum bicolor* plants. *Plant Growth Regulation*, *78*(1), 121-131. https://doi.org/10.1007/s10725-015-0079-1

Fageria, N. K., dos Santos, A. B., & Moraes, M. F. (2010). Influence of urea and ammonium sulfate on soil acidity indices and lowland rice production. *Communications in Soil Science and Plant Analysis, 41*(13), 1565-1575. https://doi.org/10.1080/00103624.2010.485237

Flexas, J., Bota, J., Loreto, F., Cornic, G., & Sharkey, T. D. (2004). Diffusive and metabolic limitations to photosynthesis under drought and salinity in C3 plants. *Plant Biology*, *6*(3), 269-279. https://doi.org/10.1055/s-2004-820867

Gahoonia, T. S., Claassen, N., & Jungk, A. (1992). Mobilization of phosphate in different soils by ryegrass supplied with ammonium or nitrate. *Plant and Soil*, *140*(2), 241-248. https://doi.org/10.1007/BF00010600

Giorda, L., & Ortiz, S. (2012). *El cultivo de sorgo en la región semiárida central de Córdoba: aportes al sistema de producción ganadera.* INTA Manfredi.

González, F. J., Martínez, A. L., & Pérez, R. M. (2019). Efecto del yeso agrícola en la mejora de los suelos salinos y en el rendimiento de los cultivos. *Revista de Ciencia y Tecnología Agrícola*, *12*(2), 85-94. https://doi.org/10.1234/rcta.2019.12.2.85

Hadi, M. R., & Karimi, N. (2012). El papel del calcio en la tolerancia a la sal de las plantas. *Revista de Nutrición Vegetal*, *35*(6), 905-927. https://doi.org/10.1080/01904167.2012.717158

Jacoby, R., Peukert, M., Succurro, A., Koprivova, A., & Kopriva, S. (2017). The role of soil microorganisms in plant mineral nutrition-current knowledge and future directions. *Frontiers in Plant Science*, *8*. https://www.frontiersin.org/journals/plant-science/articles/10.3389/fpls.2017.01617

Kalaji, H. M., Bąba, W., Gediga, K., Goltsev, V., Samborska, I. A., Cetner, M. D., Dimitrova, S., Piszcz, U., Bielecki, K., Karmowska, K., Dankov, K., & Kompała-Bąba, A. (2018). Chlorophyll fluorescence as a tool for nutrient status identification in rapeseed plants. *Photosynthesis Research*, *136*(3), 329-343. https://doi.org/10.1007/s11120-017-0467-7

Kissel, D. E., Cabrera, M. L., & Paramasivam, S. (2008). Ammonium, ammonia, and urea reactions in soils. In J. S. Schepers & W. R. Raun (Eds.). *Nitrogen in agricultural systems* (p. 101-155). American Society of Agronomy. https://doi.org/10.2134/agronmonogr49.c4

Lawlor, D. W., & Cornic, G. (2002). Photosynthetic carbon assimilation and associated metabolism in relation to water deficits in higher plants. *Plant, Cell & Environment*, *25*(2), 275-294. https://doi.org/10.1046/j.0016-8025.2001.00814.x

Liu, C., Gu, W., Li, B., Feng, Y., Liu, C., Shi, X., & Zhou, Y. (2024). Screening key sorghum germplasms for low-nitrogen tolerance at the seedling stage and identifying from the carbon and nitrogen metabolism. *Frontiers in Plant Science, 15*. https://doi.org/10.3389/fpls.2024.1340509

Marschner, P., & Rengel, Z. (2012). Nutrient availability in soils. In P. Marschner (Ed.). *Marschner's mineral nutrition of higher plants* (3rd ed., p. 315-330). Academic Press. https://doi.org/10.1016/B978-0-12-384905-2.00012-1

Naeem, A., Deppermann, P., & Mühling, K. H. (2023). Ammonium fertilization enhances nutrient uptake, specifically manganese and zinc, and growth of maize in unlimed and limed acidic sandy soil. *Nitrogen, 4*(2), 239-252. https://doi.org/10.3390/nitrogen4020017

Pierre, W. H. (1928). Nitrogenous fertilizers and soil acidity: I. Effect of various nitrogenous fertilizers on soil reaction. *Agronomy Journal*, *20*(3), 254-269. https://doi.org/10.2134/agronj1928.00021962002000030006x

RAGT Semillas Argentina, (2025, febrero 24). Sorgo, una herramienta versátil para la conversión de reservas forrajeras. RAGT Semillas Argentina. https://ragt-semillas.com.ar/sorgo-unaherramienta-versátil-para-la-conversión-de-reservas-forrajeras

Ranaweera, Y., & De Silva, R. C. L. (2021). A laboratory study on the effects of fertilizer addition on mobilization, percolation, and leaching of calcium ions in soils of the Anuradhapura district. *International Conference on Applied and Pure Sciences*.

Rengasamy, P. (2010). Soil processes affecting crop production in salt-affected soils. *Functional Plant Biology*, *37*(7), 613-620. https://doi.org/10.1071/FP09249

Sachdev, S., Ansari, S. A., Ansari, M. I., Fujita, M., & Hasanuzzaman, M. (2021). Abiotic stress and reactive oxygen species: Generation, signaling, and defense mechanisms. *Antioxidants, 10*(2). https://doi.org/10.3390/antiox10020277

Saqib, M., Abbas, G., & Akhtar, J. (2020). Root-mediated acidification and resistance to low calcium improve wheat (*Triticum aestivum*) performance in saline-sodic conditions. *Plant Physiology and Biochemistry*, *156*, 201-208. https://doi.org/10.1016/j.plaphy.2020.09.001

Sharma, S., Gupta, N., Chakkal, A. S., Sharma, N., Alamri, S., Siddiqui, M. H., & Haider, F. U. (2023). Changes in enzyme activities in salt-affected soils during the incubation study of diverse particle sizes of rice straw. *Agriculture*, *13*(9), Article 1694. https://doi.org/10.3390/agriculture13091694

Sparks, D. L. (2003). The chemistry of saline and sodic soils. In D. L. Sparks (Ed.), *Environmental soil chemistry* (2nd ed., p. 285-300). Academic Press. https://doi.org/10.1016/B978-012656446-4/50010-4

Stirbet, A., & Govindjee, G. (2011). On the relation between the Kautsky effect (chlorophyll *a* fluorescence induction) and Photosystem II: Basics and applications of the OJIP fluorescence transient. *Journal of Photochemistry and Photobiology B: Biology, 104*(1-2), 236-257. https://doi.org/10.1016/j.jphotobiol.2010.12.010

Strasser, R. J., Tsimilli-Michael, M., & Srivastava, A. (2004). Analysis of the chlorophyll *a* fluorescence transient. In G. C. Papageorgiou & Govindjee (Eds.). *Chlorophyll a fluorescence: A signatura of photosynthesis* (p. 321-362). Springer Netherlands. https://doi.org/10.1007/978-1-4020-3218-9_12

Sui, N., Yang, Z., Liu, M., & Wang, B. (2015). Identification and transcriptomic profiling of genes involved in increasing sugar content during salt stress in sweet sorghum leaves. *BMC Genomics*, *16*(1), 534. https://doi.org/10.1186/s12864-015-1760-5

Suzuki, Y., Ohsaki, K., Takahashi, Y., Wada, S., Miyake, C., & Makino, A. (2023). The behavior of photosystems II and I is modulated by N partitioning to Rubisco in mature leaves acclimated to low N levels and in senescent leaves in rice. *Plant and Cell Physiology, 64*(1), 55-63. https://doi.org/10.1093/pcp/pcac139

Tupa-Andrade, L.; Caro-Castro, J.; León-Quispe, J. (2025). Isolation of Polyhydroxyalkanoate (PHA)-Producing *Azotobacter* spp. from Crop Rhizospheres Located in Lima, Peru. *Revista de la Facultad de Ciencias Agrarias. Universidad Nacional de Cuyo. 57*(2): 45-56. DOI: https://doi.org/10.48162/rev.39.170.

Wakeel, A. (2013). Potassium–sodium interactions in soil and plant under saline-sodic conditions. *Journal of Plant Nutrition and Soil Science, 176*(3), 344-354. https://doi.org/10.1002/jpln.201200417

Zhang, H., Xu, N., Wu, X., Wang, J., Ma, S., Li, X., & Sun, G. (2018). Effects of four types of sodium salt stress on plant growth and photosynthetic apparatus in sorghum leaves. *Journal of Plant Interactions, 13*(1), 506-513. https://doi.org/10.1080/17429145.2018.1526978.

Growth and Foliar Alkaloid Content of *Clitoria ternatea* under Different Irrigation Frequencies

Desarrollo y contenido foliar de alcaloides de la conchita azul (*Clitoria ternatea*) con diferentes frecuencias de riego

Tatiana Gavilanez-Buñay [1*], Juan Pio Salazar-Arias [2], Jorge Luis Ramirez de la Rivera [3]

Originales: *Recepción:* 05/03/2025 - *Aceptación:* 25/09/2025

ABSTRACT

Clitoria ternatea is widely used in tropical livestock farming. This study evaluates the agronomic performance and alkaloid content of *C. ternatea* under different irrigation frequencies in protected cultivation. A randomized block design with controlled manual irrigation was implemented with five treatments, four replicates, and five experimental units per treatment. Treatments included daily irrigation (T0), irrigation every two days (T1), every three days (T2), every four days (T3), and every five days (T4). We evaluated plant height, leaf and internode number, leaf area, green and dry matter yield, and alkaloid content. Irrigation every three or four days generally resulted in the highest values for the measured variables compared to the control. Reduced irrigation frequency affects the agronomic performance of *C. ternatea* in protected cultivation. Agronomic indicators were highest under irrigation every three or four days. Alkaloid content did not vary with irrigation frequency.

Keywords
alkaloids • height • leaf area • number of leaves • yield

https://doi.org/10.48162/rev.39.187

1 Universidad Técnica de Cotopaxi. Facultad de Ciencias Agropecuarias y Recursos Naturales. Calle los Almendros y Pujilí. La Maná. Cotopaxi. C. P. 050202. Ecuador.
* tatiana.gavilanez@utc.edu.ec
2 Universidad Técnica de Cotopaxi. Facultad de Ciencias Agropecuarias y Recursos Naturales. Vía Salache. km 7,53 sector La Florida. Latacunga. C. P. 050107. Ecuador.
3 Universidad de Granma. Facultad de Ciencias Agropecuarias. Carretera a manzanillo Km 171/2. Bayamo. Granma. Código Postal: 85 100. Cuba.

Licenses Creative Commons
Attribution - Non Commercial - Share Alike

Resumen

La *Clitoria ternatea* constituye una de las especies de mayor uso en la ganadería del trópico. El objetivo de este trabajo es evaluar el comportamiento agronómico y los alcaloides de la *C. ternatea* al aplicar diferentes frecuencias de riego en cultivo protegido. Se empleó un diseño en bloques al azar. Se emplearon cinco tratamientos con cuatro repeticiones cada uno, con cinco unidades experimentales cada una. Los tratamientos consistieron en diferentes frecuencias de riego, sin riego (T0), cada dos días (T1), cada tres (T2), cuatro (T3) y cada cinco (T4). Se evaluaron las variables altura de la planta, número de hojas y entrenudos, área de la hoja, rendimiento de materia verde y seca de la planta, así como los alcaloides. Las frecuencias de riego después de tres y cuatro días mostraron los mayores valores para las diferentes variables evaluadas, con respecto al control y resto de los tratamientos. La disminución de la frecuencia de riego no afectó el comportamiento agronómico de la *C. ternatea* en cultivo protegido. Los indicadores agronómicos fueron mayores para las frecuencias de riego de tres y cuatro días. Por otra parte, el contenido de alcaloides no varió en dependencia de la frecuencia de riego.

Palabras clave
alcaloides • altura • área de la hoja • número de hojas • rendimiento

Introduction

In Latin America and the Caribbean, legumes are grown with economically important crops to promote sustainable agricultural and livestock production systems (14, 20). *C. ternatea* (Fabaceae) is widely used in tropical livestock farming due to its adaptability, productivity, and nutritional value (22). These benefits improve animal diets and help meet feed demand during the dry season. They also promote the use of sustainable animal production techniques compatible with environmental protection.

However, in the tropics, the agronomic performance, yield, and chemical composition of this species are highly variable. This variability is influenced by plant age, management practices (especially irrigation and fertilization), and edaphoclimatic conditions (3, 23).

A previous study in Ecuador showed that plant quality decreases with age (10). However, as this research was conducted during the rainy season, it did not address irrigation effects. Furthermore, scarce information describes how irrigation affects the development and foliar alkaloid content of *C. ternatea* in Ecuador's various climatic conditions. Thus, this study aims to evaluate the agronomic performance and alkaloid content of *C. ternatea* under different irrigation frequencies in protected cultivation.

Materials and methods

Site and Experiment

The study was conducted at the Technical University of Cotopaxi's experimental area, El Triunfo sector, La Maná Cantón. This site has a maximum temperature of 30°C, a minimum of 17°C, relative humidity of 86.83%, average annual rainfall of 3029.30 mm, 735.70 light hours per year, and sandy loam soil (7). The experiment lasted 70 days, and irrigation was applied manually.

Seed Collection and Storage

Seeds were collected at the Sacha Wiwa Experimental Center, treated, and stored in the Germplasm Bank of the Technical University of Cotopaxi Extension, La Maná. Seeds were stored at 6.50% humidity and 4°C until sowing.

Soil Preparation, Sewing and Transplanting

Soil in the research area contains 6.5% organic matter and has a pH of 6.5; therefore, no amendments were necessary. Seeds were sown during the dry season (July) in polystyrene

trays with 200 cells filled with common substrate from the experimental center. One seed was placed in each cell. Twenty days after sowing, seedlings with two to three true leaves were transplanted into polyethylene bags, one seedling per bag. These were immediately arranged according to the experimental design with guides for their climbing nature. All this work was carried out at the final study site. Weeds were controlled manually, and the area was disinfected by solarization (19).

The crop was protected with transparent plastic to prevent rain from interfering with treatments. Sides were covered with dark saran. Treatments were arranged on tables, one meter above the ground. Each table was divided into five sections, each representing a replicate. Variables were measured 10 days after transplanting.

Experimental Design and Treatments

The structured design with controlled manual irrigation had five treatments, four replicates and five experimental units, totalizing 100 plants. Treatments included daily irrigation (T0), irrigation every two days (T1), every three days (T2), every four days (T3), and every five days (T4).

Plant Height, Number of Leaves, and Leaf Area

Plant height was measured from the stem base to the tip of the terminal bud using a measuring tape, expressed in cm. Leaf number was averaged from 10 plants randomly selected per treatment. Leaf area was determined using the Smart Petiole application, calculating leaf area from scanned images. These variables were evaluated at 10, 20, 30, 40, and 50 days.

Node Number, Green and Brown Matter, and Alkaloid Content

Internode number was determined at 40 and 50 days after transplanting. Green and dry matter yields were measured by weighing 10 randomly selected plants per treatment at 50 days after emergence. Fresh weights were measured using a semi-analytical balance (precision: 0.01 mg). Dry matter was determined in an air-circulation oven (1). Results were expressed in tons (2).

Alkaloid content was determined using Dragendorff's reagent by mixing (a) 0.8 g pentahydroxy bismuth nitroxide in 40 ml distilled water and 10 ml acetic acid, and (b) 0.8 g potassium iodide in distilled water. The bismuth nitrate solution was prepared by dissolving 10 mg $Bi(NO3)3{\cdot}5H2O$ in 5 mL concentrated nitric acid, then diluting to 100 mL with distilled water. Additionally, 3% thiourea and 1% disodium sulfide were required.

Alkaloid solutions were diluted in acidic, acid-alcoholic, and basic-alcoholic media (21). All solutions were centrifuged, and the precipitate was washed with alcohol and re-centrifuged. The resulting precipitate was mixed with 5 mL thiourea solution, and the compound formed was measured spectrophotometrically. Results were expressed as moles of alkaloids per gram (21).

Statistical Analysis

Analysis of variance (ANOVA) was performed, and means were compared using Tukey's test ($p \leq 0.05$). Normality was assessed using the Kolmogorov-Smirnov test, and homogeneity of variances was tested using Bartlett's test.

Results

Plant Height

At 10 days, treatment T4 showed the greatest plant height ($p<0.05$), with significant differences compared to other treatments. T1, T2, and T3 did not differ significantly, with values ranging from 10.36 to 10.60 cm. The control treatment had the lowest height, significantly different from the others (table 1, page 4).

Table 1. Height of *C. ternatea* (cm) according to evaluation days.

Tabla 1. Altura de la *C. ternatea* expresada en cm según días de evaluación.

Treatments	Age (days)				
	10	20	30	40	50
T0	9.30c	10.60c	13.05c	25.90c	40.45c
T1	10.36b	13.76b	17.89b	38.50a	48.82b
T2	10.52b	14.92a	17.04b	17.30d	30.71d
T3	10.60b	12.00b	21.54a	36.50ab	40.25c
T4	12.401a	15.01a	17.87b	33.80b	70.80a
EE±	0.89	0.45	1.23	2.83	3.57
P	0.0002	0.0012	0.0023	0.0001	0.0001

Different letters in the same column indicate statistical differences for p<0.05.

T0= daily irrigation, T1= irrigation every two days, T2= irrigation every three days, T3= irrigation every four days, T4= irrigation every five days.

Letras desiguales en una misma columna difieren significativamente para p<0,05.

T0= irrigación diaria, T1= irrigación cada dos días, T2= irrigación cada tres días, T3= irrigación cada cuatro días, T4= irrigación cada cinco días.

At 20 days, T2 and T4 reflected the highest values (p<0.05). T1 and T3 showed no differences between while T0 presented the lowest value (10.60 cm), significantly different from the rest (Table 1). At 30 days, T3 reached 21.54 cm (highest, significant value). Treatments T1, T2 and T4, ranging between 17.0 and 17.89 cm, did not differ from each other. The lowest value was shown by T0 (table 1).

Treatment T1 yielded the highest value at 40 days (38.50 cm), significantly differing from the others, while T3 and T4 did not differ from each other, and T2 showed the lowest height (17.30 cm). However, at 50 days, T4 reached the highest value, T0 and T3 ranged between 40.25 and 40.40 without significant differences, and T2 was the shortest (table 1).

Number of Leaves

At 10 days, treatment T3 had the greatest number of leaves (p<0.05) with 11.60, not significantly different from T2. T1, T2, and T4 did not differ significantly. The control (T0) had the lowest number of leaves, although this was not significantly different from T1 (table 2). After 20 days, the highest value was reached by T3 with significant differences compared to the rest. Treatments T0, T1, T2 and T4 showed no differences between themselves, with values between 11 and 12.40.

Table 2. Number of leaves of *C. ternatea* according to evaluation days.

Tabla 2. Número de hojas de *C. ternatea* según días de evaluación.

Treatments	Age (days)				
	10	20	30	40	50
T0	9.00c	12.00b	14.20d	24.60b	41.20b
T1	9.40bc	12.40b	16.40c	27.60a	38.40b
T2	10.20ab	11.00b	18.60b	18.201c	27.40c
T3	11.60a	14.50a	22.20a	20.80c	48.00a
T4	9.40bc	12.40b	17.00bc	27.80a	41.40b
EE±	0.45	1.78	2.23	2.11	3.56
P	0.0001	0.0002	0.0019	0.0029	0.0013

Different letters in the same column indicate statistical differences for p<0.05

T0= daily irrigation, T1= irrigation every two days, T2= irrigation every three days, T3= irrigation every four days, T4= irrigation every five days.

Letras desiguales en una misma columna difieren significativamente para p<0,05.

T0= irrigación diaria, T1= irrigación cada dos días, T2= irrigación cada tres días, T3= irrigación cada cuatro días, T4= irrigación cada cinco días.

Treatment T3 reached the highest value ($p<0.05$) at 30 days, with significant differences in contrast to the rest. However, T2 and T4 did not show differences between themselves, the control reflected the lowest height and was differentiated from the rest. At 40 days, T1 and T4 reached the highest numbers of leaves with significant differences compared to the rest. Consequently, T2 and T3 were the lowest, without significant differences between them. Thus, at 50 days, T3 reached the highest value (48), with significant differences from the rest. However, T0, T1 and T4 showed no differences, while T2 showed the lowest number of leaves (table 2, page 4).

Leaf Area

At 10 days, T2 and T3 showed the greatest leaf area ($p<0.05$), although T2 did not differ from T4. The lowest leaf area values were observed in T0 and T1, ranging between 3.28 and 3.64 cm^2. At 20 days, T2 and T3 did not show differences showed the highest values, while T4 did not present significant differences compared to T3 (table 3). The lowest value was from T0 with 3.35 cm^2.

Treatment T4 reflected the highest value leaf area at 30 days (8.13 cm^2) with significant differences with respect to T0, T1 and T3. T2 did not show differences with respect to T3, showing values between 6.99 and 7.79 cm^2. The smallest area was reflected by T0. At 40 days, T2 and T3 did not show significant differences, ranging between 14.90 cm^2 and 16.02.

At 50 days, control and T4 reflected the lowest values, 8.90 and 9.74 cm^2, respectively, while T3 showed the significantly highest leaf area (table 3).

Table 3. Leaf area according to evaluation days.

Tabla 3. Área de las hojas según días de evaluación.

Treatments	Leaf area (cm^2)				
	Age (days)				
	10	20	30	40	50
T0	3.28±0.10c	3.35±0.33c	4.14±0.34d	5.36±0.63c	8.90±0.62c
T1	3.64±0.24c	5.14±0.53b	5.18±0.54c	8.95±0.82b	13.12±2.27b
T2	5.67±0.23ab	6.75±0.35a	7.79±0.42ab	14.90±0.58a	14.40±1.67ab
T3	6.38±0.41a	6.54±0.32ab	6.99±0.31b	16.02±0.59a	16.84±3.78a
T4	5.19±0.12b	5.84±0.74b	8.13±0.83a	7.29±0.66bc	9.74±2.89c
EE±	0.24	0.32	0.89	1.89	1.58
P	0.0029	0.0034	0.0012	0.0002	0.0041

Different letters in the same column indicate statistical differences for $p<0.05$.

T0= daily irrigation, T1= irrigation every two days, T2= irrigation every three days, T3= irrigation every four days, T4= irrigation every five days.

Letras desiguales en una misma columna difieren significativamente para $p<0,05$.

T0= irrigación diaria, T1= irrigación cada dos días, T2= irrigación cada tres días, T3= irrigación cada cuatro días, T4= irrigación cada cinco días.

Internode Number

At 40 days, T4 had the maximum internodes (6.70, $p<0.05$), significantly different from the other treatments, which ranged from 4.70 to 5.26. At 50 days, internode number was not significantly different among treatments, ranging from 5.58 to 6.68 (figure 1, page 6). At 50 days, the number of knots did not reflect differences between treatments, with values between 5.58 and 6.68 (figure 1, page 6).

Yield and Alkaloid Content

At 50 days, treatment T2 achieved the highest green matter yield, although not significantly different from T0 and T4. For dry matter, treatments T0, T1, and T2 did not differ significantly. The lowest yields were observed in T3 and T4 (figure 2, page 6).

Different letters in bars differ significantly for p<0.05.

Letras distintas en columnas difieren significativamente para p<0,05.

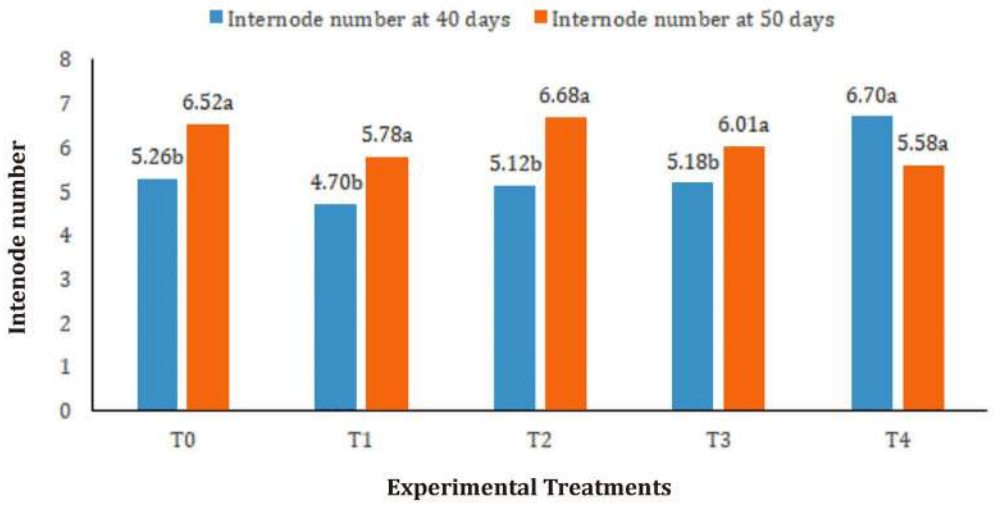


Figure 1. Internode number of *C. ternatea* at 40 and 50 Days according to Experimental Treatments.

Figura 1. Número de internudos de *C. ternatea* a los 40 y 50 días según los tratamientos experimentales.

Different letters in bars differ significantly for p<0.05.

Letras distintasen columnas difieren significativamenbte poara p<0,05.

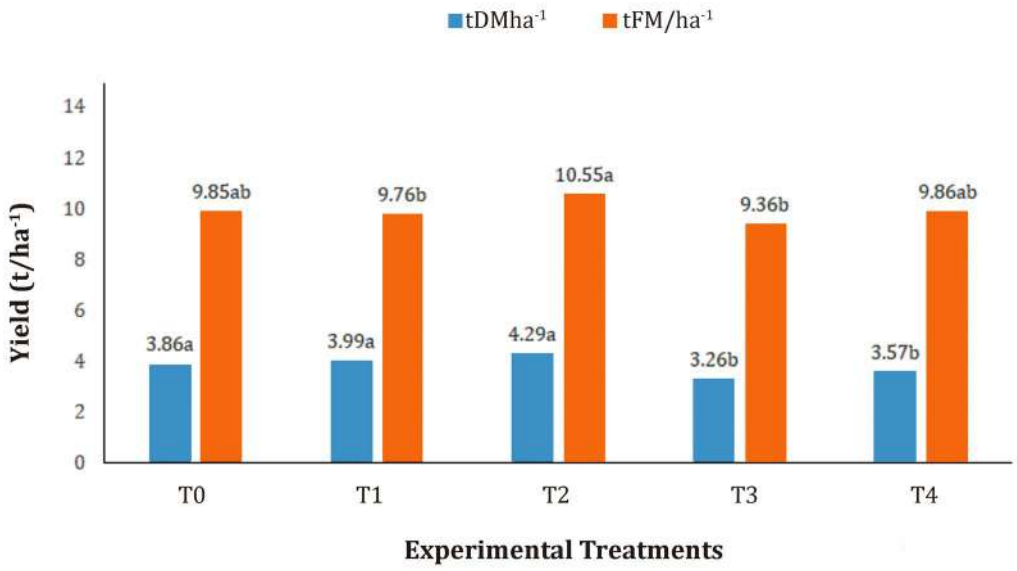


Figure 2. Fresh (FM) and Dry Matter (DM) of *C. ternatea* after 50 days of evaluation

Figura 2. Rendimiento de materia fresa y seca de *C. ternatea* después de 50 días de evaluación.

Alkaloids reached their highest value for T2 (watering every three days) with 14.2 g/kg^{-1} DM. Treatments T0 and T4 did not show differences between them. The lowest value was reached by T1 with 2 g/kg^{-1} DM (figure 3, page 7).

Different letters differ significantly for p<0.05.

Letras distintas en las barras difieren significativamente para p<0,05.

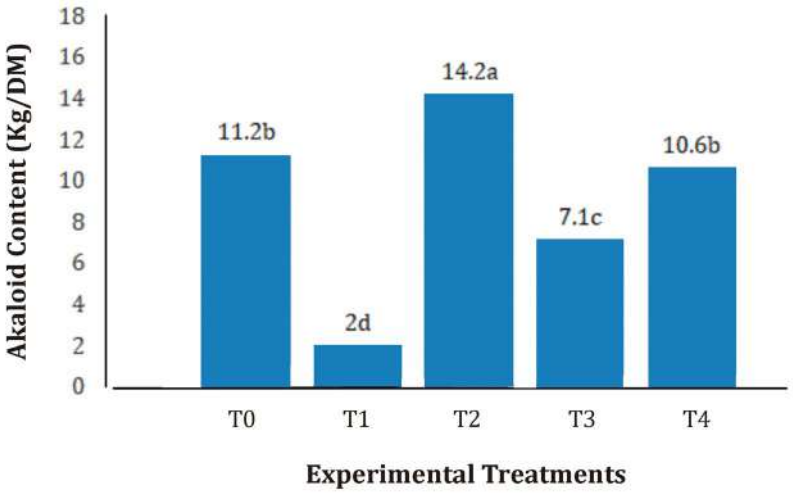


Figure 3. Alkaloid content of *C. ternatea* after 50 days of evaluation.

Figura 3. Alcaloides de *C. ternatea* después de 50 días de evaluación.

Discussion

Maximum plant height was achieved when *Clitoria ternatea* received irrigation every four or five days, with T4 reaching 48.50 cm at 50 days. These results differ from those reported by other authors (17), who observed plant heights ranging from 10.37 to 18.67 cm at 30 days and from 18.86 to 31.8 cm at 45 days under tropical conditions. Such discrepancies underscore the critical role of both irrigation management and environmental variables in modulating vegetative growth. Optimal water supply and climate conditions directly affect physiological processes, promoting stem elongation and overall development in *C. ternatea* (4, 13).

Leaf number increased as plants matured, with the highest value recorded in T3 (48 leaves at 50 days). According to previous studies (11), before 75 days, *C. ternatea* predominantly allocates photoassimilates to roots and young leaves, supporting the observed increase in leaf production and, consequently, biomass accumulation. This pattern also aligns with the trends noted for leaf area and internode development in this study.

Leaf area reached its maximum when irrigation occurred every three or four days and plant age exceeded 40 days, as similarly documented in previous studies (10). However, leaf area expansion and biomass production in *C. ternatea* depend on age, environmental factors, and agronomic practices. Irrigation management is a decisive factor in cell expansion, while excessive moisture induces root anoxia (17). Our findings highlight the necessity of balancing irrigation to optimize physiological performance and yield of *C. ternatea.*

Distinct values for leaf area in *C. ternatea* have been documented (18). An expanded leaf area enhances light interception and carbon assimilation (24, 25). Nevertheless, several agronomic and environmental factors-including irrigation regime, precipitation patterns, and organic fertilization-modulate the agronomic performance of *C. ternatea.*

In our investigation, optimal vegetative vigor and yield were measured when irrigation intervals ranged from three to four days. Environmental conditions and crop management practices, particularly irrigation frequency, affect organ differentiation and elongation (8, 24).

Yields exceeded 3.26 t DM ha^{-1} at 50 days, demonstrating the productive potential of *C. ternatea* under optimized irrigation. Literature indicates that, under adequate irrigation, this species may achieve up to 30 t ha^{-1} $year^{-1}$; however, reduced rainfall and limited soil moisture substantially decrease productivity (10). The highest yields in this study resulted from irrigation every three days, underscoring the importance of precise water

management. Productivity in *C. ternatea* varies with seasonality, genotype, agronomic practices, and environmental variables like humidity and soil properties (9). These findings highlight the necessity of conducting field trials under diverse irrigation regimes to validate and potentially improve productivity.

Yield results obtained in this study exceed those documented by various authors for *C. ternatea* under irrigated conditions. Previous reports indicate yields ranging from 1.6 to 2.5 t ha^{-1}, as well as 1.3 t ha^{-1} at 60 days, and 0.86 t ha^{-1} of dry matter in grass-legume associations involving three rows of signal grass and two rows of *C. ternatea* (12, 25, 26). Several factors may explain these discrepancies. Low planting densities and full sunlight exposure enhance photosynthesis. This, along with an expanded root system, promotes higher growth rates and biomass production under adequate soil moisture (8, 15).

Alkaloid concentrations measured align with those reported for other legume species and tree crops. Literature cites values between 0.28 and 11 g kg^{-1}, noting that secondary metabolite content depends on plant age, defense mechanisms, nutrient status, and edaphoclimatic factors (27). In this study, alkaloid levels ranged from 12 to 14 g kg^{-1}, with the highest value recorded in plants irrigated every three days. These findings suggest that, under optimal agronomic management, *C. ternatea* can accumulate substantial quantities of alkaloids, enhancing its functional and nutritional value.

Environmental contexts strongly affect the synthesis of secondary metabolites. Climate and soil properties modulate the presence and concentration of bioactive compounds. Stressful deficiencies or excesses in edaphoclimatic factors often upregulate the biosynthesis of compounds like alkaloids. For instance, increased wind speed accelerates evaporation of essential oils, while higher transpiration rates facilitate the upward movement of tropane alkaloids from roots to canopies (5, 6). This research corroborates these observations and emphasizes the importance of integrated environmental and agronomic management for optimizing yield and quality in *C. ternatea* (16).

Conclusions

Reducing irrigation frequency affects the agronomic performance of *Clitoria ternatea* under protected conditions. In fact, most agronomic variables-including plant height, leaf number, leaf area, and biomass yield-reached their highest values when irrigation occurred every three or four days. These findings indicate that watering within this interval optimizes vegetative growth and productivity by avoiding drought and excessive soil moisture.

Given that daily irrigation didn't enhance growth parameters compared to less frequent regimes under protected conditions, future research should assess whether such intensive watering is justified under field conditions. Alkaloid stability across all irrigation treatments further suggests that secondary metabolite accumulation in *C. ternatea* remains largely unaffected by variations in watering frequency within the tested range.

The evidence presented here supports the strategic management of irrigation schedules according to crop developmental stage and physiological indicators. This approach enables producers to optimize yield and resource use efficiency without compromising quality.

References

1. AOAC (Association of Official Analytical Chemists). 2016. Official Methods of Analysis of AOAC International. 20th Ed. George W. Latimer Jr (ed).
2. Boutin, R. 2023. Protocolo de rendimiento real en Kg/Ha. https://www.finagro.com.co/sites/default/files/protocolo_de_muestreo_para_la_operacion_de_la_poliza.pdf, (accessed on September 15th 2023).
3. Castrejón-Pineda, F. A.; Corona-Gochi, L.; Rosiles-Martínez, R.; Martínez-Pérez, P.; Lorenzana-Moreno, A. V.; Arzate-Vázquez, L. G. 2023. Características nutrimentales de gramíneas, leguminosas y algunas arbóreas forrajeras del trópico mexicano: fracciones de proteína (A, B1, B2, B3 y C), carbohidratos y digestibilidad *in vitro*. Universidad Nacional Autónoma de México: https://papimes.fmvz.unam.mx/proyectos/manuales_nutricion/Manual, (accessed on September 18th 2023).

4. Espinoza-Coronel, A. L.; Franco Ochoa, D. A.; Fajardo Espinoza, P. G.; Real Goya, G. E.; Pincay-Ganchozo, R. A. 2020. Nexo Agropecuario. 8(2): 43-50. https://www.researchgate.net/publication/347507134
5. Estrada-Jiménez, P. M.; Ramírez, J. L.; Verdecia, D. M. 2019. Aplicación de la minería de datos en la estimación de componentes fotoquímicos. ROCA Revista Científico-Educaciones de la provincia de Granma. 15(2): 177-186.
6. Holopainen, J. K.; Virjamo, V.; Ghimire, R. P.; Blande, J. D.; Julkunen-Titto, R.; Kivimäenpää, M. 2018. Climate change effects on secondary compounds of forest trees in the Northern Hemisphere. Frontiers in Plant Science. 9: 1445. DOI: https://doi.org/10.3389/fpls.2018.01445
7. Instituto Nacional de Meteorología e Hidrología. 2023. Las condiciones agrometeorológicas del Cantón La Maná. http://www.inamhi.gob.ec, (accessed on September 12nd 2023).
8. Jácome-Gómez, L. R.; Ramírez-Villalobos, M. 2021. Incidencia del sombreado, biorreguladores y bioestimulante en el desarrollo y rendimiento del pasto Mombaza (*Panicum maximum* Jacq.). Rev. Fac. Agron. (LUZ). 38 (2): 382-403. https://www.produccioncientificaluz.org/index.php/agronomia/ article/view/35505
9. Jamil, N.; Naqiuddin, M.; Mohd, N.; Paee, F. 2018. Influences of enviromental conditions to phytoconstituents in *Clitoria ternatea* (butterfly pea flower): A review. J. Sci Technol. 10: 208-228. DOI: http://10.30880/jst.2018.10.02,029
10. Luna Murillo, R.; Chacón Marcheco, E.; Ramírez de la Ribera, J.; Espinoza Coronel, A.; Guevara Santana, J.; Cedeño Troya, D. M.; López Cedeño, K. M. 2015. Evaluación del Kudzú (*Pueraria phaseloides*) y la *Clitoria ternatea* en diferentes estados de madurez. Revista Electrónica de Veterinaria. 16(10): 1-9. http://www.veterinaria.org/revistas/redvet/n101015.html
11. Macías-Pettao, R.; Tapia-Ramírez, S.; Pincay-Ganchozo, R.; Álvarez-Perdomo, G. 2021. Respuesta agronómica y composición química de *Clitoria ternatea* l. en el subtrópico. Nexo Agropecuario. 9(2): 13-18.
12. Mahfouz, H.; Megawer, E. A.; Maher, A.; Shaaban, A. 2020. Integrated effect of planting dates and irrigation regimes on morpho-physiological response, forage yield and quality, and water use efficiency of clitoria (*Clitoria ternatea* L.) in arid region. Arch. Agron. Soil Sci. 66 (2): 152-167. DOI: https://doi.org/10.1080/03650340.2019.1605165
13. Moraes, A.; Medeiros, S.; Fagundes, I. 2021. Estresse hídrico em plantas: uma revisão. Research, Society and Development. 10(15): 1-7. DOI: http://dx.doi.org/10.33448/rsd-v10i15.23155
14. Muñoz-González, J. C.; Huerta-Bravo, M.; Lara-Bueno, A. 2016. Producción y calidad nutrimental de forrajes en condiciones del Trópico Húmedo de México. Revista mexicana de Ciencias Agrícolas. 7(SPE16): 3315-3327.
15. Paniagua, L.; Arias, L. Alpízar, A.; Castillo, M.; Camacho, M.; Padilla, J.; Campos, M. 2018. Efecto de la densidad de siembra y edad de rebrote en la producción y composición bromatológica de *Tithonia diversifolia* (Hemsl.) A. Gray. Pastos y Forrajes. 43(4): 275-283. http://scielo.sld.cu/scielo.php?script=sci_arttext&pid=S0864-03942020000400275&l-ng=es&tlng=es
16. Piccinetti, C.; Eöry, C. A.; Prieto, G. M.; Vallejo, D. A.; Enrico, J. M.; Salvagiotti, F.; Perticari, A. 2024. Selection of *Rhizobium leguminosarum* strains via symbiotic and production variables in *Pisum sativum* L. Revista de la Facultad de Ciencias Agrarias. Universidad Nacional de Cuyo. Mendoza. Argentina. 56(1): 1-11. DOI: https://doi.org/10.48162/rev.39.118
17. Pincay-Ganchozo, R.; Luna-Murillo, R.; Espinosa-Cunuhay, K.; Espinales-Suárez, H. 2021. Escarificación química y biológica en la emergencia y crecimiento de *Clitoria ternatea*. Centro Agrícola. 48(3): 53-59.
18. Ramírez-Villalobos, M.; Urdaneta-Fernández, A.; Suárez, H.; Iglesias-Gómez, J. 2023. Distribución de materia seca, área foliar y calidad nutricional en dos genotipos de *Clitoria ternatea* L. Pastos y Forrajes. 46(2): 1-9.
19. Rendón, J. 2023. Capacidad extractora de cadmio en materiales genéticos de cacao procedentes de la colección del Instituto Nacional de Investigaciones Agropecuaria- EETP. http://repositorio.utc.edu.ec/handle/27000/8572, (accessed on September 11st 2023).
20. Renté-Martí, O.; Pablos-Pablo, R.; Corrales-Vila, Y. 2020. *Canavalia ensiformis* (L): en propiedades químicas de un suelo fluvisol diferenciado. Revista científica del Amazonas. 3(6): 65-75.
21. Rosas-Quina, Y. 2020. Efecto del tamaño de partícula en la extracción de alcaloides del tarwi (*Lupinus mutabilis*) Sweet) por método convencional. Peruvian Agricultural Research. 2(1). http://doi.org/10.51431/par.v2i1.619
22. Shamnad, J. 2019. Mineral and nutritional potential of *Clitoria ternatea* L. variants as forage. J. Trop. Agric. 57(2): 163-166. http://jtropag.kau.in/index.php/ojs2/article/view/867
23. Sosa-Montes, E.; Alejos-de la Fuente, J. I.; Pro-Martínez, A.; González-Cerón, F.; Enríquez-Quiroz, J. F.; Torres-Cardona, María G. 2020. Composición química y digestibilidad de cuatro leguminosas tropicales mexicanas. Rev. Mex. Cienc. Agríc. 11 (spe24): 211-220, DOI: https://doi.org/10.29312/remexca.v0i24.2371
24. Taiz, L.; Zeiger, E.; Møller, I. M.; Murphy, A. 2015. Plant physiology and development. Sunderland. 15-34.
25. Turnos, J. L. 2021. Influence of light intensity on the growth and yield of blu ternate (*Clitoria Sp*.) Asian Journal of Fundamental and Applied Sciences. 2(2): 1-14.

26. Santana Cabrera, J. A.; Lozada Caisa, M. A.; Gavilánez Buñay, T. C.; Salazar Arias, J. P.; Chuquitarco Esmeraldas, V. A. 2022. Evaluación del extracto de *Clitoria ternatea* como bioestimulante en el cultivo de frijol. Ciencia Latina Revista Científica Multidisciplinar. 6(4): 1931-1945. DOI: https://doi.org/10.37811/cl_rcm.v6i4.2719
27. Verdecia, D.; Herrera-Herrera, R.; Torres, E.; Sánchez, A.; Hernández- Montiel, L.; Herrera, R.; Ramírez, J. L.; Bodas, R.; Giráldez, F.; Guillaume, J.; Uvidia, H.; López, S. 2021. Primary and secondary metabolites of six species of trees, shrubs and herbaceous legumes. Cuban Journal of Agricultural Science. 5(1): 1-17.

Yield and Development of Winter and Spring Rapeseed (*Brassica napus* L.) at Different Sowing Dates in Temperate Environments

Desarrollo y rendimiento de colza (*Brassica napus* L.) invernal y primaveral ante distintas fechas de siembra en ambientes templados

Miguel Pereyra Iraola, Mateo Zubiri, José Luis Bodega, María Luján Nagore, Gastón Darwich, Roberto Dionisio Martínez *

Originales: *Recepción:* 04/06/2024- *Aceptación:* 18/10/2024

ABSTRACT

Optimal sowing dates should match the crop-critical period with favorable conditions. In rapeseed, growth stages change among spring and winter cultivars. This study characterized changes in rapeseed phenology with varying sowing dates to determine critical periods in both winter and spring cultivars. The trial took place in Balcarce, Argentina, where a winter-type variety and a spring-type were sown on eight different dates in a randomized complete block design with three replicates. Phenology was monitored weekly, and yield was evaluated at the end of the season. Changes in sowing dates and cultivars led to variations in the timing of critical periods. Considering the experimental conditions, the optimal sowing window was between April and July for sowing either rapeseed cultivar. However, the winter variety did not bloom for sowing dates after July, while the spring variety showed yield reductions due to frosts for sowing dates before the end of April. Changes in sowing date resulted in differences in timing and duration of vegetative and reproductive stages, generally leading to shorter crop cycles. However, in late sowing, winter cultivars lengthened their life cycle to the point of not reaching flowering during the growing season.

Keywords
autumn sowing date • winter sowing date • vernalization • frost

https://doi.org/10.48162/rev.39.186

Universidad Nacional de Mar del Plata. Facultad de Ciencias Agrarias. Ruta 226. km 73.5. Balcarce. C. P. 7620. Argentina. * rmartinez@mdp.edu.ar

Licenses Creative Commons Attribution - Non Commercial - Share Alike

Resumen

La fecha óptima de siembra debe hacer coincidir el período crítico del cultivo con condiciones favorables. Existen diferencias en la ubicación de las etapas de desarrollo de colza entre las variedades primaverales e invernales. El presente estudio se realizó para caracterizar los cambios en la fenología de la colza al variar la fecha de siembra para determinar el momento del período crítico en ambas variedades invernales y primaverales. El ensayo se llevó a cabo en Balcarce, Argentina, donde se sembraron una variedad tipo invernal y otra de tipo primaveral en ocho fechas diferentes. Se utilizó un diseño de bloques completos al azar con tres repeticiones y se monitoreó la fenología semanalmente, además de evaluar el rendimiento de cada tratamiento al final del ciclo. El período crítico se desplazó a diferentes períodos dependiendo de la fecha de siembra y la variedad. Bajo las condiciones experimentales, hubo una ventana ambiental óptima entre abril y julio para sembrar, tanto la variedad primaveral como la invernal. Sin embargo, la variedad invernal no floreció en siembras posteriores a julio, y la variedad primaveral experimentó reducciones en el rendimiento debido a las heladas en siembras antes del fin de abril. Las variedades ante las diferentes fechas de siembra presentaron diferencias tanto en la ubicación como en la duración de las etapas vegetativas y reproductivas, tendiendo a acortar su ciclo. Sin embargo, en las siembras más tardías, la variedad invernal alargó su ciclo hasta el punto de no alcanzar la floración durante la temporada de crecimiento.

Palabras clave
fecha de siembra otoñal • fecha de siembra invernal • vernalización • heladas

Introduction

Brassica napus L., commonly known as rapeseed or canola (particularly the "double-zero" variety with low erucic acid and glucosinolates), holds substantial economic value, primarily attributed to its edible oil and significance in bioenergy (18). Over the last decade, rapeseed has been cultivated on approximately 35 million hectares globally (38), with key production regions in the European Union, Asia, and North America (35). Effective optimization of rapeseed crop productivity depends on selecting the sowing date and cultivar type. Rapeseed cultivars are categorized into winter and spring varieties (37). Winter cultivars require vernalization and are sown in the autumn, with their development rate being temperature-dependent within specific ranges (5, 10, 21, 32). Winter cultivars are mainly cultivated in areas that meet the required temperature thresholds, particularly in Northern Europe, the United States, and China. In contrast to winter cultivars, spring cultivars do not require vernalization and are sown at later dates (16). Primary production areas for spring cultivars include Canada, with minor cultivation areas in India and South America at earlier sowing dates (17). Nevertheless, no significant differences in productivity have been reported between winter and spring cultivars in environments that fulfill their specific requirements (31). However, a wider period of sowing dates could modify cultivar relative performance.

Rapeseed development has various growth stages, from leaf rosette formation to seed maturation. Commonly used phenological scales for the study of rapeseed growth and development are Silvester-Bradley and Makepeace (1984) and Arnoud (1989). Temperature plays a primary role in determining the duration of growing stages (12, 34), although rapeseed exhibits a long-day photoperiodic response (26). The number of leaves is contingent on the length of the vegetative phase, although immature pods can also perform photosynthetic functions (28). Plants can develop multiple floral branches, which form pods containing oil-rich seeds (19). The optimal sowing date is one where the crop critical period matches with the most favorable environmental conditions. This critical period starts with the onset of flowering, lasting approximately four weeks, and is a crucial phase during which pod numbers per plant and flower abortion levels are determined (22). Additionally, crop physiological status during the first half of seed filling is a key factor (27). Regardless of the cycle duration and available water supply, which can affect the productivity of any

crop, rapeseed, in particular, exhibits a high sensitivity to elevated temperatures during the flowering period (24, 29). Furthermore, the crop remains vulnerable to frost events even during the seed-filling stage (31). Late sowings are not recommended because as temperature increases during seed filling, seed oil content decreases (13, 36).

In temperate environments, grain yield can reach 4000 kg ha^{-1} under optimal conditions (10, 15). Where winters are mild, it is feasible to use either early-sown spring genotypes or winter varieties (11, 16). Nevertheless, inappropriate sowing dates could potentially shorten the crop cycle for both types of cultivars (7). The success of the rapeseed crop depends on choosing a suitable sowing date to avoid delays in flowering and suboptimal environmental conditions during seed filling. In temperate regions, winter varieties should have autumn sowing dates, and spring varieties should have winter sowing dates. However, meteorological and operational factors could delay the sowing date and compromise the optimal conditions for crop growth. Therefore, there is a need to evaluate how different sowing dates could modify the phenology and stages of the rapeseed crop using both spring and winter cultivars across a wide range of dates. Moreover, it is crucial to analyze how the management of the sowing date optimizes crop yield depending on the type of cultivar. This study aimed to characterize changes in rapeseed phenology by varying sowing dates to determine the timing of critical periods and yield in both winter and spring cultivars.

Materials and methods

The experiment was conducted during the 2015/2016 growing season at the Experimental Research Station in Balcarce, Province of Buenos Aires, Argentina (37°45' S-58°18' W) 130 meters above sea level. Two rapeseed cultivars were sown: a winter type (Vectra, from QualityCrops) and a spring type (Bioaureo 2386, from Nuseeds), using an experimental seeder under conventional tillage. Sowing was conducted at a high density to establish the initial plant stand, and thinning was performed after crop emergence to achieve the target density (70 pl/m^2). Experimental design consisted of randomized complete blocks with three replicates, conducted in parallel strips across eight different sowing dates, corresponding to different days of year (DOY): April 23, 2015 (F1: DOY 113), May 13, 2015 (F2: DOY 141), June 1, 2015 (F3: DOY 152), June 24, 2015 (F4: DOY 175), July 10, 2015 (F5: DOY 191), August 5, 2015 (F6: DOY 217), August 27, 2015 (F7: DOY 239), and September 14, 2015 (F8: DOY 257). Each experimental unit had seven furrows 5 m long with 0.21 m distance between furrows, with the total surface area of each experimental unit being 7.35 m^2.

Throughout the crop development, phenology was closely monitored twice a week, with a specific focus on the rosette stages with 4 (B4) to 6 (B6) developed leaves, the onset of stem elongation (D1), flowering (F1), and physiological maturity (MF), following the European phenological classification INRA-CETIOM (4). Each growth stage was considered to start when 50% of the plants showed their specific characteristics. Thermal sum calculations were calculated using a base temperature of 0°C (21). Meteorological data, including air temperature, incident radiation, precipitation, and potential evapotranspiration, were obtained from a meteorological station located approximately 500 meters from the experimental site. To estimate the water deficit throughout the crop growing season, a water balance was conducted using potential evapotranspiration (ETP) calculated through the Penman-Monteith method (2).

The trial was monitored weekly to ensure disease and weed control. In addition to phenology tracking, the yield of each treatment was determined. At the end of the growing season, harvesting was conducted by collecting 1-meter from each of the three central rows within the plots. Harvested seeds were then processed using a stationary thresher, and their weight was recorded to calculate the hectare yield based on the harvested area.

All the variables were analyzed using the statistical software INFOSTAT (8). An analysis of variance was performed, and the Fisher Least Significant Difference (LSD) test for mean comparison was used, with a significance level of $P < 0.05$.

Results and discussion

Environmental Conditions

Rainfall was comparatively low during June, September, and December. However, there was a soil profile recharge in August. The water balance analyzed the relationship between rainfall and potential evapotranspiration (figure 1). Mild water deficits were consequently recorded in May, with moderate deficits in September and November, and severe deficits persisting in December. Water deficits may affect flowering and later grain filling under some sowing dates.

Blue columns represent accumulated monthly rainfall, orange columns denote atmospheric demand as potential evapotranspiration (ETP), and light blue columns illustrate the resulting balance from their difference.

Las precipitaciones acumuladas al mes en columnas azules, la demanda atmosférica en forma de evapotranspiración potencial (ETP) en columnas naranjas y el saldo resultante de su diferencia en columnas celestes.

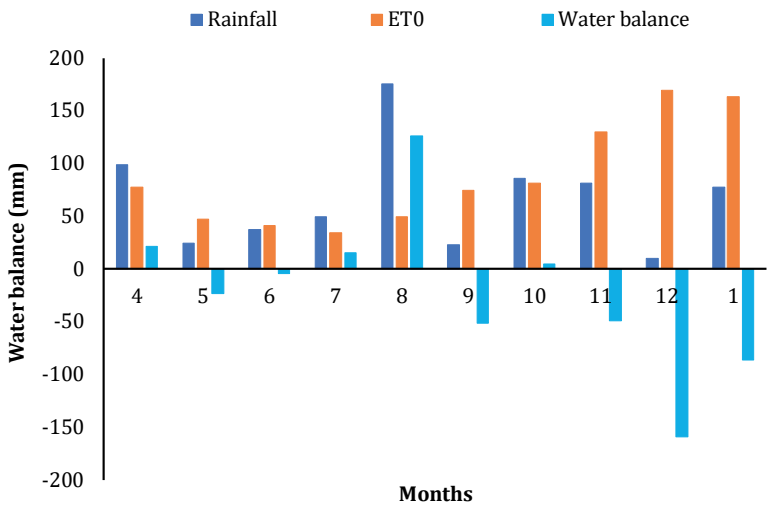


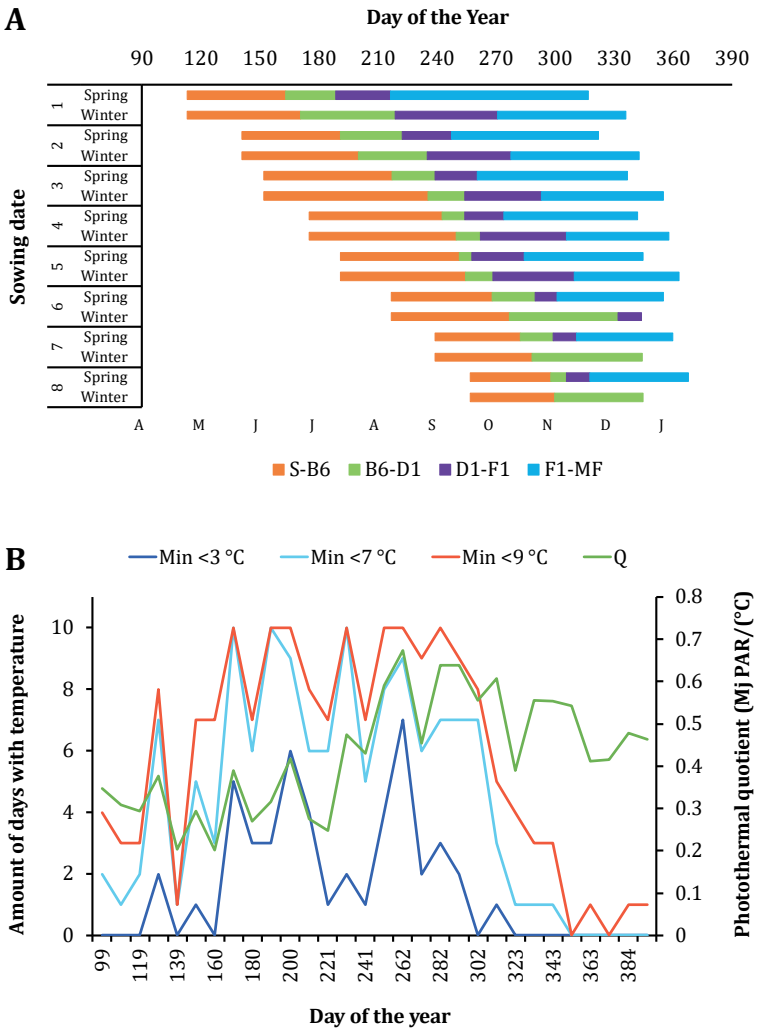
Figure 1. Water balance during the 2015-16 season for Balcarce, in the Buenos Aires province, Argentina.

Figura 1. Balance hídrico durante la temporada 2015-16 para Balcarce, provincia de Buenos Aires, Argentina.

Crop Development

As the sowing date was delayed, the average length of the crop cycles became shorter (figure 2A, page 5). The winter cultivar generally exhibited a longer cycle than the spring cultivar, but after the sixth sowing date, the winter cultivar did not complete its cycle. Critical growth periods occurred at different times when changing the sowing date and between the cultivars. These results align with previous studies from the 2008/2009 season in Paraná, where the cultivars exhibited different responses due to the delayed sowing dates (7).

From the fifth sowing date onward, the growth cycle of the winter cultivar changed from shortening to extending because the vernalization requirements were not satisfied. Vernalization-requiring cultivars increase their development rate as temperature accumulates from 4°C to 9°C. From the 250th day of the year (coinciding with the emergence of the winter cultivar sown on the sixth sowing date), a noticeable decrease in the number of days with minimum temperatures below 7 and 9°C was observed (figure 2B, page 5). Consequently, the winter variety sown after July did not flower by the time of harvest of the other treatments.



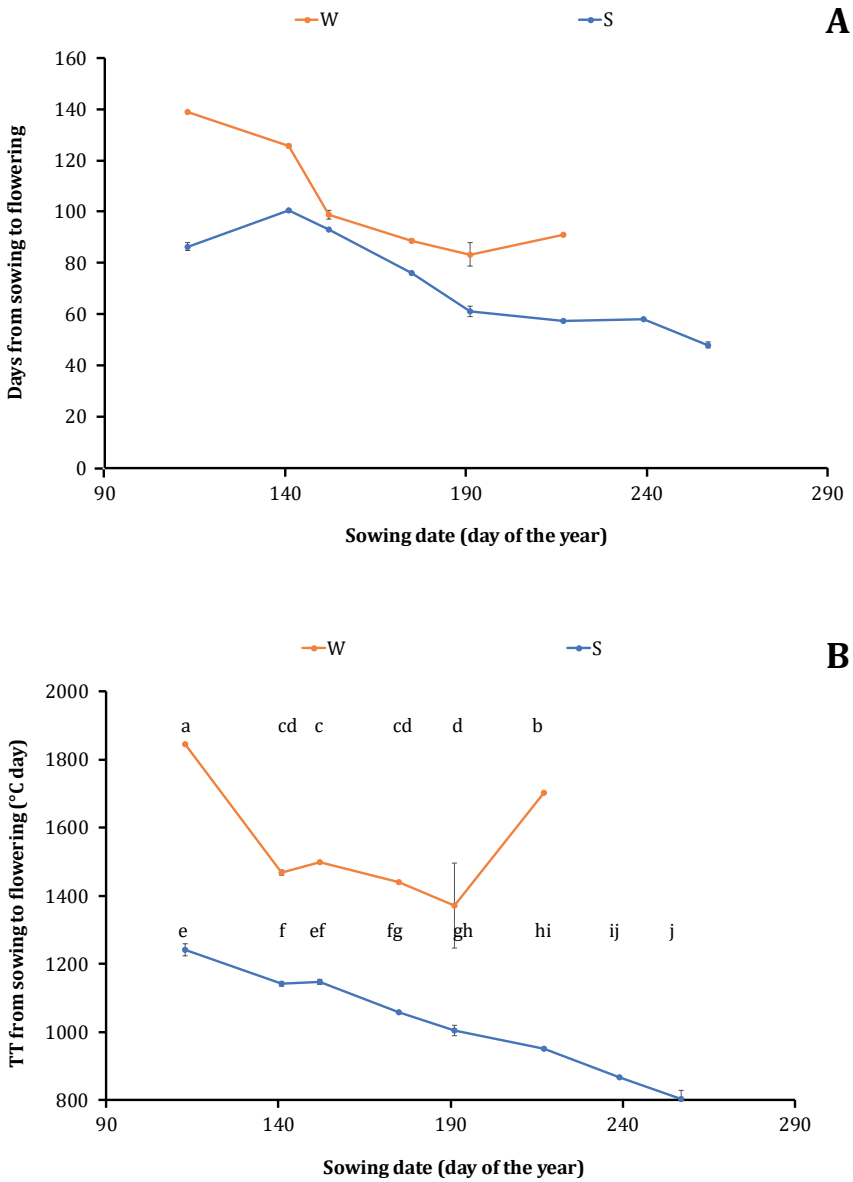
2B Number of days per decade with minimum temperatures below 3 (blue), 7 (light blue), and 9°C (red) and photothermal quotient (dashed green) for the year 2015.

2B Número de días por década con temperaturas mínimas inferiores a 3 (azul), 7 (azul claro) y 9°C (rojo) y cociente fototérmico (verde discontinuo) para el año 2015.

Figure 2A. Duration of the stages Sowing-6 leaves (S-B6 in red), 6 leaves-to inflorescence period (B6-D1 in green), appearance of inflorescence-beginning of flowering (D1-F1 in purple) and flowering - physiological maturity (F1-MF in light blue) expressed in days of the year for two cultivars analyzed and eight sowing dates evaluated.

Figura 2A. Duración de las etapas Siembra - 6 hojas (S-B6 en rojo), 6 hojas - aparición de la inflorescencia (B6-D1 en verde), aparición de la inflorescencia - inicio de floración (D1-F1 en morado) y floración - madurez fisiológica (F1-MF en celeste) expresado en días del año para los dos cultivares analizados y las ocho fechas de siembra evaluadas.

The duration from emergence to flowering period expressed in days presented a significant interaction between the sowing date and cultivar type ($p \leq 0.0001$). For the spring cultivar, the vegetative period was reduced for seven of the eight sowing dates because of delayed sowing (figure 3A, page 6). The winter cultivar also tended to shorten its vegetative period when the sowing date was delayed, up to its fifth sowing date (corresponding to July). From the seventh sowing date onward, the winter cultivar did not flower before the harvest date of the other treatments. These results partially align with results obtained by Takashima *et al.* (2013), who assessed a narrower range of sowing dates. Furthermore, the winter cultivar accumulated a higher thermal sum for the emergence-flowering period ($p \leq 0.0001$) than the spring cultivar on all sowing dates. In the spring cultivar, the vegetative period expressed in thermal units shortened as the sowing date was delayed (figure 3B page 6), whereas the winter cultivar displayed a similar trend up to the fifth sowing date (corresponding to July), after which the thermal sum for phenological change significantly increased.



Each point represents the average date of three repetitions. Different letters indicate significant differences between means of treatment.

Cada punto representa la fecha promedio de las tres repeticiones. Letras diferentes indican diferencias significativas entre las medias de los tratamientos.

Figure 3. Duration of the Sowing-Flowering period expressed in days **3A** and in thermal time **3B** for two cultivars analyzed (winter in red and spring in blue) and eight sowing dates evaluated expressed according to the day of the year in which sowing took place.

Figura 3. Duración del período siembra - floración expresado en días **3A** y expresado en unidades de tiempo térmico **3B** para los dos cultivares analizados (invernal en rojo y primaveral en azul) y las ocho fechas de siembra evaluadas expresadas según el día del año en que se realizaron.

Shortening the vegetative period in the spring cultivar would be compatible with a quantitative photoperiodic effect. In crops with a quantitative response to long-day photoperiod, increases in day length from June 21st to December 21st imply reductions in thermal sums required for growth stage change up to a threshold where the thermal sum is fixed. Since the threshold of approximately 14 hours proposed by Nanda *et al.* (1996) is not reached in the studied sowing dates, inductive photoperiod is not achieved. Hence, the thermal time to flowering was shortened by gradually delaying

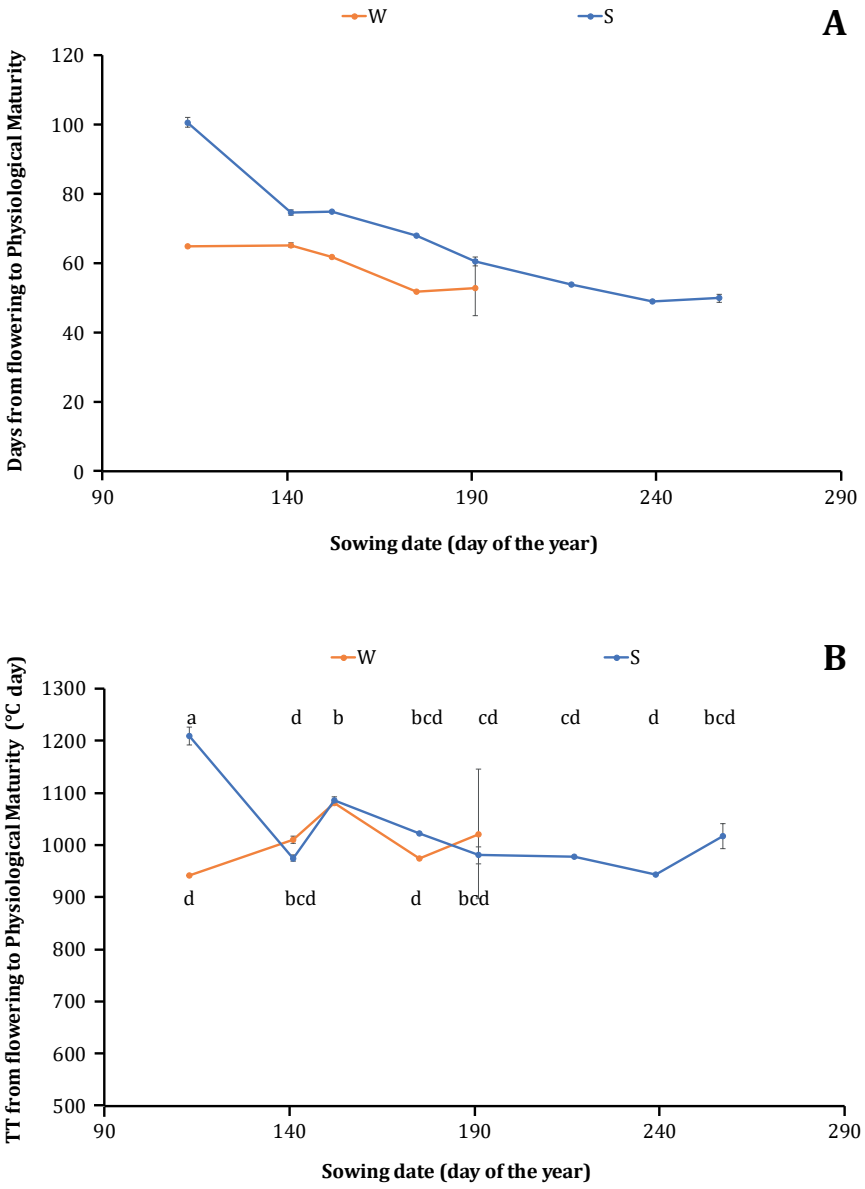
the sowing date due to the increased day length. At sowing dates where the day length does not exceed 14 hours, changes in day length caused by different sowing dates will be proportional to changes in thermal sum until flowering. In the winter cultivar, starting from the fifth sowing date, thermal sums shift from decreasing with delayed sowing to extending due to their vernalization requirements. Sensitivity to this factor also varies among cultivars (25), and it is unknown what the threshold temperature for vernalization of the analyzed cultivar is or within which period the stimulus is captured. Although cultivars requiring vernalization have accelerated development rates due to temperature accumulation between the range of 4°C to 9°C, the upper defined limit is at 13°C (11). Among plants in which flowering is promoted by the accumulation of cold hours, the effective temperature range is 1-7°C (21). In previous studies on rapeseed varieties, the optimal vernalization temperature was reported within the range of 6-9°C (33). Therefore, sowing winter cultivars after August 5th in the southeastern Buenos Aires region will not allow the accumulation of sufficient cold hours to meet the vernalization requirement for flowering during the growing season.

On the same sowing date, the spring cultivar showed a longer seed-filling duration than the winter cultivar. The duration from flowering to physiological maturity, expressed in days, exhibited an interaction between the sowing date and cultivar type ($p \leq 0.0060$). Both cultivars gradually reduced their filling period duration (figure 4A, page 8). Significant differences were determined among the combinations of sowing date and cultivar for the duration from the flowering to physiological maturity period expressed in thermal time ($p \leq 0.0013$). The spring cultivar sown in April had the longest seed-filling period, while the remaining combinations of sowing dates and cultivars did not show significant differences in the duration of the period expressed as thermal time, with an approximate value of 1000°C day (figure 4B, page 8). The findings suggest that the spring cultivar, when sown on the earliest date, may prolong its grain-filling period in thermal time because of occasional frosts during the reproductive phase. This consideration is important because the spring cultivar flowered 50 days earlier than the winter cultivar on the same sowing date (figure 2A, page 5). The hypothesis regarding the frost effect suggests that the occurrence of frosts may extend grain filling by inducing senescence in main branches, which results in greater development of lateral pods and a delay in crop maturity. It was hypothesized that postponing the sowing date by 20 days after March 1st would decrease the number of frost days by one during the critical period (31).

Crop Yield

Sowing dates that resulted in the highest yields were May (date 2) for winter varieties and the end of June (date 4) for spring varieties ($p \leq 0.0001$). For the experimental conditions, an optimal sowing timeframe for both types of rapeseed cultivars was determined to be between late April and July (figure 5, page 9). Notably, the winter variety failed to flower when sown late, while the spring variety experienced reduced yields due to early frosts when sown too early. Consequently, the highest yields were achieved during a specific flowering window between day 270 and 300 of the year, roughly from mid-September to October, with yields exceeding 5000 kg ha^{-1}. These findings are consistent with prior studies showing increases in grain yields for spring varieties when sowing dates were delayed (15). However, in later sowing dates, the highest yield was associated with the shorter-cycle variety, as observed in a previous study 7. Our findings contrast those previously reported by Agostini (2011), who suggested that environments with longer grain-filling periods would lead to higher returns. Therefore, studying how different cultivar types respond to various environmental variables when sowing dates are adjusted becomes crucial for optimizing critical periods and increasing crop yield (23).

Towards the end of September, the water scenario (figure 1, page 4), and photothermal conditions improve, and frost incidence decreases, making it the optimal time for the critical period (figure 2B, page 5). During this period, the photothermal quotient (Q) increases, enhancing radiation capture and allowing for a high accumulation of carbohydrates. The potential photothermal effect suggests that Q could also be used to explain changes in yield in rapeseed, as is the case in various species (3, 6, 9). In addition to the photothermal component, post-flowering rainfall is crucial in rainfed crops and was positively associated with yield and grain oil content (29, 33). Under our experimental conditions, water availability was favorable during October, making it the ideal time for the critical period to take place.



Each point represents the average date of three repetitions. Different letters indicate significant differences between means of treatment.

Cada punto representa la fecha promedio de las tres repeticiones. Letras diferentes indican diferencias significativas entre las medias de los tratamientos.

Figure 4. Duration of the period from Flowering to Physiological Maturity expressed in days **4A** and in thermal time **4B** for two cultivars analyzed (winter in red lines and spring in blue lines) and eight sowing dates evaluated expressed according to the day of the year in which were carried out.

Figura 4. Duración del período de Floración a Madurez Fisiológica expresado en días **4A** y expresado en tiempo térmico **4B** para los dos cultivares analizados (invernal en rojo y primaveral en azul) y las ocho fechas de siembra evaluadas expresadas según el día del año en que se realizaron.

Each point represents the average data of three repetitions. Different letters indicate significant differences between means of treatments (P<0.05).

Cada barra representa el rendimiento promedio de las tres repeticiones y su error estándar. Letras diferentes indican diferencias significativas entre las medias de los tratamientos (P<0,05).

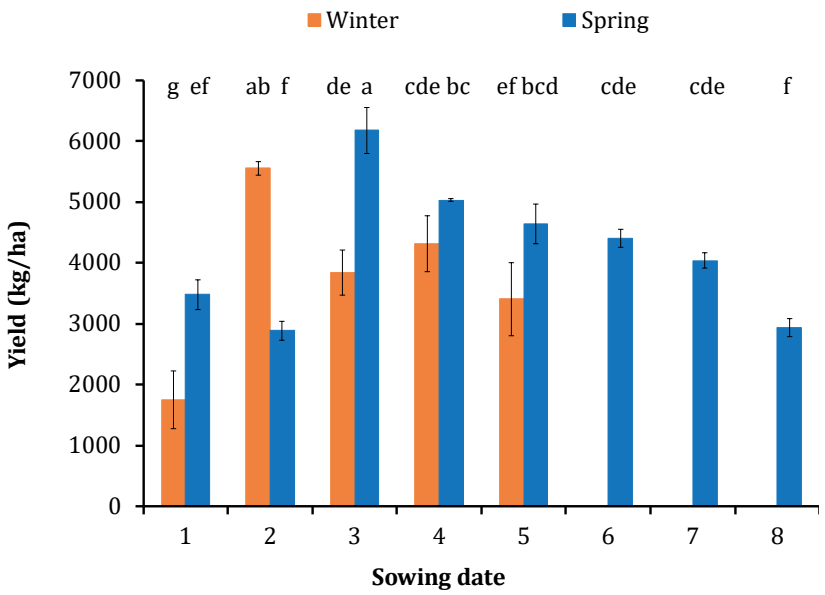


Figure 5. Grain yield expressed in kilograms per hectare on a dry basis for the two cultivars analyzed (winter in orange and spring in blue) and the eight sowing dates evaluated.

Figura 5. Rendimiento expresado en kilogramos por hectárea en base seca para los dos cultivares analizados (invernal en naranja y primaveral en azul) y las ocho fechas de siembra evaluadas.

In summary, variations in sowing dates and cultivar selection influenced the timing of the critical period. Alterations in sowing dates resulted in shifts in the flowering date, ranging from day 200 to day 300, thus delaying the flowering period from June to approximately October. The optimal sowing dates identified in this research differ slightly from those recommended for no-tillage systems in the region, which typically occur in March and April. The study was conducted under conventional tillage in only one season, potentially mitigating frost damage during crop emergence with sowing dates after May. Winter cultivars show less flexibility in sowing dates than spring varieties, as they may not flower in late sowings due to the absence of vernalization conditions. For the evaluated experimental conditions, the only observed limitation in the sowing date of spring cultivars is to avoid planting before April due to the high risk of frequent frost during the flowering period.

Conclusion

Changes in sowing date presented differences in both location and duration of vegetative and reproductive stages, tending to shorten their cycle. However, in late sowing, winter cultivars lengthened their cycle to the point of not reaching flowering during the growing season. For the tested environmental experiment conditions, optimal sowing dates were between the end of April and July for both spring and winter cultivars.

References

1. Agosti, M. B. 2011. Fertilización nitrógeno-azufrada y variabilidad genotípica en el rendimiento y la calidad del grano en colza-canola (*Brassica napus* L.). Tesis Magister. Universidad de Buenos Aires. 130 p.
2. Allen, R. G.; Pereira, L. S.; Raes, D.; Smith, M. 1998. Crop evapotranspiration: guidelines for computing crop water requirements. In: FAO Irrigation and Drainage Paper N° 56. FAO. Rome. Italy. 300 p.

3. Arisnabarreta, S.; Miralles, D. J. 2008. Critical period for grain number establishment of near isogenic lines of two- and six-rowed barley. Field Crops Research. 107: 196-202. https://doi.org/10.1016/j.fcr.2008.02.009
4. Arnoud, F. 1989. Colza: selection, varietés. Cahier Technique. CETIOM. París, Francia. 28 p.
5. Bouché, F.; Woods, D. P.; Amasino, R. M. 2017. Winter memory throughout the plant kingdom: Different paths to flowering. Plant Physiology. 173(1): 27-35. https://doi.org/10.1104/pp.16.01322
6. Cantagallo, J. E.; Chimenti, C. A.; Hall, A. J. 1997. Number of seed per unit area in sunflower correlates well with a phototermal quotient. Crop Science. 37: 1780- 1786. https://doi.org/10.2135/cropsci1997.0011183X003700060020x
7. Coll, L.; Larrosa, L. M. 2010. Efecto de la fecha de siembra y el ciclo sobre el rendimiento de colza. Actualización Técnica N° 1. EEA INTA Paraná. 36 p.
8. Di Rienzo, J. A.; Casanoves, F.; Balzarini, M. G.; Gonzalez, L.; Tablada, M.; Robledo, C. W. 2008. InfoStat, Grupo InfoStat. FCA. Universidad Nacional de Córdoba. Argentina.
9. Fischer, R. A. 1985. Number of kernels in wheat crops and the influence of solar radiation and temperature. Journal of Agriculture Science. Cambridge. 105: 447-461. https://doi.org/10.1017/S0021859600056495
10. Gómez, N. V.; Miralles, D. J. 2011. Factors that modify early and late reproductive phases in oilseed rape (*Brassica napus* L.): Its impact on seed yield and oil content. Industrial Crops and Products. 34: 1277-1285. https://doi.org/10.1016/j.indcrop.2010.07.013
11. Gómez, N. V.; Miralles, D. J.; Mantese, A. I.; Menéndez, Y. C.; Rondanini, D. P. 2018. Colza: un cultivo con historia en la FAUBA. Universidad de Buenos Aires. Facultad de Agronomía; Agronomía & Ambiente. 38(1): 23-36.
12. Habekotté, B. 1997. Evaluation of seed yield determining factors of winter oilseed rape (*Brassica napus* L.) by means of crop growth modelling. Field Crops Research. 54: 137-151. https://doi.org/10.1016/S0378-4290(97)00044-0
13. Hocking, P. J.; Kirkegaard, J. A.; Angus, J. F.; Gibson, A. H.; Koetz, E. A. 1997. Comparison of canola, Indian mustard and Linola in two contrasting environments. I. Effects of nitrogen fertilizer on dry-matter production, seed yield and seed quality. Field Crops Research. 49: 107-125. https://doi.org/10.1016/S0378-4290(96)01063-5
14. Iriarte, L. B. 2014. Cultivo de colza: fecha de siembra, densidad y distancia entre surcos. INTA Barrow. 11 p.
15. Iriarte, L. B.; Valetti, O. 2008. Cultivo de Colza. INTA. Buenos Aires. 152 p.
16. Iriarte, L. B.; López, Z. B. 2014. El cultivo de colza en Argentina. Situación actual y perspectivas. 1° Simposio Latinoamericano de Canola. Passo Fundo. Brasil. 1-7.
17. Kirkegaard, J. A.; Lilley, J. M.; Berry, P. M.; Rondanini, D. P. 2021. Canola. In: Sadras VO and Calderini DF. Crop Physiology Case Histories for Major Crops, eds and (Academic Press). 518-549.
18. Lin, L.; Allemekinders, H.; Dansby, A.; Campbell, L.; Durance-Tod, S.; Berger, A.; Jones, P. J. 2013. Evidence of health benefits of canola oil. Nutr. Rev. 71: 370-385. https://doi.org/10.1111/nure.12033
19. McWilliam, S. C.; Stafford, J. A.; Scott, R. K.; Norton, G.; Stokes, D. T. 1995. The relationship between canopy structure and yield in oilseed rape. In: Proceedings of the 9th International Rapeseed Congress. Cambridge. UK. 491-493.
20. Mendham, N. J.; Salisbury, P. A. 1995. Physiology: crop development, growth and yield. In: Kimber D.; McGregor, D. I. (Eds.), Brassica Oilseed, Production, Utilization, Camb. 11-64.
21. Michaels, S.; Amasino, R. 2000. Memories of winter: vernalization and the competence to flower. Plant Cell Environ. 23: 1145–1154. https://doi.org/10.1046/j.1365-3040.2000.00643.x
22. Mingeau, M. 1974. Comportement du colza e printemps a la sécheresse. Informations Techniques (Paris, France). 36: 1-11.
23. Miralles, D. J.; Ferro, B.; Slafer, G. 2001. Developmental responses to sowing date in wheat, barley and rapeseed. Field Crops Research. 71: 211-223. https://doi.org/10.1016/S0378-4290(01)00161-7
24. Morrison, M. J.; Stewart, D. W. 2002. Heat stress during flowering in summer brassica. Crop Science. 42: 797-803. https://doi.org/10.2135/cropsci2002.7970
25. Murphy, L.; Scarth, R. 1991. Vernalization response of spring canola (*Brassica napus* L.) In: Mc Gregor DI (eds.). Proceedings of the Eight International Rapeseed Congress. Saskatoon, Saskatchewan. Canadá. 1764-1768.
26. Nanda, R.; Bhargava, S.; Tomar, D.; Rawson, H. M. 1996. Phenological development of *Brassica campestris*, *B. juncea*, *B. napus* and *B. carinata* grown in controlled environments and from 14 sowing dates in the field. Field Crops Res. 46: 93-103. https://doi.org/10.1016/0378-4290(95)00090-9
27. Permingeat, M. P. 2013. Rendimiento de colza 00: determinación del período crítico. Tesis de grado. Facultad de Ciencias Agrarias. Universidad de Mar del Plata. Argentina. 20 p.
28. Rondanini, D. P.; Menendez, Y. C.; Gomez, N. V.; Miralles, D. J.; Botto, J. F. 2017. Vegetative plasticity and floral branching compensate low plant density in modern spring rapeseed. Field Crops Research. 210: 104-113. https://doi.org/10.1016/j.fcr.2017.05.021
29. Secchi, M. A.; Fernandez, J. A.; Stamm, M. J.; Durrett, T.; Prasad, P. V. V.; Messina, C. D.; Ciampitti, I. A. 2023. Effects of heat and drought on canola (*Brassica napus* L.) yield, oil, and protein: a meta-analysis. Field Crops Res. 293. Article 108848. 10.1016/j. fcr.2023.108848

30. Silvester-Bradley, R.; Makepeace, R. J. 1984. A code for stages of development in oilseed rape (*Brassica napus* L.). Aspects of Applied Biology. 6: 399-419.
31. Takashima, N. E.; Rondanini, D. P.; Puhl, L. E.; Miralles, D. J. 2013. Environmental factors affecting yield variability in spring and winter rapeseed genotypes cultivated in the southeastern Argentine Pampas. European Journal of Agronomy. 48: 88-100. https://doi.org/10.1016/j.eja.2013.01.008
32. Tommey, A. M.; Evans, E. J. 1991. Temperature and daylength control of flower initiation in winter oilseed rape (*Brassica napus* L.). Annals of Applied Biology. 118: 201-208. https://doi.org/10.1111/j.1744-7348.1991.tb06098.x
33. Walton, G.; Si, P.; Bowden, B. 1999. Environmental impact on canola yield and oil. In: Proceedings of the 10th International Rapeseed Congress. Camberra, Australia. http://www. regional.org.au/au/gcirc/2/136.htm (Accessed: Sept 2023).
34. Weymann, W.; Bottcher, U.; Sieling, K.; Kage, H. 2015. Effects of weather conditions during different growth phases on yield formation of winter oilseed rape. Field Crops Res. 173: 41-48. https://doi.org/10.1016/j.fcr.2015.01.002
35. Woźniak, E.; Waszkowska, E.; Zimny, T.; Sowa, S.; Twardowski, T. 2019. The rapeseed potential in Poland and Germany in the context of production, legislation, and intellectual property rights. Front Plant Sci. 2019 Nov 5;10:1423. doi: 10.3389/fpls.2019.01423. PMID: 31749825; PMCID: PMC6848278.
36. Yaniv, Z.; Schafferman, D.; Zur, M. 1995. The effect of temperature on oil quality and yield parameters of high- and low-erucic acid Cruciferae seeds (rape and mustard). Industrial Crops and Products. 3: 247-251. https://doi.org/10.1016/0926-6690(94)00041-V
37. Zhang, Z.; Cong, R. H.; Ren, T.; Li, H.; Zhu, Y.; Lu, J. W. 2020. Optimizing agronomic practices for closing rapeseed yield gaps under intensive cropping systems in China. Journal of Integrative Agriculture. 19(2020): 1241-1249. https://doi.org/10.1016/S2095-3119(19)62748-6
38. Zheng, Q.; Liu, K. 2022. Worldwide rapeseed (*Brassica napus* L.) research: A bibliometric analysis during 2011-2021. Oil Crop Science. 7(4): 157-165. https://doi.org/10.1016/j.ocsci.2022.11.004.

Conflict of Interest

The authors declare the absence of any commercial or financial relationships that could be construed as a potential conflict of interest.

Physiological and Biochemical Responses of *Neltuma ruscifolia* under Na_2SO_4 Stress

Respuestas fisiológicas y bioquímicas de *Neltuma ruscifolia* bajo estrés con Na_2SO_4

Diego Ariel Meloni [1*], José Aliçandro Bezerra da Silva [2], María Judith Ochoa [1], Julia Andrea Lescano [1]

Originales: *Recepción:* 22/04/2024 - *Aceptación:* 15/03/2025

ABSTRACT

Salt stress limits plant production in arid and semi-arid zones. Although Na_2SO_4 is frequent in saline soils, most studies on plant physiological responses to salt stress were conducted using NaCl. This study aimed to determine the effect of Na_2SO_4 salt stress on physiological and biochemical responses in *Neltuma ruscifolia*. Increasing concentrations of Na_2SO_4 were added to 6-month-old plants grown hydroponically in 25% Hoagland nutrient solution. After 60 days of saline treatments, biomass, cysteine concentration, gas exchange, mineral composition, abscisic acid and salicylic acid concentrations, and antioxidant enzyme activity were determined. It is concluded that 200 mmol L^{-1} Na_2SO_4 is the threshold for *N. ruscifolia* seedling growth. Growth inhibition can be attributed to altered ionic homeostasis and photosynthesis inhibition after stomatal closure. Nevertheless, the species shows adaptive responses to this salt. Stomatal closure and increased foliar concentrations of abscisic acid contribute to water economy, while cysteine synthesis reduces sulfate toxicity. In parallel, salt stress induces salicylic acid accumulation in leaves, increasing the activity of antioxidant enzymes that prevent oxidative stress.

Keywords
ion homeostasis • phytohormones • antioxidant enzymes • photosynthesis • salinity stress

https://doi.org/10.48162/rev.39.188

1 Universidad Nacional de Santiago del Estero. Facultad de Agronomía y Agroindustrias. INDEAS. Av. Belgrano (S) 1912. 4200- Santiago del Estero. Argentina. * dmeloniunse@gmail.com
2 Universidade Federal do Vale São Francisco. Av. Antônio Carlos Magalhães 510. Juazeiro. BA. Brazil.

Licenses Creative Commons
Attribution - Non Commercial - Share Alike

Resumen

El estrés salino limita la producción vegetal en zonas áridas y semiáridas. Aunque el Na_2SO_4 es muy frecuente en suelos salinos, la mayoría de los estudios sobre las respuestas fisiológicas de las plantas al estrés salino se realizaron utilizando NaCl. El objetivo de este trabajo fue determinar el efecto del estrés salino con Na_2SO_4, sobre las respuestas fisiológicas y bioquímicas en *Neltuma ruscifolia*. Se adicionaron concentraciones crecientes de Na_2SO_4 a plantas de 6 meses, cultivadas hidropónicamente en solución nutritiva de Hoagland al 25%. Después de 60 días de tratamientos salinos, se determinó la biomasa, la concentración de cisteína, el intercambio gaseoso, la composición mineral, las concentraciones de ácido abscísico y salicílico, y la actividad de enzimas antioxidantes. Se concluye que el umbral para el crecimiento de plántulas de *N. ruscifolia* es 200 mmol L^{-1} Na_2SO_4. La inhibición del crecimiento puede atribuirse a alteraciones en la homeostasis iónica y a la inhibición de la fotosíntesis, debido al cierre de los estomas. Sin embargo, la especie muestra respuestas adaptativas a esta sal. Por lo tanto, el cierre de los estomas, asociado con mayores concentraciones foliares de ácido abscísico, contribuye a la economía del agua. La síntesis de cisteína reduce la toxicidad del ion sulfato absorbido por las raíces. Por otro lado, el estrés salino induce la acumulación de ácido salicílico en las hojas y un aumento de la actividad de enzimas antioxidantes, que pueden prevenir el estrés oxidativo.

Palabras clave

homeostasis iónica • fitohormonas • enzimas antioxidantes • fotosíntesis • estrés salino

Introduction

Approximately 7% of world land surface (7 million hectares) is affected by salinization (16). This situation worsens in arid and semi-arid areas due to global climate change, inadequate irrigation practices, and deforestation (9, 22, 26). Arid and semi-arid areas with sodic saline soils present high concentrations of NaCl, Na_2SO_4, or Na_2CO_3 (30). Given that NaCl is the most abundant salt in these soils, it has starred numerous studies on plant physiological responses to salt stress (31). However, sulfates strongly affect several countries like Canada, USA, Mexico, Australia and central Argentina (10, 15).

Neltuma ruscifolia (ex *Prosopis ruscifolia*) is a colonizing species with many ecotypes, from shrubby forms to 16m tall trees. It is distributed in the southeast of Bolivia, west of Paraguay, north and center of Argentina, and the extreme south of the State of Mato Grosso do Sul in Brazil (14, 34). Its wood is used to manufacture poles and tool handles, and its fruits are suitable as fodder and for human consumption (14).

N. ruscifolia tolerance to NaCl has been previously studied (18). *N. ruscifolia* seedlings can develop up to concentrations of 400 mmol L^{-1} NaCl (equivalent to seawater), showing higher aerial and root biomass than the control. Higher concentrations caused seedling death after seven days. This high tolerance to NaCl was attributed to canopy exclusion abilities, compartmentalizing the salt in the roots, and to the activity of antioxidant enzymes (17). However, the species tolerance to Na_2SO_4 and its associated physiological responses are unknown.

Salinity can inhibit plant growth through osmotic or ion-specific effects. It can produce nutrient imbalance, alterations in endogenous levels of phytohormones and oxidative damage (37). Greater sensitivity to Na_2SO_4 than to NaCl has been reported in *Prosopis strombulifera*, a species phylogenetically related to *N. ruscifolia* (27). This response was correlated with decreased K, Ca, P, and Mg leaf concentrations and damaged photosynthetic apparatus (27, 30). SO_4^{-2} increased the concentrations of abscisic and salicylic acids and the activity of antioxidant enzymes (10). The accumulation of abscisic acid would have a protective role against dehydration, whereas salicylic acid would signal SO_4^{-2} damage.

This study aimed to determine the effect of Na_2SO_4 salt stress on physiological and biochemical responses in *Neltuma ruscifolia*. We hypothesize that *N. ruscifolia* tolerates high Na_2SO_4 concentrations. Affected ion homeostasis and photosynthesis determine growth thresholds. Hormonal (increased abscisic and salicylic acid concentrations) and antioxidant responses seem to contribute to Na_2SO_4 tolerance in this species.

Materials and Methods

Study Site

N. ruscifolia seeds were harvested in January 2022 in Maco village, Santiago del Estero (27°51'20" S - 64°13'27" W). The region has a subtropical climate with a dry season and absolute maximum and minimum temperatures of 45°C and -10°C, respectively (5). In this region, *N. ruscifolia* forms secondary forests (vinalares), naturally distributed in flooding areas of the Dulce and Salado rivers and on the margins of salt marshes (7). Soils originate from loessial silts and are saline-sodic, with a higher proportion of sodium chlorides and sulfates (12).

Plant Material

Seeds were scarified in concentrated sulfuric acid for 10 min and rinsed with running water for 30 min. Then, they were sown with paper towels, watered with 25% Hoagland nutrient solution, and incubated in a growth chamber at 26°C and 12 h photoperiod. The seedlings were grown hydroponically in 15 L containers with 25% Hoagland nutrient solution (12 seedlings per container). The pH was adjusted daily to 6.5 by adding HCl or KOH 1N. The trial was conducted under greenhouse conditions, with 26°C and 6 MJ m^{-2} solar irradiance. After six months of age, Na_2SO_4 was added, initiated by pulses of 50 mmol L^{-1} every 24 h, until concentrations of 50, 100, 150, 200, 250, or 300 mmol L^{-1} Na_2SO_4 were achieved. The control consisted of a 25% Hoagland nutrient solution. After 60 days of cultivation, gas exchange was measured, and roots and aerial parts were separated and dried at 60°C in a forced ventilation oven for biomass and mineral composition determinations. Cysteine, antioxidant enzymes, and phytohormones were determined with leaf samples.

Mineral Composition

Plant material was ground in a Wiley-type mill and sieved through a 40-mesh screen. Subsequently, digestion was carried out with nitric acid and perchloric acid (87:13 v/v). Mineral composition was determined by inductively coupled plasma mass spectrometry. Results were expressed as mg g DW^{-1} (8).

Cysteine Determinations

Leaves were homogenized in a mortar with liquid nitrogen and HCl 0.1 N. The homogenate was centrifuged at 15,000 g for 30 min at 5°C. Cysteine concentration was quantified in the supernatant according to Riemenschneider *et al.* (2005) and expressed as nmol g FW^{-1}.

Gas Exchange

Gas exchange measurements were performed using an infrared gas analyzer in an open system (IRGA-LCpro+ System ADC, BioScientific Ltd.), with an Arabidopsis leaf chamber, under conditions of saturating artificial light (1000 µmol m^{-2} s^{-1}) and ambient CO_2 concentration. We measured net photosynthesis (A), stomatal conductance (g_s), intercellular CO_2 concentration (C_i), and transpiration (E).

Enzymatic Determinations

Leaves were homogenized in a mortar with liquid nitrogen and 25 mM HEPES buffer pH 7.8, containing 0.2 mM Na_2EDTA, 2 mM ascorbate, and 2% (m/v) polyvinylpyrrolidone. The homogenate was centrifuged at 12,000 g and 4°C for 20 min. Subsequently, the supernatant was separated, and the soluble protein concentration was determined according to Bradford (1976). In this supernatant, enzymatic activities were also quantified.

Superoxide dismutase activity (SOD, EC1.15.11) was quantified according to Giannopolitis and Ries (1977). The reaction mixture had 100 mM phosphate buffer pH 7.4, 1 mM EDTA, 10 mM methionine, 50 µM riboflavin, and 75µM NBT. After inciting 15 min under a 15-W fluorescent tube, absorbance was read at 560 nm in spectrophotometer. One unit of SOD consisted of the amount of enzyme required to inhibit half the photoreduction of nitro blue tetrazolium chloride. SOD activity was expressed as U mg^{-1} protein min^{-1}.

Ascorbate peroxidase activity (APX, EC1.11.11) was determined according to Nakano and Asada (1981). The reaction mixture contained 50 mM phosphate buffer pH 7.5, 100 µl

of each EDTA, ascorbate, enzyme, and H_2O_2. Absorbance was recorded at 290 nm for 2 min, and an extinction coefficient of 2.8 mM^{-1} cm^{-1} was used for calculation. APX activity was expressed as µmol ascorbate mg^{-1} protein min^{-1}.

Abscisic (ABA) and Salicylic Acids (SA)

Phytohormones were extracted and quantified according to Durgbanshi *et al.* (2005). Lyophilized leaves (50 mg DW) were homogenized in a mortar with liquid nitrogen and 3 mL ultrapure water. Next, 25 µL of a mixture of standards containing 100 ng [$^2H_6$] ABA and 100 ng [$^{13}C_6$] SA was added and centrifuged at 8,000 g for 15 min. The supernatant was partitioned with diethyl ether, and the organic phase was evaporated in a vacuum at 37°C. Dried extracts were resuspended in 1 mL methanol.

Thirty µL of this solution were directly injected in the Ultra Performance Liquid Chromatography (UPLC) system coupled to a Triple Quadrupole Mass Spectrometer (TQD Mass Spectrometer coupled to an Acquity LC, Waters Milford, MA, USA) through an orthogonal Z-spray electrospray interface. Separation was performed with a reverse phase C18 column (Gravity, 50 × 2.1 mm 1.8 µm particle size, Macherey-Nagel GmbH, Germany), using a methanol: water gradient, both supplemented with 0.1% acetic acid at a flow rate of 0.3 mL min^{-1} (11). Calibration curves were constructed using known amounts of pure standard samples to determine phytohormone concentrations. ABA and SA concentrations were expressed in µg g DW^{-1}.

Experimental Design and Statistical Analysis

A completely randomized experimental design with five replications was used. The experimental unit was represented by a 15 L container with 12 seedlings. After checking homoscedasticity and normality, the results were analyzed using ANOVA and the Tukey test.

Results and Discussion

Seedlings could grow up to salt concentrations of 200 mmol L^{-1} Na_2SO_4 (figure 1). Higher salt concentrations resulted in chlorosis and seedling death before the end of the trial. Aerial growth was more sensitive than root growth. Aerial growth was reduced at 100 mmol L^{-1} Na_2SO_4, while root growth was reduced at 150 mmol L^{-1} Na_2SO_4. These results differ from those reported for the species in NaCl, in which growth threshold was 400 mmol L^{-1} NaCl (18).

Vertical bars represent mean standard deviation (n=5). For each organ, different letters indicate significant differences according to the Tukey test at 5%.

Las barras verticales representan la desviación estándar de la media (n=5). Para cada órgano, letras diferentes indican diferencias significativas según el test de Tukey al 5%.

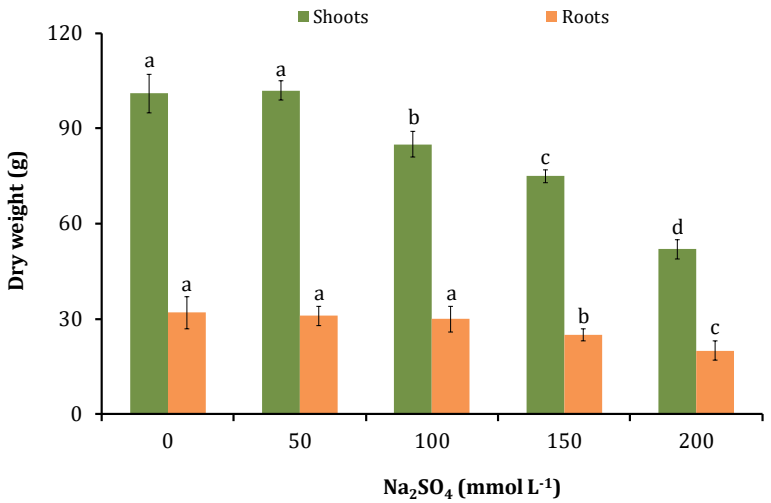


Figure 1. Dry matter of aerial part and roots of *Neltuma ruscifolia* seedlings grown hydroponically in increasing concentrations of Na_2SO_4.

Figura 1. Materia seca de parte aérea y raíces de plántulas de *Neltuma ruscifolia* cultivadas hidropónicamente en concentraciones crecientes de Na_2SO_4.

Neltuma ruscifolia excluded Na from the aerial part up to 100 mmol L^{-1} Na_2SO_4, compartmentalizing in the roots (table 1). However, SO_4 accumulated in leaves in all saline treatments.

Table 1. Mineral composition (mg g DW^{-1}) in leaves and roots of *N. ruscifolia* seedlings grown in increasing concentrations of Na_2SO_4.

Tabla 1. Composición mineral (mg g MS^{-1}) en hojas y raíces de plántulas de *N. ruscifolia* cultivadas en concentraciones crecientes de Na_2SO_4.

Na_2SO_4	Na	S	Mg	Ca	K
Leaves					
0	2.93 ± 0.51 a	2.62 ± 0.15 a	0.71 ± 0.23 a	9.21 ± 2.10 a	23.42 ± 5.32 a
50	3.45 ± 0.63 a	5.48 ± 0.57 b	0.64 ± 0.15 a	8.50 ± 1.43 a	24.11 ± 6.20 a
100	3.15 ± 0.71 a	8.11 ± 1.19 c	0.68 ± 0.09 a	8.92 ± 2.67 a	21.85 ± 4.73 a
150	5.01 ± 2.24 b	10.23 ± 1.82 d	0.47 ± 0.11 b	6.34 ± 1.93 b	14.35 ± 3.89 b
200	11.92 ± 3.40 c	11.54 ± 2.30 e	0.39 ± 0.07 c	4.11 ± 0.59 c	11.68 ± 1.54 c
Roots					
0	4.18 ± 0.37 a	1.71 ± 0.21 a	0.91 ± 0.12 a	8.73 ± 0.53 a	29.31 ± 0.98 a
50	6.17 ± 0.42 b	2.58 ± 0.17 b	0.61 ± 0.09 b	5.36 ± 1.08 b	26.83 ± 0.53 b
100	9.08 ± 0.25 c	3.75 ± 0.43 c	0.54 ± 0.02 c	4.04 ± 0.36 c	22.12 ± 0.73 c
150	15.69 ± 1.98 d	4.99 ± 0.33 d	0.39 ± 0.09 d	2.99 ± 0.66 d	14.56 ± 1.08 d
200	20.51 ± 3.10 e	6.84 ± 0.52 e	0.21 ± 0.07 e	1.27 ± 0.24 e	11.87 ± 0.69 e

Different letters indicate significant differences among treatments according to the Tukey test at 5%.

Letras diferentes indican diferencias significativas entre tratamientos según el test de Tukey al 5%.

Plant tolerance to salt stress depends on the species and the type of salt. In *Brassica rapa* (31) and *Aeluropus littoralis* (4), Na_2SO_4 was more toxic than NaCl. The opposite was observed in *Oryza sativa* (15) and *Chenopodium quinoa* (25). In *Allium cepa*, both salts had the same inhibitory effect on growth (1). Reginato *et al.* (2014) reported that *Strombocarpa strombulifera* (ex *Prosopis strombulifera*), a shrub species distributed from the Arizona desert to Argentine Patagonia, behaved as a halophyte to NaCl but was quite sensitive to Na_2SO_4.

It has been reported that Neltuma species respond to salinity through anatomical modifications that allow minimizing detrimental effects. Bravo *et al.* (2016) reported that stress increases the number of root cortex cell strata and decreases the diameter of xylem vessels in *N. ruscifolia*. The increased number of cortex cells suggests a greater capacity for toxic ion storage. Decreasing diameter of xylem vessels increase cavitation resistance at low water potentials in saline soils. In *Strombocarpa strombulifera*, salt stress produces suberization and early endodermis lignification, contributing to ionic entrance control in the root (26).

The increase in Na concentrations in the aerial part and roots was accompanied by a reduction in Mg, Ca, and K concentrations (table 1). These results agree with Reginato *et al.* (2019) in *S. strombulifera,* in which Na_2SO_4 produced a significant decrease in foliar Ca and Mg concentrations, correlating with growth inhibition and senescence. According to Ahmadizadeh *et al.* (2016), the accumulation of Na and SO_4^{2-} causes ionic imbalance and compromises uptake of other essential nutrients, such as K and Ca. The antagonism between Ca and Na ions has been attributed to the nonselective cation channels in cell membranes (NSCC), allowing the entry of both cations without discriminating one from the other (27, 32).

All salt treatments increased foliar cysteine concentrations (figure 2, page 6). Thus, in the 200 mmol L^{-1} Na_2SO_4 treatment, cysteine concentrations were six times higher than in the control.

Vertical bars represent mean standard deviation (n=5).

Different letters indicate significant differences according to the Tukey test at 5%.

Las barras verticales representan la desviación estándar de la media (n=5).

Letras diferentes indican diferencias significativas según el test de Tukey al 5%.

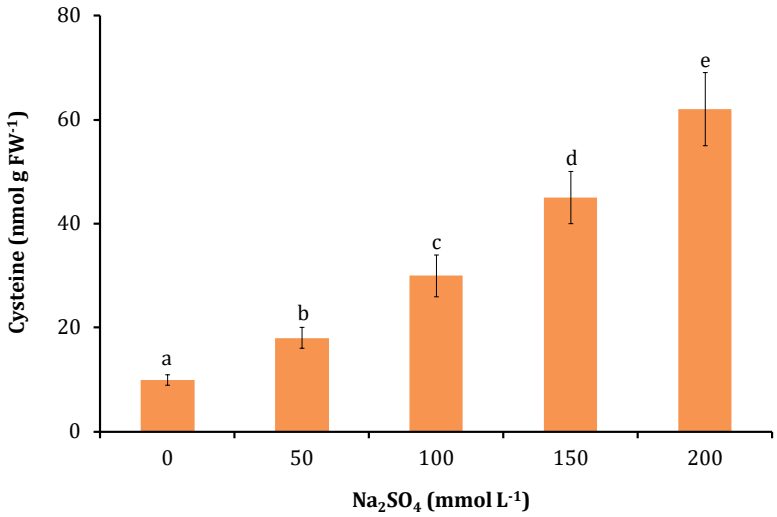


Figure 2. Cysteine concentration in leaves of *N. ruscifolia* seedlings grown in increasing concentrations of Na_2SO_4.

Figura 2. Concentración de cisteína en hojas de plántulas de *N. ruscifolia* cultivadas en concentraciones crecientes de Na_2SO_4.

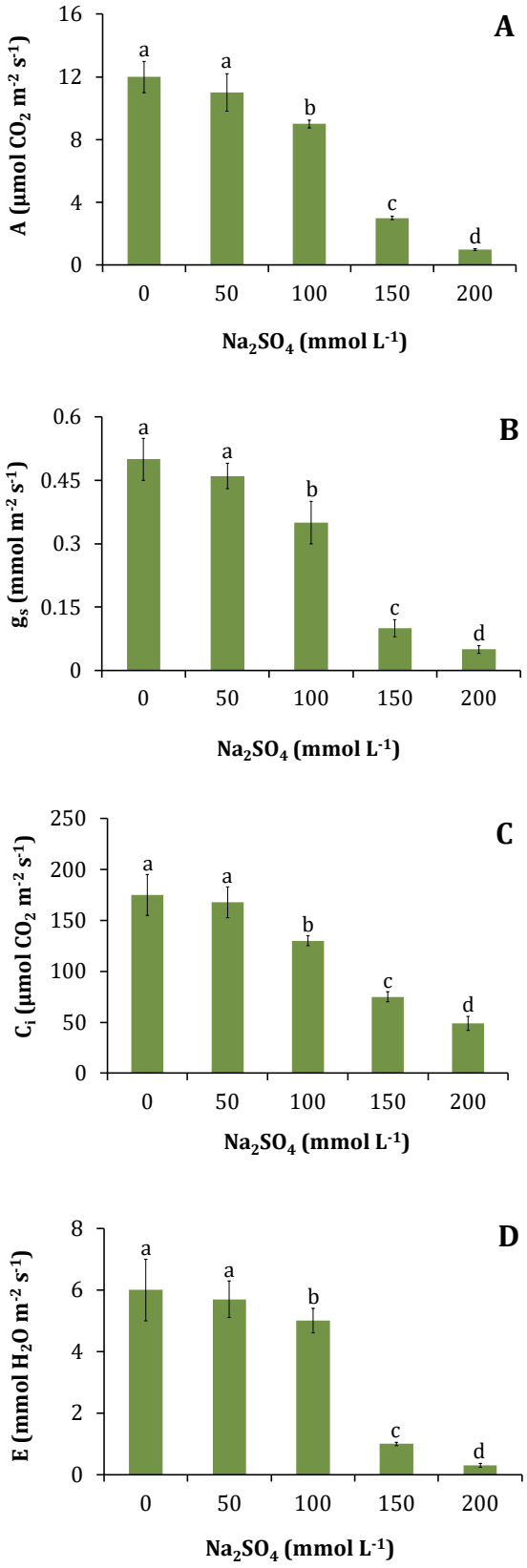
Sulfate is stored in the vacuoles of root and xylem parenchyma cells or transported via xylem to the aerial part (Takahashi *et al.*, 2011). Once in leaves, sulfate is again stored in vacuoles or reduced to sulfite in chloroplasts. Sulfite can be involved in cysteine synthesis in a reaction catalyzed by cysteine synthase. This mechanism incorporates sulfite into organic compounds, avoiding its inhibitory effect on mitochondrial respiration. Cysteine is a highly reactive thiol and helps maintain redox homeostasis in plants subjected to different abiotic stresses (39). Reginato *et al.* (2019) also reported increased foliar cysteine concentrations in *S. strobulifera* under Na_2SO_4 stress.

Salinity inhibited photosynthesis and stomatal conductance at 100 mmol L^{-1} Na_2SO_4 (figure 3A, B, page 7), causing internal CO_2 concentration (figure 3C, page 7) and transpiration (figure 3D, page 7) to decrease.

Photosynthesis can be inhibited by salinity due to stomatal and nonstomatal limitations. The latter include inhibition of Rubisco activity, decreased photosynthetic pigment concentration, and alterations at photochemical level (17). In the present case, salt stress simultaneously reduced net photosynthesis, stomatal conductance, and internal CO_2 concentration. Therefore, in this study, photosynthesis inhibition can be attributed to stomatal closure. In agreement with these results, in *Neltuma alba* the photochemical stage of photosynthesis was only inhibited by concentrations over 400 mM NaCl (20). In *S. strombulifera*, photosynthesis response to salt stress depends on the type of salt. Thus, whereas NaCl did not affect maximum quantum yield of photosystem II, Na_2SO_4 produced a significant reduction of this variable, indicating photoinhibition (29).

Concentrations over 50 mmol L^{-1} Na_2SO_4 produced a significant increase in foliar ABA (figure 4A, page 8). In the 200 mmol L^{-1} Na_2SO_4 treatment, ABA concentration was 100% higher than the control.

Phytohormones play a key role in plant physiological responses under stress conditions. In saline stress, ABA gains particular ecophysiological importance as it causes stomatal closure and reduces transpiration (35). Under water and salt stress, ABA works as a signal from the root to the aerial part, increasing water economy through stomatal closure and reduced leaf expansion (38). In *S. strombulifera*, Na_2SO_4 significantly increases foliar ABA concentrations (10), suggesting that ABA accumulation in leaves would be protective against dehydration.

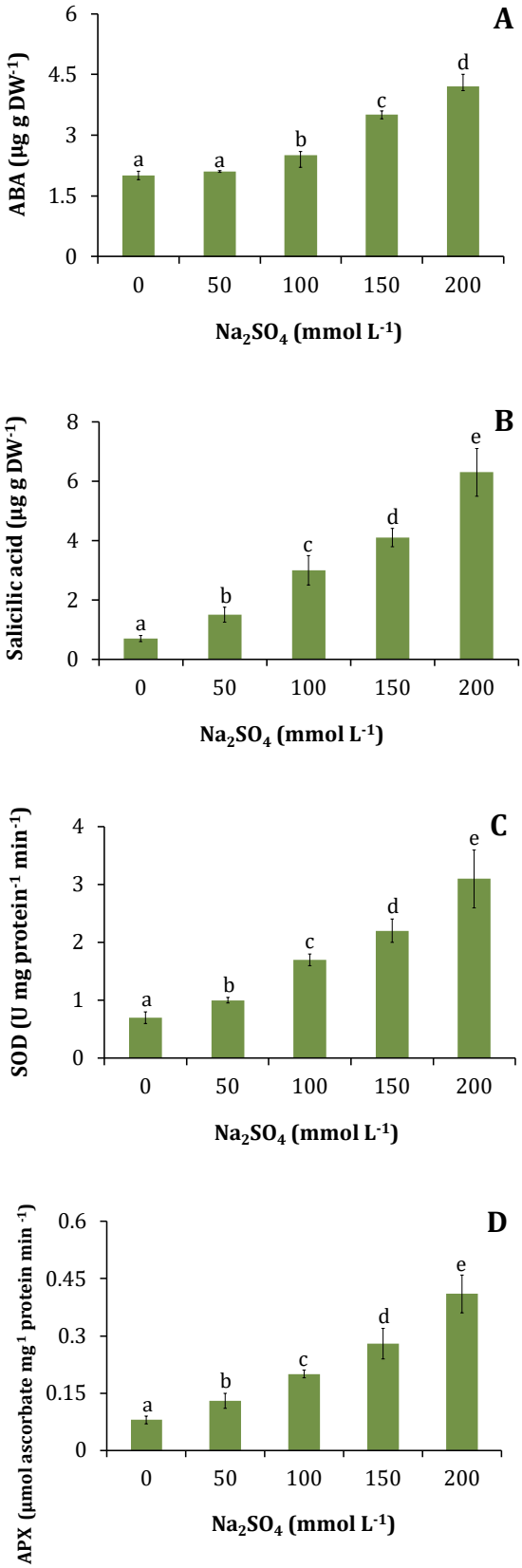


Vertical bars represent mean standard deviation (n=5). Different letters indicate significant differences according to the Tukey test at 5%.

Las barras verticales representan la desviación estándar de la media (n=5). Letras diferentes indican diferencias significativas según el test de Tukey al 5%.

Figure 3. Net photosynthesis (A), stomatal conductance (B), internal CO_2 concentration (C), and transpiration (D) in *N. ruscifolia* seedlings grown in increasing concentrations of Na_2SO_4.

Figura 3. Fotosíntesis neta (A), conductancia estomática (B), concentración interna de CO_2 (C) y transpiración (D) en plántulas de *N. ruscifolia* cultivadas en concentraciones crecientes de Na_2SO_4.



Vertical bars represent mean standard deviation (n=5). Different letters indicate significant differences according to the Tukey test at 5%.

Las barras verticales representan la desviación estándar de la media (n=5). Letras diferentes indican diferencias significativas según el test de Tukey al 5%.

Figure 4. Abscisic acid (A), salicylic acid (B), superoxide dismutase activity (C), and ascorbate peroxidase activity (D) in *N. ruscifolia* seedlings grown in increasing concentrations of Na_2SO_4.

Figura 4. Concentración de ácido abscísico (A), concentración de ácido salicílico (B), actividad superóxido dismutasa (C) y actividad peroxidasa (D) en plántulas de *N. ruscifolia* cultivadas en concentraciones crecientes de Na_2SO_4.

All salt concentrations significantly increased foliar SA concentrations (figure 4B, page 8). Discrepancies exist regarding the role of SA in regulating plant tolerance to salt stress. In *Vigna angularis* seedlings, SA mitigated the inhibitory effect of salt stress on photosynthesis and growth. This response was associated with increased tissue antioxidant activity (2). In contrast, SA was not involved in NaCl tolerance of the halophytes *Lycium humile* and *S. strombulifera*, nor was it identified as a stress signal (10, 24).

It has been suggested that SA induce antioxidant enzymes or alter the expression of their genes (21). In agreement with that observation, all salt concentrations increased the activities of SOD and APX enzymes (figure 4 C, D, page 8). However, according to Miura *et al.* (2013), low SA concentrations improve antioxidant capacity, whereas high concentrations produce oxidative stress and cell death. In agreement with these results, the high tolerance of *N. ruscifolia* to NaCl was attributed in part to its high antioxidant capacity due to the activities of SOD and peroxidase enzymes and polyphenols (19). Reginato *et al.* (2021) also reported significant increases in SOD and APX activities in leaves of *S. strombulifera* seedlings subjected to salt stress with Na_2SO_4.

Conclusions

N. ruscifolia growth threshold is 200 mmol L^{-1} Na_2SO_4. Growth inhibition can be attributed to affected ionic homeostasis and inhibition of photosynthesis due to stomatal closure. Nevertheless, the species shows adaptive responses to this salt. Thus, stomatal closure associated with increased foliar ABA concentrations contributes to water economy. Cysteine synthesis reduces sulfate toxicity when absorbed by the roots. On the other hand, salt stress induces SA accumulation in leaves and increases antioxidant activity, preventing oxidative stress. These characteristics demonstrate the high potential of the species for afforestation schemes on sodic saline soils.

References

1. Aghajanzadeh, T. A.; Reich, M.; Hawkesford, M. J.; Burow, M. 2019. Sulfur metabolism in *Allium cepa* is hardly affected by chloride and sulfate salinity. Archives of Agronomy and Soil Science. 65: 45-95. https://doi.org/10.1080/03650340.2018.1540037
2. Ahanger, M. A.; Aziz, U.; Alsahli, A. A.; Alyemeni, M. N.; Ahmad, P. 2019. Influence of exogenous salicylic acid and nitric oxide on growth, photosynthesis, and ascorbate-glutathione cycle in salt-stressed *Vigna angularis.* Biomolecules. 26: 42. https://doi.org/10.3390/biom10010042
3. Ahmadizadeh, M.; Vispo, N. A.; Calapit-Palao, C. D. O.; Pangaan, I. D.; Viña, C. D.; Singh, R. K. 2016. Reproductive stage salinity tolerance in rice: a complex trait to phenotype. Indian Journal of Plant Physiology. 21: 528-536. https://doi.org/10.1007/s40502-016-0268-6
4. Barhoumi, Z. 2018. Physiological response of the facultative halophyte, *Aeluropus littoralis*, to different salt types and levels. Plant Biosystems. 153: 298-305. https://doi.org/10.1080/11263504.2018.1478901
5. Boletta, P.; Ravelo, A.; Planchuelo, A.; Grilli, M. 2006. Assessing deforestation in the Argentine Chaco. Forest Ecology and Management. 228: 108-114. https://doi.org/10.1016/j.foreco.2006.02.045
6. Bradford, M. M. 1976. A rapid and sensitive method for the quantitation of microgram quantities of protein utilizing the principle of protein-dye binding. Analytical Biochemistry. 72: 248-54. https://doi.org/10.1006/abio.1976.9999
7. Bravo, S. J.; Pece, M.; del Corro, F.; Ojeda Brozovich, F.; Lepiscopo, M. 2016. Anatomical changes in roots and hypocotyls of *Prosopis ruscifolia* (Fabaceae) seedlings exposed to saline stress. Revista de Biología Tropical. 64: 1007-1017.
8. Chrysargyris, A.; Xylia, P.; Botsaris, G.; Tzortzakis, N. 2017. Antioxidant and antibacterial activities, mineral and essential oil composition of spearmint (*Mentha spicata* L.) affected by the potassium levels. Industrial Crops and Products. 103: 202-212. https://doi.org/10.1016/j.indcrop.2017.04.010
9. Dalzotto, D.; Sharry, S.; Piñuel, L.; Boeri, P. (en prensa). Challenges in germination of *Neltuma caldenia* in semi-arid regions: optimization of germination protocols, influence of saline stress and seed quality. Revista de la Facultad de Ciencias Agrarias. Universidad Nacional de Cuyo. Mendoza. Argentina.

10. Devinar, G.; Llanes, A.; Masciarelli, O.; Luna, V. 2013. Different relative humidity conditions combined with chloride and sulfate salinity treatments modify abscisic acid and salicylic acid levels in the halophyte *Prosopis strombulifera*. Plant Growth Regulation. 70: 247-256. https:// doi.org//10.1007/s10725-013-9796-5
11. Durgbanshi, A.; Arbona, V.; Pozo, O.; Miersch, O.; Sancho, J. V.; Gómez-Cadenas, A. 2005. Simultaneous determination of multiple phytohormones in plant extracts by liquid chromatography-electrospray tandem mass spectrometry. Journal of Agricultural and Food Chemistry. 53: 8437-8442. https://doi.org/10.1021/jf050884b
12. Galizzi, F.; Angueira, C.; Prieto, D. 1999. Suelos de la planta piloto de drenaje del INTA, Santiago del Estero. Revista Quebracho. 7: 52-60.
13. Giannopolitis, N.; Ries, S. K. 1977. Superoxide dismutase. I. Occurrence in higher plants. Plant Physiology. 59: 309-314. https://doi.org/10.1104/pp.59.2.309
14. Giménez, A. M.; Moglia, J. G. 2003. Árboles del Chaco Argentino. Guía para el reconocimiento dendrológico. Editorial El Liberal. Argentina. 307p.
15. Irakoze, W.; Vanpee, B.; Rufyikiri, G.; Dailly, H.; Nijimbere, S.; Lutts, S. 2019. Comparative effects of chloride and sulfate salinities on two contrasting rice cultivars (*Oryza sativa* L.) at the seedling stage. Journal of Plant Nutrition. 42: 1-15. https://doi.org/10.1080/01904167.2019.1584222
16. Li, J.; Pu, L.; Han, M.; Zhu, M.; Zhang, R.; Xiang, Y. 2014. Soil salinization research in China: Advances and prospects. Journal of Geographical Science. 24: 943-960.
17. Meloni, D. A. 2017. Fisiología Vegetal: respuestas de especies leñosas al estrés salino. Editorial Universidad Nacional de Santiago del Estero, Argentina. 165 p.
18. Meloni, D. A.; Gulotta, M. R.; Martínez, C. A. 2008a. *Prosopis ruscifolia* Griseb. (vinal) tolera concentraciones salinas equivalentes al agua de mar y excluye iones tóxicos de la parte aérea. Revista Quebracho. 16: 32-40.
19. Meloni, D. A.; Gulotta, M. R.; Oliva Cano, M. A. 2008b. El estrés salino incrementa la actividad de enzimas antioxidantes y la concentración de polifenoles en vinal (*Prosopis ruscifolia* G.). Revista Quebracho. 15: 27-31.
20. Meloni, D. A.; Gulotta, M. R.; Silva, D. M.; Arraiza, M. P. 2019. Effects of salt stress on germination, seedling growth, osmotic adjustment, and chlorophyll fluorescence in *Prosopis alba* G. Revista de la Facultad de Ciencias Agrarias. Universidad Nacional de Cuyo. Mendoza. Argentina. 51(1): 69-78.
21. Miura, K.; Okamoto, H.; Okuma, E.; Shiba, H.; Kamada, H.; Hasegawa, P. M.; Murata, Y. 2013. SIZ1 deficiency causes reduced stomatal aperture and enhanced drought tolerance via controlling salicylic acid-induced accumulation of reactive oxygen species in Arabidopsis. Plant Journal. 73: 91-104. https://doi.org/10.1111/tpj.12014
22. Munns, R.; Gilliham, M. 2015. Salinity tolerance of crops-what is the cost? New Phytology. 208: 668-673. https://doi.org/10.1111/nph.13519
23. Nakano, Y.; Asada, K. 1981. Hydrogen peroxide is scavenged by ascorbate-specific peroxidase in spinach chloroplasts. Plant Cell Physiology. 22: 867-880. https://doi.org/10.1093/oxfordjournals.pcp.a076232
24. Palchetti, M. V.; Llanes, A.; Reginato, M.; Barboza, G.; Luna, V.; Cantero, J. J. 2020. Germination responses of *Lycium humile*, an extreme halophytic Solanaceae: understanding its distribution in saline mudflats of the southern Puna. Acta Botanica Brasilica. 34: 540-548. https://doi.org/10.1590/0102-33062020abb0034
25. Peterson, A.; Murphy, K. 2015. Tolerance of lowland quinoa cultivars to sodium chloride and sodium sulfate salinity. Crop Science. 55: 331-338. https://doi.org/10.2135/cropsci2014.04.0271
26. Piraino, S.; Roig, F. A. 2024. Landform heterogeneity drives multi-stemmed *Neltuma flexuosa* growth dynamics. Implication for the Central Monte Desert forest management. Revista de la Facultad de Ciencias Agrarias. Universidad Nacional de Cuyo. Mendoza. Argentina. 56(1): 26-34. DOI: https://doi.org/10.48162/rev.39.120
27. Reginato, M.; Sosa, L.; Llanes, A.; Hampp, E.; Vettorazzi, N.; Reinoso, H.; Luna, V. 2014. Growth responses and ion accumulation in the halophytic legume *Prosopis strombulifera* are determined by Na2SO4 and NaCl. Plant Biology. 16: 97-106. http://dx.doi.org/10.1111/plb.12001
28. Reginato, M.; Travaglia, C.; Reinoso, H.; Garello, F.; Luna, V. 2015. Anatomical modifications in the halophyte *Prosopis strombulifera* caused by salt mixture. Flora. 218: 75-85. https://doi.org/10.1016/j.flora.2015.11.008
29. Reginato, M.; Turcio, E. T.; Luna, V.; Papenbrock, J. 2019. Differential effects of NaCl and Na2SO4 on the halophyte *Prosopis strombulifera* are explained by different responses of photosynthesis and metabolism. Plant Physiology and Biochemistry. 11: 306-314. https://doi.org/10.1016/j.plaphy.2019.05.027
30. Reginato, M.; Cenzano, A. M.; Arslan, I.; Furlán, A.; Varela, C.; Cavallin, V.; Papenbrock, J.; Luna, V. 2021. Na2SO4 and NaCl salts differentially modulate the antioxidant systems in the highly stress tolerant halophyte *Prosopis strombulifera*. Plant Physiology and Biochemistry. 167: 748-762. https://doi.org/10.1016/j.plaphy.2021.09.003
31. Reich, M.; Aghajanzadeh, T.; Helm, J.; Parmar, M. J.; Hawkesford, S.; De Kok, L. J. 2017. Chloride and sulfate salinity differently affect biomass, mineral nutrient composition and expression of sulfate transport and assimilation genes in *Brassica rapa*. Plant and Soil. 411: 319-32. https://doi.org/10.1007/s11104-016-3026-7

32. Reich, M.; Aghajanzadeh, T.; Parmar, S.; Hawkesford, M. J.; De Kok, L. J. 2018. Calcium ameliorates the toxicity of sulfate salinity in *Brassica rapa*. Journal of Plant Physiology. 231: 1-8. https://doi.org/10.1016/j.jplph.2018.08.014
33. Riemenschneider, A.; Nikiforova, V.; Hoefgen, R. De Kok, L. J.; Papenbrock, J. 2005. Impact of elevated H2S on metabolite levels, activity of enzymes and expression of genes involved in cysteine metabolism. Plant Physiology and Biochemistry. 43: 473-483. https://doi.org/10.1016/j.plaphy.2005.04.001
34. Sigrist, M. R.; Stefanello, T. H.; de Souza, C. S.; Vargas, W.; Almeida, K. S. M.; Laroca, S.; Mansano, V. F. 2018. Phenology and pollination ecology of *Prosopis rubriflora* (Leguminosae, Mimosoideae), a species from the semi-arid Brazilian Chaco. Brazilian Journal of Botany. 41: 103-115. https://doi.org/10.1007/s40415-017-0433-9
35. Singh, V. P.; Prasad, S. M.; Bosch, S. M.; Müller, M. 2017. Phytohormones and the regulation of stress tolerance in plants: current status and future directions. Frontiers in Plant Science. 8: 1871. https://doi.org/10.3389/fpls.2017.01871
36. Takahashi, H.; Kopriva, S.; Giordano, M.; Saito, H.; Hell, R. 2011. Sulfur assimilation in photosynthetic organisms: molecular functions and regulations of transporters and assimilatory enzymes. Annual Review of Plant Biology. 62: 157-184. https://doi.org/10.1146/annurev-arplant-042110-103921
37. van Zelm, E.; Zhang, Y.; Testerink, C. 2020. Salt tolerance mechanisms of plants. Annual Review of Plant Biology. 71:403-433. https://doi.org/10.1146/annurev-arplant-050718-100005
38. Wilkinson, S.; Kudoyarova, G. R.; Veselov, D. S.; Arkhipova, T. N.; Davies, W. J. 2012. Plant hormone interactions: innovative targets for crop breeding and management. Journal of Experimental Botany. 63: 3499-3509. https://doi.org/10.1093/jxb/ers148
39. Zagorchev, L.; Seal, C. E.; Kranner, I.; Odjakova, M. A. 2013. Central role for thiols in plant tolerance to abiotic stress. International Journal of Molecular Science. 14:7405-7432. https://doi.org/10.3390/ijms14047405

Acknowledgments

The authors thank the Consejo de Investigaciones Científicas y Tecnológicas de la Universidad Nacional de Santiago del Estero (CICyT-UNSE) for funding.

Calcium Chloride as a Regulator of Floral Stem Bending in Cut-Flower Gerbera (*Gerbera jamesonii* L.)

Cloruro de calcio como regulador de la curvatura del tallo floral en gerberas de corte (*Gerbera jamesonii* L.)

Analia Verónica Puerta [1], Carlos Alberto Bouzo [2], Gunther Mantilla [1*]

Originales: *Recepción:* 16/07/2025 - *Aceptación:* 09/04/2026

ABSTRACT

Gerbera is an ornamental plant with vibrant and striking colours. However, postharvest stem bending reduces commercial quality and limits vase life by impairing water uptake. Calcium plays a key role in regulating and strengthening the stem structure, thereby reducing curvature and preserving tissue integrity. This study evaluated the effects of calcium chloride ($CaCl_2$) on histochemical, metabolic and structural traits associated with vase life quality in *Gerbera jamesonii* L. *cv.* 'Ruby Red'. Plants were cultivated under greenhouse conditions in a soilless system, and two vase solutions were applied postharvest: 0 and 0.5 g L^{-1} $CaCl_2$. Measurements were conducted over 17 days in a postharvest room. The 0.5 g L^{-1} $CaCl_2$ treatment significantly enhanced postharvest quality by extending vase life by 7 days, preserving stem length, increasing tissue calcium content, and promoting favourable histochemical and structural attributes. The findings contribute to the understanding of flower stem physiology and offer an effective strategy to enhance postharvest quality in gerbera.

Keywords
cut flower • postharvest quality • stem turgor loss • water uptake • vase life

https://doi.org/10.48162/rev.39.216

1 Instituto de Floricultura. Centro de Investigación en Recursos Naturales (INTA). De los Reseros y Nicolas Repetto. Hurlingham. Argentina. * mantilla.gunther@inta.gob.ar
2 Universidad Nacional del Litoral. Facultad de Ciencias Agrarias. Cátedra de Fisiología Vegetal. Santa Fe. Argentina.

Licenses Creative Commons
Attribution - Non Commercial - Share Alike

Resumen

La gerbera es una planta ornamental con colores vibrantes y llamativos. Sin embargo, la curvatura del tallo poscosecha reduce la calidad comercial y limita la vida en florero al afectar la absorción de agua. En este sentido, el calcio ayuda a regular y fortalecer la estructura del tallo, reduciendo su curvatura y protegiendo la integridad estructural del tejido. Este estudio evaluó los efectos del cloruro de calcio ($CaCl_2$) en los caracteres histoquímicos, metabólicos y estructurales asociados con la calidad de vida en florero en *Gerbera jamesonii* L. *cv.* 'Ruby Red'. Las plantas se cultivaron en condiciones de invernadero en un sistema sin suelo, y se aplicaron dos soluciones de florero poscosecha: 0 y 0,5 g L^{-1} $CaCl_2$. Las mediciones se realizaron durante 17 días en una cámara de poscosecha. El tratamiento con 0,5 g L^{-1} $CaCl_2$ mejoró significativamente la calidad poscosecha al extender la vida en florero en 7 días, preservar la longitud del tallo, aumentar el contenido de calcio en el tejido y promover atributos histoquímicos y estructurales favorables. Los hallazgos contribuyen a la comprensión de la fisiología del tallo floral y ofrecen una estrategia eficaz para mejorar la calidad poscosecha de la gerbera.

Palabras clave

flor de corte • calidad poscosecha • pérdida de turgencia del tallo • consumo de agua • vida en florero

Introduction

Gerbera is a genus of perennial ornamental plants widely cultivated for cut flower production. However, its postharvest longevity is compromised by premature stem bending, a critical quality disorder that affects its commercial acceptance (Alikhani *et al.*, 2021). Stem bending in gerbera is primarily associated with water imbalance, insufficient mechanical strength, and degradation of cell wall components of the stem during vase life (Manzoor *et al.*, 2024).

The maintenance of stem rigidity is closely related to the integrity of cell walls and middle lamella, where calcium (Ca^{2+}) plays a fundamental role by forming cross-links with pectins, enhancing tissue firmness and preventing cell disintegration (Wdowiak *et al.*, 2024). In addition, calcium participates in signaling pathways regulating senescence and stress responses, thereby contributing to postharvest stability (Ge *et al.*, 2019).

Postharvest treatments based on calcium supplementation have been widely studied as a strategy to improve stem strength and extend vase life in cut flowers. Cheng *et al.* (2020) demonstrated that calcium delays structural degradation and reduces membrane permeability. Similarly, García-González *et al.* (2022) reported an increase in mechanical resistance and stem firmness in gerbera when calcium was supplied in vase solutions. Mohammadi *et al.* (2024) also confirmed the effectiveness of Ca^{2+} treatments in reducing bending incidence and preserving cytological integrity. Milani *et al.* (2019) observed that calcium application improved the mechanical properties of cell walls, contributing to higher postharvest longevity in gerbera flowers. The study aimed to evaluate the effects of $CaCl_2$ and its relationship with histochemical, metabolic, and structural traits associated with vase life quality in cut flowers *Gerbera jamesonii* L. *cv.* 'Ruby Red'.

Materials and Methods

Experimental Design and Treatment Application

The experiment was conducted using *G. jamesonii cv.* 'Ruby Red' plants grown in a greenhouse during the summer. Seedlings were purchased from Florist Holland and transplanted individually in December into 12-L black polyethylene pots containing a soilless substrate composed of *Sphagnum* peat moss and perlite (3:2, v/v). A drip fertigation system with a flow rate of 2 L h^{-1} was used, with one emitter installed per pot.

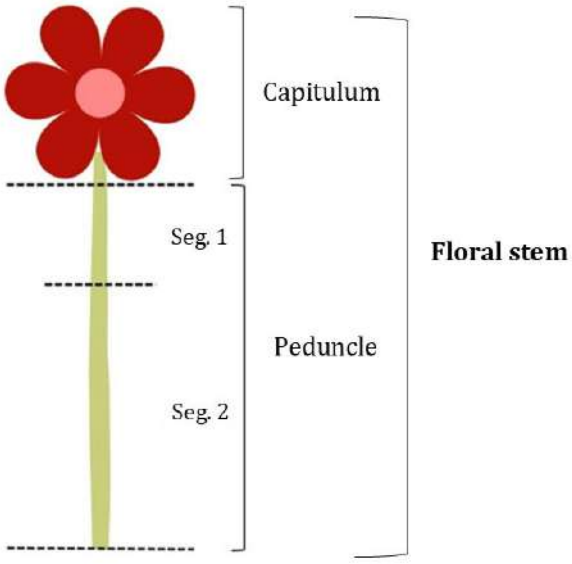
Harvesting was carried out at the same floral developmental stage -when 1-3 rows of male florets were visible- to ensure uniform maturity across harvest times. The floral stems were cut diagonally to a length of 35 cm from the base of the floral head. Then weighed and placed in 250 mL Erlenmeyer flasks, each containing 200 mL of the designated treatment solution. The flasks were sealed with plastic film to reduce evaporation. Two treatments were applied: distilled water (control, T1) and an aqueous solution of $CaCl_2$ at 0.5 g L^{-1} (T2). Postharvest settings were maintained at 20 ± 2°C, 65% relative humidity, and a 12-hour photoperiod using white fluorescent lamps (900 lux). The calcium chloride and water solutions were maintained throughout the vase life, without replacement. Ten flower stems were used for each treatment. Therefore, 30 stems were evaluated for each treatment, and the experimental unit was the vase.

Measurements were performed at two time points: at the beginning (Initial) and at the end (Final) of the postharvest period. Day 0 corresponded to the day of harvest and placement of the stems in the vase solution. The endpoint was defined as the termination of vase life, characterized by visual signs of loss in commercial quality (Mohsin *et al.*, 2023), including visible symptoms and reduced visual appeal compromising the commercial acceptance of the product, such as curvature of the floral stem, wilting of the inflorescences, signs of dehydration, and the fall of the first ray florets. The end-of-life date was recorded when at least 50% of the flowers showed senescence symptoms, indicating unsuitability for marketing or ornamental use.

To compare the evolution of parameters during vase life, a Daily Variation Rate (DVR) was calculated for each measurement. The coefficient was derived from the mean values at the initial and final time points, divided by the mean vase life of each treatment according to the formula:

DVR = (Final mean value - Initial mean value) / Mean vase life

A positive DVR indicates an increase in the variable over time, while a negative DVR denotes a reduction relative to the initial value. The control treatment (stems held in distilled water without calcium supplementation) was subjected to the same sampling procedures and DVR calculation to provide a baseline for comparison. Measurements were conducted on the capitulum and along two segments of the floral stem: segment 1 (0-15 cm below the capitulum) and segment 2 (15-35 cm) (figure 1).



Capitulum, Segment 1 (Seg. 1) and 2 (Seg. 2) of the peduncle.

Capítulo, Segmento 1 (Seg. 1) y 2 (Seg. 2) del pedúnculo.

Figure. 1. Parts of the floral stem.

Figura. 1. Partes del tallo floral.

Study of Vase Life and Quality of Flowers

Vase life was considered terminated when the floral stem exhibited noticeable deterioration, including peduncle bending or ligule wilting, or abscission (Mohsin *et al.*, 2023). Bending severity was assessed using a three-grade scale: Grade I (0°-45°), Grade II (45°-90°), and Grade III (>90°), following the scale adapted from Celikel & Reid (2002) for cut flowers.

Calcium content in the capitulum and segments 1 and 2 was determined according to Bárbaro *et al.* (2024). Stem length was recorded again at the end of the vase life period. Individual floral stem weight and water uptake were determined using a digital scale (Ohaus SP402, USA). Water consumption was calculated by weighing the flasks with and without the floral stem at both time points and pH and electrical conductivity in the solution vase were determined using a digital conductivity meter (Orion Thermo Scientific, 145, USA) and pH meter (Horiba, M-12, Japan). Soluble sugar concentrations were analysed in 10 stems per treatment, assessing the entire floral stem. Samples were preserved in liquid nitrogen, ground, and centrifuged at 6500 rpm for 5 minutes at 4°C (Thermo Scientific Heraeus Primo R, France). The supernatant was filtered for analysis. Sucrose, D-glucose, and D-fructose contents were quantified using UV-spectrophotometry with enzymatic BioAnalysis kits (Boehringer Mannheim/R-Biopharm, Darmstadt, Germany). Absorbance was measured at 340 nm (Perkin Elmer, USA).

Anatomical characteristics of peduncle segments 1 and 2 were examined using transverse sections. Ten peduncle samples per treatment were randomly selected from flowers exhibiting the average curvature response of each treatment, ensuring that the analysed tissues were representative of the overall postharvest condition. Samples were fixed in FAA solution (formaldehyde, alcohol, acetic acid) for 48 hours, stored in 70% ethanol, and dehydrated through an ethanol series. Cross-sections (8-10 µm thick) were stained with safranin-fast green and mounted in Canada balsam. Observations were made using a fluorescent microscope (Olympus BX50, Japan) at 4× magnification, and images were captured with CellSens Standard Imaging Software.

Additionally, the peduncle surface area and cell sections from segment 1 (curvature zone) were analysed at the beginning and end of the experiment using a stereoscopic magnifying glass (Olympus SZX9, 25×). Images of representative samples were processed with CellSens Standard Imaging Software. The total peduncle area, pith area, and cellular tissue area (μm^2) were measured using the "2-point circle" and "rotated ellipse" tools. The proportions of cellular tissue and pith relative to the total peduncle area were calculated according to the formula:

Tissue proportion= Mean tissue area (μm^2) /Total area (μm^2)

Pith proportion = Mean pith area (μm^2) /Total area (μm^2).

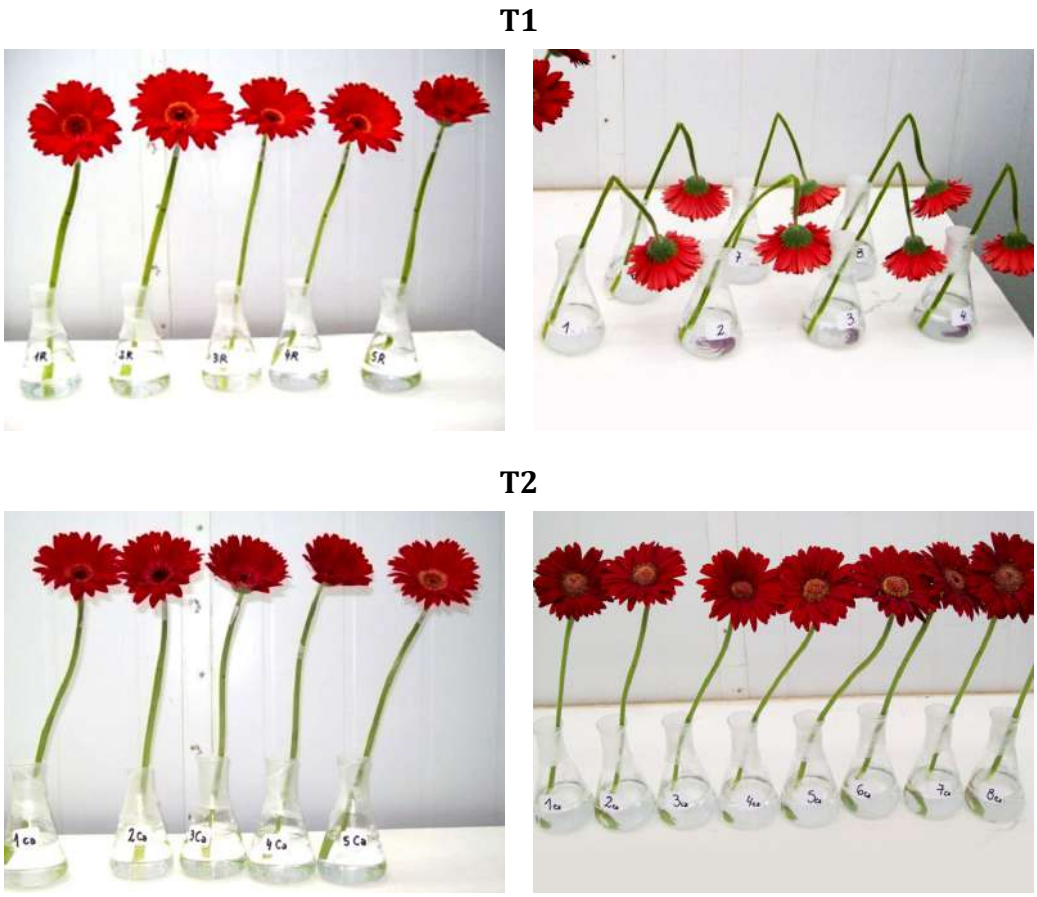
Statistical Analysis

The experimental design was completely randomized with three replicates per treatment, using 10 floral stems per treatment [T1, control: floral stems kept in distilled water, T2: floral stems kept in aqueous solution of $CaCl_2$, at 0.5 g L^{-1}]. Measurements were subjected to analysis of variance (ANOVA), and when differences between means were detected, they were compared using Tukey's test at a 95% significance level (Di Rienzo *et al.*, 2020).

Results and Discussion

Floral stems maintained in distilled water (T1) exhibited peduncle bending, whereas stems placed in the calcium solution (T2) remained upright throughout the evaluation period. The incorporation of calcium into the vase solution effectively prevented bending and extended vase life by 7 days. In T1, peduncle bending defined the end of vase life, occurring 10 days after harvest. The degree of curvature in treatment was highly pronounced, exceeding 120°. Floral stems in water showed a degree III curvature (126.25°), making them

unsuitable for commercialization as cut flowers. In contrast, in T2, the curvature changed by less than 1° from the initial measurement (5.50°) (degree I), thereby maintaining their commercial quality. The vase life was 17 days, and its end was due to flower opening and the subsequent ligule drop (figure 2).



T1 (floral stems kept in distilled water) and T2 (floral stems kept in $CaCl_2$ solution), at the Initial (left) and Final (right) of the experiment, 17 days after harvest, in *G. jamesonii cv.* 'Ruby red'.

T1 (tallos florales mantenidos en agua destilada) y T2 (tallos florales mantenidos en solución de $CaCl_2$), al inicio (izquierda) y al final (derecha) del experimento, 17 días después de la cosecha, en *G. jamesonii cv.* 'Ruby red'.

Figure 2. Effect of vase solution on stem curvature degree and floral opening.
Figura 2. Efecto de la solución de florero sobre el grado de curvatura del tallo y apertura floral.

The floral stems kept in the calcium solution showed no peduncle bending at any point during their postharvest life and exhibited an increase in calcium content in their tissues, including the capitulum and segments 1 and 2 (figure 2; table 1, page 6). The effect of calcium was also evident in the length of the floral stem, as the stems maintained in the calcium solution retained their length during vase life (35.48 cm). In contrast, stems maintained in water showed a significant increase in length (40.33 cm), particularly in the distal portion, which coincided with the bending zone. Furthermore, the daily variation rate (DVR) of length was significantly higher, 0.4 cm d^{-1}. While in the stem kept in calcium, it was 0.03 cm. d^{-1}.

Table 1. Calcium content in the capitulum and in segments 1 and 2 of the floral stem at the beginning of the experiment (initial Ca content) and daily variation rate of calcium content (DVR Ca) in stems kept in water (control) and $CaCl_2$ solution (0.5 g L^{-1}) during the postharvest experiment of *G. jamesonii cv.* 'Ruby red'.

Tabla 1. Contenido de calcio en el capítulo y en los segmentos 1 y 2 del tallo floral al inicio del experimento (contenido inicial de Ca) y tasa de variación diaria del contenido de calcio (DVR Ca) en tallos mantenidos en agua (control) y en solución de $CaCl_2$ (0,5 gL^{-1}) durante el experimento de poscosecha de *G. jamesonii cv.* 'Ruby red'.

Lowercase letters indicate statistically significant values in columns (p<0.05).

Letras minúsculas en columnas indican valores estadísticamente diferentes (p<0,05).

Treatments	Initial Ca content (meq L^{-1})			DVR Ca (meq L^{-1} d^{-1})		
	Capitulum	Segment 1	Segment 2	Capitulum	Segment 1	Segment 2
Water	0.244 a	0.197 a	0.250 a	0.001 a	0.004 a	0.004 a
$CaCl_2$ solution	0.213 a	0.189 a	0.239 a	0.331 b	0.143 b	0.081 b

The results obtained support the idea that calcium plays a relevant role in preserving stem architecture by acting as a structural modulator at the cellular level (Alikhani *et al.*, 2021, Cheng *et al.*, 2020). Furthermore, a functional interaction between calcium and auxin can be hypothesized, in which the Ca^{2+} may influence hormonal signalling pathways, potentially attenuating the gravitational response and contributing to stem postural stability (Hartmann *et al.*, 2021).

Additionally, the floral stems kept in water (T1) exhibited a higher water uptake and a higher rate of fresh weight loss (table 2). Since evaporation was controlled by sealing the tops of the vases, the observed weight loss is primarily attributed to transpiration. The results indicate a higher transpiration rate (T1), suggesting a greater metabolic rate compared to T2.

Table 2. Vase solution uptake, daily variation rate (DVR) of vase solution uptake, initial fresh weight in the entire floral stem (FW) and DVR of FW in stems kept in water (control) and $CaCl_2$ solution (0.5 g L^{-1}) during the postharvest experiment of *G. jamesonii cv.* 'Ruby red'.

Tabla 2. Absorción de la solución de florero, tasa de variación diaria (TDR) de la absorción de la solución de florero, peso fresco inicial del tallo floral (PF) y TDR de PF en tallos mantenidos en agua (control) y en solución de $CaCl_2$ (0,5 gL^{-1}) durante el experimento de poscosecha de *G. jamesonii cv.* 'Ruby red'.

Lowercase letters indicate statistically significant values in columns (p<0.05).

Letras minúsculas en columnas son estadísticamente diferentes (p<0,05).

Treatments	Solution uptake (mL)	DVR - Solution (mL d^{-1})	Initial FW (g)	DVR-FW (mL d^{-1})
Water	45.30 a	4.50 a	20.95 a	-0.35 a
$CaCl_2$ solution	41.20 a	2.42 b	21.04 a	-0.21 b

Several studies have indicated calcium deficiency can cause loss of firmness in stems and leaves, negatively affecting the structural rigidity of tissues (Park *et al.*, 2022). The incorporation of calcium in postharvest treatments has shown positive effects by reinforcing cellular structure and reducing the incidence of curvature and other disorders related to mechanical integrity loss (Tonooka *et al.*, 2023). Such effects arise from the stabilizing role of calcium, which strengthens both the cell wall and the plasma membrane by interacting with pectin in the cell wall (Xia *et al.*, 2025), thereby increasing rigidity and helping maintain tissue shape (Parvin *et al.*, 2019).

Thus, an increase in fresh mass is a clear indicator of greater water retention capacity, higher turgidity, and reduced stem bending. A lower daily water loss and a lower transpiration rate in the T2 (table 2, page 6).

The main route of water loss in cut flowers occurs through stomata. In Gerbera sp. flowers, stomata are distributed on different parts of the flower (Huang *et al.*, 2018). An increase in cytosolic free calcium promotes the efflux of K^+ and anions, leading to a marked decrease in osmotic potential and a consequent loss of guard cell turgidity, ultimately resulting in stomatal closure (Gupta *et al.,* 2023). This effect, produced by endogenous calcium, can be replicated by exogenous supply, such as the application of $CaCl_2$ provided by $CaCl_2$ (Ciriello *et al.*, 2024). Thus, results could explain the lower weight loss observed in gerbera in the T2 treatment (table 2, page 6), prolonging vase life by reducing the incidence of stem bending (Timalsina *et al.*, 2023). Park and Kim (2022) reported that pre-harvest spraying with $CaCl_2$ in Gerbera 'Harmony' increased stem hardness, internal calcium content, and cellular pectin levels, improving the tissue's ability to resist water loss.

The effect of calcium was also evident in postharvest sugar metabolism, showing a positive relationship with the physiological performance of stems during vase life. At the beginning of the experiment, sugar concentrations in the floral stems did not differ significantly between treatments. However, throughout the vase life period, a progressive decline in sugar levels was observed in both treatments; this reduction was more pronounced in the control (T1) compared with the calcium-treated stems (T2) (table 3).

Table 3. Sugar content expressed on a fresh weight (FW) in the entire floral stem at the beginning of the experiment (initial sugar content) and daily variation rate of sugar content (DVR sugar content) in stems kept in water (control) and $CaCl_2$ solution (0.5 g L^{-1}) during the postharvest experiment of *G. jamesonii* cv. 'Ruby red'.

Tabla 3. Contenido de azúcar expresado en peso fresco (PF) en el tallo floral al inicio del experimento (contenido inicial de azúcar) y tasa de variación diaria del contenido de azúcar (contenido de azúcar DVR) en tallos mantenidos en agua (control) y en solución de $CaCl_2$ (0,5 gL^{-1}) durante el experimento de poscosecha de *G. jamesonii* cv. 'Ruby red'.

Treatments	Initial sugar content (mg g^{-1} FW)			DVR sugar content (mg g^{-1} FW d^{-1})		
	Sacarose	Glucose	Fructose	Sacarose	Glucose	Fructose
Water	8.86 a	8.24 a	1.11 a	0.28 a	-0.47 a	-0.99 a
$CaCl_2$ solution	8.94 a	8.06 a	1.34 a	0.10 b	-0.20 b	-0.60 b

Lowercase letters indicate statistically significant values in columns ($p<0.05$).

Letras minúsculas en columnas son estadísticamente diferentes ($p<0,05$).

The difference suggests that stems in T1 consumed their available sugars more rapidly, likely to meet energy demands and sustain postharvest stress responses, which may have accelerated senescence. In contrast, stems in T2 exhibited a slower rate of sugar depletion, indicating greater metabolic stability and reduced tissue collapse.

The observed correlation between sugar content and stem bending can be attributed to the dual role of carbohydrates in plant metabolism. Besides serving as energy substrates, they act as osmotic regulators, maintaining cellular water balance and turgor (Borghi & Fernie, 2017).

Furthermore, variations in carbohydrate content during vase life have been reported to result from a redistribution among different sugar types. Thus, a decline in certain sugar forms may be accompanied by an increase in others, reflecting active transport and metabolic conversion processes within stem tissues (Kim and Oh, 2021). Previous studies have also suggested an accumulation of certain low-molecular-weight polysaccharides in the bending zone of cut gerbera stems during vase life, potentially contributing to structural and functional alterations associated with peduncle curvature (Cheng *et al.*, 2020; Ali and Asal, 2023).

Previous studies have shown that the presence of carbohydrates can extend vase life (Seyed Hajizadeh *et al.*, 2024, Verdonk *et al.*, 2023), since they play a key role in plant metabolism (Perik *et al.*, 2012), giving rigidity and firmness to the stems without weight loss, as T1 where low tissue resistance was evident (Tang *et al.*, 2023) and a decrease in sugars.

The results of the morphochemical determinations presented here are consistent with the histological characterization and help explain the effect of using the calcium solution in the postharvest process (figure 3, and figure 4, page 9). Histological sectioning revealed possible changes in the anatomical structure of the stem floral in T1 and T2 during the postharvest life.

Figure 3 shows the histological characteristics of T1 (floral stems kept in water) and T2 (floral stems kept in calcium solution) at the beginning of the experiment. In both treatments, an unilayered epidermis and a cortex composed of parenchymal cells with collateral vascular bundles of various sizes were observed. The vascular bundles were surrounded by sclerenchyma caps at the phloem and xylem poles, while in the sclerification stage, forming a continuous ring of sclerified cells. The sclerenchyma cells are arranged in caps (Crang *et al.*, 2018) and have thicker walls than collenchyma. They are separated by parenchyma cells and contain small intercellular spaces.

ace: ring of sclerified cells, ce: sclerenchyma cap, cx: cortex, ep: epidermis, fl: phloem, hvch: small vascular bundle, hvg: large vascular bundle, hvm: medium vascular bundle, m: medulla, pm: medullary parenchyma, ri: interfascicular region, xil: xylem, pca: flattened cortical parenchyma, pma: flattened medullary parenchyma, pxila: flattened xylem parenchyma, xil: xylem.

ace: anillo de células esclerificadas, ce: casquete esclerenquimático, cx: corteza, ep: epidermis, fl: floema, hvch: haz vascular pequeño, hvg: haz vascular grande, hvm: haz vascular mediano, m: médula, pm: parénquima medular, ri: región interfascicular, xil: xilema, pca: parénquima cortical aplanado, pma: parénquima medular aplanado, pxila: parénquima xilemático aplanado, xil: xilema.

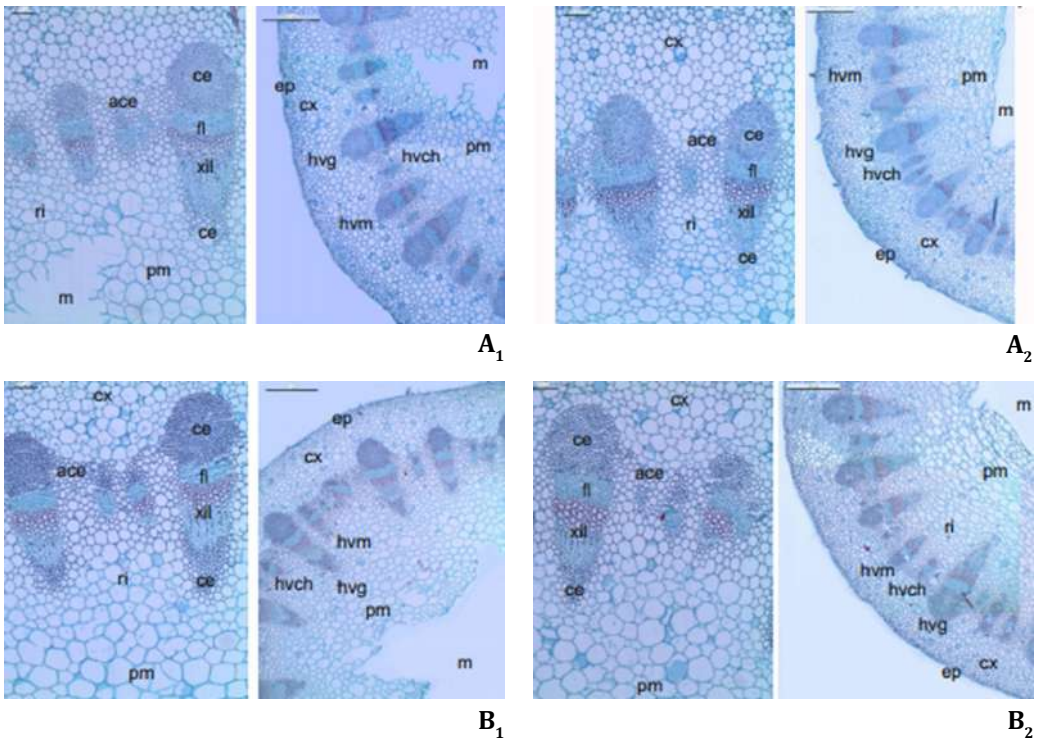


Figure 3. Histological section of the floral stem of T1 (floral stems kept in water) and T2 (floral stems kept in $CaCl_2$ solution), at the beginning of the postharvest experiment, showing the distal region or segment 1 (A1 and A2) and the basal region or segment 2 (B1 and B2) in *G. jamesonii cv.* 'Ruby red'.

Figura 3. Corte histológico del tallo floral de T1 (tallos florales mantenidos en agua) y T2 (tallos florales mantenidos en solución de $CaCl_2$), al inicio del experimento poscosecha, mostrando la región distal o segmento 1 (A1 y A2) y la región basal o segmento 2 (B1 y B2) en G. jamesonii *cv.* 'Ruby red'.

ace: ring of sclerified cells, ce: sclerenchyma cap, cx: cortex, ep: epidermis, fl: phloem, hvch: small vascular bundle, hvg: large vascular bundle, hvm: medium vascular bundle, m: medulla, pm: medullary parenchyma, ri: interfascicular region, xil: xylem, pca: flattened cortical parenchyma, pma: flattened medullary parenchyma, pxila: flattened xylem parenchyma, xil: xylem.

ace: anillo de células esclerificadas, ce: casquete esclerenquimático, cx: corteza, ep: epidermis, fl: floema, hvch: haz vascular pequeño, hvg: haz vascular grande, hvm: haz vascular mediano, m: médula, pm: parénquima medular, ri: región interfascicular, xil: xilema, pca: parénquima cortical aplanado, pma: parénquima medular aplanado, pxila: parénquima xilemático aplanado, xil: xilema.

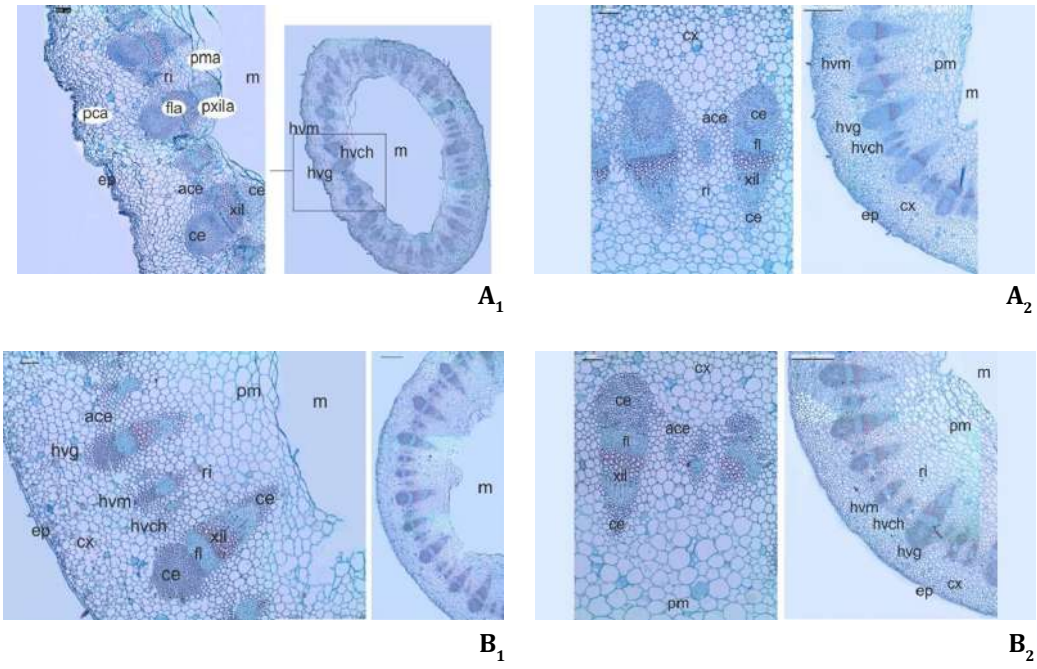


Figure 4. Histological section of the floral stem of T1 (floral stems kept in water) and T2 (floral stems kept in $CaCl_2$ solution) at the end of the postharvest experiment, showing the distal region or segment 1 (A1, A2) and the basal region or segment 2 (B1, B2) in *G. jamesonii cv.* 'Ruby red'.

Figura 4. Corte histológico del tallo floral de T1 (tallos florales mantenidos en agua) y T2 (tallos florales mantenidos en solución de $CaCl_2$) al final del experimento poscosecha, mostrando la región distal o segmento 1 (A1, A2) y la región basal o segmento 2 (B1, B2) en *G. jamesonii cv.* 'Ruby red'.

The differentiation of tissues forming the vascular bundles, starting with the sclerenchyma in the adaxial region, allowed for the visualization of thicker walls in all tissues, and their cells in longitudinal view appeared ellipsoidal. The study showed uniformity in histology between segments 1 and 2. However, there are significant differences in the organization and arrangement of the cortex, as well as the shapes and sizes of cells between the tissues at the end of the vase life experiment (figure 4).

Although cell disintegration at the end of the vase life occurred in both treatments, the process was more pronounced in segment 1 of the T1 treatment, which also showed a lower degree of sclerenchymatization (figure 4, and figure 5, page 10).

The pith cavity in T1 was significantly larger than T2. Measurements of pith and tissue proportion in segment 1, taken at the beginning and end of the postharvest experiment, revealed a marked increase in pith proportion in T1 during vase life, accompanied by a significant reduction in tissue proportion (figure 6, page 10; table 4, page 11). Additionally, the increase in medulla size may be associated with the disintegration of cells near it (Wang *et al*., 2023), which could explain the bending observed in the stems.

The calcium-treated stems showed less expansion of the medullary cavity and a smaller reduction in cellular tissue compared with stems kept in water (figure 4, page 11, figure 6, page 10 and table 4, page 11). The evidence suggests that calcium contributes to reduced cell disintegration and increased stem firmness, thereby preventing bending. A higher proportion of supporting tissue and lignin in the mid-stem is associated with reduced stem curvature (Abd-Elkader *et al.*, 2020; Lear *et al.*, 2022). Overall, the pattern reinforces the idea that calcium enhances stem strength by increasing lignin content and promoting its association with pectin in the cell wall (Balk *et al.*, 2023).

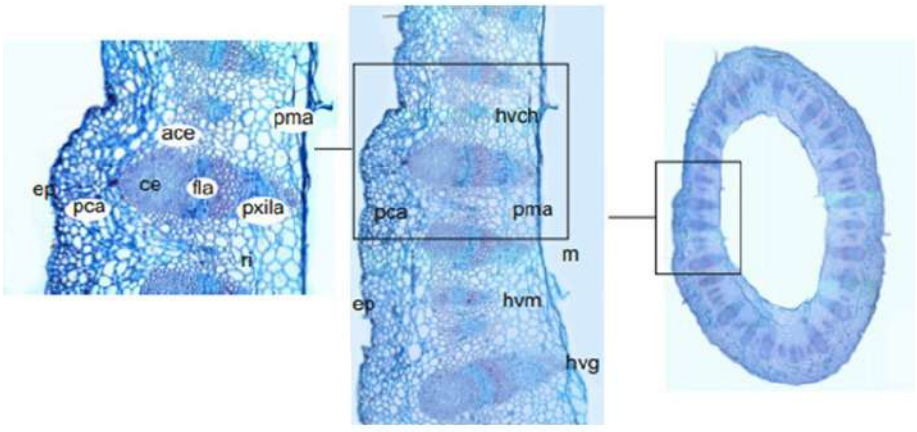


Figure 5. Histological section of the floral stem of T1 (floral stems kept in water) at the end of the postharvest experiment, showing cellular disintegration in the bending zone (segment 1) in *G. jamesonii* cv. 'Ruby red'.

Figura 5. Corte histológico del tallo floral de T1 (tallos florales mantenidos en agua) al final del experimento poscosecha, mostrando desintegración celular en la zona de flexión (segmento 1) en *G. jamesonii* cv. 'Ruby red'.

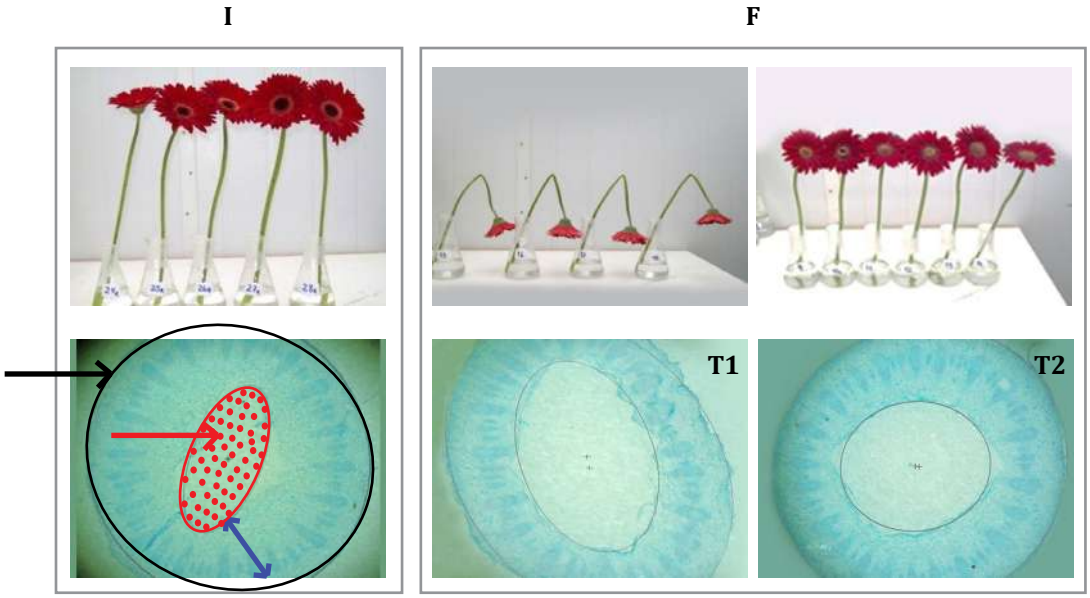


Figure 6. Histological section of segment 1 of floral stems and measurement of total area (black arrow), pith area (red arrow), and Tissue area (blue arrow) in T1 (floral stems kept in water) and T2 (floral stems kept in $CaCl_2$ solution) at Initial (I) and Final (F) of the postharvest experiment in *G. jamesonii* cv. 'Ruby red'.

Figura 6. Corte histológico del segmento 1 de tallos florales y medición del área total (flecha negra), área de médula (flecha roja) y área de tejido (flecha azul) en T1 (tallos florales mantenidos en agua) y T2 (tallos florales mantenidos en solución de CaCl2) al inicio (I) y al final (F) del experimento poscosecha en *G. jamesonii* cv. 'Ruby red'.

Table 4. Relative proportion of tissue (tissue) and relative proportion of pith (pith) in segment 1 of the floral stem at the beginning (Initial) and end (Final) of the postharvest experiment in stems kept in water (control) and $CaCl_2$ solution (0.5 g L^{-1}) during the postharvest experiment of *G. jamesonii* cv. 'Ruby red'.

Tabla 4. Proporción relativa de tejido (tejido) y proporción relativa de médula (médula) en el segmento 1 del tallo floral al inicio (Inicial) y final (Final) del experimento de poscosecha en tallos mantenidos en agua (control) y en solución de CaCl2 (0,5 gL^{-1}) durante el experimento de poscosecha de *G. jamesonii* cv. 'Ruby red'.

Treatments	Initial		Final	
	Tissue	Pith	Tissue	Pith
Water	87.20	9.20	61.09 a	38.90 a
$CaCl_2$ solution	87.20	9.20	75.17 b	24.82 b

Lowercase letters indicate statistically significant values in columns ($p<0.05$).

Letras minúsculas en columnas son estadísticamente diferentes ($p<0,05$).

The interaction between calcium and pectin, particularly through the formation of calcium-pectate complexes, plays a crucial role in maintaining cell wall integrity and resistance to enzymatic degradation. Thus, it can reduce cavity expansion and preserve vascular function, ensuring adequate water transport and maintaining turgor during postharvest life (Sun *et al.*, 2025).

Consequently, the anatomical stabilization provided by calcium could delay stem bending by preserving both the mechanical strength and water continuity in the tissue (Delmer *et al.*, 2024).

Histological analyses confirm a close relationship between the higher calcium content observed in the floral stems kept in calcium solution (T2) and their greater cellular integrity, which contributes to the prevention of stem bending, maintaining superior structural integrity and firmness, exhibiting no bending. Parenchymatous and sclerified cells in these treated tissues displayed reduced compression and enhanced sclerenchyma integrity. In contrast to floral stems kept in distilled water (T1), which bent due to the loss of structural support. Calcium treatment effectively preserved the turgidity and stability of the floral stems.

Calcium is known to stabilize cell walls by forming cross-links with pectic acids, strengthening the middle lamella, and maintaining membrane integrity, which reduces cell disintegration (Mohsin *et al.*, 2023). Furthermore, during vase life, the pH and electrical conductivity (EC) of the vase solution containing stems kept in distilled water (T1) increased significantly (EC: initial 2.6 to final 30.94 µS cm^{-1}; pH: initial 5.5 to final 6.58), suggesting ion leakage from damaged tissues. Associated with the loss of membrane selectivity and increased permeability due to senescence-induced degradation (Ehsanimehr *et al.*, 2024).

In contrast, the calcium treatment (T2) showed no significant variations in EC or pH during vase life and maintained membrane stability and ionic homeostasis. These results align with previous findings indicating that calcium mitigates ion leakage by preserving the integrity of plasma membranes and regulating ion transport across cells (El-Bana *et al.*, 2023).

Numerous studies have identified calcium as a key stabilizer of membrane integrity, contributing to wall rigidity by binding to pectins in the middle lamella (Narwal *et al.*, 2024, Taiz *et al.*, 2018). In T2, the calcium absorbed by the tissues (table 1, page 6) may have enhanced membrane stability, delayed senescence processes, and supported cell compartmentalization, thereby reducing or preventing electrolyte leakage.

The results underscore the role of calcium in sustaining metabolic activity and structural stability, thereby maintaining stem firmness and integrity over time. Overall, the findings from this experiment provide meaningful insights into the physiological effects of calcium treatment, consistent with recent research seeking technological alternatives to extend the postharvest life of *Gerbera jamesonii* (Granados *et al.*, 2025).

Conclusions

There is a direct relationship between the calcium content in the vase solution and the histochemical, metabolic, and structural characteristics in the postharvest quality of *Gerbera jamesonii* L. cv. 'Ruby Red'. Calcium application has proven to be a critical factor in improving the quality and structural resilience floral stem. The evidence findings indicate that adequate calcium supplementation not only strengthens the physical structure of stems but also supports more harmonious and efficient plant development.

References

Abd-Elkader, H. H., Massoud, H. Y., El-Baz, T. T., El-Erian, M. A. (2020). Effect of amino acids spray on growth, flowering and keeping quality of *Gerbera jamesonii* L. as a pot plant. *Journal of Plant Production, 11*(2), 201-206. https://doi.org/10.21608/jpp.2020.79110

Ali, K. K., & Asal, K. N. A. (2023). Effect of Foliar Application of Calcium and Nano-Chitosan on the Growth of Rose Seedlings. *IOP Conference Series: Earth and Environmental Science, 1158*(4), 42032. https://doi.org/10.1088/1755-1315/1158/4/042032

Alikhani, T. T., Tabatabaei, S. J., Torkashvand, A. M., Talei, D. (2021). Silica nanoparticles and calcium on the histological characteristics and stem bending in Gerbera cut flowers. *Ornamental Horticulture*, *27*(3), 334-343. https://doi.org/10.1590/2447-536x.v27i3.2308

Balk, M., Sofia, P., Neffe, A. T., Tirelli, N. (2023). Lignin, the Lignification Process, and Advanced, Lignin-Based Materials. *International Journal of Molecular Sciences*, *24*(14), 11668. https://doi.org/10.3390/ijms241411668

Bárbaro, L. A., Rubio, E., Karlanián, M. A. & Iwasita, B. E. (2024). Substrate pH Management Strategies in the Production of Yerba Mate Seedlings (*Ilex paraguariensis* A. St.-Hil.). *Chilean journal of agricultural & animal sciences*, *40*(3), 530-544**.** https://dx.doi.org/10.29393/chjaas40-44emlb40044

Borghi, M., Fernie, A. R. (2017). Floral Metabolism of Sugars and Amino Acids: Implications for Pollinators' Preferences and Seed and Fruit Set. *Plant Physiol.,75*(4): 1510-1524. doi:10.1104/pp.17.01164.

Çelikel, F. G., Reid, M. S. (2002). Storage temperature affects the quality of cut flowers from the *Asteraceae. HortScience*, *37*(1), 148-150. https://doi.org/10.21273/hortsci.37.1.148

Cheng, G., Wang, L., He, S., Liu, J., Huang, H. (2020). Involvement of pectin and hemicellulose depolymerization in cut gerbera flower stem bending during vase life. *Postharvest Biology and Technology*, *167*, 111231. https://doi.org/10.1016/j.postharvbio.2020.111231.

Ciriello, M., Campana, E., Colla, G., De Pascale, S., Rouphael, Y. (2024). Preharvest calcium application boosts the biostimulatory effect of protein hydrolysate by improving the postharvest life of gerbera cut flower. *Scientia Horticulturae*, *331*, 113140. https://doi.org/10.1016/j.scienta.2024.113140

Crang, R., Lyons-Sobaski, S., Wise, R. (2018). Parenchyma, Collenchyma, and Sclerenchyma. In: *Plant Anatomy.* Springer, Cham. https://doi.org/10.1007/978-3-319-77315-5_6

Delmer, D., Dixon, R. A., Keegstra, K., Mohnen, D. (2024). The plant cell wall-dynamic, strong, and adaptable-is a natural shapeshifter. *Plant Cell, 1;36*(5):1257-1311. https://doi: 10.1093/plcell/koad325.

Di Rienzo, J. A., Casanoves, F., Balzarini, M. G., González, L., Tablada, M. (2020). InfoStat versión 2020. Grupo InfoStat, FCA, Universidad Nacional de Córdoba. http://www.infostat.com.ar

Ehsanimehr, N., Hosseinifarahi, M., Abdipour, M. (2024). Improving postharvest quality and vase life of cut rose flowers by pre-harvest foliar co-applications of γ-aminobutyric acid and calcium chloride. *Sci Rep,* 14, 14520. https://doi.org/10.1038/s41598-024-64021-8

El-Bana, H. S., & Ennab, H. A. (2023). Post-harvest application of some calcium forms to improve quality and shelf life of mandarin fruits during storage. *Alexandria Journal of Agricultural Sciences*, *68*(3), 141-151.https://doi.org/10.21608/alexja.2023.222162.1039

García-González, A., Soriano-Melgar, L. D. A. A., Cid-López, M. L., Cortez-Mazatán, G. Y., Mendoza-Mendoza, E., Valdez-Aguilar, L. A., Peralta-Rodríguez, R. D. (2022). Effects of calcium oxide nanoparticles on vase life of Gerbera cut flowers. *Scientia Horticulturae*, *291*, 110532. https://doi.org/10.1016/j.scienta.2021.110532

Ge, Y., Lai, Q., Luo, P., Liu, X., Chen, W. (2019). Transcriptome profiling of *Gerbera hybrida* reveals that stem bending is caused by water stress and regulation of abscisic acid. *BMC Genomics*, *20*(1). https://doi.org/10.1186/s12864-019-5961-1

Granados Ortiz, S. A.; Visentini, F. F.; Panigo, E. S.; Muñoz, F. F.; Malano, J. P.; Derita, M. G.; Daurelio, L. D.; Bouzo, C. A.; Pérez Rubin, A. A.; Céccoli, G. (2025). Green Synthesis and Foliar Application of Copper Nanoparticles in Sunflower (*Helianthus annuus* L.) to Improve Physiological Parameters and Yield. *Revista de la Facultad de Ciencias Agrarias. Universidad Nacional de Cuyo. 57*(2): 187-198. DOI: https://doi.org/10.48162/rev.39.182

Gupta, S., Kaur, N., Kant, K., Jindal, P., Ali, A., Naeem, M. (2023). Calcium: A master regulator of stress tolerance in plants. *South African Journal of Botany*, *163*, 580-594. https://doi.org/10.1016/j.sajb.2023.10.047

Hartmann, F. P., Tinturier, E., Julien, J.-L., Leblanc-Fournier, N. (2021). Between Stress and Response: Function and Localization of Mechanosensitive Ca2+ Channels in Herbaceous and Perennial Plants. *International Journal of Molecular Sciences*, *22*(20), 11043. https://doi.org/10.3390/ijms222011043

Huang, X., Lin, S., He, S., Lin, X., Liu, J., Chen, R., Li, H. (2018). Characterization of stomata on floral organs and scapes of cut 'Real' Gerberas and their involvement in postharvest wáter loss. *Postharvest Biology and Technology*, *142*, 39-45. https://doi.org/10.1016/j postharvbio.2018.04.001

Kim, J., & Oh, W. (2021). Cold Storage Period of Bulbs Influences Their Sugar Contents and Post-Storage Growth and Flowering in *Lilium* Oriental Hybrids. *Agriculture*, *11*(11), 1080. https://doi.org/10.3390/agriculture11111080

Lear, B., Casey, M., Stead, A. D., Rogers, H. J. (2022). Peduncle necking in *Rosa hybrida* induces stressrelated transcription factors, upregulates galactose metabolism, and downregulates phenylpropanoid biosynthesis genes. *Frontiers in Plant Science*, *13*. https://doi.org/10.3389/fpls.2022.874590

Manzoor, A., Bashir, M. A., Naveed, M. S., Akhtar, M. T., & Saeed, S. (2024). Postharvest Chemical Treatment of Physiologically Induced Stem End Blockage Improves Vase Life and Water Relation of Cut Flowers. *Horticulturae, 10*(3), 271. https://doi.org/10.3390/horticulturae10030271

Milani, M., Pradella, E. M., Heintze, W., Schafer, G., & Bender, R. J. (2019). The effects of supplemental nitrogen and calcium on the quality and postharvest life of cut gerbera. *Ornamental Horticulture, 25*(4), 365-373. https://doi.org/10.1590/2447-536X.v25i4.2028

Mohammadi, M., Ranjbar, M. E., Eghlima, G. (2024). Impact of gibberellic acid and calcium chloride treatments on neck bending prevention and vase life extension of Gerbera cut flowers. *Journal of Plant Growth Regulation, 43*(4), 1093-1102. https://doi.org/10.1007/s00344-023-11164-z

Mohsin, R. M., Asal, K. A., Kamaluddin, A. A., Zaky, A. A. (2023). Genotypes and storage duration effects on the quality of cut flower-Gerbera (*Gerbera jamesonii* Hook). *Sabrao J. Breed. Genet, 55*(1), 260-267. https://doi.org/10.54910/sabrao2023.55.1.24

Narwal, P., Negi, N. P. (2024). Exogenous Calcium Enhances Osmotic Regulation, Photosynthetic Machinery and Stomatal Characteristics in Banana Under Dehydration Stress. *Indian Journal of Agricultural Biochemistry*, *37*(1), 24-30. https://doi.org/10.5958/0974-4479.2024.00004.4

Park, J., Kim, W. S. (2022). Preharvest Spraying of CaCl2 Alleviates the Scape Bending of Gerbera 'Harmony' Flowers by Strengthening the Pectin Crosslinks through Ca2+ Bonds. *Horticulturae*, *8*(6), 523. https://doi.org/10.3390/horticulturae8060523

Parvin, K., Nahar, K., Hasanuzzaman, M., Bhuyan, M. H. M. B., Fujita, M. (2019). Calcium-Mediated Growth Regulation and Abiotic Stress Tolerance in Plants. In: Hasanuzzaman, M., Hakeem, K., Nahar, K., Alharby, H. (eds). *Plant Abiotic Stress Tolerance*. Springer, Cham. https://doi org/10.1007/978-3-030-06118-0_13

Perik, R. R., Razé, D., Harkema, H., Zhong, Y., Van Doorn, W. G. (2012). Bending in cut *Gerbera jamesonii* L. flowers relates to adverse water relations and lack of stem sclerenchyma development, not to expansion of the stem central cavity or stem elongation. *Postharvest Biology and Technology, 74*, 11-18. https://doi.org/10.1016/j.postharvbio.2012.06.009

Seyed Hajizadeh, H., Bayrami Aghdam, S., Fakhrghazi, H., Karakus, S., Kaya, O. (2024). Physico-Chemical Responses of Alstroemeria spp. cv. Rebecca to the presence of Salicylic Acid and Sucrose in vase solution during postharvest life. *BMC Plant Biology, 24*(1). https://doi.org/10.1186/s12870-024-04814-1

Sun, M., Wang, F., Ci, J., Liu, Y., Li, K., Wang, D., Yu, W., Zhuang, Y., & Xiao, Y. (2025). Effects of Different Calcium Preparations on Fresh-Cut Quality and Storage Quality of Starkrimson Apple. *Plants*, *14*(9), 1293. https://doi.org/10.3390/plants14091293

Taiz, L., Zeiger, E., Møller, I, Murphy, A. (2018). *Fundamentals of Plant Physiology*. Oxford University Press. 561 p.

Tang, Y., Lu, L., Sheng, Z., Zhao, D., Tao, J. (2023). An R2R3-MYB network modulates stem strength by regulating lignin biosynthesis and secondary cell wall thickening in herbaceous peony. *The Plant Journal, 113*(6), 1237-1258, doi: 10.1111/tpj.16107.

Timalsina, S., Poudel, P. R., Acharya, A. K., Pathak, R., & Pun, U. K. (2023). Effect of calcium chloride and floral preservatives in the vase life of gerbera cut flower. *Nepal Agriculture Research Journal*, *15*(1), 125-135. https://doi.org/10.3126/narj.v15i1.51538

Tonooka, M., Homma, Y., Toyoizumi, T., Ichimura, K. (2023). Stem bending in cut Gerbera under the condition of suppressing bacterial proliferation is associated with the weakening of the stem strength. *Scientia Horticulturae, 319*, 112153, doi: 10.1016/j.scienta.2023.112153

Verdonk, J. C., Van Ieperen, W., Carvalho, D. R. A., Van Geest, G., Schouten, R. E. (2023). Effect of preharvest conditions on cut-flower quality. *Front. Plant Sci., 14*, 1281456. doi: 10.3389/fpls.2023.1281456

Wang, L., Chen, Y., Wu, M., Dai, F., Ye, M., Chen, F., Huang, H. (2023). Involvement of lignin deposition and cell wall degradation in stem senescence of Chinese flowering cabbage during storage. *Postharvest Biology and Technology*, *198*, 112256. https://doi.org/10.1016/j.postharvbio.2023.112256

Wdowiak, A., Podgórska, A. & Szal, B. (2024). Calcium in plants: an important element of cell physiology and structure, signaling, and stress responses. *Acta Physiol Plant,* 46, 108. https://doi.org/10.1007/s11738-024-03733-w

Xia, C., Cao, Y., Gan, W., Lin, H., Li, H., Lin, F., Lu, Z., Chen, W. (2025). Optimal Vase Solution for Gerbera hybrid Cut Flower Keeping Fresh by Activating SA and Cytokinin Signaling and Scavenging Reactive Oxygen Species. *Biology, 14*(1), 18. https://doi.org/10.3390/biology14010018

Effects of Climate Change on Nine Rainfed *Zea mays* Races in Chiapas, Mexico

Efectos del cambio climático sobre nueve razas de temporal de *Zea mays* en Chiapas, México

Alejandro Vázquez Moreno [1], Tamara Mila Rioja Paradela [2, 3 *], Arturo Carrillo Reyes [2, 3], Carolina Orantes García [4], Eduardo Espinoza Medinilla [4]

Originales: *Recepción:* 30/07/2024 - *Aceptación:* 14/04/2025

ABSTRACT

Maize cultivation (*Zea mays)* is essential for Mexico from a nutritional, cultural and economic perspective. Scientific literature ignores the impact of anthropogenic causes of climate change on rainfed cultivation of *Z. mays* in Chiapas, Mexico, one of the poorest states in the country. Therefore, we modeled the feasibility of rainfed cultivation for nine races of rainfed maize for the years 2060 and 2100. The MaxEnt 4.4.4 algorithm modeled maize cultivation under two scenarios (4.5 and 8.5) for 2060 and 2100. Model inputs were 12 bioclimatic variables, 3 climatic variables, and 1 elevation variable. All layers were obtained from the WorldClim 2.1 project. By 2060, the suitable area for rainfed cultivation of the nine *Z. mays* races would drastically decrease under both modeled scenarios. By 2100, this area will decrease for seven races, and disappear for the Olotillo and Olotón races. To the best of our knowledge, this is the first study providing fundamental information on how climate change will negatively impact the nine *Z. mays* races in Chiapas, Mexico. This enables the development of sustainable management protocols or conservation strategies.

Keywords
bioclimatic variables • climatic variables • elevation • MaxEnt 4.4.4 • rainfed maize races

https://doi.org/10.48162/rev.39.192

1 Universidad de Ciencias y Artes de Chiapas. Facultad de Ingeniería. Programa de Maestría en Ciencias en Desarrollo Sustentable y Gestión de Riesgos. Tuxtla Gutiérrez. Libramiento Norte Poniente N° 1155. Colonia Lajas Maciel. C. P. Chiapas. México.
2 Universidad de Ciencias y Artes de Chiapas. Facultad de Ingeniería.
* tamararioja@gmail.com
3 Oikos. Conservación y Desarrollo Sustentable AC. Calle Bugambilias N° 5. Colonia Bismark. C. P. 29267. San Cristóbal de las Casas. Chiapas. México.
4 Universidad de Ciencias y Artes de Chiapas. Instituto de Ciencias Biológicas.

Licenses Creative Commons
Attribution - Non Commercial - Share Alike

Resumen

El cultivo de maíz (*Zea mays*) es de gran importancia para la población de México desde una perspectiva nutricional, cultural y económica. La literatura científica carece de información sobre el impacto del cambio climático antropogénico en el cultivo de temporal de *Z. mays* en Chiapas, México, uno de los estados más pobres del país. Es por ello que modelamos la viabilidad del cultivo de temporal para nueve razas de maíz de temporal para los años 2060 y 2100. Se utilizó el algoritmo MaxEnt 4.4.4 para modelar bajo dos escenarios (4.5 y 8.5) para el 2060 y el 2100. El modelo se alimentó con 12 variables bioclimáticas, 3 variables climáticas y una variable de elevación. Todas las capas se obtuvieron del proyecto WorldClim 2.1. Se proyecta que el área adecuada para el cultivo de temporal de las nueve razas de *Z. mays* disminuirá drásticamente para 2060 bajo los escenarios 4.5 y 8.5. Para el año 2100, bajo los mismos escenarios, la superficie se reducirá para siete razas, mientras que en las razas de maíz Olotillo y Olotón desaparecerá por completo. Por primera vez, se proporciona información fundamental sobre cómo el cambio climático impactará negativamente a las nueve razas de *Z. mays* en Chiapas, México, lo que permitirá desarrollar protocolos de manejo sustentable y/o estrategias de conservación.

Palabras clave

variables bioclimáticas • variables climáticas • elevación • MaxEnt 4.4.4 • razas de maíz de temporal

Introduction

Agriculture is the primary source of global food supply (7). However, this activity is severely threatened by anthropogenic causes of climate change, especially for rainfed crops (21). Increases in environmental temperature, changes in precipitation patterns, and drought events often reduce crop production area (34).

Maize (*Z. mays)* constitutes an essential food in Mexico. It is a highly nutritious source consumed in various presentations, holding particular socio-cultural value for indigenous people and the whole population (24, 32).

Maize production is relevant for national and international markets (44). However, in southeastern Mexico, most rainfed maize areas are being abandoned given social issues, changes in land use, poor technological implementation, and inadequate public policies (55). In Chiapas, farmers are vulnerable to these changes. Aimed at sustaining rainfed maize production, many have resorted to hybrid seeds, declining native varieties and losing ancestral techniques in favor of contemporary ones (31).

Mexico's maize races are cataloged in 7 racial groups based on morphology, adaptation types, and genetic traits (20, 51, 52). Within these groups, the National Commission for Knowledge and Use of Biodiversity (2020) reports a total of 64 races, 59 of which are native. In Chiapas, 11 races have been documented, with 9 having geographical records associated with rainfed agriculture: Zapalote Chico, Cubano Amarillo, Tepecintle, Zapalote Grande, Tuxpeño, Vandeño, Comiteco, Olotón and Olotillo (10), specimens registry of the National Biodiversity Information System (www.snib.mx/).

No study has yet analysed the impact of climate change on cropping areas for these maize races in the state of Chiapas, Mexico. This information is crucial considering approximately 88% of total maize production in Chiapas depends on rain cycles (30). Each race is cultivated in distinct environmental conditions, adapted to specific temperature, precipitation, and elevation (3, 6, 11, 36, 56). Therefore, this study aims to determine whether these races will be differently affected by climate change and provide insights for sustainable management plans (49, 57). This, considering reproductive and adaptation strategies, and cultural practices preventing their disappearance (33).

Materials and Methods

Study Area

The study area encompassed the entire state of Chiapas, located in southeastern Mexico. It borders the state of Tabasco to the north, Veracruz and Oaxaca to the west, the Pacific Ocean to the south, and Guatemala to the east. It spans 74,415 km^2 (13) and lies between 17°59' to 14°32' N and 90°22' to 94°14' W.

Annual precipitation varies widely across the state, ranging from 800 to 2,500 mm. Variations in the north range from 1,500 to 2,500 mm and between 1,500 and 2,000 mm in the south. In the central part of the state, most areas register annual precipitation between 800 and 1,200 mm, while in the rest of the state, precipitation ranges from 1,200 to 1,500 mm (54).

Chiapas held the first place in harvested maize area from 2010 to 2021. However, now the state ranked 6th in national production volume with 1.3 million tons (45).

Database of Spatial Records for Nine Maize Races (*Z. mays*) in Chiapas

Georeferenced records for the nine maize races were obtained from scientific databases such as the 2023 Geoinformation Portal from the National Commission for the Knowledge and Use of Biodiversity (2023), the Biodiversity Information Facility (www.gbif.org/es/), COMPADRE (https://compadre-db.org/; COMPADRE Plant Matrix Database 2023), and the Specimen Register of the National System of Information on Biodiversity (www.snib.mx/).

After removing all duplicated records or those with erroneous coordinates (42), we defined 1,215 records for the Comiteco race, 60 for Cubano Amarillo, 209 for Olotillo, 456 for Olotón, 77 for Tepecintle, 1,159 for Tuxpeño, 63 for Vandeño, 13 for Zapalote Chico, and 40 for Zapalote Grande, totaling 3,292 presence records.

Finally, using the "spThin" package in R software and RStudio, the spatial correlation among the presence data for the nine maize races was reduced through 100 iterations (2, 47, 50).

Environmental Layers for the Nine Rainfed Maize Races

Environmental layers for minimum, maximum, and average monthly temperatures, monthly cumulative rainfall, elevation and 19 bioclimatic variables were obtained to determine suitable environmental conditions for the nine rainfed maize races in Chiapas. These layers correspond to cultivating periods for each race in Chiapas. The cropping season for the Zapalote Chico race occurs from May (planting) to August (harvest) (3, 28, 36). In contrast, Cubano Amarillo, Tepecintle, Vandeño, Tuxpeño, and Zapalote Grande extend from May to October (11), while Comiteco, Olotón, and Olotillo races grow from May to December (3, 11).

All layers were obtained from the WorldClim 2.1 project (18). Each environmental variable consists of a georeferenced raster layer with a spatial resolution of 30 seconds (~1 km^2) (19). Layers were cropped using the georeferenced boundary of the state of Chiapas using R software and its graphical interface, RStudio (47, 50).

Current Feasibility of the Nine Rainfed Maize Races

To determine current feasibility of the nine maize races, the model was calibrated to the current scenario using the Maxent 4.4.4 algorithm operating on presence data of a particular species to predict its geographical distribution based on maximum entropy (14).

The calibration area was Chiapas, with 75% of presence records used for training and 25% for evaluation. The model was configured with a logistic function and ten cross-validation replicates (41).

A Jackknife test assessed variable contributions, while predictive capacity was evaluated using the area under the curve (AUC) (39). Any replicates under 0.9 were discarded. Then, pixel reclassifications of the resulting raster layer of each replicate (.asc) allowed obtaining a binary map (0 = no feasibility for the nine rainfed maize races, 1 = feasibility for the nine rainfed maize races) using the 10th percentile presence value as cut-off point (27).

Using QGIS version 3.285 (43), the binary map was multiplied for each cross-validation replicate, obtaining a unique raster for each maize race. Binary maps (rasters) were polygonised, and each polygon on the map was dissolved to obtain surface areas in hectares and generate maps of regional feasibility for the nine rainfed maize races.

Feasibility of the Nine Rainfed Maize (*Z. mays*) Races Under Climate Change Scenarios

Feasibility of the nine rainfed maize races in Chiapas under climate change scenarios (2041-2060 and 2081-2100) was modeled using the same presence records and environmental variables as the current scenario. Similarly, the same parameters were used in MaxEnt.

The HadGEM3-GC31-LL circulation model and the 4.5 and 8.5 greenhouse gas (GHG) concentration pathways were used (46). These scenarios represent different projections of the future (38). The Shared Socioeconomic Pathways (SSP) 245 scenario (GHG concentration pathway 4.5) anticipates a middle-of-the-road pathway where trends continue their historical patterns without significant deviations (38). The SSP 585 scenario (GHG concentration pathway 8.5) assumes low population growth and includes rapid technological change, paired with intensive use of fossil fuels, implying higher levels of greenhouse gas emissions (16).

Results

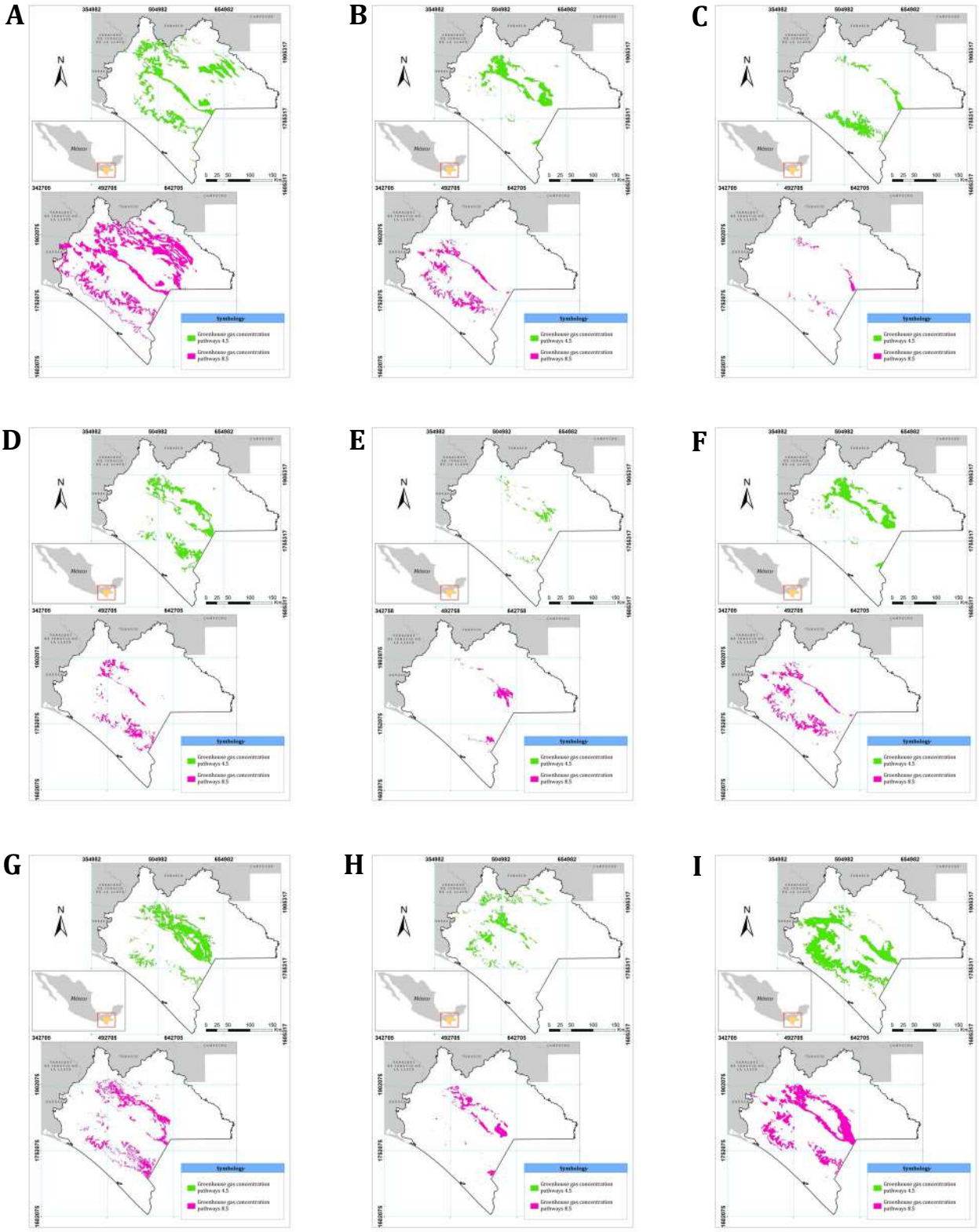
Feasibility of the Nine Rainfed Maize (*Z. mays*) Races in Chiapas Under Climate Change Scenarios

According to the MaxEnt model, by 2060 under the 4.5 concentration pathway (SSP 245) scenario, the suitable area for rainfed cultivation will shrink for all nine maize races (table 1; figure 1, page 5). The Olotón race will be most affected, with a projected cultivation area of 6,356 ha, followed by Comiteco, with a projected area of 79,303 ha. Under the 8.5 concentration pathway (SSP 585) scenario, all races will experience similar declines, with Olotón reduced to 990 ha.

Table 1. Feasibility of rainfed cultivation area for nine maize races (*Zea mays*) in 2060 and 2100 under two greenhouse gas concentration pathway scenarios (4.5 and 8.5) in Chiapas, Mexico.

Tabla 1. Superficie de factibilidad de cultivo de temporal de nueve razas de maíz (*Z. mays*) para los escenarios de vía de concentración de 4.5 y 8.5 al año 2060 y 2100, en Chiapas, México.

Race	Feasibility of *Z. mays* rainfed area (Ha)				
	Current scenario	2060 scenario		2100 scenario	
		SSP 245	SSP 585	SSP 245	SSP 585
Comiteco	314,691	79,303	94,946	155,059	6,440
Cubano Amarillo	853,238	439,710	218,085	363,489	19,167
Olotillo	632,659	294,904	61,246	34,086	0
Olotón	286,507	6,356	990	16,425	0
Tepecintle	3,401,913	383,029	319,876	287,384	264,114
Tuxpeño	1,242,256	622,971	454,994	591,708	172,365
Vandeño	1,953,746	305,520	184,916	921,418	164
Zapalote Chico	4,846,495	728,708	1,267,441	368,273	490,703
Zapalote Grande	1,969,184	913,752	760,014	84,283	16,568



A: Zapalote Chico, B: Olotón, C: Olotillo, D: Cubano Amarillo, E: Comiteco, F: Tepecintle, G: Tuxpeño, H: Vandeño, I: Zapalote Grande.

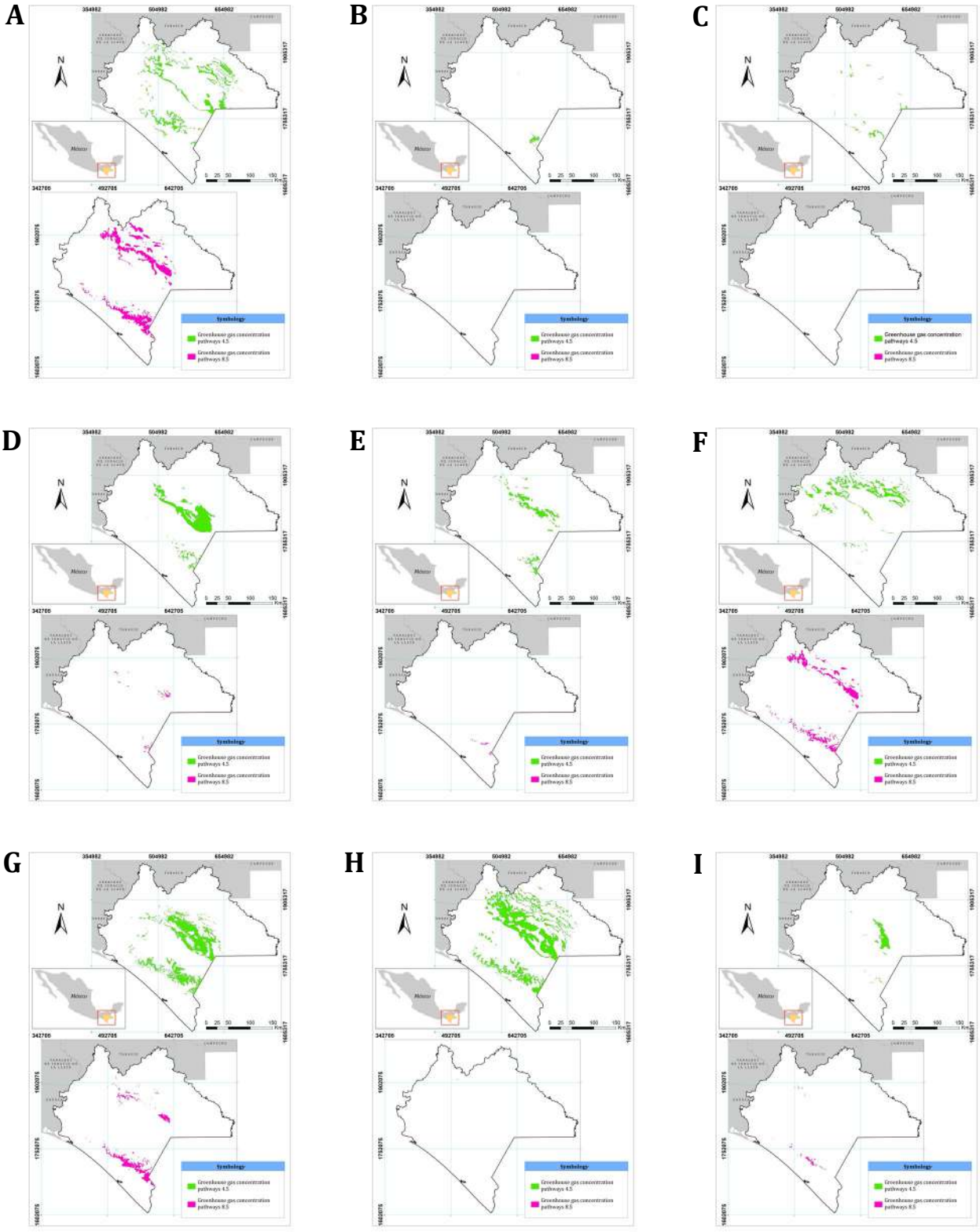
Figure 1. Feasibility of rainfed areas for nine maize (*Zea mays*) races in 2060 under two greenhouse gas concentration pathway scenarios (4.5 and 8.5) in Chiapas, Mexico.

Figura 1. Factibilidad de la superficie de temporal para las nueve razas de maíz estudiadas (*Z. mays*) para el año 2060, bajo dos escenarios de trayectorias de concentración de gases de efecto invernadero (4.5 y 8.5), en Chiapas, México.

The variables that contributed the most to the 2060 model under the 4.5 concentration pathway scenario were: "maximum temperature of the warmest month" (Bio 5), explaining 74% of modeling results for the Zapalote Chico race; "mean diurnal range" (Bio 2), contributing 22.8%, 26.6%, 30.2%, and 16.4% for the Cubano Amarillo, Tuxpeño, Vandeño, and Comiteco races, respectively; "average precipitation for December" with 20.4% and 21.6% for the Tepecintle and Zapalote Grande races, respectively; "precipitation seasonality" (Bio 15) contributing 22.2% for the Olotillo race; and finally, "average minimum temperature for June", contributing 39.3% for the Olotón race. Under the 5.8 concentration pathways, the most influential variables were: "maximum temperature of the warmest month" (Bio 5), contributing 92.6% for the Zapalote Chico race; "mean diurnal range" (Bio 2), with 27%, 34.5%, 31.3%, and 15.4% for Cubano Amarillo, Tuxpeño, Vandeño, and Comiteco, respectively; "average precipitation for December" with 19.2% and 21.8% for Tepecintle and Zapalote Grande, respectively; "precipitation seasonality" (Bio 15), contributing with 21.5% for the Olotillo race; and finally, "average minimum temperature for June" contributing 40.1% for the Olotón race.

According to the MaxEnt model in the concentration pathway scenario 4.5 (SSP 245), similarly to the 2060 scenario, in the 2100 scenario, all nine maize races will experience a rainfed area reduction (table 1, page 4; figure 2, page 7). The Olotón race will drastically reduce its area to 16,425 ha. In the concentration pathway scenario 8.5 (SSP 585), the rainfed area of nine maize races will be significantly reduced, with the Olotillo and Olotón races disappearing by the year 2100.

The variables that most contributed to the 2100 model, in the concentration pathway scenario 4.5, were "maximum temperature of the warmest month" (Bio 5) with 59.3% contribution for the Zapalote Chico race, "mean diurnal range" (Bio 2) with 22.2%, 34.7%, 34.9%, 16.9%, and 23% for the Cubano Amarillo, Tuxpeño, Vandeño, Comiteco, and Olotillo races respectively, "average precipitation for October" with 21.5% for the Zapalote Grande race, "average precipitation for December" with 21.7% for the Tepecintle race, and finally, "average minimum temperature for June" with 40.8% for the Olotón race. For the concentration pathways 5.8 were "maximum temperature of the warmest month" (Bio 5) with 89.1% contribution for the Zapalote Chico race, "mean diurnal range" (Bio 2) with 25.9%, 31.5%, 31.3%, 17.2%, and 19.8% for the Cubano Amarillo, Tuxpeño, Vandeño, Comiteco, and Olotillo races respectively, "average precipitation for October" with 23.4% for the Zapalote Grande race, "average precipitation for December" with 13.4% for the Tepecintle race, and finally, "average minimum temperature for June" with 36.9% for the Olotón race.



A: Zapalote Chico, B: Olotón, C: Olotillo, D: Cubano Amarillo, E: Comiteco, F: Tepecintle, G: Tuxpeño, H: Vandeño, I: Zapalote Grande.

Figure 2. Feasibility of rainfed area for nine maize (*Z. mays*) races in 2100, under two greenhouse gas concentration pathway scenarios (4.5 and 8.5), in Chiapas, Mexico.

Figura 2. Factibilidad de la superficie de temporal para las nueve razas de maíz estudiadas (*Z. mays*) para el año 2100 bajo dos escenarios de trayectorias de concentración de gases de efecto invernadero (4.5 y 8.5), en Chiapas, México.

Discussion

Chiapas has the largest maize cultivation area in all of Mexico (approximately 900,000 hectares), ranking fourth in national production, with 294,468 maize producers. Rainfed maize accounts for 98% of this area (33). However, climate change may reduce rainfed areas, limiting production and threatening food security for Chiapas' rural population (1). As a result, communities may lose physical, social and economic access to many maize races, reducing the availability of safe and nutritious food (19).

According to the MaxEnt model, climate change will significantly impact feasibility of cultivation areas for the 9 maize races in Chiapas, as suggested for other regions of Mexico (22, 30, 55) and other countries (4, 9, 17). For example, the feasible rainfed area for the Zapalote Chico race decreases drastically under climate change scenarios, dropping from 4,846,495 ha to 728,708 ha by 2060 and to 368,273 ha by 2100 with the 4.5 concentration pathway (figure 3 and figure 4, page 9), due to increased maximum temperatures of the warmest month (Bio 5) and decreased precipitation of the warmest quarter (Bio 18). Additionally, the feasible rainfed area for Olotón and Olotillo also decreases drastically under climate change scenarios. Olotón rainfed area decreases from 286,507 ha to 6,356 ha by 2060 and to 16,425 ha by 2100 with the 4.5 concentration pathway, while the Olotillo rainfed area decreases from 632,659 ha to 294,904 ha by 2060 and to 34,086 ha by 2100 with the 4.5 concentration pathway. But, by 2100, under the 8.5 concentration pathway, these two maize races will disappear from Chiapas after the influence of mean diurnal range and the increasing average minimum temperature for June, as for Zapalote Chico.

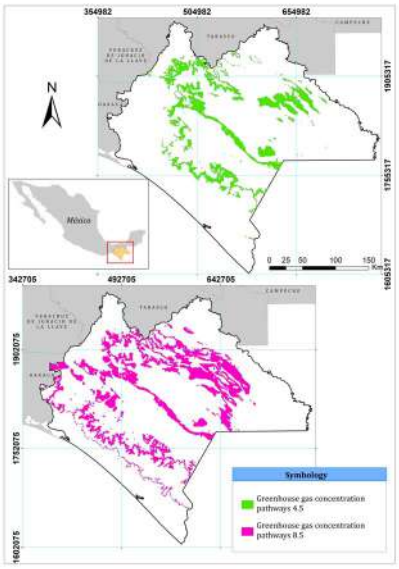


Figure 3. Feasibility of rainfed areas for the Zapalote Chico maize race (*Z. mays*) by 2060 under two greenhouse gas concentration pathway scenarios (4.5 and 8.5), in Chiapas, Mexico.

Figura 3. Factibilidad de la superficie de temporal para la raza de maíz Zapalote Chico (*Z. mays*) para el año 2060 bajo dos escenarios de trayectorias de concentración de gases de efecto invernadero (4.5 y 8.5), en Chiapas, México.

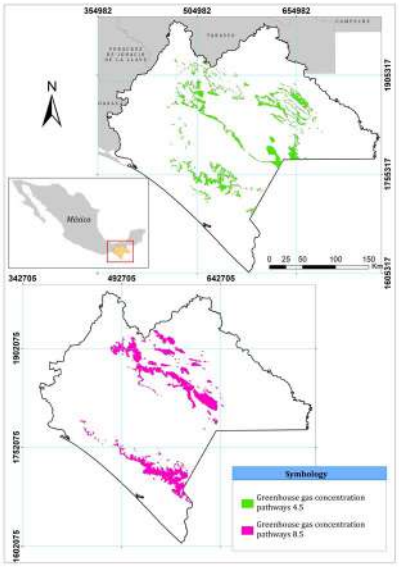


Figure 4. Feasibility of rainfed areas for the Zapalote Chico maze race (*Z. mays*) by 2100 under two greenhouse gas concentration pathway scenarios (4.5 and 8.5) in Chiapas, Mexico.

Figura 4. Factibilidad de la superficie de temporal para la raza de maíz Zapalote Chico (*Z. mays*) para el año 2100 bajo dos escenarios de trayectorias de concentración de gases de efecto invernadero (4.5 y 8.5), en Chiapas, México.

Suitable environmental conditions in Chiapas, derived from the MaxEnt model, under the current scenario for rainfed Zapalote Chico race are temperatures ranging from 8.2°C to 29.1°C, accumulated precipitation from 80.3 mm to 2,092 mm, and an elevation ranging from -2 to 2,155 m.a.s.l (3, 6, 36). Suitable environmental conditions in Chiapas, derived from the Maxent model for the current scenario and rainfed cultivation of Olotón race, are temperatures ranging from 4.4°C to 21.1°C, accumulated precipitation from 282.2 mm to 1,630 mm, and an elevation ranging from 384 to 2,732 m.a.s.l., while for Olotillo race, suitable conditions include ambient temperatures from 4.7°C to 26.1°C, accumulated precipitation from 196.1 mm to 1,695 mm, and elevations from 112.7 meters to 2,302 m a. s. l. (3, 6, 36).

Currently, the geographic areas of Chiapas meet these environmental conditions, allowing optimal development of all 9 races (6, 11), preventing both water and thermal stress (42). However, the increase in temperature due to climate change will shorten the cultivation period by accelerating growth rates (25). Exposure to high temperatures causes severe damage and cellular collapse (8), leading to pollination failure, fruit abortion and reduced load, promoting vegetative growth (15). This ultimately results in significant losses of aerial biomass, poor seed production, and reduced grain yield expressed as fewer grains per cob, and therefore, lower overall yields (26, 48).

High temperatures and less rainfall will negatively impact rainfed cultivation of these races in Chiapas. Water is essential for plant growth (5), and a limiting resource in rainfed cultivation. Reduced precipitation causes water stress and plant death when transpiration exceeds cavitation thresholds (29). Transpiration is closely associated with CO_2 exchange for photosynthesis and is essential for plant growth and development (53). On the other hand, reduced precipitation further delays stigma exposure (pollen release), leading to reduced crop productivity (58).

Rainfed maize cultivation is fundamental for food security in Chiapas and Latin America, contributing to local and regional economic growth (7). Beyond its economic importance, maize holds deep cultural significance for various ethnic groups, playing an integral role in their worldview, ranging from traditional cuisine to its use in sacred rituals (6). Nutritionally, maize is closely associated with nixtamalization, a process that involves treating it with lime. This technique enhances calcium bioavailability and improves protein assimilation, allowing for the preparation of tortillas, an essential and highly nutritious staple (40).

This study shows how climate change will negatively impact nine rainfed maize races in Chiapas, offering key insight for future sustainable management protocols and/or conservation actions (23). However, a more comprehensive long-term cohort study should also consider social, economic, and cultural factors. Recognizing the importance of the social context in such research will value both subjective experiences and the understanding of sociocultural realities (35).

Conclusions

Our results suggest that the nine maize (*Z. mays*) races currently grown in Chiapas, Mexico, will experience a dramatic decrease in their rainfed cultivation area under climate change scenarios for the years 2060 and 2100.

Supplemmentary Material

https://docs.google.com/document/d/14UogbVdf2wcb2ZcKhiJ0GMOhjxBhTUN9/edit?usp=sharing&ouid=111310786017351827239&rtpof=true&sd=true

References

1. Ahumada, R.; Velázquez, G.; Flores, E.; Romero, J. 2014. Impactos potenciales del cambio climático en la producción de maíz. Rev. Investigación y Ciencia. 61: 48-53.
2. Aiello-Lammens, M. E.; Boria, R. A.; Radosavljevic, A.; Vilela, B.; Anderson, R. P. 2015. spThin: an R package for spatial thinning of species occurrence records for use in ecological niche models. Ecography. 38: 541-545. DOI: https:// doi.org/10.1111/ecog.01132
3. Aragón, F.; Taba, S.; Hernández, J. M.; Figueroa, J. D.; Serrano, V. 2004. Informe final del Proyecto CS002: Actualización de la información sobre maíces criollos de Oaxaca. Secretaria de Agricultura, Ganadería, Desarrollo Rural, Pesca y Alimentación. México. D. F. http://www.conabio.gob.mx/institucion/proyectos/resultados/InfCS002.pdf (fecha de consulta: 14/11/2023).
4. Avilés, M. 2022. Zonificación agroecológica del cultivo de maíz (*Zea mays*) y su adaptabilidad a los posibles cambios climáticos del Cantón Buena Fé, Provincia Los Ríos. Rev. Multidiscipinar. 6(6): 6484-6501. DOI: 10.37811/cl_rcm.v6i6.3900
5. Azcón-Bieto, J.; Talón, M. 2013. Fundamentos de Fisiología Vegetal. Barcelona. Ed. McGRAW-HILL. 639 p.
6. Brush, S. B.; Perales, H. 2007. A maize landscape: Ethnicity and agro-biodiversity in Chiapas, Mexico. Rev. Agriculture, Ecosystems & Environment. 121: 211-221. DOI: https://doi.org/10.1016/j.agee.2006.12.018
7. Bula, A. 2020. Importancia de la agricultura en el desarrollo socio-económico. https:// observatorio.unr.edu.ar/wp-content/uploads/2020/08/Importancia-de-la-agricultura-en-el-desarrollo-socio-econ%C3%B3mico.pdf (Fecha de consulta: 27/02/2024).
8. Chaves-Barrantes, N. F.; Gutiérrez-Soto, M. V. 2017. Respuesta al estrés por calor en los cultivos. II. Tolerancia y tratamiento agronómico. Rev. Agronomía Mesoamericana 1: 255-271. DOI: https://doi.org/10.15517/am.v28i1.21904
9. Chimborazo, E. 2020. Modelación de nichos ecológicos bajo dos escenarios de cambio climático para maíz Chulpi (*Zea mays*) en la provincia de Cotopaxi, en el período 2019-2020. Tesis de grado de Ingeniería en Medio Ambiente. Facultad de Ciencias Agropecuarias y Recursos Naturales. Universidad Técnica de Cotopaxi. Ecuador. 71 p.
10. Comisión Nacional para el Conocimiento y Uso de la Biodiversidad (CONABIO). 2011. Base de datos del proyecto global "Recopilación, generación, actualización y análisis de información acerca de la diversidad genética de maíces silvestres en México". https://www.biodiversidad.gob.mx/diversidad/proyectoMaices (Fecha de consulta: 20/03/2023).
11. Comisión Nacional para el Conocimiento y Uso de la Biodiversidad (CONABIO). 2020. Razas de maíz en México. https://www.biodiversidad.gob.mx/diversidad/alimentos/maices/razas-de-maiz (Fecha de consulta: 18/03/2023).
12. Comisión Nacional para el Conocimiento y Uso de la Biodiversidad (CONABIO). 2023. Portal de información geográfica. http://www.conabio.gob.mx/informacion/gis/ (Fecha de consulta: 06/02/2023).
13. Comité de Información Estadística y Geografía (CEIEG). 2024. Datos Geográficos del Estado de Chiapas. Disponible en: https://ceieg-test.subseplan.chiapas.gob.mx/info-geografica (Fecha de consulta: 29/07/2023).
14. Cruz-Cárdenas, G.; Villaseñor, J. L.; López-Mata, L.; Martínez-Meyer, E.; Ortíz, E. 2014. Selección de predictores para el modelado de la distribución de especies en MaxEnt. Rev. Chapingo serie Ciencias forestales y del ambiente. 2: 187-201. DOI: https://doi.org/10.5154/r.rchscfa.2013.09.034

15. Dol, G.; Huvermann, R. 2020. Interacciones entre plantas y polinizadores a altas temperaturas. https://www.koppert.mx/content/mexico/noticias/2020/2020_10_19__Informaci%C3%B3n_importante_sobre_sistemas_de_polinizaci%C3%B3n_natural_en_altas_temperaturas/Interacciones_entre_plantas_y_polinizadores_a_altas_temperaturas.pdf (fecha de consulta: 21/03/2024).
16. Escoto, A.; Sánchez, L.; Gachuz, S. 2017. Trayectorias Socioeconómicas Compartidas (SSP): nuevas maneras de comprender el cambio climático y social. Rev. Estudios demográficos y urbanos. 32 (3): 669-693. DOI: http://dx.doi.org/10.24201/edu.v32i3.1684
17. Esperanza, M. 2013. Efectos del cambio climático en el rendimiento de tres cultivos mediante el uso del modelo AquaCrop. Instituto de Hidrología, Meteorología y Estudios Ambientales. Colombia.
18. Fick, S. E.; Hijmans, R. J. 2017. WorldClim 2: new 1-km spatial resolution climate surfaces for global land areas. International Journal of Climatology. DOI: 10.1002/joc.5086
19. Food and Agriculture Organization of the United Nations (FAO). 2008. Climate change and food security: A framework document. https://web.archive.org/web/20220325152622id_/https://www.fao.org/3/k2595e/k2595e00.pdf (accessed July 2023).
20. Goodman, M. M.; McK Bird, R. 1977. The races of maize IV: tentative grouping of 219 Latin American races. Rev. Econ Bot. 31: 204-221. DOI: https://doi.org/10.1007/BF02866591
21. Granados-Ramírez, R.; Longar, M. P. 2008. Variabilidad pluvial, agricultura y marginación en el estado de Michoacán. Rev. Análisis económico 54: 283-303.
22. Guajardo-Panes, R. A.; Granados-Ramírez, G. R.; Sánchez-Cohen, I.; Barradas-Miranda, V. L.; Gómez-Rojas, J. C.; Díaz-Padilla, G. 2018. Rendimientos de maíz (*Zea mays* L.) en escenarios de cambio climático en la región de la antigua, Veracruz-México. Rev. Agrociencias. 5: 725-739.
23. Ibarra-Montoya, J. L.; Rangel-Peraza, G.; González-Farias, F. A.; Anda, J.; Martínez-Meyer, E.; Macias-Cuellar, H. M. 2012. Uso del modelado de nicho ecológico como una herramienta para predecir la distribución potencial de *Microystis sp* (cianobacteria) en la Presa Hidroeléctrica de Aguamilpa, Nayarit, México. Rev. Ambi-Agua. 1: 218-234. DOI: http://dx.doi.org/10.4136/ambi-agua.607
24. Kato, T. A.; Mapes, C.; Mera, L.; Serratos, J.; Bye, R. A. 2009. Origen y diversificación del maíz. Ediciones Universidad Nacional Autónoma de México y Comisión Nacional para el Conocimiento y Uso de la Biodiversidad. 116p.
25. Kumar, S. N.; Aggarwal, P. K.; Rani, S.; Jain, S.; Saxena, R.; Chauhan, N. 2011. Impac of climate change on crop productivity in Western Ghats, coastal and northeastern regions of India. Current Science. 3: 332-341.
26. Lawlor, D. W. 2005. Plant responses to climate change: Impacts and adaptation. p. 81-88. DOI: 10.1007/4-431-31014-2_10
27. Liu, C.; Berry, P. M.; Dawson, T. P.; Pearson, R. G. 2005. Selecting thresholds of occurrence in the prediction of species distribution. Ecography. 28: 385-393. DOI: https://doi.org/10.1111/j.0906-7590.2005.03957.x
28. López-Romero, G.; Santacruz-Varela, A.; Muñoz-Orozco, A.; Castillo-González, F.; Córdova-Téllez, L.; Vaquera-Huerta, H. 2005. Caracterización morfológica de poblaciones nativas de maíz del Itsmo de Tehuantepec, México. Rev. Interciencia. 5: 284-290.
29. Luna-Flores, W.; Estrada-Medina, H.; Jiménez-Osornio, J. J.; Pinzón-López, L. L. 2012. Efecto del estrés hídrico sobre el crecimiento y eficiencia del uso del agua en plántulas de tres especies arbóreas caducifolias. Rev. Terra latinoamericana. 4: 343-353.
30. Magaña, A. L. 2014. Evaluación integral de los impactos de la variabilidad y el cambio climático en la agricultura de maíz en el estado de Michoacán. Tesis de grado en maestría en administración integral del ambiente. EL Colegio de la Frontera Norte. Tijuana. México. 157 p.
31. Martínez, E. 2015. Maíz, milpa, milperos y agricultura campesina en Chiapas. Resumen de tesis de grado en doctor en Desarrollo Rural. División de Ciencias Sociales y Humanidades. Universidad Autónoma Metropolitana. Xochimilco. 81 p.
32. Massieu, Y.; Lechuga, J. 2002. EL maíz en México: biodiversidad y cambios en el consumo. Rev. Análisis económico. 36: 281-303.
33. Mercer, K. L.; Perales, H. 2019. Estructura de la adaptación local a lo largo del paisaje: tiempo de floración y aptitud en variedades locales de maíz mexicano *(Zea mays* L. subsp. mays). Rev. Genetic Resources and Crop Evolution. 66: 27-45. DOI: https://doi.org/10.1007/s10722-018-0693-7
34. Nelson, G. C.; Rosegrant, M. W.; Koo, J.; Robertson, R.; Sulser, T.; Zhu, T.; Ringler, C.; Msangi, S.; Palazzo, A.; Batka, M.; Magalhaes, M.; Valmonte-Santos, R.; Ewing, M.; Lee, D. 2009. Cambio climático: El impacto en la agricultura y los costos de adaptación. Washington, D. C. Ediciones Instituto Internacional de Investigación sobre políticas alimentarias. 23 p. DOI: 10.2499/0896295370
35. Noriega, B. S.; Rodríguez, R. E.; López, I. A.; Buchi, C. S.; Girón, M. H.; Flores, M. A. 2021. Importancia del contexto social para la investigación. Revista científica del Sistema de Estudios de Posgrado. 1: 77-87. DOI: https://doi.org/10.36958/sep.v4i1.77
36. Nuricumbo, A. 2015. Zapalote Chico: Soberanía alimentaria en el Itsmo de Tehuantepec, México. Facultad de Ciencias. Universidad de Vigo. Tesis de grado doctoral en Ciencia y Tecnología Agroalimentaria. España. 83 p.

37. Olivo, M. L.; Soto-Olivo, A. 2010. Comportamiento de los gases de efecto invernadero y las temperaturas atmosféricas con sus escenarios de incremento potencial. Revista de la Universidad Experimental Politécnica. 57: 221-230.
38. O'Neill, B. C.; Tebaldi, C.; Vuuren, D. P.; Eyring, V.; Friedlingstein, P.; Hurtt, G.; Knutti R.; Kriegler, E.; Lamarque, J. F.; Lowe, J.; Meehl, G. A.; Moss, R.; Riahi, K.; Sanderson, B. M. 2016. The Scenario Model Intercomparison Project (ScenarioMIP) for CMIP6. Geoscientific Model Development. 9: 3461-3482. DOI: 10.5194/gmd-9-3461-2016
39. Palma-Ordaz, S.; Delgadillo-Rodríguez, J. 2014. Distribución de ocho especies exóticas de carácter invasor en el estado de Baja California, México. Botanical Sciences. 92(4): 587-597.
40. Perales, H. 2012. Maíz: nuestra herencia y responsabilidad. Ecofronteras. 46: 2-5.
41. Phillips, S. J.; Anderson, R. P.; Schapire, R. E. 2006. Maximum entropy modeling of species geographic distributions. Ecological Modelling. 190: 231-259. DOI: https://doi.org/10.1016/j.ecolmodel.2005.03.026
42. Pozo-Gómez, D. M.; Orantes-García, C.; Sánchez-Cortéz, M. S.; Rioja-Paradela, T.; Carrillo-Reyes, A. 2022. Potential distribution of *Croton guatemalensis*: A model with reproductive biology data. Botanical Sciences. (100)2: 291-299. DOI: https://doi.org/10.17129/botsci.2865
43. QGIS.org. 2023. QGIS Geographic Information System. QGIS Association. http://www. qgis.org (Accessed June 2023).
44. Quevedo, D. C.; Cervantes, J.; Noriero, L.; Zepeda, J. M. 2017. Maíz: Sustento de vida en la cultura Teenek. Comunidad Tamaletom, Tancanhuitz, S.L.P, México. Revista de Geografía Agrícola 58: 5-19.
45. Ramírez, O.; Ibarra, D. G.; Gutiérrez, A. 2023. Análisis económico de la producción de maíz en Chiapas, México, en la región Frailesca. Revista Científica Multidisciplinar. 4: 423-437. DOI: https://doi.org/10.37811/cl_rcm.v7i4.6879
46. Ramírez-Magil, G.; Botello, F.; Navarro-Martínez, A.; Ramírez-Magil, G.; Botello, F.; Navarro-Martínez, A. 2020. Idoneidad de hábitat para *Swietenia macrophylla* en escenarios de cambio climático en México. Rev. Madera y bosques. 3. DOI: https://doi.org/10.21829/myb.2020.2631954
47. R Core Team. 2022. R: A Language and Environment for Statistical Computing. R Foundation for Statistical Computing. https://www.R-project.org/ (Accessed May 2023).
48. Rincón-Tuexi, J. A.; Castro-Nava, S.; López-Santillán, J. A.; Huerta, A. J.; Trejo-López, C.; Briones-Encinia, F. 2006. Temperatura alta y estrés hídrico durante la floración en poblaciones de maíz tropical. Revista Internacional Botánica Experimental. 75: 31-40.
49. Rivera, D. A. 2020. Impacto del cambio climático en la distribución potencial de especies nativas de interés agrícola en México. Instituto de Ciencias. Benemérita Universidad Autónoma de Puebla. Tesis de grado en maestría en Manejo Sostenible de Agroecosistemas. Puebla. 62 p.
50. RStudio Team. 2022. RStudio: Integrated Development Environment for R. RStudio. PBC. Boston.
51. Ruiz, J, A.; Durán, N.; Sánchez, J. J.; Ron, J.; González, D. R.; Holland, J. B.; Medina, G. Climatic rdaptation and ecological descriptors of 42 Mexican maize races. Crop Science. 48: 1502-1512. DOI: https://doi.org/10.2135/cropsci2007.09.0518
52. Sánchez, J, J.; Goodman, M. M.; Stuber, C.W. 2000. Isozymatic and morphological diversity in the races of maize of Mexico. Economic Botany. 54: 43-59. DOI: https://doi.org/10.1007/BF02866599.
53. Santiago, A. 2010. Aspectos básicos de la fisiología en respuesta a estrés y el clima como condicionante del mismo en las plantas. https://exa.unne.edu.ar/biologia/ fisiologia.vegetal/Aspectosb%C3%A1sicosfisiolog%C3%ADarespuestaestr%C3%A9s.pdf (fecha de consulta: 12/11/2023).
54. Sistema Nacional de Información sobre Biodiversidad (SNIB). 2023. Precipitación anual en México (1910-2009). http://www.conabio.gob.mx/informacion/gis/?vns=gis_root/clima/precip/preanu13gw (fecha de consulta: 25/02/2023).
55. Soto, L.; Jiménez, G.; Lerner, T. 2008. Diseño de sistemas agroforestales para la producción y la conservación. Ediciones El Colegio de la Frontera Sur. 90 p.
56. Tinoco-Ruedas, J.; Gómez-Díaz, J.; Monterroso-Rivas, A. 2011. Efectos del cambio climático en la distribución potencial del maíz en el estado de Jalisco, México. Rev. Terra Latinoamericana. 29(2): 161-168.
57. Ureta, C.; Martínez-Meyer, E.; Perales, H. R.; Álvarez-Buylla E. 2011. Projecting the effects of climate change on the distribution of maize races and their wild relatives in Mexico. Mexico. Global Change Biology. DOI: https://doi.org/10.1111/j.1365-2486.2011.02607.x
58. Zarco, E.; González, V. A.; López, M. C.; Salinas Y. 2005. Marcadores fisiológicos de la tolerancia a sequía en maíz (*Zea mays* L.). Rev. Agrociencia. 5: 517-528.

Radial Growth Dynamics and Drought Resilience in *Pinus pinea* L. Plantations from Central-Western Argentina: Implications for Forestry Development

Dinámica del crecimiento radial y resiliencia a la sequía de *Pinus pinea* L. en plantaciones del centro-oeste argentino: implicancias forestales

Sergio Piraino [1, 2*], Luciano Diaz Dentoni [3], Fidel Alejandro Roig [1, 2, 4]

Originales: *Recepción:* 20/05/2025 - *Aceptación:* 21/10/2025

ABSTRACT

Forests play a crucial role in ecological stability, carbon sequestration, habitat provision and economy. As climate change intensifies, increasing drought frequency and severity challenge our understanding of forest resilience. Based on this premise, we examined radial growth dynamics and drought response of *Pinus pinea* L. in Mendoza Province in both mesic and xeric conditions. Using dendrochronological techniques, we assessed the long and short-term effects of soil and atmospheric drought on radial growth trends at two irrigated plantations with contrasting environments. Growth dynamics reflected differences in soil, climate, and irrigation. Growth rates were significantly higher at the mesic stand, which received nearly twice the precipitation and irrigation compared to xeric one. In contrast, growth at the xeric site was strongly limited by early-summer atmospheric drought, while late-growing season soil moisture and climatic conditions affected tree-ring development at the mesic site. Growth resilience to extreme events experienced site dependence, with edaphic drought exerting a stronger negative effect than atmospheric dry spells at the mesic stand. Our results underscore the importance of integrating short- and long-term drought assessment into *P. pinea* management strategies and support the potential of stone pine plantations in extra-Mediterranean South America for sustainable forestry under changing climatic conditions.

Keywords
climate change • forest management • Mendoza • tree-rings

https://doi.org/10.48162/rev.39.191

1 Instituto Argentino de Nivología, Glaciología y Ciencias Ambientales. Consejo Nacional de Investigaciones Científicas y Técnicas (IANIGLA CONICET). Laboratorio de Dendrocronología e Historia Ambiental. Av. Dr. Adrian Ruiz Leal. Parque Gral. San Martín. M5500 Mendoza. Argentina.
2 Universidad Nacional de Cuyo. Facultad de Ciencias Agrarias. Cátedra de Economía y Política Agraria. Almirante Brown 500. M5528AHB. Chacras de Coria. Mendoza. Argentina.
* spiraino@fca.uncu.edu.ar; spiraino@mendoza-conicet.gob.ar
3 Universidad Nacional de Cuyo. Facultad de Ciencias Agrarias. Almirante Brown 500. M5528AHB. Chacras de Coria. Mendoza. Argentina.
4 Universidad Mayor. Facultad de Ciencias. Hémera Centro de Observación de la Tierra. Camino La Pirámide 5750. Huechuraba. Santiago.Chile.

Licenses Creative Commons
Attribution - Non Commercial - Share Alike

Resumen

Los bosques son esenciales en la estabilidad ecológica, la captura de carbono, la provisión de hábitats y de recursos económicos. Ante el aumento de la frecuencia y severidad de las sequías asociado al cambio climático, comprender la resiliencia forestal resulta crucial. Este estudio analizó mediante métodos dendrocronológicos los efectos a corto y largo plazo de las sequías edáficas y atmosféricas sobre el crecimiento radial de *Pinus pinea* L. en dos plantaciones irrigadas bajo condiciones ambientales contrastantes en el centro-oeste argentino. Los patrones de crecimiento reflejaron diferencias ambientales y de manejo. Las tasas de crecimiento fueron significativamente mayores en el rodal mésico, que recibió casi el doble de precipitación e irrigación que el xérico. En este último, el crecimiento se vio limitado por sequías atmosféricas de comienzo del verano, mientras que en el mésico influyeron las sequías edáficas y climáticas al final de la temporada de crecimiento. La resiliencia ante eventos extremos mostró dependencia del sitio, con un efecto negativo más marcado de la sequía edáfica en el rodal mésico. Los resultados destacan la necesidad de integrar evaluaciones multitemporales de sequía en el manejo de *P. pinea* y su potencial para un desarrollo forestal sostenible en regiones extra-Mediterráneas de Sudamérica.

Palabras clave
cambio climático • manejo forestal • Mendoza • anillos de crecimiento de árboles

Introduction

Forests maintain ecological balance by storing carbon, regulating water cycles, and providing habitat for numerous species (Barnes *et al.*, 1997). Recent climatic shifts have increased the focus on the resilience of natural and planted forests under abiotic disturbances (Johnstone *et al.*, 2016). Drought threatens forest health and productivity, as dry spells become more frequent and intense (IPCC, 2023). Extreme drought events have severely impacted forests, reducing growth rates and increasing tree mortality (Allen *et al.*, 2010).

Due to their genetic uniformity, plantation forests may respond differently to dry spells than natural woodlands (Camarero *et al.*, 2021; Navarro-Cerrillo *et al.*, 2023). Their capacity to withstand and recover from a drought event dictates their long-term sustainability and broader environmental and economic values. Even considering that forest plantations only cover about 7% of the global forest area, they significantly contribute to mitigating deforestation impacts on natural woodlands (FAO, 2020). This provides particular importance to the in-depth understanding of their drought resilience.

Drought stress manifests in two primary forms: atmospheric drought, driven by low humidity and high evaporative demand, and edaphic drought, characterized by depleted soil water (Mishra & Singh, 2010). These conditions can occur separately or together, each uniquely impacting plant growth (Knutzen *et al.*, 2017). Disentangling these responses is key to predicting how trees will perform in a changing climate.

Forest responses to extreme drought can be assessed by analyzing long- and short-term growth trends. Long-term trends reveal climate-growth relationships, while short-term responses measure resilience, that is, the capacity to withstand and recover from dry spells (Lloret *et al.*, 2011). Dendrochronology provides a powerful method for investigating tree growth responses to ecological variables, allowing us to reconstruct growth trends and identify periods of stress, thereby illuminating species' resilience and adaptability (Piraino, 2020; Piraino *et al.*, 2022, 2024).

Pinus pinea L. (stone pine), a conifer prized for its edible seeds, holds significant ecological and economic value (Mutke *et al.*, 2012). In its native Mediterranean range, the species now suffers drought-related decline in cone yield (Calama *et al.*, 2020). Climate models project a contraction of its suitable habitat and a negative trend in radial growth (Mechergui *et al.*, 2021; Natalini *et al.*, 2024). Establishing extra-Mediterranean plantations could help offset the impending global shortfall in nut production.

Growers have successfully introduced stone pine to southern South America (Chile and Argentina) (Muñoz *et al.*, 2012), where it adapts well to diverse conditions and promises economic benefits from non-timber products (Loewe-Muñoz *et al.*, 2012). Recent studies have analyzed tree-ring variability and its relationship with climate trends and extremes in Chilean plantations under typical Mediterranean conditions (Loewe Muñoz *et al.*, 2024ab). However, no research has yet reconstructed radial growth dynamics in Argentina, where the species thrives in semi-arid environments (Calderón *et al.*, 2008; Diaz Dentoni, 2024).

This study aims to investigate how *P. pinea* radial growth interacts with drought conditions in two irrigated plantations located in Argentina's Mendoza Province. We hypothesize that drought events significantly suppress growth, with the stronger effects during extreme dry years. Our findings will clarify the potential of this species for forestry in extra-Mediterranean regions, especially as climate change threatens its native range.

Material and Methods

Study Site Characteristics

We selected two sites for this study: Dique Yaucha (hereafter YAU; 34°00'03" S, 69°07'03" W) and Malargüe (hereafter MAL: 35°35'55" S, 69°31'37" W), both located in southern Mendoza Province (figure 1, page 4). These plantations represent the only undisturbed adult artificial forests in the region (Piraino *et al.*, 2021).

At both sites, stone pine seedlings were planted between the late 1980s and early 1990s, forming a monospecific plantation with a spacing of 3x3 m between rows and trees. The plantations are situated at similar elevations (1213 m a. s. l. for YAU vs 1470 m a. s. l. for MAL). The YAU site is characterized by semi-arid conditions, with mean annual temperature of 15°C, and total annual precipitation of 335 mm (figure 1, page 4). In contrast, MAL grows under Mediterranean-type climate, with mean annual temperature and total annual precipitation values of 12.6°C and 610 mm, respectively (figure 1, page 4). Soils are gravelly to sandy with good permeability at YAU, and loam to clay loam of alluvial origin at MAL. Both plantations receive supplementary irrigation: approximately 300-350 mm annually at YAU and 500-600 mm at MAL, evenly distributed across the irrigation season (September-July; current and projected upper river water balance 2020-2021; G. Aguado, *personal communication*). According to this characterization, we considered YAU and MAL sites xeric and mesic, respectively.

Dendrochronological Sampling and Tree-Ring Chronology Development

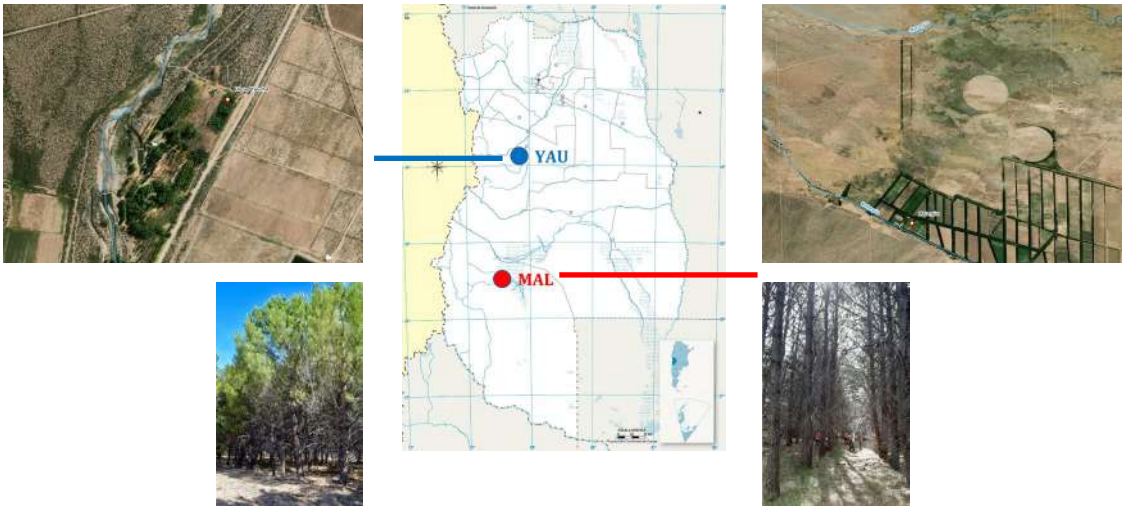
During the austral spring of 2021 and 2022, we extracted one core per tree at breast height (approximately 1.30 m above soil level) from 16 individuals at YAU and 10 at MAL, respectively, by using a 5.15 mm increment borer. We selected sampled trees based on their health status. Cores were glued onto wooden mounts, and the transverse section was polished with progressively finer sandpaper to highlight ring boundaries. Samples were scanned at 1200 dpi, and tree-ring width (TRW) was measured to 0.001 mm precision with CooRecorder software (Maxwell & Larsson, 2021). Calendar years were assigned following Schulman's convention for the Southern Hemisphere (Schulman, 1956).

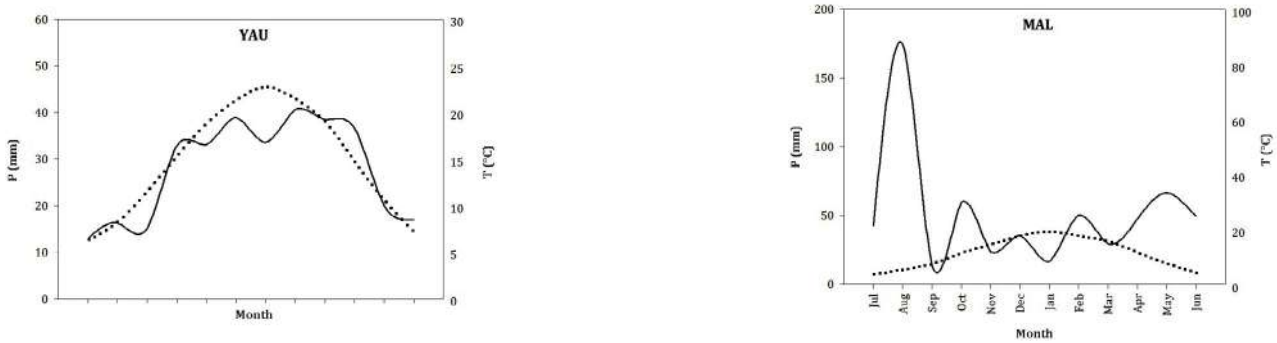
TRW series were statistically validated with COFECHA software (Holmes, 1983). Two indices were calculated: 1) the mean correlation among individual series (MC); and 2) mean sensitivity (MS), the relative year-to-year variability in TRW, reflecting the species' sensitivity to environmental factors (Speer, 2010).

After statistical validation, individual chronologies were standardized to remove the low-frequency, age-related trends and highlight the high-frequency climate signal (Speer, 2010). Raw TRW series were detrended using a 20-years spline with a 50% frequency cutoff applied in ARSTAN40c software (Cook & Krusic, 2008). We used the standardized residual chronology version for all drought-growth analyses to minimize bias from non-climatic trends (Villalba & Veblen, 1997).



Source/Fuente: IGN





Precipitation and temperature data belong to the INTA San Carlos (Dique Yaucha: 33.73°S, 69.1°W; http://siga.inta.gob.ar/#/), and Malargüe Aero (Malargüe: 35.48°S; 69.58°W; http://www.meteomanz.com/) gauge stations, covering the 2000-2020 period. T: monthly mean air temperature; P: monthly total rainfall. Gray dot line refers to monthly mean air temperature, and black solid line to monthly total rainfall.

Los datos de precipitación y temperatura pertenecen a las estaciones climáticas INTA San Carlos (Dique Yaucha: 33.73°S, 69.1°O; http://siga.inta.gob.ar/#/) y Malargüe Aero (Malargüe: 35.48°S; 69.58°O; http://www.meteomanz.com/), y cubren el período 2000-2020. T: temperatura media mensual del aire; P: precipitación total mensual. La línea de puntos grises indica la temperatura media mensual del aire, y la línea negra continua, la precipitación total mensual.

Figure 1. Geographical location of the sampled sites and Ombrothermic diagram drawn according to the methods of Bagnouls & Gaussen (1953).

Figura 1. Ubicación geográfica de los sitios muestreados y diagrama ombrotérmico elaborado según los métodos de Bagnouls & Gaussen (1953).

Statistical Analyses

To assess differences in TRW trends among sites under varying environmental conditions, we compared the raw ring-width site chronologies for the common period 1992-2020 with a Kruskal-Wallis test hosted in the InfoStat software (Di Rienzo *et al.*, 2021). Then, we used site and individual- standardized chronologies to evaluate the effect of drought on growth at long and short-term timescales. For the long-term analysis, correlation functions were calculated between the standardized site-chronologies and two datasets: SPEI (Standardized Precipitation Evaporation Index; Vicente-Serrano *et al.*, 2010), and soil moisture at 100 cm depth (SM100). Monthly values of both datasets were obtained from the KNMI Climate Explorer for 1901-2018 (SPEI) and 1979-2016 (SM100) (Trouet & Van Oldenborgh, 2013; http://climexp.knmi.nl/). Correlation functions were computed with DENDROCLIM2002 for the common period 1992-2016 (n = 25) (Biondi & Waikul, 2004). We selected this interval because the YAU chronology began in 1992 and SM100 data ended in 2016. Based on prior research, stone pine plantations in South America (Loewe-Muñoz *et al.*, 2022), a 13-month time-window was selected, spanning June of the year preceding growth through June of the growth year. No monthly irrigation data were available, which prevented direct comparison between supplementary water inputs and ring development.

We assessed short-term growth responses to extreme drought using the line of full resilience (LFR; Schwarz *et al.*, 2020). The LFR approach evaluates the relationship between resistance and recovery *sensu* Lloret *et al.*, 2011; see below for mathematical definitions. and compares it with the theoretical scenario of full resilience (Schwarz *et al.*, 2020). This method provides an integrated assessment of tree capacity to withstand drought stress (Schwarz *et al.*, 2020).

We defined drought years based on the significant monthly windows identified by the correlation function analysis, which we used to calculate annual series for SPEI and SM100. We classified years with SPEI or SM100 values in the lowest 5th percentile as extreme drought events. For these events, we calculated tree-level resistance (R_t) and recovery (R_c) indices as $R_t = TRI_d/TRI_pre_d$ and $R_c = TRI_post_d/TRI_d$. TRI is the standardized tree-ring index, *d* refers to the drought year, and *pre* and *post* denote the year before and after extreme dry spell, respectively (Lloret *et al.*, 2011). Short p*re* and *post* time windows were chosen to minimize overlap among consecutive drought events (see Results). Finally, Finally, we calculated the LFR as $R_c = 1/R_t$.

Results

We developed two tree-ring chronologies from 10 (MAL) and 16 (YAU) wood samples (table 1 and figure 2, page 6). The chronologies covered 1991-2020 at MAL and 1992-2021 at YAU (table 1, page 6). Mean annual raw TRW (mTRW) was significantly higher at MAL than at YAU stand ($H = 8.35$; $p = 0.0039$; data not shown). Tree-ring statistics showed higher MC and MS values for YAU (table 1, page 6).

Correlation function analyses revealed that radial growth at both sites was significantly influenced by long-term drought conditions, although responses differed between stands (figure 3, page 6). At MAL, standardized growth was positively related to late spring (June; JUN) SPEI and SM100. At YAU, SPEI positively influenced ring width during December (DEC) of the year of growth, while no significant relationship emerged with SM100 (figure 3, page 6).

Based on these results, we selected JUN-SM100 and JUN-SPEI to identify extreme drought events at MAL, and DEC-SPEI at YAU stand. Statistical analyses identified three extreme drought events at MAL (MAL-SM100 2010: MAL-SPEI 2012; MAL-SPEI 2014) and two at YAU (YAU-SPEI 2003 and YAU -SPEI 2011) (figure 4, page 7). We excluded the YAU -SPEI 2003 event, as trees were likely in their seedling phase.

LFR analysis revealed contrasting responses among stands (figure 5, page 8). At YAU, only 6% of trees displayed full resilience to the 2011 extreme drought. At MAL, no tree exhibited full resilience to the 2010 SM100 event. In contrast, LFR values were comparable between the MAL-SPEI 2012 (LFR = 40%) and the MAL-SPEI 2014 (LFR = 50%) events (figure 5, page 8).

Table 1. Characteristics of the tree-ring chronologies.

Tabla 1. Características de las cronologías de anillos de crecimiento.

Site	N	Period	mTRW (mm/year)	MC	MS
YAU	16	1992-2021	0.41	0.57	0.37
MAL	10	1991-2020	0.72	0.55	0.18

N: Number of sampled trees per site. Period: time range of the sampled cores. mTRW: mean annual tree-ring width value. MC: mean correlation between series at each stand. MS: mean sensitivity.

N: Número de árboles muestreados por sitio. Period: rango temporal de las muestras. mTRW: valor medio anual del ancho de anillo. MC: correlación media entre series en cada rodal. MS: sensibilidad media.

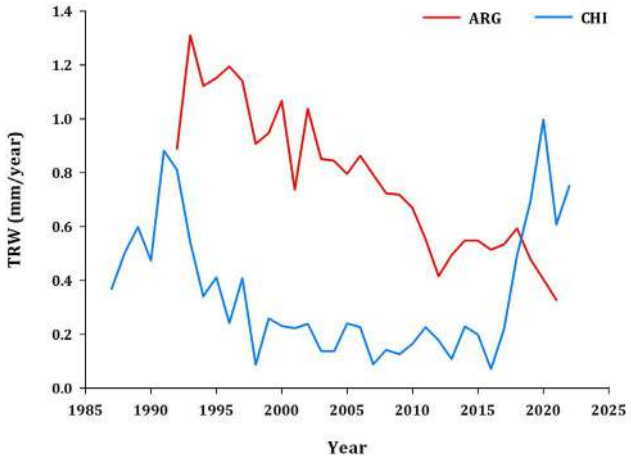
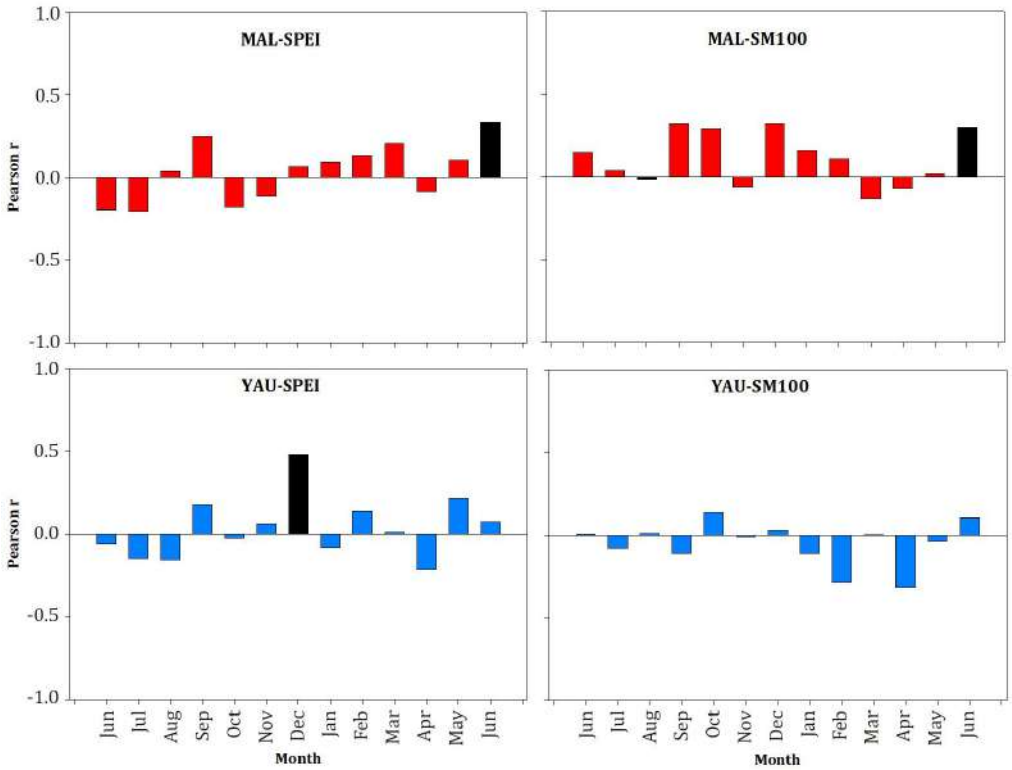


Figure 2. Raw tree-ring width (TRW) site chronologies of the sampled stone pine plantations.

Figura 2. Cronologías de datos brutos de ancho de anillo (TRW) de las plantaciones de pino piñonero muestreadas.

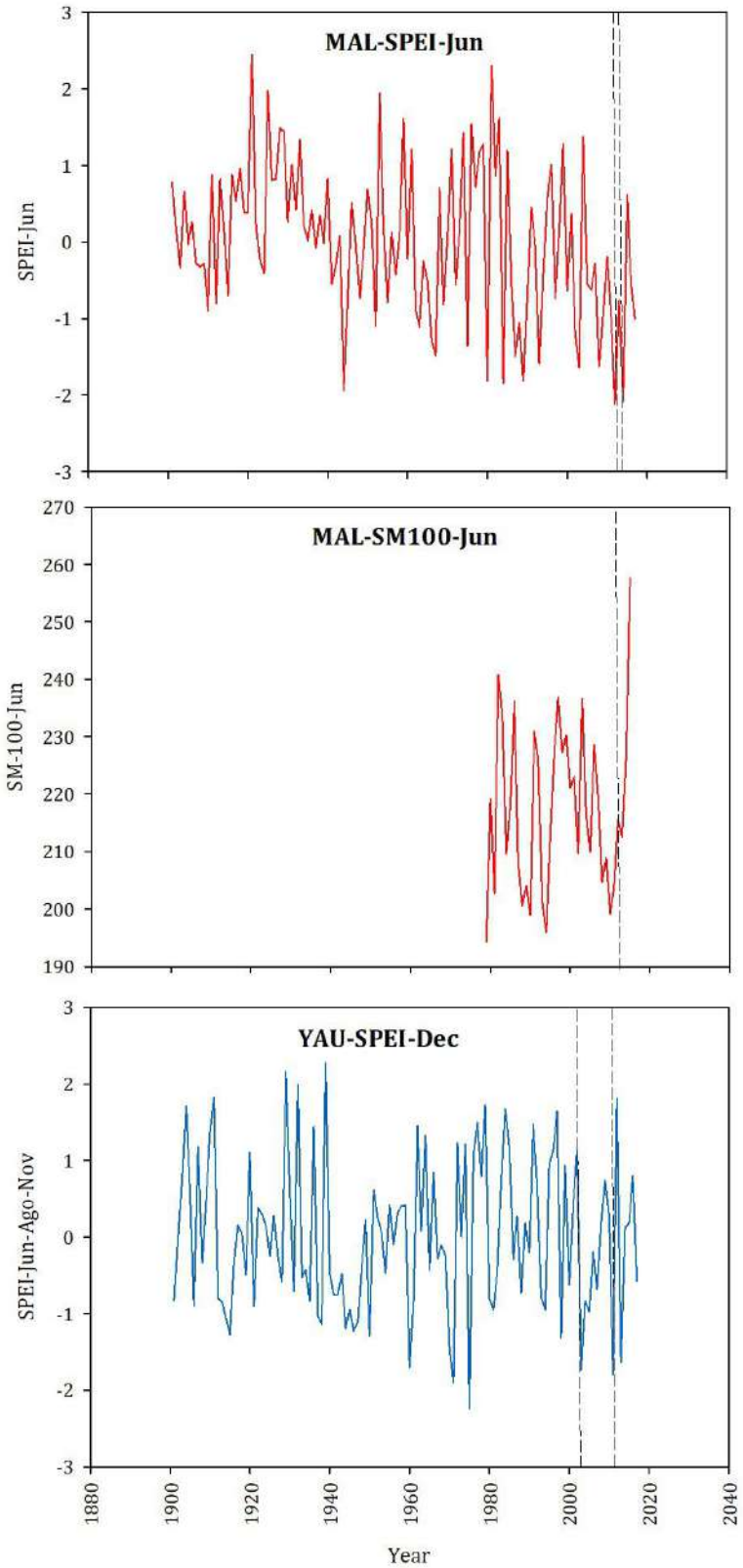


Black bars refer to significant Pearson *r* values at $p < 0.05$ level.

Las barras negras indican valores de correlación de Pearson significativos por $p < 0,05$.

Figure 3. Correlation functions results between each residual chronology and monthly SPEI and SM100 values for the common period 1992-2016.

Figura 3. Resultados de las funciones de correlación entre cada cronología residual y los valores mensuales de SPEI y SM100 para el período común 1992-2016.

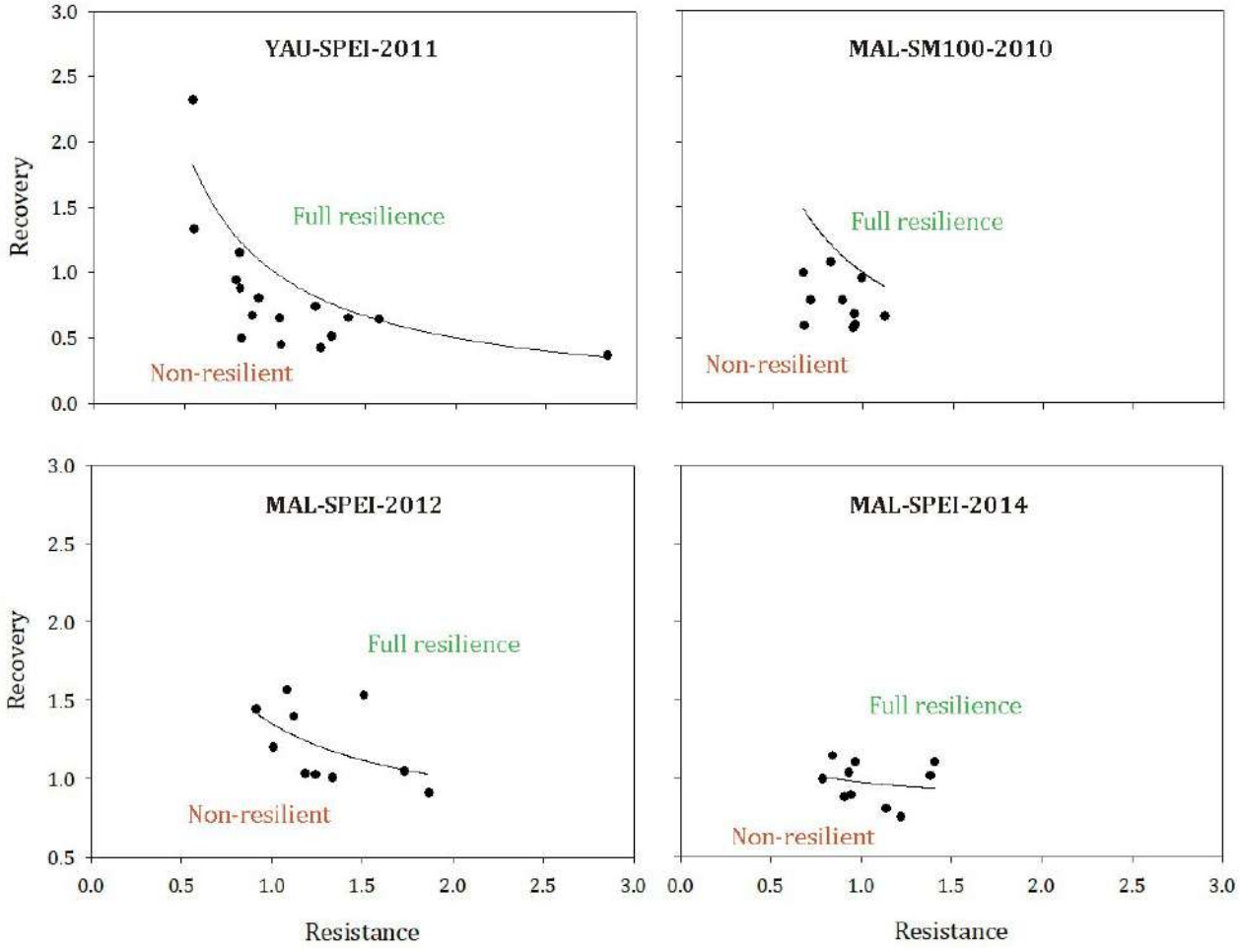


Vertical lines refer to local extreme drought events.

Las líneas verticales indican los eventos locales de sequía extrema.

Figure 4. Historical series of SPEI and SM100 at each site based on correlation function results.

Figura 4. Series históricas de SPEI y SM100 por cada sitio, basadas en los resultados de las funciones de correlación.



Dots located above the LFR correspond to trees exhibiting full resilience (Resilience = 1.0).
Los puntos situados por encima de la LFR corresponden a los árboles que exhiben resiliencia plena (Resiliencia = 1.0).

Figure 5. Comparison of the relationship between observed tree-level mean values of R_t and R_c and the hypothetical function (black curve) representing the LFR across all R_t values, for the analyzed extreme atmospheric and edaphic drought events.

Figura 5. Comparación de la relación entre los valores medios observados a nivel de árbol de R_t y R_c y la función hipotética (curva negra) que representa la LFR a lo largo de todos los valores de R_t, para los eventos analizados de sequía atmosférica y edáfica extrema.

DISCUSSION

This study provided novel information of how stone pine growing in an extra-Mediterranean region responds to atmospheric and edaphic drought across multiple timescales. Previous research addressed the species' dendroclimatological signal and resilience to extreme climatic events in Chile (Loewe-Muñoz *et al.*, 2024ab), but no studies had explored these dynamics under the environmental conditions of central-western Argentina. Our findings offer new insights of *P. pinea* growth and drought resilience beyond its native Mediterranean habitat, confirming the species' adaptability to new climatic contexts.

Although our sample size was relatively small, it well represented growth dynamics of both populations. At MAL, sampled trees accounted for 85% of the original plantation (n = 12). At YAU, the tree-ring chronology reliably captured stand-level growth, with an Expressed Population Signal (EPS; Wigley *et al.*, 1984) exceeding the 0.85 threshold, indicating strong agreement between sampled trees and the overall population (data not shown).

The mean correlation coefficient among individual series fell within the range reported in literature, confirming the robustness of our ring-width measurements (Natalini *et al.*, 2016; Piraino *et al.*, 2013). At YAU, MS was twice as high as at MAL. Theoretically, MS should reflect MC variability, since both indices are strongly related (Fritts *et al.*, 1965). Nevertheless, MC differed only slightly between stands. The higher irrigation regime at MAL likely explained the differences in MS values by reducing growth sensitivity to environmental variability. This interpretation agrees with previous studies in Central European conifer comparing irrigated and non-irrigated woodlands (Feichtinger *et al.*, 2014; Rigling *et al.*, 2003).

Mean TRW at both sites exceeded values previously reported (Mechergui *et al.*, 2021). This pattern likely reflects both the relatively young age of the plantations, with trees probably still at their juvenile growth phase, and the benefit of irrigation, which can extend the growing season, enhance nutrient mobility, and increase primary production (Feichtinger *et al.*, 2014; Loewe-Muñoz *et al.*, 2024a). The higher mTRW at MAL compared with YAU further reflects the more favorable water balance at that site (precipitation + irrigation: see Materials and Methods).

Our analyses of drought-radial growth relationships across timescales indicated that irrigation did not fully decouple growth from climate, suggesting that the supplementary water was likely insufficient (Perulli *et al.*, 2019). This limitation was particularly evident at YAU, where radial growth benefited only during the early phases of ring development. These results have practical implications for managing future plantations in semi-arid central-west Argentina. However, the lack of systematic irrigation records prevented statistical evaluation of watering effect. For future *P. pinea* plantations in Mendoza, we recommend monitoring irrigation at least monthly to enable direct comparison between radial growth dynamics and water supply.

Correlation function analyses provided quantitative evidence of the species' distinct responses to atmospheric and edaphic drought. At MAL, radial growth correlated with high soil moisture and wet atmospheric conditions at the end of the growing season. In contrast, at YAU, ring width responded positively to early summer (December) SPEI. Previous studies in the Mediterranean range reported similar patterns, showing that radial growth benefits from low evapotranspiration during the growing season and from abundant precipitation before cambium reactivation (Mechergui *et al.*, 2021). Physiologically, *P. pinea* is a drought-tolerant species, capable of reducing photosynthetic activity during water stress through root mortality, stomata control, and biomass allocation (Mechergui *et al.*, 2021). Nevertheless, drought constrains tree growth by reducing sap flow and significantly decreasing stem increment (Mechergui *et al.*, 2021; Piraino, 2020). Our findings confirm that, regardless of irrigation, the species' radial growth remains constrained by unfavorable environmental conditions during the growing period (Loewe-Muñoz *et al.*, 2024b; Piraino, 2020).

Analysis of annual SPEI and SM100 series identified several extreme drought events that impacted growth dynamics at both sites. At MAL, edaphic dry spells exerted stronger short-term effects on growth than atmospheric droughts. This difference may reflect the direct impact of soil water deficit on roots uptake, whereas atmospheric drought primarily affects transpiration and leaf water potential, which may not immediately restrict stem growth if surface soil moisture remains sufficient (Berauer *et al.*, 2024). Future studies should integrate physiological data from both root and stem levels, along with site-specific infiltration rates, to better characterize the species responses to different drought types.

Conclusion

Our study provides critical baseline data on the radial growth and drought resilience of *P. pinea*, establishing a foundation for evaluating its potential for forestry development beyond Mediterranean environments. These findings are especially relevant for Mendoza Province, where current forestry focuses almost exclusively on medium-quality wood production from more water-demanding species like as *Populus* spp. Expanding *P. pinea* cultivation would diversify local forestry and could yield substantial economic benefits under the semi-arid conditions of central-western Argentina.

References

Allen, C. D., Macalady, A. K., Chenchouni, H., Bachelet, D., McDowell, N., Vennetier, M., Kitzberger, T., Rigling , A., Breshears, D. D., Hogg, E. H., Gonzalez, P., Fensham, R., Zhang, Z., Castro, J., Demidova, N., Lim, J. N., Allard, G., S., Running S. W., Semerci, A., Cobb, N. (2010). A global overview of drought and heat-induced tree mortality reveals emerging climate change risks for forests. *Forest ecology and management, 259*(4), 660-684.

Bagnouls, F. (1953). Saison sèche et indice xérothermique. *Bull Soc His nat Toulouse, 88,* 193-239.

Barnes, B. V., Zak, D. R., Denton, S. R., & Spurr, S. H. (1997). *IForest ecology* (N° Ed. 4, p. xviii+-774).

Berauer, B. J., Steppuhn, A., & Schweiger, A. H. (2024). The multidimensionality of plant drought stress: The relative importance of edaphic and atmospheric drought. *Plant, Cell & Environment, 47*(9), 3528-3540.

Biondi, F., & Waikul, K. (2004). DENDROCLIM2002: A C++ program for statistical calibration of climate signals in tree-ring chronologies. *Computers & geosciences, 30*(3), 303-311.

Calama, R., Gordo, J., Mutke, S., Conde, M., Madrigal, G., Garriga, E., Arias, M. J., Piqué, M., Gandía, R., Monterno, G., Pardos, M. (2020). Decline in commercial pine nut and kernel yield in Mediterranean stone pine (*Pinus pinea* L.) in Spain. *Forest-Biogeosciences and Forestry, 13*(4), 251.

Calderón, A., Bustamante, J. A., Riu, N., Perez, S. (2008). Conifers behaviour under irrigation in the Yaucha dam. Mendoza, Argentina. *Revista de la Facultad de Ciencias Agrarias. Universidad Nacional de Cuyo. 40*(1): 67-72. https://bdigital.uncu.edu.ar/app/navegador/?idobjeto=2676

Camarero, J. J., Gazol, A., Linares, J. C., Fajardo, A., Colangelo, M., Valeriano, C., Sánchez-Salguero, R., Sangüesa-Barreda, G., Granda, E., Gimeno, T. E. (2021). Differences in temperature sensitivity and drought recovery between natural stands and plantations of conifers are species-specific. *Science of the Total Environment, 796*, 148930.

Cook, E. R., & Krusic, P. J. (2008). *A tree-ring standardization program based on detrending and autoregressive time series modeling, with interactive graphics (ARSTAN)*. http://www. ldeo. columbia. edu/res/fac/trl/public/publicSoftware. html

Diaz Dentoni, L. (2024). *Análisis de la dinámica de crecimiento de Pinus pinea l. en dos parcelas bajo riego en la provincia de Mendoza.* Tesis de grado. FCA-UNCuyo. 34p.

Di Rienzo, J., Casanoves, F., Balzarini, M., Gonzalez, L., Tablada, M., Robledo, C. (2021). *InfoStat version 2021*.

FAO (Food and Agriculture Organization). (2020). *Global Forest Resources Assessment 2020: Main report*. FAO, Rome.

Feichtinger, L. M., Eilmann, B., Buchmann, N., & Rigling, A. (2014). Growth adjustments of conifers to drought and to century-long irrigation. *Forest Ecology and Management, 334*, 96-105.

Fritts, H. C., Smith, D. G., Cardis, J. W., & Budelsky, C. A. (1965). Tree-ring characteristics along a vegetation gradient in northern Arizona. *Ecology, 46*(4), 393-401.

Holmes, R. L. (1983). Computer-assisted quality control in tree-ring dating and measurement. *Tree-Ring Bulletin, Vol. 43.* 1-10.

IPCC (2023). *Sections. In: Climate Change 2023: Synthesis Report. Contribution of Working Groups I, II and III to the Sixth Assessment Report of the Intergovernmental Panel on Climate Change* [Core Writing Team, H. Lee and J. Romero (eds.)]. IPCC. p. 35-115.

Johnstone, J. F., Allen, C. D., Franklin, J. F., Frelich, L. E., Harvey, B. J., Higuera, P. E., Mack, M. C., Meentemeyer, R. K., Metz, M. R., Perry, G. L. W., Schoennagel, T., Turner, M. G. (2016). Changing disturbance regimes, ecological memory, and forest resilience. *Frontiers in Ecology and the Environment, 14*(7), 369-378.

Knutzen, F., Dulamsuren, C., Meier, I. C., & Leuschner, C. (2017). Recent climate warming-related growth decline impairs European beech in the center of its distribution range. *Ecosystems, 20*, 1494- 1511.

Lloret, F., Keeling, E. G., & Sala, A. (2011). Components of tree resilience: effects of successive low-growth episodes in old ponderosa pine forests. *Oikos, 120*(12), 1909-1920.

Loewe Muñoz, V., Delard, C., González González, M., Mutke, S., Fuentes Díaz, V. (2012). Introducción del pino piñonero (*Pinus pinea* L.) en Chile. *Ciencia & Investigación Forestal,18*(2), 39-52.

Loewe-Muñoz, V., Del Río, R., Delard, C., Balzarini, M. (2022). A detailed time series of hourly circumference variations in *Pinus pinea* L. in Chile. *Annals of Forest Science. 79*(1): 4.

Loewe-Muñoz, V., Del Río, R., Delard, C., Cachinero-Vivar, A. M., Camarero, J. J., Navarro-Cerrillo, R., & Balzarini, M. (2024a). Resilience of *Pinus pinea* L. trees to drought in Central Chile based on tree radial growth methods. *Forests, 15*(10), 1775.

Loewe-Muñoz, V., Cachinero-Vivar, A. M., Camarero, J. J., Río, R. D., Delard, C., & Navarro-Cerrillo, R. M. (2024b). Dendrochronological analysis of Pinus pinea in Central Chile and South Spain for sustainable forest management. *Biology, 13*(8), 628.

Maxwell, R. S., & Larsson, L. A. (2021). Measuring tree-ring widths using the CooRecorder software application. *Dendrochronologia, 67,* 125841.

Mechergui, K., Saleh Altamimi, A., Jaouadi, W., & Naghmouchi, S. (2021). Climate change impacts on spatial distribution, tree-ring growth, and water use of stone pine (*Pinus pinea* L.) forests in the Mediterranean region and silvicultural practices to limit those impacts. *iForest-Biogeosciences and Forestry, 14*(2), 104.

Mishra, A. K., & Singh, V. P. (2010). A review of drought concepts. *Journal of hydrology, 391*(1-2), 202- 216.

Muñoz, V. F. L., Delard, C., González, M. V. G., Mutke, S., & Díaz, V. C. F. (2012). Introducción del pino piñonero (*Pinus pinea* L.) en Chile. *Ciencia & Investigación Forestal, 18*(2), 39-52.

Mutke, S., Calama, R., González-Martínez, S. C., Montero, G., Javier Gordo, F., Bono, D., & Gil, L. (2012). Mediterranean stone pine: botany and horticulture. *Horticultural reviews, 39*(1), 153-201.

Natalini, F., Alejano, R., Vázquez-Piqué, J., Pardos, M., Calama, R., & Büntgen, U. (2016). Spatiotemporal variability of stone pine (*Pinus pinea* L.) growth response to climate across the Iberian Peninsula. *Dendrochronologia, 40*, 72-84.

Natalini, F., Alejano, R., Pardos, M., Calama, R., & Vázquez-Piqué, J. (2024). Declining trends in long-term *Pinus pinea* L. growth forecasts in Southwestern Spain. *Dendrochronologia, 88,* 126252.

Navarro-Cerrillo, R. M., Cachinero-Vivar, A. M., Pérez-Priego, Ó., Cantón, R. A., Begueria, S., & Camarero, J. J. (2023). Developing alternatives to adaptive silviculture: Thinning and tree growth resistance to drought in a Pinus species on an elevated gradient in Southern Spain. *Forest Ecology and Management, 537*, 120936.

Perulli, G. D., Peters, R. L., von Arx, G., Grappadelli, L. C., Manfrini, L., & Cherubini, P. (2019). *Learning from the past to improve in the future: tree-ring wood anatomy as retrospective tool to help orchard irrigation management*. In IX International Symposium on Irrigation of Horticultural Crops 1335 (p. 179-188).

Piraino, S. (2020). Assessing *Pinus pinea* L. resilience to three consecutive droughts in central-western Italian Peninsula. *iForest-Biogeosciences and Forestry, 13*(3), 246.

Piraino, S., Camiz, S., Di Filippo, A., Piovesan, G., & Spada, F. (2013). A dendrochronological analysis of *Pinus pinea* L. on the Italian mid-Tyrrhenian coast. *Geochronometria, 40*, 77-89.

Piraino, S., Cignoli, F. N., Robledo, S., & Pérez, S. (2021). Un pino mediterráneo en Sudamérica: situación actual y potencialidad de *Pinus pinea* L. en territorio argentino. *Experticia, 12*(1). 7-10. https://revistas.uncu.edu.ar/ojs3/index.php/experticia/article/view/5041

Piraino, S., Molina, J. A., Hadad, M. A., & Roig, F. A. (2022). Resilience capacity of *Araucaria araucana* to extreme drought events. *Dendrochronologia, 75*, 125996.

Piraino, S., Hadad, M. A., Ribas-Fernández, Y. A., & Roig, F. A. (2024). Sex-dependent resilience to extreme drought events: implications for climate change adaptation of a South American endangered tree species. *Ecological Processes, 13*(1), 24.

Rigling, A., Brühlhart, H., Bräker, O. U., Forster, T., & Schweingruber, F. H. (2003). Effects of irrigation on diameter growth and vertical resin duct production in *Pinus sylvestris* L. on dry sites in the central Alps, Switzerland. *Forest Ecology and Management, 175*(1-3), 285-296.

Schulman, E. (1956). *Dendroclimatic changes in semiarid America*. University of Arizona.

Schwarz, J., Skiadaresis, G., Kohler, M., Kunz, J., Schnabel, F., Vitali, V., & Bauhus, J. (2020). Quantifying growth responses of trees to drought-A critique of commonly used resilience indices and recommendations for future studies. *Current Forestry Reports, 6,* 185-200.

Speer, J. H. (2010). *Fundamentals of tree-ring research*. University of Arizona Press.

Trouet, V., & Van Oldenborgh, G. J. (2013). *KNMI* Climate Explorer: a web-based research tool for high-resolution paleoclimatology. *Tree-Ring Research, 69*(1), 3-13.

Vicente-Serrano, S. M., Beguería, S., & López-Moreno, J. I. (2010). A multiscalar drought index sensitive to global warming: the standardized precipitation evapotranspiration index. *Journal of climate, 23*(7), 1696-1718.

Villalba, R., & Veblen, T. T. (1997). Spatial and temporal variation in Austrocedrus growth along the forest steppe ecotone in northern Patagonia. *Canadian Journal of Forest Research, 27*(4), 580-597.

Wigley, T. M., Briffa, K. R., & Jones, P. D. (1984). On the average value of correlated time series, with applications in dendroclimatology and hydrometeorology. *Journal of Applied Meteorology and climatology, 23*(2), 201-213.

Climatic Normals in Chacras de Coria. Evolution of Air Temperature for the 1959-2020 Period

Normales climáticas de Chacras de Coria. La evolución de la temperatura del aire para el período 1959-2020

Carlos Alejandro Flores *, Adriana Inés Caretta, Nora Beatriz Martinengo

Originales: *Recepción:* 19/03/2025 - *Aceptación:* 19/12/2025

ABSTRACT

Air temperature data registered from 1959 to 2020 by the Chacras de Coria meteorological station (32°59' S Lat.; 68°52' W Long.) were analyzed to characterize the site and identify trends considering the climate change scenario. We ensured quality and homogeneity of the time series following the procedures of the Standard World Meteorological Organization, calculating reference (1961-1990) and regulatory (1991-2020) climatological normals. The ClimPACT package detected trends in temperature-related indices, including extreme values, daily thermal amplitude, and degree days. The results reveal that the 1991-2020 period was 0.6°C warmer than 1961-1990. Significant increases were observed in average minimum (0.12°C/decade) and average maximum (0.20°C/decade) temperatures. Extreme minimum and maximum temperatures also increased by 0.11°C/decade and 0.33°C/decade, respectively, resulting in fewer cold nights (-0.49%/decade) and more hot days (1.6%/decade). Daily temperature ranges increased by 0.11°C/decade, and degree days by 52 DD/decade. These findings are consistent with global warming evidence. A corrected and homogenized database spanning over 60 years is available for future climatological studies.

Keywords
climatology • climate change • ClimPACT

https://doi.org/10.48162/rev.39.210

Universidad Nacional de Cuyo. Facultad de Ciencias Agrarias. Almirante Brown 500. Chacras de Coria. M5528AHB. Mendoza. Argentina. * cflores@fca.uncu.edu.ar

Licenses Creative Commons
Attribution - Non Commercial - Share Alike

Resumen

Se analizaron datos de temperatura del aire (1959-2020) de la estación meteorológica Chacras de Coria (32°59' Lat. S; 68°52' Long. O) para caracterizar el sitio e identificar tendencias bajo el escenario de Calentamiento Global y Cambio Climático. Se aplicaron procedimientos estándar de la Organización Meteorológica Mundial para asegurar la calidad y homogeneidad de las series temporales, calculando normales climatológicas de referencia (1961-1990) y regulatorias (1991-2020). Se utilizó el paquete ClimPACT para detectar tendencias en índices asociados a la temperatura, incluyendo valores extremos, amplitud térmica diaria y Grados Día. Los resultados revelan que el período 1991-2020 fue 0,6°C más cálido que 1961-1990. Se observaron incrementos significativos en las temperaturas mínimas promedio (0,12°C/década) y máximas promedio (0,20°C/década). Los valores extremos de temperaturas mínimas y máximas también aumentaron a razón de 0,11°C/década y 0,33°C/década respectivamente, lo que se tradujo en menos noches frías (-0,49%/década) y más días calurosos (1,6%/década). La amplitud térmica diaria creció 0,11°C/década, y los Grados Día en 52 GD/década. Estos hallazgos concuerdan con la evidencia global de calentamiento. Una base de datos de más de 60 años, corregida y homogeneizada, está disponible para futuros estudios climatológicos.

Palabras clave
climatología • cambio climático • ClimPACT

Introduction

Since 1959, the Chacras de Coria weather station located at 32°59' S. Lat.; 68°52' W. Long. (Facultad de Ciencias Agrarias - Universidad Nacional de Cuyo) has generated a rich heritage of high-quality meteorological data. This allowed us to establish climatological normals and calculate indices to analyze the evolution of Climatic Elements (CE), such as air temperature and precipitation, which are crucial for understanding Climate Change (CC). Chacras de Coria is strategically located within the Mendoza River oasis, an area recently zoned under edaphoclimatic criteria as a region of high variability, where this site is part of one of the highland zones characterized by a warm climate and cold nights (Córdoba *et al.*, 2025).

Climate Change refers to a statistically significant variation in the climate state. Climate Change can be caused by natural internal processes or external forcing. The latter are persistent anthropogenic changes in the atmospheric composition or land use. Thus, the increasing Greenhouse Gas (GHG) emissions generate heterogeneous impacts at the space-time scale. Changes observed from these situations become evident in the CE (9).

Globally, each successive decade has been warmer since 1990. Historical records indicate that the 2011-2020 decade was the warmest, with significant margins for both land and ocean temperatures. These temperature increases, along with sea acidification, level rise, ice masses loss, and more intense and frequent extreme events, are related to anthropogenic CC, especially linked to higher GHG concentrations (24).

This study calculated air temperature normals and investigated this CE in Chacras de Coria during the 1959-2020 period, characterizing this site and detecting trends.

Materials and Methods

Daily maximum and minimum air temperature values from January 1st, 1959, to December 31st, 2020, were used. Observations were made daily at 9:00, 15:00, and 21:00 h local time. The data was analyzed using the ClimPACT package. This package provides the frequency, duration, and magnitude of climate extremes relevant to agriculture and food security, health, and water resources. Such indices, designed to track heat waves, droughts, and precipitation extremes, are monthly and annually available. ClimPACT uses historical daily values of maximum and minimum temperature and daily precipitation to calculate over 60 different climate indices (4, 20).

Climate data is considered homogeneous when all serial fluctuations express real CE variability. Data are typically assumed free of instrumentation, coding or processing errors. However, meteorological and climatological data are usually heterogeneous and erratic. These errors can be systematic, affecting a complete set of observations, or random, like the differences in parallax between observers reading a mercury barometer. These are known as over- or under-error observations and can be independent or correlated. Independent errors in consecutive observations are considered random, while dependent errors are correlated from one observation to the next (23). Therefore, we evaluated and homogenized the climatic normals and proposed indices.

Data Quality Evaluation

Quality evaluation verifies that the reported data is representative and not contaminated by unrelated factors (23). This evaluation is performed before testing homogenization, since outliers can affect this latter process.

The 1961-1990 data were established as the base period as suggested by the WMO, considered the standard reference period for long-term climate change assessments. These years allow the user to calculate percentile thresholds (21).

ClimPACT reports outlier data based on interquartile ranges (IQR) defined as the difference between the 75th and 25th percentiles. In this study, outliers were defined as those values 3x IQR above p75 or below p25. Using the IQR to identify outliers avoids affecting the process by larger outliers, making a single evaluation process sufficient (4).

Histograms of decimal values also helped to identify rounding biases. Other anomalies addressed were, (i) events of 4 or more consecutive equal values of minimum and maximum temperatures, (ii) repeated dates, (iii) values over 50°C, (iv) dates on which maximum and minimum temperature differences with the previous day were 20°C or more, (v) dates when maximum temperature was lower than minimum temperature and (vi) number of missing values for each variable and year. Incorrect values were amended and recorded in a change log file after consulting the original meteorological logs. With a corrected database, a second data quality analysis process reviewed the generated files, assuring data rigor. Finally, homogenization tests were executed.

Homogeneity

Climate time series often exhibit spurious or “non-climatic” jumps as well as gradual modifications due to changes in station location, environment, exposure, instrumentation, or observing practices. These heterogeneities can seriously affect extreme values. Therefore, station historical metadata is crucial for solving these problems (25).

A reliable analysis of a climate time series relies on data consistency over time. This need is addressed by statistically testing data homogeneity and defining a consequent homogenization process. Considering daily data is highly variable compared to monthly or annual data, adjusting homogeneity can be arduous. In a homogeneity test, the null hypothesis considers the series analysed is homogeneous, while the alternative hypothesis considers it presents, at least, one change point (22). We tested homogeneity with the RHtestsV4 software based on the RHtestsV3 software package with the addition of quantile matching adjustments estimated with reference series (19).

Methods based on penalized maximum t-test (PMT) or F (PMF) can identify and fit multiple change points in a time series. While the PMT test uses reference stations required for homogeneity analysis, the PMF test can be used as an absolute method when no neighbouring stations can be used in the comparison, as in this study (17, 18).

For the homogenization analysis, we used the corrected file, previously transformed to fit the RHtestsV4 package, according to the quality control criteria already explained. This file was loaded with the requested parameters, including the missing data code and confidence level.

Climatological Normals

Considering the rapid pace of climate change and the need for up-to-date information for operational purposes, at the 17th World Meteorological Congress in 2015, the WMO introduced a novel approach to 30-year data periods. The standard climatological normal

shifted from non-overlapping 30-year periods (1931-1960, 1961-1990, 1991-2020) to more recent 30-year periods beginning with a year ending in 1 and ending with a year finishing in 0. The period from 1961 to 1990 was retained as normal reference for long-term climate change assessments (21). We calculated the climatological normals for 1961-1990 (reference normal) and 1991-2020. The new approach now considers series that partially overlap and are updated every 10 years (2001-2030, 2011-2040, 2021-2050).

Due to the COVID-19 pandemic restrictions, 2020 data presented some discontinuities. However, the WMO concluded that a random distribution of missing days over a month generated 95% confidence interval corresponding, on average, to 11% of the standard deviation of the underlying daily values of 5 missing days, and 17% of the standard deviation of 10 days missing. This is equivalent, for example, to a few tenths of a degree Celsius for typical standard deviation values, considering daily maximum and minimum temperatures. However, when a substantial number of missing days are consecutive, additional uncertainty arises, given certain autocorrelation in most daily meteorological parameters (21).

A monthly value associated with the average of the daily values of a particular month was not calculated when any of the following criteria were met: (i) observations were missing for 11 or more days in a month or (ii) observations were missing for five or more consecutive days in the month. Likewise, a normal or average for a given month considered at least 24 of the 30 years, that is, at least 80% of the years averaging a period (21, 23). Furthermore, a remaining "suspicious or incorrect" value after undergoing the control process was considered missing within the series.

After data quality and homogeneity tests, the primary climatological parameters were obtained using InfoStat (2020).

The Indexes

ClimPACT provides 60 standardized indices that compare results across periods, regions, and different source data sets. Trends calculated by ClimPACT are based on Sen's slope (15), a nonparametric test, and reflect the median slope of all ordered pairs in a data set. Since it is less affected by outliers, it is also more appropriate for calculating trends in extreme values, such as those from climatic elements, compared to other common trend estimators like least squares. The 95% confidence intervals are calculated for the slope, along with lower and upper limits (4).

The evaluated indices were: (i) TNn: minimum temperature in a month ("temperature of the coldest night in the month") (°C); (ii) TNm: average daily minimum temperature (°C); (iii) TMm: average daily temperature (°C); (iv) TXm: average daily maximum temperature (°C); (v) TXx: maximum temperature in the month ("temperature of the hottest day") (°C); (vi) TN10p: percentage of days in which the minimum temperature is below the 10th percentile ("percentage of days with cold night temperatures", %); (vii) TX90p: percentage of days where the maximum temperature is above the 90th percentile ("percentage of days with hot daytime temperatures", %); (viii) DTR: average difference between daily maximum temperature and daily minimum temperature ("daily average thermal amplitude", °C); (ix) GDDgrow10: Grow Degree Days (Lower Developmental Threshold = 10°C); and (x) FD: number of days with frost (number of days in which the minimum temperature is equal or below 0°C).

Results and Discussion

Our results did not present change points for a confidence level of 0.99; therefore, the series was considered homogeneous.

Climatological Normals

Tables 1 and 2 (page 5), show Mean daily air temperatures (TMm) and Standard Deviations (S.D.) for 1961-1990 and 1991-2020. Tables 3 and 4 (page 5), show TNm and TNn values and their date of occurrence for 1961-1990 and 1991-2020. Table 5 (page 5) and table 6 (page 6), show TXm and TXx values and their date of occurrence for 1961-1990 and 1991-2020.

Table 1. Mean daily air temperatures (TMm) and Standard Deviations (S.D.) (°C) (1961-1990).
Tabla 1. Medias diarias (TMm) y Desviaciones Estándar (D.E.) (°C) (1961-1990).

	Jan.	Feb.	Mar.	Apr.	May.	Jun.	Jul.	Aug.	Sep.	Oct.	Nov.	Dec.	Annual
TMm	22.2	21.0	18.3	14.6	10.6	7.1	6.8	9.0	11.5	15.6	18.7	21.3	14.7
S.D.	0.8	0.9	1.0	1.4	1.2	1.4	1.1	1.2	1.2	0.8	1.3	1.2	5.6

Table 2. Mean daily air temperatures (TMm) and Standard Deviations (S.D.) (°C) (1991-2020).
Tabla 2. Medias diarias (TMm) y Desviaciones Estándar (D.E.) (°C) (1991-2020).

	Jan.	Feb.	Mar.	Apr.	May.	Jun.	Jul.	Aug.	Sep.	Oct.	Nov.	Dec.	Annual
TMm	23.4	21.7	19.3	14.8	10.9	7.8	7.0	9.4	12.4	16.0	19.3	22.1	15.3
S.D.	1.0	1.2	1.0	1.1	1.2	1.1	1.3	1.3	1.2	1.4	1.1	1.2	5.8

Table 3. TNm and TNn values and their date of occurrence (°C) (1961-1990).
Tabla 3. Valores de TNm y TNn y su fecha de ocurrencia (°C) (1961-1990).

	Jan.	Feb.	Mar.	Apr.	May.	Jun.	Jul.	Aug.	Sep.	Oct.	Nov.	Dec.
TNm	15.4	14.4	12.1	8.2	3.9	0.5	0.1	1.8	4.4	8.5	11.6	14.4
TNn	4.6	3.8	-1.4	-4.2	-7.0	-8.7	-9.2	-7.0	-5.8	-2.8	-1.4	3.3
Day	18	11	29	27	30 & 31	13	1	13	2	5	9	20
Year	'90	'77	'64	'89	'88	'67	'89	'78	'66	'72	'80	'80

Table 4. TNm and TNn values and their date of occurrence (°C) (1991-2020).
Tabla 4. Valores de TNm y TNn y su fecha de ocurrencia (°C) (1991-2020).

	Jan.	Feb.	Mar.	Apr.	May.	Jun.	Jul.	Aug.	Sep.	Oct.	Nov.	Dec.
TNm	16.5	14.9	12.8	8.4	4.7	1.0	0.0	2.0	5.2	8.7	12.0	14.8
TNn	4.5	4.8	0.0	-3.9	-5.5	-8.0	-11.8	-7.7	-5.3	-2.0	-0.8	1.6
Day	10	21	31	14	31	26 & 7	22	14	17	5	4	25
Year	'19	'03	'98	'08	'93	'11 & '12	'10	'99	'13	'20	'92	'02

Table 5. TXm and TXx values and their date of occurrence (°C) (1961-1990).
Tabla 5. Valores de TXm y TXx y su fecha de ocurrencia (°C) (1961-1990).

	Jan.	Feb.	Mar.	Apr.	May.	Jun.	Jul.	Aug.	Sep.	Oct.	Nov.	Dec.
TXm	28.9	27.6	24.5	21.0	17.3	13.7	13.5	16.2	18.7	22.6	25.8	28.2
TXx	36.2	36.1	34.4	30.5	28.5	26.8	31.3	29.0	32.5	35.2	36.5	37.0
Day	16 & 3	4	17	6	17	11	28	22	11	12	9	17
Year	’61 & ’89	’72	’63	’67	’67	’75	’79	’88	’86	’85	’67	’75

Table 6. TXm and TXx values and their date of occurrence (°C) (1991-2020).
Tabla 6. Valores de TXm y TXx y su fecha de ocurrencia (°C) (1991-2020).

	Jan.	Feb.	Mar.	Apr.	May.	Jun.	Jul.	Aug.	Sep.	Oct.	Nov.	Dec.
TXm	30.2	28.5	25.8	21.3	17.1	14.6	14.0	16.8	19.6	23.2	26.5	29.3
TXx	41.3	39.9	37.0	31.8	31.4	33.2	29.2	32.9	35.2	35.7	37.7	40.2
Day	30	18	4	13	1	21	26	29	22	29	8	24
Year	’98	’99	’98	’11	´97	´99	´99	´97	´18	´09	´12	´12

Average Daily Temperature (TMm)

Annual mean air temperatures (tables 1 and 2, page 5), show that the 1991-2020 period was 0.6°C warmer than the previous 30-year period. The SD also increased in the second period by 0.2°C, implying more frequent or extremely high temperatures, as mean values have also escalated. This is confirmed by comparing TNm, TNn, TXm, and TXx values in tables 3, 4, 5 (page 5) and table 6; figure 1).

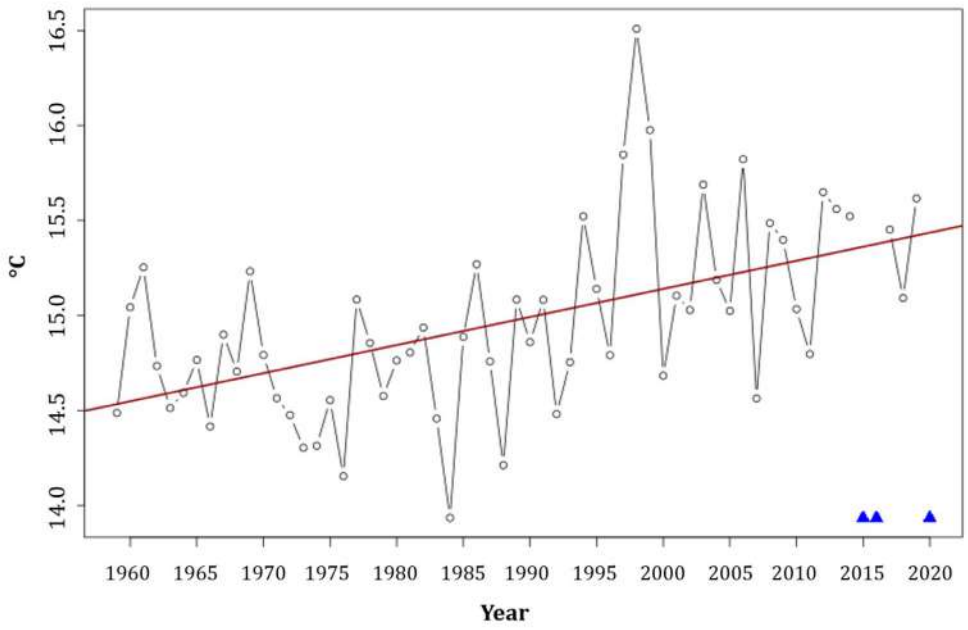


Figure 1. Sen’s slope of annual average daily temperatures (1959-2020).
Figura 1. Pendiente de Sen de las temperaturas medias diarias anuales (1959-2020).

Average daily temperatures registered a highly significant increase of 0.15°C per decade (*p-value* <0.00001). The greatest contribution occurred during the summer quarter (DJF) with 0.25 °C.decade$^{-1,}$ and the winter quarter (JJA), the lowest with 0.09°C.decade^{-1}.

In Argentina, average increase in mean annual temperatures was approximately 0.7°C between 1961 and 2020, which gives an estimated increase of 0.12°C per decade, close to the 0.15°C per decade (1959-2020) obtained for our site. The global increase was 1°C in the same period, giving an estimate of 0.17°C per decade (1).

Average Daily Minimum Temperature (TNm)

Average daily minimum temperatures are significantly increasing at a rate of 0.12°C per decade (*p-value* <0.00001). All quarters had positive slopes, except for winter (JJA), whose slope was zero. The trends (°C.decade^{-1}) were 0.22 (DJF), 0.12 (MAM), and 0.11 (SON). Other authors have also reported increased average annual temperatures in the Cuyo Region in 1960 - 2010 (3) and in the Humid Pampa Region in 1936-2019, particularly attributable to higher minimum temperatures in spring and summer (9) (figure 2).

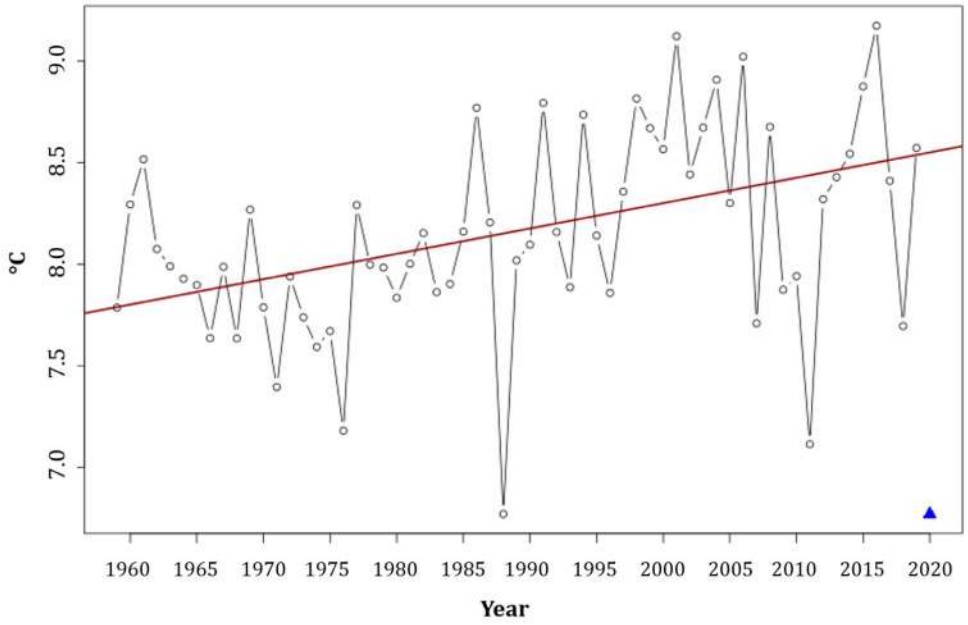


Figure 2. Sen's slope of the annual average daily minimum temperatures (1959-2020).
Figura 2. Pendiente de Sen de las temperaturas mínimas medias diarias (1959-2020).

Minimum Monthly Value of Daily Minimum Temperature (TNn)

The "temperature of the coldest night" shows a tendency to register an increase of 0.11°C per decade (*p-value* = 0.37), where the greatest contribution is registered during the winter quarter (JJA) with a 0.12°C per decade increase, and the lowest during springtime (SON) with a 0.05°C per decade increase. TNn also records increases in the "humid pampas" (9), in the Cuyo region (3), and appears in the analysis of extreme temperature trends in Argentina (11) (figure 3, page 8).

Percentage of Days with Minimum Temperatures Under the 10th Percentile

The percentage of cold nights (TN10p) decreased 0.49 percentage points per decade (*p-value* = 0.04). The winter quarter (JJA) showed no trend, while the other quarters had values of -1.03 (DJF), -0.22 (MAM), and -0.42 (SON) (%.decade^{-1}). In central Argentina, a lower percentage of cold nights has also been observed from October to January and in March and June (12) (figure 4, page 8).

Average Daily Maximum Temperature (TXm)

Average maximum temperatures registered a significant increase of 0.2°C per decade (*p-value* <0.000), with particular contribution from the spring and summer quarters with 0.21 and 0.31°C.decade^{-1}, respectively. However, in a general provincial analysis, no significant positive trend was observed between 1997 and 2017 (8). In a more detailed analysis, only north and south Mendoza recorded significant increases of 0.5°C in 1960-2010 (3) (figure 5, page 9).

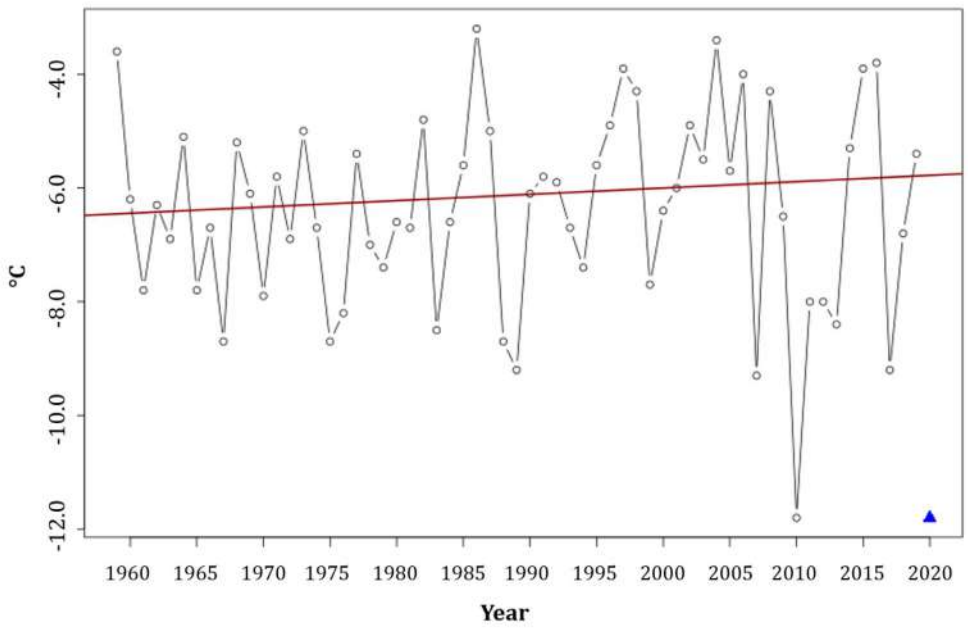


Figure 3. Sen' s slope of the annual coldest daily minimum temperatures (1959-2020).
Figura 3. Pendiente de Sen de las temperaturas mínimas diarias absolutas (1959-2020).

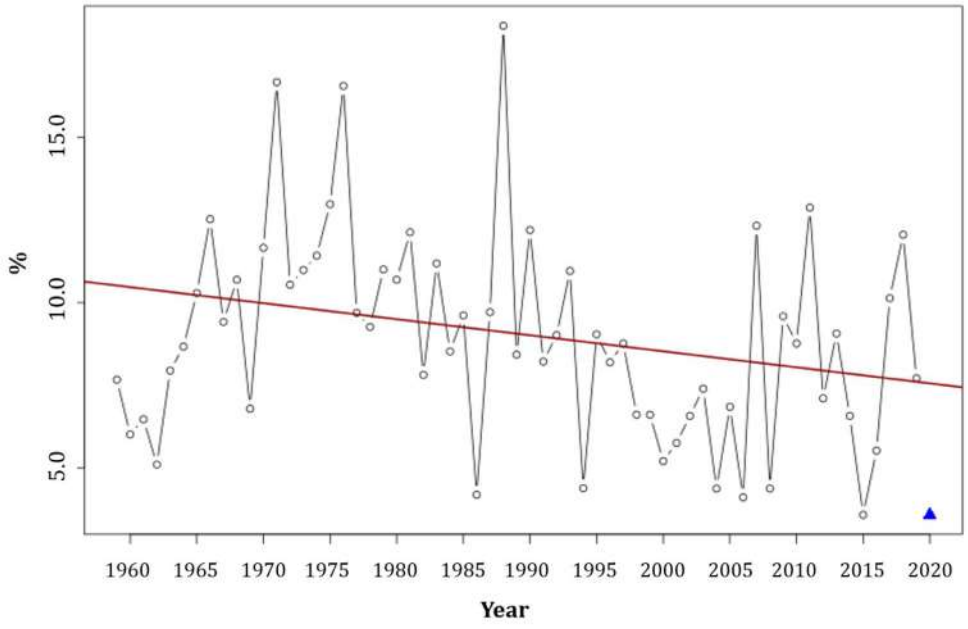


Figure 4. Sen's slope of the annual percentage of cold nights (1959-2020).
Figura 4. Pendiente de Sen del porcentaje anual de noches frías (1959-2020).

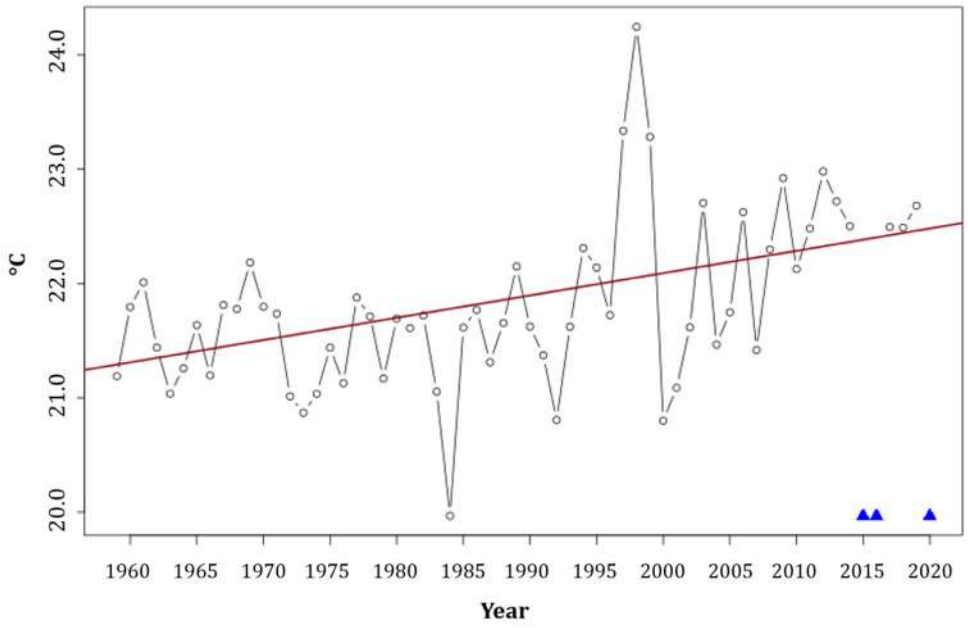


Figure 5. Sen´s slope of the annual average of daily maximum temperatures (1959-2020).
Figura 5. Pendiente de Sen temperaturas máximas medias diarias anuales (1959-2020).

Monthly Maximum Value of Daily Maximum Temperature (TXx)

Maximum temperatures of the warmest days registered a highly significant increase of 0.33°C per decade (*p-value* <0.000). The four quarters presented positive slopes, although the spring quarter (SON) contributed the least, with an increase of 0.24°C decade^{-1}. Increasing maximum temperatures were also recorded in nearby areas, such as northwestern Argentina, with October having the highest frequency (2) (figure 6).

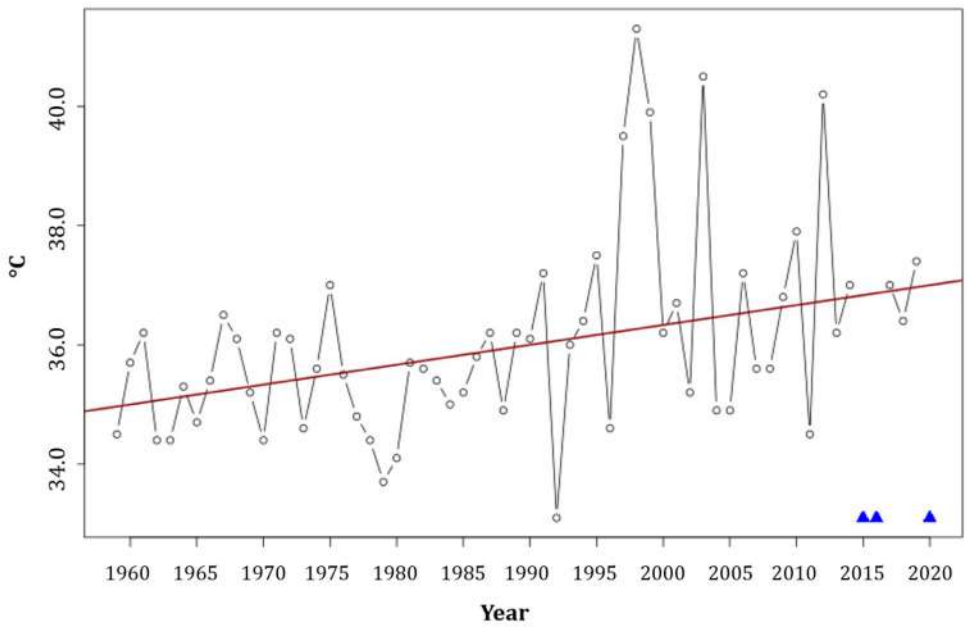


Figure 6. Sen´s slope of the annual warmest daily maximum temperatures (1959-2020).
Figura 6. Pendiente de Sen de las temperaturas máximas absolutas diarias (1959-2020).

The detected increase in both maximum and minimum temperatures suggests a growing pressure on crop water demand due to intensified evapotranspiration. This historical thermal trend provides a fundamental input for modeling future scenarios within the methodological framework of Farreras *et al.* (2026). Integrating these projections would allow for estimating the future evolution of the Water Footprint (WF), evaluating how increased irrigation requirements will impact water security and social welfare in the Mendocinian Northern Oasis.

Percentage of Days with Maximum Temperatures Over the 90th Percentile

The annual fraction of days with hot daytime temperatures (TX90p) rose at a rate of 1.6% per decade (*p-value* <0.000), with the DJF quarter contributing the most (3.10%.decade^{-1}) compared with the JJA quarter (0.99 %.decade^{-1}). Spring and fall show similar trends, 1.31 and 1.40%.decade^{-1} respectively. In central Argentina, increases in the percentage of TX90p have been recorded in March, August, and November (12), along with increasing heat waves in Mendoza (3). Between 1941 and 2000, and every 20 years, alternations of the hot extremes were observed, corresponding to an increase in the last years of the 20th century (14). Had this pattern continued, it should have decreased between 2001 and 2020; however not observed in this analysis (figure 7).

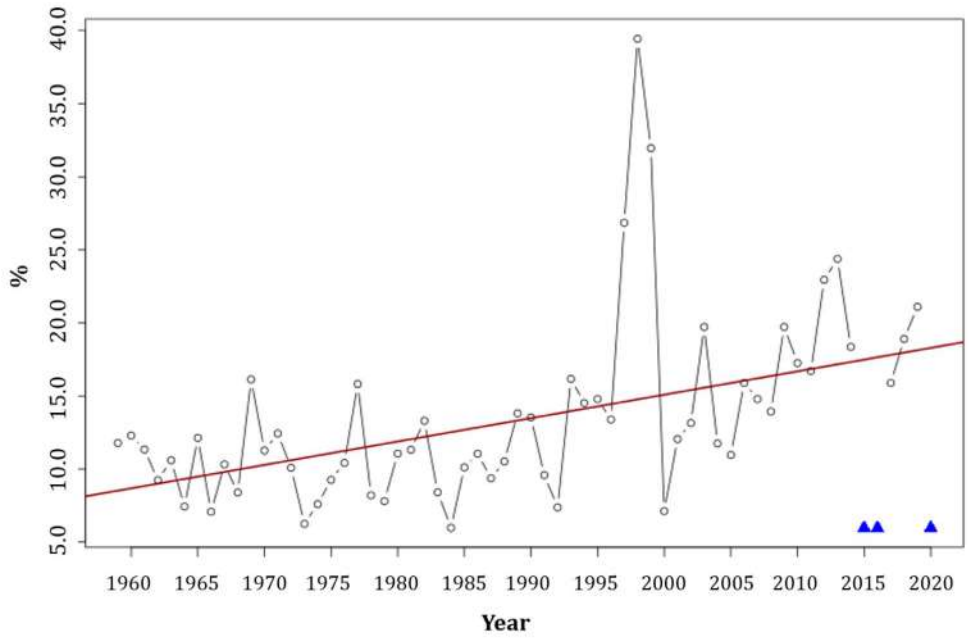


Figure 7. Sen' s slope of the annual percentage of hot daytime temperatures (1959-2020).
Figura 7. Pendiente de Sen porcentaje de máximas mayores al percentil 90 (1959-2020).

Daily Thermal Range (DTR)

The daily thermal range increased 0.11°C per decade (*p-value*= 0.013), with the winter period contributing the most (0.25°C decade^{-1}).

In 2021, the IPCC reported a declining trend for global DTR, mainly during 1960-1980 (6). In Argentina, a similar decrease was reported in the thermal amplitude due to the decreasing extremes of maximum and minimum temperatures from 1941 to 2000 (14) or given to minimum temperatures increasing more than maximum ones, particularly in central Argentina. This asymmetrical growth of maximum and minimum temperatures would lead to reduced daily ranges, mainly due to warmer nights (2).

Nevertheless, later studies showed that the global observed DTR trend was reversed during 1980-2021, significantly growing at a rate of 0.091 ± 0.008°C per decade. The trend

was dominated by a faster rate of increasing daily maximum air temperature. A 0.063 ± 0.012°C per decade global land DTR trend was reported due to a faster rate of rising daily maximum air temperature (6). This data also agrees with our observations since the growing trend of TXm is 66.6% greater than TNm (figure 2, page 7 and figure 5, page 9). Analogous results were reported in Colombia for the 1981-2020 period (10) (figure 8).

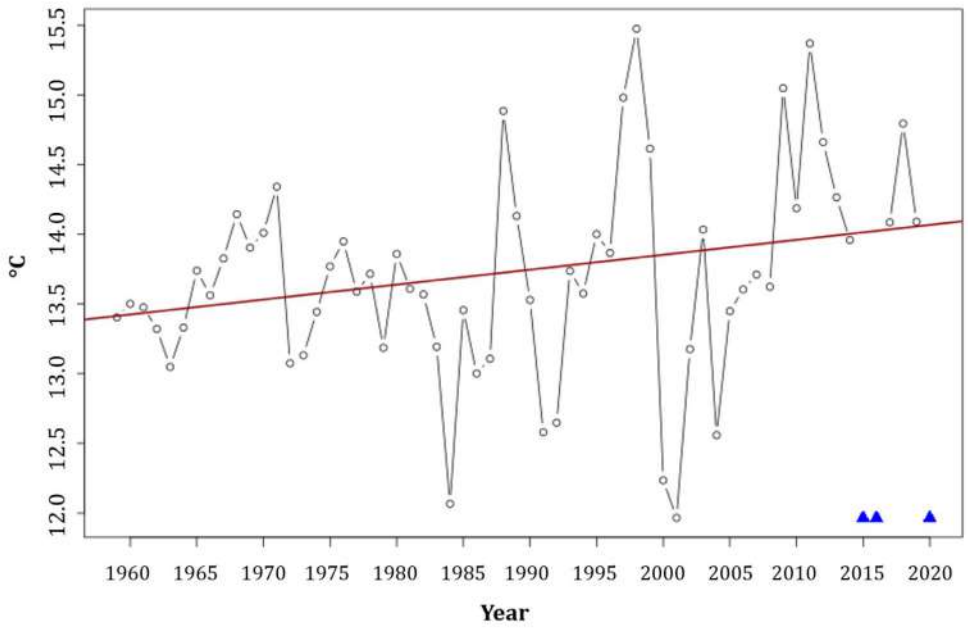


Figure 8. Sen's slope of the mean annual daily temperature range (DTR) (1959-2020).
Figura 8. Pendiente de Sen amplitud térmica media diaria anual (DTR) (1959-2020).

Annual Accumulation of Degree Days Base 10 °C (gddgrow10)

The annual sum of the differences between average daily temperatures (TMm) and a base value of 10°C, where TMm > 10°C, measures heat accumulation to predict development rates of ectothermic organisms. In this case, we found a highly significant incremental rate of 52 Degree Days per decade (*p-value* <0.000) (figure 9, page 12).

Number of Days with Frost (FD)

Based on the 1959-2019 data, the site presented an annual average of 47.3 ± 12.1 days with frosts. Figure 10 (page 12) shows the monthly distribution of days with frosts. In both cases, 2020 was discarded from the analysis, given missing data for March, April, May, June, and August (figure 10, page 12).

No significant increase in days with meteorological frost was observed for our study site. The Sen slope was 0.024 (*p-value* = 0.765), and the frost regime remained practically constant during the analyzed period. However, a joint analysis for Mendoza and San Juan provinces showed a downward trend in annual frost frequency (1), as found in the humid pampas for 1981-2000 (14) (figure 11, page 13).

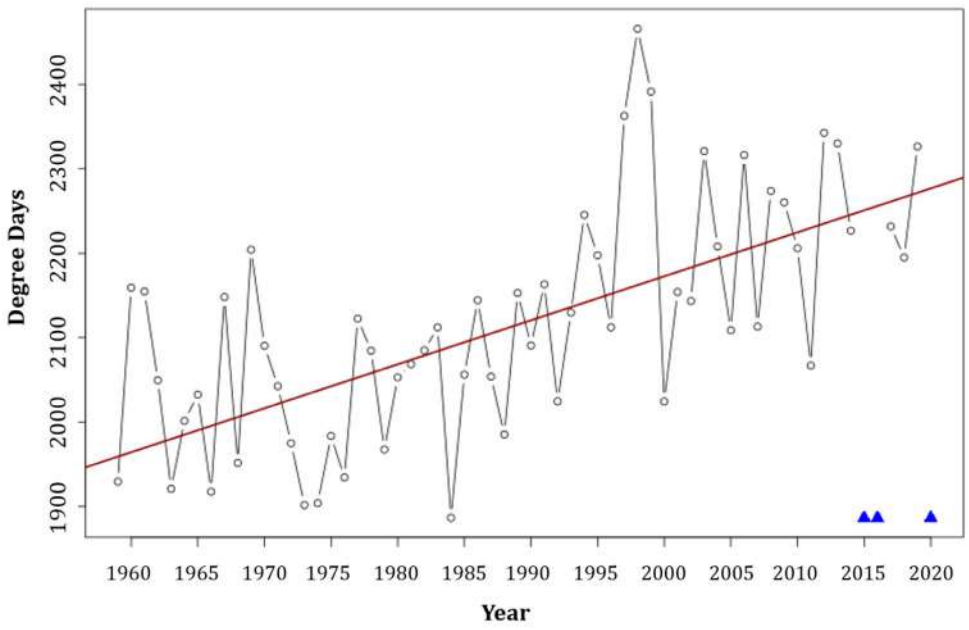


Figure 9. Sen's slope of the annual accumulation of Degree Days base 10°C (1959-2020).
Figura 9. Pendiente de Sen de la acumulación anual de grados día base 10°C (1959-2020).

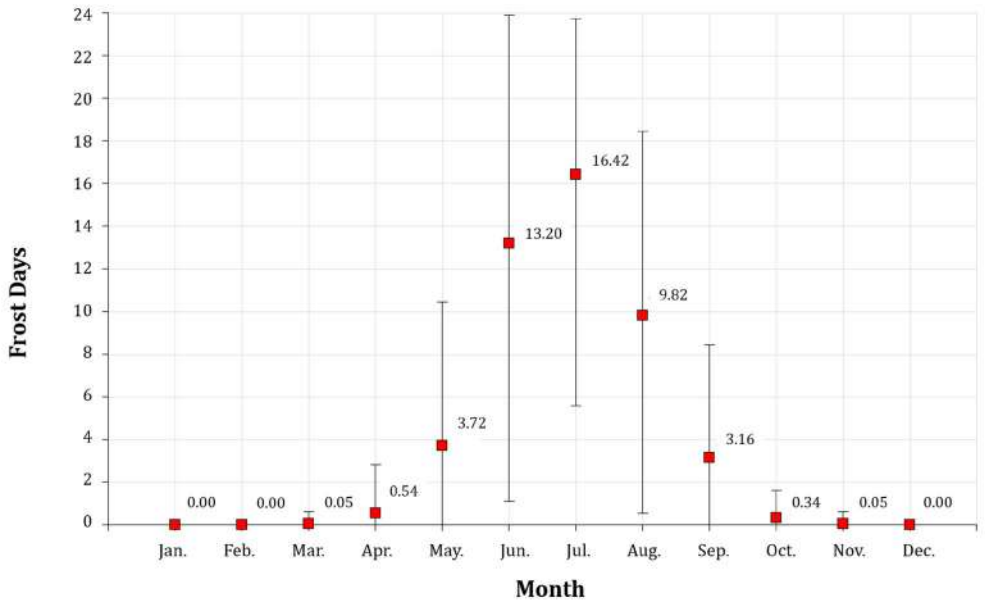


Figure 10. Distribution of days with frosts and non-parametric prediction intervals (1959-2019).
Figura 10. Distribución de días con heladas e intervalos de predicción no paramétrica (1959-2019).

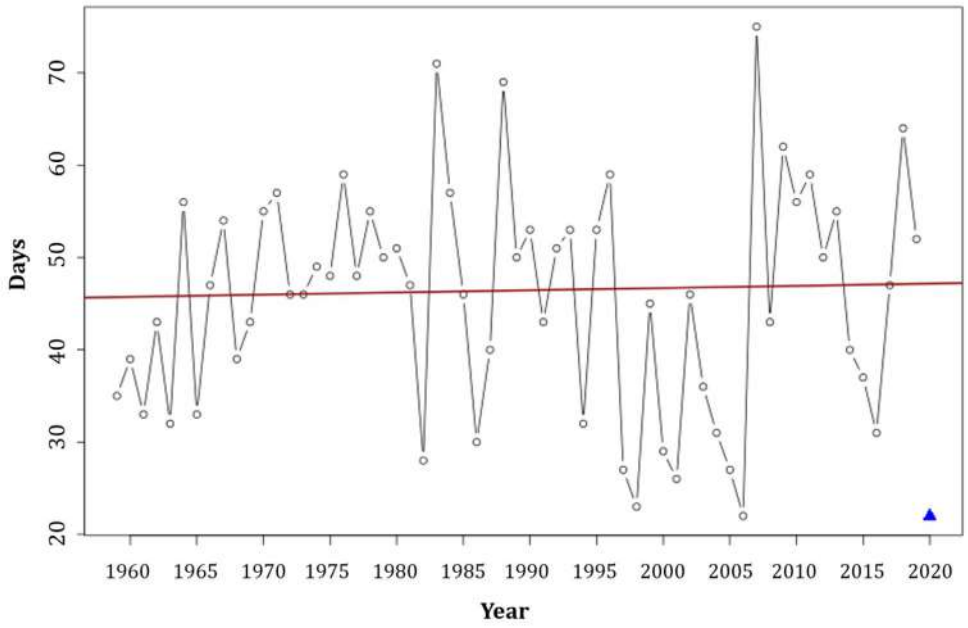


Figure 11. Sen' s slope of days with meteorological frosts (1959-2020).
Figura 11. Pendiente de Sen de días con heladas meteorológicas (1959-2020).

Conclusions

We present the 1961-2020 trends for the main indices suggested by the WMO for global warming and climate change. Although these trends should not be extrapolated beyond the period considered, they constitute a solid comparison basis for the next climate normal (2001-2030). Our results confirm the progressive increase in temperatures observed globally. Winter, and more frequently, summer are the most affected seasons. Changing temperature parameters are evidenced by increasing maximum and minimum temperatures, decreasing percentage of cold nights (TN10p), and increasing percentage of warmer days (TX90p).

The significantly larger availability of Degree Days based on 10°C also indicates greater energy availability, shortening cycles of ectothermic organisms as long as extreme temperatures, especially maximum temperatures, do not become stressful. Thus, impacts on growth rates of ectothermic organisms should be expected, as well as effects of extremely high temperatures on their physiology and behavior.

Trends found at our local level agree with those worldwide. Although both minimum and maximum temperatures are increasing, higher values observed in the daily thermal range are explained by a greater increase in maximum temperatures than in minimum temperatures.

References

1. Alabar, F.; Valdiviezo Corte, M.; Moreno, C.; Hurtado, R. 2022. Temperaturas extremas registradas en estaciones del noroeste argentino. XIX Reunión Argentina de Agrometeorología: Producción Armónica y Sustentable. Asociación Argentina de Agrometeorología. https://www.siteaada.org/_files/ugd/ cf1a17_2f530752296445dc92edabb44abeeecc.pdf
2. Aneise, A. J.; Möhle, E.; Risaro, D. B.; Schteingart, D. 2024. Cambio climático. Argendata. Fundar. https://argendata.fund.ar/topico/cambio-climatico/. Retrieved June 19th, 2025.
3. Araneo, D. 2015. Foro de Cambio Climático. Efectos del Cambio Climático en Mendoza y propuestas de adaptabilidad. UNCUYO-ONU. https://www.uncuyo.edu.ar/centroasuntosglobales/upload/foro-de-cambio-climatico-presentacion-diego-araneo.pdf
4. Commission for Climatology (CCl). 2024. Expert Team on Climate Risk and Sector-Specific Climate Indices (ETCRSCI). Climpact user guide. https://github.com/ARCCSS-extremes/climpact/blob/master/www/user_guide/Climpact_user_guide.md. Retrieved February 27th, 2024.

5. Córdoba, M.; Vallone, R.; Paccioretti, P.; Corvalán, F.; Balzarini, M. 2025. Data-driven Method for the Delimitation of Viticultural Zones: Application in the Mendoza River Oasis, Argentina. Revista de la Facultad de Ciencias Agrarias. Universidad Nacional de Cuyo. Mendoza. Argentina. 57(2): 57-68. DOI: https://doi.org/10.48162/rev.39.171
6. Di Rienzo, J. A.; Casanoves, F.; Balzarini, M.; Gonzalez, L.; Tablada, M.; Robledo, C. W. 2020. InfoStat versión 2020. Centro de Transferencia InfoStat. FCA. Universidad Nacional de Córdoba.
7. Farreras González, V. I.; Lauro, C.; Abraham, L.;Salvador, P. F. 2026. Social Welfare Effects of Water Security Improvements in Arid Regions: The Case of Mendoza, Argentina. Revista de la Facultad de Ciencias Agrarias. Universidad Nacional de Cuyo. e8916. DOI: https://doi.org/10.48162/rev.39.195
8. Huang, X.; Dunn, R. J.; Li, L. Z.; McVicar, T. R.; Azorin-Molina, C.; Zeng, Z. 2023. Increasing Global Terrestrial Diurnal Temperature Range for 1980-2021. Geophysical Research Letters, 50(e2023GL103503). doi.org/https://doi.org/10.1029/2023GL103503
9. IPCC. 2013. Annex III: Glossary [Planton, S. (ed.)]. In: Climate Change 2013: The Physical Science Basis. Contribution of Working Group I to the Fifth Assessment Report of the Intergovernmental Panel on Climate Change [Stocker, T. F., D. Qin, G.-K. Plattner, M. Tignor, S.K. Allen, J. Boschung, A. Nauels, Y. Xia, V. Bex and P.M. Midgley (eds.)]. Cambridge University Press.
10. Mulena, G. C.; Araneo, D. C. 2018. Variabilidad y tendencia de los extremos de temperatura sobre la provincia de Mendoza, Argentina. CONGREMET XIII. https://cenamet.org.ar/congremet/wp-content/uploads/2018/11/T0099_MULENA.pdf
11. Müller, G. V.; Lovino, M. A.; Sgroi, L. C. 2021. Observed and Projected Changes in Temperature and Precipitation in the Core Crop Region of the Humid Pampa, Argentina. Climate. 9(3): 40. https://doi.org/10.3390/cli9030040
12. Ruiz Murcia, J. F.; Melo Franco, J. Y.; Herrera Aponte, S. M.; Fonseca Gutiérrez, E. K.; Vega Burgos, A. 2023. Cálculo de indicadores (evidencias) de cambio climático para Colombia 1981-2020. IDEAM-METEO / 004-2023. Instituto de Hidrología, Meteorología y Estudios Ambientales. Grupo de modelamiento numérico de tiempo y clima. Grupo de gestión de datos y red meteorológica. IDEAM.
13. Rusticucci, M.; Barrucand, M. 2004. Observed trends and changes in temperature extremes over Argentina. Journal of Climate. 17(20): 4099-4107.
14. Rusticucci, M.; Barrucand, M.; Collazo, S. 2016. Temperature extremes in the Argentina central region and their monthly relationship with the mean circulation and ENSO phases. International Journal of Climatology. 37(6): 3003-3017. https://doi.org/10.1002/joc.4895
15. Sen, P. K. 1968. Estimates of the Regression Coefficient Based on Kendall's Tau. Journal of the American Statistical Association. 63(324): 1379-1389. doi.org/10.1080/01621459.1968.10480934
16. Tencer, B.; Rusticucci, M. 2012. Analysis of interdecadal variability of temperature extreme events in Argentina applying EVT. Atmósfera. 25(4): 327-337. http://www.scielo.org.mx/scielo.php?script=sci_arttext&pid=S0187-62362012000400002&lng=es&tlng=en
17. Wang, X. L. 2008a. Accounting for autocorrelation in detecting mean-shifts in climate data series using the penalized maximal t or F test. J. Appl. Meteor. Climatol. (47): 2423-2444. doi.org/10.1175/2008JAMC1741.1
18. Wang, X. L. 2008b. Penalized maximal F-test for detecting undocumented mean-shifts without trend-change. J. Atmos. Oceanic Tech. V (3): 368-384. doi.org/10.1175/2007/JTECHA982.1
19. Wang, X. L.; Feng, Y. 2013. RHtestsV4 User Manual. Climate Research Division, Atmospheric Science and Technology Directorate. Science and Technology Branch Environment. http:// etccdi.pacificclimate.org/software.shtml
20. WMO and Green Climate Fund (GCF) Secretariats. 2022. Developing the Climate Science Information for Climate Action WMO-No. 1287. World Meteorological Organization. https://library.wmo.int/idurl/4/53280
21. World Meteorological Organization. 2017. WMO Guidelines on the Calculation of Climate Normals WMO-No. 1203. World Meteorological Organization. https:// library.wmo.int/viewer/55797/download?file=1203_en.pdf&type=pdf&navigator=1
22. World Meteorological Organization. 2020. Guidelines on Homogenization WMO-No. 1245. World Meteorological Organization. https://library.wmo.int/ idurl/4/57130
23. World Meteorological Organization. 2023. Guide to Climatological Practices WMO-No. 100. World Meteorological Organization. https://library.wmo.int/ idurl/4/60113
24. World Meteorological Organization. 2023. The Global Climate 2011-2020. A decade of accelerating climate change. WMO-No. 1338. World Meteorological Organization. https:// library.wmo.int/idurl/4/68585
25. Zwiers, F. W.; Zhang, X. 2009. Guidelines on Analysis of extremes in a changing climate in support of informed decisions for adaptation WMO/TD-No. 1500. World Meteorological Organization. https://library.wmo.int/idurl/4/48826

Predictive Modeling of Effective Electrical Conductivity for Irrigation Water in Mendoza, Argentina

Modelo predictivo de conductividad eléctrica efectiva para aguas de riego en Mendoza, Argentina

Daniela Virginia Cónsoli *, María Flavia Filippini

Originales: *Recepción:* 25/09/2025- *Aceptación:* 12/03/2026

ABSTRACT

This study develops five predictive models based on regression trees to estimate the Effective Electrical Conductivity (CEE) of irrigation water in the Green Belt of Mendoza, Argentina. Using 468 water samples and physicochemical measurements from the Chachingo and Pescara canals, the models incorporate between one and six predictor variables. The most prominent model includes values of Actual Electrical Conductivity (CEA), calcium, magnesium, and bicarbonate ions, with a correlation coefficient of 0.99 and a mean absolute error of 26.5 µS cm^{-1}. CEE is a key indicator for assessing water quality in areas with moderately soluble salts. These models provide a cost-effective tool for identifying salinity risks in irrigation water of varying quality. Their simplicity and robustness make them suitable for Mendoza or other regions with similar conditions, supporting efficient water resource management in agriculture.

Keywords
effective electrical conductivity • irrigation water • regression trees • water quality • salinity • green belt

https://doi.org/10.48162/rev.39.214

Universidad Nacional de Cuyo. Facultad de Ciencias Agrarias. Departamento de Ingeniería Agrícola. Almirante Brown 500. M5528AHB. Chacras de Coria. Mendoza. Argentina. * dconsoli@fca.uncu.edu.ar

Licenses Creative Commons
Attribution - Non Commercial - Share Alike

Resumen

Este estudio desarrolla cinco modelos predictivos basados en árboles de regresión para estimar la Conductividad Eléctrica Efectiva (CEE) del agua de riego en el Cinturón Verde de Mendoza, Argentina. Utilizando 468 muestras de agua y mediciones fisicoquímicas de los canales Chachingo y Pescara, los modelos emplean entre 1 y 6 variables predictoras. El modelo más destacado incluye valores de Conductividad Eléctrica Actual (CEA), iones calcio, magnesio y bicarbonatos, con un coeficiente de correlación de 0,99 y un error absoluto medio de 26,5 μS cm^{-1}. La CEE es crucial para evaluar la calidad del agua en áreas con sales de mediana solubilidad. Estos modelos permiten a productores, técnicos e investigadores realizar análisis más económicos, facilitando la identificación de riesgos salinos en aguas de calidad variable. Su simplicidad y robustez los hacen aplicables no solo en Mendoza, sino también en otras regiones con condiciones similares, contribuyendo al manejo eficiente de los recursos hídricos en la agricultura.

Palabras clave

conductividad eléctrica efectiva • agua de riego • árboles de regresión • calidad del agua • salinidad • cinturón verde

Introduction

The arid province of Mendoza critically relies on the efficient management of water resources, primarily originating from snowmelt in the Andean mountain range. This water availability has enabled the development of agricultural oases that occupy only 4% of the provincial territory but concentrate 98% of the population and agro-industrial activities. Within this framework, irrigation water quality in the Northern Oasis -where the Green Belt is located- is key for the production of vegetables and fruits that supply the Mendoza Metropolitan Area and other national markets. However, the increasing water demand from agricultural, industrial, and urban sectors has exacerbated water quality problems (Zuluaga *et al.*, 2011), driving the continuous development of strategies to promote rational use and sound management of the resource across productive sectors (Ardila & Saldarriaga, 2013).

Irrigation water systems in arid regions are characterized by strong spatial variability and environmental heterogeneity, requiring analytical approaches capable of capturing complex interactions and spatial dependence (Ciardullo *et al*., 2025).

Globally, agriculture is the largest consumer of freshwater and major driver of surface and groundwater degradation (FAO, 1997). In Mendoza, regional geochemical characteristics -particularly the presence of moderately soluble salts- limit the applicability of international classifications, such as the Riverside system modified by Thorne-Peterson (1954, 1996) and the FAO guidelines (Ayers & Wescot, 1987), which also inform the Ente Provincial del Agua y Saneamiento criteria (EPAS, 1995). In contrast, the classification proposed by Wainstein (1968) adapts the Riverside scheme [modified by Thorne-Peterson], incorporating Effective Electrical Conductivity (CEE), gypsum content, and the role of drainage in eliminating sodium excess (Avellaneda *et al.*, 2004). Nevertheless, calculating CEE requires a complete physicochemical analysis, and budgetary constraints often hinder its practical use.

Defining CEE in the study area provides a more accurate interpretation of water quality, considering moderately soluble salts strongly influence water chemistry. This underscores the importance of estimating CEE using a reduced set of easily accessible, low-cost variables. We address this methodological gap with regression trees to predict CEE based on various physicochemical variables.

A decision tree is an algorithm that analyzes information and establishes associations between profiles (independent variables) and a target outcome (dependent variable) (Díaz-Martínez *et al.*, 2021). The response may be categorical (classification trees) or continuous (regression trees). These trees generate recursive partitions through classification rules until a final classification, identifying profiles (terminal nodes) and probabilities (Cardona Hernández, 2004). These techniques offer certain advantages

over other multivariate classification or prediction methods. The first advantage is their non-parametric nature, without assumptions about the distribution of predictor variables, their relationship with the response, or possible interactions. A decision tree makes optimal choices from a probabilistic perspective (Díaz-Martínez *et al.*, 2021). Generally, the inherent logic of decision trees makes them simpler to interpret than other multivariate regression methods (Calle & Sánchez-Espigares, 2007). This methodology has proven effective in data mining, allowing segmentation and classification of large volumes of information to predict variables of interest, such as CEE. Consequently, water quality can be assessed using a limited number of physicochemical variables, facilitating resource monitoring.

In recent years, data-driven approaches integrating multiple environmental variables and machine-learning techniques have proven effective for analyzing complex agro-environmental systems, enabling the identification of key drivers and improving the interpretation of spatial variability (Córdoba *et al.*, 2025).

This methodology offers new perspectives on water quality that might be applied in other regions with similar geochemical conditions. To date, no scientific studies have proposed methodological alternatives for estimating CEE beyond the traditional approach proposed by Wainstein (1968), based on the CEE calculation developed by Nijensohn (1961).

This study advances knowledge concerning irrigation water quality, particularly in areas requiring more tailored and accessible approaches. The predictive model of Effective Electrical Conductivity (CEE) aimed to optimize water classification in the Mendoza Green Belt and provide a practical tool to inexpensively evaluate water quality, supporting more efficient and sustainable water resource management.

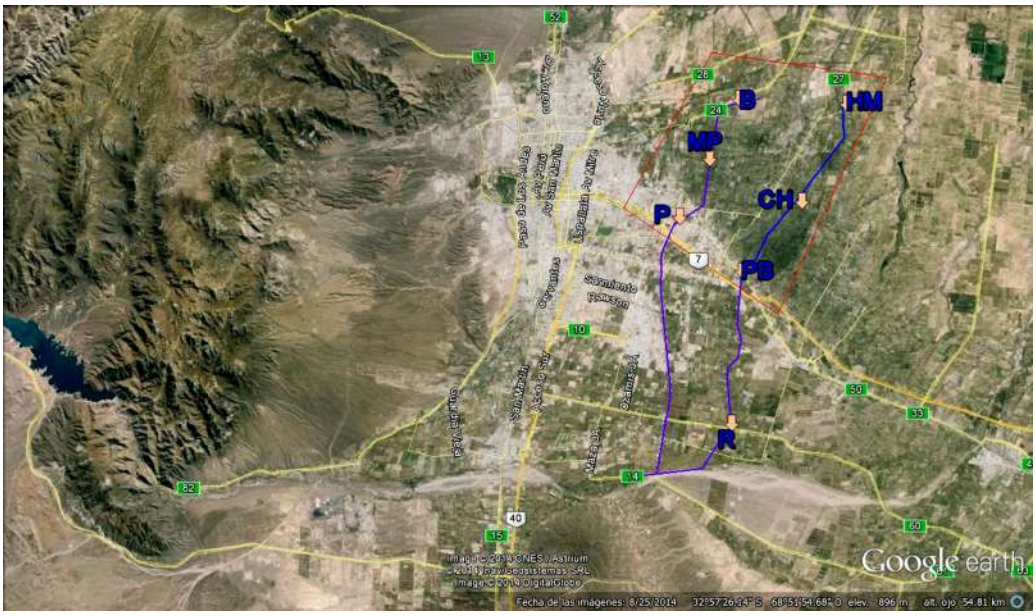
Materials and Methods

The study area is located within the Mendoza Green Belt (approximate coordinates 32°53’ S - 68°42’ W), a region devoted to intensive vegetable production that includes the districts of Los Corralitos, La Primavera, Km 8, Mundo Nuevo, and Las Violetas. The area has a semi-arid climate, with scarce rainfall concentrated in summer (200-250 mm annually), extreme temperatures, and frequent winter frosts (Ramos *et al.*, 2017). Soils have high organic matter and a shallow water table (Akil, 2020). Since the commissioning of the Potrerillos Dam in 2003, irrigation management in this area shifted from a traditional system with irregular water availability to a more controlled and efficient approach.

This study considers a prior monitoring work conducted between 1999 and 2013 by Facultad de Ciencias Agrarias (FCA) and Instituto Nacional del Agua (INA), with a large dataset for the study area (Cónsoli, 2015). During this period, water samples were collected monthly or bimonthly at fixed points in the Mendoza Green Belt, specifically in the Chachingo and Pescara canals. Samples were analyzed to determine: Actual Electrical Conductivity (CEA), pH, calcium (Ca^{2+}), magnesium (Mg^{2+}), sodium (Na^{+}), potassium (K^{+}), carbonate (CO_3^{2-}), bicarbonate (CO_3H^{-}), chloride (Cl^{-}), and sulfate (SO_4^{2-}) (Official Methods of Analysis of AOAC International, 1995). Nitrates (NO_3^{-}) and phosphates (PO_4^{3-}) were measured using a HACH 2010 spectrophotometer, while heavy metals such as lead (Pb), copper (Cu), cadmium (Cd), and zinc (Zn) were quantified using atomic absorption spectrophotometry. Based on these analyses, additional parameters were calculated, including Effective Electrical Conductivity (CEE), Sodium Adsorption Ratio (SAR), and the alkali coefficient (K), as established by Hardman-Miller (Avellaneda *et al.*, 2004). Furthermore, water quality classifications were performed using the Riverside classification as modified by Thorne and Peterson (1954, 1996) and the regional classification for irrigation water proposed by Wainstein (1968).

Sampling Sites

Figure 1 (page 4) shows the sampling points in the field. Each site was assigned a short name and abbreviation for easy identification.



The green belt area of Mendoza is indicated in red. Source: authors' elaboration based on Google Earth.

El área del cinturón verde de Mendoza se indica en rojo. Fuente: elaboración propia a partir de Google Earth.

Figure 1. Image of the study area with georeferenced points and a sketch of the Pescara and Chachingo channels (in blue).

Figura 1. Imagen de la zona de estudio con puntos georreferenciados y croquis de los canales Pescara y Chachingo (en azul).

The sampling points along the Chachingo Canal (or Canal Vertientes Corralitos) include: *Route 60* (R), at Canal-Route 60 intersection; *Puente Blanco* (PB), at canal-Carril Nacional (National Drive), where water enters the Green Belt; *Chachingo* (CH), located in the middle section of the canal, east Corralitos; and *Hijuela Montenegro* (HM), final section of Chachingo Canal.

For the Pescara Canal, the Route 60 (R) point was the starting reference, since Chachingo and Pescara canals receive water from the Mendoza River within a few meters of each other. We sampled Pescara (P), at canal entrance to the Mendoza Green Belt, at canal-Carril Nacional (National Road); Matus and Pescara (MP), in the middle section of the canal, downstream from the Industrial Drainage Inspection of the Pescara Collector (Departamento General de Irrigación, DGI); and Becases (B), at the end of the canal, named after a nearby farm.

Water Characterization

Waters in the study area are generally classified as "low sodium hazard" (S1) and, according to the Riverside classification, exhibit "medium salinity" (C3), suggesting their use in soils with moderate to good permeability. In addition to selecting crops with moderate to high salt tolerance, regular leaching irrigations are recommended to prevent hazardous salt accumulation. According to Wainstein's classification (1968), waters are generally grouped as "moderately saline" (C3) or "medium saline" (C4), with C3 waters being suitable for all crops. In salt-sensitive plants, soils without moderate to good permeability must be leached. The C4 waters are suitable for soils with lower permeability but need adequate drainage. Alternatively, moderately tolerant crops should be used with leaching irrigation.

Towards the canals' most distant points, increased salinity and sodicity reduce irrigation suitability. These waters are classified according to Wainstein (1968) as C4 "medium saline" (15% increase in EC relative to the initial point), C5 "distinctly saline" (45%), and C6 "strongly saline" (90%), with a sodium hazard of S2 "moderate risk" (SAR exceeding 4.4 and Na^{+} values 3.9 times higher than the initial levels). In most cases, soil gypsum mitigates this hazard. However, in fine-textured soils with restricted drainage, the sodium hazard remains considerable, being most critical towards the end of the Pescara Canal, where the proportion of moderately soluble salts is lower.

Predictive Model: Regression Trees

Using data mining techniques to construct predictive models with regression trees, we obtained equations to estimate Effective Electrical Conductivity (CEE) as a function of related variables, based on Cónsoli (2015). Predictor variables were selected by degree of correlation with CEE, determination complexity, and cost. This analysis established different combinations of predictor variables varying in number (Cónsoli, 2015). This study determined correlations among quantitative measurements, descriptive and validation statistical techniques for continuous and nominal variables, and a clustering strategy to identify water quality patterns from joint measurements. Initially, Artificial Neural Networks (ANN) were applied to include missing data in the database (26 values for heavy metals and 27 for nitrates and phosphates, before 2008).

The data set used for model development consisted of 468 water samples, each with 16 analyzed parameters and others calculated from measurement results. These instances were employed in the training phase, where CEE was to be predicted.

Modeling was conducted in two phases. In the first training phase, the algorithm known as M5P (Holmes *et al.*, 1999; Quinlan, 1993; Wang & Witten, 1997), which implements a regression tree model also referred to as a "model tree", was used to build a predictive model from the measured data. The minimum number of instances per leaf node was set at 4, with pruning and unfiltered predictions. The resulting regression tree contained intermediate nodes representing queries about attribute values, and leaf nodes containing linear models (LM) to calculate CEE.

The model validation phase included a cross-validation technique (Dietterich, 1997) with ten folds to evaluate model performance. This approach divides the dataset into 10 subsets. In each iteration, 9 subsets are used for training and 1 for validation. Metrics such as correlation coefficients, mean absolute errors, and relative squared errors assessed fit and generalization ability. Both phases used the open-source tool Waikato Environment for Knowledge Analysis (WEKA, Hall *et al.*, 2009).

Results and Discussion

Figure 2 represents a correlation plane associating the measured variables (Cónsoli, 2015).

The variables associated with component 1 (horizontal) include the alkali coefficient (K), CEA, CEE, SAR o RAS, and most of the ions present in the water. There is also variation related to component 2 (vertical), comprising the variables pH, PO_4^{3-}, and CO_3^{2+}.

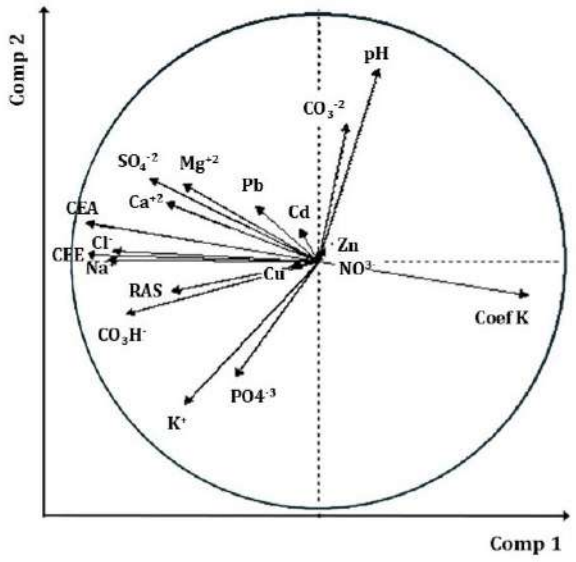


Figura 2. Plano de correlación de las variables cuantitativas.

Figure 2. Correlation plane of the quantitative variables.

The figure 2 (page 5) shows that CEA, CEE, and all ions except CO_3^{2-} were significantly correlated. As CEA and CEE increased, Cl^- (high to near-perfect linear correlation), SO_4^{2-}, Na^+, Mg^{2+}, Ca^{2+}, and HCO_3^- (moderately high correlation), K^+, PO_4^{3-}, and SAR (moderately low correlation), also tended to increase ($p < 0.01$). As expected from a theoretical standpoint, an inverse and statistically significant correlation was observed between CEA and the K coefficient ($p < 0.01$); that is, as CEA increases, K tends to decrease, requiring fewer irrigations to salinize the soil. Ions with major preponderance in waters from the study area, Cl^-, SO_4^{2-}, Na^+, Mg^{2+}, Ca^{2+}, and HCO_3^-, strongly influenced CEA.

Considering CEE, correlations are similar to those found with CEA, but stronger for CO_3H^- (almost perfect correlation) and moderately high for Mg^{2+}. The lack of correlation between CEA or CEE and pH is corroborated.

Heavy metals, NO_3^-, and PO_4^{3-} show no significant relationships. Correlation between PO_4^{3-} and K^+ is moderately low. CO_3^{2-} is the only ion not correlated with any variable, possibly due to its low presence in Mendoza waters. Statistical validation showed that the moderately low relationship between CO_3^{2-} and pH is the only one for this anion. The pH is inversely correlated with K^+ ($p < 0.01$). The alkali coefficient (K) is negatively correlated with several variables, indicating its value decreases with increasing Cl^-, CEA, CEE (high to perfect correlation), SO_4^{2-}, CO_3H^-, and Na^+ (moderately high correlation).

These correlations (Cónsoli, 2015) are crucial to validate the use of regression trees to predict CEE from a reduced set of physicochemical variables in irrigation water. Thus, figure 2 (page XXX) illustrates high correlations between CEE and CEA, Cl^-, SO_4^{2-}, Na^+, Mg^{2+}, Ca^{2+}, and HCO_3^- reinforcing their selection as key predictors, excluding other variables from the model.

CEE Prediction Models

To the best of our knowledge, no previous studies have used similar methodologies to predict CEE in this area or other regions. This lack of methodological background highlights the need for innovative solutions such as regression trees, which provide accurate predictions adapted to local conditions. Our study is a pioneer, contributing knowledge on irrigation water quality and potential application in other regions with similar conditions.

To build the training set from numerical data, regression trees were developed from measurements focusing on variables that accurately predicted the numerical value of CEE in future instances. Ions showing high positive correlations with CEE were CEA, CO_3H^-, Cl^-, SO_4^{2-}, Ca^{2+}, Mg^{2+}, and Na^+ (Cónsoli, 2015). These variables were fundamental for the proposed models. However, SO_4^{2-} was excluded because its determination is costly and laborious, prioritizing those easy to measure. Based on this selection, different models were trained by progressively reducing the number of variables until an approach based exclusively on CEA to predict CEE.

Table 1 (page 7) shows the five generated models (M1, M2, M3, M4, and M5) rules and equations for each case. Table 2 (page 8) provides a comparative overview of the training and validation phases for each model.

M1, M2, M3, and M4 generated identical rules: if CEA is less than or equal to 1292.5 µS cm^{-1}, LM1 equation is to be applied, whereas if CEA exceeds this value, LM2 equation should be used (table 1, page 7). Equations depend on variables considered in each model. Although M5 includes more variables and has a good correlation coefficient, its complexity makes it less practical.

M5 predicts CEE as a function of CEA, Ca^{2+}, Mg^{2+}, CO_3H^-, Na^+, and Cl^-, using 11 equations depending on the values of these variables and presenting more complex rules (figure 3, page 8). A correlation coefficient of 0.99, absolute error of 21.5 µS cm^{-1} in the training phase and 26.7 µS cm^{-1} in validation, prove this model to be highly accurate.

Subsequently, other models were generated by eliminating variables. First, Cl^- was excluded given its costly determination. In this way, M4 uses CEA, Ca^{2+}, Mg^{2+}, CO_3H^-, and Na^+, and is simplified to only two equations (table 1, page 7), with a correlation coefficient of 0.99 and an absolute error of 27 µS cm^{-1}, a very satisfactory performance.

In M3, Na^+ was also excluded since its analysis requires a flame photometer. This model, based on CEA, Ca^{2+}, Mg^{2+}, and CO_3H^-, achieved a correlation coefficient of 0.99 and an absolute error of 26.5 µS cm^{-1} with only two equations, enhancing practicality without losing accuracy.

Table 1. Linear Models (LM), rules and equations to predict CEE in each case.
Tabla 1. Modelos Lineales (LM) con las reglas y ecuaciones para predecir la CEE en cada caso.

Models	LM rule sets	Corresponding formulas for each case
M1	CEA <= 1292.5 : $LM1_{(1)}$	CEE = 0.9768 * CEA + 21.8862
	CEA > 1292.5 : $LM2_{(1)}$	CEE = 0.7417 * CEA + 310.5959
M2	CEA <= 1292.5 : $LM1_{(2)}$	CEE = 1.0219 * CEA - 0.3337 * Ca^{+2} - 0.1346 * Mg^{+2} + 20.8534
	CEA > 1292.5 : $LM2_{(2)}$	CEE = 1.08 * CEA - 2.7262 * Ca^{+2} - 1.1744 * Mg^{+2} + 380.2531
M3	CEA <= 1292.5 : $LM1_{(3)}$	CEE = 1.0147 * CEA - 0.3315 * Ca^{+2} - 0.1069 * Mg^{+2} + 0.0371 * CO_3H^- + 21.1215
	CEA > 1292.5 : $LM2_{(3)}$	CEE = 0.9978 * CEA - 2.5839 * Ca^{+2} - 0.751 * Mg^{+2} + 0.4818 * CO_3H^- + 329.4153
M4	CEA <= 1292.5 : $LM1_{(4)}$	CEE = 1.0147 * CEA - 0.3315 * Ca^{+2} - 0.1069 * Mg^{+2} + 0.0371 * CO3H- + 21.1215
	CEA > 1292.5 : $LM2_{(4)}$	CEE = 0.9978 * CEA- 2.5839 * Ca^{+2} - 0.751 * Mg^{+2} + 0.4818 * CO_3H^- + 329.4153
M5	CEA <= 1292.5: $LM1_{(5)}$	CEE = 1.0147 * CEA- 0.3315 * Ca^{+2} - 0.1069 * Mg^{+2} + 0.0371 * CO_3H^- + 21.1215
	CEA > 1292.5 y <= 1355: $LM2_{(5)}$	CEE = 0.6026 * CEA - 1.273 * Ca^{+2} - 0.1259 * Mg^{+2} + 0.1687 * CO_3H^- + 695.5064
	CEA > 1355 y <= 1472.5 ; Ca^{+2} <=189: $LM3_{(5)}$	CEE = 0.8979 * CEA - 1.5034 * Ca^{+2} - 0.1259 * Mg^{+2} + 0.1856 * CO_3H^- + 342.7067
	CEA > 1355 y <= 1472.5 ; Ca^{+2} > 189; CO_3H^- <=204.35: $LM4_{(5)}$	CEE = 0.6803 * CEA - 2.2181 * Ca^{+2} - 0.1259 * Mg^{+2} + 0.3066 * CO_3H^- + 741.6139
	CEA > 1355 y <= 1472.5 ; Ca^{+2} > 189; CO_3H^- >204.35: $LM5_{(5)}$	CEE = 0.6803 * CEA - 2.3326 * Ca^{+2} - 0.1259 * Mg^{+2} + 0.2875 * CO_3H^- + 771.7037
	CEA > 1472.5 y <= 1759 ; Ca^{+2} <= 217: $LM6_{(5)}$	CEE = 0.892 * CEA - 1.3212 * Ca^{+2} - 0.1259 * Mg^{+2} + 0.3454 * CO_3H^- - 0.0404 * Cl^- + 290.3693
	CEA > 1472.5 y <= 1759 ; Ca^{+2} > 217 y <= 245: $LM7_{(5)}$	CEE =0.9936 * CEA - 2.9687 * Ca^{+2} + 0.121 * Mg^{+2} + 0.2135 * CO_3H^- - 0.3672 * Cl^- + 504.9899
	CEA > 1472.5 y <= 1759 ; Ca^{+2} > 245: $LM8_{(5)}$	CEE = 0.9712 * CEA- 1.4499 * Ca^{+2} + 0.3773 * Mg^{+2} + 0.2135 * CO_3H^- - 1.4054 *Cl^- + 304.5196
	CEA > 1759 y <= 1892 ; Ca^{+2} <= 218: $LM9_{(5)}$	CEE = 0.9632 * CEA + 0.1412 * Na^+ - 2.1807 * Ca^{+2} - 0.4294 * Mg^{+2} + 0.2992 * CO_3H^- + 358.7019
	CEA > 1759 y <= 1892 ; Ca^{+2} > 218: $LM10_{(5)}$	CEE = 1.0206 * CEA - 3.3314 * Ca^{+2} - 0.3184 * Mg^{+2} + 0.593 * CO_3H^- + 415.8853
	CEA > 1892: $LM11_{(5)}$	CEE = 1.0711 * CEA - 0.3053 * Na^+ - 3.1189 * Ca^{+2} - 0.8342 * Mg^{+2} + 0.5663 * CO_3H^- + 332.8886

Electrical conductivities are expressed in µS cm^{-1} and ion concentrations in mg L^{-1}.

The subscript in parentheses refers to the model used.

Las conductividades eléctricas se expresan en µS cm^{-1} y las concentraciones de iones en mg L^{-1}.

El subíndice entre paréntesis hace referencia al modelo empleado.

Tabla 2. Métricas de las etapas de entrenamiento y validación, para los 5 modelos generados para predecir la Conductividad Eléctrica Efectiva (CEE).

Table 2. Metrics from the training and validation stages, for the 5 models generated to predict Effective Electrical Conductivity (CEE).

Model		M1	M2	M3	M4	M5
Variables		CEA	CEA, Ca^{2+}, Mg^{2+}	CEA, Ca^{2+}, Mg^{2+}, CO_3H^-	CEA, Ca^{2+}, Mg^{2+}, CO_3H^-, Na^+	CEA, Ca^{2+}, Mg^{2+}, CO_3H^-, Na^+, Cl^-
Number of rules		**2**	**2**	**2**	**2**	**11**
Training set evaluation	Correlation coefficient	0.9699	0.9891	0.9922	0.9922	0.9953
	Mean absolute error	62.0428	33.7285	28.1542	28.1542	21.5275
	Mean squared error	100.7367	60.8372	51.6089	51.6089	39.9993
	Relative absolute error	18.8396%	10.2418%	8.5492%	8.5492%	6.5369%
	Relative squared error	24.3504%	14.7058%	12.4751%	12.4751%	9.6688%
Cross-validation	Correlation coefficient	0.9691	0.9881	0.9916	0.9914	0.9913
	Mean absolute error	62.6744	33.1415	26.5318	27.0827	26.7222
	Mean squared error	102.0014	63.6402	53.6790	54.2490	54.4405
	Relative absolute error	18.9145%	10.0017%	8.0070%	8.1733%	8.0645%
	Relative squared error	24.5397%	15.3107%	12.9142%	13.0514%	3.0974%

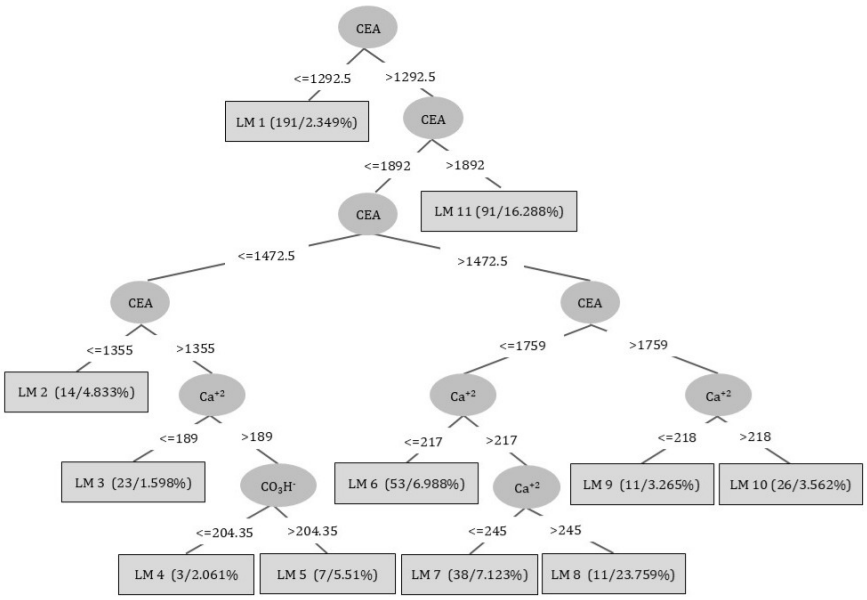


Figure 3. Regression tree of Model 5 (M5): rules of the 11 generated Linear Models (LM), support and confidence values.

Figura 3. Árbol de regresión del Modelo 5 (M5), que muestra las reglas de los 11 Modelos lineales (LM) generados, con soporte y confianza.

In M2, only Ca^{2+} and Mg^{2+} were used together with CEA, excluding CO_3H^-. This model showed a slightly lower correlation coefficient (0.989) and a higher absolute error (33 µS cm^{-1}).

Finally, M1 used only CEA to predict CEE, obtaining a correlation coefficient of 0.9699 and an absolute error of 62 µS cm. Although less accurate, M1 is useful when detailed ionic analyses are unavailable, allowing an acceptable estimation of CEE with minimal resources.

These models can be implemented using simple software or spreadsheets to calculate CEE from basic measurements, enabling rapid and inexpensive evaluations.

Although M5 showed the best results in the training phase, cross-validation metrics of M3 were superior. This difference between training and validation suggests that M5 may have been overfit during training, limiting its generalization capacity. On the other hand, M3 is easier to apply, with only two rules or LMs compared with 11 rules in M5.

Cross-validation in this study provided a reliable assessment of the developed predictive models. This technique divides data into training and testing subsets, allowing for the identification of null overfitting. In this way, a more accurate estimate of model performance under different conditions is obtained, reducing the risk of overfitting. Cross-validation enables the identification of models with greater generalization capacity (Velásquez *et al.*, 2013), reinforces predictive robustness, and provides greater confidence, independent of data particularities.

When the same procedure obtained a model including almost all quantified variables (CEA, Ca^{2+}, Mg^{2+}, CO_3H^-, Na^+, Cl^-, pH, SAR o RAS, K^+, CO_3^{2-}, Pb, Cu, Zn, Cd, alkali coefficient K, and classification indices such as Riverside and Wainstein, 1968), we obtained eight rules, an absolute error of 70 µS cm^{-1} and a correlation coefficient of 0.98. This demonstrates that including a larger number of variables does not necessarily improve accuracy and may cause overfitting Rodriguez Murillo (2019).

Among all models, M3 stands out for sufficient accuracy and significant operational simplicity. M3 includes only the variables CEA, Ca^{2+}, Mg^{2+}, and CO_3H^-, significantly reducing analytical complexity without sacrificing predictive accuracy.

Compared with M4, which includes an additional variable (Na^+), M3 maintains a similar level of accuracy while eliminating the need for a flame photometer, thus simplifying the process and reducing operational costs. Likewise, compared with M5, which incorporates up to 11 complex equations, M3 uses only two equations, easing its implementation.

Considering M2, although simpler by excluding the variable CO_3H^-, shows a higher absolute error (33 µS cm^{-1}) and a slightly lower correlation coefficient (0.9890), representing a clear loss of precision. M1, based exclusively on CEA, offers the greatest simplicity, but its lower accuracy limits it to preliminary estimates in contexts with severe resource constraints.

In conclusion, M3 emerges as the best option, combining accuracy and ease of application. This makes it an optimal tool for predicting CEE in various agronomic and environmental applications.

Prediction of CEE as a Function of CEA, Ca^{2+}, Mg^{2+}, and CO_3H^- According to Model 3:

Representation of Inputs and Outputs

A: Set of attributes or input (independent) variables: CEA, Ca^{2+}, Mg^{2+}, and CO_3H^-.

V: Set of possible values of the attributes (table 3, page 10).

E: Set of 468 training instances described in terms of A, V, and a numerical value of CEE that belongs to E.

Parameters of the M5P Algorithm and Learned Model

Figure 4 (page 10), shows the regression tree generated using the M5P algorithm. This model contains two rules or linear models (LMs), with a relative squared error of 12.5% in the training data. The correlation coefficient is high, reaching 0.9922.

The rules and equations derived from the model are as follows:

- If CEA <= 1292.5: LM1(3)

CEE = 1.0147 * CEA - 0.3315 * Ca^{+2} - 0.1069 * Mg^{+2} + 0.0371 * CO_3H^- + 21.1215

- If CEA > 1292.5: LM2(3)

CEE = 0.9978 * CEA - 2.5839 * Ca^{+2} - 0.751 * Mg^{+2} + 0.4818 * CO_3H^- + 329.4153

Table 3. Inputs and continuous output of Model 3 to predict Effective Electrical Conductivity (CEE).

Tabla 3. Descripción de entradas y salidas continuas del Modelo 3 para predecir la Conductividad Eléctrica Efectiva (CEE).

Electrical conductivities are expressed in µS cm^{-1} and ion concentrations in mg L^{-1}.

Las conductividades eléctricas se expresan en µS cm^{-1} y las concentraciones de iones en mg L^{-1}.

Sample	Minimum	Maximum	Mean
CEA	599.0000	3200.0000	1470.3000
Ca^{+2}	24.0000	424.0000	183.6000
Mg^{+2}	8.5000	140.0000	40.3000
CO_3H^-	12.2000	780.8000	238.4000
CEE	599.0000	2805.4000	1376.5000

Electrical conductivities are expressed in µS cm^{-1}.

Las conductividades eléctricas se expresan en µS cm^{-1}.

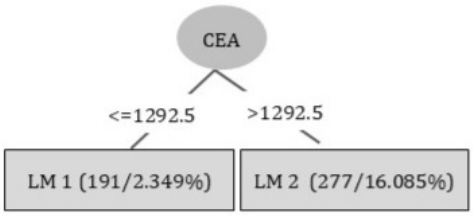


Figure 4. Regression tree of Model 3 (M3) to predict Effective Electrical Conductivity (CEE) as a function of CEA, Ca^{+2}, Mg^{+2} and CO_3H^-, with support and confidence.

Figura 4. Árbol de regresión del Modelo 3 (M3) para predecir Conductividad Eléctrica Efectiva (CEE) en función de CEA, Ca^{+2}, Mg^{+2} y CO_3H^-, con soporte y confianza.

Validation

M3 performance shows solid predictive capacity. The correlation coefficient, which evaluates the statistical relationship between predicted and observed values, is 0.9916, indicating an excellent fit. The prediction error is 8%, considered reasonable. The mean absolute error is 26 µS cm^{-1} of CEE, highly acceptable for evaluating irrigation water.

Conclusions

The predictive model of CEE, developed through regression trees, is effective, precise, and accessible for evaluating irrigation water quality in the Mendoza Green Belt.

Five models were developed, using from one to six variables (CEA). All models showed robust performance, confirming applicability in diverse scenarios. This versatility allows resource optimization while reducing costs compared to traditional analytical methods.

Model 3 stood out for simplicity and performance, predicting CEE from four key physicochemical variables: CEA, Ca^{2+}, Mg^{2+}, and CO_3H^-. The rules generated by the regression trees offer replicability and adaptability in contexts with specific geochemical characteristics.

The proposed approach improves risk interpretation in irrigation waters containing salts of medium solubility, as it is adapted to local geochemical conditions and overcomes limitations of international classification systems. This methodology provides practical alternatives, contributing to the sustainable and efficient management of water resources in Mendoza and similar regions.

These simple equations reduce analytical costs and facilitate frequent monitoring, reserving detailed ionic analyses for particular situations. Future research should focus on comparative studies to evaluate model performance in varied contexts and on refining predictor variables according to local conditions. Expanding the dataset to other regions will also help validate model adaptability, ensuring broader applicability in agricultural water management.

References

Akil, N. N. (2020). *Zonificación del cinturón verde de Mendoza en base a las funciones ecosistémicas*. Tesina de grado. Universidad Nacional de Cuyo. Facultad de Ciencias Agrarias. Biblioteca Digital UNCUYO. https://bdigital.uncu.edu.ar/15559

Ardila, A. N. & Saldarriaga, J. (2013) Formulación de un índice global de calidad de aguas residuales para riego. *Av. Cien. Ing., 4*(3), 11-26.

Avellaneda, M.; Bermejillo, A.; Mastrantonio L. E. (2004). *Aguas de riego calidad y evaluación de su factibilidad de uso*. EDIUNC.

Ayers, R. S. & Westcot, D. W. (1987). La calidad del agua en la Agricultura. *Serie FAO Riego y Drenaje 29*(1).

Calle, M. L. & Sánchez-Espigares, J. A. (2007). Árboles de clasificación y regresión en la investigación Biomédica. *Medicina Clínica*, *129*(18), 702-706. https://doi.org/10.1157/13112516

Cardona Hernández, P. A. (2004). Aplicación de árboles de decisión en modelos de riesgo crediticio. *Revista Colombiana de Estadística, 27*(2), 139-151. https://revistas.unal.edu. co/index.php/estad/article/view/28808

Ciardullo, V. F.; Gennari, A. J. (2025). Agricultural Land Valuation-Hedonic Pricing and Geostatistical Advances: A State-of-the-Art Review. *Revista de la Facultad de Ciencias Agrarias. Universidad Nacional de Cuyo. 57*(2): 224-236. https://doi.org/10.48162/rev.39.185

Cónsoli, D. V. (2015). *Evolución de la contaminación del agua de riego y clasificación de su calidad dentro del cinturón verde de Mendoza*. Tesis de maestría no publicada. Maestría en Riego y Drenaje. Universidad Nacional de Cuyo.

Córdoba, M.; Vallone, R.; Paccioretti, P.; Corvalán, F.; Balzarini, M. (2025). Data-driven Method for the Delimitation of Viticultural Zones: Application in the Mendoza River Oasis, Argentina. *Revista de la Facultad de Ciencias Agrarias. Universidad Nacional de Cuyo. 57*(2): 57-68. DOI: https://doi.org/10.48162/rev.39.171

Díaz-Martínez, M. A., Ahumada-Cervantes, M. de los A., & Melo-Morín, J. P. (2021). Árboles de decisión como metodología para determinar el rendimiento académico en educación superior. *Revista Lasallista de Investigación, 18*(2), 94-104. https://revistas.unilasallista.edu.co/index.php/rldi/article/view/2724

Dietterich, T. G. (1997). Machine-learning research. *AI Magazine, 18*(4), 97.

Ente Provincial del Agua y Saneamiento (EPAS). (1995). *Normas de calidad de aguas*. Documento preliminar. Mendoza. Argentina.

FAO. (1997). *Lucha contra la contaminación agrícola de los recursos hídricos*. Estudio FAO Riego y Drenaje. 55 p. Por Ongley, E. D. GEMS/Water Collaborating Centre Canadá Centre for Inland Waters. http://www.fao.org/docrep/w2598s/w2598s00.htm#Contents

Hall, M., Frank, E., Holmes, G., Pfahringer, B., Reutemann, P., & Witten, I. H. (2009). *T*he WEKA Data Mining Software: An Update. *ACM SIGKDD Explorations Newsletter*, *11*(1). Recuperado de https://www. kdd.org/exploration_files/p2V11n1.pdf

Holmes, G., Hall, M., Frank, E. (1999). Generating Rule Sets from Model Trees. In: Foo, N. (eds) *Advanced Topics in Artificial Intelligence (AI 1999)*. Lecture Notes in Computer Science, vol 1747. Springer, Berlin, Heidelberg. https://doi.org/10.1007/3-540-46695-9_1

Nijensohn, L. (1961). Calidad de aguas de riego (Capítulo 14). En *Primer curso nacional de manejo de riego: Riego y drenaje*. Mendoza, Argentina.

Official Methods of Analysis of AOAC International. (1995). 16 th Edition. Volumen I.

Quinlan, J. R. (1993). *C4.5: Programs for Machine Learning*. Morgan Kaufmann. Quinlan, J. R.

Ramos, R. A., Bottesi, M. C., & Quinteros, J. R. (2017). *Estimación del avance urbano sobre la interfase urbano-rural del oasis norte de la provincia de Mendoza.* INTA. https://repositorio.inta.gob.ar/xmlui/handle/20.500.12123/43

Rodríguez Murillo, N. A. (2019). *Análisis de validación cruzada bajo diferentes condiciones de ruido*. Tesis de Maestría en Ingeniería Industrial. Tecnológico Nacional de México. 84 p.

Thorne, D. W., & Peterson, H. B. (1954). *Técnica de Riego* (Versión Española, 1963). México.

Thorne. D. W. & Peterson H. B. (1996). *Técnica de Riego Fertilidad y Explotación de los Suelos*. Editorial Continental.

Velásquez, J. D., Fonnegra R., Y., & Villa G., F. A. (2013). Pronóstico de series de tiempo con redes neuronales regularizadas y validación cruzada. *Revista Vínculos, 10(1)*, 267-279. https://doi.org/10.14483/2322939X.4702

Wainstein, P. (1968). *Clasificación de las aguas de riego de Mendoza*. Informes Científicos y Técnicos N°15. Instituto de Suelos y Riego.

Wang, Y., & Witten, I. (1997). Induction of model trees for predicting continuous classes. In *Proceedings of the Poster Papers of the ECML*. 128-137.

Zuluaga, J. M., Drovandi, A. A., Bermejillo, A. I., Filippini, M. F., Cónsoli, D. V., Salcedo, C. E., Valdes, A. E., & Morsucci, A. L. (2011). *Diagnóstico de la calidad del recurso hídrico en el cinturón verde de Mendoza, Argentina*. XVI Congreso Nacional de Irrigación. Asociación Nacional de Especialistas en Irrigación. Culiacán.

Translocation and Experimental Adaptation of *Distichia muscoides* Cushions in a Wetland Impacted by Acid Rock Drainage, Ancash, Peru

Translocación y adaptación experimental de cojines de *Distichia muscoides* en un bofedal impactado con drenaje ácido de roca, Áncash, Perú

Maria Cristina Otoya Fernández [1*], Yeidy Montano [2], Marilín Sánchez-Purihuamán [3], Pedro M. Tapia [4], Junior Caro-Castro [5], Carmen Carreño-Farfán [6]

Originales: *Recepción:* 27/02/2024 - *Aceptación:* 23/09/2024

ABSTRACT

The deglaciation of the Andean mountain range negatively impacts ecosystems and water bodies, primarily increasing the concentration of heavy metals. However, their concentration can be reduced by applying bioremediation techniques. The objective of this study was to evaluate the effect of the translocation and adaptation of *Distichia muscoides* cushions in a wetland impacted by acid rock drainage in a high Andean region. For this purpose, the characteristics of water, peat, and *D. muscoides* tissue were compared in two wetlands, and the behavior of translocated *D. muscoides* was evaluated based on the bioaccumulation and translocation factors of metals. The quantification of Al, Fe, and Mn in peat, root, and aerial tissue of *D. muscoides* showed higher concentration values after the translocation of the cushions. Additionally, the bioaccumulation factor classified the transplanted cushions as accumulators of Al, Cu, As, Fe, Mn, and Zn, while the translocation factor classified the cushions as phytoextractors of Al, As, Cr, Fe, Mn, and Zn, and phytostabilizers of Pb and Cu. It is concluded that translocated and adapted *D. muscoides* cushions have potential for the bioremediation of wetlands contaminated with acid rock drainage.

Keywords
Bioremediation • wetland • acid rock drainage • *Distichia muscoides* • heavy metals

https://doi.org/10.48162/rev.39.190

1 Universidad Nacional Pedro Ruiz Gallo. Facultad de Ciencias Biológicas. Laboratorio de Investigación Biotecnología Microbiana. Lambayeque-Perú. *crisotofer13@gmail.com
2 Instituto Nacional de Investigación en Glaciares y Ecosistemas de Montaña. Huaraz. Ancash-Perú.
3 Universidad Nacional Pedro Ruiz Gallo. BlyME: BS-CA. Grupo de Investigación Biodiversidad y Manejo Ecológico del Bosque Seco y Cultivos Tropicales. Lambayeque-Perú.
4 Universidad Peruana Cayetano Heredia. Facultad de Ciencias e Ingeniería. Lima-Perú.
5 Universidad Nacional Mayor de San Marcos. Facultad de Ciencias Biológicas. Laboratorio de Ecología Microbiana. Lima-Perú.
6 Universidad Nacional Pedro Ruiz Gallo. BlyME: BS-CA. Facultad de Ciencias Biológicas. Laboratorio de Investigación Biotecnología Microbiana. Lambayeque-Perú.

Licenses Creative Commons
Attribution - Non Commercial - Share Alike

Resumen

La desglaciación de la cordillera andina impacta de manera negativa los ecosistemas y cuerpos de agua, incrementando la concentración de metales pesados como principal consecuencia; sin embargo, su concentración puede ser disminuida aplicando técnicas de biorremediación. El objetivo de este trabajo fue evaluar el efecto de la translocación y adaptación de cojines de *Distichia muscoides* en un bofedal impactado con drenaje ácido de roca en una región altoandina. Para ello, se compararon las características del agua, turba y tejido de *D. muscoides* en dos bofedales, evaluando el comportamiento de *D. muscoides* traslocados basados en los factores de bioacumulación y traslocación de metales. La cuantificación de Al, Fe y Mn en turba, tejido radicular y aéreo de *D. muscoides* demostró mayores valores de concentración después de la traslocación de los cojines. Por otro lado, el factor de bioacumulación calificó los cojines trasplantados como acumuladores de Al, Cu, As, Fe, Mn, Zn, mientras que el factor de traslocación calificó a los cojines como fitoextractores de Al, As, Cr, Fe, Mn, Zn, y fitoestabilizadores de Pb y Cu. Se concluye que los cojines de *D. muscoides* traslocados y adaptados tienen potencial para la biorremediación de bofedales contaminados con drenaje ácido de roca.

Palabras clave

Biorremediación • bofedales • drenaje ácido de roca • *Distichia muscoides* • metales pesados

Introduction

The Huascaran Biosphere Reserve is a natural heritage site located in Ancash, Peru, encompassing an area of 1,155,800 hectares. This includes the core area, Huascaran National Park (HNP), which contains 95% of the Cordillera Blanca (11). Between 1962 and 1970, the Cordillera Blanca covered 723 km^2 and 658 km^2, respectively (6). However, by 2016, the glacial area had decreased to 448.81 km^2, representing a 38.2% reduction and a loss of 277.45 km^2 (38). Additionally, in the Santa River, which is fed by western glaciers, heavy metals have been detected at levels exceeding the Maximum Permissible Limits (MPL) of the Environmental Quality Standards (EQS) for Water. This contamination results from glacial erosion, rock weathering, and anthropogenic activity (18, 39).

The retreat of Andean glaciers exposes rock material that typically contains sulfide minerals (pyrite), which, when oxidized and leached, generates acid rock drainage (ARD) with an acidic pH and high metal concentrations, impacting water bodies and ecosystems (17). The ARD formation process begins when sulfide minerals, exposed to atmospheric oxygen, become unstable and oxidize (34). The oxidation of pyrite, the main mineral responsible for ARD generation, requires oxygen and water and can be accelerated by microbial action. Metals in ARD originate from the oxidation of sulfides and the dissolution of acid-consuming minerals. ARD has an acidic pH, a high concentration of sulfates, and primarily dissolved metals such as iron (Fe) and aluminum (Al). However, trace metals like lead (Pb), zinc (Zn), copper (Cu), cadmium (Cd), manganese (Mn), cobalt (Co), and nickel (Ni) can reach high concentrations on certain occasions (38). Heavy metals are persistent pollutants because they bioaccumulate, are not biodegradable, and are highly toxic even at low concentrations, affecting plants, animals, and humans (27).

Wetlands are characteristic of the tropical and subtropical Andes (5, 36), where cushion plants such as *Distichia muscoides* and *Oxychloe andina* are found. These are primary species of the Andean Altiplano with the capacity to store water and elevate it above the groundwater level (31). These cushion plants regulate water release, act as sinks for organic carbon, and promote wildlife (7, 20). However, they are threatened by glacial retreat (20), overgrazing, anthropogenic extraction, and heavy metal contamination from ARD (10, 31, 36). Previous studies conducted in the Cordillera Blanca, Ancash, Peru, have demonstrated the effectiveness of transplanting species like *D. muscoides* to accelerate the bioremediation of environments impacted by ARD (17, 38).

Based on previous evidence, bioremediation is proposed as a solution, involving the application of microorganisms, plants, or derived enzymes for environmental restoration.

This approach relies on the biological entities' ability to reduce or eliminate contaminants (12). Phytoremediation, the use of plants for bioremediation, allows them to absorb, mobilize, and accumulate heavy metals and other contaminants through strategies like phytoextraction, phytostabilization, and phytovolatilization (16, 28). In phytoextraction, metals are absorbed by roots, transported, and accumulated in stems and leaves. Phytostabilization reduces contaminant mobility and prevents migration to groundwater (24, 30). Phytovolatilization involves the absorption of metals by roots, transport via the xylem, and release from the aerial parts of plants (23).

The response of plants to heavy metals classifies them as excluders, indicators or accumulators. Excluders have lower metal accumulation in their above-ground parts compared to the soil concentration. Indicators maintain a direct relationship between metal concentration in their above-ground parts and the soil. Accumulators have higher metal concentrations in their above-ground parts compared to the soil. To implement phytoremediation through phytostabilization, excluder plants are used, which accumulate metals in their roots, while for phytoextraction, accumulator plants are necessary to transport metals to their above-ground parts (1, 16, 24).

Plants like *D. muscoides* are efficient for the stabilization and extraction of heavy metals (17); however, it is necessary to analyze the technical, ecological, and economic feasibility before their use, considering the conditions of the damaged ecosystem and the possibilities of application (12). Therefore, the objective of this study was to evaluate the effect of translocating and establishing *D. muscoides* cushions in a wetland impacted by ARD located in the Ancash region, Peru, aiming to remediate ARD-affected wetlands. The specific objectives were: a) to compare the characteristics of wetlands unaffected and affected by ARD, b) to monitor the adaptation of translocated *D. muscoides* cushions by comparing the concentration of heavy metals, and c) to determine the behavior of translocated cushions in an ARD-impacted wetland.

Materials and Methods

Comparison of Wetlands Affected and Unaffected by ARD

Study Area

The study was conducted within HNP, in the district of Catac, province of Recuay, Ancash region. Two wetlands were selected, designated as wetland 1 and 2, both predominantly populated with *D. muscoides* cushions. Three zones (A, B, and C) were established within each wetland (figure 1, page 4), based on pH conditions (3.95-7.27), temperature (8.7-14.7°C), altitude (4506-4818 meters above sea level), and the condition of the *D. muscoides* cushions. For sampling in each zone of both wetlands, nine sampling points were considered (A1, A2, A3, B1, B2, B3, C1, C2, and C3) with a 50 cm separation between them. Each wetland involved nine samples of root tissue, nine of aerial tissue, three water samples, and three peat samples.

Sampling of Water from the Wetlands

Water quality was assessed according to the National Protocol for the Quality of Natural Bodies of Surface Water (3). In each wetland, three water samples were collected in October 2021. Five-hundred mL of water were collected using sterile polyethylene bottles placed at the imaginary triangle center formed by the three sampling points. The samples were taken against the water flow direction at a depth of 20-30 cm, with the addition of 1 mL of nitric acid as a chemical preservative. Physicochemical parameters such as pH and temperature were measured in each wetland water sample using a handheld meter (HANNA HI8424 model).

Sampling of Peat, Root and Foliage of D. muscoides

Sampling of organic peat was conducted following the established technique in the Peruvian Soil Sampling Guide (21). Nine cushions of *D. muscoides* were selected in each wetland, one per sampling point, at a depth of 30 cm. From each cushion, a rectangle of 20x15 cm consisting of peat, roots, and aerial tissue was extracted. In the laboratory, peat samples from each zone (three sampling points) were mixed, and a 300 g sample of the most decomposed peat was selected, totaling three samples per wetland. Root tissue was separated from aerial tissue, and 250 g from each rectangle was weighed, resulting in nine samples per wetland.

The concentration of heavy metals in all samples was determined using Inductively Coupled Plasma Atomic Emission Spectrometry (ICP-AES) for water according to method EMW 200.7 (19). For peat, root tissue, and aerial tissue, method 3050-B (2) was employed. Metal concentration values in water were compared with EQS fow water, Category 4, Subcategory 1 (22).

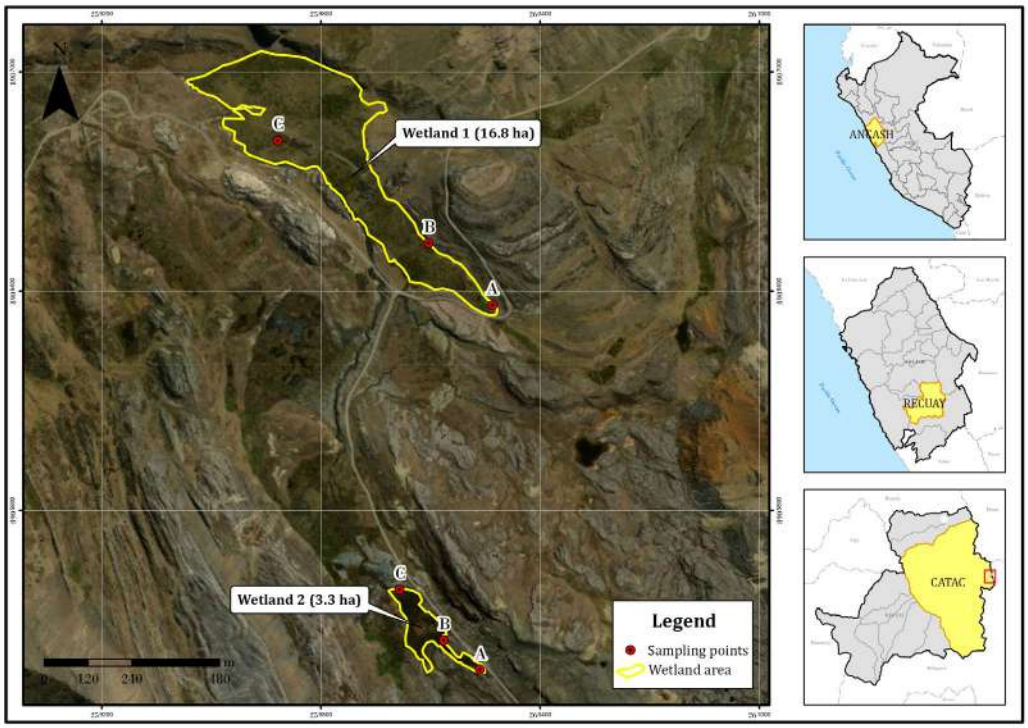


Figure 1. Location of the sampling zones in wetlands 1 and 2.

Figura 1. Ubicación de las zonas de muestreo en los bofedales 1 y 2.

Presence of Sulfate-Reducing Bacteria in the Sediment of Water Bodies

For sampling, three zones were considered in each wetland, with two sampling points in each zone (A1, A2, B1, B2, C1, and C2). Samples of 1000 g of sediment from the water bodies were collected using an auger that extracts perforated solid material (37) at a depth of 70 cm. The samples were immediately deposited into transparent glass jars and transported in a thermal box (10±1°C) to the laboratory, where enrichment of sulfate-reducing bacteria (SRB) was conducted in twelve Winogradsky columns (25).

Translocation and Adaptation of *D. muscoides* and Comparison of Heavy Metal Concentrations

Translocation and Adaptation of D. muscoides

The phase of translocation or transplantation and adaptation of *D. muscoides* took place from December 2021 to May 2022 in zone B, the experimental area of wetland 2, previously delineated (total area: 7.7 ha). This area is traversed by water from Pastoruri Creek, covering an area of 5x5 m^2 (georeferenced points E: 260088 and N: 8905452, at an altitude of 4804 meters above sea level). Eight cushions were selected from zones A and B of wetland 1, located at the edge in contact with the water, from which a rectangle (30 x 15 cm) consisting of roots, aerial tissue, and root peat was extracted to a depth of 30 cm. Among the eight rectangles extracted from the cushions, five were designated for translocation and three for the initial analysis of heavy metal concentration in peat, root tissue, and aerial tissue before transplantation. Monitoring of the adaptation of transplanted cushion rectangles was conducted over 5 months, during what is known as the rainy season due to the significant influence of wetland water levels (7). Monitoring occurred every 10 days during the first two months and subsequently every 15 days from the third to the fifth month. Vigor and persistence of green color were evaluated in each cushion rectangle.

After 5 months of transplantation, a random sampling of three cushions was conducted from among the five that were transplanted. The presence of few, moderate, or abundant roots allowed for assessing the adaptation of the cushions to the transplantation. In contrast, the absence of roots indicated inadequate adaptation of the cushions to the transplantation.

Comparison of Heavy Metal Concentrations

The concentration of heavy metals in the peat, root tissue, and aerial tissue of three *D. muscoides* cushions before translocation was compared with the concentration determined in three cushions 5 months after translocation. Additionally, the concentration of heavy metals in the peat, root tissue, and foliage of three translocated cushions was compared with that in three native cushions (not transplanted) from the wetland impacted by ARD where the translocation occurred.

Behavior of Translocated Cushions in the Wetland Impacted by ARD

The behavior of transplanted *D. muscoides* was evaluated using the bioaccumulation factor (BAF) and translocation factor (TF) (30) of the root tissue and foliage of both translocated and non-translocated *D. muscoides*.

$$\text{BAF} = \frac{\text{Concentration of root or foliage}}{\text{Concentration of peat}}$$

$$\text{TF} = \frac{\text{Concentration of foliage}}{\text{Concentration of root tissue}}$$

Statistical Analysis

The concentrations of heavy metals (mg/kg) in peat, root tissue, and foliage before and after the translocation of *D. muscoides* were analyzed using the paired Student's t-test for normally distributed samples and the Wilcoxon test for samples with a non-normal distribution. Additionally, the concentrations of heavy metals (mg/kg) in translocated and non-translocated cushions were analyzed using the one-sample Student's t-test. A significance level of 0.05 was applied to all statistical tests. The analyses were conducted using RStudio 2021.09.

Results and Discussion

Characteristics of the Studied Wetlands

Wetland 2 was classified as impacted by ARD based on the acidic pH of the water, higher concentrations of metals in both the water and tissues of *D. muscoides*, as well as the presence of sulfate-reducing bacteria (table 1, page 6).

The pH range of water in wetland 2, impacted by ARD (3.95 - 6.35), was more acidic compared to wetland 1, which showed no apparent impact from ARD (water: 7.13 - 7.30). In ARD-impacted environments, a permanent acidity (3.54-4.47) has been reported (39), or significantly lower pH (3.60-4.42) compared to non-ARD water (6.95-7.13) (15). The acidic pH is a consequence of ARD, resulting from glacier retreat and subsequent oxidation of exposed mineralized rocks. The acidic pH increases the availability of dissolved metal ions in the water, thereby increasing toxicity to living organisms (38).

Neutralization reactions also influence ARD. While most carbonate minerals dissolve rapidly, hydrolysis of Fe or Mn, following the dissolution of their respective carbonates and subsequent precipitation, can generate acidity (34). The concentration of metals in the water of wetland 2 (Fe, Mn, Zn) was higher than in wetland 1. 0.4844 mg/L of Mn was quantified in wetland 2, contrasting with wetland 1 (0.0002 mg/L), a value that exceeds the EQS for water, Category 4 (22).

Regarding water temperature, the ranges were similar in wetlands 1 and 2 (10.5 - 12.3°C and 8.7 - 14.7°C, respectively). Similarly, in the Quillcay basin, Ancash region, it was determined that water temperature remained constant throughout the year at different sampling points, thus not contributing to differences in water quality found in potentially ARD-affected and unaffected areas (15).

Table 1. Concentration of heavy metals (mg/kg) in *D. muscoides* from the evaluated wetlands.

Tabla 1. Concentración de metales pesados (mg/kg) en *D. muscoides* procedentes de los bofedales evaluados.

Heavy metal	Water (n=3) (mg/L)	Peat (n=3) (mg/kg)	Root tissue (n=9) (mg/kg)	Foliage (n=9) (mg/kg)
Wetland 1				
Aluminum (Al)	0.0200±0.01	2.0000±0.09	2.000±0.05	2.00±0.00
Cadmium (Cd)	0.0029±0.00	4.0500±3.35	4.1844±1.67	4.00±2.25
Copper (Cu)	0.0010±0.00	1.4500±0.77	2.636±3.56	2.04±1.08
Iron (Fe)	0.6520±0.55	1545.80±191.53	1020.81±83.07	774.56±237.44
Manganese (Mn)	0.0002±0.00	119.86±10.40	118.218±12.02	74.91±27.23
Lead (Pb)	0.0060±0.00	9.720±1.98	22.112±17.15	5.99±2.04
Zinc (Zn)	0.0267±0.00	7.020±4.75	72.125±10.27	35.60±9.29
Wetland 2				
Aluminum (Al)	0.0200±0.00	2.000±0.05	2.000±0.00	2.000±0.00
Cadmium (Cd)	0.0009±0.00	11.520±1.75	14.230±7.20	5.110±3.94
Copper (Cu)	0.0010±0.05	13.170±6.25	4.190±1.35	3.130±1.09
Iron (Fe)	2.8807±0.59	16980.97±148.55	6583.57±90.60	7830.47±864.16
Manganese (Mn)*	0.4844±0.43	106.630±8.19	136.50±14.34	183.11±48.30
Lead (Pb)	0.0060±0.04	51.9000±7.90	19.790±5.86	15.64±3.11
Zinc (Zn)	0.0643±0.03	161.7400±16.8	80.34±7.67	93.29±7.23

*Peruvian EQS: Category 4, subcategory 1: 0.2 mg/L.

*ECA peruano: Categoría 4, subcategoría 1: 0,2 mg/L.

The concentration range of metals in the peat (Cd, Cu, Fe, Pb, Zn), root tissue (Cu, Fe, Zn, Cd, Mn), and foliage (Cd, Fe, Mn, Zn) in wetland 2 was higher than that in wetland 1 (table 1). Fe and Al are the main metals dissolved in ARD, as previously reported by Zimmer *et al.* (2018). However, the high concentration of heavy metals in the peat and tissues of *D. muscoides* suggests that these plants are adapted to decontamination efforts (10). Al, Fe, and Mn are the heavy metals quantified in higher concentrations in *D. muscoides* exposed to ARD in an artificial wetland, with other metals such as Cu, Cd, Fe, Ni, and Zn also present (17).

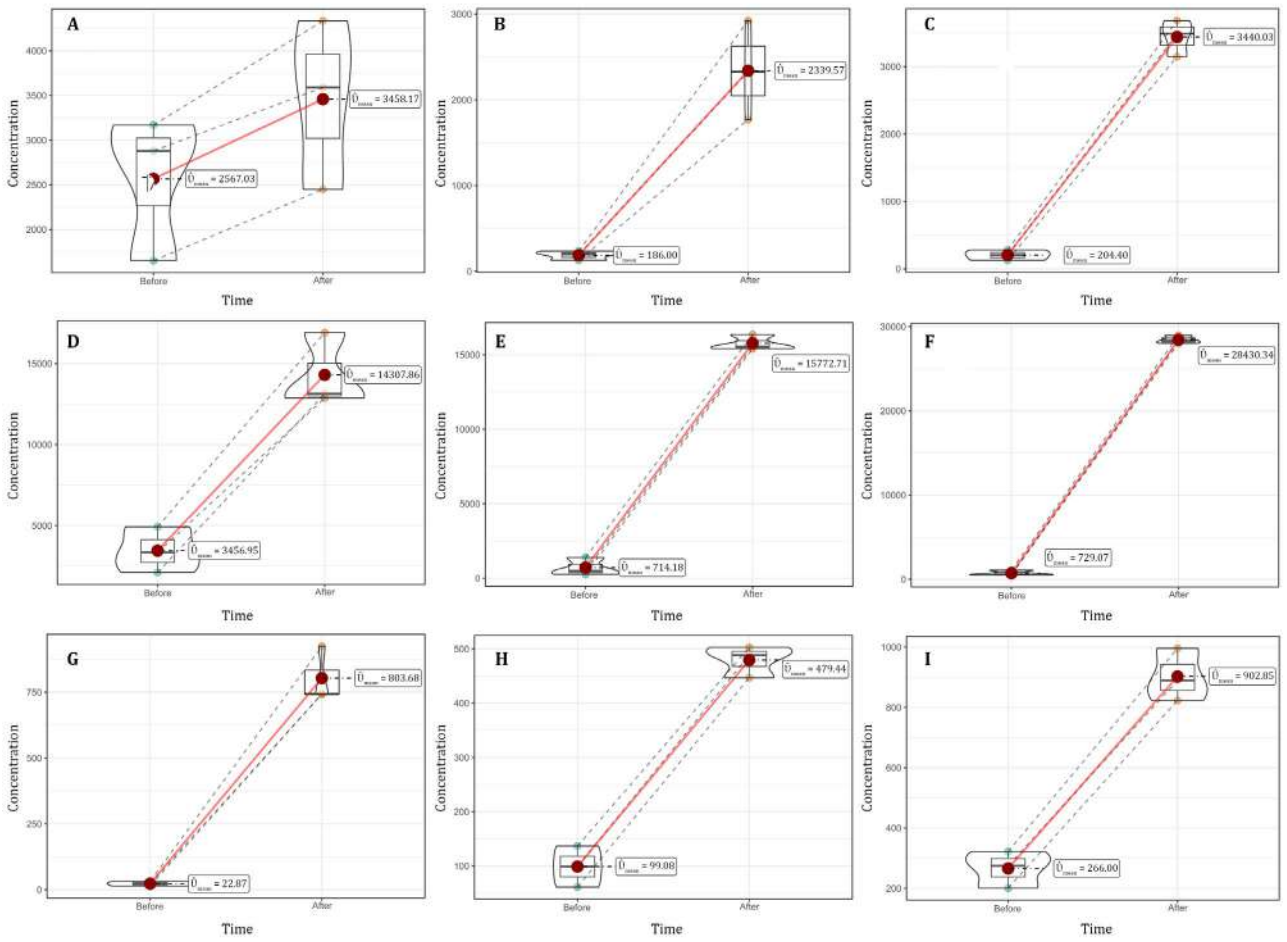
Regarding the Winogradsky columns from sediment in water bodies, several characteristics were observed related to coloration, gas production, and turbidity, verifying the presence of sulfate-reducing bacteria (BSR), similar to Winogradsky columns processed with residual sludge from wastewater treatment (25). The black coloration of the sulfate-reducing zone results from sulfide precipitation with reduced metals such as iron, which deposits at the bottom of the columns (29). BSR produce approximately 2 moles of alkalinity per mole of reduced sulfate, thereby neutralizing the pH of acidic waters. Additionally, the generated bicarbonate ions consume protons and raise the pH of acidic water (8, 33). In Wetland 2, the presence of BSR was confirmed in 66.7% of the Winogradsky columns, compared to 16.67% in columns prepared from wetland 1 samples. This difference may be attributed to the greater impact of ARD in wetland 2. As a consequence of increased oxidation of sulfide minerals, sulfate concentrations rise, which are used as electron acceptors by BSR, while organic matter in lower layers of the peat serves as a carbon source (38).

Translocation and Adaptation of *D. muscoides* and Comparison of Heavy Metal Concentrations

From days 20 to 80, the vigor and green color persisted in all cushions. By day 100, there was no discernible difference in vigor and color due to flooding. From days 120 to 160, a blackish coloration appeared on the edges and middle tissue of all translocated rectangles. At day 160, it was determined that the green coverage ranged from 34.3% to 97.9%, and the black coverage from 2.1% to 65.7% in the translocated cushions, compared to 100% green

coverage in the controls. The major radius of the translocated cushions ranged from 26 to 38 cm, and the minor radius from 21 to 44 cm, compared to 30-32 cm and 20-21 cm in the non-translocated controls. Additionally, a regular to abundant number of roots was observed in the translocated cushions compared to the abundant root presence in the controls.

The growth of *D. muscoides* is very slow, requiring more than 5 months for translocated cushions to develop morphology similar to non-translocated ones. A growth rate of 1-2 cm per year has been reported, with an increase in height of more than 1 cm in summer and less than 1 cm in winter over 6 months (7). In contrast, the root production of *D. muscoides* was 2000-2800 g m-2 year^{-1}, a range that exceeds other cushion species such as *Plantago rigida*, which produces 1000-1080 g m-2 year^{-1} (32). In areas with shallow and stable water tables, *D. muscoides* is dominant and exhibits a high capacity for peat accumulation, owing to its abundant underground biomass that can facilitate the adaptation of translocated plants (26). The establishment of translocated *D. muscoides* cushions was evidenced by both growth and the accumulation of metals in their tissues. Thus, it was demonstrated that translocation is a technique with potential for the recovery of impacted wetlands, as also corroborated by Luna (2018), who collected and transplanted *D. muscoides* cushions to artificial wetlands and determined a growth of 3.3 cm in roots and 2.8 cm in foliage after 9 months. Additionally, the pH of ARD at the inlet of the wetland was 2.9-3.6 and at the outlet was 3.87-5.30, indicating a decrease in water acidity, although the level achieved was lower than the EQS for water (6.5-8.5).



A. Al (peat). B. Al (root). C. Al (foliage). D. Fe (peat). E. Fe (root). F. Fe (foliage). G. Mn (peat). H. Mn (root). I. Mn (foliage).
A. Al (turba). B. Al (raíz). C. Al (follaje). D. Fe (turba). E. Fe (raíz). F. Fe (follaje). G. Mn (turba). H. Mn (raíz). I. Mn (follaje).

Figure 2. Concentration of heavy metals (mg/kg) in *D. muscoides* before and after transplantation (five months).
Figura 2. Concentración de metales pesados (mg/kg) en *D. muscoides* antes y después del trasplante (cinco meses).

Cushions Before and After Translocation

The t-Student analysis for related samples revealed statistically significant differences ($p<0.05$) in the concentrations of Al, Fe, and Mn in peat, root tissue, and foliage before and after transplantation. The concentrations of these metals were higher after transplantation (figure 2, page 7).

In contrast, the concentrations of Cr and Ar in peat, root tissue, and foliage before and after transplantation were statistically equal (table 2, $p > 0.05$). On the other hand, concentrations of Pb were statistically different in peat; those of Zn were statistically different in root and aerial tissues; and those of Cu differed in peat and foliage. However, the Wilcoxon analysis showed that Cu concentrations in root tissue before and after transplantation were statistically equal ($p > 0.05$).

Table 2. Concentrations of heavy metals (mg/kg) before and after transplantation of *D. muscoides*.
Tabla 2. Concentraciones de metales pesados (mg/kg) antes y después del trasplante de *D. muscoides.*

Heavy metal	Cushions before transplantation			Cushions after transplantation		
	Peat (n=3)	Root tissue (n=3)	Foliage (n=3)	Peat (n=3)	Root tissue (n=3)	Foliage (n=3)
Arsenic (As)	13.84±7.22	3.09±0.16	3.00±0.00	9.32±0.99	5.95±1.71	16.65±2.17
Copper (Cu)	22.4±1.21	4.59±0.85	2.75±0.50	5.40±0.82	6.09±0.388	3.42±0.10
Chromium (Cr)	3.52±0.13	1.00±0.00	1.00±0.00	1.90±0.12	0.66±0.01	1.72±0.05
Lead (Pb)	74.84±30.32	6.47±3.08	8.42±1.94	5.74±0.83	4.36±0.38	4.22±0.09
Zinc (Zn)	376.43±59.4	71.56±16.01	58.63±6.60	21.32±0.24	23.95±3.09	27.49±1.78

The presence of metals in *D. muscoides* tissues before and 5 months after translocation demonstrated that macrophytes can easily absorb bioavailable metals (As, Cd, Cu, Se, Ni, Zn), moderately bioavailable metals (Co, Fe, Mn, Hg), and poorly bioavailable metals (Cr, Pb) from water sediments, accumulating, translocating, and eventually storing them (4, 35). This capacity persisted in the translocated *D. muscoides* cushions. The ability to accumulate metals in translocated *D. muscoides* cushions corresponds with Luna (2018), who quantified Al, Cd, Cu, Fe, Mn, Ni, and Zn in plants of this species 9 months after transplantation to artificial wetlands.

Translocated and non-Translocated Cushions in the ARD-Impacted Wetland

The t-Student analysis of a single sample demonstrated that the concentration of heavy metals was statistically different ($p<0.05$) in the peat, root tissue, and foliage of *D. muscoides* in the ARD-impacted wetland (figure 3, page 9). The concentrations of Al, Fe, Cr, As, Zn, Cu, and Mn were higher in the foliage of translocated *D. muscoides* cushions compared to the peat and root tissue. In contrast, the concentrations of Al, Fe, Pb, Cr, and As in the peat and root tissue of non-translocated cushions were higher than in the foliage. These results indicate the absorption and movement of metals within the plant tissues of translocated *D. muscoides* cushions, where the concentrations of Cu in peat, root tissue, and foliage; Zn in peat and root tissue; and Al, Fe, Pb, Cu, and As in foliage were higher than in non-translocated cushions. The accumulation and translocation of Al, Cd, Cu, Fe, Mn, Ni, and Zn have previously been demonstrated in translocated *D. muscoides* to an artificial wetland (17). In contrast, the concentration of Mn was lower in the peat, root tissue, and foliage of translocated cushions compared to non-translocated cushions, a result that may be related to the duration of non-translocated cushions in the ARD-impacted wetland 2, where the concentration of Mn in water, root tissue, and foliage was higher than in wetland 1, which was not impacted.

Behavior of Translocated Cushions in the ARD-Impacted Wetland

The bioconcentration and translocation factors used to evaluate bioremediation capacity (1, 9, 10, 14) demonstrated the absorption of heavy metals, as well as their translocation to the foliage in transplanted *D. muscoides* cushions (17), highlighting their potential for phytoremediation of these contaminants (14). The BAF indicates the phenotypic trait of

heavy metal accumulation in plant tissues and their potential for phytoextraction (14), while the TF provides information on contaminant mobility within plants (10). The BAF of heavy metals in foliage classified both translocated and non-translocated cushions as excluders (BAF < 1) of Al, Cu, Cr, Pb, and accumulators (BAF 1-10) of Mn and Zn (figure 4). A previous study identified *D. muscoides* as an accumulator of Zn and a hyperaccumulator of Al and Mn (17). The difference between that study and the present one may be attributed to the use of an artificial wetland in the former, where plants were exposed to a constant flow of ARD for 9 months, unlike the natural wetland used in the present study over 5 months. Additionally, manure was applied during the implementation of the artificial wetland, providing microorganisms that may promote plant growth and activity (13).

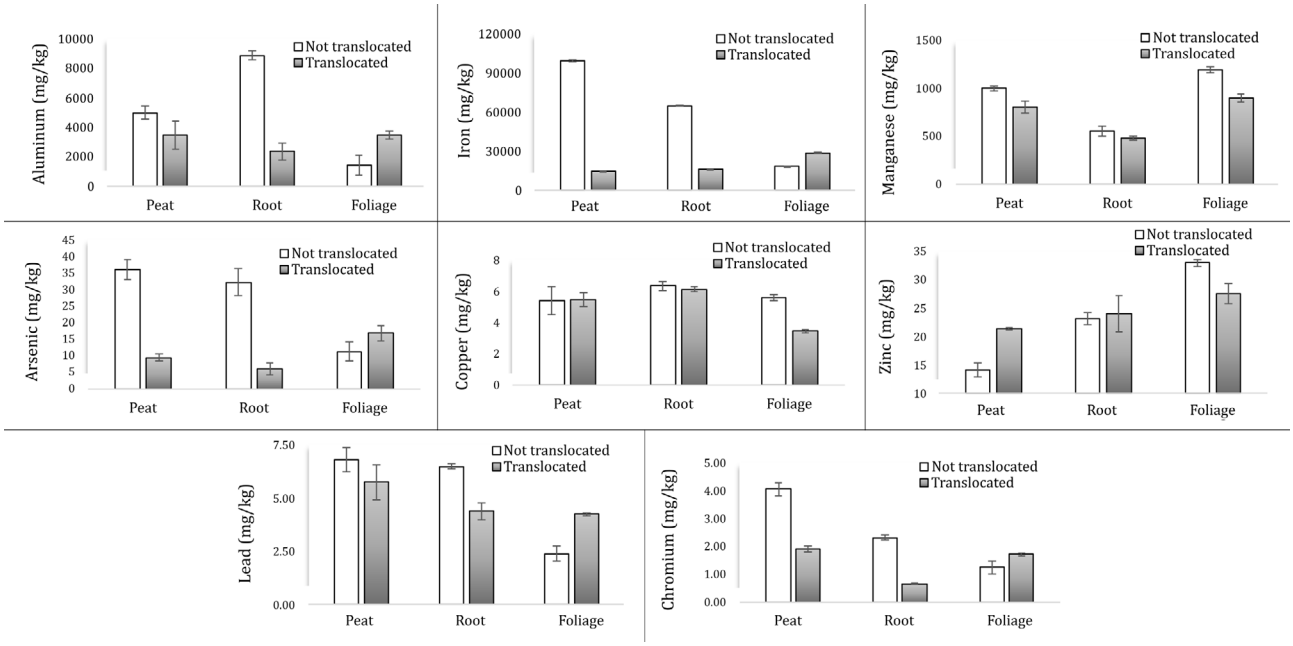


Figure 3. Concentration of heavy metals (mg/kg) in non-translocated and translocated *D. muscoides* cushions.

Figura 3. Concentración de metales pesados (mg/kg) en cojines de *D. muscoides* no translocados y translocados.

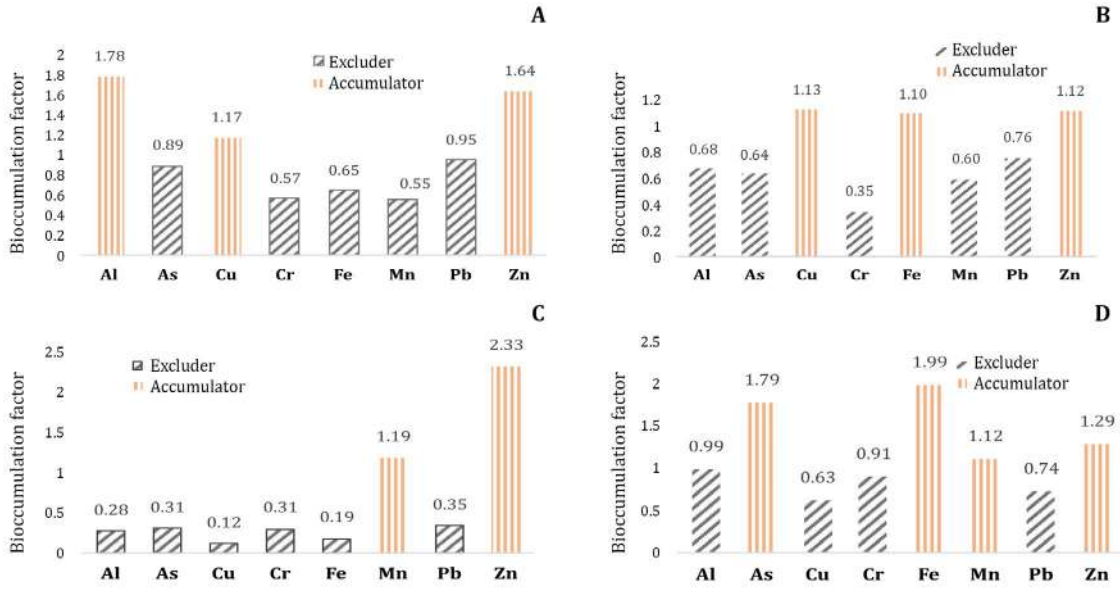


Figure 4. Bioaccumulation factor in root tissue in non-translocated cushions (A), translocated cushions (B), and in foliage in non-translocated cushions (C) and translocated cushions (D) of *D. muscoides.*

Figura 4. Factor de bioacumulación en tejido radicular en cojines no translocados (A), translocados (B), y en follaje en cojines no translocados (C) y translocados (D) de *D. muscoides.*

The BAF of metals in root tissue classified both translocated and non-translocated cushions as excluders of As, Cr, Mn, and Pb, and accumulators of Cu and Zn. The highest BAF values in roots corresponded to Fe (1.10), Cu (1.13), and Zn (1.12), which were higher than for other heavy metals (0.34-0.75). This contrasts with the values observed in *T. latifolia*, where BAF values for Ni and Zn drastically decreased, metals that reached higher concentrations (42.2 and 107 mg/kg) in wetland sediments compared to Cr (30.1 mg/kg), Cu (33.2 mg/kg), and Pb (39.3 mg/kg). This decrease is related to negative regulation or the plant's capacity to reduce or suppress a response to stimuli. At low environmental concentrations of metals, the plant can retain them; however, when concentrations increase chronically, tissues may not effectively control bioaccumulation (9). While an inverse relationship between BAF and the concentration of major metals was observed in *T. latifolia*, this relationship was not observed in *D. muscoides* regarding Fe, Cu, and Zn, metals that were found in higher concentrations in wetland 2 impacted by ARD.

The translocation factor of metals equally classified transplanted and non-transplanted cushions as phytoextractors (TF > 1) of Mn and Zn, and phytostabilizers (TF < 1) of Pb and Cu (figure 5). This aligns with the classifications attributed to *T. latifolio* as a phytoextractor of Zn, but contrasts with these plants as phytostabilizers of As, Cr, and Ni (9). Regarding Al, As, Fe, and Cr, the translocation factor classified transplanted cushions as phytoextractors, whereas non-transplanted cushions were classified as phytostabilizers. In phytoremediation, metals absorbed by the roots are transported and accumulated in the foliage, thereby permanently reducing these contaminants in peat or soil. In phytostabilization, metal mobilization is reduced, preventing migration into groundwater; however, contaminants remain in the peat or soil (24, 30).

This study had several limitations, including aspects of experimental design (such as the study area and sample size), challenges during experiment execution (such as inaccessibility to the experimental zone due to flooding and the slow growth of *D. muscoides*), and logistical issues (such as entry and handling of plants in the protected area and transportation of samples to the laboratory). Despite these challenges, the data obtained and analyzed were sufficient to determine the experimental positive effect of translocation and adaptation of *D. muscoides* cushions in a ARD-impacted wetland.

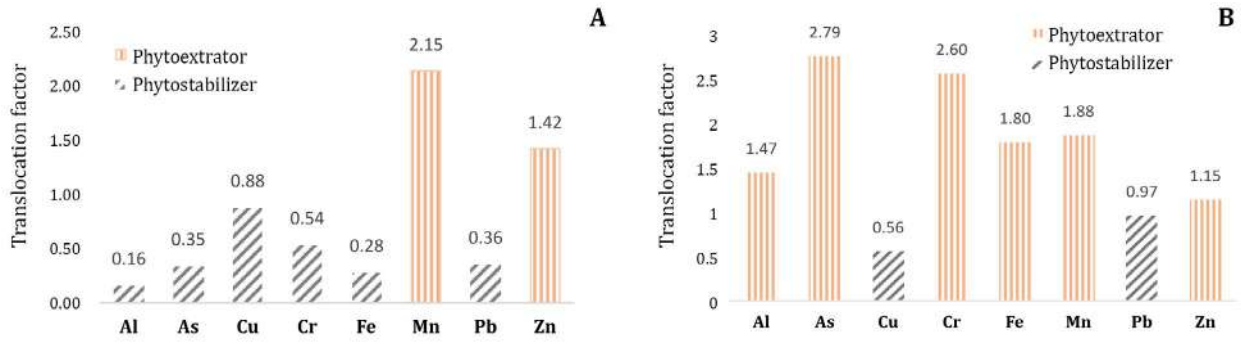


Figure 5. Translocation factor of non-translocated (A) and translocated (B) cushions of *D. muscoides*.

Figura 5. Factor de traslocación de cojines no traslocados (A) y traslocados (B) de *D. muscoides*.

Conclusion

The translocated cushions of *D. muscoides* adapted to the ARD-impacted wetland, promoting the phytoextraction and phytostabilization of heavy metals over the five months of evaluation. Particularly notable is the accumulation of Mn and Zn in the aerial plant tissue, alongside the accumulation and stabilization of Pb and Cu in the root tissue. The concentrations of some metals at certain points showed a higher standard deviation from the mean; however, these outliers had little effect on the overall results. This confirms *D. muscoides'* phytoremediation activity in extracting heavy metals from the environment, thereby preventing their deposition in the soil and surrounding water. They are proposed as suitable candidates for bioremediating ARD-impacted wetlands. However, larger-scale studies are needed that encompass a broader sample size, evaluate the concentration of heavy metals in water throughout the study period, and cover both wet and dry periods of the wetland to obtain more definitive results. Finally, special attention is emphasized on the concentration of Mn, which was the metal with the highest concentration in the evaluated wetlands.

References

1. Alcalá Jáuregui, J. A.; Rodríguez Ortiz, J. C.; Filippini, M. F.; Martínez Carretero, E.; Hernández Montoya, A.; Rojas Velázquez, A. N.; Méndez Cortés, H.; Beltrán Morales, F. A. 2022. Metallic elements in foliar material and fruits of three tree species as bioindicators. Revista de la Facultad de Ciencias Agrarias. Universidad Nacional de Cuyo. Mendoza. Argentina. 54(2): 61-72. DOI: https://doi.org/10.48162/rev.39.083
2. Arsenic, A. M.; Beryllium, A. M.; Chromium, B. N.; Cobalt, C. P.; Iron, C. S.; Lead, C. S.; Thallium, I. Z. 1996. Method 3050B acid digestion of sediments, sludges, and soils 1.0 scope and application. United States Environmental Protection Agency (EPA). Washington. DC. USA. 1-12.
3. Autoridad Nacional del Agua (ANA). 2011. Protocolo Nacional de Monitoreo de la calidad en cuerpos naturales de agua superficial. Ministerio de Agricultura. Perú. https://hdl. handle. net/20.500.12543/215 (Accessed May, 2023).
4. Awa, S.; Hadibarata, T. 2020. Removal of heavy metals in contaminated soil by phytoremediation mechanism: A Review. Water, air, Soil Pollut. 231-47. https://doi.org/10.1007/s11270-020-4426-0
5. Benfield, A.; Yu, Z.; Benavides, J. 2021. Environmental controls over Holocene carbon accumulation in *Distichia muscoides*-dominated peatlands in the eastern Andes of Colombia. Quaternary Science Reviews. 251: 106687. https://doi.org/10.1016/j.quascirev.2020.106687
6. Chávez, J.; Gonzales, J.; Iparraguirre, J. 2023. El impacto del cambio climático en la evolución glaciar desde la pequeña edad de hielo, en la vertiente occidental de la subcuenca Ranrahirca (Cordillera Blanca, Ancash). Tesis de grado en Ingeniería Ambiental y Recursos Naturales. Facultad de Ingeniería Ambiental y Recursos Naturales. Universidad Nacional del Callao. Perú. 156 p.
7. Cooper, D.; Kaczynski, K.; Slayback, D.; Yager, K. 2015. Growth and organic carbon production in peatlands dominated by *Distichia muscoides*, Bolivia, South America. Artic, Antarctic, and Alpine Research. 47(3): 505-510. https://doi.org/10.1657/AAAR0014-060
8. Ding, X.; Qian, L.; Juang, W.; Liu, H.; Yiming, A.; Zha, M.; Qu, J.; Jiang, Z. 2024. Review of bacterial sulfate reduction in lacustrine deposition and its identification in the Jimsar Sag, Junggar Basin. Marine and Petroleum Geology. 163: 106801. https://doi.org/10.1016/j.marpetgeo.2024.106801
9. Haghnazar, H.; Sabbagh, K.; Johannesson, K.; Pourakbar, M.; Aghayani, E. 2023. Phytoremediation capability of *Typha latifolia* L. to uptake sediment toxic elements in the largest coastal wetland of the Persian Gulf. Marine Pollution Bulletin. 188: 114699. https://doi.org/10.1016/j.marpolbul.2023.114699
10. Heisi, H.; Awosusi, A.; Nkuna, R.; Matambo, T. 2023. Phytoextraction of anthropogenic heavy metal contamination of the Blesbokspruit wetland: Potential of wetland macrophytes. Journal of Contaminant Hydrology. 253: 104101. https://doi.org/10.1016/j.jconhyd.2022.104101
11. Hirsh, M. 2016. Compilación sistemática de la situación actual en bofedales, bosques, paisajes, calidad de agua y praderas en la reserva de biósfera Huascarán, región Áncash. USAID, Instituto de montaña conservación, cultura, comunidad AID-527-A-14-00001. 39 p.
12. Hussein, S.; Qurbani, K.; Ahmed, S.; Tawfeeq, W.; Hassan, M. 2024. Bioremediation of heavy metals in contaminated environments using *Comamonas* species: A narrative review. Bioresource Technology Reports. 25: 101711. https://doi.org/10.1016/j.biteb.2023.101711
13. Janaki, M.; Kirupanantha, P.; Senthil, S.; Stanley, V.; Al Farraj, D.; Aljeidi, R.; Arokiyaraj. S. 2024. Beneficial role of *Burkholderia cepacia* in heavy metal bioremediation in metal-polluted soils and enhance the tomato plant growth. Biocatalysis and Agricultural Biotechnology. 57: 103032. https://doi.org/10.1016/j.bcab.2024.103032

14. Jara-Peña, E.; Gómez, J.; Montoya, H.; Sánchez, T.; Tapia, L.; Cano, N.; Dextre, A. 2017. Acumulación de metales pesados en *Calamagrostis rigida* (Kunth) Trin ex Steud. (Poaceae) y *Myriophyllum quitense* Kunth (Haloragaceae) evaluadas en cuatro humedales altoandinos del Perú. Arnaldoa. 24(2): 583-598. http://dx.doi.org/10.22497/arnaldoa.242.24210
15. La Matta, F. 2020. Influencia del drenaje ácido de roca en la comunidad de macroinvertebrados bentónicos, índices bióticos de calidad de agua y grupos funcionales alimenticios en ríos y cabeceras de La Cordillera Blanca (Subcuenca de Quillcay, Áncash). Tesis de grado en Biología. Facultad de Ciencias y Filosofía. Universidad Peruana Cayetano Heredia. Lima. Perú. 118 p.
16. López, M.; Morales, O. 2022. Fitorremediación de suelos contaminados por metales pesados: una revisión. Revista de Ciencia y Tecnología El Higo. 12(2): 15-28. https://doi.org/10.5377/elhigo.v12i2.15197
17. Luna, E. 2018. Biorremediación utilizando *Distichia muscoides* y *Calamagrostis glacialis* del drenaje ácido de roca proveniente del nevado de Pastoruri-2015. Tesis de grado en Ingeniería Ambiental. Facultad de Ciencias del Ambiente. Universidad Nacional Santiago Antúnez de Mayolo. Ancash. Perú. 103 p.
18. Magnússon, R.; Cammeraat, E.; Lücke, A.; Jansen, B.; Zimmer, A.; Recharte, J. 2020. Influence of glacial sediments on the chemical quality of surface water in the Ulta valley, Cordillera Blanca, Perú. Journal of Hydrology. 587: 125027. https://doi.org/10.1016/j.jhydrol.2020.125027
19. Martín, T. D.; Brockhoff, C. A.; Creed, J. T.; EMMC Methods Work Group. 1994. Methods EMW 200.7: Methods for the determination of metals in environmental samples. U.S. Environmental Protection Agency Cincinnati, Ohio. Methods Work Group. Revision 4.4. 1-58.
20. Martínez, V.; Benavides, J. 2023. Carbon balance shift in mountain peatlands along a gradient of grazing disturbance in the tropical Andes (Colombia). Plant Ecology. 224: 1049-1058. https://doi.org/10.1007/s11258-023-01356-8
21. Ministerio del Ambiente (MINAM). 2016. El Perú y el cambio climático, tercera comunicación nacional del Perú a la Convención Marco de las Naciones Unidas sobre cambio climático. https://www.gob.pe/institucion/minam/informes-publicaciones/2653-el-peru-y-el-cambio-climatico-tercera-comunicacion-nacional-del-peru (Accessed March, 2023).
22. Ministerio del Ambiente (MINAM). 2017. Decreto Supremo N° 004-2017. Estándares de Calidad Ambiental (ECA) para Agua y establecen Disposiciones Complementarias. https://www.gob.pe/institucion/minam/normas-legales/3671-004-2017- minam (Accessed March, 2023).
23. Narváez, C.; Kalinhoff, C.; Sánchez, A. 2024. Potencial del arbusto *Lantana camara* L. (Verbenaceae) para la fitoestabilización y volatilización de mercurio. Revista Internacional de Contaminación Ambiental. 40: 95-103. https://doi.org/10.20937/RICA.54790
24. Oggero, A.; Nakayama, H.; Ávalos, C.; Garcia, I.; Benítez, J.; Ayala, J.; Elkhalili, R., Peralta, I. 2021. Eficiencia de la absorción de cobre (Cu) y cromo (Cr), una propuesta de fitorremediación de efluentes mediada por *Typha domingensis*. Revista de la Sociedad Científica del Paraguay. 26(2): 100-113. https://doi.org/10.32480/rscp.2021.26.2.100
25. Orrego, S. 2019. Eficiencia de consorcios de bacterias sulfato reductoras en la degradación anaerobia de hidrocarburos aromáticos del petróleo en microcosmos, junio-octubre de 2018. Tesis de maestría en Ciencias en Ingeniería Ambiental. Universidad Nacional Pedro Ruiz Gallo. Lambayeque. Perú. 83 p.
26. Oyague, E.; Cooper, D.; Ingol, E. 2022. Effects of land use on the hydrologic regime, vegetation, and hydraulic conductivity of peatlands in the central Peruvian Andes. Journal of Hydrology. 609: 127687. https://doi.org/10.1016/j.jhydrol.2022.127687
27. Pabón, S.; Benítez, R.; Sarria, R.; Gallo, J. 2020. Contaminación del agua por metales pesados, métodos de análisis y tecnologías de remoción. Una revisión. Entre Ciencia e Ingeniería. 14(27): 9-18. https://doi.org/10.31908/19098367.1734
28. Pedraza, M. 2021. Fitorremediación en cuerpos de agua contaminados por metales pesados. Revista Científica de Biología y Conservación. 1(1): 61-78. https://doi.org/10.58720/ibs. v1i1.6
29. Rascón, J.; Corroto, F. 2020. Evolución fisicoquímica y de las bacterias de azufre en microcosmos de diferentes sistemas acuáticos de la Región Amazonas. Revista de Investigación Científica Tayacaja. 3(1). https://doi.org/10.46908/rict.v3i1.68
30. Reyna, D.; Cortés, L.; Sandino, G.; Martínez, M.; Rodríguez, L. 2022. Estudio del comportamiento de especies vegetales en un proceso de fitoestabilización para remediación de suelo contaminado por jal minero abandonado. Ciencia, Tecnología y Salud. 16(32): 52-57. https://doi.org/10.36790/epistemus.v16i32.197
31. Ruthsatz, B. 2022. Vegetación y ecología de los bofedales tropicales altoandinos en el norte de Chile. Chloris Chilensis. 25(1): 165-214.
32. Suárez, E.; Chimbolema, S.; Chimner, R.; Lilleskov, E. 2021. Root biomass and production by two cushion plant species of tropical high-elevation peatlands in the andean paramo. Mires and Peat. 27. https://doi.org/10.19189/MaP.2020.OMB.StA.2131
33. Wang, H.; Wang, X.; Zhang, Y.; Wang, D.; Long, X.; Chai, G.; Wang, Z.; Meng, H.; Jiang, C.; Dong, W.; Guo, Y.; Li, J.; Xu, Z.; Lin, Y. 2023. Sulfate-reducing bacteria-based bioelectrochemical system for heavy metal wastewater treatment: Mechanisms, operating factors, and future challenges. Journal of Electroanalytical Chemistry. 915 (15): 117945. https://doi.org/10.1016/j.jelechem.2023.117945

34. Wanner, C.; Moradi, H.; Ingold, P.; Cardenas, M.; Mercurio, R.; Furrer, G. 2023. Rock glaciers in the Central Eastern Alps-How permafrost degradation can cause acid rock drainage, mobilization of toxic elements and formation of basaluminite. Global and Planetary Change. 227: 104180. https://doi.org/10.1016/j.gloplacha.2023.104180
35. Yan, A.; Wang, Y.; Tan, S.; Yusof, M.; Ghosh, S.; Chen, Z. 2020. Phytoremediation: a promising approach for revegetation of heavy metal-polluted land. Frontiers in Plant Science. 30(11): 359. https://doi.org/10.3389/fpls.2020.00359
36. Yaranga, R. 2020. Humedal Altoandino del Perú: Diversidad florística, productividad primaria neta aérea, condición ecológica y capacidad de carga. Scientia Agropecuaria. 11(2): 213-221. https://doi.org/10.17268/sci.agropecu.2020.02.08
37. Zheng, H.; Bingjie, L.; Guocheng, L.; Zhaohui, C.; Chenchen, Z. 2019. Potential toxic compounds in biochar: Knowledge gaps between biochar research and safety, biochar from biomass and waste. Biochar from Biomass and Waste. 349-384. https://doi.org/10.1016/B978-0- 12-811729-3.00019-4
38. Zimmer, A.; Brito, M.; Alegre, C.; Sánchez, J.; Recharte, J. 2018. Implementación de dos sistemas de biorremediación como estrategia para la prevención y mitigación de los efectos del drenaje ácido de roca en la Cordillera Blanca, Perú. Revista de Glaciares y Ecosistemas de Montaña. 4(3): 57-76.
39. Zimmer, A.; Beach, T.; Luzzadder, S.; Rabatel, A.; Lopez, J.; Cruz, R.; Temme, A. 2024. Physico-chemical properties and toxicity of young proglacial soils in the Tropical Andes and Alps. Catena. 237: 107748. https://doi.org/10.1016/j.catena.2023.107748

Acknowledgement

This work was supported by the Instituto Nacional de Investigación en Glaciares y Ecosistemas de Montaña (INAIGEM). We also thank the biology laboratory of the Centro de Investigación para el Fomento Sustentable (CIFOS) for allowing the use of its facilities.

Statistical Optimization of Seed Coating in Arid-Zone Grass Species Used as Cover Crops in Woody Agroecosystems

Optimización estadística del recubrimiento de semillas en gramíneas de zonas áridas para cultivos de cobertura en agroecosistemas leñosos

Carola Meglioli [1* a], Benjamín Kuchen [2, 3 a], Leandro Ormeño [1, 3], Fabio Vazquez [2], Carlos Alberto Parera [1]

Originales: *Recepción:* 26/06/2025- *Aceptación:* 09/12/2025

ABSTRACT

Inter-row vegetative cover improves soil physicochemical properties and biodiversity but should not compete with main crop for water. Native grass species such as *Leptochloa crinita* (Lag.) P. M. Peterson & N. W. Snow, *Pappophorum caespitosum* R. E. Fr. and *Digitaria californica* (Benth.) Henrard var. californica provide forage value, require less water than conventional cover crops, and exhibit high tolerance to the edaphoclimatic conditions of arid regions. However, their small seed size hinders efficient handling and sowing. Seed coating increases seed size and weight, forming a pellet that improves handling, distribution, and protection. Nevertheless, limited information is available on coating techniques for small-seeded species. This study aims to optimize the coating process through a statistically designed experiment to evaluate key morphological and physiological seed traits. A Box-Behnken design was applied to optimize one compositional factor of the pellet and two operational parameters. Pellet traits such as size, heterogeneity, seed number, and residue were analyzed alongside germination and seedling development. Optimization was first carried out using edible amaranth seeds as a model organism and then validated with native grasses. The resulting models were statistically significant and allowed the identification of an optimal operational range. Germination was unaffected in single-seed pellets, and root growth was enhanced by the coating process. Overall, the proposed statistical methodology proved effective and broadly applicable for optimizing small-seed coating processes.

Keywords
Native seeds • *Leptochloa crinita* • *Pappophorum caespitosum* • *Digitaria californica*

https://doi.org/10.48162/rev.39.189

1 Universidad Nacional de San Juan (UNSJ). Facultad de Ciencias Exactas, Físicas y Naturales (FCEFyN). Departamento de Biología. Gabinete de Recursos Vegetales. Av. Ig. de la Roza oeste 590. Rivadavia. San Juan. Argentina. * caromeglioli@gmail.com
2 Universidad Nacional de San Juan (UNSJ). Facultad de Ingeniería (FI). Av. Libertador Oeste 1109. San Juan. Argentina.
3 Consejo Nacional de Investigaciones Científicas y Técnicas (CONICET). Godoy Cruz 2290. CABA. Argentina.
a Both authors contributed equally to this work.

Licenses Creative Commons
Attribution - Non Commercial - Share Alike

Resumen

Las coberturas vegetales interfilares mejoran las propiedades fisicoquímicas y la biodiversidad del suelo, pero no deberían competir por el agua en los cultivos. Algunas especies nativas, como Leptochloa crinita (Lag.) P. M. Peterson & N. W. Snow, *Pappophorum caespitosum* R. E. Fr. y *Digitaria californica* (Benth.) Henrard var. californica, ofrecen valor forrajero, requieren menos agua que cultivos de cobertura convencionales y presentan alta tolerancia a las condiciones edafoclimáticas del árido. No obstante, el pequeño tamaño de sus semillas dificulta su manejo. El recubrimiento incrementa tamaño y peso de las mismas, formando un pellet que facilita su manipulación, distribución y protección. Sin embargo, hay escasa información sobre el recubrimiento de semillas pequeñas. Este estudio busca optimizar dicho proceso mediante diseño experimental y evaluar variables morfológicas y fisiológicas clave. Se aplicó un diseño Box-Behnken para optimizar un factor de composición del pellet y dos factores operativos. Se evaluaron características del pellet como tamaño, heterogeneidad, cantidad de semillas y residuo, así como la germinación y desarrollo de plántulas. La optimización se realizó con semillas de amaranto de consumo humano como organismo modelo y fue validada en gramíneas nativas. Los modelos resultaron significativos y permitieron definir una zona operativa óptima. La germinación no se vio afectada en pellets de una semilla, más aún el crecimiento radicular se vio beneficiado por el proceso de recubrimiento. Finalmente, la metodología estadística utilizada demostró ser aplicable y eficaz para optimizar el recubrimiento de semillas.

Palabras clave

Semillas nativas • *Leptochloa crinita* • *Pappophorum caespitosum* • *Digitaria californica*

Introduction

Some agronomic management practices in woody crops like vineyards, olive groves, almond orchards, and walnut plantations can act as regionally significant drivers of soil degradation. Inter-row areas in these systems, particularly under pressurized irrigation, are often classified as “degraded areas” due to prolonged soil exposure to erosive forces (Chen *et al*. 2010).

Inter-row cover crops provide multiple agro-environmental benefits reducing weed competition, enhancing biodiversity, improving nutrient cycling, and serving as green manure (Rubio-Asensio *et al.* 2022; Thioye *et al.* 2021; Tomaz *et al.* 2021). However, in semi-arid regions, conventional cover crops may compete with main crop for water and nutrients. This limitation encourages the use of native species, which generally possess deep root systems, lower water requirements, and superior adaptation to local edaphoclimatic conditions (Pornaro *et al*. 2022; Massa Decon & Pérez, 2025).

Native grasses such as *Leptochloa crinita* (Lag.) P. M. Peterson & N. W. Snow, *Pappophorum caespitosum* R. E. Fr. and *Digitaria californica* (Benth.) Henrard var. californica are valued for their tolerance to drought, aridity and salinity, rapid establishment, and low water use (Kozub *et al*. 2018; Vega-Riveros *et al*. 2020). *D. californica* has already been used successfully as an inter-row species (Ferrari & Parera, 2015), while *L. crinita* and *P. caespitosum* have been employed as forage grasses (Marinoni *et al*. 2019). Nevertheless, these native species produce small, lightweight seeds (often less than 1 mm), with variable shapes (Carballo *et al*. 2005; Ramírez-Segura *et al*. 2022), making them difficult to handle and sow (Pedrini *et al*. 2017). Germination rates also improve significantly when floral residues are removed, exposing caryopsis (Meglioli *et al*. 2024).

Seed coating intends to overcome these challenges. By enclosing the caryopsis within a protective layer, coating increases seed size, enhances mechanical and distribution, and reduces damage during sowing (Afzal *et al*. 2020; Pedrini *et al*. 2017). Moreover, it can improve germination and plant establishment (Pedrini *et al*. 2017). Coating mixtures of native species may also improve agroecosystem resilience and stability by increasing functional diversity (Madsen *et al*. 2012).

Although seed coating technologies have been primarily developed for major agricultural species (Pedrini *et al*. 2017), there is limited literature regarding suitable coating material and operational parameters for small native grasses. In addition, many studies on seed coating lack robust experimental design (Rajeshwari *et al*. 2020). Statistical experimental design and response surface methodology provide powerful tools to analyze factor interactions, reduce experimental effort, and model complex biological responses (Pedrozo *et al*. 2024; Leardi, 2009).

Here, we hypothesized that the coating process would not negatively affect the germination of *L. crinita*, *P. caespitosum*, and *D. californica*. To test this hypothesis, the present study optimized key factors in the mechanical coating of small amaranth seeds a model organism due to its similar morphology (Zubillaga *et al*. 2024). The optimized conditions were then validated with the target native grasses by evaluating pellet size, seed conglomeration, and germination performance.

This study provides an original integrative approach, combining statistical optimization with the use of a model organism. Focusing on seed-level responses, the research explores variability and highlights how pellet composition and seed number influence germination and early seedling development.

Materials and Methods

Plant Material

Because obtaining spikelet-free grass seeds is a labor-intensive process and a consistent seed supply was required for process optimization, commercial amaranth seeds were used as a model due to their morphological similarity to native grasses (Xavier *et al*. 2019).

For validation, seeds of *L. crinita*, *P. caespitosum*, and *D. californica* (*Poaceae*) were provided by the native species germplasm bank (ARG1416) at the Plant Resources Cabinet from Universidad Nacional de San Juan (UNSJ). Seeds were mechanically scarified and air-cleaned to obtain naked caryopses.

Seed Coating Optimization Procedure and Factors

Lavanya *et al*. (2011) described for mechanisms of pellet formation: nucleation, coalescence, layering, and abrasion. In the present study, nucleation was excluded because the seed served as the nucleus. Coalescence refers to the formation of larger particles from multiple nuclei; layering involves the successive addition of powder layers; and abrasion encompasses the material exchange between forming particles.

Based on previous reports and acknowledging that the sequential addition of filler and binder significantly affects final pellet size (Rajeshwari *et al*. 2020), the process was structured into 16 coating stages (table 1).

Table 1. Seed coating stages.

Tabla 1. Etapas del recubrimiento de semillas.

Stage	1	2	3	4	5	6	7	8	9	10	11	12	13	14	15	16
Binder	X	X	X	X	X	X	X	X	X	X	X	-	X	-	X	-
CO_3Ca	X	-	X	X	X	X	X	-	X	X	X	X	X	X	-	-
Clay	-	X	-	-	-	-	-	X	-	-	-	-	-	-	X	X

Quantitative and qualitative properties of the coating materials (table 2, page 4) were selected following ecological and sustainability criteria, key principles for ecological restoration (Hoose *et al*. 2019).

Table 2. Quantitative and qualitative factors considered.
Tabla 2. Factores cuantitativos y cualitativos considerados.

Factors related	References for factor and level consideration	Qualitative	Quantitative	Quantity	Unit
Seed	Rotary coater	Fixed	Fixed	30	g/proc.
Filler	Kangsopa *et al.* 2018	Fixed	Fixed	8.8/4.2	g/ stage
Binder	Afzal *et al.* 2020	Fixed	Variable	1.6 - 2.4	mL
Colorant	Afzal *et al.* 2020	Fixed	Fixed	1	g
Process	Working equipment		Fixed	16	stages
Pressure	Rotary coater		Fixed	1	atm
Temperature	Rotary coater		Fixed	25	°C
Plate speed	Pasha *et al.* 2016		Variable	490 - 630	rpm
Atomizer disc speed	Pasha *et al.* 2016		Fixed	420	rpm
Stage time	Just *et al.* 2013		Variable	30 - 40	sec/ stage

* Factors were considered under ecological restrictions

* Los factores se evaluaron dentro de restricciones ecológicas.

Filler: A 70:30 (w/w) mixture of calcium carbonate and diatomaceous earth (Kangsopa *et al*. 2018). White clay (kaolin) was used as a surface-smoothing agent (Romo-Campos & Guzmán Valle, 2019). Binder: Gum arabic (25% w/v), a natural water-soluble polysaccharide with a viscosity of 156.7 cP at 25°C, was used. Colorant: A food-grade powder dye was added for visual differentiation. After reviewing literature, it was decided to optimize three independent variables: plate rotational speed (490, 560, and 630 rpm), binder volume (1.6, 2, and 2.4 mL), and stage time (30, 35, and 40 s).

Evaluated Responses on the Optimization and Validation

Thirty pellets were randomly selected for measurement. Pellet size was determined by recording the major and minor diameters (mm) using a digital caliper. Size heterogeneity was calculated as the standard deviation of these diameters. To determine the number of seeds per pellet, each pellet was gently crushed, and the enclosed seeds were counted under a stereomicroscope. The amount of residue was quantified by collecting and weighing (g) the material adhered to the drum and plate of the rotary coater after coating. This value was subtracted from the total input weight of filler and binder to estimate the proportion of material loss.

Numerical Optimization of Multiple Responses

Using the fitted models, a numerical multi-response optimization was performed. The objectives were to: maximize pellet size, minimize the number of seeds per pellet (target = 1), minimize size heterogeneity, and minimize residue amount.

Pellet Validation

A single optimal point derived from the numerical optimization was selected to validate the desirability function and predictive models. For this purpose, a mixture of 30 g of cleaned caryopses was prepared, comprising 10 g each of *L. crinita*, *P. caespitosum*, and *D. californica*.

Additional Responses Evaluated during Validation

Dissolution: Pellets were placed on germination paper moistened and saturated with distilled water. The time required for complete disintegration was recorded.

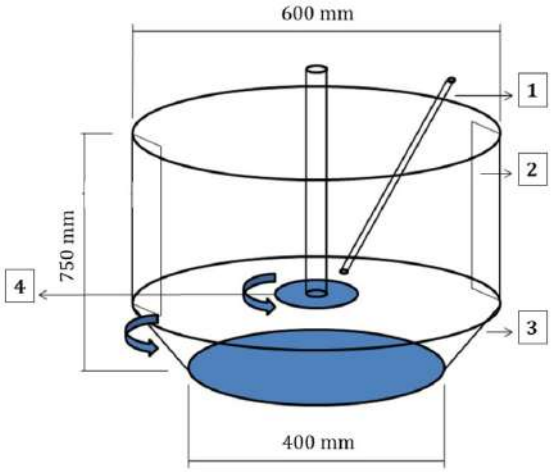
Fragmentation: Pellets were placed in a 15 mL Falcon tube and subjected to continuous vibration for 1 min using a vortex shaker (Arcano) at 800 rpm. The number of broken pellets was counted (modified from Rajeshwari *et al*. 2020).

Germination Responses

To evaluate the effect of coating on germination, 30 pellets were sown in sterile Petri dishes lined with germination paper moistened with 6 mL of distilled water. Treatments included (four replicates each): caryopses (control), consisting of 10 seeds from each native species; single-seed pellets, diameter < 1.6 mm; and multi-seed pellets (conglomerates), diameter between 1.6 and 2.8 mm, containing an average of five seeds per pellet (150 seeds total) (Hoose *et al*. 2019). Plates were incubated in a germination chamber at 25°C under a 12 h light/dark cycle for five days. Germination was recorded when radicle emergence was visible, and shoot and radicle lengths were measured with a caliper.

Equipment

The coating process was performed using a rotary coater (SATEC Concept model ML 2000, SATEC Equipment GmbH, Germany (figure 1).



1- liquid pipeline, 2- baffles, 3- rotary coater plate, 4- atomizer disc.

1- Conducto para líquido. 2- Deflectores. 3- Plato giratorio recubridor. 4- Disco atomizador.

Figure 1. Schematic representation of the rotary coater (SATEC Concept model ML 2000).
Figura 1. Esquema interno. Modelo Concept SATEC ML 2000.

Statistical Analysis

All experimental design (Box-Behnken) and analyses were performed using Design-Expert 7.0.0 (Stat-Ease Inc., USA). Model significance, lack of fit, adequacy, precision, robustness, and numerical optimization were assessed. ANOVA assumptions, outliers, and data transformations were also analyzed to ensure model validity.

Results

Seed Coating Optimization

Table 3 summarizes the factor level used in the Box–Behnken experimental design and the corresponding responses obtained from the coating process for each experimental run.

Table 3. Box–Behnken design showing variation in plate speed, stage duration, and binder volume, and their corresponding responses: pellet size, seed number, residue amount, and size heterogeneity.

Tabla 3. Diseño Box-Behnken: Variación de factores: velocidad del plato, tiempo por etapa y cantidad de aglutinante; y resultados de la optimización: tamaño del pellet, cantidad de semillas, cantidad de residuo y heterogeneidad del tamaño.

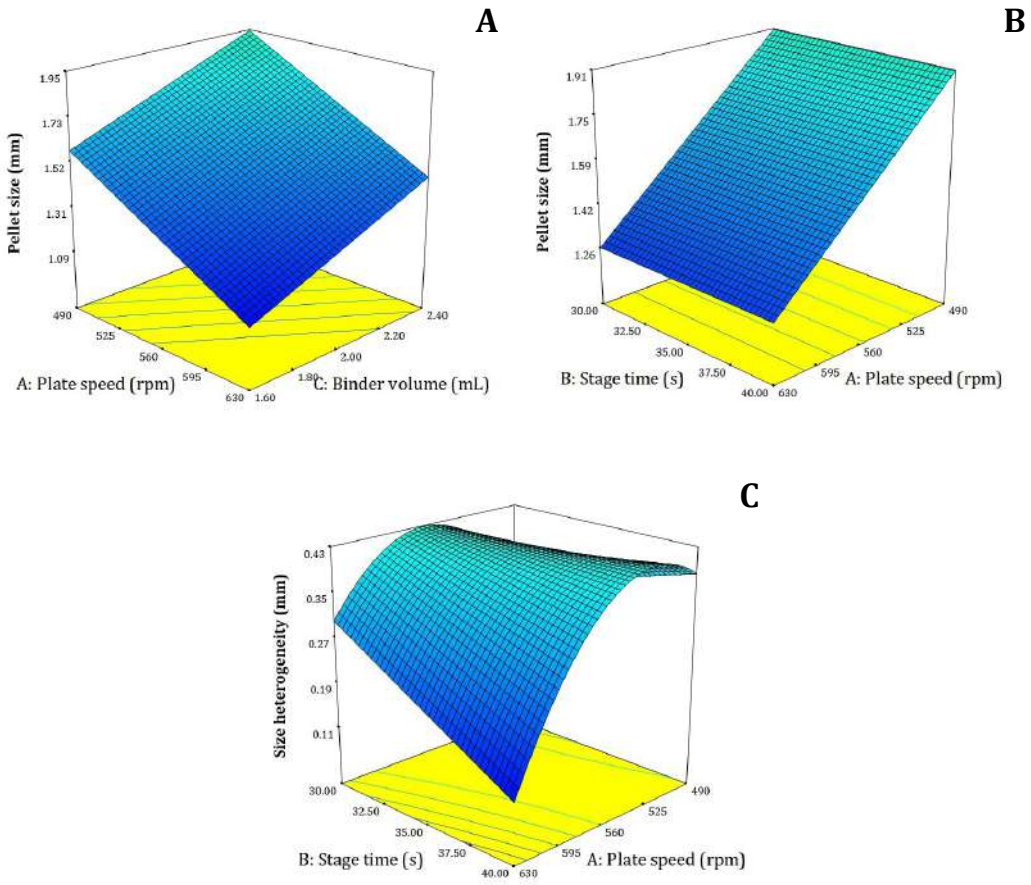
	Factors			Responses			
Run	**Plate rotational speed (rpm)**	**Stage time (s)**	**Binder amount (mL)**	**Pellet size (mm)**	**Number of seeds (*posteriori* rounded)**	**Residue amount (g)**	**Size heterogeneity standard deviation (mm)**
1*	560	35	2	1.58	0.9	64.89	0.35
2*	630	30	2	1.28	0.8	42.98	0.29
3	630	35	2.4	3.99	6.9	0	0.90
4	560	35	2	1.9	2.8	63.89	1.26
5	490	35	2.4	2.37	4	80.9	0.55
6*	560	35	2	1.74	1.2	24.02	0.44
7*	630	40	2	1.07	0.9	71.12	0.11
8	560	40	1.6	1.85	2.3	63.74	0.63
9*	490	30	2	1.68	1.1	95.46	0.27
10*	560	30	2.4	1.83	0.8	130.52	0.27
11*	560	30	1.6	1.32	1.2	79.82	0.60
12*	490	40	2	1.5	1	83.75	0.38
13*	490	35	1.6	1.73	1.3	77.36	1.01
14	560	40	2.4	1.57	1.6	87.56	0.60
15*	630	35	1.6	1.09	0.9	87.68	0.33

*Runs for single-seed pellet size model.

*Corridas para el modelo de tamaño de pellets de una semilla.

Modeling of Responses

Pellet size data were analyzed in two subsets: (A) single-seed pellets (figure 2A, page 4) and (B) all data combined (figure 2B, page 7), including multi-seed (conglomerate) pellets (Hoose *et al*. 2019). All response models were significant (table 4, page 7) and showed no lack of fit unless otherwise indicated. Adjusted and predicted R^2 values were consistent, and ANOVA assumptions were met.



(A) Single-seed pellets; (B) combined dataset (single- and multi-seed pellets); (C) size heterogeneity (standard deviation) of single-seed pellets. Binder volume fixed at 2 mL.

A- Tamaño del pellet con una sola semilla. B- Todos los datos, tamaños de pellets con una y múltiples semillas. C- Heterogeneidad del tamaño en pellets de una sola semilla (desviación estándar). Volumen de aglutinante fijo en 2 mL.

Figure 2. Influence of the evaluated factors on pellet size.
Figura 2. Influencia de los factores evaluados sobre el tamaño del pellet.

Table 4. Responses and models/ Statistical summary of the fitted models.
Tabla 4. Respuestas y modelos/ Resumen estadístico de los modelos ajustados.

Response	Adj. R^2	Model
(A) Pellet size: Single-seed pellets	0.61	Pellet size = 2.57 - 3.5*10 $^{-3}$ * P_S + 0.45 * B_V
(B) Pellet size: All data	0.42	Pellet Size = 4.16 - 4.60*10^{-3} * P_S
Size heterogeneity: Single-seed pellets	0.96	Size Heterogeneity = - 6.88 + 0.02 * P_S + 0.35 * S_T - 2.43 * B_V - 2.08*10 $^{-4}$ * P_S * S_T + 9.99*10^{-3} * P_S * B_V - 0.11 * S_T * B_V - 2.78*10^{-5} * P_S ^{2}
Size heterogeneity: All data		No Fit
Number of seeds Bartlett, M. S. (1947).	0.36	Sqrt (Number of seeds) = - 0.26 + 0.76 * B_V
Residue amount	0.63	Residue amount = - 1704.79 + 3.13 * P_S + 960.47 * B_V - 1.69 * P_S * B_V

* (P_S: Plate speed, B_V: Binder volume, S_T: Stage time)

* (P_S: Velocidad del plato, B_V: Volumen del aglutinante, S_T: Tiempo de etapa).

Pellet Size and Size Heterogeneity

Models indicated that increasing the rotational speed of the rotary coater plate reduced pellet size (figure 2A-B, page 7). Conversely, greater binder volume increased pellet size for single-seed pellets (figure 2A, page 7).

Size heterogeneity (figure 2C, page 7) was analyzed only for single-seed pellets, since combining single-and multi-seed data was better represented by the overall mean (mean = 0.54). Longer stage duration and higher rotation speed reduced size variability among pellets.

Number of Seeds per Pellet

The model describing the number of seeds per pellet was significant (adjusted R^2 = 0.36; figure 3). Although predictive precision was moderate, the model adequately represented overall behavior (Pedrozo *et al*. 2024). Increasing binder volume led to the formation of conglomerates.

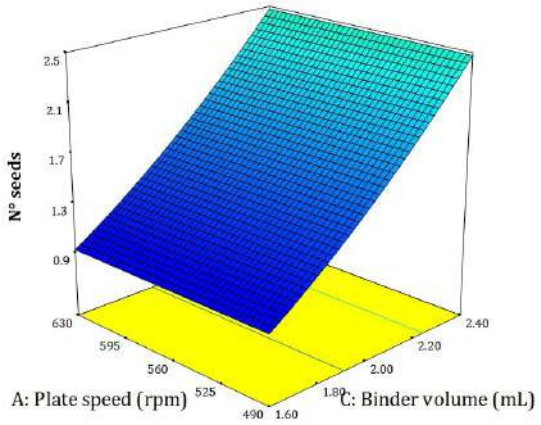


Figure 3. Influence of the evaluated factors on the number of seeds per pellet.

Figura 3. Influencia de los factores evaluados sobre la respuesta de cantidad de semillas.

Amount of Residue

During coating, some material adhered to the rotary drum and plate, contributing to residue accumulation (figure 4).

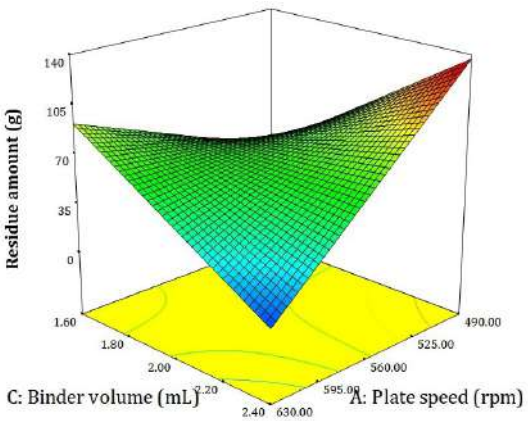


Figure 4. Effect of evaluated factors on the residue adhered to the rotary coater drum and plate at the end of process.

Figura 4. Influencia de los factores evaluados sobre la cantidad de residuo adherido al tambor y al plato de la peletizadora al final del proceso.

The smallest amounts of residue occurred at high plate rotation speed and maximum binder volumes, which coincided with the formation of conglomerates. Conversely, low plate speeds combined with high binder volumes produced the largest residues.

Residue per experiment ranged from 0 to 140 g, averaging 43% of total input mass.

Multi-Response Optimization

A simultaneous optimization was performed using desirability criteria for the following responses: pellet size (maximize, importance: +++), size heterogeneity (minimize, +), number of seeds (minimize, ++++), and amount of residue (minimize, ++). The optimal compromise solution is shown in figure 5. All models used corresponded to the complete dataset (single- and multi-seed pellets).

Pellet size (maximize +++), size heterogeneity(minimize+), amount of seed (minimize +++++), and amount of residue (minimize ++).

Tamaño del pellet (maximizar +++), Heterogeneidad del tamaño (minimizar +), Cantidad de semillas (minimizar +++++), y Cantidad de residuo (minimizar ++).

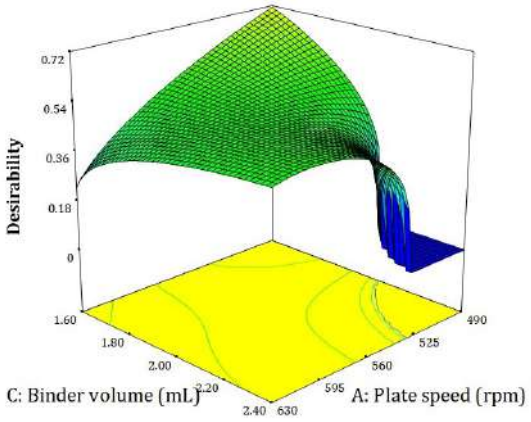


Figure 5. Multiple-response optimization based on experimenter-defined criteria.

Figura 5. Optimización de múltiples respuestas según criterios del experimentador.

Maximum desirability was achieved at low plate speed and low binder volume. A marked decrease in desirability occurred under conditions of low plate speed and high binder volumes, corresponding to zones of formation of conglomerates and high residue accumulation.

Prediction and Validation

Model predictions were validated using the following optimized conditions: plate speed = 595 rpm, binder volume = 2.2 mL, and stage duration = 35 s (overall desirability: 0.51). Validation used caryopses of *L. crinita*, *P. caespitosum*, and *D. californica* (table 5, page 10).

Pellets were classified into four size categories, and validation results were calculated as weighted means based on proportional mass. Two additional responses were also evaluated: fragmentation and dissolution time.

Weighted means: pellet size = 1.38 mm; number of seeds per pellet = 3.15; heterogeneity (SD) = 0.36. Single-response value: amount of residue = 25% at the end of the process.

Predicted values for these conditions are presented in table 6 (page 10).

All validation results fell within the 95% confidence intervals predicted by the models.

Germination and Seedling Performance

Pellets obtained during validation (table 6, page 10) were used to evaluate germination and early seedling development in native grasses (*L. crinita*, *P. caespitosum*, and *D. californica)*.

Germination

No significant differences were detected in germination percentage between control caryopses and single-seed pellets (figure 6, page 10). However, multi-seed (conglomerate) pellets showed a 20% reduction compared to both control and single-seed treatments.

Table 5. Validation responses: Pellet size, size heterogeneity, and number of seeds after classification into four size categories, expressed as weight percentage of the total mix. Additional responses: Fragmentation and dissolution time.

Tabla 5. Respuestas de validación: Tamaño del pellet, heterogeneidad del tamaño y número de semillas tras el tamizado en cuatro tamaños, y porcentaje de representación del total de la mezcla en peso. Respuestas adicionales: Fragmentación y disolución.

Size category	Size average (mm)	Size heterogeneity (standard deviation size)	Number of seeds (mean)	Percentage representation (% by weight)	Fragm. (%)	Dissol. (s)
Fine	1.1	0.12	1	34	50	< 3
Medium	1.2	0.09	1.4	43	60	< 3
Coarse	1.6	0.62	5.4	18	30	< 3
Very coarse	2.85	0.58	9.2	5	0	< 3

*Fragm.: violent fragmentation; Dissol.: pellet dissolution time.

*Fragm.: Fragmentación violenta, Dissol.: Tiempo de disolución del pellet.

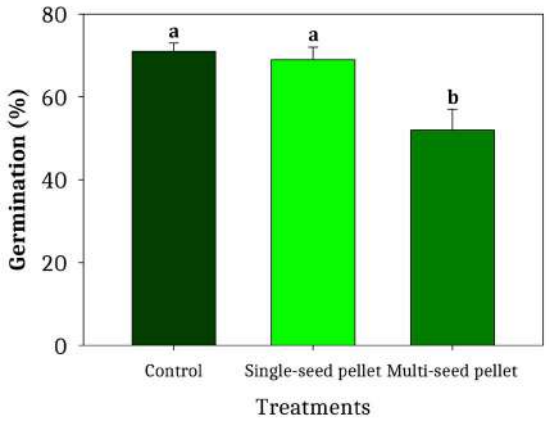
Table 6. Model-predicted responses under optimal conditions (plate speed 595 rpm; binder volume 2.2 mL; stage time 35 s).

Tabla 6. Predicción de las respuestas del pellet bajo las condiciones: velocidad del plato (595 rpm), volumen de aglutinante (2,2 mL), tiempo por etapa (35 segundos).

Response	Prediction	95% CI low	95% CI high	Validation (weighted mean)
Seed size	1.42	1.22	1.62	1.38
Seed quantity	2.22	1.37	3.28	3.15
Heterogeneity	0.54	0.36	0.71	0.36
Amount of residue	43.21	21.15	65.26	25*

* Single response, not weighted mean.

* Respuesta individual, no promedio ponderado.



Bars indicate: standard deviation; different letters denote significant differences (Fisher's LSD, α < 0.05).

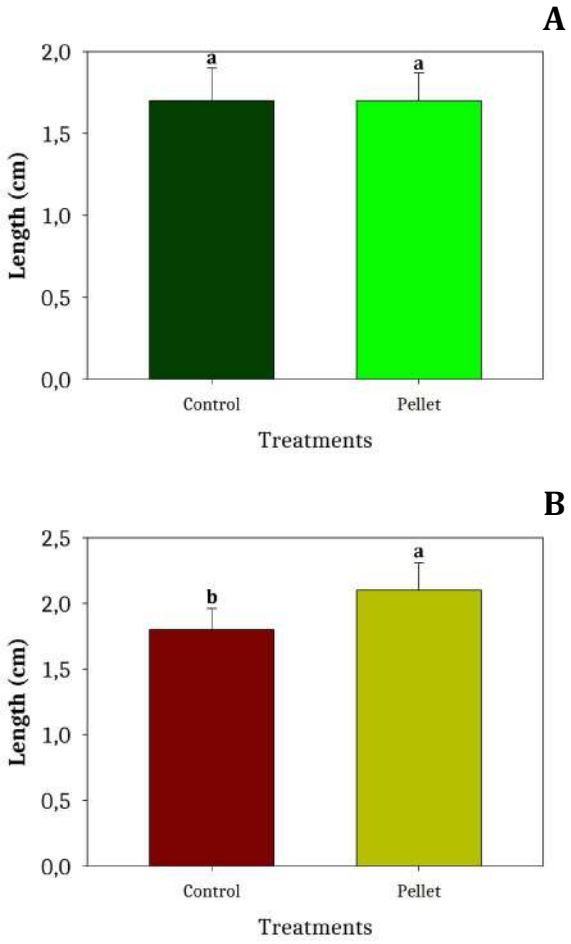
Las barras indican la desviación estándar. Letras diferentes indican diferencias significativas (LSD de Fisher, α < 0,05).

Figure 6. Germination percentages for caryopses (control), single-seed pellets, and multi-seed pellets. Species: *L. crinita*, *P. caespitosum*, and *D. californica*.

Figura 6. Porcentajes de germinación obtenidos en los tratamientos de cariopses (control), pellets de una semilla y pellets de múltiples semillas. Especies: *L. crinita*, *P. caespitosum* y *D. californica*.

Shoot and Radicle Length

Shoot and radicle length results are shown in figure 7. Shoot length did not differ significantly among treatments. In contrast, radicle length was significantly greater in pelleted seeds (2.12 ± 0.17 cm) than in controls (1.78 ± 0.11 cm).



Bars represent standard deviation; different lowercase letters indicate significant differences (Fisher's LSD, α < 0.05).

Las barras indican la desviación estándar. Letras minúsculas diferentes indican diferencias significativas (LSD de Fisher, α < 0,05).

Figure 7. (A) Shoot and (B) radicle length in caryopses (control) and pellet treatments for *L. crinita*, *P. caespitosum*, and *D. californica*.

Figura 7. (A) Longitud de plántula y (B) longitud de radícula para los tratamientos: cariopses (control) y pellets. Especies: *L. crinita*, *P. caespitosum* y *D. californica*.

Discussion

This study provides one of the first comprehensive descriptions of the seed-coating process for small-seeded species, detailing component quantities, proportions, processing times, and operational stages. It also represents the first statistical optimization of seed coating for native grass from arid regions. Although seed-coating technologies have been developed for decades, detailed methodological information is rarely available in the public domain, as most advances are confined to private industry (Pedrini *et al*. 2017).

Optimization of Individual Responses

The fitted models showed that the rotational speed of the coater plate had a significant influence on pellet size and homogeneity. The shear effect associated with higher speeds likely caused a reduction in pellet size (figures 2A-B, page 7) due to material detachment

from the forming pellet (Iparraguirre, 2009; Pasha *et al*. 2016). Conversely, increasing binder volume in single-seed pellets resulted in larger pellet (figure 2A, page 7), in agreement with reports from the pharmaceutical industry where higher impeller speeds reduce pellet size, whereas binder concentration increases it (Thies & Kleinebudde, 1999). Longer stage durations were associated with reduced size heterogeneity (figure 2C, page 7), in line with the findings of Just *et al*. (2013). The combination of layering and abrasion appears to benefit from extended processing times, promoting more uniform pellets. Heterogeneity also decreased with increasing plate speed, confirming the observations made by Pasha *et al*. (2016). Regarding the number of seeds per pellet (figure 3, page 8), higher binder viscosity induced by increased binder volume promoted seed adhesion and coalescence (Johansen & Shaefer, 2001; Keningley *et al*. 1997; Lavanya *et al*. 2011). For residue response (figure 4, page 8), a relevant factor considering the effort required to obtain spikelet-free native grass seeds (Meglioli *et al*. 2024), the combination of greater conglomerate mass and higher rotational speed enhanced the detachment of adhering material, reducing residue (Iparraguirre, 2009). In contrast, low speed combined with high binder volume increased adhesion to the plate and drum, resulting in higher residue levels (Johansen & Shaefer, 2001). The mean residue of 43% per run was lower than that reported by Pedrini *et al*. (2017) for *Solanum lycopersicum* (65.3%) and *Microlaena stipoides* (60.9%).

Multi-Response Optimization, Validation, and Germination in Native Seeds

Multi-response desirability analysis successfully identified optimal coating conditions. Validation confirmed both the predictive accuracy and robustness of the statistical models, as all measured values for native grass seeds fell within the 95% confidence intervals of model predictions.

Seed coating can enhance or impair seed physiology by facilitating water and nutrient uptake or, conversely, by impeding radicle emergence (Pedrini *et al*. 2017; Sprey *et al*. 2019). In the present study, germination of single-seed pellets was unaffected, in agreement with the results obtained using comparable materials (Romo-Campos & Guzmán Valle, 2019). In contrast, multi-seed pellets (conglomerates) showed reduced germination, possibly due to allelopathic interactions among seeds during germination, as reported in other grass species (Möhler *et al*. 2018). The enhanced radicle length observed in pelleted seeds may be associated with the coating components ($CaCO_3$, diatomaceous earth, kaolin), which provide calcium and silicon, elements linked to cell elongation, improved nutrient transport, and stress tolerance (Bauer *et al*. 2011; Jalal *et al*. 2023). Additionally, the high intraspecific genetic variability of native grasses (Trod *et al*. 2018; Villagra *et al*. 2011), combined with the mixed caryopses from three species, could explain the variability seen in physiological responses.

Conclusions

Validation using small-seeded native grasses confirmed the applicability, accuracy, and robustness of the statistical optimization methodology. All pellet traits fell within the predicted confidence intervals, supporting the reliability of the models. Seedling evaluations indicated that coating did not negatively affect germination, possibly due to the rapid dissolution of the coating material, and that the process positively influenced radicle elongation.

References

Afzal, I., Javed, T., Amirkhani, M., Taylor, A. G. (2020). Modern Seed Technology: Seed Coating Delivery Systems for Enhancing Seed and Crop Performance. *Agriculture*, *10*, 526. https://doi.org/10.3390/agriculture10110526

Bartlett, M. S. (1947). The Use of Transformations. *Biometrics*, *3*(1): 39-52. https://doi.org/10.2307/3001536

Bauer, P., Elbaum, R., Weiss, I. M. (2011). Calcium and silicon mineralization in land plants: transport, structure and function. *Plant Science, 180*(6), 746-756. https://doi.org/10.1016/j.plantsci.2011.01.019

Carballo, D. J., Matus, M., Betancourt, M., Ruiz, C. (2005). Manejo de Pasto I. Facultad de Ciencia Animal. Universidad Nacional Agraria. https://repositorio.una.edu.ni/id/ eprint/2425

Chen, D., Suter, H. C., Islam, A., & Edis, R. (2010). Influence of nitrification inhibitors on nitrification and nitrous oxide (N_2O) emission from a clay loam soil fertilized with urea. *Soil Biology Biochem, 42*(4): 660-664. https://doi.org/10.1016/j.soilbio.2009.12.014

Ferrari, F. N., & Parera, C. A. (2015). Germination of six native perennial grasses that can be used as potential soil cover crops in drip-irrigated vineyards in semiarid environs of Argentina. *Journal of Arid Environments*, *113*, 1-5. https://doi.org/10.1016/j.jaridenv.2014.09.002

Hoose, B. W., Call, R. S., Bates, T. H., Anderson, R. M., Roundy, B. A., Madsen, M. D. (2019). Seed conglomeration: a disruptive innovation to address restoration challenges associated with small-seeded species. *Restoration Ecology, 27*(5): 959-965. https://doi.org/10.1111/ rec.12947

Iparraguirre, L. M. (2009). *Mecánica Básica: fuerza y movimiento*. Instituto Nacional de Educación Tecnológica. http://www.bnm.me.gov.ar/giga1/ documentos/EL001845.pdf

Jalal, A., da Silva Oliveira, C. E., Galindo, F. S., Rosa, P. A. L., Gato, I. M. B., de Lima, B. H., Teixeira Filho, M. C. M. (2023). Regulatory Mechanisms of Plant Growth-Promoting Rhizobacteria and Plant Nutrition against Abiotic Stresses in *Brassicaceae* Family. *Life*, *13*, 211. https://doi. org/10.3390/ life13010211

Johansen, A., Schæfer, T. (2001). Effects of interactions between powder particle size and binder viscosity on agglomerate growth mechanisms in a high shear mixer. *European Journal of Pharmaceutical Sciences*, *12*(3), 297-309. https://doi.org/10.1016/S0928-0987(00)00182-2

Just, S., Toschkoff, G., Funke, A., Djuric, D., Scharrer, G., Khinast, J., Knop, K., Kleinebudde, P. (2013). Optimization of the inter-tablet coating uniformity for an active coating process at lab and pilot scale. *International journal of pharmaceutics*, *457*(1), 1-8. http://dx.doi. org/10.1016/j. ijpharm.2013.09.010

Kangsopa, J., Hynes, R. K., Siri, B. (2018). Lettuce seeds pelleting: A new bilayer matrix for lettuce (*Lactuca sativa*) seeds. *Seed Science and Technology, 46*(3), 521-531. https://doi. org/10.15258/ sst.2018.46.3.09

Keningley, S. T., Knight, P. C., Marson, A. D. (1997). An investigation into the effects of binder viscosity on agglomeration behaviour. *Powder Technology*, *91*(2), 95-103. https://doi.org/10.1016/ S0032-5910(96)03230-5

Kozub, P. C., Cavagnaro, J. B., Cavagnaro, P. F. (2018). Exploiting genetic and physiological variation of the native forage grass *Trichloris crinita* for revegetation in arid and semi-arid regions: An integrative review. *Grass and Forage Science, 73*(2), 257-271. https://doi.org/10.1111/ gfs.12337

Lavanya, K., Senthil, V., Rathi, V. (2011). Pelletization technology: a quick review. *International Journal of Pharmaceutical Sciences and Research*, *2*(6), 1337. http://dx.doi.org/10.13040/ IJPSR.0975-8232.2(6).1337-55

Leardi, R. (2009). Experimental design in chemistry: A tutorial. *Analytica Chimica Acta, 652*(1-2), 161-172. https://doi.org/10.1016/j.aca.2009.06.015

Madsen, M. D., Davies, K. W., Jason Williams, C. & Svejcar, T. J. (2012). Agglomerating seeds to enhance native seedling emergence and growth. *Journal of Applied Ecology*, *49*, 431-438 https:// doi.org/10.1111/j.1365-2664.2012.02118.x

Marinoni, L. D. R., Zabala, J. M., Taleisnik, E. L., Schrauf, G. E., Richard, G. A., Tomas, P. A., Giavedoni, J. A. & Pensiero, J. F. (2019). Wild halophytic species as forage sources: Key aspects for plant breeding. *Grass and Forage Science*, *74*(3), 321-344. https://doi.org/10.1111/gfs.12410

Massa Decon, A. M.; Pérez, S. 2025. Nursery Production of *Neltuma Genus* in Arid and Semiarid Regions of Argentine: a Review. Revista de la Facultad de Ciencias Agrarias. Universidad Nacional de Cuyo. Mendoza. Argentina. 57(2): 211-223. DOI: https://doi.org/10.48162/rev.39.184

Meglioli, C., Scaglia, J. A., Parera, C. A. (2024). Factores que afectan la germinación de tres pastos de zonas áridas: *Leptochloa crinita*, *Pappophorum caespitosum* y *Digitaria californica* (*Poaceae*). *Acta Botanica Mexicana*, (131). https://doi.org/10.21829/abm131.2024.2329

Möhler, H., Diekötter, T., Herrmann, J. D., & Donath, T. W. (2018). Allelopathic vs. autotoxic potential of a grassland weed-evidence from a seed germination experiment. Plant Ecology & Diversity, 11(4), 539–549. https://doi.org/10.1080/17550874.2018.1541487

Pasha, M., Hare, C., Ghadiri, M., Gunadi, A., Piccione, P. M. (2016). Effect of particle shape on flow in discrete element method simulation of a rotary batch seed coater. *Powder Technology*, *296*, 29-36. http://dx.doi.org/10.1016/j.powtec.2015.10.055

Pedrini, S., Merritt, D. J., Stevens, J., Dixon, K. (2017). Seed Coating: Science or Marketing Spin? *Trends in Plant Science, 22*(2): 106-116. https://doi.org/10.1016/j.tplants.2016.11.002

Pedrozo, L. P., Kuchen, B., Flores, C. B., Rodríguez, L. A., Pesce, V. M., Maturano, Y. P., Nally, M. C., Vazquez, F. (2024). Optimization of sustainable control strategies against blue rot in table grapes under cold storage conditions. *Postharvest Biology and Technology*, *213*, 112946. https:// doi. org/10.1016/j.postharvbio.2024.112946

Pornaro, C., Meggio, F., Tonon, F., Mazzon, L., Sartori, L., Berti, A., Macolino, S. (2022). Selection of inter-row herbaceous covers in a sloping, organic, non-irrigated vineyard. *PLoS ONE, 17*(12): e0279759. https://doi.org/10.1371/journal.pone.0279759

Rajeshwari, M., Renganayaki, P. R., Vanitha, C., Ravikesavan, R. (2020). Standardization of Pellet size for Mechanized Sowing in Foxtail Millet (*Setaria italica*). *Madras Agricultural Journal.* https://doi.org/10.29321/MAJ.2020.000370

Ramírez-Segura, E., Maldonado-Jaquez, J. A., Torres-Salas, I., Quero-Carrillo, A. R. (2022). Atributos físicos y fisiológicos de semilla de pastos nativos del México árido. *Revista fitotecnia mexicana*, *45*(4): 453-460. https://doi.org/10.35196/rfm.2022.4.453

Romo Campos, R. de L., & Guzmán Valle, J. F. G. (2019). Recubrimiento de semillas como técnica para la restauración de suelos degradados. *e-CUCBA 11*: 46-53. https://doi.org/10.32870/e-cucba.v0i11.128

Rubio-Asensio, J. S., Abbatantuono, F., Ramírez-Cuesta, J. M., Hortelano, D., Ruíz, J. L, Parra, M., Martínez-Meroño, R. M., Intrigliolo, D. S., Buesa, I. (2022). Effects of cover crops and drip fertigation regime in a young almond agroecosystem. *Agronomy*, *12*(11), 2606. https://doi.org/10.3390/ agronomy12112606

Sprey, L. M., Ferreira, S. A. D. N., Sprey, M. M. (2019). Physiological quality of pelleted Cubiu (*Solanum sessiliflorum* Dunal) seeds. *Revista Brasileira de Fruticultura*, *41*, e-075. https://doi.org/10.1590/0100-29452019075

Thies, R., Kleinebudde, P. (1999). Melt pelletisation of a hygroscopic drug in a high shear mixer: Part 1. Influence of process variables. *International journal of pharmaceutics*, *188*(2), 131-143. https://doi.org/10.1016/S0378-5173(99)00214-8

Thioye, B., Legras, M., Castel, L., Hirissou, F., Chaftar, N., Trinsoutrot-Gattin, I. (2021). Understanding arbuscular mycorrhizal colonization in walnut plantations: The contribution of cover crops and soil microbial communities. *Agriculture*, *12*(1), 1. https://doi.org/10.3390/ agriculture12010001

Tomaz, A., Coleto Martínez, J., Arruda Pacheco, C. (2021). Effects of cover crops and irrigation on 'Tempranillo' grapevine and berry physiology: an experiment under the Mediterranean conditions of Southern Portugal. *OENO One*, *55*(3), 191-208. https://doi.org/10.20870/ oeno-one.2021.55.3.4629

Trod, M. A., Tomas, P. A., Cervigni, G. D., Zabala, J. M., Marinoni, L. D., Giavedoni, J. A. (2018). Análisis de la distribución y densidad estomática en *Trichloris* (*Chloridoideae, Poaceae*), bajo diferentes regímenes hídricos. *Boletín de la Sociedad Argentina de Botánica*, *53*(4): 1-10. http:// dx.doi.org/10.31055/1851.2372.v53.n4.21979

Vega Riveros, C., Villagra, P. E., & Greco, S. A. (2020). Different root strategies of perennial native grasses under two contrasting water availability conditions: implications for their spatial distribution in desert dunes. *Plant Ecology*, *221*(7), 633-646

Villagra, P. E., Giordano, C., Alvarez, J. A., Cavagnaro, J. B., Guevara, A., Sartor, C., Passera, C. B., Greco, S. (2011). Ser planta en el desierto: estrategias de uso de agua y resistencia al estrés hídrico en el Monte Central de Argentina. *Ecología Austral*, *21*(1), 029–042. https://ojs.ecologiaaustral.com. ar/index.php/Ecologia_Austral/article/view/1294

Xavier, J. B., Andrade, D. B. D., Souza, D. C. D., Guimarães, G. C., Resende, L. V., & Guimarães, R. M. (2019). Morphological, chemical and physiological characterization of *Amaranthus* spp. Seeds. Journal of Seed Science, *41*(4), 478-487. https://doi.org/10.1590/2317-1545v41n4226286

Zubillaga, M. F.; Repupilli, J. A.; Boeri, P.; Servera, J. A.; Gallego, J. J.; Piñuel, L. (2024). Nutritional quality of amaranth (*Amaranthus*) silage in response to forage airing and addition of lactic bacteria. Revista de la Facultad de Ciencias Agrarias. Universidad Nacional de Cuyo. Mendoza. Argentina. 56(1): 117-126. DOI: https://doi.org/10.48162/rev.39.128

Conflicts of Interest

The authors declare that the research was conducted in the absence of any commercial or financial relationships that could be construed as a potential conflict of interest.

Impact of Fire on the Genetic Variability of a Natural Population of *Stylosanthes hippocampoides* (Fabaceae) in Corrientes, Argentina

Efecto de los incendios sobre la variabilidad genética de una población natural de *Stylosanthes hippocampoides* (Fabaceae) en Corrientes, Argentina

Julieta Berenice Arcangeli [1], Graciela Inés Lavia [1, 2], María Celeste Silvestri [1, 2 *]

Originales: *Recepción:* 07/03/2025 - *Aceptación:* 30/05/2025

ABSTRACT

Stylosanthes hippocampoides, a native legume forage species, was first studied by our research team in 2016 to assess genetic variability in natural populations in northeastern Argentina. Recurrent fires in the following years raised concerns about their effects on population genetics. This study aimed to evaluate and compare the genetic variability and structure of *S. hippocampoides* populations before and after fire events, and to infer whether such disturbances influence genetic diversity. Using Geographic Information System tools, we selected one fire-affected population (ASI) and one unaffected population (TC). Genetic analyses were conducted using inter-simple sequence repeat markers, and pre- and post-fire genetic statistics were compared. Greater genetic variability was observed between populations than within them. The TC population exhibited higher intra-population genetic diversity than the ASI population. Genetic variability decreased in ASI post-fire, while TC slightly increased. However, neither change was statistically significant. Genetic structure analysis consistently grouped individuals by population, regardless of fire exposure. These findings provide a foundation for future research on *Stylosanthes*, incorporating additional populations with varied fire histories and examining post-fire recovery processes.

Keywords
Stylo • NEA • ISSR • wildfires • forage legumes

https://doi.org/10.48162/rev.39.193

1 Instituto de Botánica del Nordeste (IBONE, UNNE -CONICET). Sargento Juan Bautista Cabral 2131. 3402BKG. Casilla de Correo 209. Corrientes. Argentina.
* celestesilvestri@gmail.com
2 Universidad Nacional del Nordeste (FACENA - UNNE). Facultad de Ciencias Exactas y Naturales y Agrimensura. Avenida Libertad 5470. Campus Deodoro Roca. Corrientes. Argentina.

Licenses Creative Commons
Attribution - Non Commercial - Share Alike

Resumen

Stylosanthes hippocampoides, una leguminosa forrajera nativa, fue estudiada por primera vez por nuestro equipo de investigación en 2016 para evaluar la variabilidad genética en poblaciones naturales del noreste de Argentina. Los incendios recurrentes en los años siguientes generaron interrogantes sobre sus efectos en la genética de las poblaciones. Este estudio tuvo como objetivo evaluar y comparar la variabilidad y la estructura genética de poblaciones de *S. hippocampoides* antes y después de los eventos de incendio, e inferir si tales perturbaciones influyen en la diversidad genética. Utilizando herramientas del Sistema de Información Geográfica, seleccionamos una población afectada por incendios (ASI) y otra no afectada (TC). Se realizaron análisis genéticos utilizando marcadores moleculares de inter secuencias simples repetidas, y se compararon las estadísticas genéticas anteriores y posteriores a los incendios. Se observó mayor variabilidad genética entre poblaciones que dentro de ellas. La población TC mostró una mayor variabilidad genética intrapoblacional que la población ASI. En ASI, la variabilidad genética disminuyó tras el incendio, mientras que TC mostró un ligero aumento; sin embargo, ninguno de los cambios fue estadísticamente significativo. El análisis de estructuración genética agrupó a los individuos por poblaciones, independientemente de la exposición al fuego. Estos resultados proporcionan una base para futuras investigaciones sobre *Stylosanthes,* incorporando poblaciones adicionales con historias de incendios variadas y examinando los procesos de recuperación post-incendio.

Palabras clave
Stylo • NEA • ISSR • fuego • leguminosas forrajeras

Introduction

Ecological disturbances, whether natural or anthropogenic, can alter key demographic and biological processes, ultimately affecting the distribution of genetic diversity within populations (4). Genetic variability influences all levels of biodiversity, from individual fitness and population viability to species adaptability to environmental change and even speciation. Consequently, the interaction between disturbances and genetic variability carries significant ecological and evolutionary implications (4, 19). Understanding how genetic variability fluctuates in populations exposed to recurrent disturbances is crucial for effective biodiversity conservation and management.

Since mid-2019, northeastern Argentina (NEA) has experienced negative monthly precipitation anomalies, leading to prolonged droughts (33). This situation, combined with fire use in agricultural practices as a vegetation management tool, created favorable conditions for wildfires (35). Notably, recurrent fires in the province of Corrientes affected 12% of its total area (30).

Stylosanthes Sw. (Fabaceae) comprises approximately 50 species adapted to tropical and subtropical regions of the Americas, ranging from the southern United States to Argentina. These species are valued for their use as forage (18), as well as for soil recovery (41) and ecological restoration (36). Eight *Stylosanthes* species are native to Argentina, most of which are found in the NEA (40). As part of a project to conserve native forage legumes in the NEA, our research team evaluated the genetic variability of *Stylosanthes hippocampoides* Mohlenbr. populations in 2016 (34). These populations were later affected by fires (30), providing an opportunity to examine potential genetic impacts.

Genetic consequences of fire on plant populations are diverse and context-dependent, influenced by the scale and frequency of fire events, biological traits and adaptive strategies of the species involved (3). For instance, individuals of some species can survive fire and resprout, resulting in minimal effects on genetic variability. In contrast, other species depend on the formation of seed banks and the genetic variability they preserve for post-fire regeneration (37). Moreover, fires can fragment previously continuous populations, creating barriers that isolate subpopulations. Such fragmentation is expected to reduce gene flow and increase genetic differentiation among populations (9).

In this context, this study analyses the genetic variability and structure of a natural population of *S. hippocampouides* affected by fires, comparing it with a control population not exposed to such events. This would allow inferring whether these disturbances influence population genetic variability and structure. Considering the extent of recent fires in the region, the small population sizes of *S. hippocampoides*, and the time elapsed since such events, we hypothesize that the post-fire ASI population exhibits reduced genetic variability compared to pre-fire levels, likely due to a bottleneck effect. Additionally, we expect the genetic structure of the ASI population to remain unchanged, as the elapsed time may be insufficient for spatial genetic subdivision to occur.

Materials and Methods

Stylosanthes hippocampoides is a perennial herb or sub-shrub with a prostrate to semi-erect growth habit, native to grasslands and savannas of Argentina, Brazil, Bolivia, Paraguay, and Uruguay (40). Its recorded lifespan is up to five years, with an estimated generation time of 6-12 months (23). *Stylosanthes* species are self-pollinating or predominantly self-pollinating (29).

Populations evaluated in this study were selected by overlaying geolocations of the populations assessed in 2016 by the research team (34) with fire-affected areas in Corrientes province, identified using historical satellite images from the FIRMS database (15). A fire was recorded at the ASI population site (27°27'58" S; 57°28'12" W) on September 30, 2020, with additional events occurring 0.96 km and 0.24 km away in July 2019. Based on this, the ASI population was selected. As a control, we selected a population within the Private Natural Reserve "Paraje Tres Cerros" (29°6'18" S; 56°56'10" W), which was confirmed to be unaffected by fire (figure 1, page 4). The ASI site lies on a broad roadside shoulder along National Route 12 (km 1171), about 700 meters from the Santa Isabel stream, subject to human disturbance due to routine roadside maintenance. In contrast, the TC population is located within the protected reserve, on the northern slope of Nazareno Hill. This area, characterized by dry air, high solar radiation, and sparse herbaceous vegetation, is free from human disturbance.

Sample collection was conducted in February-March 2022. Following Silvestri *et al.* (2020), we sampled approximately 10 - 15 adult individuals from each population, ensuring at least 3 meters between individuals. Total DNA was extracted from 200 mg of dry leaves from 10-11 individuals per population, following the protocol of Doyle and Doyle (1987). DNA integrity was confirmed by electrophoresis on 0.8% agarose gel in 1× TAE buffer stained with ethidium bromide (10 mg/ml), and concentration was determined by spectrophotometry. Nuclear DNA was amplified using PCR reactions with the same ISSR primers and conditions described by Silvestri *et al.* (2020). Amplified products were separated on 2% agarose gels in 1× TAE buffer at 60 V for 2 h and stained with ethidium bromide (10 mg/ml). Bands were scored as present or absent to generate a binary matrix based on homologous DNA fragments. Genetic diversity within populations was estimated using the total number of bands, number of private bands, percentage of polymorphic loci, number of different alleles, number of effective alleles, expected heterozygosity, and Shannon's information index. These indices were compared between pre-fire and post-fire periods for each population.

To assess whether differences in genetic variability were statistically significant, we compared the Shannon index and expected heterozygosity using previously published data (34). Given the non-normal distribution of the data, the non-parametric Wilcoxon-Mann-Whitney test was applied (42). Analyses were performed in the R Studio environment (28). Total genetic differentiation was analyzed at the species level, population, and by population combined with collection period using analysis of molecular variance (AMOVA) (11). Nei's distance and genetic identity indexes (21) were calculated between individuals. Based on genetic distance values, Principal Coordinate Analysis (PCoA) was used to visualize the distribution of genetic variation within and among populations. All statistical analyses and diversity indices were computed using GenAlEx 6.5 (24). Genetic differentiation within and between populations was further assessed using Bayesian clustering in STRUCTURE 2.3.4 (26), applying the admixture model with correlated allele frequencies. The analysis used a burn-in of 50,000 iterations followed by 100,000 Markov chain Monte Carlo (MCMC) replications (12). The algorithm was run 10 times for each number of genetic clusters (K), ranging from 1 to 6. The optimal number of clusters (ΔK) was determined following the method of Evanno *et al.* (2005).

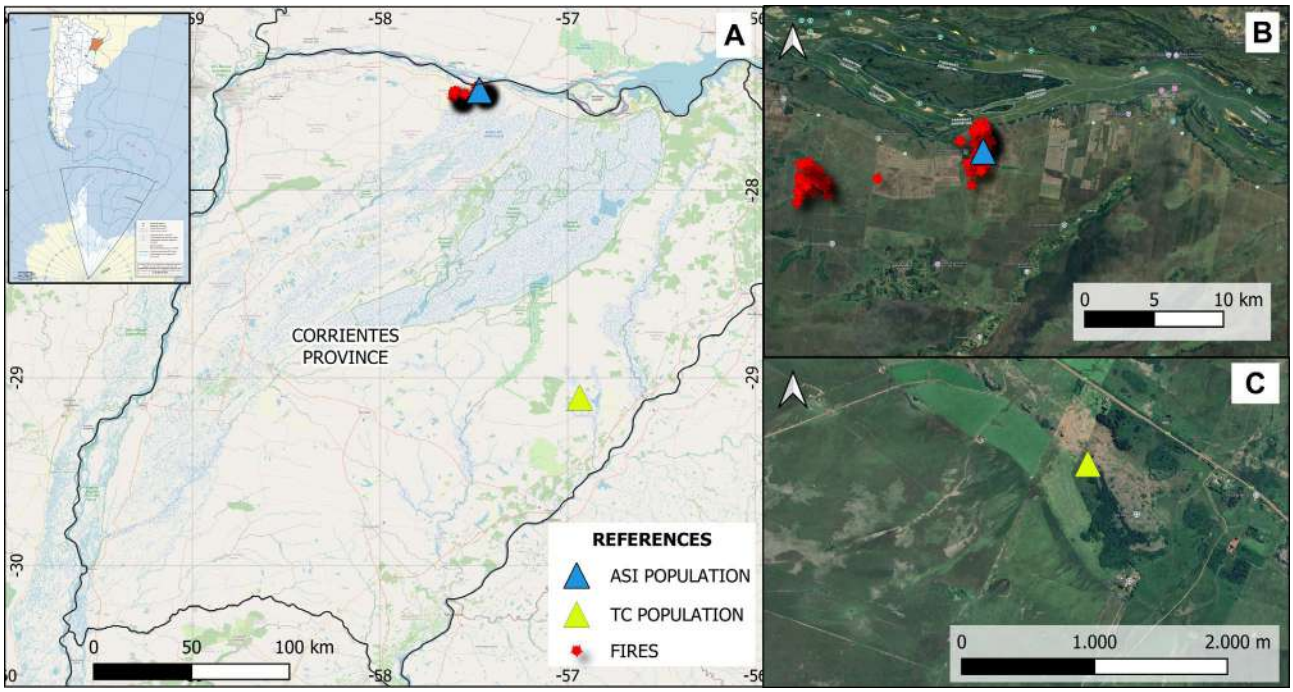


Figure 1. Location of *S. hippocampoides* populations under study and fire hotspots within a 15 km radius of the ASI population location in July 2019 and September 2020 (A). Satellite zoom of the location of the ASI population (B) and the TC population (C).

Figura 1. Localización de las poblaciones de *S. hippocampoides*, y focos de incendio en un radio de 15 km de la localización de la población ASI en julio de 2019 y septiembre de 2020 (A). Zoom satelital de la ubicación de la población ASI (B) y de la población TC (C).

Results

Genetic Variability Before and After Fire

A total of 55 loci were scored in *S. hippocampoides*, of which 62.27 % were polymorphic. At the species level, expected heterozygosity (He) was 0.25, and the Shannon index (I) was 0.37. Intrapopulation genetic diversity was lower in the ASI population compared to TC population.

Based on the same populations and molecular markers, comparisons between pre-fire (2016) and post-fire (2022) periods showed generally similar values. In the ASI population, I, He, and PLP values decreased from 0.20 to 0.17, from 0.13 to 0.11, and from 39.26% to 30.91%, respectively. Conversely, in the TC population, these indices increased: I from 0.17 to 0.23, He from 0.11 to 0.15, and PLP from 33.33% to 38.18%. The Na values increased in both populations, from 0.90 to 1.11 in ASI and 0.74 to 1.24 in TC. The Ne values slightly decreased in ASI (from 1.22 to 1.19) and increased in TC (from 1.20 to 1.27). The TNB decreased in both populations, from 69 to 44 in ASI, and from 56 to 47 in TC. The NPB remained constant in ASI (8 bands) but increased in TC from 1 to 11 bands (table 1, page 5). However, differences in I and He between pre- and post-fire periods for each population were not statistically significant according to the Wilcoxon-Mann-Whitney test (42) (ASI: $w = 3997$, $p = 0.3393$; TC: $w = 3452$, $p = 0.374$).

Table 1. Descriptive statistics of genetic variability of each population before (pre-fires, year 2016) and after fire events (post-fires, year 2022).

Tabla 1. Comparación de los estadísticos descriptivos de la variabilidad genética de cada población antes (pre incendios, año 2016) y después de los incendios (post incendios, año 2022).

Descriptive statistics	ASI population		TC population	
	Pre-fires (2016)	Post-fires (2022)	Pre-fires (2016)	Post-fires (2022)
N	9	11	8	10
TNB	69	44	56	47
NPB	8	8	1	11
Ne	1.22 (±0.03)	1.19 (±0.04)	1.20 (±0.03)	1.27 (±0.05)
Na	0.90 (±0.08)	1.11 (±0.09)	0.74 (±0.08)	1.24 (±0.09)
I	0.20 (±0.02)	0.17 (±0.03)	0.17 (±0.02)	0.23 (±0.04)
He	0.13 (±0.02)	0.11 (±0.02)	0.11 (±0.02)	0.15 (±0.03)
PPL (%)	39.26	30.91	33.33	38.18

N: Number of individuals, TNB: total number of bands, NPB: number of private bands, Ne: number of effective alleles, Na: number of different alleles, I: Shannon's information index, He: expected heterozygosity, PPL: percentage of polymorphic loci, ±: standard deviation. The genetic data of the populations from the pre-fire period were obtained from Silvestri *et al.* (2020).

N: Número de individuos, TNB: número total de bandas, NPB: número de bandas privadas, Ne: número de alelos efectivos, Na: Número de alelos diferentes, I: Índice de Shannon; He: Heterocigosis esperada, PPL: Porcentaje de Loci Polimórficos, ±: Desviación estándar. Los datos genéticos de las poblaciones del periodo pre-incendios fueron obtenidos de Silvestri *et al.* (2020)

Genetic Structure Analysis

AMOVA results showed that genetic variation was higher among populations than within them, when grouping by population alone and by population with collection period (table 2). Genetic distances between ASI2016 and ASI2022 and between TC2016 and TC2022 were 0.05 and 0.01, respectively, with corresponding genetic identity values of 0.95 and 0.998. PCoA based on individual genetic distances revealed that the first three coordinates accounted for 61.71% of total variation, with coordinates 1 and 2 explaining the largest proportion (56.73%). Coordinate 1 separates ASI and TC individuals. ASI individuals showed greater dispersion than those from TC. However, individuals within each population could not be grouped by collection period (pre- and post-fire) (figure 2, page 6).

Bayesian clustering identified two groups with the highest ΔK observed at K = 2. Individuals showed high membership coefficients to a single group corresponding to their geographic population, ASI (combined from pre- and post-fire individuals) and the TC (also including individuals from both periods) (figure 3, page 6).

Table 2. Hierarchical analysis of the genetic variability distribution estimated by AMOVA.

Tabla 2. Análisis jerárquico de la distribución de la variabilidad genética estimada por AMOVA.

Grouping	Source	Est. Var.	%	Φ*st*
Populations (ASI and TC)	Among Populations	7.59	66	0.656*
	Within Populations	3.99	34	
	Total	11.58	100	
Populations + periods (ASI2022. ASI2016. TC2022 and TC2016)	Among populations + periods	5.070	56	0.560*
	Within populations + periods	3.989	44	
	Total	9.058	100	

Est. Var**:** Estimated Variance component, %: Percentage of total variance, Φst= Phi value for each cluster, *p < 0.05.

Est. var= Componente de la varianza, **%**= Porcentaje de la varianza total, Φ***st***= Valor de *phi* para cada agrupación, *significativo p < 0,05.

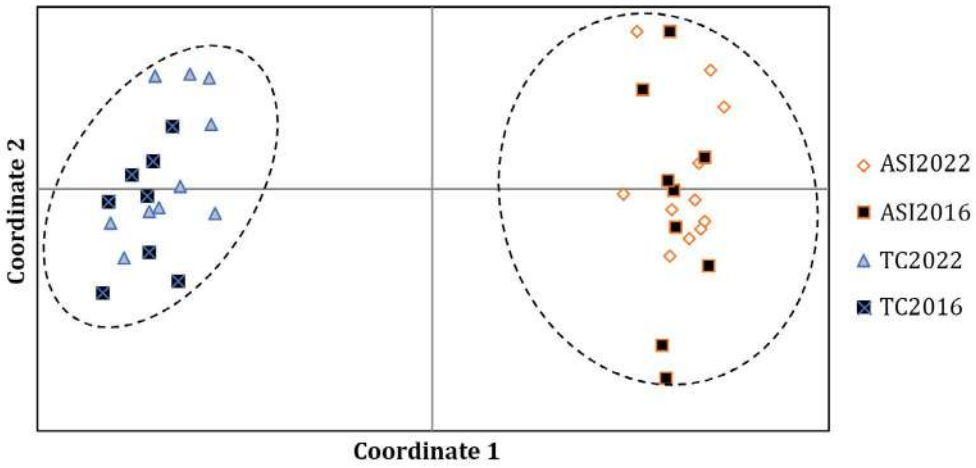


Figure 2. Principal Coordinate Analysis (PCoA) according to Nei's genetic distance between individuals of the ASI2022, ASI20116, TC2022 and TC2016 populations of *S. hippocampoides.*

Figura 2. Análisis de Coordenadas Principales (PCoA) de acuerdo a la distancia genética de Nei entre individuos de las poblaciones ASI2022, ASI20116, TC2022 and TC2016 de *S. hippocampoides.*

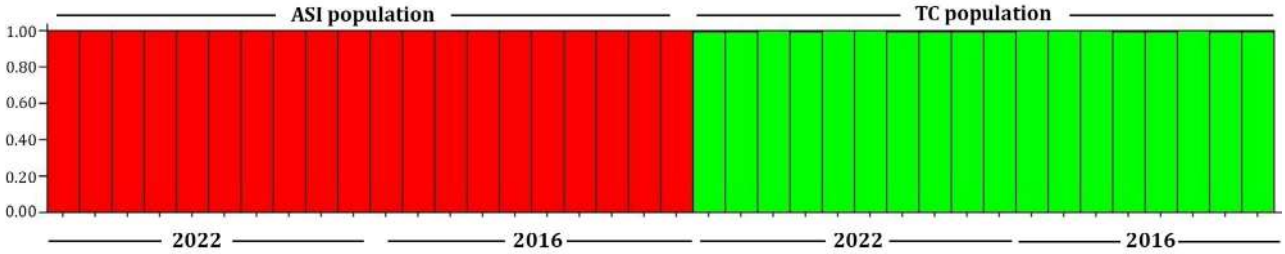


Figure 3. Bayesian clusters inferred by STRUCTURE of the populations under study of *S. hippocampoides*. Each individual is represented by a single vertical bar. Bars are partitioned into K = 2 components that represent each individual's proportional assignment to one of the genetic clusters. The populations and the collection period are indicated above and below the figure, respectively.

Figura 3. Agrupaciones Bayesianas inferidas por STRUCTURE de las poblaciones en estudio de *S. hippocampoides*. Cada individuo está representado por una barra vertical. Las barras están divididas en K = 2 componentes que representan la proporción del genoma de cada individuo asignada a un grupo genético. Las poblaciones y los periodos de colección se indican por encima y por debajo del gráfico, respectivamente.

Discussion

Our results show high genetic variability in *S. hippocampoides*, relative to values reported for this species using ISSR markers (33) and random amplified polymorphic DNA markers (17). Higher genetic diversity has been observed in other *Stylosanthes* species using ISSR markers (1, 6). These variations may result from differences in sampling and inherent genetic variability among species. For instance, Silvestri *et al.* (2020) analyzed eight populations, while we included only two. Kazan *et al.* (1993) used four individuals per population, whereas we analyzed ≥10 individuals per population. AMOVA results indicated that genetic variation is greater among populations than within populations, consistent with previous studies on *Stylosanthes* species using ISSR (1, 6, 34) and other molecular markers (5, 31, 39). This is expected given the predominant self-fertilizing reproduction of most *Stylosanthes* species. The total number of bands (TNB) in both populations was lower

than in the pre-fire evaluation, while the number of private bands (NPB) increased in the TC population and remained stable in the ASI population. These differences may be due to variations in the number of populations analyzed and differences in band interpretation between studies. We assessed two geographically distant populations, whereas Silvestri *et al.* (2020) included eight populations, two of which were from the "Tres Cerros" Natural Reserve. Since only one of these populations is included in our current analysis, the increase in NPB in the TC population can be attributed to the absence of nearby populations in both evaluations, whereas the NPB in the ASI population remained unchanged.

Following natural or artificial fire events, population genetic variability may decrease, increase, or remain unchanged. A decrease is the least commonly reported outcome (43), while increases or stability are more frequent (3, 27, 32). In our study, the ASI population showed no statistically significant changes in genetic diversity indices after fire. Genetic diversity often requires multiple generations to show significant shifts, depending on the intensity and frequency of disturbances and the degree of population fragmentation (2).

The maintenance of genetic variability may result from adaptations that mitigate fire negative effects. Like many Fabaceae species, *Stylosanthes* seeds have hard, impermeable coats that require scarification at 80°C or exposure to surfaces reaching 120°C to break dormancy and enable germination (7, 13). This trait supports the formation of persistent seed banks below the soil surface, which can store genetic material from recent and earlier pre-fire generations. Seed bank formation has been documented in *S. hippocampoides* (23), and considering its generation time and the interval between our evaluations, this mechanism is a plausible explanation for the observed genetic stability. Such a strategy enables post-fire regeneration from multi-generational seed banks rather than a few surviving individuals (3). Additionally, *Stylosanthes* species are known for drought tolerance and high colonization capacity (18), traits that promote rapid recovery after fire events.

The ASI population, located along a roadside subject to frequent burning and mowing, may be adapted to such disturbances. Banks *et al.* (2013) suggest that populations in frequently disturbed areas may rely on these conditions for persistence, as disturbance can enhance resource availability and shape community composition. In this context, the ASI population may exhibit fire adaptation, with a strong colonizing response enabled by heat-softened seeds and reduced competition. This interpretation aligns with Gardener (1980), who found that *Stylosanthes* cultivars from arid environments were more fire-resistant than those from humid coastal areas.

Bayesian clustering analysis showed a high degree of individual assignment to a single cluster, corresponding to their respective geographic populations. This pattern, along with the separation of populations along different axes in the PCoA, supports the observed genetic differentiation. The presence of private bands in both populations further indicates strong genetic identity. These findings suggest that the two sampled sites represent genetically structured and distinct populations. However, no signs of fragmentation were detected in the genetic structure of the fire-affected ASI population. Fire effects on genetic structure are often spatially heterogeneous (22), and seed bank depletion may vary depending on fire intensity and frequency (25, 38). Such dynamics can influence demographic connectivity and affect the distribution of genetic diversity within and among populations. Despite this, few studies have compared the genetic composition of seed banks and adult populations in fire-prone ecosystems (3, 9, 25). Gardener (1980) found that most *Stylosanthes* cultivars possessed sufficient seed reserves for regeneration, with the number of seedlings in each regenerating line correlating with seed quantity in the soil. Nevertheless, direct comparisons between the genetic profiles of pre-fire adults and post-fire seedlings remain scarce, making it difficult to determine whether seed banks fully preserve the genetic composition of earlier generations. The lack of changes in genetic structure in the ASI population may be explained by several biological traits of the species, such as its predominantly self-fertilizing reproduction, which limits within-population genetic variability, a short generation time that allows a rapid regeneration; a large and persistent seed bank; and the relatively brief time between fire events and post-fire sampling, which may not have been sufficient for genetic subdivision to emerge.

Given the increasing frequency and intensity of fires across the natural range of *S. hippocampoides* in recent years (14, 20, 30), future research should expand on this

study by including more populations with contrasting fire histories. Determining whether post-fire individuals originate from soil seed banks or surviving adults would also be valuable. Such information is essential for informing germplasm collection and designing effective conservation strategies.

Conclusion

Our results showed no statistically significant changes in the genetic variability indices of the ASI population after fire, nor evidence of fragmentation or alterations in its genetic structure. However, as only one fire-affected population was analyzed, our capacity to fully assess the species' response to fire is limited. This study should therefore be viewed as a preliminary step. Future research should include additional populations with contrasting fire histories and examine whether post-fire individuals originate from soil seed banks or surviving adults. Given the increasing frequency and intensity of fires in recent years in Argentina, driven by human activities and intensified by climate change, such studies are crucial for developing effective conservation strategies for native species.

References

1. Alzate-Marin, A. L.; Costa-Silva, C.; Rivas, P. M. S.; Bonifacio-Anacleto, F.; Santos, L. G.; Moraes Filho, R. M. D.; Martinez, C. A. 2019. Diagnostic fingerprints ISSR/SSR for tropical leguminous species *Stylosanthes capitata* and *Stylosanthes macrocephala*. Sci. Agr. 77(3): e20180252. https://doi.org/10.1590/1678-992X-2018-0252
2. André, T.; Lemes, M. R.; Grogan, J.; Gribel, R. 2008. Post-logging loss of genetic diversity in a mahogany (*Swietenia macrophylla* King, Meliaceae) population in Brazilian Amazonia. For. Ecol. Manag. 255: 340-345. https://doi.org/10.1016/j.foreco.2007.09.055
3. Ayre, D. J.; Ottewell, K. M.; Krauss, S. L.; Whelan, R. J. 2009. Genetic structure of seedling cohorts following repeated wildfires in the fire-sensitive shrub *Persoonia mollis* ssp. *nectens*. J. Ecol. 97(4): 752-760. https://doi.org/10.1111/j.1365-2745.2009.01516.x
4. Banks, S. C.; Cary, G. J.; Smith, A. L.; Davies, I. D.; Driscoll, D. A.; Gill, A. M.; Lindenmayer, D. B.; Peakall, R. 2013. How does ecological disturbance influence genetic diversity? Trends Ecol Evol. 28(11): 670-679. https://doi.org/10.1016/j.tree.2013.08.005
5. Barros, A. M.; Faleiro; F. G.; Shiratsuchi, L. S.; Pereira de Andrade, R.; Britto Lopes, G. K. 2005. Variabilidade genética e ecológica de *Stylosanthes macrocephala* determinadas por RAPD e SIG. Pesqui. Agropecu. Bras. 40: 899-909. https://doi.org/10.1590/S0100-204X2005000900010
6. Costa, J. C.; Fracetto, G. G. M.; Fracetto, F. G. C.; Souza, T. C.; Santos, M. V. F.; Lira Júnior, M. A. 2018. Genetic diversity in natural populations of *Stylosanthes scabra* using ISSR markers. Genet. Mol. Res. 17(1): gmr18219. https://doi.org/10.4238/gmr16039866
7. Dalzotto, D.; Sharry, S.; Piñuel, L.; Boeri, P. 2025. Challenges in germination of *Neltuma caldenia* in semi-arid regions: optimization of germination protocols, influence of saline stress and seed quality. Revista de la Facultad de Ciencias Agrarias. Universidad Nacional de Cuyo. Mendoza. Argentina. 57(1): 67-79. DOI: https://doi.org/10.48162/rev.39.152
8. Doyle, J. J.; Doyle, J. L. 1987. A rapid DNA isolation procedure for small quantities of fresh leaf tissue. Phytochemistry. 19(1): 11-15.
9. England, P. R.; Usher, A. V.; Whelan, R. J; Ayre, D. J. 2002. Microsatellite diversity and genetic structure of fragmented populations of the rare, fire-dependent shrub *Grevillea macleayana*. Mol. Ecol. 11(6): 967-977. https://doi.org/10.1046/j.1365-294X.2002.01500.x
10. Evanno, G.; Regnaut, S.; Goudet, J. 2005. Detecting the number of clusters of individuals using the software STRUCTURE: A simulation study. Mol. Ecol. 14(8): 2611-2620. https://doi.org/10.1111/j.1365-294X.2005.02553.x
11. Excoffier, L.; Smouse, P. E.; Quattro, J. M. 1992. Analysis of molecular variance inferred from metric distances among DNA haplotypes: Application to human mitochondrial DNA restriction data. Genetics. 131(2): 479-491. https://doi.org/10.1093/genetics/131.2.479
12. Falush, D.; Stephens, M.; Pritchard, J. K. 2003. Inference of population structure using multilocus genotype data: Linked loci and correlated allele frequencies. Genetics. 164(4): 1567-1587. https://doi.org/10.1093/genetics/164.4.1567
13. Fidelis, A.; Daibes, L. F.; Martins, A. R. 2016. To resist or to germinate? The effect of fire on legume seeds in Brazilian subtropical grasslands. Acta Bot. Bras. 30: 147-151. https://doi.org/10.1590/0102-33062015abb0187
14. Fidelis, A.; Zirondi, H. L. 2021. And after fire, the Cerrado flowers: a review of post-fire flowering in a tropical savanna. Flora 280:151849. https://doi.org/10.1016/j.flora.2021.151849

15. FIRMS-NASA's. Fire Information for Resource Management System. 2020. https://firms.modaps.eosdis.nasa.gov/map/#d:24hrs;@0.0,0.0,3z, (Verified 1 July 2020).
16. Gardener, C. J. 1980. Tolerance of perennating Stylosanthes plants to fire. Aust. J. Exp. Agric. Anim. Husb. 20(106): 587-593. https://doi.org/10.1071/EA9800587
17. Kazan, K.; Manners, J. M.; Cameron, D. F. 1993. Genetic relationships and variation in the *Stylosanthes guianensis* species complex assessed by random amplified polymorphic DNA. Genome. 36: 43-49. https://doi.org/10.1139/g93-006
18. Maass, B.; Sawkins, L. 2004. History, relationships and diversity among *Stylosanthes* species of commercial significance. In Chakraborty, S. (Ed). High-yielding anthracnose-resistant *Stylosanthes* for agricultural systems. CSIRO Publishing. 12-26.
19. MacDougall, A. S.; McCann, K. S.; Gellner, G.; Turkington, R. 2013 Diversity loss with persistent human disturbance increases vulnerability to ecosystem collapse. Nature. 494(7435): 86-89. https://doi.org/10.1038/nature11869
20. Naval Fernández, M. C.; Albornoz, J. V.; Bellis, L. M., Baldini, C.; Arcamone, J. R.; Silvetti, L. E.; Argarañaz, J. P. 2023 Megaincendios 2020 en Córdoba: Incidencia del fuego en áreas de valor ecológico y socioeconómico. Ecol. Austral 33: 136-151. http://dx.doi.org/10.25260/EA.23.33.1.0.2120
21. Nei, M. 1973. Analysis of gene diversity in subdivided populations. Proc. Natl. Acad. Sci. 70: 3321-3323. https://doi.org/10.1073/pnas.70.12.3321
22. Ooi, M. K. J.; Whelan, R. J.; Auld, T. D. 2006. Persistence of obligate-seeding species at the population scale: effects of fire intensity, fire patchiness and long fire-free intervals. Int. J. Wildland Fire 15: 261-269. https://doi.org/10.1071/WF05024
23. Orr, D. M. 2008. Grazing management influences the dynamics of populations of *Stylosanthes hippocampoides* (Oxley fine stem stylo). Trop. Grassl. 42(4): 193-201.
24. Peakall, R.; Smouse, P. E. 2006. GENALEX 6: Genetic analysis in Excel. Population genetic software for teaching and research. Mol. Ecol. Not. 6(1): 288-295. https://doi.org/10.1111/j.1471-8286.2005.01155.x
25. Premoli, A. C.; Kitzberger, T. 2005. Regeneration mode affects spatial genetic structure of *Nothofagus dombeyi* forests. Mol. Ecol. 14: 2319-2329. https://doi.org/10.1111/j.1365-294x.2005.02629.x
26. Pritchard, J. K.; Stephens, M.; Donnelly, P. 2000. Inference of population structure using multilocus genotype data. Genetics. 155(2): 945-959. https://doi.org/10.1093/genetics/155.2.945
27. Rajora, O. P.; Pluhar, S. A. 2003. Genetic diversity impacts of forest fires, forest harvesting, and alternative reforestation practices in black spruce (*Picea mariana*). Theor. Appl. Genet. 106(7): 1203-1212. https://doi.org/10.1007/s00122-002-1169-9
28. R Core Team. 2020. R: A language and environment for statistical computing. R Foundation for Statistical Computing v 04.2 [software]. http://www.R-project.org/
29. Santos García, M. O.; Resende, R. M. S.; Chiari, L.; Zucchi, M. I.; de Souza, A. P. 2011. Mating systems in tropical forages: *Stylosanthes capitata* Vog. and *Stylosanthes guianensis* (Aulbl.) Sw. Euphytica. 178: 185-193. https://doi.org/10.1093/aobpla/pls001
30. Saucedo, G. I.; Perucca, A. R.; Kurtz, D. B. 2023. Las causas de los incendios de principios del año 2022 en la provincia de Corrientes. Ecol Aust. 33(1): 273-284. https://doi.org/10.25260/EA.23.33.1.0.2020
31. Sawkins, M. C.; Maass, B. L.; Pengelly, C.; Newburry, H. J.; Ford-Lloyd, B. V.; Maxted, N.; Smith, R. 2001. Geographical patterns of genetic variation in two species of *Stylosanthes* Sw. using amplified fragment length polymorphism. Mol. Ecol. 10: 1947-1958. https://doi.org/10.1046/j.0962-1083.2001.01347.x
32. Segarra-Moragues, J. G.; Ojeda, F. 2010. Postfire response and genetic diversity in *Erica coccinea*: Connecting population dynamics and diversification in a biodiversity hotspot. Evolution 64(12): 3511-3524. https://doi.org/10.1111/j.1558-5646.2010.01064.x
33. Servicio Meteorológico Argentino. 2020. Informe especial por déficit de lluvias en la región noreste de Argentina. https://www.smn.gob.ar/boletines/informe-especialsequ%C3%ADa-en-el-nea (Fecha de consulta: 15 de abril 2020).
34. Silvestri, M. C.; Acuña, C. A.; Moreno, E. M. S.; Garcia, A. V.; Vanni, R. O.; Lavia, G. I. 2020. Patterns of genetic diversity and potential ecological niches of *Stylosanthes* species from northeastern Argentina. Crop Sci. 60: 1436-1449. https://doi.org/10.1002/csc2.20117
35. Smichowski, H.; Montiel, M. R.; Romero, V.; Kowalewski, M.; Contreras, F. I. 2021. Evaluación de incendios en áreas periurbanas de la ciudad de Corrientes (Argentina) durante la sequía extrema del año 2020. Pap. Geogr. 67: 151-167. https://doi.org/10.6018/geografia.486441
36. Starr, C. R.; Corrêa, R. S.; Filgueiras, T. D.; Hay, J. D.; dos Santos, P. F. 2013. Plant colonization in a gravel mine revegetated with Stylosanthes spp. in a Neotropical savanna. Land. Ecol. Eng. 9: 189-201. https://doi.org/10.1007/s11355-012-0196-1
37. Steinitz, O.; Shohami, D.; Ben-Shlomo, R.; Nathan, R. 2012. Genetic consequences of fire to natural populations. Isr. J. Ecol. Evol. 58: 205-220. https://doi.org/10.1560/IJEE.58.2-3.205
38. Uchiyama, K.; Goto, S.; Tsuda, Y.; Takahashi, Y.; Ide, Y. 2006. Genetic diversity and genetic structure of adult and buried seed populations of *Betula maximowicziana* in mixed and post-fire stands. For. Ecol. Manag. 237: 119-126. https://doi.org/10.1016/j.foreco.2006.09.037

39. Vander Stappen, J.; Van Campenhout, S.; Gama Lopez, S.; Volckaert, G. 1998. Sequencing of the internal transcribed spacer region ITS1 as a molecular tool detecting variation in the *Stylosanthes guianensis* species complex. Theor. Appl. Genet. 96: 869-877. https://doi.org/10.1007/s001220050814
40. Vanni, R. O. 2017 The genus *Stylosanthes* (Leguminosae - Dalbergiaeae) in South America. Bol. Soc. Argent. Bot. 52(3): 549-585. https://doi.org/10.31055/1851.2372.v52.n3.18033
41. Velásquez Ramírez, M. G.; del Castillo Torres, D.; Guerrero Barrantes, J. A.; Vásquez Bardales, J.; Thomas, E.; Cusi Auca, E.; Gushiken, M. C.; Muñoz Díaz, B.; Russo, R.; Corvera Gomringer, R. 2021. Soil recovery of alluvial gold mine spoils in the Peruvian Amazon using *Stylosanthes guianensis*, a promising cover crop. Land Degrad. Dev. 32(18): 5143-5153. https://doi.org/10.1002/ldr.4118
42. Wilcoxon F. 1950. Some rapid approximate statistical procedures. Ann. N. Y. Acad. Sci. 52(6): 808-814. https://doi.org/10.1111/j.1749-6632.1950.tb53974.x
43. Worth, J. R.; Jordan, G. J.; Marthick, J. R.; Sakaguchi, S.; Colhoun, E. A.; Williamson, G. J.; Motomi, I.; Bowman, D. M. 2017. Fire is a major driver of patterns of genetic diversity in two co-occurring Tasmanian palaeoendemic conifers. J. Biogeogr. 44(6): 1254-1267. https://doi.org/10.1111/jbi.12919

Acknowledgments

This work was supported by the Secretaría General de Ciencia y Técnica of the Universidad Nacional del Nordeste (Special Grant for Strategic Research in the Context of Drought and Wildfires in the Province of Corrientes. Research Group: Germplasm of Leguminous Species of Productive Interest: Conservation, Characterization, and Pre-breeding) and by PICT-2021-I-INVI-00202 (Agencia Nacional de Promoción Científica y Tecnológica, ANPCyT).

Integrating Professional and Crowdsourced Data to Address Biodiversity Knowledge Gaps in Under-Sampled Semi-Arid Wetlands

Integración de datos profesionales y colaborativos para abordar vacíos de conocimiento sobre biodiversidad en humedales semiáridos

Solana Tabeni, Joaquin Asad, Ever Tallei, Benjamin Bender, Bertilde Rossi

Originales: *Recepción:* 20/08/2025 - *Aceptación:* 20/03/2026

ABSTRACT

Arid wetlands are vulnerable ecosystems affected by natural and human factors. Their study and conservation are limited by data scarcity and sampling bias. In a wetland of west-central Mendoza, Argentina (Leyes-Tulumaya streams), we explored the contribution of plant and vertebrate records from traditional scientific sources and citizen science. Of 270 recorded species, citizen science contributed the majority of records and unique species. Similarity between databases was greatest between citizen science and literature, with birds dominating among vertebrates. The vertebrate inventory stabilized over time, although estimated richness exceeded observed richness. Accumulation curves for plants did not reach asymptote, suggesting incomplete sampling. Positive spatial autocorrelation of records was detected, indicating data clustering in lagoons. The integration and joint analysis of data sources proved crucial to obtain a more complete and robust understanding of biodiversity and its spatial distribution. Citizen science contributions, in particular, expand databases in understudied arid ecosystems, complementing traditional methods and addressing spatial and temporal information gaps.

Keywords
Monte Desert wetlands • scientific collections • citizen science • biodiversity monitoring

https://doi.org/10.48162/rev.39.215

Instituto Argentino de Investigaciones de las Zonas Áridas (IADIZA). CCT-CONICET Mendoza, UNCuyo. Gobierno de Mendoza. Av. A. Ruiz Leal s/n. Parque General San Martín. C. P. 5500. Mendoza. Argentina. * stabeni@mendoza-conicet.gob.ar

Licenses Creative Commons
Attribution - Non Commercial - Share Alike

Resumen

Los humedales áridos son ecosistemas vulnerables, afectados por factores naturales y humanos. Su estudio y conservación se ven limitados por la escasez de datos y sesgos de muestreo. En un humedal del centro-oeste de Mendoza, Argentina (Arroyos Leyes-Tulumaya), exploramos la contribución de registros de plantas y vertebrados provenientes de fuentes científicas tradicionales y ciencia ciudadana. De 270 especies registradas, la ciencia ciudadana aportó la mayoría de los registros y especies únicas. La similitud entre bases fue mayor entre ciencia ciudadana y literatura, con aves dominando los vertebrados. El inventario de vertebrados se estabilizó con tiempo, aunque la riqueza estimada superó la observada. Las curvas de acumulación para plantas no alcanzaron una asíntota, sugiriendo un muestreo incompleto. Se detectó autocorrelación espacial positiva de los registros, indicando agrupamiento de datos en las lagunas. La integración y análisis conjunto de fuentes de datos demostró ser crucial para obtener una comprensión más completa y robusta de la biodiversidad y su distribución espacial. Los aportes de la ciencia ciudadana, en particular, expanden las bases de datos en ecosistemas áridos poco estudiados, complementando métodos tradicionales y abordando brechas de información espacial y temporal.

Palabras clave
humedales del Desierto del Monte • colecciones científicas • ciencia ciudadana • monitoreo de biodiversidad

Introduction

Preserving biodiversity in arid regions poses challenges for the scientific community. It requires collaboration across scientific fields and innovative technologies. Partnerships with various societal sectors are also necessary. A major hurdle in studying biological diversity in dry regions is the scarcity of data and the challenges in acquiring it Hochachka *et al.* (2012). Ecological knowledge requires information on species distributions at different scales. However, collecting data at several scales is often costly yet essential for providing a broader context for more focused research and conservation efforts Reis *et al.* (2016). Few arid regions have sampling levels proportional to their diversity Wolf *et al.* (2022). In a scenario of accelerated expansion of agriculture, urbanization, and fragmentation, acquiring additional data is crucial to rectify environmental representation biases. This helps assess species loss and their ecological roles García-Vega & Newbold (2020).

Crowdsourced data play a significant role in biodiversity monitoring Bowler *et al.* (2022), Gouraguine *et al.* (2019). Citizen science involves the public in research, allowing non-scientists to help collect and analyze data. This approach aids biological information gathering across large areas Wolf *et al.* (2022). On the other hand, long-term ecosystem data demand funding commitments that is not always assured, impacting conservation endeavors. Citizen science data expands biodiversity databases, complementing professional data in ecosystems Galván *et al.* (2022), Klemann-Junior (2017).

South American arid wetlands are unexplored and undersampled ecosystems Reis *et al.* (2016). These ecosystems have high levels of use but little biological information. Wetlands are vital in dry regions because they provide essential surface and groundwater for communities and wildlife Pocock (2017). This study explores biodiversity data from traditional scientific methods and data arising from citizen participation strategies. We aim to: 1) compare records from different sources (*i.e.* scientific collections, literature, and citizen science observations), to analyze biodiversity knowledge; 2) analyze temporal data acquisition to assess quality and gaps; 3) explore spatial distribution of data to assess the geographical scope. We hypothesize that 1) citizen science data complement and expand traditional scientific data, 2) combining data sources reduces spatial biases, resulting in a pattern of observed richness characterized by well-sampled and undersampled areas.

Materials and Methods

Study Area

The study area encompasses the wetland system of the Leyes-Tulumaya streams. It consists of seasonal lagoons and marshes, and riparian habitats (-32.763° S -68.594° W) (figure 1).



Source/Fuente: IGN

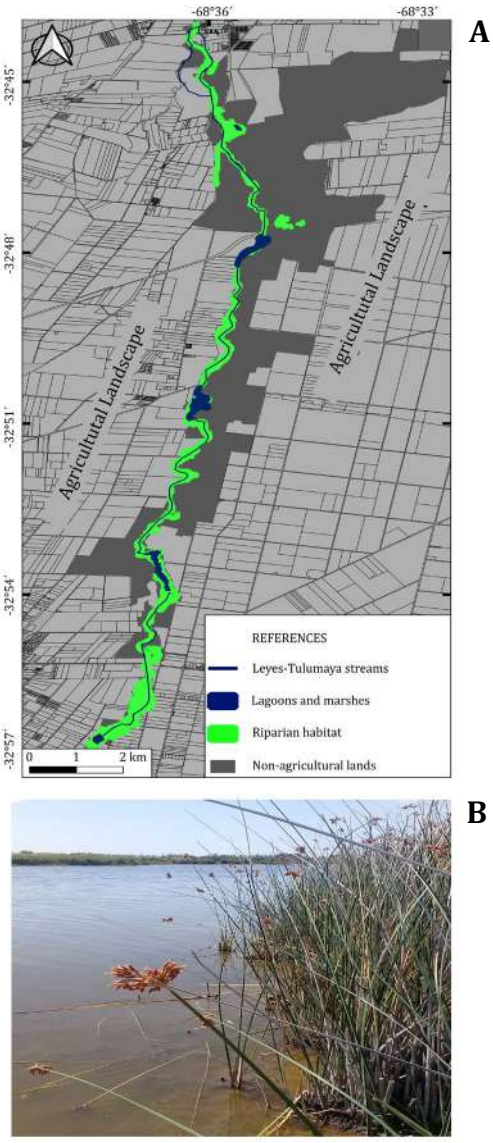


Figure 1. A. Map of study area. Wetland system of the Leyes-Tulumaya streams (Mendoza, Argentina). B. Riparian habitat and lagoon in a section of the Leyes-Tulumaya streams.

Figura 1. A. Mapa del área de estudio. Humedal de los arroyos Leyes-Tulumaya (Mendoza, Argentina). B. Hábitat ripario y laguna en una sección de los arroyos Leyes-Tulumaya.

The system is in the Mendoza River Basin within the Monte Desert biome (Mendoza). This system receives subsurface water from the Mendoza River, along with surface runoff from rain and drainage from irrigated farms and agricultural drainage. The wetland is part of the Gran Ciénaga del Bermejo. Its surface has been gradually decreasing since colonial times due to agricultural and urban expansion Prieto *et al.* (2012), Ciardullo *et al.* (2025). The wetland sits in a mosaic of urban and agricultural landscapes. Riparian habitats feature dense formations of *Scirpus californicus*, *Typha dominguensis* and *Phragmites australis*. Flooded habitats include *Salicornia* sp., *Distichlis* sp., *Juncus* spp., *Xanthium* sp. and *Suaeda* sp. Contreras & Fernandez (1980).

Data Source

We used plant and vertebrate occurrence data, the most recorded groups, to compare data from expert sampling and citizen science. We conducted bibliographic searches in Google Scholar until December 2024. The search used terms such as: Leyes Tulumaya AND wetland* OR humedal OR humedales OR sistema OR laguna*. This identified 21 articles. We chose peer-reviewed articles from scientific journals that featured these words in titles, abstracts, or keyword lists: We excluded technical reports and theses to ensure reproducibility. We expanded the search at the documentation center of the CONICET (Consejo Nacional de Investigaciones Científicas y Técnicas). After filtering and integrating both searches, we obtained 12 articles concerning wetland biodiversity.

We reviewed the scientific collections of IADIZA CONICET Mendoza. Plant records came from the herbarium collection (MERL, Mendoza Ruiz Leal). Vertebrates came from the collections of birds (CORI), mammals (CMAI), reptiles and amphibians (CHEI) and fishes (CICI). The revision covered years 1933 in plants and 1976 in vertebrates, to December 2024. We also searched non-digitized records in field notebooks of naturalists and collectors and the accession register of specimens. We obtained 38 plant and 150 vertebrate species records. For specimens lacking geographic coordinate data, the text on the label or collection card was manually inspected. Once the locality was obtained, the georeferencing protocol proposed by Zermoglio *et al.* (2020) was applied. The crowdsourced biodiversity data came from the citizen science platforms iNaturalist https://www.inaturalist.org/ and eBird https://ebird.org/home. As this wetland lacks a conservation status, its boundaries are not well defined. In order to create a polygon that encompasses all citizen-reported observations, we calculated the maximum habitat reach influenced by water in non-agricultural lands: We calculated the maximum water reach in non-agricultural lands between 1985 and 2022, in QGIS version 3.26 (figure 1, page 3). We used MapBiomas Argentina Collection 1 for land cover classifications (https://argentina.mapbiomas.org/). The polygon includes streams, lagoons, and marshes and riparian habitats. We selected iNaturalist observations of plants and vertebrate species with a research grade designation, meaning their taxonomic identification had at least two-thirds expert agreement. This search resulted in 458 species records. In addition to the iNaturalist database, we consult the eBird database. We filtered the eBird list of bird species occurring in the study area, resulting in 5450 records. We extracted scientific names, dates, and coordinates.. We manually reviewed photographs to rule out taxonomic errors. To ensure comparability across different sources, taxonomic nomenclature, was revised and aligned with GBIF (Troudet *et al.*, 2017) standards. Additionally other reference bases such as Sociedad Argentina para el Estudio de los Mamíferos https://www.sarem.org.ar/ and Flora Argentina http://www.floraargentina.edu.ar/ were consulted. Species whose geographic range did not align with the study area were excluded, along with duplicate records. Records of species with doubtful or debated taxonomy were considered only at the genus level.

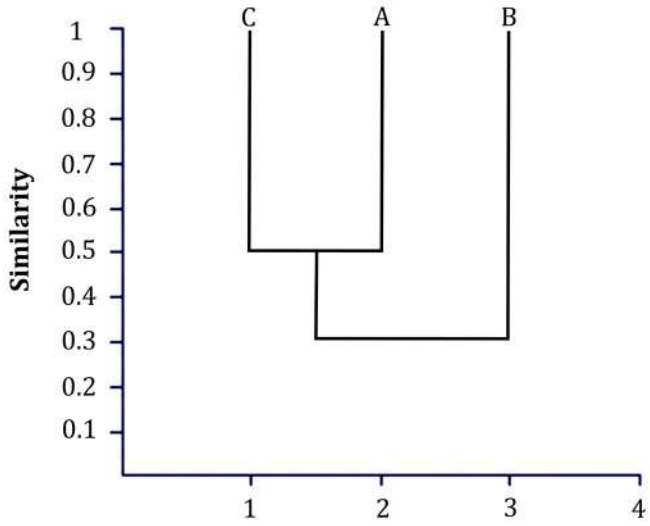
Data Analysis

We compared species composition similarity across data sources Jaccard index-based similarity matrices were used to generate dendrograms (single linkage) visualizing data source relationships. We performed clustering analysis using PAST 4.0. To test for taxonomic differences within and between datasets a we conducted a X^2 test. We integrated records to provide a first quantitative assessment of species richness and analyze the completeness of the inventory. Species records from three data sources were integrated from the first record

until December 1st, 2024. Data were grouped into 3-year periods. This resuled in 17 periods for vertebrates (1977-2024) and 15 for plants (1980-2024). We calculated species accumulation curves using the nonparametric estimators CHAO 2 and ICE Callaghan *et al.* (2021) using EstimateS 9.1.0 Colwell & Elsensohn (2014). We tested spatial autocorrelation of biodiversity records using Moran's I statistic. This index ranges from -1 to 1. High and positive values of Moran's I indicate positive autocorrelation, implying the clustering of similar values. A value close to zero indicates no autocorrelation. Moran's *I* was computed in GeoDa 0.9 (Anselin *et al.*, 2009).

RESULTS

The three datasets yielded 270 species of plants and vertebrates. Plants represented 15% and vertebrates 85% being vertebrates. Native species predominate, with only 3% being introduced (3 plant species and 6 vertebrate species). Among plants, Caryophyllales (27%) and Asterales (22%) were most abundant. Passeriformes (60%) and Charadriiformes (12%) dominated bird records. Rodentia (75%) and Carnivora (25%) prevailed in mammals. Amphibians and reptiles included Anura and Squamata. Siluriformes (33%) and Characiformes (22%) were the most frequent orders in fishes. Database similarity ranged from 0.21 to 0.66. Citizen science and literature databases showed the greatest similarity, indicating a greater number of shared species, primarily birds (57%) (figure 2).



A: scientific literature; B: biological collections; C: citizen science from the Leyes and Tulumaya streams wetland system (Mendoza, Argentina).

A: literatura científica; B: colecciones biológicas; C: ciencia ciudadana del sistema de humedales de los arroyos Leyes y Tulumaya (Mendoza, Argentina).

Figure 2. Similarity dendrogram (Jaccard index) between species databases from the Leyes and Tulumaya streams wetland system (Mendoza, Argentina).

Figura 2. Dendograma de similitud (índice de Jaccard) entre bases de datos de especies del sistema de humedales de los arroyos Leyes y Tulumaya (Mendoza, Argentina).

Citizen science data yielded the most records (232 species of vertebrates and plants). It also had the highest number of unique species. Since 2009, it contributed 72 unique vertebrates and 21 unique plants. Literature added 162 records since 1980, including 24 unique vertebrates and 3 unique plant species. Scientific collections contributed 64 species since 1976, including only 8 unique vertebrate records. Vertebrate representation did not differ significantly across databases ($X^2 = 8.96$, df = 8, $p = 0.34$). Birds comprised 92% of vertebrate records. This differed significantly from other classes ($X^2 = 1296.08$, df = 4, $p < 0.001$). Plant records, differed between databases. Magnoliopsida (dicotyledons) was prevalent in citizen science records ($X^2 = 9.15$, df = 2, $p < 0.05$). It was more abundant than Liliopsida (monocotyledons) ($X^2 = 11.57$, df = 1, $p < 0.001$) (table 1, page 6).

Table 1. Number of records of plants and vertebrates species from the Leyes and Tulumaya streams wetland system reported in the different databases.

Tabla 1. Número de registros de especies de plantas y vertebrados en el sistema de humedales de los arroyos Leyes y Tulumaya según diversas bases de datos.

Vertebrates	Scientific literature	Scientific collections	Citizen science
Birds	133	50	182
Mammals	9	2	3
Reptiles	0	1	1
Amphibians	0	0	1
Fishes	4	2	7
Plants			
Magnoliopsida	7	6	32
Liliopsida	9	3	6

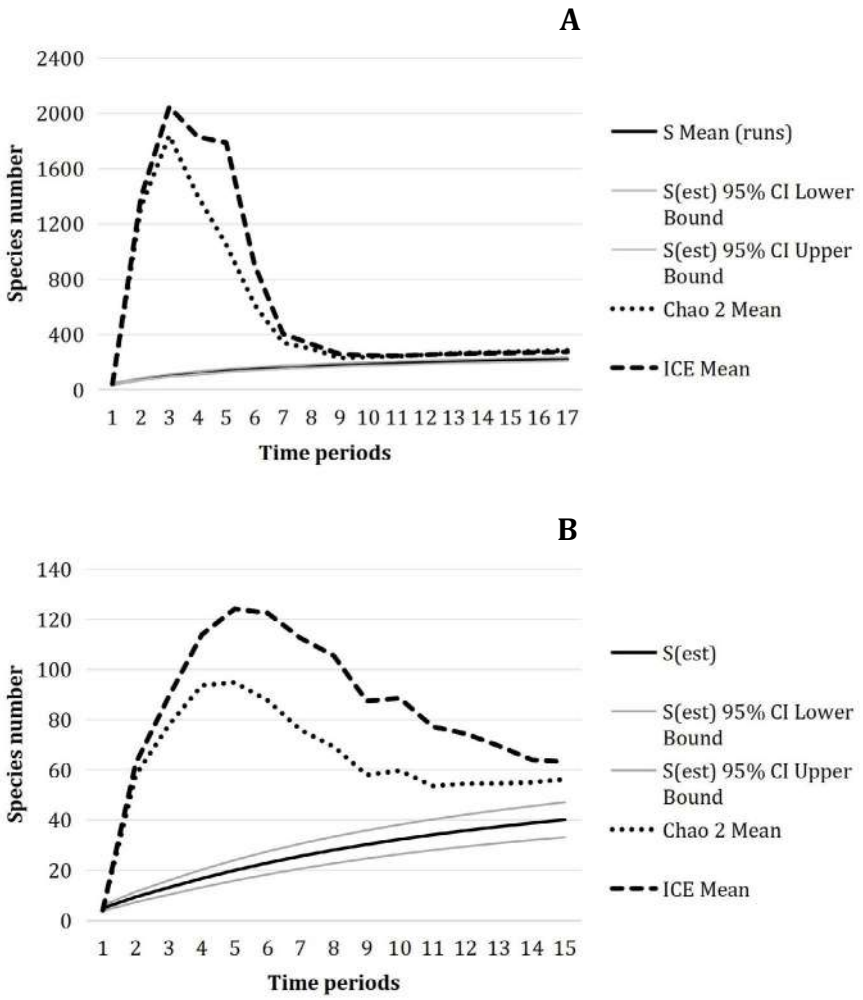
Since the first record of vertebrate species in the wetland (1976), the completeness of the inventory has evolved, as seen in the species accumulation curve (figure 3 A, page 7).

The vertebrate inventory has evolved since 1976. The non-parametric estimators ICE and Chao2 (Challaghan *et al.*, 2021) show growth in initial stages (1976-1988), followed by a stabilization. The high number of uniques in this period suggests that literature and collections were the main sources of new species (table 2, page 7).

Uniques decreased after the 2000s. This indicates diversity is approaching the asymptote. Although the decrease in uniqueness at the end of the curve suggests adequate detection of diversity, the estimated richness (ICE: 272 species, Chao2: 283 species) exceeds the observed richness (229 species). Suggesting that a dditional species may still be found. Observed plant species richness was 41. Nonparametric estimators suggested higher richness than observed. ICE values exceeded Chao2, but species accumulation curves for both exhibited high initial growth without reaching a clear asymptote (figure 3 B, page 7). The increasing average of unique species suggests incomplete sampling (table 2, page 7).

The local Moran's I statistic revealed positive spatial autocorrelation in the data distribution (Moran's I = 0.856, $p < 0.05$). This result indicates a marked tendency for similar values to cluster among neighboring sites. Sites with a higher records are geographically adjacent to other sites with high records, predominantly located in the upper-right quadrant (High-High) (figure 4 A, page 8).

Analogously, sites with lower values of species records also cluster spatially, concentrating in the lower-left quadrant (Low-Low). The distribution of species records was not random within the wetland but rather exhibits a distinctive pattern of spatial clustering. Records were higher in the wetland's lagoons (from north to south: Montenegro lagoon, Soria lagoon, La Paloma lagoon, and Viborón lagoon), while areas connecting the lagoons had fewer records (figure 4 B, page 8).



Estimated richness (S est) and confidence intervals and richness according to non-parametric estimators CHAO 2 and ICE over time.

Riqueza estimada (S est) con intervalos de confianza y riqueza según estimadores no paramétricos CHAO 2 e ICE a lo largo del tiempo.

Figure 3. Species accumulation curve for vertebrates (A) and plants (B) in the wetland system of the Leyes and Tulumaya streams.

Figura 3. Curva de acumulación de especies de vertebrados (A) y plantas (B) en el sistema de humedales de los arroyos Leyes y Tulumaya.

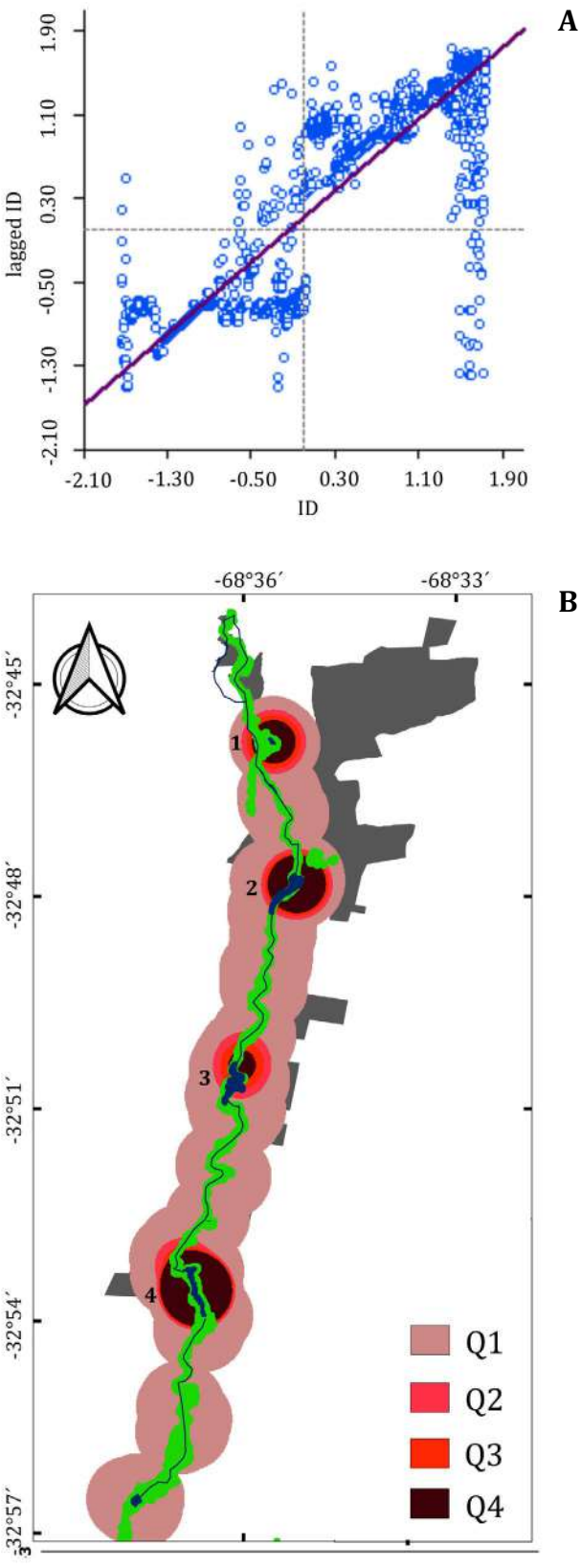
Table 2. Richness of vertebrate animals and plants observed in the Leyes and Tulumaya streams wetland system (S obs) and its upper (S (est) U) and lower (S (est) L) 95% confidence intervals, and estimated through the Chao2 and ICE indices.

Tabla 2. Riqueza de animales vertebrados y de plantas observadas en el sistema de humedales de los arroyos Leyes y Tulumaya (S obs) y sus intervalos superior (S (est) U) e inferior (S (est) L) del 95 % de confianza y estimada a través de los índices de Chao2 e ICE.

The number of unique and duplicated species in the database consisted of scientific collections, literature, and citizen science.

El número de especies únicas y duplicadas en la base de datos está compuesto por colecciones científicas, literatura y ciencia ciudadana.

Species richness	Vertebrate animals	Plants
S (obs)	229	41
S (est) 95 % L	206.04	33.01
S (est) 95 % U	233.96	46.99
Chao2 mean	283.06	56.12
ICE mean	272.59	63.11
Uniques	68	20
Duplicates	33	10



(A) The spatial distribution of vertebrate and plant records (B) in the wetland system of the Leyes and Tulumaya streams (Mendoza, Argentina). Occurrence records are presented cumulatively in quartiles (Q1 = 100%, Q2 = 75%, Q3 = 50%, Q4 = 25%). Montenegro lagoon (1), Soria lagoon (2), La Paloma lagoon (3), Viborón lagoon (4).

(A) Distribución espacial de los registros de vertebrados y plantas (B) en el sistema de humedales de los arroyos Leyes y Tulumaya (Mendoza, Argentina). Los registros de ocurrencia se presentan acumulados en cuartiles (Q1= 100 %, Q2=75%, Q3=50%, Q4=25 %). Laguna Montenegro (1), Laguna de Soria (2), Laguna de La Paloma (3), Laguna del Viborón (4).

Figure 4. Moran scatter plot showing the spatial autocorrelation of species records.

Figura 4. Diagrama de dispersión de Moran mostrando la autocorrelación espacial de los registros de especies.

Discussion

Comprehensive biodiversity inventories are crucial alongside conservation efforts. Many species vanish before they can be documented (Freitas & Gouveia, 2025). As expected in hypothesis 1, the results show increasing data from citizen scientists since the 2000s, contrasting with professional databases' peak in the 1970s-80s. A growing number of studies have yielded results consistent with our results, showing that in the last two to three decades, the global increase in data from citizen science platforms had become established as a valuable and effective resource for filling information gaps about biodiversity (Mason *et al*., 2025; Pocock *et al.*, 2017). Citizen science however does not replace systematic records or professional biological collections. Collections ensure standardized methods, taxonomic accuracy, long-term accessibility, and detailed contextual data (Suarez & Tsutsui, 2004).

Citizen contributions often focus on charismatic groups. Birds are well-represented because they are easily observed Rodriguez *et al.*, 2024. Our results also showed a predominance of bird records, contributed mainly in eBird and iNaturalist. We found no significant variation between citizen and professional databases. This suggests a natural abundance of birds for this desert wetland. Various studies indicate that opportunistic citizen science data exhibit uneven sampling over time and a bias towards charismatic taxa. Our results confirm this situation and highlight the need to implement strategies to mitigate data loss in future research. The adoption of standardized sampling protocols (Hochachka *et al*., 2012), the education and training of participants in the identification of less conspicuous taxa (Bonney et *al*., 2014), and the implementation of incentives to record underrepresented groups (Theobald *et al*., 2015) would consolidate the existing database.

In addition to the rapid accumulation of data, taxonomic bias is further exacerbated over time. Species identification from photographs, has limits by the impossibility of observing key taxonomic traits. Species-level identification in groups like small mammals, fish, or plants necessitates analysis of physical specimens. While citizen science offers new possibilities, data quality and identification challenges, reinforce the importance of expert validation and systematic collection of data (Miller & Edwards, 2016). Thus, presence of cryptic species (*e.g.*, Astyanax spp. (Pisces)) or species detectable only through specific capture techniques (*e.g.*, small rodents) in our study site, exemplifies the need for professional sampling and to expand scientific collections by adding more specimens.

In accordance with hypothesis 2, the spatial distribution of data exhibits distinctive patterns, reflecting the spatial heterogeneity of species records. Citizen science data often concentrate in accesible areas. This leaves gaps in remote or less-explored regions (Callaghan *et al.*, 2021). In turn, scientific collections and research projects can also reflect historical sampling biases, leading to uneven coverage resulting in geographical and taxonomic gaps, especially for less-studied regions or groups (Daru *et al.*, 2018). Our study revealed data clusters in four lagoon-riparian habitats and a lower number of records in the areas that connect them. Our results suggest that biodiversity hotspots reflect sampling effort rather than necessarily representing areas of greater species diversity. Skewed distribution we detected in records, as an indirect indicator of wetland accessibility, would allow these data to be used to investigate the consequences of advancing land use and habitat fragmentation that threaten species mobility in wetlands (Amezaga *et al.*, 2002). The lack of access and private ownership of the spaces that connect the lagoons and their riparian habitats could be a limiting factor resulting in the scarcity of records from citizen and research sources and would require consideration in future monitoring. Furthermore, providing spatially explicit data on species distribution in data-poor or data-free regions can greatly assist decision-makers in directing resources to priority research areas (Herrera-Lopera *et al.*, 2025). The lack of knowledge about the world's arid zone wetlands does not reflect their conservation importance. These key biodiversity areas support vulnerable populations and should be preserved due to their ecological significance and integrity (van Rees *et al.*, 2025). For example, the diversity of the bird group surveyed in our study from professional and non-professional sources reveals heterogeneity in the use of the wetland's temporal and spatial resources. This aspect has been pointed out by other previous studies that have highlighted the function of this wetland as refuge, nesting sites for migrants, and biological corridors to high-productivity areas (Tallei *et al.*, 2021).

The complementarity of professional and non-professional databases allows for the completion of species lists in the face of the urgent need for knowledge demanded by the management of wetlands in dry regions. As Callaghan *et al.* (2021) points out, redundancies and gaps in citizen science data (taxonomic, spatial, and temporal biases) also exist in professional scientific data. Our results demonstrate that the scarcity of data in certain taxonomic groups has not been covered by either citizen science or professionals, as is the case with underrepresented groups such as fish, amphibians, mammals, and, surprisingly, plants. Far from being an isolated case, our case study aligns with the patterns observed in global biodiversity databases, such as GBIF (Troudet *et al.*, 2017), as well as particularly in desert wetlands, where, for example, 60.4% of the freshwater taxa described are insects, while small mammals are largely ignored in biodiversity monitoring programs (Stephenson *et al.*, 2020).

Integrating academic and citizen science data offers the most accurate approach to understanding biodiversity by offsetting inherent biases (Díaz-Calafat *et al.*, 2024). While these data sources are largely independent operationally, citizen science observations are conceptually dependent on academic data through shared taxonomic frameworks, nomenclature, and species concepts developed by professional taxonomists. Acknowledging this linkage is essential for interpreting differences between datasets, as observed discrepancies reflect not only contrasting sampling strategies but also their integration within a common taxonomic foundation (Chandler *et al.*, 2017).Therefore, the conservation of freshwater ecosystems requires collaborative strategies between experts and citizens to expedite data collection, incorporate it into public databases to prioritize the conservation of their invaluable biodiversity and contribute to ecosystem stability under extreme conditions.

Conclusions

The results obtained in the present study support the recognition of the Leyes-Tulumaya streams wetland system as an area of significant importance for conservation. The high biodiversity documented in these habitats, immersed in an arid ecosystem, suggests considerable potential for the identification of taxa not yet recorded. Furthermore, it is evident that the contributions derived from citizen science initiatives constitute an invaluable tool for expanding the information available in understudied arid ecosystems, by complementing conventional research methods and addressing data deficits at both spatial and temporal levels. The information generated by this study provides an important basis for the development of management actions aimed at conserving the biodiversity of these wetlands.

References

Amezaga, J. M., Santamaría, L. & Green, A. J. (2002). Biotic wetland connectivity-supporting a new approach for wetland policy. *Acta Oecologica, 23*(3), 213-222. https://doi.org/10.1016/S1146-609X(02)01152-9

Anselin, L., Syabri, I., & Kho, Y. (2009). GeoDa: an introduction to spatial data analysis. In *Handbook of applied spatial analysis: Software tools, methods and applications*. Springer. 73-89.

Bonney, R., Shirk, J. L., Phillips, T. B., Wiggins, A., Ballard, H. L., Miller-Rushing, A. J., Parrish, J. K. (2014). Next steps for citizen science. *Science, 343*(6178), 1436-1437. https://doi.org/10.1126/science.1251554

Bowler, D. E., Bhandari, N., Repke, L., Beuthner, C., Callaghan, C. T., Eichenberg, D., Henle, K., Klenke, R., Ritcher, A., Jansen, F., Bruelheide, H. & Bonn, A. (2022). Decision-making of citizen scientists when recording species observations. *Scientific reports*, *12*(1), 11069. https://doi.org/10.1038/s41598-022-15218-2

Callaghan, C. T., Poore, A. G., Mesaglio, T., Moles, A. T., Nakagawa, S., Roberts, C., Rowley, J., Vergés, A., Wilshire, J. H., Cornwell, W. K. (2021). Three frontiers for the future of biodiversity research using citizen science data. *BioScience, 71*(1), 55-63. https://doi.org/10.1093/biosci/biaa131

Chandler, M., See, L., Copas, K., Bonde, A. M., López, B. C., Danielsen, F., Legind, J. K., Masinde, S., Miller-Rushing, A. J., Newman, G., Rosemartin, A., Turak, E. (2017). Contribution of citizen science towards international biodiversity monitoring. *Biological Conservation, 213,* 280-294. https://doi.org/10.1016/j.biocon.2016.09.004

Ciardullo, F. V, & Gennari, A. J. (2025). Agricultural Land Valuation-Hedonic Pricing and Geostatistical Advances: A State-of-the-Art Review. *Revista de la Facultad de Ciencias Agrarias. Universidad Nacional de Cuyo. 57*(2): 224-236. DOI: https://doi.org/10.48162/rev.39.185

Colwell, R. K., & Elsensohn, J. E. (2014). EstimateS turns 20: Statistical estimation of species richness and shared species from samples, with non-parametric extrapolation. *Ecography*, *37*(6), 609-613. https://doi.org/10.1111/ecog.00814

Contreras, J. R., & Fernandez, A. (1980). Ecología de la avifauna de la laguna del Viborón, Departamento Maipú, Provincia de Mendoza. *Revista del Museo de Historia Natural de San Rafael, 8*, 3-14.

Daru, B. H., Park, D. S., Primack, R. B., Willis, C. G., Barrington, D. S., Whitfeld, T. J, Seidler, T. G., Sweeney, P. W., Foster, D. R., Ellison, A. M., Davis, C. C. (2018). Widespread sampling biases in herbaria revealed from large-scale digitization. *New Phytologist*, *217*(2), 939-955. https://doi.org/10.1111/nph.14855

Díaz-Calafat, J., Jaume-Ramis, S., Soacha, K., Álvarez, A., & Piera, J. (2024). Revealing biases in insect observations: A comparative analysis between academic and citizen science data. *Plos one, 19*: e0305757. https://doi.org/10.1371/journal.pone.0305757

eBird. 2021. eBird: An online database of bird distribution and abundance [web application]. eBird, Cornell Lab of Ornithology, Ithaca, New York. Available: http://www.ebird.org.

Flora Argentina. Flora vascular de la República Argentina y del Cono Sur. http://www.floraargentina.edu.ar/

Freitas, H., & Gouveia, A. C. (2025). Biodiversity futures: Digital approaches to knowledge and conservation of biological diversity. *Web Ecology*, *25*(1), 29-37. https://doi.org/10.5194/we-25-29-2025

Galván, S., Barrientos, R., & Varela, S. (2022). No bird database is perfect: citizen science and professional datasets contain different and complementary biodiversity information. *Ardeola*, *69*(1), 97-114. https://doi.org/10.13157/arla.69.1.2022.ra6

García-Vega, D., & Newbold, T. (2020). Assessing the effects of land use on biodiversity in the world's drylands and Mediterranean environments. *Biodiversity and Conservation, 29*(2), 393-408. https://doi.org/10.1007/s1053

Gouraguine, A., Moranta, J., Ruiz-Frau, A., Hinz, H., Reñones, O., Ferse, S. C., Jompa, J., & Smith, D. J. (2019). Citizen science in data and resource-limited areas: A tool to detect long-term ecosystem changes. *PLoS One, 14*: e0210007. https://doi.org/10.1371/journal.pone.0210007

Herrera-Lopera, J. M., Solé, M., & Cultid-Medina, C. A. (2025). Mapping the Missing: Assessing Amphibian Sampling Completeness and Overlap With Global Protected Areas. *Ecology and Evolution, 15*: e71137. https://doi.org/10.1002/ece3.71137

Hochachka, W. M., Fink, D., Hutchinson, R. A., Sheldon, D., Wong, W. K., & Kelling, S. (2012). Data-intensive science applied to broad-scale citizen science. *Trends in Ecology & Evolution*, *27*(2), 130-137. https://doi:10.1016/j.tree.2011.11.006

iNaturalist. 2025. iNaturalist observations. https://www.inaturalist.org/observations

Klemann-Junior, L., Villegas Vallejos, M. A., Scherer-Neto, P., & Vitule, J. R. S. (2017). Traditional scientific data vs. uncoordinated citizen science effort: A review of the current status and comparison of data on avifauna in Southern Brazil. *PloS one, 12*: e0188819. https://doi.org/10.1371/journal.pone.0188819

MapBiomas Argentina - Colección 2 de la Serie anual de Mapas de Cobertura y Uso del Suelo de Argentina, https://argentina.mapbiomas.org/

Mason, B. M., Mesaglio, T., Heitmann, J. B., Chandler, M., Chowdhury, S., Gorta, S. B. J., Grattarola, F., Groom, Q., Hitchcock, C., Hoskins, L., Lowe, S. K., Marquis, M., Pernat, N., Shirey, V. Baasanmunkh, S., & Callaghan, C. T. (2025). iNaturalist accelerates biodiversity research. *BioScience, 75(11), 953-965.* https://doi.org/10.1093/biosci/biaf104

Miller, S. E., & Edwards, S. E. (2016). Citizen Science and Entomology: An Introduction to New Possibilities and Old Challenges. *Annals of the Entomological Society of America, 109,* 629-633.

Milton, S. J., & Dean, W. R. J. (2010). Plant invasions in arid areas: Special problems and solutions: a South African perspective. *Biological Invasions, 12*(12), 3935-3948. https://doi:10.1007/s10530-010-9820-x

Pocock, M. J., Tweddle, J. C., Savage, J., Robinson, L. D., & Roy, H. E. (2017). The diversity and evolution of ecological and environmental citizen science. *PloS one*, *12*(4), e0172579. https://doi.org/10.1371/journal.pone.0172579

Prieto, M. D. R., Rojas, J. F., Castrillejo, T. N., & Hernández, F. (2012). Procesos ambientales y construcción del territorio a partir de un estudio de caso: la ciénaga del Bermejo, oasis Norte de Mendoza 1810-1930. *Revista de Historia Americana y Argentina, 47,* 175-207.

Reis, R. E., Albert, J. S., Di Dario, F., Mincarone, M. M., Petry, P., & Rocha, L. A. (2016). Fish biodiversity and conservation in South America. *Journal of Fish Biology*, *89*(1), 12-47. https://doi:10.1111/jfb.13016

Rodriguez Forti, L., Passetti, A., Oliveira, T., Lima, J., Queiros, A., Lopes, M. A. D. F., & Szabo, J. K. (2024). Declining representation of imperiled Atlantic Forest birds in community-science datasets. *Perspectives in Ecology and Conservation, 22*(3), 277-287. https://doi.org/10.1016/j.pecon.2024.02.001

SAREM. Sociedad Argentina para el Estudio de los Mamíferos. https://www.sarem.org.ar/es/lista-de-mamiferos-de-argentina-2024/

Stephenson, P. J., Ntiamoa-Baidu, Y., & Simaika, J. P. (2020). The use of traditional and modern tools for monitoring wetlands biodiversity in Africa: Challenges and opportunities. *Frontiers in Environmental Science, 8*, 61. https://doi.org/10.3389/fenvs.2020.00061

Suarez, A. V., & Tsutsui, N. D. (2004). The value of museum collections for research and society. *BioScience*, *54*(1), 66-74. https://doi.org/10.1641/0006-3568(2004)054[0066:TVOMCF]2.0.CO;2

Tallei, E., Benavidez, A., Schaaf, A., Isola, P., & Zanotti, M. (2021). Seasonal dynamics of waterbirds from a relict wetland in the central Monte Desert, Argentina. *Neotropical Biology and Conservation, 16*(2), 333-349. https://doi:10.3897/neotropical.16.e61672

Theobald, E. J., Ettinger, A. K., Burgess, H. K., DeBey, L. B., Schmidt, N. R., Froehlich, H. E., Wagner, C., HilleRisLambers, J., Tewksbury, J., Harsch, M. A., Parrish, J. K. (2015). Global change and local solutions: Tapping the unrealized potential of citizen science for biodiversity research. *Biological Conservation, 181,* 236-2. https://doi.org/10.1016/j.biocon.2014.10.021

Troudet, J., Grandcolas, P., Blin, A., Vignes-Lebbe, R., & Legendre, F. (2017). Taxonomic bias in biodiversity data and societal preferences. *Scientific reports, 7*(1), 9132. https://doi.org/10.1038/s41598-017-09084-6

van Rees, C. B., Geist, J., & Arthington, A. H. (2025). Grasping at water: a gap-oriented approach to bridging shortfalls in freshwater biodiversity conservation. *Biological Reviews, 100*(5), 1970-1991. https://doi.org/10.1111/brv.70030

Wolf, S., Mahecha, M. D., Sabatini, F. M., Wirth, C., Bruelheide, H., Kattge, J., Moreno, A., Martínez, K. M., & Kattenborn, T. (2022). Citizen science plant observations encode global trait patterns. *Nature ecology & evolution, 6*(12), 1850-1859. https://doi.org/10.1038/s41559-022-01904-x

Zermoglio, P. F., Chapman, A. D., Wieczorek, J. R., Luna, M. C., Bloom, D. A. (2020). Georeferencing Quick Reference Guide. Copenhagen: GBIF Secretariat. https://doi.org/10.35035/e09p-h128

Acknowledgements

This work was financed with funds from CONICET Argentina (PIP 2022-2024 00318CO).

Social Welfare Effects of Water Security Improvements in Arid Regions: The Case of Mendoza, Argentina

Efectos sobre el bienestar social de mejoras en la seguridad hídrica en regiones áridas: el caso de Mendoza, Argentina

Verónica Inés Farreras González [1, 2*], Carolina Lauro [1], Laura Abraham [3], Pablo Federico Salvador [2]

Originales: *Recepción:* 03/06/2025- *Aceptación:* 26/09/2025

ABSTRACT

Water security is a critical challenge in Mendoza, Argentina, an arid region that faces rising water demand and uncertainty caused by climate change. Agriculture consumes 90% of the fresh water in the region, while vineyards occupy just over 60% of the cultivated area. This study estimates the social welfare effects of an improvement in water security achieved by reallocating water from vineyards to other uses. We used a multidisciplinary approach, applying benefit transfer to estimate social welfare changes and water footprint to quantify shifts in water availability. Our findings suggest that a water security policy in the Mendocinian Northern Oasis can result in an average 21-percentage-point increase in annual water availability for other uses. This equals an average household welfare gain of 17.43 US dollars per year (95% CI: 8.40-35.64) at 2024 prices over the next 30 years. This study offers a framework for regions worldwide facing similar challenges of water scarcity, increasing water demand, and climate change. Moreover, it can support the design of more informed water management strategies to ensure long-term water security.

Keywords

water security • social welfare • benefit transfer method • water footprint • water reallocation • arid regions • mendocinian northern oasis

https://doi.org/10.48162/rev.39.195

1 Instituto Argentino de Nivología, Glaciología y Ciencias Ambientales (CCT-CONICET-Mendoza). Av. Ruiz Leal s/n. Parque General San Martín. 5500 Mendoza. Argentina.

2 Universidad Nacional de Cuyo. Facultad de Ciencias Económicas. M5502JMA. Mendoza. Argentina. * vfarreras@mendoza-conicet.gob.ar

3 Universidad Nacional de Cuyo. Facultad de Ciencias Agrarias. Cátedra de Administración Rural. Almirante Brown 500. M5528AHB. Chacras de Coria. Mendoza. Argentina.

Licenses Creative Commons Attribution - Non Commercial - Share Alike

Resumen

La seguridad hídrica es un desafío crítico en Mendoza, Argentina, una región árida que enfrenta una creciente demanda de agua y la incertidumbre generada por el cambio climático. La agricultura consume el 90% del agua dulce mientras que los viñedos ocupan más del 60% de la superficie cultivada. Este estudio estima los efectos sobre el bienestar social de una mejora en la seguridad hídrica mediante la reasignación de agua de viñedos a otros usos. Aplicamos un enfoque multidisciplinario, usando transferencia de beneficios para estimar cambios en el bienestar social y la huella hídrica para cuantificar variaciones en la disponibilidad de agua. Nuestros resultados sugieren que una política de seguridad hídrica en el Oasis Norte Mendocino puede generar un aumento promedio de 21 puntos porcentuales en la disponibilidad anual de agua para otros usos, lo que equivale a una ganancia anual promedio en bienestar de 17,43 USD por hogar (IC 95%: 8,40-35,64), a precios de 2024, durante los próximos 30 años. Este estudio ofrece un marco replicable en otras regiones con desafíos similares de escasez y creciente demanda hídrica, contribuyendo al diseño de estrategias de gestión del agua más informadas para garantizar la seguridad hídrica a largo plazo.

Palabras claves

seguridad hídrica • bienestar social • método de la transferencia de beneficios • huella hídrica • reasignación del agua • regiones áridas • oasis norte de Mendoza

Introduction

On the eastern side of the Central Andes, mountain rivers flow through the Mendocinian landscapes, providing vital water resources to the region. As population and urban growth accelerate in an area where water demand is increasing, climate change is introducing greater uncertainty and variability in water availability (Lauro *et al.*, 2022). If climate models prove accurate and current water management policies remain unchanged, Mendoza -a historically arid region- may become even drier in coming decades (Rivera *et al.*, 2020). This scenario could exacerbate existing water scarcity, intensifying current challenges and threatening human welfare.

Currently, agriculture consumes approximately 90% of the fresh water in Mendoza (Duek, 2018). In this context, ensuring secure, sustainable and profitable food production while conserving water for alternative uses, including environmental preservation, requires improvements in agricultural water management efficiency (Pérez Blanco *et al.*, 2020).

In response, recent efforts in Mendoza have focused on aligning water distribution with crop water requirements to improve water management efficiency (Villodas *et al.*, 2023). However, previous studies, such as that of Morábito *et al.* (2005), had already addressed key aspects of this issue. Such efforts could enhance water security by conserving agricultural water to reallocate to other uses, potentially improving social welfare. However, the implications of these strategies for Mendocinian citizens' welfare remain unclear.

Understanding the social welfare effects of water security management can provide crucial insights. For instance, if society were to intervene to enhance water security, what would be the maximum it would invest in water systems matching crop requirements? Alternatively, what economic compensation might society consider offering if the reforms necessary to achieve water security result in unintended consequences for certain users? Addressing these questions highlights the importance of economic valuation in public policy decisions.

Economic valuation is widely applied to estimate the monetary value of changes in people's welfare resulting from ecological or environmental shifts (Carson *et al.*, 1993). However, to our knowledge, this approach has not been applied to assess how changes in water security -through increased water availability and reallocation- affect welfare. The closest studies have addressed the economic valuation of certain aspects of water security, the role of prices in managing water scarcity, and governance issues (Farreras *et al.*, 2017; Farreras and Abraham, 2020; Katz, 2016; Pellegrini *et al.*, 2023; Pérez Blanco *et al.*, 2020 and Zetland, 2021). Other related studies examine overexploitation, demand quantification

for various uses, and the impacts of climate variability on water supply (Castex *et al.*, 2015; Konapala *et al.*, 2020; Lauro *et al.*, 2021; Rivera *et al.*, 2021).

Motivated by the importance of economic valuation in decision-making, our study combines economic and hydrological data from 2010 to 2020 in a case study. Our main aim is to estimate the changes in citizens' welfare in the Mendocinian Northern Oasis due to improved water security. This improvement comes from reallocating water from vineyards -which cover just over 60% of the cultivated area- to industry, municipal areas, and non-viticultural crops. These changes are achieved while maintaining or even increasing grapevine production. The percentage of water allocated for the population is not included within the percentage of water available to other uses. This is because Mendoza Water Law 1884, which remains in effect, prioritises water supply for the population over other uses (DGI, 2016b).

This study provides a framework for regions worldwide facing similar water scarcity challenges. By assessing social welfare effects of an improvement in water security, it offers critical insights for decision-makers, policymakers, and resource managers in comparable global contexts. These insights support the design of more informed water management strategies, ensuring long-term water security.

Materials and Methods

Study Area

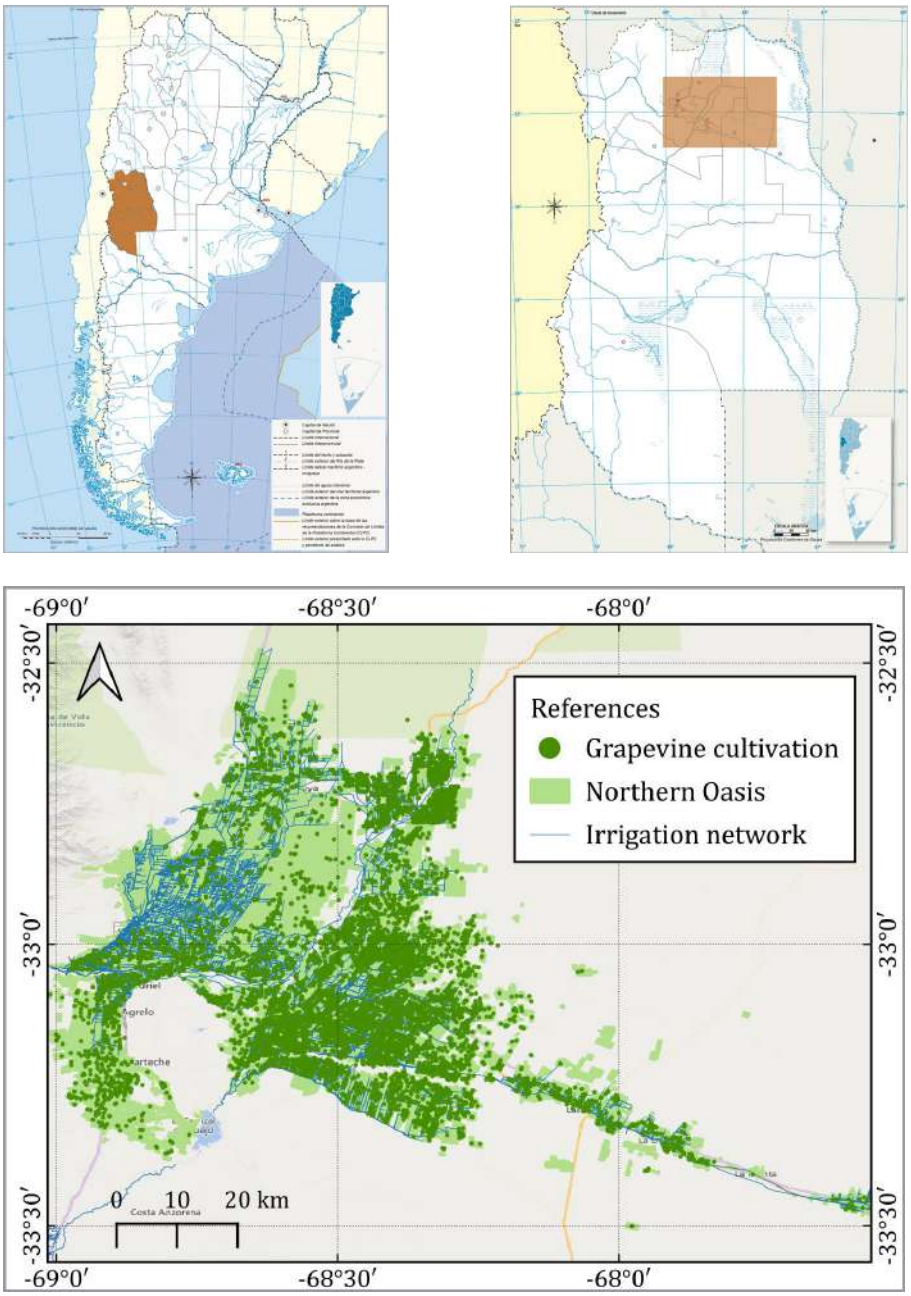
Because of the region's dry climate, most agricultural and urban areas in Mendoza are confined to small parts of the territory. These oases were established using an irrigation system of ditches and canals that carefully follows the topography of the region. This system makes the most of the water coming from mountain rivers, whose streamflow is the result of melting snow and Andean glaciers. It is also supported by groundwater boreholes (Monnet *et al.*, 2022; Morábito *et al.*, 2007). In Mendoza, the irrigation water is managed as a common resource through political and collective processes. Therefore, long-term water security depends on strong institutions and deep reforms (Zetland, 2021).

Between 2010 and 2020, mountain rivers in Mendoza experienced a significant hydrological deficit due to reduced snowfall associated with climate variability and climate change (Rivera *et al.*, 2021). Under different global warming scenarios, climate projections for components of the hydrological cycle in the Central Andes indicate further reductions in snowfall and river flows. These effects will undoubtedly impact the availability of water resources, highlighting the need for efficient water use (Castex *et al.*, 2015; Rivera *et al.*, 2020).

Our area of study, the Mendocinian Northern Oasis irrigated by the Mendoza and Tunuyán Inferior Rivers, is home to more than half of the province's total population (figure 1, page 4). This region is characterised by an arid and semi-arid climate. The average annual minimum and maximum temperatures are 11°C and 23°C, respectively, with an annual rainfall of 267 mm (SMN, 2024). The soils are classified as typical Torrifluvents with a loamy texture (INTA, 1990).

Although agricultural landscapes exhibit considerable crop diversity, grapevine crops -*Vitis vinifera*- are predominant, covering just over 60% of the cultivated area (INDEC, 2018). Among the diverse grape varieties grown, three dominate nearly 50% of the vineyards: Malbec (22.36%), Bonarda (11.75%), and Cereza (11.50%). The average annual grape production between 2008 and 2017 was approximately 1.1 million tonnes (INV, 2020).

Given the extensive area of vineyards in the oasis, the efficient use of water is crucial. However, around 75% of grape-growing farms rely on surface irrigation systems, one of the least water-efficient methods compared to pressurised systems (INDEC, 2018). Furthermore, the water distribution system disregards crop-specific requirements, delivering the same amount of water per hectare regardless of actual needs. Consequently, regional challenges related to water scarcity are further exacerbated by current management, increasing uncertainty in the availability at the oasis level and hindering efficient allocation. This underscores the need for sustainable and efficient water management to ensure long-term water security.



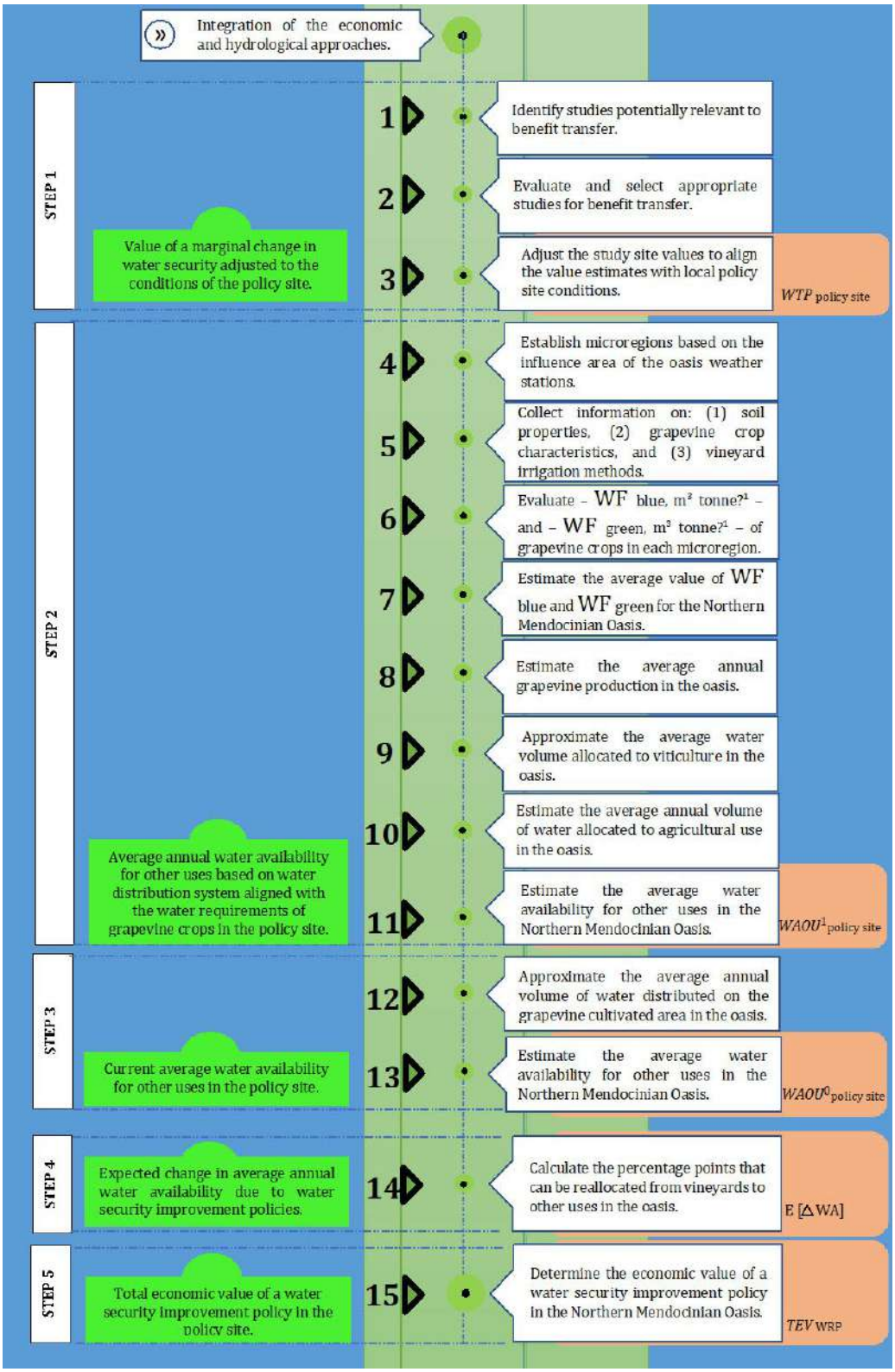
Source: Own elaboration based on data from the National Sanitary Registry of Agricultural Products (RENSPA), the Territorial Environmental Information System (SIAT), and the National Geographic Institute (IGN).

Fuente: Elaboración propia basada en datos del Registro Nacional Sanitario de Productores Agropecuarios (RENSPA), el Sistema de Información Ambiental Territorial (SIAT) y el Instituto Geográfico Nacional (IGN).

Figure 1. Farm units with grapevine cultivation in the Mendocinian Northern Oasis.

Figura 1. Explotaciones agropecuarias con cultivo de vid en el Oasis Norte de Mendoza.

In this study, we adopted a multidisciplinary approach. The benefit transfer method (BTM), widely used in the field of economics, was applied to extrapolate values obtained from a previous study site to a policy site. These values were used to predict welfare changes in the Mendocinian Northern Oasis under water security policies that would reallocate agricultural water to other uses. Additionally, a hydrological approach -specifically, the water footprint (WF) methodology proposed by Hoekstra *et al.* (2011)- was employed to estimate changes in water availability for these alternative uses. This integrated approach, used to estimate the total economic value (TEV) of a water security improvement policy, is summarised below and illustrated in figure 2 (page 5).



Source: Own elaboration.

Fuente: Elaboración propia.

Figure 2. Methodological framework integrating economic and hydrological approaches to estimate the TEV of a water security improvement policy.

Figura 2. Esquema metodológico que combina enfoques económico e hidrológico para estimar el valor económico total de una política de mejora de la seguridad hídrica.

First, we identified potential study sites to infer the change in citizens' welfare in the Mendocinian Northern Oasis resulting from a water security improvement policy. Since welfare is assumed to derive from the preferences satisfaction, it can be quantified using the willingness to pay (WTP). To enhance welfare change prediction accuracy, we adjusted the estimated WTP at the study site to align with the policy site conditions. The process is formally outlined as follows:

$$WTP_{policy\ site} = WTP_{study\ site} \times F \quad (1)$$

Where $WPT_{policy\ site}$ represents the value of a marginal change in water security -achieved through a policy that conserves agricultural water for reallocation to other uses- adjusted to the policy site's conditions. $WPT_{study\ site}$ refers to the value of a water security change estimated in one or more previous studies, which requires adjustment. F, the adjustment factor, accounts for these differences.

Factor *F* may represent different types of adjustments, depending on the similarity between the study and the policy sites. The degree of similarity is crucial in determining both the extent and the nature of these adjustments (Boutwell and Westra, 2013; Johnston *et al.*, 2021).

Second, we calculated the average annual water availability for other uses ($WAOU^{1}_{study\ site}$). This calculation was based on the water distribution system aligned with the water requirements of grapevine crops in the Mendocinian Northern Oasis. To achieve this, we first estimated the WF of grapevine crops and determined the required volume of water according to their specific needs. The steps involved in this estimation are outlined below.

Initially, specific data on rainfall, minimum and maximum temperatures, and relative humidity were collected from six weather stations in the Mendocinian Northern Oasis (2010-2020). Then, we used these data to divide the oasis into six climatic microregions based on each station's influence area. As a result, each microregion retains the name of its corresponding weather station.

The WF is an environmental indicator that accounts for the average volume of water required according to the water needs of crops, expressed per unit of product, *i.e.*, volume per unit of mass (m^3 $tonne^{-1}$).

The WF is calculated as the ratio between the volume of crop water use (CWU, m^3 ha^{-1}) throughout the entire crop growth period -from sprouting to harvest- and crop yield (Y, tonne ha^{-1}). The CWU is the volume of water required to compensate for a crop's evapotranspiration losses and to prevent crop water stress. This CWU can be divided into two components: the blue CWU -irrigation water- and the green CWU- effective rain.

For this research, we estimated the blue CWU (CWU_{blue}, m^3 ha^{-1}) and the green CWU (CWU_{green}, m^3 ha^{-1}) for each of the six microregions. The green and blue CWU were calculated from the accumulation of daily evapotranspiration (ET, mm day^{-1}) during the growing period, from sprouting to harvest. To perform these estimations, we used the CROPWAT program (FAO, 2024). For this, we incorporated meteorological data (table 1, page 7), grapevine crop parameters (Allen *et al.*, 1998; Civit *et al.*, 2018; Rodriguez *et al.*, 2000), and sandy loam soil properties estimated with the Soil Water Characteristics software (USDA, 2024).

Using the blue and green CWU values for each of the six microregions, the specific blue and green WF of vineyards at the microregion level was inferred separately from Equations (2) and (3) (page 7), respectively.

$$\mathrm{WF}_{blue\ i} = \frac{1}{2} \sum_{j=1}^{2} \left(\frac{\mathrm{CWU}_{blue\ i}}{\mathrm{Y}_i} \right)_j, \quad (2)$$

Where $WF_{blue\ i}$ represents the average blue WF in the *i*-th microregion, taking into account both surface and pressurised irrigation systems; $CWU_{blue\ i}$ is the blue CWU in the *i*-th microregion; Y_i is the yield per hectare in the *i*-th microregion; and j is the irrigation method, ranging from 1 to 2 (specifying, j = 1 surface and j =2 pressurised irrigation systems). The distinction in the irrigation systems was considered using various crop coefficients (Kc) to account for the differences in water requirements between surface (j = 1) and pressurised (j = 2) irrigation methods.

Table 1. Location of weather stations and average meteorological data (2010-2020).
Tabla 1. Ubicación de las estaciones meteorológicas y datos promedio (2010-2020).

Weather station	Altitude (m a. s. l.)	Latitude S	Longitude W	Rainfall (mm)	Minimum temperature (°C)	Maximum temperature (°C)	Relative humidity (%)
Russel	850	-33.01	-68.75	12.80	1.50	30.90	48.30
Junín	653	-33.12	-68.48	20.80	1.20	33.40	57.70
Medrano	708	-33.17	-68.64	22.00	8.80	24.60	45.60
Jocolí	900	-32.60	-68.60	11.40	1.30	33.60	44.40
Perdriel	960	-33.12	-68.91	23.70	-0.90	29.80	45.90
Las Violetas	960	-32.81	-68.60	13.20	1.30	31.60	46.40

Source: Own elaboration based on data from the Agriculture and Climate Contingencies Agency (DACC, 2021) of Mendoza province.
Fuente: Elaboración propia basada en datos de la Dirección de Agricultura y Contingencias Climáticas (DACC, 2021) de la provincia de Mendoza.

$$WF_{green\ i} = \frac{1}{2}\sum_{j=1}^{2}\left(\frac{CWU_{green\ i}}{Y_i}\right)_j, \quad (3)$$

Where $WF_{green\ i}$ represents the average green WF in the *i*-th microregion, taking into account both surface and pressurised irrigation systems; $CWU_{green\ i}$ is the green CWU in the *i*-th microregion; Y_i is the yield per hectare in the *i*-th microregion; and j is the irrigation method, ranging from 1 to 2 (specifying, *j* = 1surface and *j* =2 pressurised irrigation systems).

Then, the average values for both the blue and green WF were calculated at the oasis level, formally:

$$WF_{blue} = \frac{1}{6}\sum_{i=1}^{6} WF_{blue\ i}, \quad (4)$$

Where WF_{blue} represents the average blue WF at oasis level; $WF_{blue\ i}$ the blue WF in the *i*-th microregion; and *i* the microregion, ranging from 1 to 6. Each *i* represents a distinct microregion within the oasis.

$$WF_{green} = \frac{1}{6}\sum_{i=1}^{6} WF_{green\ i}, \quad (5)$$

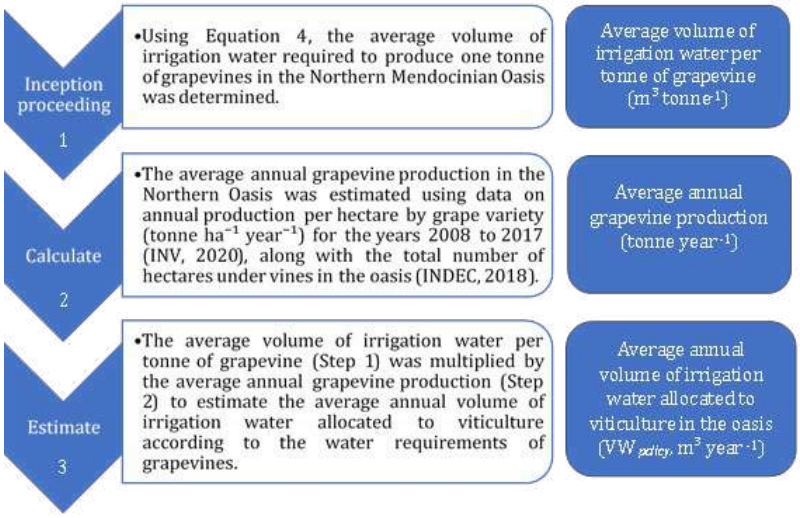
Where WF_{green} represents the average green WF at oasis level; $WF_{green\ i}$ the green WF in the *i*-th microregion; and *i* the microregion, ranging from 1 to 6. Each *i* represents a distinct microregion within the oasis.

Once the average values for the blue WF (m^3 $tonne^{-1}$) were calculated at the oasis level (Equation 4), the water availability for other uses ($WAOU^1_{policy\ site}$) in the oasis was derived from Equation (6):

$$WAOU^1_{policy\ site} = \{1 - [\frac{VW_{policy}}{AW}]\} \times 100, \quad (6)$$

Where $WAOU^1_{policy\ site}$ represents the average annual percentage of water availability for other uses that could be achieved at the policy site, if the water distribution system were aligned with the water requirements of grapevine crops; VW_{policy} corresponds to the average annual volume of water allocated to viticulture in the oasis (m^3 $year^{-1}$); and AW (agricultural water) is the average annual volume of water allocated to agricultural use (m^3 $year^{-1}$).

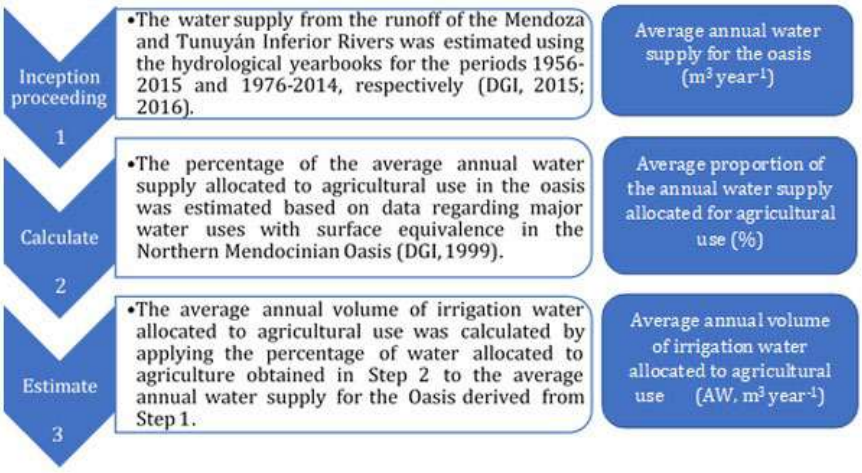
Figure 3 and figure 4, illustrate the respective processes used to estimate the average annual irrigation water volumes allocated to viticulture (VW_{policy}, m^3 $year^{-1}$) and agriculture (AW, m^3 $year^{-1}$) in the oasis.



Source: Own elaboration.
Fuente: Elaboración propia.

Figure 3. Process for estimating the average annual volume of irrigation water allocated to viticulture in the Mendocinian Northern Oasis.

Figura 3. Proceso para estimar el volumen promedio anual de agua de riego asignado a la viticultura en el Oasis Norte de Mendoza.



Source: Own elaboration.
Fuente: Elaboración propia.

Figure 4. Process for estimating the average annual volume of irrigation water allocated for agricultural use in the Mendocinian Northern Oasis.

Figura 4. Proceso para estimar el volumen promedio anual de agua de riego asignado al uso agrícola en el Oasis Norte de Mendoza.

Next, we calculated the current average annual water availability for other uses in the policy site, formally:

$$WAOU^{0}_{policy\ site} = \left\{1 - \left[\frac{VW_{current}}{\text{AW}}\right]\right\} \times 100, \quad (7)$$

Where $WAOU^{0}_{policy\ site}$ represents the average annual percentage of current water availability for other uses in the policy site; $VW_{current}$ (Equation 8) is the current average annual volume of water allocated to viticulture (m^3 $year^{-1}$); and AW is the average annual volume of water allocated to agricultural use (m^3 $year^{-1}$) in the oasis.

$$VW_{current} = \left(\frac{AW}{A_{agr.}}\right) A_{vit.}, \quad (8)$$

Where $VW_{current}$ represents the current average annual volume of water allocated to viticulture in the policy site; AW is the average annual volume of water allocated to agricultural use (m^3 $year^{-1}$); Avit. (ha) is the area under vines in the oasis; and Aagr. (ha) is the total cultivated area in the oasis (INDEC, 2018).

We then calculated the percentage points that could be reallocated from vineyards to other uses in the oasis. This was based on increased water availability and its subsequent reallocation following the implementation of a water security improvement policy (Equation 9).

$$\text{E}\left[\Delta\, WA\right] = WAOU^{1}_{policy\ site} - WAOU^{0}_{policy\ site}, \quad (9)$$

Where $E\ [\Delta WA]$ denotes the expected change in average annual water availability resulting from the water security improvement policy; $WAOU^{1}_{policy\ site}$ is the average annual percentage of water availability for other uses that could be achieved in the policy site if the water distribution system were aligned with the water requirements of grapevine crops; and $WAOU^{0}_{policy\ sity}$ is the average annual percentage of current water availability for other uses in the policy site.

Finally, we estimated the TEV of a water security improvement policy in the Mendocinian Northern Oasis by applying Equation (10):

$$\text{TEV}_{WRP} = \text{E}\left[\Delta\, WA\right] \times WTP_{policy\ site}, \quad (10)$$

Where $E\ [\Delta WA]$ is the expected change in average annual water availability resulting from water security improvement policies; and $WTP_{policy\ site}$ is the value of a marginal change in water security -achieved through a policy that conserves agricultural water for reallocation to other uses- adjusted to the conditions of the policy site.

Results and Discussion

The results follow five methodological stages to predict the TEV of a water security improvement policy in the Mendocinian Northern Oasis (figure 2, page 5). The practical implications of these results are discussed in the context of water security management, focusing on efficient agricultural water allocation and conservation strategies.

Value of a Marginal Change in Water Security Adjusted to the Conditions of the Policy Site

According to Rosenberger and Loomis (2003) and Johnston *et al*. (2021), the study site was selected for its similarity to the policy site in four categories. These categories are: (i) socio-economic characteristics, (ii) biophysical conditions, (iii) proposed environmental changes, and (iv) economic valuation objectives.

A comprehensive literature review was then conducted to identify potential study sites that met these criteria. This process led to the selection of the study by Farreras and Abraham (2020). They estimated the welfare effects of adapting viticultural management practices to climate change in the Mendocinian Northern Oasis. The study applied the discrete choice experiment (DCE) method, a valuation technique consistent with welfare economic theory (Bennett and Blamey, 2001). This method relies on society's stated maximum WTP to avoid or accept a marginal change in the quantity or quality of an environmental good's attribute. This is achieved through the design of hypothetical markets presented via questionnaires. Additionally, the use of the DCE at the study site allows for the identification of marginal values for specific environmental attributes and has been shown to perform better than other economic valuation methods when benefit transfers are required (Hanley *et al.*, 1998).

Surveys at the study site were conducted in spring 2017. A representative sample of citizens of the Northern Oasis of Mendoza was interviewed. The sample consisted of randomly selected individuals aged between 24 and 80 years, all residing in cities with populations of over 10,000 inhabitants. Approximately 90% of those approached agreed to be interviewed. The interviews were conducted face-to-face in the respondents' homes, resulting in 678 valid observations.

Environmental Attributes and Levels Used at the Study Site

The study valued three attributes related to adapting vineyard practices to climate change in Mendoza: (1) water availability for other uses, (2) use of chemical fertilisers, and (3) use and conservation of biodiversity. Given the objective of this study, the primary attribute of interest is the availability of water for other uses.

The attribute had four levels-41% (business-as-usual, BAU), 53%, 65%, and 76%. These represent the average water available in 30 years for other uses: industry, public areas (green spaces, urban trees), and irrigation of non-vineyard crops. These levels ranged from the value expected under a BAU scenario to values above the BAU level. The BAU level shows the situation projected in 30 years from now under non-adaptive management practices in Mendocinian vineyards. Other levels show potential outcomes from adapting viticultural practices to climate change.

Marginal Benefit or Value to Be Transferred

The study by Farreras and Abraham (2020) estimated that a representative citizen of the Mendocinian Northern Oasis was, on average, willing to pay 13.05 (95% CI: 6.24-27.28) Argentine pesos [0.74 (95% CI: 0.35-1.55) US dollars] per household annually for an additional percentage point in water availability for other uses, at 2017 prices subject to adjustment for inflation, over the next 30 years. Figures in parentheses indicate the limits of the 95% confidence interval.

Adjustment Process

We adjusted the estimated values at the study site to align with the conditions of the policy site, following the methodology of Rolfe *et al.* (2015). Their study demonstrated that transferring values between similar sites requires straightforward adjustments. Since the study and policy sites coincide, inflation was the adjustment factor used to align information and ensure accurate value estimates for the policy site.

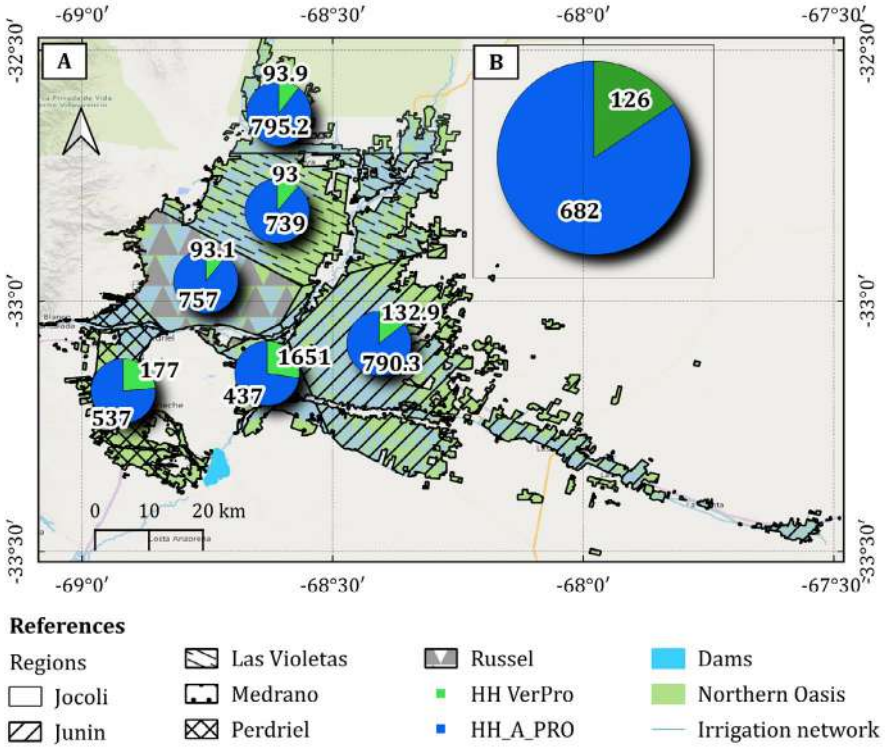
Adjustment for Inflation

The estimated values at the study site were adjusted using the Consumer Price Index (CPI). This adjustment accounts for inflation between the interview period (September 2017) and November 2024 (Equation 1, page 6). The accumulated inflation over this period was 6,393% (INDEC, 2024). Therefore, a representative citizen of the Mendocinian Northern Oasis is

estimated to be, on average, willing to pay 847.34 (95% CI: 405.16-1,771.29) Argentine pesos [0.83 (95% CI: 0.40-1.74) US dollars] per household annually for an improvement in water security equivalent to an additional percentage point in water availability for other uses, at 2024 prices over the next 30 years. Average exchange rate in November 2024: 1 US dollar equals 1,019.56 Argentinean pesos.

Average Annual Water Availability for Other Uses Based on a Water Distribution System Aligned with the Water Requirements of Grapevine Crops in the Policy Site

Using meteorological, grapevine, and soil data, we estimated the blue and green WF of vineyards at the microregional level by applying Equation [2], (page 6) and Equation [3], (page 7), respectively. Figure 5A, depicts the blue and green WF for each of the six microregions within the Northern Oasis of Mendoza.



Source: Own elaboration.
Fuente: Elaboración propia.

Figure 5. Blue and green WF (m^3 $tonne^{-1}$) (A) for each of the six microregions and (B) for the Mendocinian Northern Oasis.

Figura 5. Huella hídrica azul y verde (m^3 $tonelada^{-1}$) (A) para cada una de las seis microrregiones y (B) para el Oasis Norte de Mendoza.

Given that the crop requires more water than is provided by rainfall, the deficit is compensated through irrigation. As a result, the blue WF exceeded the green WF across all microregions. The Jocolí microregion had the highest blue WF, at 795 m^3 $tonne^{-1}$, while the Medrano microregion had the lowest, at 437 m^3 $tonne^{-1}$.

The variations in WF across microregions result from a variety of factors, including local climate conditions and agricultural management practices. This information may be particularly useful for stakeholders involved in promoting efficient water allocation and conservation strategies. For instance, a decision-maker may prioritise water distribution based on specific crops' water requirements. The analysis of the WF enables the design of distribution schemes tailored to these local needs. In this context, for the same crop and irrigation system, microregions with higher WF need more water than those with lower footprints. If resource distribution aligns with irrigation water demand, it becomes possible

to reduce water deliveries in certain microregions without compromising agricultural productivity or associated ecosystems. This approach increases water availability at the oasis scale, enabling more efficient resource reallocation and strengthening long-term water security without sacrificing productivity or ecosystem integrity (Grafton *et al.*, 2018).

Meanwhile, the Mendocinian Northern Oasis averages 682 m^3/tonne blue WF (Equation 4, page 7) and 126 m^3/tonne green WF (Equation 5, page 5), as shown in figure 5B (page 11). This highlights the dominance of irrigation water over effective rainfall in meeting the vineyard water requirements in this region.

These results partially align with previous findings in the literature. For example, Civit *et al.* (2018) estimated that the blue WF for the most important varietals in the five wine-producing regions of Mendoza ranges from 540.53 m^3 $tonne^{-1}$ to 1,020.03 m^3 $tonne^{-1}$. On a global scale, Mekonnen and Hoekstra (2011) reported an average blue WF of 608 m^3 $tonne^{-1}$ in viticulture production for the period 1996-2005. Similarly, Herath *et al.* (2013) documented blue WFs of 601 m^3 $tonne^{-1}$ and 611 m^3 $tonne^{-1}$ in vineyards in the Gisborne and Marlborough regions of New Zealand, respectively. These findings emphasise reliance on irrigation in viticulture. About 84% of vineyard water needs were met through irrigation during the analysed period. This underscores the need for sustainable water resource management.

We estimated that, under a water distribution system aligned with the grapevine crops' water requirements, 69% of water could, on average, be available annually for other uses (Equation 6, page 7; figure 6A). This estimate is based on the average annual water volumes allocated to viticulture (figure 3, page 8) and agriculture (figure 4, page 8).

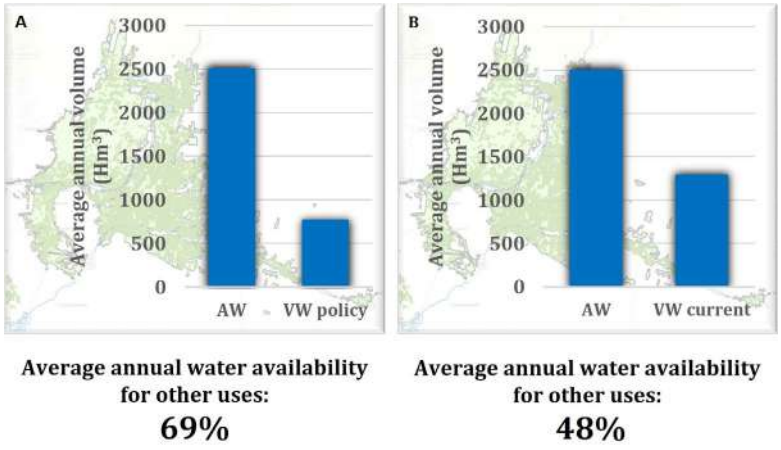


Figure 6. Average annual percentage of water availability for other uses in the Mendocinian Northern Oasis estimated under (A) the implementation of a water security improvement policy and (B) the current water management.

Figura 6. Porcentaje promedio anual de disponibilidad hídrica para otros usos en el Oasis Norte de Mendoza estimado bajo (A) la implementación de una política de mejora de la seguridad hídrica y (B) la gestión hídrica actual.

Current Average Water Availability for Other Uses in the Policy Site

We estimated that, on average, 48% of water is currently available annually for other uses in the Mendocinian Northern Oasis (Equation 7, page 9; figure 6B). This estimate is based on current average annual water volumes allocated to viticulture (Equation 8, page 9) and agriculture (figure 4, page 8).

Expected Change in Average Annual Water Availability Due to a Water Security Improvement Policy

Next, we estimated the average percentage points of irrigation water that could be reallocated from vineyards to other uses under a water security improvement policy (Equation 9, page 9). The average reallocation was estimated at 21 percentage points. This volume could be redistributed to industry, municipal spaces (green areas, urban trees), and irrigation of non-viticultural crops.

Total Economic Value of a Water Security Improvement Policy in the Policy Site

Assuming unitary price elasticity, the TEV of reallocating an average of 21 percentage points of water from vineyards to other uses can be estimated. This is calculated by multiplying the 21-percentage-point change by the value of a one-percentage-point increase in water availability for other uses.

Applying Equation [10] (page 9), a water security policy that increases average annual water availability for other uses by 21 percentage points corresponds to an average household welfare gain of ARS 17,794.14 [USD 17.43] per year at 2024 prices (95% CI: ARS 8,508.36-37,197.09 [USD 8.40-36.54]) over the next 30 years.

Direct comparisons are difficult due to differing units used to estimate WTP (*e.g.*, per hectare, time horizon). However, this finding aligns with Pellegrini *et al.* (2023), who estimated social welfare changes associated with improvements in specific water security components. Based on their literature review, they reported households' willingness to pay between 9.68 and 209.66 US dollars per year for water purification services. For biodiversity habitat conservation, willingness to pay ranged from 17.23 to 106.40 US dollars. For cultural services such as aesthetic and recreational benefits, willingness to pay ranged from 17.23 to 156.99 US dollars. WTP in the study of Pellegrini *et al.* (2023) are expressed in Euros. We expressed them in US dollars using the average 2023 daily Euro - USD exchange rate published, 1.08268509, by www.macrotrends.net

Our study adopts a comprehensive approach to value a water security improvement policy, explicitly addressing water reallocation to alternative uses. This analysis helps fill a gap by providing a broader perspective that accounts for welfare associated with overall water security enhancement.

Conclusions

Globally, many regions face severe water scarcity, worsened by global changes increasing uncertainty and variability in water availability. In this context, a paradigm shift in water resource management is crucial. Aligning water allocation with crop requirements improves management efficiency and strengthens long-term water security, while protecting agricultural productivity and the integrity of ecosystems. Understanding the benefits of such strategies is essential for their successful implementation. This study addresses this gap by estimating the changes in social welfare resulting from improved water security.

A distinctive contribution of our study lies in the estimation of social welfare changes resulting from water security improvements, expressed in monetary terms. This information is particularly valuable for decision-makers, policymakers, and natural resource managers. For example, with a fixed budget for a water security improvement policy, decision-makers can evaluate whether the costs outweigh the monetary benefits provided to citizens. Similarly, this estimation allows policymakers to allocate resources efficiently and justify major water security reforms to stakeholders and the public by emphasising socio-economic benefits.

Our study found that the TEV of a water security improvement policy in the Northern Mendocinian Oasis -resulting in a 21-percentage-point average increase in the annual water availability for other uses- is equivalent to an average household welfare gain of ARS 17,794.14 [USD 17.43] per year at 2024 prices (95% CI: ARS 8,508.36-37,197.09 [USD 8.40-36.54]) over the next 30 years.

These findings offer decision-makers a robust basis for assessing the costs and benefits of investments in water security, thereby enabling more informed public policy decisions.

Following the guidance of experts in BTM, the method was carefully applied to ensure a state-of-the-art implementation. Recognising that transfer errors often arise from differences between study and policy sites, we prioritised ensuring similarity across four categories: (i) socio-economic characteristics, (ii) biophysical conditions, (iii) proposed environmental changes, and (iv) economic valuation objectives. This approach aimed to minimise transfer errors and establish benefit transfer as a robust tool for obtaining the TEV of a water security improvement policy.

Nevertheless, data limitations led to restrictive assumptions. For instance, the estimation of water reallocation from vineyards to other uses relied solely on surface water data. This may have resulted in an underestimation of the policy's TEV. Similarly, the WF estimation of vineyards did not account for inefficiencies in the irrigation system, potentially leading to an overestimation of the policy's TEV. Therefore, our results should be interpreted as approximations, within the context of these limitations.

In summary, this study demonstrates that social welfare is expected to increase through the implementation of water security improvement policies. It provides a framework for regions worldwide where irrigation water is a common resource facing challenges like water scarcity, rising water demand, and climate change. By assessing social welfare effects of an improvement in water security, it offers critical insights for decision-makers, policymakers, and resource managers in comparable global contexts. These insights support the design of more informed water management strategies, ensuring long-term water security.

References

Allen, R. G., Pereira, L. S., Raes, D. & Smith, M. (1998). *Crop evapotranspiration: Guidelines for computing crop water requirements* (FAO Irrigation and Drainage Paper N° 56). Food and Agriculture Organization of the United Nations.

Bennett, J. & Blamey, R. (2001). *The choice modelling approach to environmental valuation* (p. 269). Edward Elgar Publishing.

Boutwell, J. L. & Westra, J. V. (2013). Benefit transfer: A review of methodologies and challenges. *Resources, 2*(4), 517-527. https://doi.org/10.3390/resources2040517

Carson, R. T., Carson, N., Alberini, A., Flores, N. & Wright, J. (1993). *A bibliography of contingent valuation studies and papers*. Natural Resources Damage Assessment.

Castex, V., Morán, E. & Beniston, M. (2015). Water availability, use and governance in the wine producing region of Mendoza, Argentina. *Environmental Science & Policy, 48*, 1-8. https://doi.org/10.1016/j.envsci.2014.12.008

Civit, B., Piastrellini, R., Curadelli, S. & Arena, A. P. (2018). The water consumed in the production of grapes for vinification (*Vitis vinifera*): Mapping the blue and green water footprint. *Ecological Indicators, 85*, 236-243.

Dirección de Agricultura y Contingencias Climáticas. (2021). *Informe técnico* [Dataset].

Departamento General de Irrigación. (1999). *Plan hídrico para la provincia de Mendoza. Bases y propuestas para el consenso de una política de estado*. Gobierno de Mendoza.

Departamento General de Irrigación. (2015). *Balance hídrico río Tunuyán Inferior* (Cap. 5, p. 129).

Departamento General de Irrigación. (2016a). *Balance hídrico río Mendoza* (Cap. 4, p. 128).

Departamento General de Irrigación. (2016b). *Aquabook*. http://aquabook.agua.gob.ar/

Duek, A. E. (2018). Escenarios de uso sostenible del recurso hídrico en el sector agrícola de Mendoza. *4° Encuentro de Investigadores en Formación en Recursos Hídricos*, 11. https://www.ina.gov.ar/ifrh-2018/pdf/IFRH_2018_paper_4.pdf

Farreras, V., Riera, P., & Salvador, P. F. (2017). Environmental valuation with periodical payments in high-inflation economies: An Argentinean case study. *Ecological Economics, 138*, 56-63. https://doi.org/10.1016/j.ecolecon.2017.03.028

Farreras, V., & Abraham, L. (2020). Valuation of viticultural adaptation to climate change in vineyards: A discrete choice experiment to prioritize trade-offs perceived by citizens. *Wine Economics and Policy, 9*(2), 99-112.

Food and Agriculture Organization of the United Nations. (2024). *CROPWAT 8.0 for Windows* [Computer software]. https://www.fao.org/land-water/databases-and-software/cropwat/en/

Grafton, R. Q., Williams, J., Perry, C. J., Molle, F., Ringler, C., Steduto, P., Udall, B., Wheeler, S. A., Wang, Y., Garrick, D., & Allen, R. G. (2018). The paradox of irrigation efficiency. *Science, 351,* 748-750.

Hanley, N., Wright, R. E., & Adamowicz, V. (1998). Using choice experiments to value the environment. *Environmental and Resource Economics, 11*: 413-428. https://doi.org/10.1023/A:1008287310583

Herath, I., Green, S., Singh, R., Horne, D., van der Zijpp, S., & Clothier, B. (2013). Water footprinting of agricultural products: A hydrological assessment for the water footprint of New Zealand's wines. *Journal of Cleaner Production, 41,* 232-243.

Hoekstra, A. Y., Chapagain, A. K., Aldaya, M. M., & Mekonnen, M. M. (2011). *The water footprint assessment manual: Setting the global standard*. Routledge. https://waterfootprint.org/resources/TheWaterFootprintAssessmentManual_English.pdf

Instituto Nacional de Estadísticas y Censo. (2018). *Censo Nacional Agropecuario 2018. Cuadros estadísticos*. https://www.indec.gob.ar/indec/web/Nivel4-Tema-3-8-87

Instituto Nacional de Estadísticas y Censo. (2024). [Dataset]. https://www.indec.gob.ar/ftp/cuadros/economia/sh_ipc_12_24.xls

Instituto Nacional de Tecnología Agropecuaria. (1990). *Atlas de Suelos de la República Argentina*.

Instituto Nacional de Vitivinicultura. (2020). *Relevamiento Vitivinícola Argentino-Sector Primario*. https://www.argentina.gob.ar/inv/vinos/estadisticas/regiones-vitivinicolas

Johnston, R. J., Boyle, K. J., Loureiro, M. L., Navrud, S., & Rolfe, J. (2021). Guidance to enhance the validity and credibility of environmental benefit transfers. *Environmental and Resource Economics, 79,* 575-624. https://doi.org/10.1007/s10640-021-00574-w

Katz, D. (2016). Undermining demand management with supply management: Moral hazard in Israeli water policies. *Water, 8*(4), 159. https://doi.org/10.3390/w8040159

Konapala, G., Mishra, A. K., Wada, Y., & Mann, M. E. (2020). Climate change will affect global water availability through compounding changes in seasonal precipitation and evaporation. *Nature Communications, 11,* 3044. https://doi.org/10.1038/s41467-020-16757-w

Lauro, C., Vich, A. I. J., Otta, S., Moreiras, S. M., Vaccarino, E., & Bastidas, L. (2021). Recursos hídricos superficiales de la vertiente oriental de los Andes Centrales (28°-37°S) en contexto de variabilidad hidroclimática. *Boletín de Estudios Geográficos, 116*, 45-71.

Lauro, C., Vich, A. I. J., Rivera, A., Otta, S., Moreiras, S. M., Bastidas, L., & Vaccarino, E. (2022). Patrones de variabilidad hidroclimática en los Andes Centrales (30-37°S) de Argentina. *Geoacta, 44*(1), 1-22.

Mekonnen, M., & Hoekstra, A. Y. (2011). The green, blue and grey water footprint of crops and derived crop products. *Hydrology and Earth System Sciences, 15*(5), 1577-1600. https://doi.org/10.5194/hess-15-1577-2011

Monnet, M., Vignola, R., & Aliotta, Y. (2022). Smallholders' water management decisions in the face of water scarcity from a socio-cognitive perspective: Case study of viticulture in Mendoza. *Agronomy, 12*(11), 2868. https://doi.org/10.3390/agronomy12112868

Morábito, J., Mirábile, C., Salatino, S., Pizzuolo, P., Chambouleyron, J., & Fasciolo, G. (2005). *Eficiencia de riego actual y potencial en el área regadía del río Mendoza*. https://repositorio.ina.gob.ar/items/cd398433-7fa6-4b9c-adb9-0b7ebc2dcb97

Morábito, J., Mirábile, C., & Salatino, S. (2007). Eficiencia del riego superficial, actual y potencial, en el área de regadío del río Mendoza (Argentina). *Ingeniería del Agua, 14*, 199-214. https://doi.org/10.4995/ia.2007.2912

Pellegrini, E., Dalmazzone, S., Fasolino, N. G., Frontuto, V., Gizzi, P., Luppi, F., Moroni, F., Raggi, M., Zanni, G., & Viaggi, D. (2023). Economic analysis under the Water Framework Directive: The state of the art and way forward. *Water, 15*(23), 4128. https://doi.org/10.3390/w15234128

Pérez Blanco, C. D., Hrast Essenfelder, A., & Perry, C. (2020). Irrigation technology and water conservation: A review of the theory and evidence. *Review of Environmental Economics and Policy, 14*(2).

Rivera, J. A., Naranjo Tamayo, E., & Viale, M. (2020). Water resources change in Central-Western Argentina under the Paris Agreement warming targets. *Frontiers in Climate, 2*, 587126. https://doi.org/10.3389/fclim.2020.587126

Rivera, J., Lauro, C., & Otta, S. (2021). Cuantificación del déficit hidrológico reciente en la región de Cuyo a partir de indicadores de caudales bajos. *Boletín de Estudios Geográficos, 116*, 23-44.

Rodríguez, J., De la Iglesia, F., & Ocvirk, M. (2000). Fenología de cultivares de vid (*Vitis vinífera* L.) en Luján de Cuyo. *Revista de la Facultad de Ciencias Agrarias, Universidad Nacional de Cuyo, 32*(2), 15-24. http://bdigital. uncu.edu.ar/11001

Rolfe, J., Windle, J., & Johnston, R. J. (2015). Applying benefit transfer with limited data: Unit value transfers in practice. In R. J. Johnston, J. Rolfe, R. S. Rosenberger, & R. Brouwer (Eds.), *Benefit transfer of environmental and resource values: A guide for researchers and practitioners* (p. 381-398). Springer.

Rosenberger, R., & Loomis, J. (2003). Benefit transfer. In P. Champ, K. Boyle, & T. Brown (Eds.), *A primer on nonmarket valuation* (p. 445-482). Kluwer Academic Publishers.

Servicio Meteorológico Nacional. (2024). *Estadísticas climatológicas normales período 1991-2020*. https://www.smn.gob.ar/descarga-de-datos

United States Department of Agriculture. (2024). *Soil water characteristics* (Version 6.02.72) [Computer software]. https://www.ars.usda.gov/research/software/download/?softwareid=492&modecode=80-42-05-10

Villodas, R., Andino, M., Baduí, M. T., & Marinelli, S. (2023). Distribución de riego en función de la demanda-cuenta de agua. *XXVII Congreso Nacional del Agua*, Buenos Aires, Argentina.

Zetland, D. (2021). The role of prices in managing water scarcity. Water Security, 12, 100081. https://doi.org/10.1016/j.wasec.2020.100081

Acknowledgements

We sincerely thank the two anonymous referees for their valuable contributions, which have greatly improved the quality of this article. We also acknowledge the support of the Secretaría de Investigación, Internacionales y Posgrado (SIIP) at Universidad Nacional de Cuyo through project SIIP: 06/D006-T1.

Determinants of Agricultural Land Prices in the Mendoza River Basin: A Spatial Hedonic Analysis with Emphasis on Irrigation Water

Determinantes del precio de la tierra agrícola en la Cuenca del Río Mendoza: un análisis hedónico espacial con énfasis en el agua de riego

Vanina Fabiana Ciardullo [1*], Alejandro Juan Gennari [1], María Eugenia Martinez Fagliano [1], Patricia Lilian Winter [1], Juan Matías Elissonde [2]

Originales: *Recepción:* 24/09/2025 - *Aceptación:* 16/12/2025

ABSTRACT

This research examines the determinants of agricultural land prices in the Mendoza River Basin, with emphasis on the marginal contribution of irrigation water as a strategic resource in an arid context. An original georeferenced database of 297 cultivated rural properties (2003-2024) was compiled, using advertised asking prices expressed in 2024 constant US dollars. A mixed spatial hedonic model with a log-log functional form was applied, incorporating hierarchical random effects (district nested within department), exponential spatial correlation, and heterogeneous variance across districts. The results indicate that properties with definitive surface irrigation rights command prices approximately 21% higher than comparable properties that rely exclusively on groundwater, confirming surface irrigation water as a pivotal economic asset. Soil quality and productive improvements increase land values by approximately 20% and 21%, respectively. In contrast, land size and distance to urban centres have significant negative effects (elasticities of -0.39 and -0.47). These findings highlight the central role of surface irrigation water as an economic asset and indicate a territorially segmented land market. The proposed methodology provides empirical evidence to support the design and implementation of water management and land-use planning policies in irrigated agricultural regions.

Keywords
hedonic pricing • farmland value • irrigation water • land characteristics • geostatistics • arid regions • river basins

https://doi.org/10.48162/rev.39.205

1 Universidad Nacional de Cuyo. Facultad de Ciencias Agrarias. Cátedra de Economía y Política Agraria. Almirante Brown 500. M5528AHB. Chacras de Coria. Mendoza. Argentina. * vciardullo@fca.uncu.edu.ar
2 Universidad Nacional de Cuyo.

Licenses Creative Commons
Attribution - Non Commercial - Share Alike

Resumen

Esta investigación examina los determinantes del precio de la tierra agrícola en la Cuenca del Río Mendoza, con énfasis en la contribución marginal del agua de riego como recurso estratégico en un contexto árido. Se compiló una base de datos georreferenciada original de 297 propiedades rurales cultivadas (2003-2024), utilizando precios de oferta publicados expresados en dólares estadounidenses constantes de 2024. Se aplicó un modelo hedónico espacial mixto con forma funcional log-log, que incorpora efectos aleatorios jerárquicos (distrito anidado en departamento), correlación espacial exponencial y varianza heterogénea entre distritos. Los resultados indican que las propiedades con derechos definitivos de riego superficial presentan precios aproximadamente un 21% superiores a los de propiedades comparables que dependen exclusivamente de agua subterránea, lo que confirma al agua de riego superficial como un activo económico fundamental. La calidad del suelo y las mejoras productivas incrementan el valor de la tierra en aproximadamente un 20% y un 21%, respectivamente. En contraste, el tamaño del predio y la distancia a centros urbanos ejercen efectos negativos significativos (elasticidades de -0,39 y -0,47). Estos hallazgos subrayan el papel central del agua de riego superficial como activo económico y revelan la existencia de un mercado territorialmente segmentado. La metodología propuesta aporta evidencia empírica para apoyar el diseño e implementación de políticas de gestión del agua y de planificación del uso del suelo en regiones agrícolas irrigadas.

Palabras clave

precio hedónico • valor de la tierra agrícola • agua de riego • características del terreno • geoestadística • regiones áridas • cuencas hidrográficas

Introduction

Land valuation in irrigated arid regions is a complex and multidimensional process in which physical (soil quality, topography), productive (crop type, farm improvements and infrastructure), institutional (irrigation rights and reliability), and territorial factors (accessibility, proximity to urban centres) interact to actively shape prices (Caballer & Guadalajara, 2005). In such settings, water scarcity and supply variability are binding constraints that affect both expected agricultural productivity and the formation of land prices. The institutional architecture of irrigation -combining surface canals, wells, legal water rights, and conveyance efficiency- together with pronounced spatial heterogeneity in soil quality, productive specialization and accessibility, yields segmented markets in which territorial and water-related attributes translate into price differentials across farms (Caballer & Guadalajara, 2005).

These features are particularly pronounced in the Mendoza River Basin, the province's main agricultural oasis. Urban expansion into peri-urban fringes, increasing fragmentation of farm structures, pressure on the availability and quality of irrigation water, and growing competition for land uses collectively shape market dynamics in which price signals reflect agricultural returns, locational services (access to roads and markets), climate risk (hail) and edaphic quality. The interplay between natural endowment (soils, water), capital investment (on-farm improvements, pressurized irrigation) and accessibility tends to reinforce intra-basin territorial gaps, making consistent quantitative evidence essential to guide water management and land-use planning.

These territorial dynamics are consistent with evidence from irrigated areas in the neighbouring San Martín Department, where declining irrigation water availability and irrigation management constraints have intensified land-use pressures and contributed to rural abandonment (Guida-Johnson *et al.*, 2024).

Analytically, hedonic price theory posits that the price of a heterogeneous asset can be decomposed into the implicit values of its observable attributes (Rosen, 1974). Applied to farmland, the literature repeatedly documents positive effects of irrigation availability/reliability, soil quality and productive infrastructure, alongside negative effects associated with distance to urban centres and, frequently, parcel size when the outcome

is expressed as price per hectare (Chicoine, 1981; Decimavilla & Sperlich, 2008; Fraser & Hilder, 2007; Gracia *et al.*, 2004; Huang *et al.*, 2006; Palmquist & Danielson, 1989). Previous studies consistently report sizeable and robust irrigation premia across alternative functional forms: approximately 15-20% in Mediterranean land markets (Sardaro *et al.*, 2020), around 29% for the adoption of drip irrigation systems (Donoso *et al.*, 2013), and up to 63% in Spanish estimates (Caballer & Guadalajara, 2005).

Complementary evidence also reports implicit unit values for irrigation water, ranging from about USD 9-44 per acre-foot in the United States (Faux & Perry, 1999) to €3.46/m^3 (capital value) and €0.14-0.35/m^3 (rental value) in the Guadalquivir Basin (Berbel & Mesa, 2007), underscoring water's role as an economic asset capitalised into agricultural land prices. In this context, high-value perennial crops (vineyards, fruit orchards) and on-farm improvements (including pressurized irrigation) tend to raise prices, whereas adverse environmental conditions (*e.g.*, salinity) and greater remoteness from markets reduce them (Decimavilla & Sperlich, 2008; Fraser & Hilder, 2007; Gracia *et al.*, 2004; Huang *et al.*, 2006; Mukherjee & Schwabe, 2014).

A central methodological issue is the spatial dimension of land markets. In many irrigated environments, prices exhibit spatial autocorrelation and territorial heterogeneity (administrative hierarchies, irrigation associations and farmer-managed irrigation boards), violating independence and homoskedasticity assumptions in OLS and potentially biasing coefficients and standard errors (Guadalajara *et al.*, 2019). Consequently, spatial specifications -spatial-lag and spatial-error models, mixed-effects structures, and log-log generalizations- are increasingly used to capture neighbourhood spillovers and improve fit and inference relative to OLS (Guadalajara *et al.*, 2019; Huang *et al*, 2006; Mukherjee & Schwabe, 2014). In arid irrigated regions in particular, water quality -with emphasis on salinity and supply variability- emerges as a key price determinant and a source of omitted-variable bias if ignored (Mukherjee & Schwabe, 2014). Yet, most empirical evidence still comes from developed countries, and there is a dearth of studies integrating hedonic approaches with spatial econometrics for arid Latin American settings; recent work in Argentina advances mapping and prediction under different frameworks and aims (Córdoba *et al.*, 2021).

Recent reviews reinforce this diagnosis. Ciardullo & Gennari (2025) indicate that previous studies highlight the importance of incorporating irrigation-water attributes, spatial dependence, and territorial heterogeneity into hedonic models, as these factors are regarded as relevant for explaining price formation in arid regions. Their review also identifies major methodological gaps in Argentine empirical research, particularly the limited valuation of irrigation water rights and the scarce integration of geostatistical and spatial-econometric tools into hedonic approaches. In this context, the development of spatially explicit models that quantify the contribution of irrigation water and other territorial attributes to land values in the Mendoza River Basin becomes especially relevant.

In sum, the state of the art indicates that (i) irrigation water -as a scarce environmental resource- has an implicit value systematically capitalised into farmland prices; (ii) soil quality and productive improvements increase value; (iii) accessibility (distance) and negative externalities reduce it; and (iv) spatial dependence and territorial heterogeneity must be modelled explicitly to obtain valid, policy-relevant elasticities and inferences (Caballer & Guadalajara, 2005; Guadalajara *et al*., 2019; Huang *et al.*, 2006; Mukherjee & Schwabe, 2014; Rosen, 1974). Against this backdrop, the present article undertakes a spatial hedonic analysis based on a mixed log-log specification for the Mendoza River Basin, integrating water-related attributes (type of supply), productive features, and territorial factors, and quantifying the marginal effects and price differentials that characterise its segmented land market.

The general objective of this study is to analyse and quantify the determinants of agricultural land prices in the Mendoza River Basin, with particular emphasis on the marginal contribution of irrigation water in an arid irrigated setting, by estimating a spatial hedonic mixed log-log model that explicitly captures spatial dependence and territorial heterogeneity and yields policy-relevant elasticities and price differentials.

Hypotheses of the Study

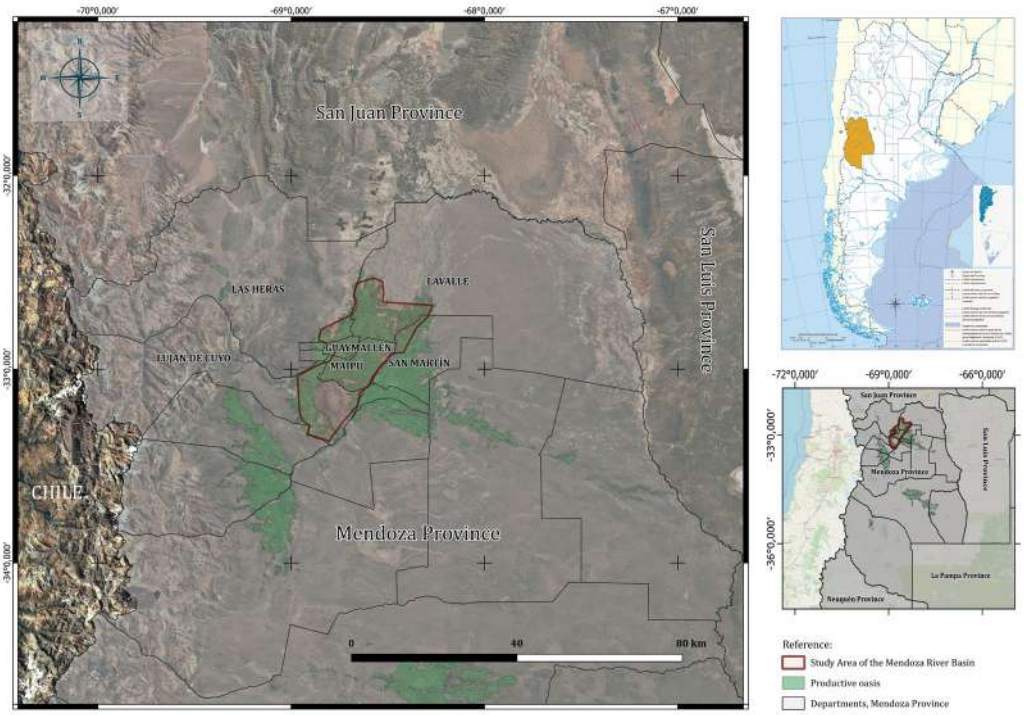
Building on the theoretical expectations summarised above, the study advances the following central hypothesis:

H1. Properties with secure surface irrigation rights command higher land prices than otherwise comparable properties that rely exclusively on groundwater, reflecting the capitalisation of irrigation water as a scarce and strategic economic asset.

Materials and Methods

Study Area

The Mendoza River Basin, located in Mendoza, Argentina, is the most important irrigated system in the province, encompassing the departments of Las Heras (including its high-mountain area), Lavalle, Guaymallén, Maipú, Luján de Cuyo, parts of San Martín, and the urban areas of Capital and Godoy Cruz. The study area corresponds specifically to the agricultural production zones of the basin, supplied by both surface and groundwater resources, while excluding high-mountain environments and fully urbanised areas (figure 1). This agricultural territory exhibits pronounced heterogeneity in soil quality, irrigation infrastructure, and productive specialisation. Vineyards predominate in Maipú and Luján de Cuyo -often complemented by enotourism and high-value agribusinesses- while Lavalle and Las Heras are characterised by more diversified cropping systems, including horticulture and forages. Spatial variability across the study area is shown in figure 2 (page 5), which maps (a) asking farmland prices per hectare (constant 2024 USD, by range) and (b) irrigation water supply type.



Author's elaboration based on georeferenced data from the National Geographic Institute (IGN), Argentina.

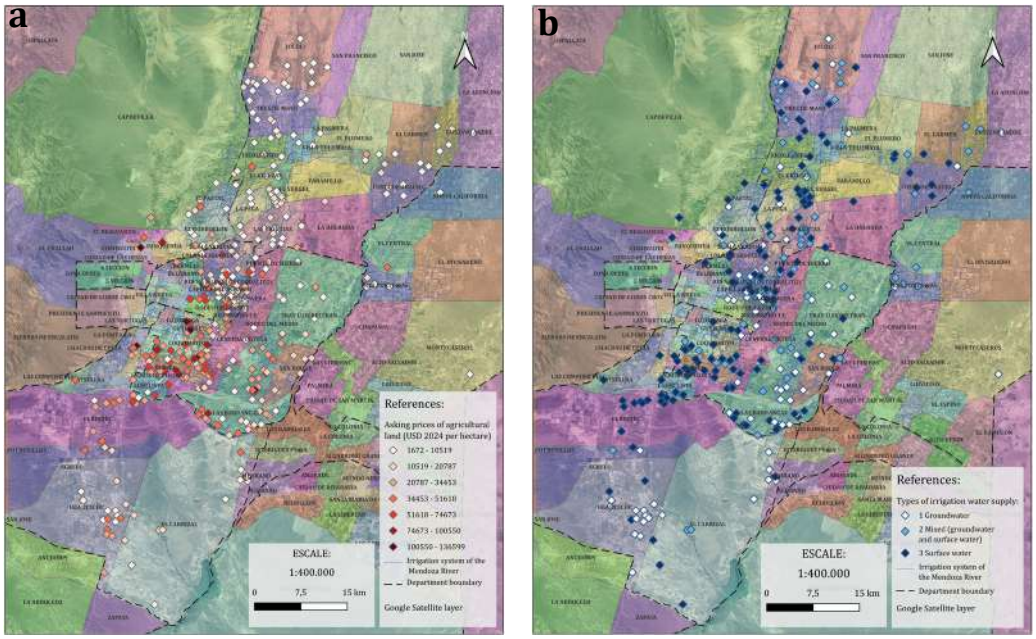
Source: National Geographic Institute (IGN, 2025). Environmental and Territorial Information System (SIAT). Google Satellte and Open Street Map.

Elaboración propia a partir de datos georreferenciados del Instituto Geográfico Nacional (IGN), Argentina.

Fuente: Instituto Geográfico Nacional (IGN, 2025). Sistema de Información Ambiental y Territorial (SIAT). Google Satellite y OpenStreetMap.

Figure 1. Map of the Study Area in the Mendoza River Basin, Mendoza Province, Argentina.

Figura 1. Mapa del área de estudio en la Cuenca del Río Mendoza, Provincia de Mendoza, Argentina.



(a) Advertised asking prices per hectare (2024 constant USD, by range); (b) Irrigation water by supply type (surface, groundwater, mixed).

Source: Our elaboration.

(a) Precios de oferta publicados por hectárea (USD constantes de 2024, por rango); (b) Agua de riego según tipo de abastecimiento (superficial, subterráneo, mixto).

Fuente: Elaboración propia.

Figure 2. Cultivated Rural Properties in the Mendoza River Basin.

Figura 2. Propiedades rurales cultivadas en la Cuenca del Río Mendoza.

Database Construction

The dataset was constructed from advertised asking prices published in classified listings from major provincial newspapers and real estate portals (Inmoclick, Cocucci, Contacto, Argenprop) covering the period 2003-2024. For 2003-2013, data were reconstructed from the physical archive of Los Andes newspaper and collected using a systematic sampling strategy -the second and fourth Sundays of May, August, and November- to avoid seasonal distortions (*e.g.*, harvest effects). For 2014-2024, the database was updated at five-year intervals (2018 and 2024), ensuring temporal coverage while maintaining consistency with the sampling framework.

A total of 297 cultivated rural properties were included. All advertised asking prices are standardised to constant 2024 US dollars using the U.S. CPI-U index (Bureau of Labor Statistics; data from the Federal Reserve Bank of Minneapolis). The study excludes parcels with evident peri-urban conversion potential to focus on agricultural land markets. Screening combined municipal zoning regulations, proximity to urban boundaries with public services, and explicit marketing language in the advertisements (*e.g.*, "suitable for subdivision", "residential estates", "developments", industrial/commercial, per-square-meter quotations, swimming pool, scenic views, detailed urban buildings).

The resulting dataset provides a cross-sectional sample of homogenised property values suitable for estimating static econometric models of farmland prices. Following Caballer and Guadalajara (2005), this approach responds to the structural limitation of low transaction frequency in rural land markets by constructing a single standardized reference period. Property prices are expressed in constant 2024 dollars, allowing the model to capture market values at a given moment in time. Accordingly, the econometric specification is formulated as a static cross-sectional model in spatial terms, under the assumption that temporal variables are fixed at a single value. This design enables robust estimation of the marginal contribution of attributes, particularly irrigation water, to agricultural land values.

Building on this framework, the explanatory variables were organized into four groups, selected based on economic theory, prior hedonic evidence, and data availability.

Physical attributes included total farm area (hectares), a cultivated area index (share of the holding under cultivation), crop type (viticultural, fruit, or horticultural), productive improvements (buildings such as a farmhouse and/or shed, and productive facilities such as a packing house, greenhouse, or small-livestock unit), and water-supply type (surface, groundwater, or mixed). Territorial attributes comprised department and district, distance to the urban centre (Mendoza kilometre zero, km 0), soil quality by irrigation suitability from the Instituto Nacional de Tecnología Agropecuaria (INTA) (2025) in collaboration with the Departamento General de Irrigación (DGI, Government of Mendoza Province), hail risk from the Dirección de Contingencias Climáticas (DCC, Government of Mendoza Province), and surface-water quality from the Instituto Nacional del Agua (INA, Argentina). The economic context captured departmental gross regional product (GRP) from the Dirección de Estadísticas e Investigaciones Económicas (DEIE, Government of Mendoza Province); departmental billed revenue for 2024 varietal grape production -computed as the cash and financed average price weighted by output in quintals- and the departmental average varietal grape price, both compiled by the Bolsa de Comercio de Mendoza (BCM, 2024). Finally, the social context included population density (per km^2, 2022) and the population growth rate (2010-2022) from the Instituto Nacional de Estadísticas y Censos (INDEC, Argentina). See Table A.1 in Appendix for the complete list of variables.

Spatial Hedonic Model: Specification and Estimation

We estimated a spatial hedonic mixed (multilevel) model with a log-log functional form:

$$\ln P_i = \alpha + \sum_j \beta_j \ln X_{ij} + \sum_m \gamma_m D_{im} + u_{d(i)} + \varepsilon_i,$$

where

P_i = price per hectare (2024 USD) of property *i*

lnX_{ij} = continuous covariates in natural logs interpreted as elasticities

D_{im} = dummies are dummy variables, with percentage effects computed as 100[exp(γm)-1]

$u_{d(i)}$ = random intercept for district *d* nested within department ($u_d \sim N(0,\sigma^2_u)$)

ε_i = residuals with exponential spatial correlation structure (*corExp*) based on inter-point distances in the project CRS.

To address heteroscedasticity, we incorporated a variance identity function (*varIdent*) that allows residual variance to differ by district. This specification corrects for systematic variability in error dispersion across territorial units, improving the reliability of estimated standard errors.

We fitted the models using the *nlme* package in R. Competing specifications of fixed effects, random structures, and correlation families were compared using maximum likelihood (ML) and information criteria (AIC/BIC). Final estimates and standard errors are reported under restricted maximum likelihood (REML), with 95% confidence intervals derived from Wald approximations using nlme's degrees-of-freedom. Diagnostics included residual analysis, assessment of heteroscedasticity, and checks for residual spatial autocorrelation (Moran's I).

Continuous regressors were log-transformed and then mean-centred (after logging) to preserve the elasticity interpretation of βj\beta_jβj and improve numerical stability; no standard deviation scaling was applied. Mean-centring shifts the intercept but does not affect slope coefficients, while SD scaling would alter the elasticity interpretation.

Modelling Strategy

We followed a three-step strategy to structure inference and robustness: i) Exploratory analysis and baseline OLS (m_lin); ii) Main specification (m0F1_log); iii) Alternative specifications.

- Exploratory analysis and baseline OLS (m_lin). Descriptive statistics and ANCOVA guided variable screening and coding. We then estimated an exploratory log-log OLS on the 297 constant-price observations to obtain a transparent baseline (elasticities/signs) and to inspect residual patterns.

- Main specification (m0F1_log). The preferred model is the mixed log-log spatial specification described above, with district random effects (nested in department), *corExp* residual correlation and *varIdent* heteroscedasticity. Model selection among random and correlation structures used ML; inference is reported under REML.

- Alternative specifications for robustness.
  - A GAM ($\ln P_i \sim_s (\ln Dist) +_s (\ln Area) + \cdots$)
  - was estimated to assess potential non-linearities and check the stability of coefficient signs and significance.
  - A model with Matérn residual correlation was fitted as an alternative to the exponential (*corExp*) structure to test sensitivity to the choice of spatial covariance family.

Model comparisons drew on adjusted R^2, explained deviance, and residual diagnostics. The spatial mixed model (m0F1_log) was ultimately retained for its combination of interpretability (elasticities) and superior overall fit.

Results

Descriptive Statistics and Preliminary Analysis

Descriptive statistics reveal marked territorial segmentation. Average land prices range from USD 8,620/ha in Lavalle (88 cases) to USD 27,526/ha in Maipú (101 cases). All property prices are expressed in constant 2024 US dollars. The complete table of descriptive statistics is provided in Appendix A2.

To examine the role of agricultural attributes, ANCOVA models were estimated to compare adjusted mean prices across crop types and irrigation water sources. Results show that crop type exerts a significant influence on market values (table 1): vineyards and fruit orchards command premiums of roughly USD 2,600/ha relative to horticultural land. Similarly, irrigation water access strongly differentiates land values (table 2): properties supplied with surface or mixed water achieve higher adjusted prices than those relying exclusively on groundwater.

Table 1. Comparison of adjusted mean prices by crop type (ANCOVA results, Fisher's LSD, α = 0.05).

Tabla 1. Comparación de medias ajustadas de precios según tipo de cultivo (resultados de ANCOVA, LSD de Fisher, α = 0,05).

Crop Type (Tipo_Cult2)	Adjusted Means	S.E.	
Viticultural (3)	18,784	1,903	A
Olive-Fruit (2)	18,744	1,939	A
Horticultural (1)	16,175	1,985	B

Means sharing a common letter are not significantly different (p > 0.05). Source: Own elaboration.

Las medias que comparten una misma letra no presentan diferencias estadísticamente significativas (p > 0,05). Fuente: Elaboración propia.

Table 2. Comparison of adjusted mean prices by type of irrigation water supply (ANCOVA results, Fisher's LSD, α = 0.05).

Tabla 2. Comparación de medias ajustadas de precios según tipo de abastecimiento de agua de riego (resultados de ANCOVA, LSD de Fisher, α = 0,05).

Irrigation Water Supply (Agua_Riego6)	Adjusted Means	S.E.	
Surface (3)	19,658	2,076	A
Mixed (2)	18,231	1,921	A
Groundwater (1)	15,814	1,890	B

Means sharing a common letter are not significantly different (p > 0.05). Source: Own elaboration.

Las medias que comparten una misma letra no presentan diferencias estadísticamente significativas (p > 0,05). Fuente: Elaboración propia.

Exploratory OLS baseline (m_lin)

An exploratory log-log OLS model was estimated on the 297 constant-price observations (2024 USD). Predictors included quantitative covariates (log-transformed continuous variables, interpreted as elasticities) and categorical attributes (dummy indicators, interpreted as percentage premia relative to the reference category, 100[exp(β)-1]). The model attains adjusted R^2 = 0.524, with AIC = 541.80 and BIC = 567.89.

Results highlight the central role of irrigation water, crop type, and productive improvements. Properties supplied by surface or mixed irrigation command an estimated premium of about 27% relative to groundwater; permanent crops (viticulture or fruit orchards) are associated with a 22% premium compared to horticultural land; and buildings or productive facilities imply a 16% premium. Soil quality shows a positive but statistically insignificant effect (≈ +7%).

Continuous variables exhibit the expected negative elasticities: for distance to the urban centre (β = -0.445), a 10% increase reduces prices by ≈ 4.5%, and doubling distance lowers values by ≈ 26-27%. For farm size (β = -0.299), a 10% increase reduces prices by ≈ 3.0%, and doubling area lowers values by ≈ 18-19%. Departmental GRP has a small but positive and statistically significant effect (β = 0.037).

Taken together, these results confirm that access to irrigation water, permanent crops, and on-farm improvements are dominant price determinants, while larger and more distant farms are penalized in the land market. However, because this model does not account for spatial autocorrelation or hierarchical territorial structure, it motivated the transition to the spatial mixed-effects log–log model (m0F1_log), estimated on the same 297 cases.

Spatial Hedonic Mixed Model (m0F1_log)

The preferred specification is a multilevel spatial hedonic model (MLM) with a log-log functional form, estimated on the full sample of 297 properties. The estimated coefficients are presented in table 3. The final econometric specification (m0F1_log) includes district-level random effects and an exponential spatial correlation structure, and is expressed as follows:

$$\begin{aligned}\ln(\text{Price}_i) = {} & 10.7438 + 0.1055 \cdot \text{CropType}_i + 0.1908 \cdot \text{Improvements}_i \\ & + 0.1793 \cdot \text{SoilQuality}_i + 0.1887 \cdot \text{IrrigationWaterSource}_i \\ & - 0.4698 \cdot \ln(\text{Distance}_i) - 0.3948 \cdot \ln(\text{FarmSize}_i) \\ & + 0.0199 \cdot \ln(\text{GRP}_{d(i)}) + u_{d(i)} + \varepsilon_i\end{aligned}$$

Table 3. Estimated coefficients of the spatial mixed log-log hedonic model (m0F1_log).
Tabla 3. Coeficientes estimados del modelo hedónico espacial mixto log-log (m0F1_log).

Attribute	Estimated coefficient	Standard error	t-value	p-value	Significance	Elasticity / % Effect
(Intercept)	10.7438	0.2725	39.434	0.0000	***	-
Crop type	0.1055	0.0247	4.275	0.0000	***	**≈ +11.1%**
Productive improvements	0.1908	0.0013	141.853	0.0000	***	**≈ +21.0%**
Soil quality	0.1793	0.0456	3.936	0.0003	***	**≈ +19.6%**
Irrigation water source	0.1887	0.0375	5.032	0.0000	***	**≈ +20.8%**
Distance to urban centre (log)	-0.4698	0.0770	-6.104	0.0000	***	**Elasticity: -0.47**
Farm size (log)	-0.3948	0.0225	-17.581	0.0000	***	**Elasticity: -0.39**
Departmental GRP (log)	0.0199	0.0114	1.751	0.0869	.	**Elasticity: +0.02**

Significance / Significancia: *** p < 0.001; ** p < 0.01; * p < 0.05; . p < 0.1.

Properties supplied by surface or mixed irrigation command an estimated premium of ≈21%, equivalent to ≈USD 3,951/ha when evaluated at the sample mean price of USD 18,996/ha, relative to groundwater-dependent properties. Permanent crops (viticulture and fruit orchards) exhibit a premium of ≈11%, corresponding to ≈USD 2,108/ha, compared to horticultural land. Productive improvements (*e.g.*, buildings and facilities) show the largest effect, increasing land values by ≈21%, or ≈USD 3,989/ha at the mean. Importantly, soil quality also emerges as a significant determinant once spatial dependence and hierarchical structure are modelled explicitly. While the baseline OLS specification (m_lin) suggests a positive but statistically insignificant effect, the spatial mixed model estimates a ≈20% premium (≈USD 3,723/ha) for properties with adequate soils. This contrast reflects the gains in efficiency and reduced bias achieved when accounting for spatial correlation and administrative hierarchy, factors that otherwise inflate residual variance and dampen significance in non-spatial models.

Continuous variables behave as expected. The elasticity for distance to the urban centre is -0.470, implying that a 10% increase in distance reduces land prices by about 4.7% (≈USD -893/ha), while doubling distance leads to a decline of ≈ 27-28% (≈USD -5,129/ha). Farm size elasticity is also negative (-0.395): a 10% increase in area reduces land prices by ≈ 3.9% (≈USD -746/ha), and doubling area lowers values by ≈ 19-20% (≈USD -3,799/ha). Departmental GRP has a small positive effect (0.020, significant at the 10% level), implying an increase of ≈2% (≈USD 380/ha) for a 10% rise in local economic activity.

Goodness-of-fit metrics confirm the adequacy of this specification (table 4). The model achieves a log-likelihood of -231.8, with AIC = 581.5 and BIC = 797.9. The random-effects structure captures territorial heterogeneity: the district-level random intercept shows meaningful variability (SD ≈ 0.192), while the department-within-district component is negligible. The exponential spatial correlation (*corExp*) presents an estimated range of 0.0274 and a small nugget effect (0.00205), indicating limited residual spatial dependence once fixed and random effects are accounted for.

Table 4. Goodness-of-fit metrics and model parameters for the spatial hedonic mixed model (m0F1_log).

Tabla 4. Medidas de bondad de ajuste y parámetros del modelo hedónico espacial mixto (m0F1_log).

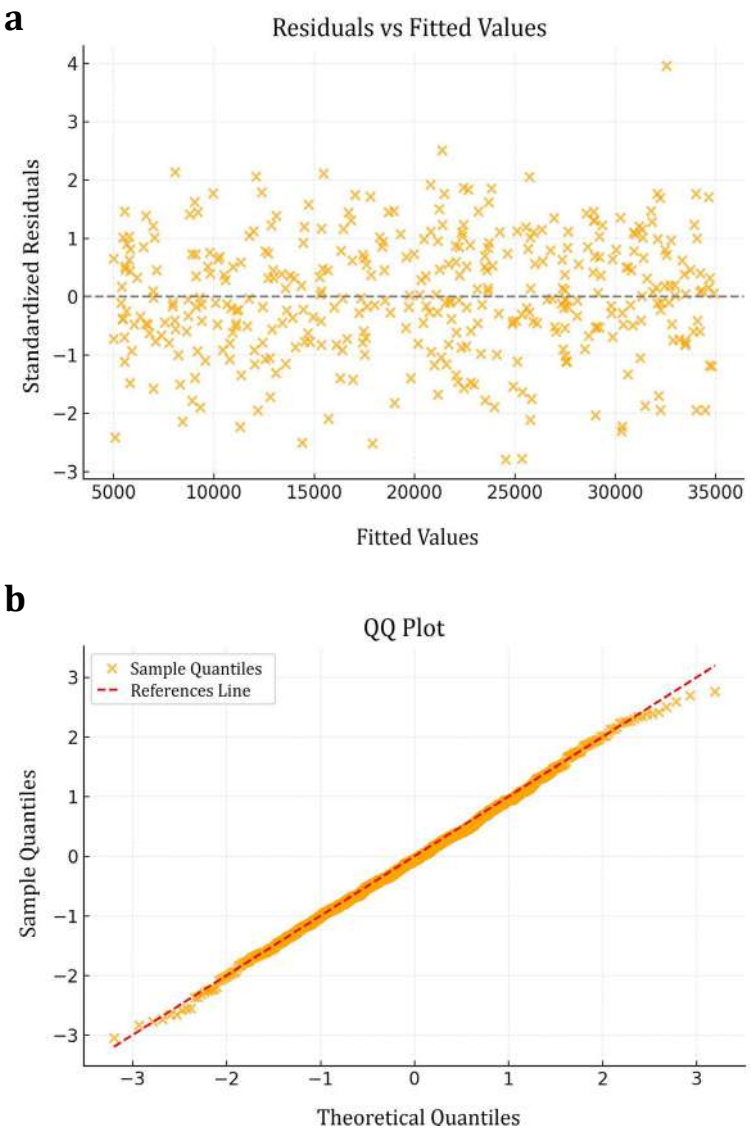
Metric	Value
AIC	581.536
BIC	797.8552
Log-likelihood	-231.768
Random SD (District)	0.191895
Random SD (Depto %in% District)	0.002291
Range (spatial correlation, *corExp*)	0.0274
Nugget (spatial correlation, *corExp*)	0.00205

Source: Authors' calculations using hierarchical linear mixed-effects modelling (lme) in R.

Cálculos de los autores utilizando modelos lineales mixtos jerárquicos (lme) en R.

Residual diagnostics further support model adequacy. The scatterplot of predicted values against studentized residuals shows no systematic patterns, confirming homoscedasticity. Similarly, the normal Q-Q plot indicates approximate normality of residuals, with only minor deviations in the tails. These diagnostics (figure 3, page 10) strengthen confidence in the reliability of the model's inference.

Taken together, these findings demonstrate that irrigation water, crop type, soil quality, and productive improvements are the strongest determinants of farmland values in the Mendoza River Basin, while larger and more distant farms are systematically penalized. The inclusion of hierarchical random effects and spatial correlation provides a more robust inference framework than non-spatial alternatives, supporting the reliability of the spatial mixed log-log model (m0F1_log).



(a) scatterplot of predicted values *vs.* studentized residuals, (b) normal Q-Q plot of residuals.

Source: Own elaboration.

(a) diagrama de dispersión de valores predichos *vs.* residuos estudentizados, (b) gráfico Q-Q normal de los residuos.

Fuente: Elaboración propia.

Figure 3. Residual diagnostic plots for the spatial mixed log-log model (m0F1_log).

Figura 3. Gráficos de diagnóstico de residuos para el modelo hedónico espacial mixto log-log (m0F1_log).

Predictive Validation

The predictive performance of the preferred spatial mixed model (m0F1_log) was assessed using two cross-validation schemes: random 5-fold and spatial leave-one-cluster-out (k-means, k=5). In the random cross-validation, the model achieved RMSE = 14.18 USD (±1.97) and MAE = 10.03 USD (±1.33), both below the observed standard deviation of land prices (17,230 USD/ha). These error metrics are computed in the log-price estimation scale, consistent with the log-log specification of the model and therefore serve as relative indicators of predictive performance rather than absolute monetary errors. In the spatial cross-validation, which is more demanding as training and test sets come from different geographic clusters, the model attained RMSE = 13.87 USD (±6.58) and MAE = 9.74 USD (±4.45).

In both cases, predictive errors were substantially lower than the overall price dispersion, confirming that the model significantly reduces uncertainty compared to a naïve mean-based estimator. The slightly superior performance under spatial validation suggests robust generalization to unobserved geographic areas, attributable to the inclusion of spatial correlation (exponential structure) and hierarchical random effects (district/department).

Residual Diagnostics and Spatial Autocorrelation

Residual diagnostics indicate that the model adequately accounts for spatial dependence. Moran's I test on normalized residuals (k = 8 nearest neighbours) yielded a statistic close to zero (I = -0.014, p = 0.66), showing no significant spatial autocorrelation. This confirms that the spatial correlation and hierarchical effects embedded in m0F1_log successfully captured the underlying spatial structure of farmland prices.

Additional graphical checks -including the Moran's I, Moran Scatterplot, LISA maps, and the empirical semivariogram- also showed no residual spatial patterns, reinforcing the robustness of the specification. Together, these results validate both the predictive capacity and the spatial adequacy of the model, supporting its use for territorial applications and policy analysis. Full results are reported in Appendix: Moran's I test (Table A.3), LISA cluster map and Moran scatterplot (Figure A.1a and A.1b) and residual semivariograms (Figure A.2a and A.2b).

Comparative Analysis with Alternative Models

Two sets of comparative results are presented to evaluate alternative hedonic specifications.

First, table 5 reports the explanatory performance of the models in terms of adjusted R^2 and explained deviance. The results highlight the improvement from the baseline OLS (m_lin) to the spatial GAM and finally to the mixed spatial log-log model (m0F1_log), which attains the highest explanatory power (>99% deviance explained) while preserving interpretability in terms of elasticities.

Table 5. Comparative performance of hedonic models by functional form and explanatory power.

Tabla 5. Comparación de modelos hedónicos según la forma funcional y el desempeño explicativo.

Source: Authors' elaboration based on a dataset of 297 properties (2024 constant USD).

Elaboración de los autores sobre la base de un conjunto de datos de 297 propiedades (USD constantes de 2024).

Model	adjusted R^2	explained deviance
Lineal (lm)	0.524	53.6 %
GAM espacial	0.574	59.8 %
m0F1_log	0.927	>99 %

Second, table 6 (page 12), provides a more comprehensive comparison of specifications and diagnostics across alternative hedonic models. This extended summary includes the baseline OLS, intermediate mixed-effects models, the final spatial mixed log-log model, and robustness checks with GAM and Matérn specifications. The comparison highlights both methodological differences and empirical performance, justifying the selection of m0F1_log as the preferred specification.

In summary, the comparative evidence confirms that although both the GAM and Matérn specifications yield consistent results, the spatial mixed log-log model (m0F1_log) remains the preferred specification. It combines robust performance, parsimony, and superior explanatory power, while retaining the advantage of directly interpretable elasticities, making it the most suitable model for applied analysis of agricultural land values.

Table 6. Comprehensive comparison of spatial hedonic models: specifications and diagnostics.

Tabla 6. Comparación integral de modelos hedónicos espaciales: especificaciones y diagnósticos.

Model	Functional form	Spatial structure	Adjusted R^2 / Pseudo-R^2	Comments
m_lin	Log-log (**OLS**)	No spatial structure	**0.52**	Baseline model. Elasticities are directly interpretable. Does not account for spatial autocorrelation or territorial hierarchy. Serves as a comparative benchmark.
m0F1	Linear (**spatial mixed**, no logs)	Hierarchical (Department/ District) + exponential spatial correlation + heteroskedasticity by district	**0.71**	Incorporates hierarchical and spatial structure. Coefficients in monetary units. Substantial improvement over OLS.
m0F1_ log	Log-log (**spatial mixed**, final model)	Hierarchical (Department/ District) + exponential spatial correlation + heteroskedasticity by district	**0.75**	Final model. Coefficients interpretable as elasticities. Robust, parsimonious, and with strong predictive performance. Recommended for practical applications.
GAM	Semiparametric	Bivariate spatial smoother *s(Xj, Yj)*	**0.57**	Introduces non-linear effects. The spatial smoother is significant. Does not outperform **m0F1_log**. Greater complexity without material gains.
Matérn	Log-log	Hierarchical + Matérn spatial correlation (continuous field)	**≈ 0.74**	Captures localised spatial dependence. Fit like **m0F1_log**. Supports robustness of results under an alternative spatial covariance.

Source: Authors' elaboration based on a dataset of 297 properties (2024 constant USD).

Elaboración de los autores sobre la base de un conjunto de datos de 297 propiedades (USD constantes de 2024).

Discussion

The analysis confirms that farmland values in the Mendoza River Basin arise from the combination of water, productive, territorial, and socioeconomic attributes, in line with hedonic theory and previous empirical evidence. The estimated elasticities and percentage impacts provide a transparent assessment of the relative importance of each factor, offering insights that are both statistically rigorous and territorially relevant. These results support the study's central hypothesis that secure access to surface irrigation water is capitalised into agricultural land prices.

Irrigation Water as a Key Economic Attribute

One of the most robust findings concerns irrigation water. Properties supplied by surface or mixed sources command a price premium of approximately 21% relative to those relying exclusively on groundwater -an effect that amounts to roughly USD 3,951/ha at the sample mean. This result emphasises the critical role of water availability, quality, and security of supply in determining land values, especially in semi- arid regions such as western Argentina, where agricultural productivity fundamentally depends on water availability.

The finding is consistent with international evidence reporting positive capitalization of irrigation water rights into land values (Mallios *et al.*, 2009; Demetriou, 2015; Palmquist & Danielson, 1989).

Crop Type and Market Segmentation

Crop type is another key determinant. Permanent crops -viticulture, olive groves, and fruit orchards- are valued more highly than horticultural land, reflecting an ≈11% premium (≈USD 2,108/ha). This premium aligns with the long-term profitability and market stability associated with perennial crops, which are often integrated into high-value agribusiness and enotourism chains. The capitalization of crop type into land values confirms prior findings in Mediterranean and Latin American agricultural markets (Huang *et al.*, 2006; Palmquist & Danielson, 1989), where perennial systems systematically capture higher implicit rents.

Productive Improvements and Infrastructure

Infrastructure also plays a decisive role. Properties with productive improvements -such as buildings or productive facilities- exhibit premiums of around 21% (≈USD 3,989/ha). These results indicate that the market values not only the physical assets but also their capacity to lower entry barriers and enable immediate productive use. This interpretation is consistent with evidence from other Argentine regions (Marcolini Tulliani, 2015), where infrastructure is understood as an asset that signals future profitability and reduces investment uncertainty.

Soil Quality and Agronomic Suitability

Soil quality, often neglected in market analyses, plays a decisive role. Properties with soils of adequate to marginal suitability (classes 2-3) are valued around 20% higher (≈USD 3,723/ha) than those with poor soils (class 4). Although soil quality was not statistically significant in the non-spatial OLS model, its significance in the spatial specification reflects the efficiency gains from incorporating hierarchical random effects and spatial correlation. This result reinforces the need to integrate edaphic indicators into valuation and land-use planning, consistent with evidence from Huang *et al.* (2006).

Farm Size and Scale Effects

Farm size exhibits the expected inverse relationship with land value. The negative elasticity ($\beta = -0.395$) shows that larger holdings receive systematically lower per-hectare prices: a 10% increase in size reduces land values by approximately 3.9%, while doubling farm size leads to a decline of around 19-20%. This pattern reflects economies of scale and weaker market demand for large properties, consistent with international evidence (Bastian *et al.*, 2002; Maddison, 2000).

Distance and the Urban Gradient

Accessibility strongly influences land values. Distance to Mendoza city displays a negative elasticity ($\beta = -0.470$): a 10% increase in distance lowers land prices by approximately 4.7%, while doubling distance leads to a decline of around 27-28%. This finding accords with Von Thünen's classical rent theory (1826/1966) and corroborates recent spatial studies highlighting the importance of accessibility to services, infrastructure, and markets in shaping agricultural land values.

Socioeconomic Context: Departmental GRP

Departmental GRP exerts a small but positive influence on land values. Although the effect is only marginally significant at the 10% level ($p = 0.10$), its positive sign is consistent with the expectation that more economically dynamic territories tend to command higher agricultural land values. While not definitive, this pattern reinforces the interpretation of land markets as embedded within broader territorial development dynamics (Greene, 2011; Gujarati, 2003).

Geostatistical Modeling and Spatial Patterns

The spatial mixed model (m0F1_log) shows no significant global spatial autocorrelation in the residuals (Moran's I, $p > 0.05$), indicating that the principal determinants operate relatively uniformly across the study area. Accordingly, geostatistical interpolation methods such as ordinary kriging or regression kriging were not applied, as these techniques require spatial dependence in the residual structure. Even so, descriptive maps reveal marked inter-departmental price differences -higher in Maipú and Luján de Cuyo and lower in Lavalle- likely reflecting contrasts in irrigation infrastructure, market access, and agroecological conditions.

Cross-validation results further demonstrate the model's predictive strength. RMSE values of approximately 14 in the log-price estimation scale remain far below the observed price dispersion (standard deviation ≈17,230 USD/ha), evidencing substantial gains in predictive accuracy relative to a naïve benchmark. Both random and spatial validation schemes produce consistent results, underscoring the robustness of the specification and its suitability for applied land-market analysis in arid irrigated regions.

Conclusions

This study provides new empirical evidence on the determinants of agricultural land values in the Mendoza River Basin by integrating hedonic spatial econometrics with geostatistical validation. The results show that irrigation water, crop type, productive improvements, and soil quality are the dominant drivers of land values, while larger and more remote farms are systematically penalised. The strong premiums associated with perennial crops, productive improvements, and especially surface or mixed irrigation water emphasise the strategic importance of these attributes in arid agricultural systems. These results are consistent with the study's central hypothesis, demonstrating that secure access to surface irrigation water is a key determinant of land values in arid contexts.

Methodologically, the findings demonstrate the importance of modelling spatial correlation and hierarchical structure. Soil quality, which was not statistically significant in a non-spatial OLS framework, became significant once spatial dependence was accounted for, illustrating the risks of biased or inefficient inference in models that ignore spatial processes. This reinforces the relevance of spatial econometric approaches for land-valuation research in heterogeneous and water-scarce regions.

From a policy perspective, the study highlights the close connection between land values and secure access to irrigation water, along with investments in permanent crops and infrastructure. These insights are particularly relevant for territorial planning, water allocation, and agricultural investment decisions in semi-arid environments where water is a binding constraint.

The spatial mixed log–log model (m0F1_log) achieved robust explanatory and predictive performance, providing a reliable framework for the economic valuation of agricultural land in water-scarce contexts. By combining econometric rigour with spatial realism, the study contributes to both the scientific literature and the design of evidence-based land and water policies in arid regions.

Future research could compare land prices between properties with and without access to irrigation water to better inform water governance and territorial development.

Supplemmentary Material

https://drive.google.com/file/d/1V77HtChvbDmympq9GpUh8CFouaV6Oxl6/view?usp=drive_link

References

Bastian, C. T., McLeod, D. M., Germino, M. J., Reiners, W. A. & Blasko, B. J. (2002). Environmental amenities and agricultural land values: A hedonic model using geographic information systems data. *Ecological Economics*, *40*(3), 337-349. https://doi.org/10.1016/S0921-8009(01)00278-6

Berbel, J., & Mesa, P. (2007). Valoración del agua de riego por el método de precios quasi-hedónicos: aplicación al Guadalquivir. *Economía Agraria y Recursos Naturales, 7*(14), 127-144.

Bolsa de Comercio de Mendoza. (2024). *Estadística de los Mercados-Uva varietal*. https://bcmdz.com.ar/servicios/tasa-estadistica#mercados

Caballer Mellado, V., & Guadalajara Olmeda, N. (2005). Modelos econométricos de valoración de la tierra de uso agrícola: Una aplicación al Estado español. *Revista española de Estudios Agrosociales y Pesqueros, 205*, 13-38.

Chicoine, D. L. (1981). Farmland values at the urban fringe: An analysis of sale prices. *American Journal of Agricultural Economics*, *63*(3), 530–537.

Ciardullo, V. F., & Gennari, A. J. (2025). Agricultural Land Valuation-Hedonic Pricing and Geostatistical Advances: A State-of-the-Art Review. *Revista de la Facultad de Ciencias Agrarias. Universidad Nacional de Cuyo. 57*(2), 224-236. https://doi.org/10.48162/rev.39.185

Córdoba, M., Carranza, J. P., Piumetto, M., Monzani, F., & Balzarini, M. (2021). A spatially based quantile regression forest model for mapping rural land values. *Journal of Environmental Management*, 289, 112509.

Decimavilla, E., & Sperlich, S. (2008). Urban pressure and land value in Spain: A hedonic pricing approach. *Agricultural Economics Review, 9*(1), 22-33.

Demetriou, D. (2015). A GIS-based hedonic price model for agricultural land. In D. G. Hadjimitsis, K. Themistocleous, S. Michaelides, & G. Papadavid (Eds.), Proceedings of SPIE. *The International Society for Optical Engineering, 9535*, 95350B. https://doi. org/10.1117/12.2192498

Departamento General de Irrigación. (2016). *Balance Hídrico Río Mendoza*. DGI.

Departamento General de Irrigación, Mekorot Israel National Water Co., & Consejo Federal de Inversiones. (2023). *Plan Maestro para el sector hídrico de la provincia de Mendoza: Informe 1. Estudio de la situación actual del sector hídrico*. https://www.irrigacion.gov.ar/web/wp-content/uploads/2025/03/1-PLAN-MAESTRO-PARA-EL-SECTOR-H%C3%8DDRICO-Informe-1-MENDOZA.pdf

Dirección de Agricultura y Contingencias Climáticas. Gobierno de Mendoza. (2010). *Índice de siniestralidad por granizo*. https://www.mendoza.gov.ar/contingencias/

Dirección de Estadísticas e Investigaciones Económicas. Ministerio de Gobierno, Infraestructura y Desarrollo Territorial. Gobierno de Mendoza. (2024). *Participación del Producto Bruto Geográfico por Departamento.* https://deie.mendoza.gov.ar/

Donoso, G., Cancino, J., & Foster, W. (2013). Farmland values and agricultural growth: The case of Chile. *Economía Agraria y Recursos Naturales, 13*(2), 33-52. https://doi.org/10.7201/earn.2013.02.02

Faux, J., & Perry, G. M. (1999). Estimating irrigation water value using hedonic price analysis: A case study in Malheur County, Oregon. *Land Economics*, *75*(3), 440-452.

Federal Reserve Bank of Minneapolis. (2024). *Consumer Price Index, 1913.* https://www.minneapolisfed.org/about-us/monetary-policy/inflation-calculator

Fraser, I., & Hilder, C. (2007). Vineyard capitalisation: A hedonic analysis of wine grape growing properties. *Australian Journal of Agricultural and Resource Economics*, *51*(1), 1-17.

Gracia, A., Pérez y Pérez, L., Sanjuán, A., & Barreiro Hurle, J. (2004). Análisis hedónico de los precios de la tierra en la provincia de Zaragoza. *Estudios Agrosociales y Pesqueros, 202*, 51-69.

Greene, W. H. (2011). *Econometric Analysis* (7th ed.). Pearson. *(Note: the 7th edition was published in the United States in 2011, and in its international version in 2012; the content is identical.).*

Guadalajara, H., García, L., & Rodríguez, J. (2019). Assessing the localization impact on land values: A spatial hedonic study. *Spanish Journal of Agricultural Research*, *17*(3), e0110. https://doi.org/10.5424/sjar/2019173-14961

Guida-Johnson, B.; Vignoni, A. P.; Migale, G. M.; Aranda, M. A.; Magnano, A. (2024). Rural abandonment and its drivers in an irrigated area of Mendoza (Argentina). *Revista de la Facultad de Ciencias Agrarias. Universidad Nacional de Cuyo. 56*(1): 35-47. DOI: https://doi.org/10.48162/rev.39.121

Gujarati, D. N. (2003). *Basic econometrics* (4th ed.). McGraw-Hill.

Huang, H., Miller, G., Sherrick, B., Gómez, M. (2006). Factors influencing Illinois farmland values. *American Journal of Agricultural Economics*, *88*(2), 458-470.

Instituto Geográfico Nacional. (2025). Información geoespacial. *Capas SIG*. https://www.ign.gob.ar/NuestrasActividades/InformacionGeoespacial/CapasSIG

Instituto Nacional de Tecnología Agropecuaria & Departamento General de Irrigación. Gobierno de Mendoza. (2025). *Clasificación de suelos y aptitud de riego de la Provincia de Mendoza.*

Maddison, D. J. (2000). A hedonic analysis of agricultural land prices in England and Wales. *European Review of Agricultural Economics*, *27*(4), 519-532. https://doi.org/10.1093/erae/27.4.519

Mallios, Z., Papageorgiou, A., Latinopoulos, D., & Latinopoulos, P. (2009). Spatial hedonic pricing models for the valuation of irrigation water. *Global NEST Journal, 11*(4), 575-582.

Marcolini Tulliani, S. B., Verón Medina, C. S., & Goytia García, M. D. (2015). Rentabilidad y precio de la tierra agrícola: un estudio sobre la región pampeana argentina. *CAPIC Review*, *13*(1), 21-30.

Mukherjee, M., & Schwabe, K. A. (2014). Where's the salt? A spatial hedonic analysis of the value of groundwater to irrigated agriculture. *Agricultural Water Management*, *145,* 110-122.

Palmquist, R. B., & Danielson, L. E. (1989). A hedonic study of the effects of erosion control and drainage on farmland values. *American Journal of Agricultural Economics*, *71*(1), 55-62.

Rosen, S. (1974). Hedonic prices and implicit markets: Product differentiation in pure competition. *Journal of Political Economy*, *82*(1), 34-55. https://doi.org/10.1086/260169

Sardaro, R., La Sala, P., & Roselli, L. (2020). Land pricing in rural development: The role of irrigation and territorial policies. *Land Use Policy, 94*, 104531.

von Thünen, J. H. (1966). Isolated state: An English edition of Der isolierte Staat. (P. Hall, Ed. & Trans.). Pergamon Press. (Original work published 1826).

Farmers' Fertilizer Use Behaviour: Evidence from Western Part of Türkiye

Análisis de los factores que afectan al comportamiento de los agricultores frente al uso de fertilizantes: datos de la parte occidental de Turquía

Murside Cagla Ormeci Kart [1*], Kenan Ciftci [2], Sule Isin [1]

Originales: *Recepción:* 09/02/2024 - *Aceptación:* 23/07/2025

ABSTRACT

Fertilizer use has been important for decades. Recent records show significant increases in their usage. Excessive and unconscious applications threaten human and environmental health and cause economic losses. This study aims to identify farmers' fertilizer use behaviour in Izmir province. In 2016, survey data were collected using a structured questionnaire concerning farmers' views and attitudes regarding fertilizer use. Seven factors were identified, explaining 80.34% of total variability, determining farmers' behaviour in the study area by cluster analysis. Farmers in the region were classified into four groups. The largest group, "environment and health-oriented", comprised 38.8% of the farmers. We concluded that farmers consider environmental sensitivity regarding fertilizer applications; however, environmental awareness should be further developed.

Keywords
cluster • farmer decisions • factor analysis • fertilizer • input choices

https://doi.org/10.48162/rev.39.194

1 Ege University. Faculty of Agriculture. Department of Agricultural Economics. 35100. Bornova/İzmir. Türkiye. * cagla.kart@ege.edu.tr
2 Van Yüzüncü Yıl University. Faculty of Agriculture. Department of Agricultural Economics. 65080. Tuşba/Van. Türkiye.

Licenses Creative Commons Attribution - Non Commercial - Share Alike

Resumen

El uso de fertilizantes ha sido importante por décadas. Los registros recientes muestran grandes incrementos en el uso de fertilizantes. El uso excesivo e inconsciente de fertilizantes amenaza la salud humana y ambiental y causa pérdidas económicas. Este estudio tiene como objetivo identificar el comportamiento de uso de fertilizantes de los agricultores en la provincia de Izmir. En 2016, se recopiló datos de encuestas utilizando un cuestionario estructurado sobre las opiniones y actitudes de los agricultores en relación con el uso de fertilizantes. Siete factores explican el 80,34% de la variabilidad total, determinando el comportamiento de los agricultores en el área de estudio mediante análisis de conglomerados. Los agricultores de la región se clasificaron en cuatro grupos. El grupo más grande, "orientado al medio ambiente y la salud", comprendía el 38,8% de los agricultores. Concluimos que los agricultores consideran la sensibilidad ambiental respecto de las aplicaciones de fertilizantes; sin embargo, la conciencia ambiental aguarda por mayor desarrollo.

Palabras clave

conglomerados • decisiones de los agricultores • análisis factorial • fertilizantes • elección de insumos

Introduction

Agriculture has taken its present form after various stages in human history. The development of agriculture-based industries, soilless agriculture, irrigation techniques and major scientific developments has led to revolutionary changes in agriculture aimed at increasing yields. For production enhancement, soil protection, agrochemical use, and improved agricultural technology constitute distinct factors (17). Undoubtedly, fertilization is one major practice aimed at increasing production and food, with shares in crop production of approximately 58% (4, 19). Today, producing desired quantities and qualities is not possible without using fertilizers (20).

Recent records show significant increases in fertilizer usage. Excessive and unconscious use of fertilizers threatens human and environmental health and causes economic losses. Overuse of chemical fertilizer and soil quality are common issues in both developed and developing countries. In Türkiye, several studies have examined fertilizer use behaviour. Farmers often rely on personal experience to determine fertilizer type and quantity (1, 6, 8, 9, 10, 13, 15, 20).

Western Türkiye, characterized by diverse soil types including alluvial, clay, and sandy soils, is highly fertile and supports a wide range of agricultural activities. The region experiences a Mediterranean climate with hot, dry summers and mild wet winters, growing crops such as olives, grapes, figs, and citrus fruits. Agricultural practices in this region follow both traditional methods and modern techniques, including irrigation systems, greenhouses, and organic farming practices. The combination of favourable soil characteristics, climate, and advanced agricultural practices makes Western Türkiye a key area for agricultural production (14, 16). This study aimed to identify farmers' fertilizer use behaviour. Our objectives are to:

- explore farmers' attitudes towards fertilizers effects on production and the environment, and to,
- classify farmers according to their fertilizer purchasing and usage behaviour.

Materials and methods

Considering crop pattern and level of production intensity, in 2016 we selected Menemen (38°36' N 27°04' E), Torbali (38°9' N 27°21' E), and Tire (38°5' N 27°44' E), districts of Izmir province (figure 1, page 3).

Data were collected using a structured questionnaire concerning farmers' views and attitudes regarding fertilizer use.

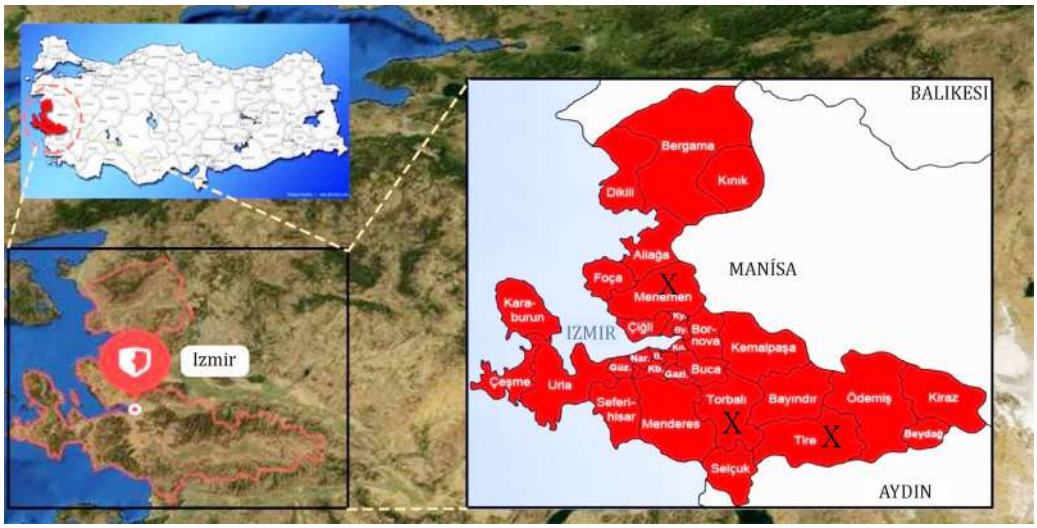


Figure 1. Study area.
Figura 1. Area de studio.

Using equation 1 (11), the sample size was 165, at 99% confidence interval and with a 10% margin of error.

$$n = \frac{\mathrm{N\ p\ (1-p)}}{(N-1)\sigma_{px}^2 + p(1-p)} \quad (1)$$

We conducted interviews with 32 farmers (19.4%) in Menemen, 46 farmers (27.9%) in Torbalı, and 87 farmers (52.7%) in Tire. Our analysis involved descriptive statistics, absolute and relative distributions, cross tables, simple averages, and statistical comparisons. Additionally, we asked the farmers to indicate agreement or disagreement regarding several statements related to fertilizer issues. Options included "strongly agree", "agree", "neutral", "disagree", and "strongly disagree" (Likert-type scale).

Factor analysis is one of the multivariate analysis techniques frequently used in various fields, especially in the social sciences. We use factor analysis to reduce the number of attitudinal and behavioural variables in fertilizer use, easing interpretation. The question set with 38 statements on fertilizer use was then reduced to 31 statements and seven factor dimensions. Finally, using scores obtained from factor analysis, we clustered the farmers.

Cluster analysis is used for sociological data and homogeneous research groups based on behaviour, attitude, and opinion. The analysis groups and distinguishes comparable units, separating them from different units, creating variables with 'great' similarity within each cluster (2, 3, 5, 7). Hierarchical clustering (HC) segments objects based on similarity (12, 18).

Results and Discussion

Socio-Economic Characteristics of the Farmers

Table 1 (page 4) shows general characteristics of farmers. Average age was 50 years old, with the youngest farmer being 21 and the oldest farmer being 78 years old. On average, farmers had approximately eight years of education and 27 years of experience. Additionally, average household size was four people, with two individuals from each family engaged in agricultural work.

Table 1. General information about farmers.
Tabla 1. Información general sobre los agricultores.

	Min.	Max.	Mean	Std. Dev.
Age (years)	21	78	50.30	13.128
Agricultural experience (years)	3	60	26.72	14.116
Education (years)	2	17	7.72	3.598
Household size (person)	1	12	3.99	1.737
Household member engaged in agricultural work (person)	1	12	1.94	1.607

Note: derived from research.
Nota: derivado de la investigación.

Land Structure and Crop Pattern

Average farm size was 13.65 ha, irrigated land size was 13.40 ha, non-irrigated land size was 0.25 ha, and 6.88 average number of plots. Almost 40.22% of field area, 11.04 hectares, is dedicated to cotton cultivation, while 38.23% is used for grain maize, 11.96% for wheat, 10.33% for silage maize (second crop), 7.43% for silage maize, 1.18% for barley, 1.00% for alfalfa, and 3.35% for other cereals (second crop). Regarding orchards, 59.02% of 0.61 hectare is dedicated to peach production, 29.51% to olives, and the rest are vineyard (table 2).

Table 2. Land structure and crop patterns.
Tabla 2. Estructura de la tierra y modelos de producción.

	Mean	%
Farm size (ha)	**13.65**	**100.00**
Irrigated land (ha)	13.40	98.17
Non-irrigated land (ha)	0.25	1.83
Total number of parcels	**6.88**	**-**
Cotton area (ha)	4.44	40.22
Maize (grain) area (ha)	4.22	38.23
Wheat area (ha)	1.32	11.96
Maize (silage) area (ha)	0.82	7.43
Barley area (ha)	0.13	1.18
Alfalfa area (ha)	0.11	1.00
Maize (silage) area (ha) - second crop	1.14	10.33
Cereals area(ha) - second crop	0.37	3.35
Total field area*	**11.04**	**113.70**
Processing tomato area (ha)	0.68	34.00
Watermelon area (ha)	0.26	13.00
Melon area (ha)	0.16	8.00
Table tomato area (ha)	0.05	2.50
Other vegetable area (ha)	0.85	42.50
Vegetable area (ha) - second crop	0.30	15.00

Note: derived from research. * Due to the second crops, the sum of percentages is more than 100.
Nota: derivado de la investigación.
* La superficie total del campo es superior a 100 debido a cultivos secundarios.

Total vegetable area*	**2.00**	**115.00**
Peach orchard (ha)	0.36	59.02
Vineyard area (ha)	0.07	11.47
Olive orchard (ha)	0.18	29.51
Total orchard area (ha)	**0.61**	**100.00**

Note: derived from research. * Due to the second crops, the sum of percentages is more than 100.

Nota: derivado de la investigación.

* La superficie total del campo es superior a 100 debido a cultivos secundarios.

Factor Dimensions Related to Fertilizer Use

Factors related to fertilizer use practices were assessed using a five-point Likert scale (table 3). We defined ranges as 1.00-1.49 strongly disagree, 1.50-2.49 disagree, 2.50-3.49 neutral, 3.50-4.49 agree, and 4.50-5.00 strongly agree.

Table 3. Factor dimensions determining farmers' attitudes towards fertilizer use.

Tabla 3. Dimensiones de los factores que determinan las actitudes de las explotaciones en cuanto al uso de fertilizantes.

Dimension name	Variables	Av.	Factor loading
Health &Nature	Excessive use of phosphorus fertilizers harms human health	3.8606	0.904
	Excessive use of phosphorus fertilizers leads to water pollution	3.7394	0.881
	Excessive use of potassium fertilizers harms human health	3.9152	0.877
	Excessive use of phosphorus fertilizers harms animals	3.6606	0.852
	Excessive use of potassium fertilizers leads to water pollution	3.8182	0.851
	Excessive use of potassium fertilizers harms animals	3.6909	0.847
	Excessive use of phosphorus fertilizers damages soil fertility	3.9333	0.837
	Excessive use of potassium fertilizers damages soil fertility	3.9394	0.824
	Excessive use of nitrogenous fertilizers leads to water pollution	3.9818	0.810
	Excessive use of phosphorus fertilizers harms crops	3.9758	0.794
	Excessive use of potassium fertilizers harms crops	4.0364	0.781
	Excessive use of nitrogenous fertilizers harms human health	4.0545	0.780
	Excessive use of nitrogenous fertilizers damages soil fertility	4.2242	0.721
	Excessive use of nitrogenous fertilizers harms crops	4.2121	0.706
Materiality	If crop support increases, I will use more fertilizer	2.6121	0.911
	If fertilizer support increases, I will use more fertilizer	2.5879	0.906
	If I expect an increase in crop prices, I will use more fertilizer	2.6242	0.884
	If fertilizer price is low, I will use more fertilizer	2.6121	0.869

Note: derived from research. KMO: 0.782 Bartlett's Test of Sphericity: 6204.316682 Sig: 0.000 Variance Explained: 80.343.

Nota: derivado de la investigación. KMO: 0,782 Prueba de esfericidad de Bartlett: 6204,316682 Sig: 0,000 Varianza explicada: 80,343.

Usage behaviour for own-consumption crops	I use less phosphorus fertilizer to the crops I consume	2.1758	0.982
	I use less nitrogenous fertilizer to the crops I consume	2.1455	0.980
	I use less potassium fertilizer to the crops I consume	2.2424	0.969
Yield expectation	The more phosphorus fertilizer I use, the crop yield will increase	2.2000	0.903
	The more nitrogenous fertilizer I use, the crop yield will increase	2.2242	0.902
	The more potassium fertilizer I use, the crop yield will increase	2.2485	0.886
Necessity	If I do not use any phosphorus fertilizers, I will not be able to get any crop	3.3879	0.944
	If I do not use any potassium fertilizers, I will not be able to get any crop	3.4061	0.924
	If I do not use any nitrogenous fertilizers, I will not be able to get any crop	3.6606	0.914
Legal regulation	Those who use fertilizer consciously should be rewarded	3.9939	0.822
	Excessive fertilizer use should be penalised	3.2606	0.822
Awareness	I use fertilizer consciously	4.2364	0.823
	Environmentally friendly production is my primary goal	4.3576	0.748

Note: derived from research. KMO: 0.782 Bartlett's Test of Sphericity: 6204.316682 Sig: 0.000 Variance Explained: 80.343.

Nota: derivado de la investigación. KMO: 0,782 Prueba de esfericidad de Bartlett: 6204,316682 Sig: 0,000 Varianza explicada: 80,343.

Factor analysis generally requires sample sizes four or five times larger than the number of variables. This study used data from 165 farmers responding to 31 variables using the Likert scale. The hypothesis "the population correlation matrix is a unit matrix" was rejected based on Bartlett's Test of Sphericity (6204.316682). Additionally, the Kaiser-Meyer-Olkin (KMO) statistic was 0.782 (KMO ≥ 0.5), indicating that factor analysis was appropriate.

Seven identified factors explained 80.34% of variability, determining fertilizer use behaviour in the study area (table 3). The first factor, "health and nature" exerts the greatest influence and encompasses statements such as "Excessive use of fertilizers harms human health" "Excessive use of fertilizers leads to water pollution", "Excessive use of fertilizers harms animals" "Excessive use of fertilizers damages soil fertility", and "Excessive use of fertilizers harms crops".

The second factor, "materiality" includes statements as "If crop support increases, I will use more fertilizer", "If fertilizer support increases, I will use more fertilizer", "If I expect an increase in crop prices, I will use more fertilizer" and "If fertilizer price is low, I will use more fertilizer".

The third factor, "usage behaviour for own-consumption crops" includes the statements "I use less phosphorus/nitrogenous/potassium fertilizer to the crops I consume".

The fourth factor, called "yield expectation" has a weaker impact and is influenced by the statement "The more nitrogenous/phosphorus/potassium fertilizer I use, the crop yield will increase".

The fifth factor, referred to as "necessity" includes the statements "If I do not use any phosphorus/ potassium/nitrogenous fertilizers, I will not be able to get any crop."

The sixth factor, named "legal regulation" encompasses the statements "Those who use fertilizer consciously should be rewarded" and "Those who use excessive fertilizer should be penalised."

The final factor, called "awareness" has the least effect and involves "I use fertilizer consciously " and "Environmentally friendly production is my primary goal."

Farmers Classification According to Fertilizer Use Behaviour

Farmers were categorized according to factor dimensions. Cluster analysis identified four groups: "unconscious", "support oriented", "environment and health oriented" and "return oriented".

Each dimension represents distinct motivational or perceptual factors influencing fertilizer use behaviour. Table 4 includes individual items or statements grouped under factor dimensions. The Kruskal-Wallis test was applied to determine statistically significant differences among group regression scores. When examining dimensions determining fertilizer usage behaviour within different groups, variations arise in materiality, yield expectation, necessity, legal regulation, and awareness.

The "environment and health-oriented" group is the largest, comprising 38.8% of farmers. Farmers largely associate excessive use of fertilizers (phosphorus, potassium, and nitrogen) with negative consequences for soil, water, human and animal health. The environmental and health-oriented group generally reports higher agreement (scores around 4.2-4.5), suggesting stronger alignment with sustainability.

Table 4. Farmers' groups according to fertilizer use and behaviour dimensions.

Tabla 4. Grupos de agricultores según las dimensiones de uso de fertilizantes y comportamiento.

Statements / dimensions	Unconscious	Support oriented	Environment and health orientated	Return oriented
Health & Nature	**-0.25455**	**-0.24211**	**0.25255**	**0.02230**
Excessive use of phosphorus fertilizers harms human health	3.51	3.52	**4.25**	3.81
Excessive use of phosphorus fertilizers leads to water pollution	3.31	3.52	**4.09**	3.70
Excessive use of potassium fertilizers harms human health	3.54	3.48	**4.27**	4.05
Excessive use of phosphorus fertilizers harms animals	3.23	3.30	**4.19**	3.42
Excessive use of potassium fertilizers leads to water pollution	3.46	3.55	**4.22**	3.68
Excessive use of potassium fertilizers harms animals	3.26	3.27	**4.12**	3.70
Excessive use of phosphorus fertilizers damages soil fertility	3.60	3.67	**4.31**	3.81
Excessive use of potassium fertilizers damages soil fertility	3.60	3.52	**4.36**	3.90
Excessive use of nitrogenous fertilizers leads to water pollution	3.57	3.70	**4.34**	4.00
Excessive use of phosphorus fertilizers harms crops	3.63	3.85	**4.47**	3.51
Excessive use of potassium fertilizers harms crops	3.54	3.79	**4.56**	3.79
Excessive use of nitrogenous fertilizers harms human health	3.80	3.67	**4.30**	4.25
Excessive use of nitrogenous fertilizers damages soil fertility	4.00	3.85	**4.55**	4.23
Excessive use of nitrogenous fertilizers harms crops	3.80	4.06	**4.56**	4.16

Note: derived from research. * Significant for p<0.01 according to the Kruskal-Wallis test.

Nota: derivado de la investigación. * Significativo para p<0,01 según la prueba de Kruskal-Wallis.

Materiality*	**-0.26676**	**0.74373**	**-0.79963**	**1.09000**
If crop support increases. I will use more fertilizer	2.26	**4.21**	1.25	3.99
If fertilizer support increases. I will use more fertilizer	2.00	**4.36**	1.20	4.08
If I expect an increase in crop prices. I will use more fertilizer	2.40	**4.06**	1.33	3.90
If the fertilizer price is low. I will use more fertilizer	2.26	**4.27**	1.33	3.78
Usage behaviour for own consumption crops	**-0.07091**	**-0.00700**	**0.15503**	**-0.21845**
I use less phosphorus fertilizer to the crops I consume	1.91	2.33	**2.45**	1.77
I use less nitrogenous fertilizer to the crops I consume	1.89	2.27	**2.42**	1.77
I use less potassium fertilizer to the crops I consume	1.97	2.39	**2.45**	1.99
Yield expectation*	**0.12140**	**1.17888**	**-0.30481**	**-0.71648**
The more phosphorus fertilizer I use. the crop yield will increase	2.26	**4.21**	1.41	1.69
The more nitrogenous fertilizer I use. the crop yield will increase	2.31	**4.33**	1.42	1.60
The more potassium fertilizer I use. the crop yield will increase	2.29	**4.39**	1.48	1.57
Necessity	**0.01293**	**0.35980**	**0.09723**	**-0.56208**
If I do not use any phosphorus fertilizers. I will not be able to get any crop	3.29	**4.18**	3.52	2.49
If I do not use any potassium fertilizers. I will not be able to get any crop	3.11	**4.24**	3.55	2.64
If I do not use any nitrogenous fertilizers. I will not be able to get any crop	3.97	**4.33**	3.69	2.57
Legal regulation*	**-0.73179**	**0.13614**	**0.39622**	**-0.12842**
Those who use fertilizer consciously should be rewarded	2.63	**4.76**	4.47	3.76
Excessive fertilizer use should be penalised	2.23	3.36	**3.81**	3.21
Awareness*	**-1.05106**	**0.42491**	**0.30105**	**0.10599**
I use fertilizer consciously	3.11	4.52	**4.70**	4.26
Environmentally friendly production is my primary goal	3.40	**4.70**	4.62	4.55
Number of farmers	**35**	**33**	**64**	**33**
Percentage %	**21.2**	**20.0**	**38.8**	**20.0**
The rate of soil analysis (%)	**37.14**	27.27	31.25	24.24

Note: derived from research. * Significant for p<0.01 according to the Kruskal-Wallis test.

Nota: derivado de la investigación. * Significativo para p<0,01 según la prueba de Kruskal-Wallis.

Other items / statements				
Excessive use of nitrogenous fertilizers harms animals	3.43	3.39	**4.20**	3.95
Profit maximization is my primary goal	4.49	**4.79**	4.47	4.53
We must raise awareness about the harms of fertilizers	4.17	**4.88**	4.66	4.66
Soil analysis should be done for conscious fertilizer use	4.34	4.61	4.55	**4.72**
Expert advice should be taken and implemented for conscious fertilizer use	4.03	4.21	**4.73**	4.49
Soil analysis should be made mandatory by government	3.69	4.33	**4.34**	4.29
If there is no soil analysis support. I will not do soil analysis	3.29	**3.76**	2.95	3.42

Note: derived from research. * Significant for p<0.01 according to the Kruskal-Wallis test.

Nota: derivado de la investigación. * Significativo para p<0,01 según la prueba de Kruskal-Wallis.

Farmers in the "unconscious" group exhibit the lowest levels of awareness and legal regulation. Additionally, this group demonstrates a negative attitude towards "health and nature" "materiality" and "usage behaviour for own consumption crops".

Farmers in the second group, called "support oriented" exhibit positive behaviour towards "yield expectation", "necessity", "materiality", "legal regulation", and "awareness" in fertilizer use. In other words, farmers in this group have environmental concern, but use fertilizers to achieve higher yields. The "support oriented" group" highly rates statements regarding material incentives (*e.g.*, "If crop support increases, I will use more fertilizer") reflecting a reliance on external incentives, like subsidies. Conversely, the environment and health-oriented dimension scores are notably lower.

Farmers categorized as "environment and health-oriented" score higher than other groups in terms of "health and nature", "usage behaviour for own consumption crops" and "legal regulation". However, they hold negative attitudes towards "materiality" and "yield expectation" dimensions.

Farmers in the last group, "return oriented", have a strong positive association with the "materiality" dimension. Farmers in this group use fertilizers based on fertilizer price, crop price and subsidies.

Legal statements emphasize the importance of regulatory frameworks and awareness campaigns. The environment and health-oriented dimension strongly supports these initiatives, while the unconscious group disagrees. Notably, "I use fertilizer consciously" scores highest in the health-oriented group, underscoring commitment to sustainability.

Conclusion

This study identified farmers' fertilizer use behaviours in Izmir. We determined farmers' tendencies regarding fertilizer use behaviours, and environmental concern. Although farmers show moderate environmental sensitivity, they should gain further awareness.

Worldwide demand for food and the consequent demand for higher yields increase day by day. Fertilizers are emerging as an essential element for increased production. But excessive fertilizer use has negative technical, environmental and economic effects. Therefore, education and extension services should aim at raising consciousness, while the agricultural policies to be implemented should not only ensure economic sustainability in agricultural production but also incorporate environmentally friendly measures.

References

1. Aydin, B.; Ozkan, E.; Kayali, E.; Atav, V.; Gurbuz, M. A.; Kursun, I.; Kayhan, I. E. 2022. Comparative analysis of the opinions of the producers regarding fertilization practices and subsidies in Edirne and Tekirdağ Provinces. Journal of Agriculture Engineering. 374: 43-55.
2. Bynen, E. J. 1973. Cluster Analysis: Survey and Evaluation of Techniques. Tilburg University Press. 112p.
3. Cuhadar, M.; Atis, E. 2021. The analysis underlying factors affecting farmers' attitudes towards drought. Turkish Journal of Agriculture and Natural Sciences. 8(1): 1-7.
4. Eraslan, F.; Nal, A.; Gunes, A.; Erdal, I.; Coskan, A. 2010. Chemical fertilizer production and consumption status, problems, solution suggestions and innovations in Türkiye, Proceedings of Turkish Chamber of Agricultural Engineers; Agricultural Engineering VII. Technical Congress. Ankara. 955-972.
5. Etumnu, C.; Gray, A. W. 2020. A clustering approach to understanding farmers' success strategies. Journal of Agricultural and Applied Economics. 52(3): 335-351.
6. Gozener, B.; Sayili, M.; Yurdabakan, M. 2016. Fertilizer use condition in important products: Tokat city Kazova district example. Journal of Agricultural Faculty of Gaziosmanpasa University. 33(2): 41-47.
7. Hyland, J. J.; Jones, D. L.; Parkhill, K. A.; Barnes, A. P.; Williams, A. P. 2016. Farmers' perceptions of climate change: identifying types. Agriculture and Human Values. 33(2): 323-339.
8. Kadioglu, B. 2021. Investigation of possible links between soil pollution and chemical fertilizer use. Journal of Mus Alparslan University Agricultural Production and Technologies. 1(2): 26-38.
9. Kilic, O.; Eryilmaz, G. A.; Cakır, S. 2021. Environmental sensitivity of fruit producers toward chemical fertilizer and pesticide use in Zonguldak Province. Anadolu J Agr Sci. 36(1): 113-121.
10. Kiziloglu, R.; Kizilaslan, N. 2017. Fertilizer use the condition of cultivator province center in Kahramanmaras, Turkish Journal of Agriculture-Food Science and Technology. 5(1): 18-23.
11. Newbold, P. 1995. Statistics for business and economics. Prentice-Hall International, Upper Saddle River.
12. Nguyen, L. L. H.; Khuu, D. T.; Halibas, A.; Nguyen, T. Q. 2024. Factors that influence the intention of smallholder rice farmers to adopt cleaner production practices: An empirical study of precision agriculture adoption. Evaluation Review. 48(4): 692-735.
13. Ozalp, B.; Guldal, H. T. 2017. Sensitiveness of maize producers on to environmental and human health in terms of hybrid seed, chemical fertilizer and pesticide: case of Adana. Turkish Journal of Agricultural Economics. 23(1): 13-24.
14. Ozturk, M.; Altay, V.; Gonenç, T. M.; Unal, B. T.; Efe, R.; Akcicek, E.; Bukhari, A. 2021. An overview of olive cultivation in Turkey: botanical features, eco-physiology and phytochemical aspects. Agronomy. 11(2): 295.
15. Sipahi, C.; Kizilaslan, H. 2003. The study of acquire and apply chemical fertilizer on Artova area of Tokat province. Journal of Agricultural Faculty of Gaziosmanpasa University (JAFAG). 20(1): 17-25.
16. Turkes, M.; Sahin, S. 2024. Will olive groves have a future under climate change conditions in the North Aegean sub-region, a Mediterranean agricultural environment of Turkey? Turkish Journal of Agriculture-Food Science and Technology. 13(1): 43-58.
17. Wagan, S. A.; Memon, Q. U. A.; Chunyu, D.; Jingdong, L.; 2018. A comparative study on agricultural production efficiency between China and Pakistan using data envelopment analysis (DEA). Custos e Agronegocio on Line. 14: 169-190.
18. Wawire, A. W.; Csorba, Á.; Tóth, J. A.; Michéli, E.; Szalai, M.; Mutuma, E.; Kovács, E. 2021. Soil fertility management among smallholder farmers in Mount Kenya East region. Heliyon. 7(3).
19. Welte, E. 1973. Profitability and optimal use of mineral fertilizer in forms of different cropping potential. Pontificiae Academial Screntiarum Scripta Varia. 38: 403-426.
20. Yilmaz, H.; Demircan, V.; Gul, M. 2009. Determination of information sources of producers on chemical fertilizer use and evaluation in terms of agricultural extension. Journal of Suleyman Demirel University Faculty of Agriculture. 4(1): 31-44.

Funding

We are grateful to Ege University Scientific Research Projects Coordination (BAP) which was supported this study under the project number 2013-ZRF-017.

Conflict of Interest

The authors declare no competing interests.

Author Contribution Statement

All authors contributed equally to the design and implementation of the research, to the analysis of the results and to the writing of the manuscript.

First Record of Potential Vectors (Hemiptera: Auchenorrhyncha) of *Xylella fastidiosa* in Olive Groves from Argentina

Primer registro de potenciales vectores (Hemiptera: Auchenorrhyncha) de *Xylella fastidiosa* en olivares de Argentina

Bárbara S. Defea [1, 2 *], Angelo Mazzaglia [3], Susana L. Paradell [2], Gabriela Lucero [4], Álvaro Foieri [2], Pablo Pizzuolo [4], Oscar Peñaloza [5], Eduardo G. Virla [6], Stefano Speranza [3]

Originales: Recepción: 06/08/2025 - Aceptación: 15/04/2026 *Nota Científica*

ABSTRACT

This study aimed to identify potential vectors of the bacterium *Xylella fastidiosa* in olive orchards in La Rioja Province, Argentina. Hoppers (Hemiptera: Auchenorrhyncha) were collected during the spring of 2019 from localities with a high incidence of this pathogen in olive trees and associated spontaneous vegetation. Of the 14 species identified, eight tested positive for *X. fastidiosa* subsp. *pauca*. The ability to transmit this xylem-inhabiting bacterium is directly linked to the feeding habits of its vectors. The xylem-feeding species *Bucephalogonia xanthophis* (Berg), *Ciminius albolineatus* (Taschenberg), and *Notozulia entreriana* (Berg) tested positive and are confirmed carriers of *X. fastidiosa*. Consequently, these species may be considered potential vectors in olive orchards in La Rioja and represent suitable candidates for further epidemiological studies aimed at confirming their role as effective vectors of the bacterium.

Keywords

Cercopidae • Cicadellidae • Cicadellinae • molecular detection • olives • olive quick decline

https://doi.org/10.48162/rev.39.218

1 Centro de Estudios Parasitológicos y de Vectores (CONICET-UNLP-CICPBA). Boulevard 120 s/n (1900). La Plata. Buenos Aires. Argentina. * bdefea@cepave.edu.ar
2 Universidad Nacional de La Plata. Facultad de Ciencias Naturales y Museo. División Entomología. Av. 60 y 122 s/n (1900). La Plata. Buenos Aires. Argentina.
3 Università degli Studi della Tuscia. Dipartimento di Scienze Agrarie e Forestali. Italia.
4 Universidad Nacional de Cuyo. Facultad de Ciencias Agrarias. Almirante Brown 500 (M5528AHB). Chacras de Coria. Luján de Cuyo. Mendoza. Argentina.
5 Universidad Nacional de La Rioja. Centro de Investigación e Innovación Tecnológica. Argentina. Av. Luis M. De La Fuente S/N. Ciudad de La Rioja. La Rioja. Argentina.
6 Fundación Miguel Lillo - CONICET. Miguel Lillo 251 (T4000JFE). San Miguel de Tucumán. Tucumán. Argentina.

Licenses Creative Commons Attribution - Non Commercial - Share Alike

Resumen

El objetivo de este trabajo fue identificar vectores potenciales de la bacteria *Xylella fastidiosa* en plantaciones olivícolas de la provincia de La Rioja, Argentina. Las "chicharritas" (Hemiptera: Auchenorrhyncha) fueron recolectadas durante la primavera de 2019 en localidades con alta incidencia de este patógeno en plantas de olivos y la vegetación espontánea. De las 14 especies identificadas, ocho resultaron positivas para *X. fastidiosa* subsp. *pauca*. La capacidad de transmisión de esta bacteria, que se aloja en los vasos xilemáticos, está directamente relacionada con el hábito alimenticio de sus vectores. Las especies alimentadoras del xilema *Bucephalogonia xanthophis* (Berg), *Ciminius albolineatus* (Taschenberg) y *Notozulia entreriana* (Berg) resultaron positivas y se confirman como portadoras de *X. fastidiosa*. Consecuentemente, podrían considerarse como potenciales vectores de olivos en La Rioja y son las candidatas apropiadas para nuevos estudios epidemiológicos que permitan confirmar su rol como vectores de la bacteria.

Palabras clave

Cercopidae • Cicadellidae • Cicadellinae • detección molecular • olivos • declinamiento rápido del olivo

Introduction

Xylella fastidiosa Wells is a gram-negative bacterium belonging to the family Xanthomonadaceae that affects a wide range of plant species, including agricultural and ornamental crops worldwide (Redak *et al*., 2004). It has caused significant economic losses in South America and Europe (Castro *et al*., 2021) and represents a global threat to woodycrops (Rapicavoli *et al*., 2018). In the Americas, different subspecies of *X. fastidiosa* are associated with diseases such as Citrus Variegated Chlorosis, Pierce's disease of grapevine, and Olive Quick Decline (OQD), among others (Haelterman *et al*., 2015; Rapicavoli *et al*., 2018; Redak *et al*., 2004). In Argentina, citrus and almond crops are among the most affected (Carciofi *et al*., 2023; Nome *et al*., 1992). In 2013, the subspecies *pauca* was detected in olive plants, leading to significant losses in key production areas of La Rioja and Córdoba provinces (Haelterman *et al*., 2015). Olive orchards in Argentina cover approximately 67,000 ha, ranking second among fruit crops in cultivated area. La Rioja Province leads both planted area (26,000 ha) and production (138,000 t), followed by San Juan, Catamarca, and Mendoza provinces (FOA, 2024). In La Rioja, olive cultivation represents one of the oldest and most socioeconomically important productive sectors. Although Argentina is currently the leading producer and exporter of olive oil and table olives in the Americas, national production has declined in recent years. The incidence of *X. fastidiosa* in olive orchards in La Rioja (Arauco Department) has reached 100%, constituting a major phytosanitary constraint with a negative impact on local production (Ministerio de Desarrollo Productivo Argentina, 2022).

The main vectors of *X. fastidiosa* are two groups of xylem-sap-feeding hemipterans, commonly known as "sharpshooters" (Auchenorrhyncha: Membracoidea: Cicadellidae: Cicadellinae) and "spittlebugs" (Auchenorrhyncha: Cercopoidea: Aphrophoridae and Cercopidae) (Cornara *et al*., 2019; Redak *et al*., 2004). The ability to transmit this pathogen is directly linked to their feeding habits (Severin, 1950). Most species within Cicadellinae that have demonstrated the capacity to acquire and transmit *X. fastidiosa* have been confirmed as disease vectors in different crops, suggesting that all members of this subfamily may be considered potential vectors (Redak *et al*., 2004). Indeed, transmission may be a general trait of xylem-feeding insects, and all species with this feeding habit should be regarded as potential vectors (Lopes *et al*., 2014). In recent years, numerous additional vector species have been identified following outbreaks in olive production systems in Europe and South America (Cornara *et al*., 2019; Froza, 2022).

Information on the composition of xylem-feeding insect communities associated with olive orchards in Argentina is limited (Calahorra, 2023; Defea *et al*., 2019), and the vectors of Olive Quick Decline (OQD) in the region remain unknown. This knowledge gap has

hindered disease surveillance and the development of effective management strategies. This study aimed to confirm the presence of *X. fastidiosa* in Auchenorrhyncha species inhabiting affected olive orchards in La Rioja, Argentina.

Material and Methods

To achieve this objective, field surveys were conducted in two olive orchards severely affected by OQD-like symptoms in Aimogasta (28°35'34.90" S; 66°47'24.31" W; 825 m a. s. l.) and Villa Mazán (28°39'30.19" S; 66°31'54.38" W; 652 m a. s. l.), located 35 km apart in La Rioja Province, Argentina. Both orchards were planted with olive trees *cv.* Arauco, the cultivar most affected by OQD in the region (Tolocka *et al*., 2021). Surveys were carried out in mid-November 2019. Insects were collected using two methods: (1) sweep net sampling in the olive canopy and surrounding vegetation, and (2) light trapping using a halogen lamp and a sheet. For sweep net sampling, four trees per orchard were sampled, with four sets of 10 sweeps per tree. In addition, three 50 m transects were established in each orchard to sample spontaneous vegetation, with 100 sweeps per transect (300 sweeps per orchard). In total, seven sweep net samples were obtained per orchard per sampling date, amounting to 340 sweeps per orchard. For light trapping, a light sheet equipped with a halogen lamp was operated from 18 to 20 November, and insects were collected from twilight until 03:00 h using a manual aspirator. All captured hoppers were preserved in 70% ethanol and subsequently transferred to the laboratory for taxonomic identification and screening for *X. fastidiosa*.

Specimens were identified to the species level using the identification keys of Jones & Deitz (2009), Leal *et al.* (2016), Paladini *et al.* (2008), Young (1968, 1977), Zahniser & Dietrich (2013) and Zanol (2007). Male genitalia were dissected and cleared in 10% KOH for stereoscopic examination and subsequently preserved in glycerin. All material was deposited in the entomological collection of the Museo de La Plata, Argentina (UNLP).

For the molecular detection of *X. fastidiosa*, ethanol was carefully removed from the samples by evaporation, and insect heads were dissected from the body (Bextine *et al*., 2004) the almost exclusive foregut colonization of the bacterium (Janse & Obradovic, 2010). Heads were pooled by species, with up to five individuals per sample when available, resulting in a total of 15 samples for analysis. Total DNA was extracted using the NucleoSpin® DNA Insect kit (Macherey-Nagel, Germany) following the manufacturer's instructions.

Standard PCR reaction (25 µL) was prepared containing 12.5 µL of 2X PCR Master Mix (PCRBIO HS Taq Mix Red, PCRBIOSYSTEMS), 1 µL (400 nM) of forward primer RST31 (GCGTTAATTTTCGAAGTGATTCGATTGC), 1 µL (400 nM) of reverse primer RST33 (CACCATTCGTATCCCGGTG), 1 µL (~10 ng) of extracted DNA, and 9.5 µL of PCR-grade water. The thermic profile consisted of an initial denaturation at 95°C for 1 min, followed by 40 cycles at 95°C for 30 s, 55°C for 30 s, and 72°C for 45 s, with a final elongation at 72°C for 5 min (Minsavage *et al*., 1994). Amplicons were visualized by agarose gel electrophoresis after staining with GelRed® Nucleic Acid Gel Stain (10,000X; Biotium, Inc., USA). Samples were scored as positive when a single band of the expected size (733 bp) was clearly visible under UV light and as negative if no band or bands of different sizes were observed. DNA from *X. fastidiosa* subsp. *pauca* strain CoDiRO (CFBP 8402) served as a positive control, and PCR-grade water was used as a negative control.

It should be noted that the findings of this study were duly reported to the Servicio Nacional de Sanidad y Calidad Agroalimentaria (SENASA) through the Sistema Nacional de Vigilancia y Monitoreo de Plagas (SINAVIMO).

Results and Discussion

Due to extreme dryness during the sampling period, no hoppers were collected from olive trees or spontaneous vegetation using the sweep net method; therefore, all specimens analyzed in this study were obtained using the light sheet. A total of 324 individuals of Auchenorrhyncha were collected in La Rioja, Argentina (73 from Aimogasta and 251 from Villa Mazán). Cicadellidae was the most abundant family at both localities.

Thirteen leafhopper species and one Cercopid species were identified (table 1). The most abundant species were *Paratanus exitiosus* (Beamer), *Chlorotettix fraterculus* (Berg), and *Ciminius albolineatus* (Taschenberg), while *Curtara nebula* (Beamer) was present at both sites (table 1). In Aimogasta, four xylem-feeding species were recorded: *Bucephalogonia xanthophis* (Berg), *C. albolineatus*, *Molomea lineiceps* (Young), and *Scopogonalia osteiphera* Leal & Creão-Duarte. In contrast, in Villa Mazán, only the cercopid *Notozulia entreriana* (Berg) was identified as a xylem feeder, with the remaining species classified as phloem feeders. In Aimogasta, two known vectors of *X. fastidiosa*, *B. xanthophis* and *N. entreriana*, were detected, and *C. albolineatus* was associated with infected olive plants for the first time (figure 1, page 5). A similar species assemblage has previously been reported in Aimogasta (Defea *et al*., 2019) and Chilecito (Calahorra, 2023). Except for *Macugonalia cavifrons* (Stål), not collected in this study, the xylem-feeding species correspond to those reported by Defea *et al.* (2019). In Villa Mazán, the identified species were predominantly phloem feeders (except *N. entreriana*), belonging to the subfamilies Deltocephalinae, Iassinae, and Ledrinae (table 1). Previous studies suggest that Cicadomorpha community composition is influenced by local vegetation structure (Biedermann *et al*., 2005; Carpio *et al*., 2020). The predominance of phloem feeders, along with the presence of *N. entreriana* in Villa Mazán, may be associated with differences in vegetation cover and plant diversity between sites. The main weeds associated with olive orchards in this region belong to the families Asteraceae, Poaceae, and Solanaceae (Esteva *et al*., 2019), and include numerous species reported as hosts of *X. fastidiosa* by the European Foos Safety Authority Journal, such as *Bidens pilosa* L., *Sorghum halepense* (L.) Pers., *Cynodon dactylon* (L.) Pers., and *Hordeum vulgare* L., among others.

Table 1. Auchenorrhyncha species collected in olive crops severely affected by *Xylella fastidiosa* in La Rioja, Argentina, indicating those in which at least one specimen was infected with the bacterium.

Tabla 1. Especies de Auchenorrhyncha recolectadas en cultivos de olivo severamente afectados por *Xylella fastidiosa* en La Rioja, Argentina, en la cual se indican aquellas especies con al menos un ejemplar infectado con la bacteria.

Locality	Family	Subfamily (Tribe)	Species	Individuals	Positive for Xf
Aimogasta	Cicadellidae	Cicadellinae (Proconiini)	*Molomea lineiceps* (Young)	1	
		Cicadellinae (Cicadellini)	*Ciminius albolineatus* (Taschenberg)	46	(+)
			Bucephalogonia xanthophis (Berg)	2	(+)
			Scopogonalia osteiphera Leal & Creão-Duarte	13	
		Deltocephalinae (Opsiini)	*Opsius stactogalus* (Fieber)	4	
		Iassinae (Gyponiini)	*Curtara nebula* Delong & Freytag	7	
Villa Mazán	Cercopidae	Ichnorhininae	*Notozulia entreriana* (Berg)	3	(+)
	Cicadellidae	Deltocephalinae (Chiasmini)	*Exitianus obscurinervis* (Stål)	36	(+)
		Deltocephalinae (Hecalini)	*Spangbergiella vulnerata* (Uhler)	6	(+)
		Deltocephalinae (Athysanini)	*Paratanus exitiosus* (Beamer)	84	
		Deltocephalinae (Pendarini)	*Chlorotettix fraterculus* (Berg)	68	
		Iassinae (Gyponiini)	*Polana obliqua* Delong & Freytag	24	(+)



(A) *Bucephalogonia xanthophis*, (B) *Ciminius albolineatus*, (C) *Notozulia entreriana.*

Figure 1. Xylem-Feeding Auchenorrhyncha positive for *Xylella fastidiosa* in olive orchards of La Rioja, Argentina.

Figura 1. Auchenorrhyncha especialistas del xilema positivas para *Xylella fastidiosa* en olivares de La Rioja, Argentina.

The detection method enabled confirmation of *Xylella fastidiosa* subsp. *pauca* in multiple tested specimens (table 1, page 4). Fifty-seven percent of the identified species, including seven Cicadellidae and one Cercopidae, tested positive for the bacterium (table 1, page 4). Among the xylem-feeding species, *B. xanthophis*, *C. albolineatus* (both Cicadellini), and *N. entreriana* tested positive for *X. fastidiosa* (figure 1).

Our results are consistent with previous vector surveys and transmission studies conducted in olive groves in Italy (Cavalieri *et al*., 2018; Saponari *et al*., 2014), Brazil (Froza, 2022) and Spain (Lopes *et al*., 2014), which identified numerous species of sharpshooters and spittlebugs as the main vectors of this bacterium.

Among Cicadellinae, *B. xanthophis* is a well-known vector of *X. fastidiosa* to citrus in Brazil (Marucci *et al*., 2008) and a potential vector for coffee (Leite & Nunes, 2003). In Argentina, it has been confirmed as a carrier of the bacterium through DIVA and PCR analyses (de Coll *et al*., 2000; Dellapé *et al*., 2016) and is a predominant species in olive groves in Chilecito, La Rioja Province (Calahorra, 2023). Interestingly, in detection studies conducted on Brazilian olives, *B. xanthophis* tested negative for the bacterium (Froza, 2022). In contrast, *C. albolineatus* had not previously been associated with *X. fastidiosa* until the present study. Other Cicadellinae species, such as *C. platensis* (Berg) and *C. yana* (Young), have been reported on citrus in northern Argentina (Defea *et al*., 2022; Remes Lenicov *et al*., 1999). Further studies are required to determine the role of *C. albolineatus* in the spread of X. fastidiosa, as it was the most abundant xylem-feeding species collected that also tested positive for the bacterium.

Spittlebugs, previously considered marginal vectors, have gained increased attention following *X. fastidiosa* outbreaks in Europe, with *Philaenus spumarius* (L.) recognized as a key vector in olive crops (Cornara *et al*., 2017; Saponari *et al*., 2014). More recently, three cercopid species were confirmed as proven vectors of olives in Brazil (Froza, 2022). In the present study, *N. entreriana* was the only spittlebug collected and tested positive for *X. fastidiosa*, representing the first record of a Cercopid as a potential vector of this bacterium in Argentina.

The sharpshooter *M. lineiceps* was previously reported as positive for *X. fastidiosa* by conventional PCR in Entre Ríos Province (Dellapé *et al*., 2016). Along with *S. osteiphera*, these species have been documented as common inhabitants of olive crops in Aimogasta (Defea *et al*., 2019, 2022) and Chilecito (Calahorra, 2023). *Scopogonalia osteiphera* is abundant and frequently observed in the spontaneous vegetation of olive groves in Chilecito (Calahorra, 2023). In contrast, in the present study, both species were collected in low numbers, and all specimens tested negative for the bacterium. Nevertheless, given their reported presence in olive agroecosystems, they should be considered in future surveillance and transmission studies. The low abundance observed in our surveys may be attributed to the sparse vegetation present during the sampling period.

Numerous phloem-feeding species were collected in Villa Mazán (table 1, page 4). The leafhoppers *E. obscurinervis* (Stål), *P. exitiosus* (Beamer), and *C. fraterculus* (Berg) were among the most abundant. Notably, *Spangbergiella vulnerata* (Uhler), *Xerophloea viridis* (Fabricius), and *E. obscurinervis* are reported here for the first time in association with *X. fastidiosa*. Although previous studies have shown that phloem-feeding members of other Cicadellidae subfamilies may occasionally ingest xylem sap and acquire *X. fastidiosa*, their ability to transmit the bacterium has not yet been demonstrated (Ben Moussa *et al*., 2016; Chuche *et al*., 2017).

Conclusions

This study provides new insights into the epidemiology of *X. fastidiosa* in Argentine olive orchards. Further transmission assays are essential to confirm the species capable of acting as vectors and to identify those of epidemiological significance. In the absence of such information, effective vector monitoring and management strategies will remain limited, potentially compromising disease control and the health of olive production systems in Argentina.

References

Ben Moussa, I. E., Mazzoni, V., Valentini, F., Yaseen, T., Lorusso, D., Speranza, S. & D'Onghia, A. M. (2016). Seasonal fluctuations of sap-feeding insect species infected by *Xylella fastidiosa* in Apulian olive groves of southern Italy. *Journal of Economic Entomology, 109*(4), 1512-1518. DOI: 10.1093/jee/tow123

Bextine, B., Tuan, S. J., Shaikh, H., Blua, M., & Miller, T. A. (2004). Evaluation of methods for extracting *Xylella fastidiosa* DNA from the glassy-winged sharpshooter. *Journal of Economic Entomology, 97*(3), 757-763. DOI: 10.1093/jee/97.3.757

Biedermann, R., Achtziger, R., Nickel, H., & Stewart, A. J. (2005). Conservation of grassland leafhoppers: a brief review. *Journal of Insect Conservation*, *9*, 229-243. DOI: 10.1007/s10841-005-0531-z

Calahorra, M. A. (2023). *Monitoreo de Chicharritas y Salivazos Asociados al Agroecosistema Olivícola, Potenciales Vectores de Xylella fastidiosa en Chilecito, La Rioja (Insecta: Hemiptera: Cicadellidae, Cercopidae)*. [Tesis de Maestría, Universidad Nacional de Chilecito, Argentina]. https://repositorio.inta.gob.ar/xmlui/handle/20.500.12123/216/browse?authority=27227180086&type=author

Carciofi, I., Maspi N. & Guevara Lynch, J. P. (2023). *Cítricos dulces en Argentina. Antecedentes productivos, catalizadores tecnológicos y experiencias internacionales de la industria citrícola*. Documento N°39. Ministerio de Economía. Secretaría de Industria y Desarrollo Productivo.

Carpio, A. J., Solana, M., Tortosa, F. S., & Castro, J. (2020). Effect of cover crops in olive groves on Cicadomorpha communities. *Spanish Journal of Agricultural Research, 18*(2). DOI: 10.5424/sjar/2020182-15991

Castro, C., Di Salvo, B., & Roper, M. C. (2021). *Xylella fastidiosa*: A reemerging plant pathogen that threatens crops globally. *PLoS Pathogens, 17*(9), e1009813. DOI: 10.1371/journal.ppat.1009813

Cavalieri, V., Dongiovanni, C., Tauro, D., Altamura, G., Di Carolo, M., Fumarola, G., Saponari, M., & Bosco, D. (2018). Transmission of the CODIRO strain of *Xylella fastidiosa* by different insect species. In Proceedings *XI European Congress of Entomology*. Naples, Italy.

Chuche, J., Backus, E. A., Thiéry, D., & Sauvion, N. (2017). First finding of a dual-meaning X wave for phloem and xylem fluid ingestion: characterization of *Scaphoideus titanus* (Hemiptera: Cicadellidae) EPG waveforms. *Journal of Insect Physiology, 102*, 50-61. DOI: 10.1016/j. jinsphys.2017.01.013

Cornara, D., Cavalieri, V., Dongiovanni, C., Altamura, G., Palmisano, F., Bosco, D. & Saponari, M. (2017). Transmission of *Xylella fastidiosa* by naturally infected *Philaenus spumarius* (Hemiptera, Aphrophoridae) to different host plants. *Journal of Applied Entomology*, *141*(1-2), 80-87. DOI: 10.1111/jen.12365

Cornara, D., Morente, M., Markheiser, A., Bodino, N., Fereres, A., Redak, R. A. & Lopes, J. R. S. (2019). An overview on the worldwide vectors of *Xylella fastidiosa*. *Entomologia Generalis*, *39*(3-4), 157-181. DOI: 10.1127/entomologia/2019/0811

De Coll, O. R., Remes-Lenicov, A. M. M., Agostini, J. P., & Paradell, S. (2000). Detection of *Xylella fastidiosa* in Weedsand Sharpshooters in Orange Groves affected with Citrus Variegated Chlorosis in Misiones, Argentina. *International Organization of Citrus Virologists Conference Proceedings (1957-2010), 14*(14), 216-222. https://escholarship.org/uc/item/0x65j6dn

Defea, B., Foieri, A., & Paradell, S. (2019). Vectores de *Xylella Fastidiosa.* En Esteva Matías (Ed.), *Manual de protocolos de manejo de Plagas y patologías del olivo.* 155-172.

Defea, B., Virla, E. G., Logarzo, G. A., Cavichioli, R. R., Tapia, S., Aguirre, M. R. & Paradell, S. L. (2022). Contributions to the knowledge of the Cicadellini Sharpshooters (Hemiptera: Cicadellidae) associated with citrus orchards in Argentina. *Zootaxa, 5205*(1), 55-72. DOI: 10.11646/zootaxa.5205.1.4

Dellapé, G., Paradell, S., Semorile, L., & Delfederico, L. (2016). Potential vectors of *Xylella fastidiosa*: a study of leafhoppers and treehoppers in citrus agroecosystems affected by Citrus Variegated Chlorosis. *Entomologia Experimentalis et Applicata*, *161*(2), 92-103. DOI: 10.1111/eea.12491

Esteva, M., Banno, N., Bataglia M. J., Bonafede, F., Brizuela, M. G., Calahorra, M. A., Defea, B. S. (2019). *Manual de protocolos de manejo de plagas y patologías del olivo*. Consejo Federal de Inversiones.

FOA (Federación Olivícola Argentina). (2024). *Informe Olivícola 2018-2024*. https://federacionolivicolaargentina. com.ar/informes-anuales/

Froza, J. (2022). *Papel de espécies de cigarrinhas (Hemiptera: Auchenorrhyncha) na disseminação de Xylella fastidiosa em oliveira na Serra da Mantiqueira*. [Thesis PhD. Piracicaba, Brazil].

Gibin, D., Gutierrez Linares, A., Fasanelli, E., Pasinato, L., & Delbianco, A. (2023). Update of the Xylella spp. host plant database-systematic literature search up to 30 June 2023. *EFSA Journal, 21*(12), e8477. https://doi.org/10.2903/j.efsa.2023.8477

Haelterman, R. M., Tolocka, P. A., Roca, M. E., Guzmán, F. A., Fernández, F. D., & Otero, M. L. (2015). First presumptive diagnosis of *Xylella fastidiosa* causing olive scorch in Argentina. *Journal of Plant Pathology*, *97*(2), 393.

Janse, J. D., & Obradovic, A. (2010). *Xylella fastidiosa*: its biology, diagnosis, control and risks. *Journal of Plant Pathology, 92*(1), 35-148.

Jones, J. R., & Deitz, L. L. (2009). Phylogeny and systematics of the leafhopper subfamily Ledrinae (Hemiptera: Cicadellidae). *Zootaxa*, *2186*(1), 1-120. DOI: 10.11646/zootaxa.2186.1.1

Leal, A. H., Creão-Duarte, A. J., & Mejdalani, G. (2016). Taxonomic review of *Scopogonalia* Young, 1977 (Insecta: Hemiptera: Cicadellidae: Cicadellini) with description of six new species. *Journal of Natural History*, *50*(23-24), 1513-1542. DOI: 10.1080/00222933.2016.1166530

Leite, R. P., & Nunes, L. M. (2003). Avanços nas pesquisas sobre *Xylella fastidiosa* do café no Brasil. In *Produção integrada de café* (p. 87-101). Universidade Federal de Viçosa, Brazil.

Lopes, J., Landa, B., Fereres, A. (2014). A survey of potential insect vectors of the plant pathogenic bacterium *Xylella fastidiosa* in three regions of Spain. *Spanish Journal of Agricultural Research*, *12*(3), 795-800.

Marucci, R. C., Lopes, J. R., & Cavichioli, R. R. (2008). Transmission efficiency of *Xylella fastidiosa* by sharpshooters (Hemiptera: Cicadellidae) in coffee and citrus. *Journal of Economic Entomology*, *101*(4), 1114-1121. DOI: 10.1603/0022-0493(2008)101[1114:TEOXFB]2.0.CO;2

Ministerio de Desarrollo Productivo Argentina (2022). *Olivicultura en Argentina. Aprendiendo de la experiencia internacional: políticas públicas para el desarrollo sostenible del sector*. Doc.26. https://www.argentina.gob.ar/produccion/cep/consejo-cambio-estructural/documentos

Minsavage, G. V., Thompson, C. M., Hopkins, D. L., Leite, R. M. V. B. C. & Stall, R. E. (1994). Development of a polymerase chain reaction protocol for detection of *Xylella fastidiosa* in plant tissue. *Phytopathology*, *84*(5), 456-461. DOI: 10.1094/Phyto-84-456

Nome, S. F., Haelterman, R. M., Docampo, D. M., Prataviera, A. G., & Feo, L. D. V. D. (1992). Almond leaf scorch in Argentina. *Brazilian Phytopathology, 17*, 57-60.

Paladini, A., Carvalho, G. S., & Valério, J. R. (2008). Ultrastructure and redescription of *Notozulia entreriana* (Berg) (Hemiptera: Cercopidae). *Neotropical Entomology*, *37*, 552-557. DOI: 10.1590/S1519-566X2008000500008

Rapicavoli, J., Ingel, B., Blanco-Ulate, B., Cantu, D., & Roper, C. (2018). *Xylella fastidiosa*: an examination of a re-emerging plant pathogen. *Molecular plant pathology*, *19*(4), 786-800. DOI: 10.1111/mpp.12585

Redak, R. A., Purcell, A. H., Lopes, J. R., Blua, M. J., Mizell Iii, R. F., & Andersen, P. C. (2004). The biology of xylem fluid-feeding insect vectors of *Xylella fastidiosa* and their relation to disease epidemiology. *Annual Reviews in Entomology, 49*(1), 243-270. DOI: 10.1146/annurev.ento.49.061802.123403

Remes Lenicov, A. M., Paradell, S., De Coll, O., & Agostini, J. (1999). Cicadelinos asociados a citrus afectados por clorosis variegada (CVC) en la República Argentina (Insecta: Homoptera: Cicadellidae). *Revista de la Sociedad Entomologica Argentina*, *58*(3-4), 211-225.

Saponari, M., Loconsole, G., Cornara, D., Yokomi, R. K., De Stradis, A., Boscia, D. & Porcelli, F. (2014). Infectivity and transmission of *Xylella fastidiosa* by *Philaenus spumarius* (Hemiptera: Aphrophoridae) in Apulia, Italy. *Journal of Economic Entomology*, *107*(4), 1316-1319.

Severin, H. H. (1950). Spittle-insect vectors of Pierce's disease virus. II. Life history and virus transmission. *Hilgardia, 19*(11), 357.

Tolocka, P. A., Giolitti, F., Guzmán, F. A., Mattio, M. F., Nome, C. F., Ortega, L. I. & Haelterman, R. M. (2021). Caracterización de *Xylella fastidiosa* a partir de materiales vegetales y cepas aisladas de olivo (*Olea europaea* L.) e implementación de un sistema de diagnóstico serológico en Argentina. *Revista de investigaciones agropecuarias*, *47*(3), 380-389.

Young, D. A. (1968). Taxonomic Study of the Cicadellinae (Homoptera: Cicadellidae). Technichal Bulletin of Carolina Agricultural Experimental Station. North Carolina State University. (239, 281).

Young, D. A. (1977). Taxonomic study of the Cicadellinae (Homoptera: Cicadellidae). Part 2. New World Cicadellini and the genus Cicadella. Bulletin of Carolina Agricultural Experimental Station. North Carolina State University.

Zahniser, J. N., & Dietrich, C. (2013). A review of the tribes of Deltocephalinae (Hemiptera: Auchenorrhyncha: Cicadellidae). *European Journal of Taxonomy*, (45). DOI: 10.5852/ejt.2013.45

Zanol, K. (2007). Catalogue of the neotropical Deltocephalinae (Hemiptera: Cicadellidae). Part II-Tribe. *Acta Biol. Par., 36* (1-2): 1-46.

Acknowledgements

We thank the authorities of La Rioja Province for granting permission to collect insect specimens (Nº P4-00409-19). We are also grateful to PROIMI, and particularly to Dr. Mario Baigori, for providing access to laboratory facilities for the detection of *Xylella fastidiosa*. This work was supported by the Italian Ministry of Foreign Affairs and International Cooperation (MAECI), Italy, and the Universidad Nacional de La Plata, Argentina [11N/868].

Author contributions

BSD: conceptualization, taxonomic identification (Cicadelllinae), original draft preparation; AM and SS: molecular analysis and draft supervision; SP: taxonomic identification (Deltocephalinae, Iassinae), draft supervision; GL and PP: molecular detection, draft supervision; AF: taxonomic identification (Cercopidae), draft supervision; OP: field samplings; EV: fiel samplings, conceptualization and original draft preparation.

First Record of *Spintherophyta aurichalcea* (Germar, 1824) (Coleoptera: Chrysomelidae) Damaging *Ilex paraguariensis* (St. Hil.) Crops in Argentina

Primer registro de *Spintherophyta aurichalcea* (Germar, 1824) (Coleoptera: Chrysomelidae) dañando cultivos de *Ilex paraguariensis* (St. Hil.) en Argentina

Maria Elena Schapovaloff [1, 2*], Abel Nicolás Scherf [1], Marcos Rubén Costa [1], Maria Cecilia Gramajo [3], Diana Virginia Ohashi [4], Daniela Sofia Ayala [4]

Originales: *Recepción:* 20/12/2024 - *Aceptación:* 12/11/2025 *Scientific Note*

ABSTRACT

Ilex paraguariensis (St. Hil.), commonly known as yerba mate, is a native plant to South America and cultivated in Argentina, Brazil and Paraguay. In Argentina, yerba mate is produced and cultivated throughout the province of Misiones and northeastern Corrientes. Yerba mate is a major crop in this region, providing raw material for beverages and active compounds for the pharmaceutical industry. Yerba mate crops are attacked by different phytophagous insects that can cause significant damage. This study reports the first confirmed record of *Spintherophyta aurichalcea* (Germar, 1824) as a phytophagous insect damaging commercial *Ilex paraguariensis* plantations in Misiones and Corrientes provinces, Argentina.

Keywords
Phytophagous insects • crop damage • leaf bettles • herbivory • yerba mate

https://doi.org/10.48162/rev.39.206

1 Instituto Nacional de Tecnología Agropecuaria (INTA). EEA Montecarlo. Av. El Libertador 2472. N3384. Montecarlo. Misiones. Argentina.
2 Consejo Nacional de Investigaciones Científicas y Técnicas (CONICET). Godoy Cruz 2290. C1425FQB. Ciudad Autónoma de Buenos Aires Argentina. * schapovaloff.maria@inta.gob.ar
3 Fundación Miguel Lillo. Miguel Lillo 251. T4000JFD. San Miguel de Tucumán. Tucumán. Argentina.
4 Instituto Nacional de Tecnología Agropecuaria (INTA). EEA Cerro Azul. Ruta Nacional 14. Km. 1085. N3313 Cerro Azul. Misiones. Argentina.

Licenses Creative Commons Attribution - Non Commercial - Share Alike

Resumen

Ilex paraguariensis (St. Hil.), comúnmente conocida como yerba mate, es una planta originaria de Sudamérica y se cultiva en Argentina, Brasil y Paraguay. En Argentina la yerba mate se produce y cultiva en toda la provincia de Misiones y nordeste de la provincia de Corrientes. La yerba mate es un cultivo importante en esta región, proporcionando materia para bebidas y compuestos activos para la industria farmacéutica. Los cultivos de yerba mate son atacados por distintos insectos fitófagos que pueden ocasionar daños significativos. Este estudio reporta el primer registro confirmado de *Spintherophyta aurichalcea* (Germar, 1824) como insecto fitófago que daña plantaciones comerciales de *Ilex paraguariensis* en las provincias de Misiones y Corrientes, Argentina.

Palabras clave

Insectos fitófagos • daños a los cultivos • escarabajos de las hojas • herbivoría • yerba mate

Introduction

Yerba mate (*Ilex paraguariensis* St. Hil.) is a South American native crop, primarily cultivated in Brazil, Paraguay, and Argentina. Within Argentina, its production is concentrated across the entire province of Misiones and northeastern Corrientes, where it represents one of the region's most significant agricultural activities (2, 6). According to data from the Instituto Nacional de la Yerba Mate (INYM), in April 2025, 25,050,144 kg of yerba mate were distributed to the domestic market, and 3,482,132 kg were exported. Notably, the amount leaving the mills is considered a reliable indicator of product performance on store shelves (13).

Yerba mate provides raw material for beverages and bioactive compounds for the pharmaceutical industry (5, 11). Infusions of leaves are widely consumed as *mate* or *chimarrão* (hot) and *tererê* (cold) in Argentina (11), southern Brazil, Paraguay, and Uruguay. In addition to these traditional uses, yerba mate has recently been processed into beer, moisturizing creams, sweets, and other non-traditional products, contributing to its growing global popularity (29).

The expansion of yerba mate monocultures has promoted the growth of phytophagous insect populations while reducing natural enemies. As a result, some insects have shifted from occasional visitors to economically significant pests (5, 10). Iede and Machado (1989) reported 86 insect species feeding on different parts of the yerba mate plant. However, only a few are considered pests, since most occur at low population levels and cause no economic damage. According to these authors, six species are currently recognized as pests: *Hedypathes betulinus* (Klug, 1825), *Isomerida picticollis* (Bates, 1881) (Coleoptera: Cerambycidae), *Gyropsylla spegazziniana* (Lizer, 1919) (Hemiptera: Aphalaridae), *Thelosia camina* (Schaus, 1896) (Lepidoptera: Apatelodidae), *Hylesia nigricans* (Berg, 1875) (Lepidoptera: Saturniidae), and *Ceroplastes grandis* (Hempel, 1900) (Hemiptera: Coccidae) (10, 12).

The family Chrysomelidae is among the five largest Coleoptera families and ranks second among phytophagous beetles (20). Their diversity, global distribution, and feeding habits confer significant ecological and economic importance (4).

The genus *Spintherophyta* Dejean, 1836 (= *Chrysodina* Baly, according to Monrós & Bechyné, 1956), within the subfamily Eumolpinae, is widely distributed in Central and South America (24), with some species present in North America (21). About 100 species have been described (23), but information on host plants is limited (25). Species of *Chrysodina* [sic] have been reported as apple tree defoliators in Brazil (22), while in Argentina *Spintherophyta* spp. have been recorded as floral visitors of sunflower (*Helianthus annuus*) (27, 28).

The objective of this study was to report the presence and identification of a Chrysomelidae species damaging commercial *Ilex paraguariensis* crops in Argentina.

Materials and Methods

Entomofaunal monitoring was conducted in commercial yerba mate plantations at 14 sites in Misiones Province and four sites in Corrientes Province (figure 1). A small beetle species was observed from September to May during the 2021/2022 and 2022/2023 growing seasons.

The map was generated using QGIS software (v.3.24), based on data from the geographic information system of yerba mate in the Argentine Republic (INYM) and OpenStreetMap.

El mapa fue generado por los autores utilizando el software QGIS (v.3.24), con base en datos del sistema de información geográfica de la yerba mate en la República Argentina (INYM) y OpenStreetMap.



Source/Fuente: IGN

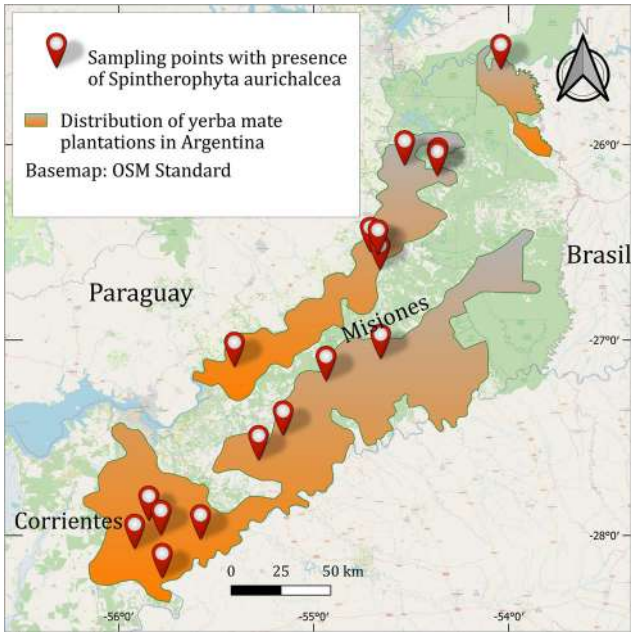
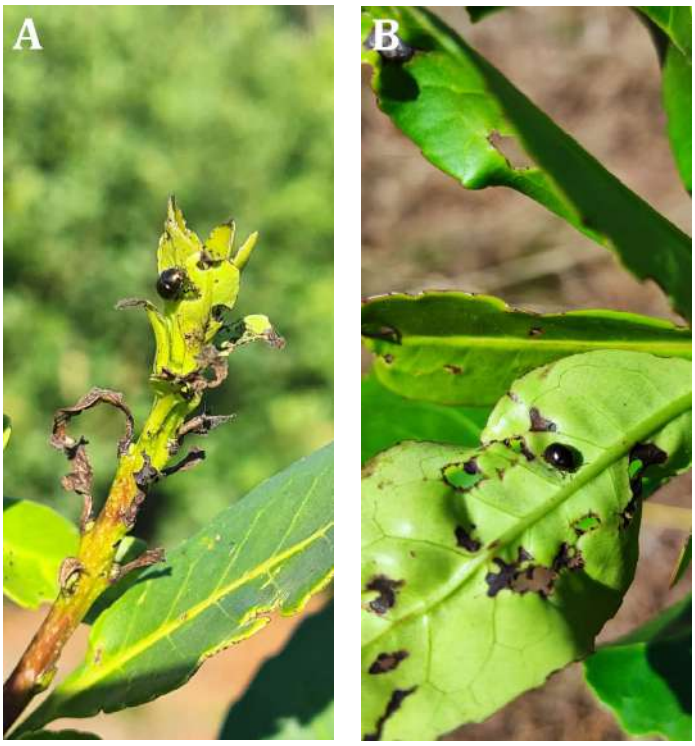


Figure 1. Sampling sites across the yerba mate cultivation area in Argentina.
Figura 1. Ubicación de los sitios de muestreo en la zona de cultivo de yerba mate en Argentina.

Adult specimens were manually collected, placed in plastic bags, and transported to the laboratory of the Montecarlo Agricultural Experimental Station of the National Institute of Agricultural Technology (INTA - EEA Montecarlo). Specimens were sent to the Miguel Lillo Foundation (FML) for taxonomic identification. Due to limited literature on this genus, the specialist compared the material with reference collections originally identified by Monrós (1951) and with the original species description by Germar (1824). All specimens were pinned and deposited in the beetle collections of the Miguel Lillo Fundation (San Miguel de Tucumán, Tucumán, Argentina) and INTA - EEA Montecarlo (Montecarlo, Misiones, Argentina).

Results and Discussion

Small beetles were collected during the sampling seasons at the 18 monitored sites in Misiones and Corrientes Provinces (figure 1). These insects caused visible damage to both young and mature yerba mate plants. The beetles were first observed feeding on tender shoots, gnawing the epidermis of apical buds. As the leaves developed, necrotic lesions appeared, resulting in characteristic damage to shoots and leaves, including necrotic and perforated areas (figure 2, page 4).



Damage to shoots (A) and damage to mature leaves (B).

Daños en brotes (A) y daños en hojas maduras (B).

Figure 2. Damage caused by *Spintherophyta aurichalcea* (Germar, 1824) to yerba mate plants.

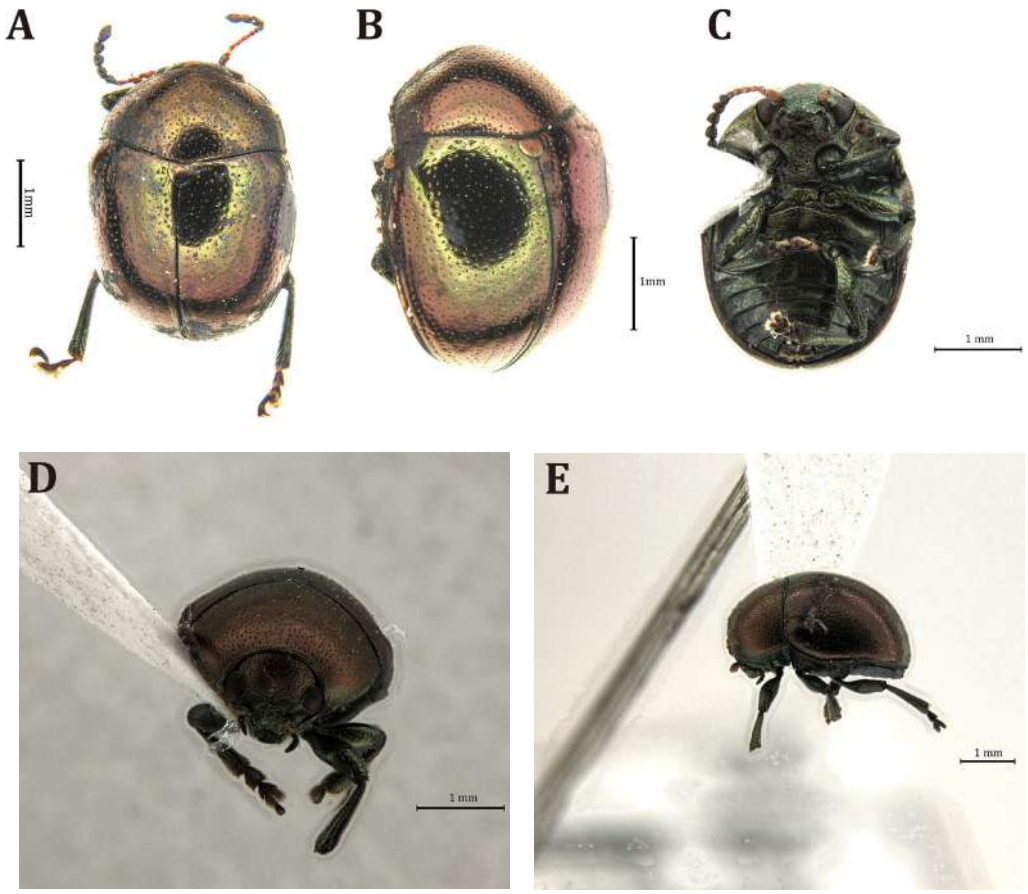
Figura 2. Daños causados por *Spintherophyta aurichalcea* (Germar, 1824) a las plantas de yerba mate.

The subfamily Eumolpinae, within the family Chrysomelidae, known as leaf beetles, comprises 12 tribes, nearly 500 genera, and approximately 7,000 species worldwide (1, 14, 24). These beetles occur on all continents except Antarctica, with a predominance in tropical and subtropical regions (14, 26). Species identification and description within many genus of Eumolpinae remain challenging (19). The considerable diversity of this group is reflected in persistent difficulties in its taxonomic classification, which several authors have described as chaotic and disorganized (8, 9, 18).

Currently, *S. aurichalcea* is classified within the genus *Spintherophyta* Dejean, 1836. It has also been referred to as [= *Chrysodina aurichalcea ab. pseudofulgurans*] Bechyné, 1949: 476; Bechyné, 1953: 128. Another species of this genus, *S. semiaurata* (Klug, 1829), has been reported in Argentina in the provinces of Córdoba, Misiones, Entre Ríos, and Buenos Aires (3). Adults of this species have been reported feeding on hibiscus flowers (*Hibiscus curtifolia L.*), peach (*Prunus persica* L.), *Citrus sp.*, blueberries and *Prosopis* sp. In Brazil, *S. semiaurata* has also been reported feeding on *I. paraguariensis*, *Prosopis* sp., strawberry flowers (*Fragaria x ananassa*), citrus (*C. sinensis, C. limon, C. reticulata*, *C. nobilis*), persimmon (*Diospyros kaki*), apple (*Malus domestica*), peach *(Prunus persica),* nectarine (*Prunus persica* var *nucipersica*), and pear (*Pyrus communis*) (12, 15, 30, 31).

Given the limited knowledge surrounding *Spintherophyta* bioecology, further research into its life cycle, natural enemies, and economic impact on yerba mate crops is essential to determine if pest control measures are necessary.

All specimens were identified as *Spintherophyta aurichalcea* (Germar, 1824) (Coleoptera: Chrysomelidae: Eumolpinae) (figure 3). This is the first report of *S. aurichalcea* causing direct damage to both nursery seedlings and mature commercial plantations of *Ilex paraguariensis* in Argentina, and, according to the available literature, the species has not previously been recorded affecting any other major crop in the country. Therefore, developing a quantitative assessment of the symptoms and damage caused by *S. aurichalcea* would be highly valuable for yerba mate cultivation, as demonstrated in recent work on the soybean black weevil, *Rhyssomatus subtilis* Fiedler (Coleoptera: Curculionidae) (17).



Dorsal view (A), semi-dorsal view (B), ventral view (C), front view (D) and lateral view (E).

Vista Dorsal (A), vista semidorsal (B), vista ventral (C), vista frontal (D) y vista lateral (E).

Figure 3. Habitus of a *Spintherophyta aurichalcea* Adult.
Figura 3. Hábito de un *Spintherophyta aurichalcea* adulto.

Conclusions

This study provides the first record of *Spintherophyta aurichalcea* (Germar, 1824) (Coleoptera: Chrysomelidae: Eumolpinae) damaging commercial *Ilex paraguariensis* crops in Argentina. The beetle was found feeding on both young shoots and mature leaves, causing necrotic and perforated areas that may compromise plant growth. Given the scarce knowledge of the bioecology of this genus, further studies are required to assess its life cycle, population dynamics, natural enemies, and potential economic impact on yerba mate production. These findings provide essential information, which results crucial for developing future monitoring and integrated pest management strategies.

References

1. Bouchard, P.; Bousquet, Y.; Davies, A.; Alonso-Zarazaga, M.; Lawrence, J.; Lyal, C.; Newton, A.; Reid, C.; Schmitt, M.; Slipinski, A.; Smith, A. 2011. Family- group names in Coleoptera (Insecta). ZooKeys. 88: 1-972. https://doi.org/10.3897/zookeys.88.807
2. Burgos, A.; Cabrera, M.; Capellari, P.; Dalurzo, H.; Dávalos, M.; Dirchwolf, P.; Dolce, N.; Fediuk, A.; Llera, V.; Maiocchi, M.; Medina, R.; Molina, S.; Pinto Ruiz, G.; Mayol M.; Tarragó, J.; Yacovich, M. 2017. Yerba mate. Reseña Histórica y Estadística. Producción e Industrialización en el siglo XXI. Ciudad Autónoma de Buenos Aires: Consejo Federal de inversiones. 310 p.
3. Cabrera, N.; Rocca, M. 2012. First records of Chrysomelidae (Insecta, Coleoptera) on blueberries in Argentina: New associations between native chrysomelids and an exotic crop. Revista de la Sociedad Entomológica Argentina. 71(1-2): 45-55.
4. Chaboo, C. 2007. Biology and phylogeny of the Cassidinae Gyllenhal *sensu lato* (tortoise and leaf-mining beetles) (Coleoptera: Chrysomelidae). Bulletin of the American Museum of Natural History. New York. 305: 1-250.
5. Chiaradia, L.; Milanez, J.; Zidko, A. 2002. Estimativa das gerações anuais de *Gyropsylla spegazziniana* (Lizer, 1917) em função de sua exigência térmica. Ciência Rural. 32(3): 385-391.
6. Daniel, O. 2009. Erva-mate: sistema de produção e processamento industrial. Dourados. MS. Universidade Federal da Grande Dourados. 288 p.
7. Germar, E. 1824. Insectorum species: novae aut minus cognitae, descriptionibus illustratae. Volumen primum, Coleoptera. Halae, Impensis J. C. Hendelii et Filii. 25: 624 p. II plates.
8. Gómez-Zurita, J.; Jolivet, P.; Vogler, A. 2005. Molecular systematics of Eumolpinae and the relationships with Spilopyrinae (Coleoptera, Chrysomelidae). Molecular phylogenetics and evolution. 34(3): 584-600. https://doi.org/10.1016/j.ympev.2004.11.022
9. Gómez-Zurita, J. 2018. Description of *Kumatoeides* gen. nov. (Coleoptera: Chrysomelidae, Eumolpinae) from New Caledonia. Zootaxa. 4521(1): 89-115. https://doi.org/10.11646/zootaxa.4521.1.4
10. Grigoletti Jr. A.; Auer, C.; Iede, E.; Soares, C. 2000. Manual de identificação de pragas e doenças da erva mate (*Ilex paraguariensis* St. Hil.). Colombo: Embrapa Florestas. Documentos. 44. 24 p.
11. Heck, C.; Mejia, E. 2007. Yerba mate tea (*Ilex paraguariensis*): A comprehensive review on chemistry, health implications, and technological considerations. Journal of Food Science. 72(9): 138-151.
12. Iede, E.; Machado, D. 1989. Pragas da erva-mate (*Ilex paraguariensis* St. Hil.) e seu controle. Boletim de Pesquisa Florestal. 18: 51-60.
13. Instituto Nacional de la Yerba Mate (INYM). (2025, June 12). https://www.inym.org.ar/
14. Jolivet, P.; Verma, K. 2008. Eumolpinae - a widely distributed and much diversified subfamily of leaf beetles (Coleoptera, Chrysomelidae). Terrestrial arthropod reviews. 1(1): 3-37. https://doi.org/10.1163/187498308X345424
15. Milleó, J.; Tesserolli de Souza, J.; Freitas Barbola, I.; Azevedo Moura, L.; Baer Pucci, M. 2013. Diversidade e sazonalidade de crisomelídeos (Coleoptera: Chrysomelidae) em pomar, no município de Ponta Grossa. Revista Brasileira de Fruticultura. 35(2): 454-463.
16. Monrós, F.; Bechyné J. 1956. Üeber einige verkannte Chrysomeliden-Namen. Entomologische Arbeiten aus dem Museum G. Frey. 7: 1118-1137.
17. Peralta, C. R.; Rinero, M.; Igarzábal, D. A.; De Rossi, R. L. 2025. First Report of the Black Soybean Weevil *Rhyssomatus subtilis* Fiedler (Coleoptera: Curculionidae) in Córdoba, Argentina. Crop Damage Estimation. Revista de la Facultad de Ciencias Agrarias. Universidad Nacional de Cuyo. Mendoza. Argentina. 57(2): 138-147. DOI: https://doi.org/10.48162/rev.39.177
18. Reid, C. 1995. A cladistic analysis of subfamilial relationships in the *Chrysomelidae sensu lato (Chrysomeloidea)*. In: Pakaluk, J., Slipinski, S.A. (Eds.), Biology, Phylogeny and Classification of Coleoptera. Papers Celebrating the 80th Birthday of Roy A. Crowson. Muzeum i Instytut Zoologii PAN. Warszawa. 559-631.
19. Riley, E. 2020. A review of the *Colaspis suilla* species group, with description of three new species from Florida (Coleoptera: Chrysomelidae: Eumolpinae). Insecta Mundi. 0830: 1-21.
20. Riley, E.; Clark, S.; Flowers, R.; Gilbert, A. 2002. Chrysomelidae Latreille 1802. In: Arnett, R., Thomas, M., Skelley, P., & Frank, H. (Eds.). American Beetles volume II: Polyphaga: Scarabaeoidea through Curculionoidea. CRC. Press LLC. 2: 617-691.
21. Riley, E.; Clark, S.; Seeno, T. 2003. Catalog of the leaf beetles of America north of Mexico (Coleoptera: Megalopodidae, Orsodacnidae and Chrysomelidae, excluding Bruchinae). The Coleopterists Society, Special Publication. 1: 1-290.
22. Santos, J.; Gonçalves, P. 2009. Principais insetos-pragas e inimigos naturais no sistema de produção orgânica de maçãs. Revista Brasileira de Agroecología. 4: 307-311.
23. Schultz, W. 1976. Review of the genus *Spintherophyta* (Coleoptera: Chrysomelidae) in North America North of Mexico. Annals of the Entomological Society of America. 69(5): 877-881.
24. Seeno, T.; Wilcox, J. 1982. Leaf beetle genera (Coleoptera: Chrysomelidae). Entomography. 1: 1-221.
25. Staines junior C. 1991. A host plant for adult *Spintherophyta globosa* (Olivier) (Coleoptera: Chrysomelidae). The Coleopterists Bulletin. 45(2): 200.
26. Strother, M.; Staines, C. L. 2008. A revision of the New World genus Fidia Baly 1863 (Coleoptera: Chrysomelidae: Eumolpinae: Adoxini). Zootaxa. 1798: 1-100. https://doi.org/10.11646/ xootaxa. 1798.1.1

27. Torreta, J.; Navarro, F.; Medan, D. 2009. Visitantes florales nocturnos del girasol (*Helianthus annuus*, Asterales: Asteraceae) en la Argentina. Revista de la Sociedad Entomológica Argentina. 68(3-4): 339-350.
28. Torreta, J.; Medan, D.; Roig Alsina, A.; Montaldo, N. 2010. Visitantes florales diurnos del girasol (*Helianthus annuus*, Asterales: Asteraceae) en la Argentina. Revista de la Sociedad Entomológica Argentina. 69(1-2): 17-32.
29. Vieira, M.; Rovaris, A.; Maraschin, M.; De Simas, K.; Pagliosa, C.; Podestá, R.; Amboni, R.; Barreto, P.; Amante, E. 2008. Chemical characterization of candy made of Erva-Mate (*Ilex paraguariensis* A. St. Hil.) residue. Journal of Agricultural and Food Chemistry. 56(12): 4637-4642. https://doi.org/10.1021/jf8011085
30. Ward, C.; O'Brien C.; O'Brien L.; Foster, D.; Huddleston, E. 1977. Annotated checklist of New World insects associated with Prosopis (Mesquite). Technical Bulletin. 1557: 115 p.
31. Zawadneak, M.; Rosado Neto, G.; Schuber, J.; Parchen, H. 2011. First Record of *Spintherophyta semiaurata* (Klug) (Coleoptera: Chrysomelidae) damaging strawberry flowers. Neotropical Entomology. 40(3): 407-408.

Acknowledgments

We thank Lic. Silvia Cordoba from the Institute the Entomology, Miguel Lillo Fundation (FML) for identifying the specimens.

Conflicts of Interest

The authors declare that they have no conflicts of interest.

Critical Point Analysis for Sustainable Management of *Cydia pomonella* (Lepidoptera: Tortricidae) in Smallholder Walnut Farms of Catamarca, Argentina

Análisis de puntos críticos en la sustentabilidad del manejo de *Cydia pomonella* (Lepidoptera: Tortricidae) en pequeñas producciones nogaleras de Catamarca, Argentina

María José Cavallo [1], María Cecilia Castilla [1, 2], Lucas Ariel Barros [1, 3], Oscar Eduardo Romero [4], Braian Vladimir Sosa [1], Martin Sebastian Espinosa [5, 6], Patricia Alejandra Diez [1, 5*]

Originales: *Recepción:* 28/02/2025 - *Aceptación:* 21/07/2025

ABSTRACT

In Argentina, 80% of walnut production is carried out by smallholder farms facing poor technology, production constraints, and substantial economic losses due to pests like *Cydia pomonella* (codling moth). We assessed sustainability risks linked to phytosanitary management on small farms in the Ambato region of Catamarca, Argentina. Our analysis included a "strong sustainability" framework with three key dimensions: ecological, economic, and sociocultural. A total of 26 indicators were related to this species' management. Using semi-structured interviews, visual aids, and field surveys across seven farms, an overall sustainability index of 1.521 was calculated, with 50% of the indicators scoring below the established threshold (on a five-level sustainability scale, the selected threshold was level two). The ecological dimension emerged as the most sustainable. Limitations included absent systematic monitoring and optimisation of treatment timing, solely with agrochemical control, weak farmer-to-farmer collaboration, and insufficient training opportunities. Cluster analysis revealed four distinct groups based on phytosanitary practices. This study highlights critical intervention points and suggests agroecological strategies to enhance sustainable pest management in smallholder walnut systems.

Keywords
codling moth • Phytosanitary management • sustainability • *Juglans regia*

https://doi.org/10.48162/rev.39.197

1 Centro Regional de Energía y Ambiente para el Desarrollo Sustentable (CONICET-UNCA). Laboratorio de Control Biológico y Biodiversidad de Insectos. C. P. 4700. Prado 366. Catamarca. Argentina.
2 Universidad Nacional de Tucumán. Facultad de Ciencias Naturales e Instituto Miguel Lillo. Instituto de Investigaciones de Biodiversidad Argentina. C. P. 4000. Miguel Lillo 251. Tucumán. Argentina.
3 Universidad Nacional de Catamarca. Facultad de Ciencias Agrarias. Cátedra Cultivos Industriales. Depto. Producción Vegetal. C. P. 4700. Av. Belgrano 300. Catamarca. Argentina.
4 Universidad Nacional de Catamarca. Facultad de Ciencias Agrarias. Cátedra Climatología agrícola. Depto. Clima, Suelo y Riego. Catamarca. Argentina.
5 Universidad Nacional de Chilecito. Departamento de Ciencias Básicas y Tecnológicas. C. P. 5360. 9 de Julio 22. Chilecito. La Rioja. Argentina. * diezpatriciaa@gmail.com
6 Consejo Nacional de Investigaciones Científicas y Técnicas. C1425FQB. Godoy Cruz 2290. Buenos Aires. Argentina.

Licenses Creative Commons
Attribution - Non Commercial - Share Alike

Resumen

En Argentina, el 80% del sector nogalero está representado por pequeños productores, con bajo nivel tecnológico, limitaciones en la producción y presencia de especies plaga como *Cydia pomonella* ("carpocapsa"), entre otros. Se evaluaron los riesgos a la sustentabilidad del manejo fitosanitario de *C. pomonella* en minifundios de Ambato (Catamarca, Argentina), considerando tres dimensiones: ecológica, económica y sociocultural, bajo un enfoque de sustentabilidad fuerte. Se identificaron 26 indicadores relacionados con el manejo de esta especie. Mediante encuestas semiestructuradas, cartillas visuales y relevamientos en siete fincas, se determinó un Índice de sustentabilidad general de 1.521, con el 50% de los indicadores por debajo del umbral establecido (de una categorización de sustentabilidad según una escala de cinco puntos, el valor umbral seleccionado fue de dos). La dimensión ecológica fue la más destacada en términos de sustentabilidad. Las limitaciones encontradas en la práctica fitosanitaria incluyeron la falta de monitoreo de *C. pomonella* que definan momentos oportunos de control, el uso de agroquímicos como única herramienta de control, ausencia de interacción entre productores y falta de capacitaciones en fitosanidad. Mediante análisis de clúster se evidenciaron cuatro grupos según sus prácticas fitosanitarias. Se detectaron puntos críticos y propusieron herramientas para promover prácticas agroecológicas para un manejo sustentable.

Palabras clave

carpocapsa • manejo fitosanitario • sustentabilidad • *Juglans regia*

Introduction

Developing sustainable agriculture requires long-term flow of goods and services to meet nutritional, socio-economic, and cultural needs, within biophysical limits defined by the natural system supporting production. Sustainability encompasses multiple, interrelated objectives that demand multidisciplinary approaches (44, 50). Understanding sustainability enables evaluating and mitigating production-based environmental impacts, while accounting for market fluctuations and supply chain vulnerabilities (21). Sustainable systems must be productive, stable, resilient, and adaptable, distributing costs and benefits equitably and fostering autonomous decision-making among stakeholders (3).

Agricultural landscapes are not isolated. Production units and the environment constitute a continuous agroecosystem. Native vegetation refuges natural enemies of insect pests, supporting biodiversity. Ecological services like biotic regulation, nutrient cycling, and pollination must be managed to maintain a dynamic equilibrium between native and introduced components (32). This management depends on farmers' knowledge and decisions (49).

Walnuts (*Juglans regia* L.) represent a major agricultural sector in Argentina. Catamarca province ranks second in national walnut production, with 4063 hectares cultivated and 2619.9 tonnes annually (47). The sector comprises a range of production systems, from large-scale farms (20%) to smallholder (80%) (29, 32, 37). These last producers manage fewer than five hectares with limited technological inputs and modest yields. Challenges such as water scarcity, labour shortage, and high logistical costs hinder sustainable practices in the region. Changes in organization of the productive sector related to financing and self-management affect marketing (16).

One productivity constraint is the codling moth (*Cydia pomonella* (Linnaeus, 1758); Lepidoptera: Tortricidae), a major pest responsible for 40% to 60% yield losses (14). Larvae penetrate fruit after hatching, causing economic damage. Conventional management relies on calendar-based applications of organophosphates and pyrethroids (8), which have led to pest resistance, environmental and biodiversity degradation while risking human health (19). Alternative control strategies, including mating disruption, biopesticides, and parasitoid-based biological control, have not been widely adopted (10, 18, 25).

Transitioning towards sustainable agriculture needs robust methodologies for sustainability assessment. These assessments must be context-sensitive, cost-effective, and capable of identifying critical constraints at different spatial scales

(field, farm, region). Since sustainability is a multidimensional concept, it is summarized through indicators (43, 44). In this way, subjective and objective indicators are measured, with the latter recorded independently of what the farmer reports (*e.g.*, vegetation cover). Two main approaches characterize sustainability. Weak sustainability allows substituting natural capital with human-made capital, while strong sustainability sees both as complementary and irreplaceable (15, 21, 38, 43). This work adopted the strong sustainability perspective.

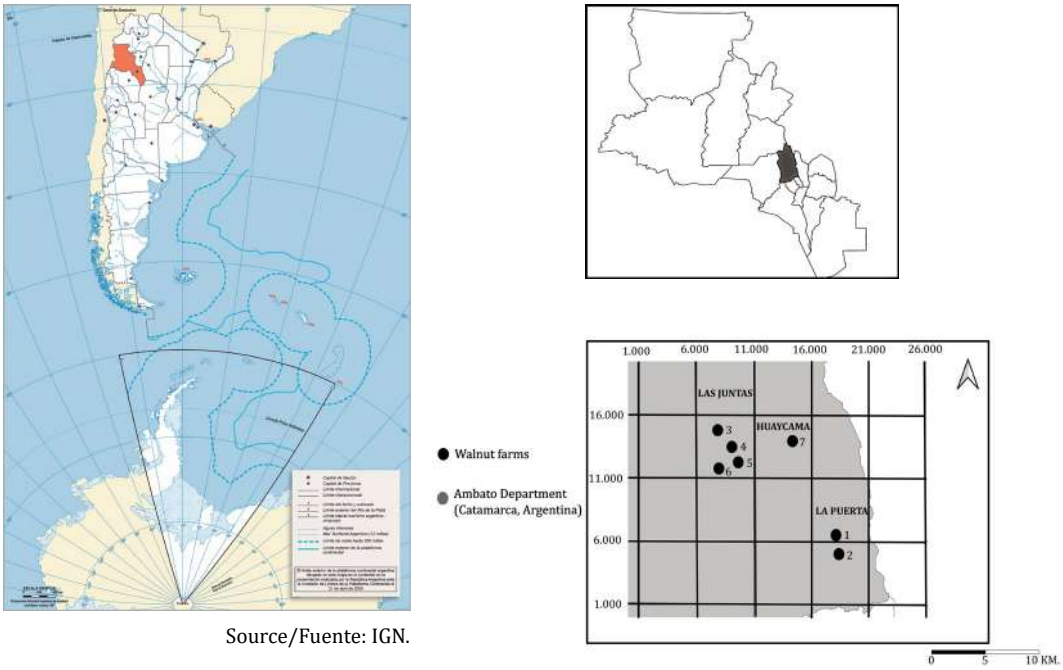
In Catamarca, previous research has addressed data on walnut varietals, types of farmers and biological aspects of *C. pomonella* (16, 32, 39, 41). To date, one study has assessed sustainability of walnut production, incorporating economic, ecological, and social dimensions within an agroecological framework (24), but no study has dealt with pest sustainable management. This study assessed the risks to sustainable phytosanitary management of *C. pomonella* by smallholder walnut farmers in Ambato (Catamarca). We employed a set of indicators and semi-structured interviews to evaluate three sustainability dimensions. (a) Ecological: Spontaneous vegetation within walnut crops supports diverse and structurally complex habitats for natural enemies of *C. pomonella*. (b) Economic: Financial losses from pest damage may exceed profits, compromising economic viability. (c) Sociocultural: Farmers largely operate in isolation and often lack knowledge about pest biology and management strategies.

This multidimensional evaluation provides insights into opportunities and constraints for sustainable pest management in smallholder agroecosystems and proposes future strategies for ecological intensification and rural resilience.

METHODOLOGY

Study Area

The study was conducted in the Ambato Department (28°10'14" S, 65°47'29" W) in Catamarca Province, Argentina, where seven smallholder walnut farms were selected as observational units (figure 1). Farms were chosen by considering average walnut production in the area and confirmed presence of *C. pomonella*. These farms exhibit notable varietal diversity, with predominant traditional 'Criolla' seed type and recently introduced lateral-bearing cultivars like 'Chandler'.



Source/Fuente: IGN.

Figure 1. Study area. Walnut farms in Ambato, Catamarca, Argentina.

Figura 1. Área de estudio. Fincas de nogales en Ambato, Catamarca, Argentina.

Indicator Development, Standardization, and Weighting.

Indicators were developed following Sarandón and Flores (2009). Table 1 shows eleven key variables related to phytosanitary management of *C. pomonella*, each associated with specific response indicators, yielding 26 sustainability indicators (Supplementary Material 1). Each indicator was scored on a five-point ordinal scale, ranging from 0 (least sustainable) to 4 (most sustainable), with 2 as analytical threshold. Relative weights were assigned to each indicator based on its perceived importance within the system. This weighting process was conducted through expert consensus in our research team (Supplementary Material 1).

Table 1. Composition of the sustainability analysis of *Cydia pomonella* management in walnut farms.

Tabla 1. Composición del análisis de sustentabilidad del manejo de *Cydia pomonella* en fincas de nogales.

Dimension	Variable	N° of indicators *
Ecological	A. On farm diversity management	6
	B. Spontaneous vegetation on farm edges	3
	C. Monitoring and regulation of *C. pomonella*	2
Economic	D. Economic investment in *C. pomonella* regulation	1
	E. Chemical control of *C. pomonella*	2
	F. Economic losses caused by *C. pomonella*	1
	G. Production marketing	2
Socio cultural	H. Extent of farmer knowledge on *C. pomonella*, alternative hosts and their regulation.	4
	I. Degree of knowledge of agrochemicals for the control of *C. pomonella*	1
	J. Social role of the farmer in relation to *C. pomonella* management	2
	k. Extent of farmer knowledge on ecosystem services for natural biological control of *C. pomonella*	2

* Details of each indicator and its categorization in Supplementary Material 1.

* Detalles de cada indicador y su categorización en Material Suplementario 1.

Estimation of Subjective Indicators in Economic and Sociocultural Dimensions

Categorical values of subjective indicators were determined after individual semi-structured interviews with the seven walnut producers between October 2023 and June 2024. The questionnaire comprised 114 questions and was supplemented by two illustrated booklets. These visual materials assessed farmers' ability to distinguish *C. pomonella* from other insects like Lepidoptera, Diptera, and Coleoptera, including natural enemies (Supplementary Material 2).

Estimation of Objective Indicators in the Ecological Dimension

Field-based ecological assessments were conducted on each farm. These included: (a) Vegetation characterization: number of plant species, cultivated and spontaneous, within each orchard and along field margins during autumn and spring. Species identification was conducted using field guides and images. Particular interest was given to Fabaceae, Asteraceae, and Apiaceae families, known to enhance the presence of natural enemies of *C. pomonella* (34, 35). (b) Vegetation cover was estimated using the square sampling method (33). Five points

per farm were randomly selected, corresponding to cardinal and central sectors (M1: North; M2: East; M3: South; M4: West; M5: center). At each point, 0.25 m^2 sampling squares were defined. Within these units, species were recorded and vegetation cover was quantified. (c) Proximity to spontaneous vegetation and habitat connectivity considered the distance from ten walnut trees per farm, randomly selected, to the nearest patch of spontaneous vegetation. Mean distance per farm was calculated.

Data Analysis

Each farm was treated as an independent unit (20), allowing for in-depth, contextual analysis and extrapolation to the broader regional context. Five categorical sustainability levels assigned to each response identified the most influential sustainability indicators as not sustainable (0%, score 0), weak (25%, score 1), moderate (50%, score 2), optimal (75%, score 3), and strongly sustainable (100%, score 4) (1). A weighted average per indicator was calculated by combining farmer proportion providing each response with the corresponding sustainability score (1, 44). The resulting values were used to generate sustainability profiles by dimension (ecological, economic, sociocultural) for each farm, and to calculate a General Sustainability Index (GSI) for the study area. Farms scoring above the threshold value of 2 were considered optimally sustainable. Equations for indicator weighting, scoring, and index calculation are provided in Supplementary Material 1. Finally, a multivariate cluster analysis (27) grouped farms according to shared indicator profiles, eliminating variables with low discriminatory power. Correlations among farm groups identified patterns of sustainability performance.

Results and Discussion

Ecological Dimension. Indicator Variability and Biodiversity Management

Based on farmer-reported data and field measurements, ecological indicators showed the greatest variability among the three evaluated dimensions (figure 2, variables 1-11, page 6). Ecological diversity management revealed moderate to high habitat complexity (table 2, page 7). Vegetation cover across farms ranged from 45% to 95%, and mean distance to the nearest spontaneous vegetation during spring-summer was under one meter. A total of 29 plant species from 13 botanical families were identified across the farms. However, only 12 of these species belonged to families previously documented as favourable for natural enemies of *C. pomonella* (23) (table 2, page 7). Notable species included *Convolvulus arvensis* L. (bindweed), *Aloysia gratissima* G. & H. (whitebrush), *Taraxacum officinale* L. (dandelion), *Melilotus albus* M. (white sweet clover), and *Ammi visnaga* L. (toothpick plant). Notably, plant spatial and temporal distributions do not result from intentional management. Rather, they establish spontaneously, primarily along farm boundaries, which may adjoin other orchards, natural landscapes, or, in some cases, expanding urban zones.

Across farms, vegetation stratification ranged from two to four layers, suggesting a potentially favourable microhabitat structure for natural enemy communities, enhancing biological control potential. Despite this, field observations and expert communications (Engineers Romero and Barros, pers. comm.) indicate low abundance and diversity of natural enemies in the study area, including *Goniozus legneri* Gordh (Hymenoptera: Bethylidae), an effective parasitoid of several lepidopteran pests, including *C. pomonella* (5, 10, 31). Several factors may account for this discrepancy. Recent urban expansion in the Ambato Department may have influenced these results (11). This area, formerly dedicated to livestock production, has undergone changes that may have negatively affected soil quality and reduced the availability of potential refuges for natural enemies. The replacement of natural vegetation likely eliminated important sources of food and shelter for beneficial fauna, disrupting the natural landscape and ecological balance. Residual effects of *agrochemicals* accumulated over recent decades, mainly pyrethroids used for *C. pomonella* control, could also contribute to these outcomes (6). In this regard, Ferrero and collaborators (2000) demonstrated the detrimental impact of organophosphates and pyrethroids on *G. legneri*, reporting reductions in longevity, oviposition capacity, and egg-laying size. Similarly, Leyton (2023) documented the harmful effects of several

insecticides (Bifenthrin, Pirimicarb, Imidacloprid) on this parasitoid species. Without adequately monitoring pest precise emergence, chemical treatments lose effectiveness, often resulting in repeated applications. Such practices disturb ecosystem balance, reduce functional biodiversity, and compromise long-term ecological sustainability. Moreover, they may contribute to developing resistant pest populations and pose risks to human health.

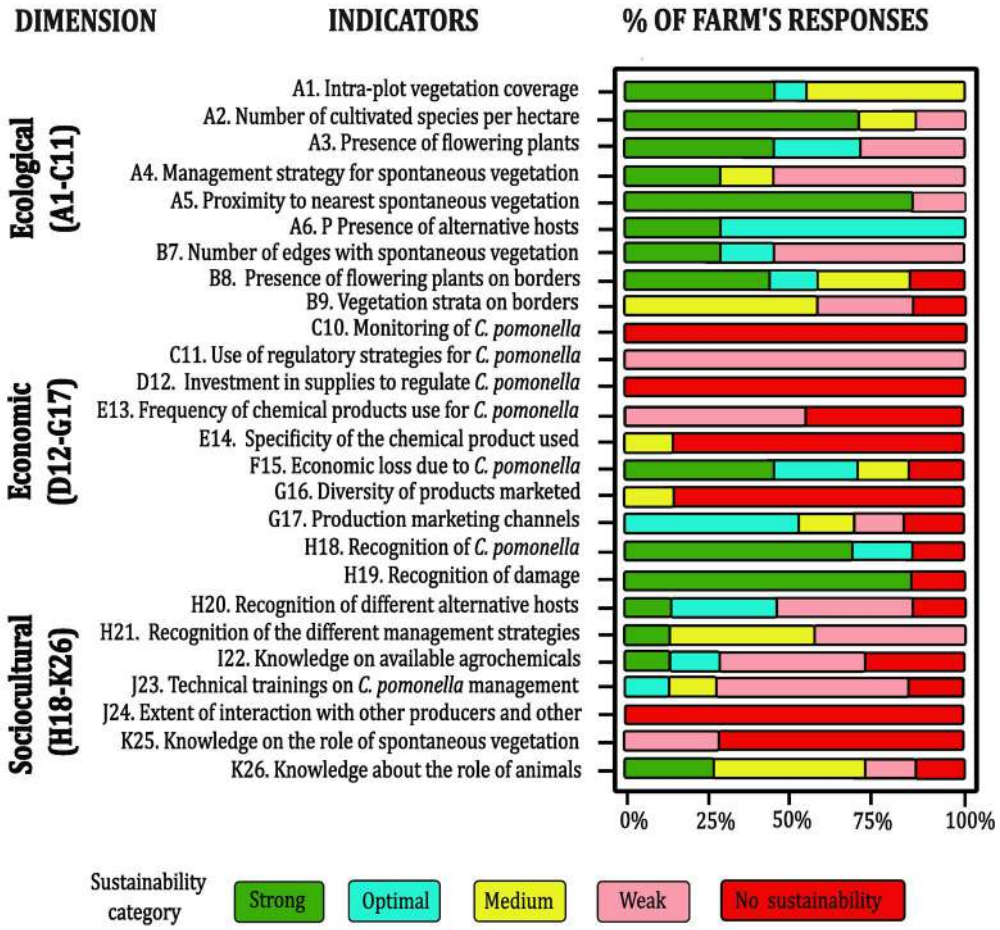


Figure 2. Percentage distribution of indicator sustainability based on farmer responses (%). All indicators are related to *Cydia pomonella* recognition and control.

Figura 2. Gráfico de distribución del porcentaje de sustentabilidad de cada indicador considerando el porcentaje de respuestas de los productores. Todos los indicadores están en función de *Cydia pomonella*, su reconocimiento y control.

Table 2. Ecological diversity on study farms.
Tabla 2. Diversidad ecológica en las fincas de estudio.

Farms	Main crop	Secondary crops	% Cob [13]	Dist. [14]	Fam. [15]	Div T. [16]	Div EN. [17]	Strata [18]
Farm 1	*Juglans regia* [1]	*Cydonia oblonga* [2], *Pronus persica* [3]	52	0	6	15	4	3
Farm 2	*J. regia*	*C. oblonga*, *Malus domestica* [4], *Pyrus sp.* [5], *Prunus domestica* [6], *Ficus carica* [7]. Forage (*Medicago sativa* [8])	45.6	3.5	7	12	6	2
Farm 3	*J. regia*	*C. oblonga*, *M. domestica*, *Pyrus* sp., *P. domestica*, *P. persica*, *Prunus dulcis* [9]. Forage (*M. sativa*, *Hordeum vulgare* [10])	54	2.5	11	17	5	4
Farm 4	*J. regia*	*C. oblonga*, pear, *P. domestica*. Forage (*Sorghum bicolor* [11], *Zea mays* [12])	94.2	0	9	14	5	2
Farm 5	*J. regia*	*C. oblonga*, *M. domestica*, *Pyrus sp*, *P. domestica*, *P. persica.* Forage (*M. sativa*)	94.8	0	13	29	12	3
Farm 6	*J. regia*	*C. oblonga*, *M. domestica*, *P. persica*	96	0	9	13	2	2
Farm 7	*J. regia*	*C. oblonga*, *Pyrus sp*, *P. persica*. Forage (*M. sativa*, *Z. mays*). Vegetable garden	73	0	10	16	4	3

1. Walnut. 2. Quince. 3. Peach. 4. Apple tree. 5. Pear tree. 6. Plum tree. 7. Fig tree. 8. Alfalfa. 9. Almond tree. 10. Barley. 11. Sorghum. 12. Corn. 13. Average percentage of vegetation cover on the farm. 14 Average distance from the walnut tree to the nearest spontaneous vegetation. 15. Number of families. 16. Total number of species. 17. Number of species belonging to the families Fabaceae, Asteraceae and Apiaceae: attractive to natural enemies (EN). 18. Number of vegetation strata.

1. Nogal. 2. Membrillo. 3. Durazno. 4. Manzano. 5. Peral. 6. Ciruelo. 7. Higo. 8. Alfalfa. 9. Almendro. 10. Cebada. 11. Sorgo. 12. Maíz. 13. Promedio de porcentaje de cobertura vegetal dentro de la finca. 14. Distancia promedio del nogal a la vegetación espontánea más cercana. 15. Número de familias. 16. Número de especies total. 17. Número de especies que pertenecen a las familias Fabaceae, Asteraceae y Apiaceae: atractivos para enemigos naturales (EN). 18. Cantidad de estratos.

Walnuts were the primary crop across all farms, accompanied by 11 secondary species, including fruit and forage crops (table 2). A common association was observed with *Cydonia oblonga* (quince), an alternative host for *C. pomonella*, with important implications for integrated pest management strategies. However, farmer perceptions of *C. oblonga* varied. In this study producers generally regarded quince as a low-priority crop, "not needing targeted control measures". Some even suggested it could constitute a trap distracting *C. pomonella* away from walnut fruits. This contrasts with Rivero *et al.* (2012) from Andalgalá (Catamarca), where farmers actively managed *C. pomonella* in quince to prevent its migration into walnut orchards. These divergent approaches highlight the need for context-specific education on host dynamics and pest ecology.

The weakest ecological sustainability indicator was absent *C. pomonella* monitoring, essential for understanding population dynamics and their effects on crop yield. Yet, extensive evidence supports the critical role of pest monitoring combined with systematic data analysis, enhancing effectiveness and sustainability of integrated pest management programs (12). Farmers reported not monitoring insects or fruit damage, nor estimating number of damaged fruits per season (figure 2, indicators C10 and C11, page 6). This limits timely and effective control strategies.

Economic Dimension: Sustainability Constraints in *C. pomonella* Management

The economic analysis revealed absent monitoring as a major limit for sustainable *C. pomonella* management. No farmer reported investing in monitoring (figure 2, D12, page 6). As a result, chemical control remains predominant across most farms, applied according to calendar schedules and without rotation of active ingredients (figure 2, E13 and E14, page 6). This facilitates the emergence of resistant pest populations, already documented in fruit-producing regions like Alto Valle (Río Negro, Neuquén) (12, 48), Chile and South Africa (7, 46). The penetration of neonate *C. pomonella* larvae into fruit makes post-infestation chemical treatments ineffective. Consequently, pest control must be precisely timed. Monitoring adult population and fruit damage, managing damage thresholds, and tracking degree-day accumulation to anticipate pest emergence have proved most effective (4, 22). However, government-led phytosanitary campaigns often proceed without prior monitoring and on broad-spectrum insecticides applied at high doses, further undermining sustainability. Previous studies in the Andalgalá region have evaluated insecticide use on walnut farms and emphasized the importance of reducing environmental and worker exposure, rotating active ingredients with distinct modes of action, and incorporating at least one compound that preserves beneficial insect populations (8, 9). Despite this, some farms in Ambato report no pest control, citing costly supplies as primary barrier.

Economic losses attributed to *C. pomonella* (figure 2, F15, page 6) are approximately 20% for half of the producers, and between 20% and 50% for the second half, consistent with Andalgalá (42). Only one producer reported losses exceeding 80%. In apple production (*Malus domestica*), a 1% fruit damage threshold per hectare has been established as economic injury level (13). However, no standardized threshold exists for walnuts. Preliminary research by our group suggests a 4% fruit loss threshold, provided monitoring is conducted regularly (Diez, pers. comm.). These thresholds imply that the sustainability assessment scale used in this study should be adjusted to reflect crop-specific economic realities more accurately, enhancing control relevance.

Alternative cultural and biological strategies remain underutilized. While collecting and destroying infested fruit (*e.g.*, by burning) is recognized as a general pest control practice (36), surveyed farmers reported this approach primarily for land clearing. In addition, the use of corrugated cardboard bands to trap diapausing larvae, a low-cost method to reduce first-generation adult populations (4), is neither considered. Biological inputs, such as *C. pomonella* granulovirus (CpGV), have shown promising results among traditional growers in Pomán and Andalgalá (40), not yet in Ambato.

Additional economic indicators detected problems related to a lack of productive diversity (figure 2, G16 and G17, page 6). Most farms only sell peeled and shelled walnuts in bulk, often at very low prices. Developing value-added products, such as candied walnuts called “nueces confitadas”, walnut oil, or walnut paste, enhances farm income and economic resilience. Similar marketing innovations have been observed in other walnut-growing regions of Catamarca, including Belén and Pomán (field interviews; Poncho Festival 2024, Catamarca).

Sociocultural Dimension: Insights into Knowledge and Systemic Challenges

Interview data revealed low sociocultural sustainability risk, as most farmers demonstrated basic knowledge of *C. pomonella* biology and field behavior (figure 2, H18-H21, page 6; table 2, page 7). This knowledge is valuable, as sustainable pest control requires understanding the pest’s life cycle and its interaction with the host (2). Participants identified the pest, recognized typical damage signs, and estimated seasonal presence in their orchards. However, as already mentioned, this knowledge is not consistently translated into practice (figure 2, D12, H21, K25, page 6). In this context, farmers are unwilling to invest in traps and

adopt a passive attitude, expecting the government to provide them. Moreover, they tend to only visually assess crop damage, without conducting actual counts that would evidence precise infestation levels. Additionally, producers did not recognize natural enemies in the brochure (parasitoids and predators). This result contrasts Rivero *et al.* (2012) in Catamarca, where nearly one-third of the producers recognized parasitoids on their farms.

Regarding alternative host species, only three farmers could identify all potential hosts of *C. pomonella*, and just one acknowledged the need to manage the pest in those crops (figure 2, H20, page 6). Most producers named only one or two hosts, primarily quince (*C. oblonga*), and believed that *C. pomonella* affected only walnut trees. Parallel assessments conducted on the same farms indicated that quince trees experienced an average fruit damage rate of 7% during the 2023-2024 season, with peak damage observed in January and February (Ing. Barros, pers. comm.). This gap between knowledge and reality may be linked to limited training opportunities and weak communication between farmers and agricultural institutions (figure 2, J23 and J24, page 6). Previous studies have shown that workshops facilitated by technical specialists can strengthen farmer networks and improve pest management outcomes (26, 32).

These findings only partially support our three hypotheses. Ecologically, although habitat structure may favour biological control, actual abundance and diversity of natural enemies seem insufficient. Economically, qualitative data suggest moderate to high pest impact, to be confirmed through quantitative assessments. Finally, socio-culturally, knowledge of the pest is not systematically applied in management decisions. This study diagnoses key limitations in *C. pomonella* control in Ambato, addressing a gap in the literature and laying the basis for more comprehensive, sustainable pest management in smallholder walnut systems.

Sustainability

The average General Sustainability Index (ISg) across the evaluated farms was 1.521, under the established threshold value of 2.0. *C. pomonella* management exhibited the highest relative sustainability in the ecological dimension (1.663), followed by the sociocultural (1.571) and economic (1.329) dimensions (table 3, page 10). These findings underscore the multifaceted nature of sustainability in pest management. As expected, farms relying exclusively on chemical control did not achieve the highest sustainability scores. In several cases, farms without control practices demonstrated comparable or even higher sustainability indices. This counterintuitive outcome can be attributed to absent monitoring practices across farms, regardless of management intensity. Control measurements without monitoring, particularly chemical applications, are often untimely, excessive, ineffective and economic-ecologically expensive. The absence of integrated monitoring systems constitutes a critical barrier for sustainable pest control.

Cluster Analysis

Cluster analysis based on the General Sustainability Index (ISg) identified four distinct groups of farms reflecting sustainability degrees (table 3, page 10). Cluster One with the highest sustainability level, comprised only Farm 2, with an ISg of 2.509, surpassing the threshold of 2.0. However, closer examination revealed that this value was driven by higher economic and sociocultural scores, while ecological performance remained limited. The producer demonstrated knowledge of *C. pomonella* management, including alternative hosts and appropriate agrochemical use. Ecological indicators on this farm revealed sparse vegetation cover, greater distances to spontaneous vegetation, and limited floral diversity from ecologically relevant plant families. At the opposite end, Cluster Two was represented by Farm 5, with the lowest sustainability score (ISg: 0.887). Unlike the other units, this farm's primary activity is livestock production, with walnut cultivation playing a minor role. Consequently, *C. pomonella* was not perceived as a significant threat, and no management strategies were implemented. Between these extremes, cluster Three included Farms 4, 6, and 7 (ISg: 1.331, 1.233, and 1.335, respectively), and Cluster Four included Farms 1 and 3 (ISg: 1.654 and 1.698, respectively). These clusters differed primarily in their ecological characteristics. Farms in Cluster Four exhibited higher vegetation cover and greater plant diversity, including flowering species and fruit crops, supporting beneficial arthropod communities. These farmers also reported greater economic losses due to *C. pomonella*, indicating pest pressure and greater economic dependency on walnut production.

Table 3. Indicator values in seven walnut farms in Ambato, Argentina, and general sustainability conditions.

Tabla 3. Valores de los indicadores empleados en siete fincas de Nogales, Ambato, Argentina y condiciones de sustentabilidad general.

Farms[1]	Variables											Sustainability values[2]			
	A	B	C	D	E	F	G	H	I	J	K	DE	DK	DSC	ISg
Farm 1	2.00	1.40	1.00	0.00	0.67	8.00	0.50	5.67	6.00	1.00	1.33	1.10	1.53	2.33	1.65
Farm 2	2.56	1.00	4.00	2.00	3.33	8.00	2.50	8.00	8.00	0.67	1.33	1.89	2.64	3.00	2.51
Farm 3	3.33	2.60	1.00	0.00	0.00	8.00	1.50	6.33	2.00	0.33	2.00	1.73	1.59	1.78	1.69
Farm 4	3.56	2.20	1.00	0.00	0.67	4.00	1.50	5.33	2.00	0.00	0.33	1.69	1.03	1.28	1.33
Farm 5	4.00	3.20	1.00	0.00	0.00	0.00	0.00	1.33	2.00	0.33	0.00	2.05	0.00	0.61	0.89
Farm 6	2.56	1.80	1.00	0.00	0.67	6.00	1.50	5.00	0.00	0.33	0.67	1.34	1.36	1.00	1.23
Farm 7	3.56	2.80	1.00	0.00	0.00	6.00	1.00	5.00	0.00	0.33	0.67	1.84	1.17	1.00	1.34
Overall average area	**3.08**	**2.14**	**1.43**	**0.29**	**0.76**	**5.71**	**1.21**	**5.24**	**2.86**	**0.43**	**0.91**	**1.66**	**1.33**	**1.57**	**1.52**

1. Walnut farms. A. On-farm diversity management. B. Spontaneous vegetation on farm edges. C. Monitoring and regulation of *C. pomonella.* D. Economic investment in *C. pomonella* regulation. E. Chemical control of *C. pomonella*. F. Economic losses caused by *C. pomonella.* G. Production marketing. H. Extent of farmer knowledge on *C. pomonella*, alternative hosts and their regulation. I. Degree of knowledge of agrochemicals for the control of *C. pomonella*. J. Social role of the farmer concerning *C. pomonella* management. k. Extent of farmer knowledge on ecosystem services for natural biological control of *C. pomonella.* 2. Results are averages of the indicators constituting each variable. DE=Ecological Dimension. DK: Economic Dimension. DSC: Socio-Cultural Dimension. ISg: General Sustainability Index. Formula. Supplementary material 1.

1. Fincas de nogales. A. Manejo de la diversidad en la finca. B. Vegetación espontánea en los bordes de la finca C. Monitoreo y regulación de *C. pomonella.* D. Inversión económica en la regulación de *C. pomonella* E. Control químico de *C. pomonella.* F. Pérdidas económicas causadas por *C. pomonella* G. Comercialización de la producción. H. Grado de conocimiento de los agricultores sobre *C. pomonella*, hospedantes alternativos y su regulación. I. Grado de conocimiento de los agroquímicos para el control de *C. pomonella.* J. Rol social del agricultor en relación con el manejo de *C. pomonell*a. k. Grado de conocimiento de los agricultores sobre los servicios ecosistémicos para el control biológico natural de *C. pomonella.* 2. Los resultados son el promedio de los indicadores que conforman la variable. DE=Dimensión Ecológica. DK: Dimensión económica. DSC: Dimensión Sociocultural. ISg: Índice de Sustentabilidad General. Fórmula. Material suplementario 1.

Conclusion

This study represents the first assessment of sustainability gaps in the phytosanitary management of *C. pomonella* among smallholder walnut farmers in Argentina. The findings highlight that effective and sustainable pest control must encompass ecological, economic, and sociocultural dimensions, rather than single-point interventions. To initiate meaningful changes, participatory frameworks must engage all relevant stakeholders, including farmers, academic researchers, and public institutions involved in agricultural policy and extension services. These workshops should be collaborative spaces for knowledge exchange, trust-building, and context-appropriate co-design management strategies. Key prevention must implement systematic pest monitoring and promote ecological practices aimed at regenerating native vegetation and enhancing habitats for natural enemies. Such efforts would strengthen ecosystem resilience and support reestablishing natural biological control mechanisms for *C. pomonella*. In parallel, enhancing market strategies through value-added products (*e.g.*, processed walnuts, specialty foods) could improve profitability, promote investment in sustainable practices, and increase resilience of walnut production systems. Ultimately, sustainability in smallholder agricultural systems depends on technical improvements in pest control and integration of holistic strategies that align ecological integrity with economic viability and social inclusion. Without adequate profitability, the relative importance of ecological and social factors diminishes, weakening long-term sustainability. Addressing vulnerabilities across all sustainability dimensions (not just one) is essential for effective management of *C. pomonella* and secure regional walnut production.

Supplemmentary Material

https://docs.google.com/document/d/1fVJGbaYYPVGXzDZbZkx76EqjtAr0z1yB/edit?usp=drive_link&ouid=111310786017351827239&rtpof=true&sd=true

References

1. Abraham, L.; Alturria, L.; Fonzar, A.; Ceresa, A.; Arnés, E. 2014. Propuesta de indicadores de sustentabilidad para la producción de vid en Mendoza, Argentina. Revista de la Facultad de Ciencias Agrarias. Universidad Nacional de Cuyo. Mendoza. Argentina. 46(1): 161-180.
2. Altieri, M. A.; Nicholls, C. I. 2007. Biodiversidad y manejo de plagas en agroecosistemas (Vol. 2). Icaria editorial.
3. Astier M.; López Ridaura, S.; Pérez E.; Masera O. R. 2002. El Marco de Evaluación de Sistemas de Manejo incorporando Indicadores de Sustentabilidad (MESMIS) y su aplicación en un sistema agrícola campesino en la región Purhepecha, México. Agroecología. 415-430.
4. Aubel, A. J. 2022. Estudios de nuevas herramientas de control de plagas de nogales con énfasis en *Cydia pomonella* en el Valle Inferior del Río Negro. Primera experiencia. Tesis final de Carrera en Ingeniería Agronómica, Facultad de Ciencias Agrarias. Universidad Nacional de Río Negro. Argentina.
5. Barros, L. A.; Espinosa, M.; Romero, O. E.; Carrizo, A.; Cavallo, M. J.; Diez, P. A. 2024. Actualización sobre la presencia natural de *Goniozus legneri* (Hymenoptera: Bethylidae) en agroecosistemas nogaleros de Catamarca y primer registro en el Departamento Famatina, Provincia de La Rioja. Revista de la Sociedad Entomológica Argentina. 83(3). DOI: 10.25085/rsea.830305.
6. Belles, C.; Cichón, L.; Di Masi, S.; Fernández, D.; Magdalena, C.; Rial, E.; Rossini M. 1996. Guía de pulverizaciones. 72 p.
7. Blomefield, T. 1994. Codling moth resistance. It is here, and how do we manage it? Deciduous Fruit Grower. 44(4): 130-132.
8. Carrizo, A.; Carrasco, F.; Aybar, S.; Leiva, S.; Matías, A. 2015. Estimación del Coeficiente de Impacto Ambiental (EIQ) en diferentes estrategias fitosanitarias en sistemas de pequeños productores de nogal, como una herramienta hacia la transición agroecológica en Catamarca, Argentina. V Congreso Latinoamericano de Agroecología-SOCLA, La Plata.
9. Casado, G. G.; Mielgo, A. A. 2007. La investigación participativa en agroecología: una herramienta para el desarrollo sustentable. Ecosistemas. 16(1).
10. Cavallo, M. J.; Romero, O. E.; Barros, L. A.; Cichón, L.; Garrido, S. A.; Diez, P. A. 2024. Functional and numerical response and mutual interference of *Goniozus legneri* (Hymenoptera: Bethylidae) on *Cydia pomonella* (Lepidoptera: Tortricidae): Its implications for biological control. Journal of Applied Entomology. 148(4): 454-463. https://doi.org/10.1111/jen.13238
11. Censo República Argentina. 2022. Resultados del Censo 2022-Catamarca. https:// censo.gob.ar/index.php/datos_definitivos_catamarca (Fecha de consulta: 27/11/2024).

12. Cichón L.; Fernández D. E. 1995. TRV Aplicación de volúmenes adecuados en cultivos de frutales de pepita. Ed. EEA Alto Valle.
13. Cichón, L.; Di Masi, S.; Fernández, D.; Magdalena, C.; Rial, E.; Rossini, M. 1996. Guía ilustrada para el monitoreo de plagas y enfermedades en frutales de pepita. Ed. INTA Centro Regional Patagonia Norte. 72 p.
14. Cichón L.; Fernández D. E.; Montagna, M. 2015. Evolución del control de carpocapsa en los últimos veinticinco años. Rev. Fruticultura y Diversificación. 51: 22-29.
15. Daly H. E 1997. De la economía del mundo lleno a la economía del mundo vacío. Ed. Goodland, R. *et al.* Medio ambiente y desarrollo sostenible. 35-50 p.
16. Errecart, V. 2012. Diagnóstico de la cadena de la nuez de nogal de las provincias de La Rioja y Catamarca. Estrategias y tácticas para mejorar su inserción en el comercio internacional. Tesis de grado de Magister, área Agronegocios y Alimentos. Universidad Nacional de Buenos Aires. Argentina.
17. Ferrero A.; Laumann R.; Gutierrez M. M.; Stadler T. 2000. Evaluación en laboratorio de la toxicidad de insecticidas en *Cydia pomonella* L. (Lepidoptera: Tortricidae) y en su enemigo natural *Goniozus* legneri Gordh (Hymenoptera: Bethylidae). Publicación de la Agricultura, Rev. de Sanidad Vegetal. Plagas. 26(4): 559-575.
18. Garrido S.; Cichón L.; Fernández D.; Azevedo C. 2005. Primera cita de la especie *Goniozus legneri* (Hymenoptera: Bethylidae) en el Alto Valle de Río Negro, Patagonia Argentina. Rev. Sociedad Entomológica Argentina. 64(1-2): 14-16.
19. Gould, F.; Brown, Z. S.; Kuzma, J. 2018. Wicked evolution: Can we address the sociobiological dilemma of pesticide resistance? Science. 360(6390): 728-732. DOI: 10.1126/science.aar378
20. Guzmán Casado G. M.; González de Molina N.; Sevilla Guzmán E. 2000. Métodos y técnicas en Agroecología, Introducción a la agroecología como desarrollo rural sostenible. 5: 149-195.
21. Harte, M. J. 1995. Ecology, sustainability, and environment as capital. Ecological Economics. 15: 157-164.
22. Huerga, M.; San Juan, S. 2005. El control de las plagas en la agricultura argentina. Estudio Sectorial Agrícola Rural-Banco Mundial/Centro de Inversiones FAO-Buenos Aires, Argentina.
23. Iermanó, M. J.; Sarandón, S. J.; Tamagno, L. N.; Maggio, A. D. 2015. Evaluación de la agrobiodiversidad funcional como indicador del potencial de regulación biótica. Aroecosistemas del sudeste bonaerense. Rev. Facultad de Agronomía. La Plata. 114(3): 1-14.
24. Juri, C.; Zárate, L. 2017. Evaluación de la sustentabilidad de una finca nogalera de un pequeño productor en Mutquin - Pomán - Catamarca. Rev. Divulgación Técnica Agrícola y Agroindustrial, Facultad de Ciencias Agrarias - UNCa. 69.
25. Keil S.; Gu H.; Dorn S. 2001. Response of *Cydia pomonella* to selection on mobility: laboratory evaluation and field verification. Ecological Entomology. 26(5): 495-501. https://doi.org/10.1046/j.1365-2311.2001.00346.x
26. Landini, F. 2022. Intercambio de experiencias y aprendizaje horizontal entre extensionistas: Fuente invisibilizada de conocimientos para la práctica. Psicoperspectivas. 21(3): 7-20. http://dx.doi.org/10.5027/
27. Lê, S.; Josse, J.; Husson, F. 2008. FactoMineR: An R package for multivariate analysis. Journal of statistical software. 25: 1-18. https://doi.org/10.18637/jss.v025.i01
28. Leyton, J. F. 2023. Efectos subletales de agroquímicos sintéticos y naturales contra *Goniozus legneri* Gordh (Hymenoptera: Bethylidae). Tesis de Magíster en Ciencias Agronómicas. Universidad de Concepción, Chile.
29. López, I.; Lovi, A.; Trejo, J. 2014. Análisis del agregado de valor en la cadena agroalimentaria de la nuez de nogal: caso Establecimiento Finca Don Manuel, Chilecito-La Rioja. Trabajo Final - Áreas de Consolidación, Ingeniería Agronómica. Universidad Nacional de Córdoba, Argentina.
30. Manetti, A.; Lara-Navarra, P.; Sánchez-Navarro, J. 2022. El proceso de diseño para generación de escenarios futuros educativos. Rev. científica iberoamericana de comunicación y educación. 30 (73). DOI: 10.3916/C73-2022-03
31. Marcucci, B.; Mazzitelli, M. E.; Garrido, S. A.; Cichón, L. I.; Becerra, V. C.; Luna, M. G. 2023. Presencia de *Goniozus legneri* (Hymenoptera: Bethylidae) y su asociación con lepidópteros plagas en el oasis cultivado Norte de la provincia de Mendoza, Argentina. Rev. Sociedad Entomológica Argentina. 82(2): 5-5.
32. Maschio. J. I. 2017. Caracterización de los productores de nogal y su relación con la calidad final del producto en la provincia de Catamarca. Cartilla de divulgación técnica. Revista de Divulgación Técnica Agrícola y Agroindustrial. 76.
33. Matteucci, S. D.; Colma, A. 1982. Metodología para el estudio de la vegetación. Programa Regional de Desarrollo, Científico y Tecnológico. 22.
34. Nicholls C. 2006. Bases agroecológicas para diseñar e implementar una estrategia de manejo de hábitat para control biológico de plagas. Agroecología. 1: 37-48.
35. Nicholls, C. I. 2008. Control biológico de insectos: un enfoque agroecológico. Ed. Universidad de Antioquia. 282 p.

36. Nievas, W. E.; Rossini, M. N.; Toranzo, J. O.; Iannamico, L. A.; Magdalena, J. C.; Fernandez, D. E.; Curetti, M. 2014. Bacteriosis del nogal (*Xanthomonas campestris* pv. juglandis) en el Valle Medio del río Negro. Repositorio EEA Alto Valle, INTA. https://repositorio.inta. gob.ar/bitstream/handle/20.500.12123/16962/INTA_CRPatagoniaNorte_EEAAltoValle_Nievas_WE_Bacteriosis_nogal_Xanthomonas_campestris_pv_juglandis.pdf?sequence=1 (fecha de consulta:20/11/2024).
37. Obschatko, E. 2009. Las explotaciones agropecuarias familiares en la República Argentina. Un análisis a partir de los datos del Censo Nacional Agropecuario 2002. Agricultura, Ganadería, Pesca y Alimentos. 68. http://repositorio.iica.int/handle/11324/6860
38. Pearce, D.; Atkinson, G. 1993. Capital theory and measure-ments of sustainable development: an indicator of weak sustainability. Ecological Economics. 8(2): 103-108.
39. Prataviera, A. G. 2000. Problemática del cultivo de la nuez de nogal en las provincias de Catamarca y La Rioja. INTA, Estación Experimental Agropecuaria Catamarca. Informe 4.
40. Quintana, G.; Cólica, J.; Fernández Gorgola, M.; Rivero, C.; Pérez, O.; Luna Mercado L. 2007. Control de Carpocapsa (*Cydia pomonella* L.) con un producto en base al virus de la granulosis (CPGV), en cultivos de nogal en Catamarca. Rev. CIZAS. 8: 39-48.
41. Quintana, G; Cólica J. 2011. Carpocapsa: plaga clave en nogal. Aspectos morfológicos y biológicos relevantes para un control adecuado. Informe Técnico INTA. 1.
42. Rivero, C.; Cólica, J.; Fernández, G. M.; Cruz, R.; Luna, M.; Rivero, A. R. 2012. El nogal: situación productiva en la localidad de El Potrero, Andalgalá, Catamarca. Rev. CIZAS. 22.
43. Sarandón, S. J. 2002. El desarrollo y uso de indicadores para evaluar la sustentabilidad de los agroecosistemas. Agroecología. 20: 393-414.
44. Sarandón, S. J.; Zuluaga, M. S.; Cieza, R.; Janjetic, L.; Negrete, E. 2006. Evaluación de la sustentabilidad de sistemas agrícolas de fincas en Misiones, Argentina, mediante el uso de indicadores. Agroecología. 1: 19-28.
45. Sarandón, S. J.; Flores, C. C. 2009. Evaluación de la sustentabilidad en agroecosistemas: una propuesta metodológica. Agroecología. 4: 19-28.
46. Sazo, L.; Araya, J. E.; Rodríguez, P. 2006. Evaluación de la susceptibilidad de *Cydia pomonella* (L.) (Lepidoptera: Tortricidae) al azinfosmetil en Chile. Boletín Sociedad Entomológica Aragonesa. 39: 451-453.
47. Secretaría de Agricultura, Ganadería, Pesca y Alimentos (SAGPyA). Informe síntesis de la economía regional: nuez del nogal. https://alimentosargentinos.magyp.gob.ar/ HomeAlimentos/economias-regionales/producciones-regionales/informes/Informe_Nuez_nogal.pdf/ (fecha de consulta 27/12/2024).
48. Soleño J.; Anguiano O. L.; Cichón L. B.; Garrido S. A.; Montagna C. M., 2012. Geographic variability in response to azinphos-methyl in field-collected populations of *Cydia pomonella* (Lepidoptera: Tortricidae) from Argentina. Pest Management Science. 68(11): 1451-1457. https://doi.org/10.1002/ps.3327
49. Tamagno, L. N.; Iermanó, M. J.; Sarandón, S. J.; Pérez, R. A. 2014. Influencia de los saberes de los agricultores familiares pampeanos sobre las decisiones productivas y tecnológicas: su relación con un manejo sustentable. Acta IX Congreso Latinoamericano de Sociología Rural. México.
50. Wezel, A.; Gemmill-Herren, B.; Bezner-Kerr, R.; Barrios, E.; Rodrigues Gonçalves, A.; Sinclair, F. 2020. Agroecological principles and elements and their implications for transitioning to sustainable food systems. A review. Agronomy for Sustainable Development. 40: 1-13. https://doi.org/10.1007/s13593-020-00646-z /

Acknowledgments

We thank the walnut farmers of Ambato for granting access to their farms and participating in the interviews. We thank Gabriel Reinoso Franchino for assistance in plant species identification, Miguel A. Garlati for general assistance, and Nahuel V. Morales Castilla and Marcos S. Macchioli Grande for language contributions.

This article was proofread by Servicio de Edición de Idioma de la Facultad de Ciencias Agrarias, UNCuyo, Mendoza.

Funding Information

The study was funded by the Agencia Nacional de Promoción Científica y Tecnológica de Argentina through "Fondo Nacional de Ciencia y Tecnología (FONCyT)" (PICT 2018-02508, PICT 2020-03499 and PICT 2021-00194) and "Fondos Complementarios para proyectos de Investigación con el Impacto en el territorio Argentino 2024 - Fundación Williams".

Biofungicide Formulation Based on *Bacillus velezensis* EM-A8 for Control of Maize Foliar Diseases

Formulación de biofungicida a base de *Bacillus velezensis* EM-A8 para el control de enfermedades foliares en maíz

Melina Sartori [1], Daiana García [1], María Fiamma Grossi Vanacore [2], Aluminé Fessia [1], Andrea Nesci [1]

Originales: *Recepción:* 29/05/2024 - *Aceptación:* 03/12/2024

ABSTRACT

The aim was to evaluate inoculum production of *Bacillus velezensis* EM-A8, a native bacterium of maize phyllosphere, antagonist to foliar pathogens *Exserohilum turcicum* and *Puccinia sorghi*. Six economic media were tested: 1) Nutrient Broth (8 $g.L^{-1}$); 2) Whole soybean flour (40 $g.L^{-1}$) + sucrose (20 $g.L^{-1}$); 3) Whole soybean flour (10 $g.L^{-1}$) + molasses (20 $g.L^{-1}$), 4) Whole soybean flour (40 $g.L^{-1}$) + molasses (10 $g.L^{-1}$); 5) Yeast extract (10 $g.L^{-1}$) + molasses (5 $g.L^{-1}$) and 6) Yeast extract (10 $g.L^{-1}$) + sucrose (5 $g.L^{-1}$). Growth was determined spectrophotometrically at 620 nm and viability was estimated. M2 showed the shortest generation time (*g* 1.22 h). M3 and M5 were selected for efficiency and a_w was modified with glycerol at 0.97. Inoculums were stored under refrigeration (5°C) and room temperature (20-25°C) for 8 months. At 5°C the viability of the antagonist at 3.3-4.5 log CFU ml^{-1} was significantly lower than at room temperature (6-6.8 log CFU ml^{-1}), where M5 showed the highest stability. The bioformulation of *B. velezensis* EM-A8 in M5 at a_w 0.97 and stored at room temperature will allow successful control of maize foliar diseases.

Keywords
biological control • formulation • growth medium • Northern leaf blight

https://doi.org/10.48162/rev.39.196

1 Universidad Nacional de Río Cuarto. Facultad de Ciencias Exactas, Físico-Químicas y Naturales. Departamento de Microbiología e Inmunología. Laboratorio de Ecología Microbiana. Consejo Nacional de Investigaciones Científicas y Técnicas (CONICET). Ruta 36 km 601. Río Cuarto 5800. Córdoba. Argentina. * msartori@exa.unrc.edu.ar
2 Universidad Nacional de Río Cuarto. Facultad de Ciencias Exactas, Físico-Químicas y Naturales. Departamento de Microbiología e Inmunología. PHD Student Laboratorio de Ecología Microbiana.

Licenses Creative Commons
Attribution - Non Commercial - Share Alike

Resumen

El objetivo fue evaluar la producción de inóculo de *Bacillus velezensis* EM-A8, bacteria nativa de la filosfera de maíz, antagonista de los patógenos foliares *Exserohilum turcicum* y *Puccinia sorghi*. Se probaron seis medios económicos: M1) Caldo Nutritivo (8 $g.L^{-1}$); M2) Harina integral de soja (40 $g.L^{-1}$) + sacarosa (20 $g.L^{-1}$); M3) Harina integral de soja (10 $g.L^{-1}$) + melaza (20 $g.L^{-1}$), M4) Harina integral de soja (40 $g.L^{-1}$) + melaza (10 $g.L^{-1}$); M5) Extracto de levadura (10 $g.L^{-1}$) + melaza (5 $g.L^{-1}$); M6) Extracto de levadura (10 $g.L^{-1}$) + sacarosa (5 $g.L^{-1}$). El crecimiento se determinó espectrofotométricamente a 620 nm y se estimó la viabilidad. M2 mostró el menor tiempo de generación (*g* 1.22 h). Por eficiencia se seleccionaron M3 y M5. Se modificó a_W a 0,97 con glicerol. Los inóculos se almacenaron en refrigeración (5°C) y a temperatura ambiente (20-25°C), durante 8 meses. A 5°C la viabilidad del antagonista se mantuvo en 3.3-4.5 log UFC ml^{-1}, significativamente menor que a temperatura ambiente (6-6.8 log UFC ml^{-1}), donde M5 mostró la mayor estabilidad. El bioformulado de *B. velezensis* EM-A8 en M5, a_W 0,97 y almacenado a temperatura ambiente, nos permitirá avanzar en el control exitoso de enfermedades foliares en maíz.

Palabras clave
control biológico • formulación • medio de crecimiento • tizón foliar del norte

Introduction

Currently, there is a strong need for environment, human and animal health-friendly alternatives to chemical compounds in agriculture. For this, previous studies in our lab selected epiphytic bacteria of maize phyllosphere with antagonist capacity against the foliar diseases Northern leaf blight produced by *Exserohilum turcicum* and Common rust produced by *Puccinia sorghi* (15, 17). Foliar applications on maize plants controlled both diseases (17). Additionally, we determined mechanisms of action and tolerance to environmental stress (18) and *in vitro* biofilm formation of the biocontrol agent (9).

Biological control is defined as the reduction of a pathogenic agent that causes a disease, through the action of live microorganisms. Practically, this control uses antagonist agents generally isolated from fruit or plant surfaces. These microorganisms, when stimulated *in situ* or artificially reintroduced into environments with the pathogens to be controlled, reduce or suppress disease development (2). A successful biocontrol product depends on the formulation process of a product composed of a biocontrol agent and ingredients to improve survival and product effectiveness (23). The formulation process can affect biocontrol efficiency, extend life, ease handling, raise compatibility with agricultural equipment and practices, and lower production costs. Formulations with high density of microorganisms and greater survival during storage are key for effective biocontrol development. For a biological product to be competitively commercialised, its shelf life should last from 6 months to a year (11, 23). Storage and packaging conditions affect product viability. Temperature modulates bacterial survival during storage (23).

The development of an economic culture medium allowing a large amount of a microbial agent at a low price must maintain control efficacy (23, 26). Low-cost medium components must provide enough energy for biosynthesis and cell maintenance (20). Numerous amendments have been utilised in experimental and commercial formulations of *Bacillus* and other biocontrol agents. Generally, amendments can be grouped as either carriers (fillers, extenders) or those improving chemical, physical, or nutritional properties (19). On the other hand, waste products from soy-based food processing are considered excellent substrates for industrial production of beneficial bacteria and metabolites. Soy waste provides high percentages of proteins (40%), carbohydrates (35%), vitamins and minerals. Soy by-products such as defatted flours are used for industrial production of beneficial bacteria and their metabolites including *Bacillus subtilis* (13, 23).

Also, molasses is a by-product of sugar cane and sugar beet. Given its low cost and contents of sugars (sucrose in 50%), nitrogen, B vitamins and minerals like iron, phosphorus, potassium, zinc, sodium, copper and magnesium, molasses constitutes one

of the most used carbon sources for industrial production of microorganisms (23, 27). Medium growths with molasses and other nitrogen sources provide the nutrients and energy necessary for a rapid cellular increase and maintenance (14, 26). Various nitrogen sources such as peptone, significantly affect the production of antifungal substances in *B. subtilis* (21, 23). Microorganisms for biocontrol are subjected to low a_w causing water stress and synthesis of compatible solutes like polyhydroxyalcohols, carbohydrates or amino acids (23).

Formulation of microbial products can be liquid (aqueous suspensions and flowables) or dry (wettable powders, dust and granules) (19). Lyophilization can maintain viability over twenty years and under no special temperature conditions (10, 25). However, post-lyophilization viability varies depending on numerous factors. This study aimed to obtain an efficient and low-cost formulation of *Bacillus velezensis* EM-A8, able to maintain high cell viability during storage, and evaluating different conditions. This *in vitro* study would provide a reliable basis for further industrial scaling.

Materials and Methods

Biocontrol Agent

Antagonist bacteria were isolated from maize leaves with disease lesions from fields of different sites in Córdoba province, Argentina. Antagonistic ability was evaluated *in vitro* and potential control agents were selected (15). These isolates were identified and deposited in the culture collection of the Department of Microbiology and Immunology, Universidad Nacional de Río Cuarto. *B. velezensis* EM-A8 Genbank accession number KY694464.1 was selected as the more effective strain in biological control of leaf blight caused by *E. turcicum* and common rust caused by *P. sorghi* (16, 17, 18).

Inoculum Preparation

B. velezensis EM-A8 inoculum was prepared from cultures grown on nutrient broth (NB) for 24 h at 140 rev min^{-1} and 25°C up to the exponential phase. Serial dilutions were performed and plated on nutrient agar (NA) to evaluate cell viability and count of colony-forming units per ml (CFU ml^{-1}).

Growth Media and Culture Conditions

The following low-cost media were used to increase viable cells of *B. velezensis* EM-A8:
1) Nutrient Broth (8 g L^{-1}) (control) (M1).
2) Whole soy flour (40 g L^{-1}) + sucrose (20 g L^{-1}) (26) (M2).
3) Whole soy flour (10 g L^{-1}) + molasses (20 g L^{-1}) (14) (M3).
4) Whole soy flour (40 g L^{-1}) + molasses (10 g L^{-1}) (26) (M4).
5) Yeast extract (10 g L^{-1}) + molasses (5 g L^{-1}) (26) (M5).
6) Yeast extract (10 g L^{-1}) + sucrose (5 g L^{-1}) (6) (M6).

All media were prepared in 250 ml flasks with 50 ml of each tested medium with 0.97 water activity (a_w) adjusted by glycerol addition (7) and autoclaved. Flasks were inoculated with 100 µl of fresh inoculum suspension of *B. velezensis* EM-A8, with an initial inoculum of 3 x 10^8 CFU ml^{-1} and incubated at 25°C under orbital agitation at 140 rev min^{-1} for 32 h.

Growth in each treatment was determined spectrophotometrically at 620 nm. Cell viability was estimated using the surface-plated method at 5, 9, 24 and 32 hours. For this, serial decimal dilutions until 10^{-9} were performed in NB. An aliquot of 0.1 ml of each dilution was spread on the surface of NA. Plates were incubated in darkness at 25°C for 24 h. Total number of viable bacteria was expressed as mean colony-forming units developed per ml of medium (CFU ml^{-1}). The experiments were replicated three times for each treatment and the assay was repeated twice. Growth parameters *g* (generation time) and *k* (constant growth rate) were calculated by linear regression of the exponential growth phase.

Viability of *B. velezensis* EM-A8 at Two Different Storage Conditions

The viability evaluation of two storage conditions was carried out for two media (M3 and M5). For this, 250 ml of each media inoculated with *B. velezensis* EM-A8 were stored at room temperature (20-25°C) and in cool storage (5°C) for 8 months (240 days). Antagonist viability was determined by plate count at different times. Sample dilutions were made in NB and spread-plated onto NA. Plates were incubated at 25°C for 24 h and the viable count was expressed as colony-forming units per ml (CFU ml^{-1}). The experiments were conducted in triplicates.

Viability of *B. velezensis* EM-A8 Under Lactose-Added

The effect of adding a post-incubation protector such as lactose was evaluated for the same media. For this assay, M1 was used as control and M3 and M5 were supplemented with 5% lactose post-incubation of *B. velezensis* EM-A8. Media were stored at room temperature and cool storage. Bacterial viability was monitored after 5 months of storage (150 days) and estimated using a surface-plated method, as previously mentioned.

Lyophilized Formulation

Since the addition of glycerol does not allow freeze-drying, flasks with M5 and not modified a_w, were inoculated with a suspension of 0.1 ml of *B. velezensis* EM-A8, incubated in an orbital shaker at 140 rev min^{-1} and 25°C for 24 h the number of colony forming units per millilitre (CFU ml^{-1}) was calculated. In order to protect cells from temperature, 5% lactose was added before lyophilization (1). The conical flasks containing inoculum were frozen directly at -20°C for 12 h and then at -80°C for 4 h. These were then connected to a freeze-dryer operating at a chamber pressure of 50.05 mbar and -45°C for 48 h.

A week later, viability of lyophilized M5 was determined. For this, 0.2 g and 1 g were rehydrated with 9 ml of NB, incubated for 1 h at room temperature and homogenised with a vortex mixer. Serial dilutions were spread-plated on the surface of NA plates. These plates were incubated at 25°C for 24 h and viable populations were counted. Survival levels were expressed as number of CFU ml^{-1} (15). The experiments were conducted in triplicates.

Statistical Analysis

ANOVA test was made for growth parameters and viable counts using InfoStat version 2012 (8). Means were compared according to the DGC test ($p > 0.05$).

Results

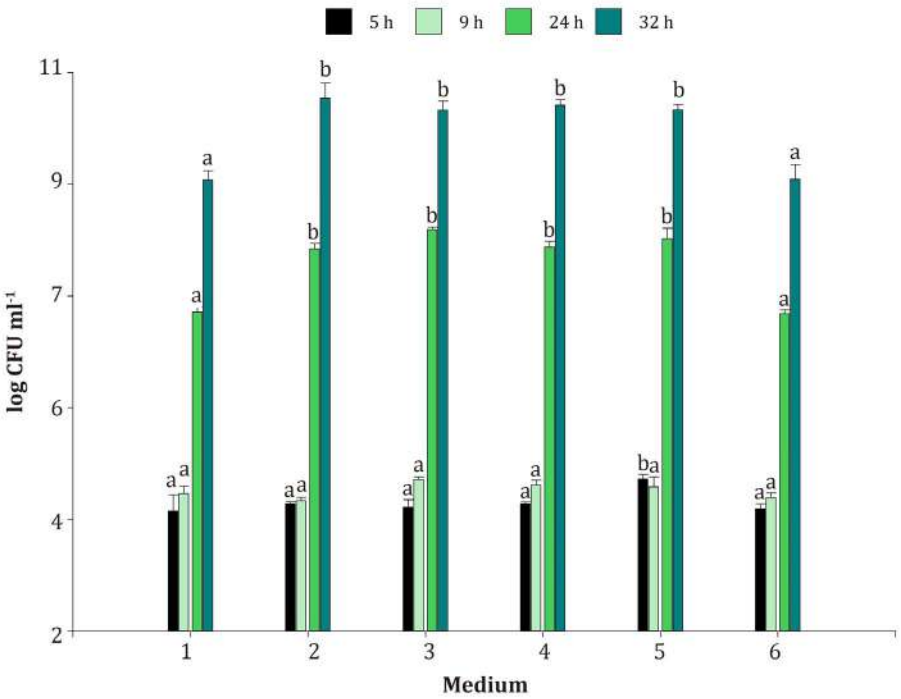
***B. velezensis* EM-A8 Growth on Low-Cost Media**

Growth data at different media and time incubation were analysed by ANOVA. All media provided high *B. velezensis* EM-A8 growth. After 9 h of incubation, no significant differences ($p<0.05$) were observed between media and time. The lowest count (4 log CFU ml^{-1}) was determined at 5 h. M5 presented a significantly higher count (f: 2,22; gl: 5; p-value 0,1192).

Significant differences were observed for *B. velezensis* EM-A8 level between culture media at 24 h (f: 40.3; gl:5: p-value <0.0001) and 32 h of incubation (f: 12.95; gl: 5; p-value 0.0002). Growth was significantly higher in M2, M3, M4 and M5 with similar counts (10.4-10.7 log CFU ml^{-1}), while the lowest count corresponded to control media (Ml) and M6 (9.3-9.7 log CFU ml^{-1}) (figure 1, page 5).

Growth parameters significantly differed among mediums (table 1, page 5). *B. velezensis* EM-A8 had the shortest generation time (*g*) in M2, followed by M3, M4, M5, M6 and M1 (control). Besides, the growth rate constant *(k)* was greater for M2, M3 and M4 with an average value of 0.55 and no significant differences among the three media ($p<0.05$). However, M1, M5 and M6 showed significant differences for *k*.

Culture media selection discarded M2 for its high soy flour content (40 g L^{-1}) and considering that M3 showed comparable growth with less soy flour content (10 g L^{-1}). We also selected M5 for growth parameters obtained in a very different media composition (yeast extract and molasses).



Different letters indicate significant differences for each medium at different incubation times according to the DGC test (P<0.05).

Datos con la misma letra no son significativamente diferentes para cada medio a diferentes tiempos de incubación según el test DGC (P<0,05).

Figure 1. Incubation of *B. velezensis* EM-A8 in different low-cost media for 32 h.

Figura 1. Incubación de *B. velezensis* EM-A8 en diferentes medios de bajo costo durante 32 h.

g: generation time.

k: constant growth rate.

Data with the same letter are not significantly different according to the DGC test (P<0.05).

g: tiempo de generación.

k: constante de la velocidad de crecimiento.

Los datos en una misma letra no son significativamente diferentes según la prueba DGC (P<0,05).

Table 1. Influence of growth media on growth parameters of *B. velezensis* EM-A8.

Tabla 1. Influencia de los medios de crecimiento en los parámetros de crecimiento de *B. velezensis* EM-A8

Media growth parameters						
	M1	**M2**	**M3**	**M4**	**M5**	**M6**
g (h)	1.52 *a*	1.22 *e*	1.26 *d*	1.27 *d*	1.36 *c*	1.43 *b*
k (h^{-1})	0.45 *D*	0.56 *A*	0.55 *A*	0.54 *A*	0.50 *B*	0.48 *C*

Viability of *B. velezensis* EM-A8 in Storage

Figure 2 (page 6), shows *B. velezensis* EM-A8 viability in M1, M3 and M5 under two different storage conditions. After 240 days of storage, viability was significantly lower in the three-growth media stored under refrigeration (5°C), showing a count average of 3.3-4.5 log CFU ml^{-1}, while viability in growth media stored at room temperature (20°C) was 6-6.8 log CFU ml^{-1}. Growth media 5 showed smaller variations in *B. velezensis* EM-A8 counts throughout storage time at room temperature.

Viability of *B. velezensis* EM-A8 Stored with Added Lactose

Lactose effect of *B. velezensis* EM-A8 viability during storage was determined in M5 at 150 days of incubation. Initial strain population was approximately 10 log (figure 3, page 6). However, after incubation, the population decreased to 4-4,5 log CFU ml^{-1} under refrigerated conditions with and without added lactose; and at room temperature at the end of the experiment, decreasing from 10 to 6 log CFU ml^{-1} with and without lactose addition.

1R (M1 with refrigeration), 3R (M3 with refrigeration), 5R (M5 with refrigeration), 1A (M1roomtemperature),3A (M3 room temperature), 5A (M5 room temperature).

1R (M1 con refrigeración), 3R (M3 con refrigeración), 5R (M5 con refrigeración), 1A (M1 temperatura ambiente), 3A (M3 temperatura ambiente), 5A (M5 temperatura ambiente).

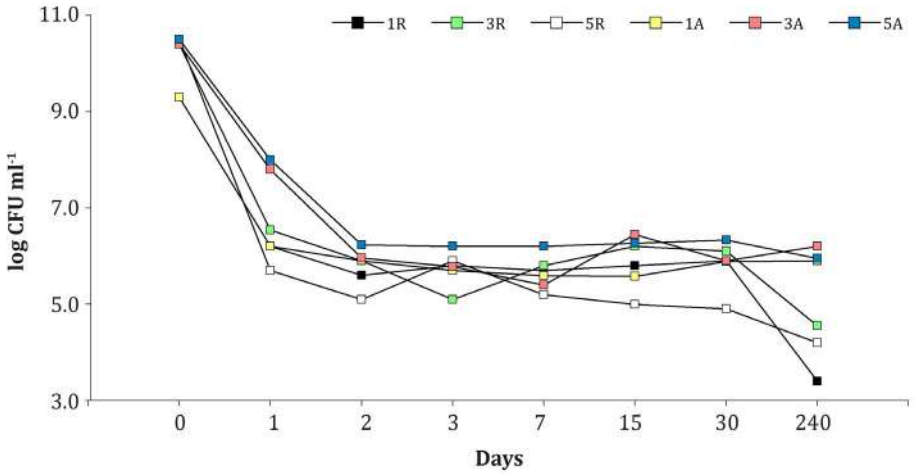


Figure 2. *B. velezensis* EM-A8 viability (CFU ml^{-1}) during storage with refrigeration (R) and room temperature (A) for 240 days. Media 1, 3 y 5.

Figura 2. Viabilidad de *B. velezensis* EM-A8 (UFC ml^{-1}) durante el almacenamiento con refrigeración (R) y temperatura ambiente (A) durante 240 días. Medios 1. 3 y 5.

Bars represent the average of three independent replications and different letters indicate significant differences (P>0.05) according to the DGC test.

Cada barra representa el promedio de tres replicaciones independientes y letras diferentes indican diferencias significativas (P>0,05) según la prueba DGC.

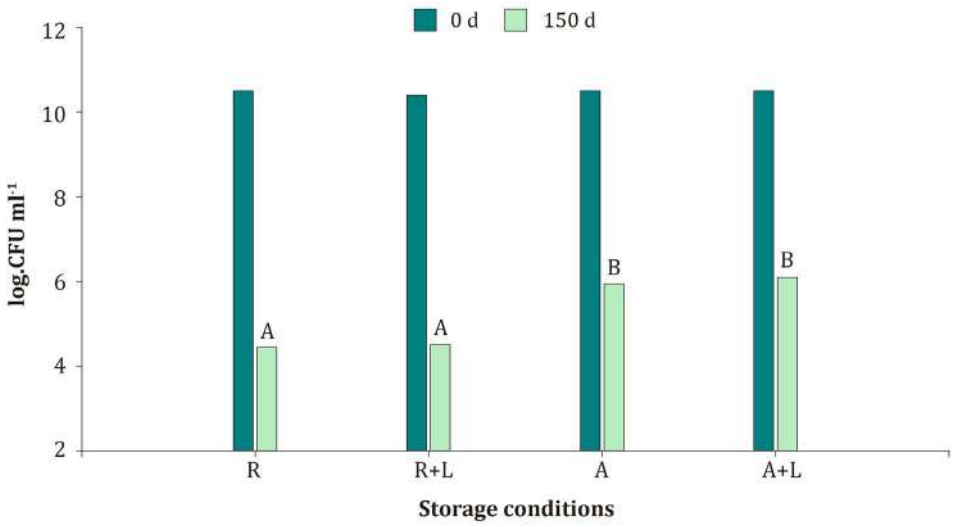


Figure 3. Viability of *B. velezensis* EM-A8 (CFU ml^{-1}) during storage under refrigeration (R) and room temperature (A), with and without lactose, at zero and 150 days.

Figura 3. Viabilidad de *B. velezensis* EM-A8 (UFC ml^{-1}) durante el almacenamiento en refrigeración (R) y temperatura ambiente (A), con adición de lactosa y sin lactosa, a cero y a los 150 días después.

Lyophilized Formulation

The initial inoculum of *B. velezensis* EM-A8, in M3 and M5 showed 5.6 x 10^9 CFU ml^{-1} before freezing. After lyophilization, each gram of rehydrated powder had 2 x 10^6 CFU ml^{-1}, indicating a significant loss of *B. velezensis* EM-A8 viability. Furthermore, the volume of liquid formulation to obtain one gram of lyophilized powder was excessive and impractical.

Discussion

The biological control of plant pathogens is an effective and eco-friendly method to manage diseases, preserving nature and human health from chemical pesticides (1). Biofungicides curb and control fungal plant pathogens by inoculating microbiota in or onto the plant. Several complex interactions among pathogen-biocontrol agents, biocontrol agent-plant, and environment play a significant role in disease control (3). In this sense, formulation determines biofungicide efficacy. Our study showed that commercial products and by-products in different media provide high growth and shelf life of *B. velezensis* EM-A8. The chosen sources of nitrogen and carbon (yeast extract, whole soy flour, sucrose, molasses) are widely described for producing beneficial microorganisms, including *B. velezensis* EM-A8 (6, 23). After one day of incubation in the studied media, cell count was 9 log. For M2, M3, M4 and M5, cell count increased by one logarithm after 32 hours, showing that *B. velezensis* EM-A8 population increased in one day of incubation and all media.

On the other hand, growth rate of *B. velezensis* EM-A8 was significantly different between M5 and M6, being higher with molasses as sugar source. Molasses concentration did not negatively affect *B. velezensis* EM-A8 growth. M3 and M4 show similar growth, even with twice the concentration of molasses in M3. However, some authors observed that high concentrations of molasses (20 and 40 g L^{-1}) did not support *B. subtilis* CPA-8 growth (26). Similar results were found by Costa *et al.* (2001) for *P. agglomerans* CPA-2, where increased molasses concentration (40 g L^{-1}) did not improve production, probably given by high toxic concentrations (6).

Regarding whole soy flour concentration, *B. velezensis* EM-A8 showed similar growth in M2 and M4 with 40 g L^{-1} and M3 with 10 g L^{-1} suggesting no influence over growth. The high concentrations of *B. velezensis* EM-A8 obtained in the whole soy flour media compared to yeast extract media showed that this carbon source promotes bacterial growth influenced by the capacity of microorganisms to use available nitrogen, similar to what Costa *et al.* (2002) and Yáñez-Mendizábal *et al.* (2012) found. However, media with whole soy flour became opaque, with lumps and debris from soy seed, complicating viability controls. On the contrary, selected media with yeast extract as nitrogen source were translucent and without lumps.

Storage temperature and media composition significantly affected *B. velezensis* EM-A8 viability, which markedly decreased in both storage conditions. After two days, the count was 4 log less than initial count. However, in both growth media (3 and 5), as well as in the control, viability remained stable throughout 8 months of storage. In all media *B. velezensis* EM-A8 cell viability showed significant difference in cold storage. In M3 and M5, viability decreased to 4 log while in the control, it decreased to 3 log. In contrast, Yáñez-Mendizabal *et al.* (2012) showed that all formulations of *B. subtilis* CPA-8 during 6 months of storage in cold and at room temperature had the same behaviour, viable cells maintained or slightly decreased around 0.2 - 0.3 log.

Contrarily, other authors demonstrated greater stability and higher microbial survival in cold-stored samples compared to those stored at room temperature (4). Moreover, it was observed that in-storage protective lactose failed to reverse viability loss of *B. velezensis* EM-A8, both in refrigeration and at room temperature. Lactose additions did not reverse viability loss, unlike previously seen (23). On the other hand, unlike other investigations (6, 10, 25), lyophilization was discarded as conservation and storage method given the amount of powder needed for later foliar application.

The viability loss of the microorganisms after the formulation and during the storage and distribution is a regular problem (23). All three liquid formulations stored at room temperature maintained stable viability in 6 log for 8 months. Practically, this finding determines such a convenient storage condition as room temperature is preferable to refrigerated storage. Formulation, production and stabilization of the biocontrol agent determines the final efficacy of a *Bacillus*-based product (19). An ideal formulation is not toxic to the host plant, easy to handle, has long shelf life, is compatible with other agrochemicals, cost-effective and stable. Formulations should work under different environmental conditions, providing reliable control of plant diseases (12). Moreover, the ability of biocontrol agents to control foliar diseases is largely affected by environmental fluctuation (12). *B. velezensis* EM-A8 is native to the phyllosphere with the advantage of being adapted to such conditions.

Agroecological management strategies would not only help in optimal recycling of nutrients and organic matter turnover, closed energy flows, and water and soil conservation but also would help in balancing pest-natural enemy populations (24). Diverse biocontrol agents have successfully contributed to the sustainable management of phytopathogens and various foliar diseases can be effectively controlled by spray application of bacterial and fungal antagonists. *Bacillus* strains are gaining enormous attention due to their ability to effectively cause disease suppression (1).

Conclusions

The liquid formulation developed from *B. velezensis* EM-A8 in growth medium with yeast extract and molasses, modified a_w with glycerol at 0.97 and stored at room temperature is a promising product and an important step towards the successful control of foliar diseases in maize.

References

1. Babbal, A.; Khasa, Y. 2017. Microbes as biocontrol agents. In: Probiotics and Plant Health. Kumas, V. (Eds). Springer. 507-551.
2. Barkai-Golan, R. 2001. Postharvest diseases of fruits and vegetables. Development and control. Elsevier, Amsterdam, The Netherlands.
3. Bonaterra, A.; Badosa, E.; Daranas, N.; Francés, J.; Roselló, G.; Montesinos, E. 2022. Bacteria as biological control agents of plant diseases. Microorganisms. 10: 1759.
4. Boza, Y.; Barbin, D.; Scamparini, A. 2004. Effect of spray drying on the quality of encapsulated cells of *Beijerinckia* sp. Process Biochemistry. 39: 1275-1284.
5. Costa, E.; Teixidó, N.; Usall, J.; Atarés, E.; Viñas, I. 2001. Production of the biocontrol agent *Pantoea agglomerans* strain CPA-2 using commercial products and byproducts. Applied Microbiology and Biotechnology. 56: 367-371.
6. Costa, E.; Teixidó, N.; Usall, J.; Atarés, E.; Viñas, I. 2002. The effect of nitrogen and carbon sources on growth of the biocontrol agent *Pantoea agglomerans* strain CPA-2. Letters in Applied Microbiology. 35: 117-120.
7. Dallyl, H.; Fox, A. 1980. Spoilage of material of reduced water activity by xerophilic fungi. Technical Series 15. London: Academic Press. 219-239.
8. Di Rienzo, J.; Casanoves, F.; Balzarini, M.; Gonzalez, L.; Tablada, M.; Robledo, C. 2012. InfoStat versión. Argentina: GrupoInfoStat, FCA, Universidad Nacional de Córdoba. http://www.infostat.com.ar
9. Fessia, A.; Sartori, M.; García, D.; Fernández, L.; Ponzio, R.; Barros, G.; Nesci, A. 2022. *In vitro* studies of biofilm-forming *Bacillus* strains, biocontrol agents isolated from the maize phyllosphere. Biofilm 4, 100097.
10. Fonseca, F.; Cenard, S.; Passot, S. 2015. Freeze-drying of lactic acid bacteria. In: Cryopreservation and Freeze-Drying Protocols. Methods in Molecular Biology, vol 1257. Wolkers, W.; Oldenhof, H. (eds) Springer, New York,
11. Kinay, P.; Yildiz, M. 2008. The shelf life and effectiveness of granular formulations of *Metschnikowia pulcherrima* and *Pichia guilliermondii* yeast isolates that control postharvest decay of citrus fruit. Biological Control. 45: 433-440.
12. Kumar, S.; Thakur, M.; Rani, A. 2014. Trichoderma: Mass production, formulation, quality control, delivery and its scope in commercialization in India for the management of plant diseases. African Journal of Agricultural Research. 9(53): 3838-3852.
13. Reis, F; Servulo, E.; De Franca, F. 2004. Lipopeptide surfactant production by *Bacillus subtilis* grown on low-cost raw materials. Applied Biochemistry and Biotechnology. 113: 899-912.
14. Sartori, M.; Nesci, A.; Etcheverry, M. 2012. Production of *Fusarium verticillioides* biocontrol agents, *Bacillus amyloliquefaciens* and *Microbacterium oleovorans*, using different growth media: evaluation of biomass and viability after freeze-drying. Food Additives and Contaminants (A). 29(2): 287-292.
15. Sartori, M.; Nesci, A.; Formento, A.; Etcheverry, M. 2015. Selection of potential biological control of *Exserohilum turcicum* with epiphytic microorganisms from maize. Revista Argentina de Microbiología. 47(1): 62-71.
16. Sartori, M.; Nesci, A.; Garcia, J.; Passone, M.; Montemarani, A.; Etcheverry M. 2017a. Efficacy of epiphytic bacteria to prevent northern leaf blight caused by *Exserohilum turcicum* in maize. Revista Argentina de Microbiología. 49(1): 75-82.
17. Sartori, M.; Nesci, A.; Montemarani, A.; Barros, G.; Garcia, J.; Etcheverry M. 2017b. Preliminary evaluation of biocontrol agents against maize pathogens *Exserohilum turcicum* and *Puccinia sorghi* in field assays. Agricultural Sciences. 8: 1003-1013.

18. Sartori, M.; Bonacci, M.; Barra, P.; Fessia, A.; Etcheverry, M.; Nesci, A.; Barros, G. 2020. Studies on possible modes of action and tolerance to environmental stress conditions of different biocontrol agents of foliar diseases in maize. Agricultural Sciences. 11: 552-566.
19. Schisler, D.; Slininger, P.; Behle, R.; Jackson, M. 2004. Formulation of *Bacillus* spp. for biological control of plant diseases. Phytopathology. 94: 1267-1271.
20. Stanbury, P.; Whitaker, A.; Hall, S. 1995. Media for industrial fermentations. In: Principles of fermentation technology. Pergamon Press, Oxford. 93-121.
21. Tabbene, O.; Slimene, I.; Djebali, K.; Mangoni, M.; Urdaci M.; Limam F. 2009. Optimization of medium composition for the production of antimicrobial activity by *Bacillus subtilis* B38. Biotechnology Progress. 25: 1266-1274.
22. Teixidó, N.; Cañamás, T. P.; Abadias, M.; Usall, J; Solsona, C.; Casals, C.; Viñas, I. 2006. Improving low water activity and desiccation tolerance of the biocontrol agent *Pantoea agglomerans* CPA-2 by osmotic treatments. Journal of Applied Microbiology. 101: 927-937.
23. Teixidó, N.; Usall, J.; Torres, R. 2022. Insight into a Successful development of biocontrol agents: production, formulation, packaging and shelf life as key aspects. Horticulturae. 8: 305.
24. Vandemeer, J. 1995. The ecological basis of alternative agriculture. Annual review of Ecology and Systematics. 26: 201-224.
25. Vermelho, A.; Moreira, J.; Junior, A.; da Silva, C.; Cardoso, V.; Akamine, I. 2024. Microbial preservation and contamination control in the baking industry. Fermentation. 10: 231. doi.org/10.3390/fermentation10050231
26. Yánez-Mendizábal, V.; Viñas, I.; Usall, J.; Torres, R.; Solsona, C.; Teixidó, N. 2012. Production of the postharvest biocontrol agent *Bacillus subtilis* CPA-8 using low-cost commercial products and by-products. Biological control. 60: 280-289.
27. Younis, M.; Hezayen, F.; Nour-Eldein, M.; Shabeb, M. 2010. Optimization of cultivation medium and growth conditions for Bacillus subtilis KO strain isolated from sugar cane molasses. American Eurasian Journal of Agricultural Environmental Science. 7: 31-37.

Acknowledgements

This study was financed by Agencia Nacional de Promoción Científica y Tecnológica (ANPCYT), FONCYT-PICT 4220/18 y PIP 2022-2024 161CO

Seed Physiological Quality and Selectivity of Pre-Emergence Herbicides in Soybean (*Glycine max* L.)

Calidad fisiológica de las semillas y selectividad de herbicidas pre-emergentes en el cultivo de soja (*Glycine max* L.)

Alessandro Guerra da Silva [1], João Victor dos Santos Caldas [1], Sérgio de Oliveira Procópio [2], Guilherme Braga Pereira Braz [1], Itamar Rosa Teixeira [3], Camila Jorge Bernabé Ferreira [1], Matheus de Freitas Souza [1], Ricardo Scheffer de Andrade Silva [1*]

Originales: *Recepción:* 16/10/2024- *Aceptación:* 13/04/2026

ABSTRACT

Seed physiological quality significantly affects crop performance. Besides proper crop establishment, pre-emergence herbicides constitute one major weed-control strategy. This study evaluated selectivity of pre-emergence herbicides in soybean sown with seeds of high and low physiological quality. The experiment was conducted in Rio Verde, Brazil, in a 4x2 randomized block design, with four replications. The treatments consisted of low and high-quality seeds combined with pre-emergence herbicides [imazethapyr + flumioxazin], diclosulam and [sulfentrazone + diuron], and a control. Plants from high-quality seeds showed better performance than those grown from low-quality seeds. This resulted in a greater emergence speed index, plant height, inter-row cover, NDVI, plant population, first pod height, thousand-grain weight, and grain yield. Regardless of seed quality, pre-emergence herbicides did not influence the evaluated traits.

Keywords
Glycine max • vigor • germination • weeds • grain yield

https://doi.org/10.48162/rev.39.217

1 Universidade de Rio Verde. Programa de Pós-graduação em Produção Vegetal. Fazenda Fontes do Saber. Campus Universitário. Rio Verde. Goiás. Brasil. CEP: 75.901-970. * ricardoscheffer@unirv.edu.br
2 Embrapa Meio Ambiente. Rodovia SP-340. Km 127,5. Tanquinho Velho. Jaguariúna. São Paulo. Brasil. CEP: 13918-110.
3 Universidade Estadual de Goiás. Instituto de Ciências Agrárias. Campus CET. Anápolis. Goiás. Brasil. CEP 75132-203.

Licenses Creative Commons Attribution - Non Commercial - Share Alike

Resumen

La calidad fisiológica de las semillas puede afectar significativamente el rendimiento de las plantas de soja. Además del adecuado establecimiento del cultivo, es necesario manejar las malezas, siendo los herbicidas pre-emergentes una de las principales opciones de control. El objetivo de este estudio fue evaluar la selectividad de herbicidas aplicados en pre-emergencia en soja sembrada con semillas de alta y baja calidad fisiológica. El experimento se implementó en campo en el municipio de Río Verde, Brasil, en un diseño factorial 4x2 en bloques al azar, con cuatro repeticiones. Los tratamientos consistieron en el uso de semillas de baja y alta calidad fisiológica combinadas con la aplicación de herbicidas [imazetapir + flumioxazina], diclosulam y [sulfentrazona + diurón] en pre-emergencia, además de un tratamiento sin herbicida. Las plantas provenientes de semillas de alta calidad fisiológica mostraron un mejor desempeño fitotécnico que las provenientes de semillas de baja calidad fisiológica. Esto resultó en aumentos en el índice de velocidad de emergencia, altura de planta, cobertura entre hileras, NDVI, población de plantas, altura de la primera vaina, peso de mil granos y rendimiento de grano. Los herbicidas aplicados en pre-emergencia no influyeron en las características evaluadas, independientemente de la calidad de las semillas.

Palabras clave
Glycine max • vigor • germinación • malezas • rendimiento de grano

Introduction

Soybean is the main oilseed grown in Brazil. Worldwide, Brazil is the largest soybean producer and exporter, with an estimated area of 47.6 million hectares in the 2024/2025 growing season and a production of approximately 169.7 million tons of grains (5).

Over the decades, Brazilian soybean production has increased, given the expansion of cultivated areas and increased productivity. However, technological difficulties like low seed quality still hinder crop maximum productivity. The use of high-physiological quality seeds ensures plant establishment and higher leaf area indices, leading to increased grain yield (3, 8). Due to metabolic processes involved in germination (7), seeds of high physiological quality have higher content of proteins, starch and soluble sugars, and greater capacity to mobilize reserves during germination, resulting in better initial performance (16). Soybean seeds with high physiological quality also exhibit quicker emergence and seedling development, resulting in rapid inter-row closure and, consequently, greater competition with weeds (6).

Noteworthy, weed interference can affect crop development. These negative effects vary with the weed community, plant density, and the period of coexistence with the crop (14). Therefore, without effective control, weed interference in soybeans can lead to significant reductions in grain yield (26).

The use of herbicides is a fundamental strategy in weed-integrated management in soybeans. The emergence and rapid spread of weeds resistant to post-emergence herbicides like glyphosate has demanded pre-emergence products (20). However, phytotoxicity after pre-emergence applications is often observed in soybean crops, stopping farmers from adopting the technology. Possible reasons for this damage in soybean plants may be related to soil properties, such as texture (2, 15), organic matter (13), and moisture (21, 31), in addition to excessive doses (4, 9), and sprayer overlapping. However, the use of seeds of low physiological quality can also contribute to the occurrence of phytotoxicity in the soybean crop. In this context, seed vigor influences seedling emergence (19) and, consequently, herbicide absorption (23).

Studies investigating the relationship between seed quality and herbicide phytotoxicity are still limited. We evaluated herbicide selectivity in pre-emergence, considering soybean seeds of high and low physiological quality.

Material and Methods

The field experiment was conducted in Rio Verde, state of Goiás, Brazil (17°47'228" S; 51°00'383" W; 769 m altitude) from December 13, 2019, to April 3, 2020. Soil physicochemical characterization included pH in $CaCl_2$: 5.2; O.M.: 32.1 and O.C.: 18.6 in $g.dm^{-3}$; P: 5.4 $mg.dm^{-3}$; K: 0.35; Ca: 1.42; Mg: 0.88; Al: 0.03; H+Al: 1.90; CEC: 4.55 and SB: 2.65 in $cmol_c.dm^{-3}$; sand, silt, and clay: 470, 80, and 450 in $g.kg^{-1}$, respectively (clay texture).

Before installing the experiment, weed chemical desiccation was carried out with two applications. The first application was 20 days before soybean sowing using glyphosate (1,440 g a.i. ha^{-1}) combined with clethodim (108 g a.i. ha^{-1}). The second application was carried out 7 days before sowing, using paraquat (400 g a.i. ha^{-1}). Both 150 L ha^{-1} applications were applied with a spraying bar. The experiment was a 2x4 randomized block design with four replications. The first factor was the physiological quality of soybean seeds, classified according to tetrazolium test (12), at high physiological quality (86% vigor and 94% viability) and low physiological quality (67% vigor and 86% viability). The second factor included three pre-emergence herbicides: [imazethapyr + flumioxazin] ([106 + 50 g a.i. ha^{-1}]), diclosulam (29.4 g a.i. ha^{-1}) and [sulfentrazone + diuron] ([210 + 420 g a.i. ha^{-1}]), and a control treatment without herbicide. Each experimental unit consisted of four sowing rows, 8.0 m long, spaced 0.5 m apart. The studied area was formed by the two central rows, disregarding 1.0 m at each end, totaling 6.0 m^2.

Soybean cultivar was NS 7007 IPRO®, with indeterminate growth and relative maturity group 7.1. Mechanical sowing was on December 13, 2019, at 2 cm depth and 17 seeds linear m^{-1}. Fertilization responded to soil chemical analysis. At sowing, the equivalent of 300 kg ha^{-1} 00-20-20 fertilizer, corresponding to 60 kg P_2O_5 and K_2O, was applied. For nitrogen supply by symbiotic N_2 fixation, seeds were inoculated with *Bradyrhizobium elkanii* (concentration of $5x10^9$ viable cells per mL) in the proportion of 0.15 L 100 kg^{-1} seeds.

Herbicides were applied after sowing using a CO_2 constant-pressure backpack sprayer (206843 Pa). The equipment consisted of a bar with four XR 110.015 VS fan spray nozzles, spaced at 0.5 m, providing a spray volume of 150 L ha^{-1}. A thermo-hygro-anemometer monitored environmental conditions during the applications (table 1). The anemometer was placed just above the plant apex at the beginning and at the end of the applications.

Table 1. Environmental conditions during herbicide application.
Tabla 1. Condiciones ambientales durante la aplicación de los tratamientos herbicidas.

Application in pre-emergence	Beginning	End
Time (t)	9:15	9:45
Temperature (°C)	25 .8	26 .0
Relative humidity (%)	74 .4	74 .1
Wind speed and direction ($km.h^{-1}$)	3 .9 E	2 .2 E
Cloudiness (%)	95	95

During the experiment, emerged weeds were manually eliminated, leaving soybean plants just exposed to the herbicides. Pest and disease management followed technical recommendations (28).

Treatment effects on soybean plant development were evaluated by calculating the emergence speed index (ESI; Equation 1; 18) in the first 10 days after emergence (DAE) until constant number of emerged plants; plant height at 7, 14, 21, 28 and 35 DAE (measurement from the soil surface to the insertion of the last fully developed trifoliate leaf in five plants per plot, randomly chosen); visual phytotoxicity at 7, 14, 21 and 28 DAE (30); normalized difference vegetation index (NDVI) at 7, 14, 21, 28 and 35 DAE, using the GreenSeeker® sensor; inter-row space closure at 35 and 42 DAE (evaluation of the percentage area covered

by foliage, considering half inter-row coverage by leaves of each adjacent row, as 100% closure); and chlorophyll *a*, *b* and total at 14, 28, and 35 DAE (measurement of the last fully developed trifoliate leaf in five plants per plot randomly chosen) using a ClorofiLOG® sensor.

$$\text{Equation 1: ESI} = \left(\frac{E_1}{N_1}\right) + \left(\frac{E_2}{N_2}\right) + \ldots \left(\frac{E_n}{N_n}\right) \quad (1)$$

where:
ESI = emergence speed index
E = Number of plants emerged each day
N = Number of days elapsed from sowing

At harvest, first pod height (distance from the ground to the insertion of the first pod, measured in five random plants), plant population (number of plants harvested), pods per plant (in five random plants), weight of a thousand grains (counting a thousand grains 13% moisture), grain yield (harvesting the plants and threshing pods, with subsequent cleaning and weighing, 13% moisture) and relative yield (yield gain in relation to the control and to the use high-quality seeds).

Statistical Analysis

Data not meeting ANOVA assumptions were transformed into $\sqrt{(x+0.5)}$: emergence speed index, NDVI at 28 and 35 DAE, inter-row cover, chlorophyll *a*, *b*, and total at 28 and 35 DAE and plant population. Data were tested by ANOVA using the F-test ($p<0.05$). Means were compared by Tukey's test ($p<0.05$). For data analysis, Sisvar software was used (10).

Results and Discussion

Physiological quality of seeds significantly influenced emergence speed (48% higher) and plant height in all evaluations, as previously seen (3, 22, 25). However, no interaction was found with pre-emergence herbicides (table 2, page 5).

Regardless of seed physiological quality, none of the pre-emergence herbicides delayed soybean emergence or reduced plant size at 7, 14, 21, 28, and 35 DAE (table 2, page 5). Thus, herbicides did not influence crop establishment, proving selectivity in pre-emergence, as previously seen (24).

At 7 and 14 DAE, and regardless of seed physiological quality, few phytotoxicity symptoms (5%) were found in soybean plants treated with herbicides [sulfentrazone + diuron], diclosulam and [imazethapyr + flumioxazin] (table 3, page 6). Later evaluations performed at 21 and 28 DAE showed no visual symptoms. Thus, a rapid recovery takes place, considering the few initial phytotoxicity symptoms. Similar results were reported by Sanchotene *et al*. (2017), who also observed mild phytotoxicity symptoms caused by the herbicides sulfentrazone, [imazethapyr + flumioxazin] and diclosulam in soybean.

The NDVI and inter-row cover significantly affected seed physiological quality in all evaluations (table 4, page 6-7). Pre-emergence herbicides caused significant effects only at 14 and 35 DAE for NDVI, without inter-row effects. Similarly, seed physiological quality and pre-emergence herbicides showed no interaction.

The use of high-quality seeds resulted in higher soybean NDVI in all evaluations (table 4, page 6-7). The highest values obtained from high-quality seeds relate to quicker emergence and initial plant growth (17).

At 14 DAE, the treatment [imazethapyr + flumioxazin] reduced soybean NDVI in relation to the control (table 4, page 6-7), probably given by mild initial phytotoxicity. At 35 DAE, this herbicide reduced NDVI values in relation to [sulfentrazone + diuron], however, none differed from the control.

Plants from high-quality seeds provided 37% higher inter-row cover at 35 DAE than plants from low-quality seeds. At 42 DAE, high-quality seed had almost completely closed inter-rows (99%). This demonstrates the importance of using high-quality seeds in faster canopy closure and consequent weed control (1).

Table 2. Emergence speed index and plant height at 7, 14, 21, 28, and 35 DAE as a function of seed physiological quality and pre-emergence herbicide application.

Tabla 2. Índice de velocidad de emergencia y altura de plantas a los 7, 14, 21, 28 y 35 días después de la emergencia (DAE) en función de la calidad fisiológica de la semilla y la aplicación de herbicidas en preemergencia.

Seed quality	Pre-emergence herbicides				
	[Sulfentrazone + diuron][1/]	Diclosulam	[Imazethapyr + flumioxazin][1/]	Control	Average
Emergence speed index					
High	46.31	45.02	46.04	44.57	45.49 a
Low	31.62	31.14	30.91	29.51	30.80 b
Average	38.97 A	38.08 A	38.48 A	37.04 A	
CV (%)			3.95		
Plant height (cm) - 7 DAE					
High	8.20	8.70	8.20	8.45	8.38 a
Low	5.95	6.05	5.70	5.65	5.83 b
Average	7.07 A	7.37 A	6.95 A	7.05 A	
CV (%)			10.88		
Plant height (cm) - 14 DAE					
High	12.75	13.30	13.55	12.85	13.11 a
Low	10.75	11.15	10.30	10.80	10.75 b
Average	11.75 A	12.22 A	11.92 A	11.75 A	
CV (%)			6.14		
Plant height (cm) - 21 DAE					
High	18,60	19.95	20.20	19.90	19.66 a
Low	17.15	17.25	17.60	16.45	17.11 b
Average	17.87 A	18.60 A	18.90 A	18.17 A	
CV (%)			5.26		
Plant height (cm) - 28 DAE					
High	28.30	28.95	27.90	28.55	28.42 a
Low	23.65	24.95	25.15	23.80	24.38 b
Average	25.97 A	26.95 A	26.52 A	26.17 A	
CV (%)			6.43		
Plant height (cm) - 35 DAE					
High	45.60	46.75	43.75	48.35	46.11 a
Low	40.85	41.05	39.15	39.05	40.02 b
Average	43.22 A	43.90 A	41.45 A	43.70 A	
CV (%)			6.51		

[1/] formulated mixture. Means followed by distinct letters, lowercase in columns and uppercase in rows, differ significantly from each other, by Tukey's test (p = 0.05). Data not meeting normality or homoscedasticity were transformed into √(x+0.5).

[1/] mezcla formulada indicada. Las medias seguidas de letras distintas, minúsculas en la columna y mayúsculas en la fila, difieren significativamente entre sí, según la prueba de Tukey al 5% de probabilidad. Los datos que no cumplían con el supuesto de normalidad se transformaron en √(x+0,5).

Table 3. Phytotoxicity in soybean plants at 7, 14, 21, and 28 DAE as a function of seed physiological quality and pre-emergence herbicides.

Tabla 3. Fitotoxicidad en plantas de soja a los 7, 14, 21 y 28 días después de la emergencia (DAE) en función de la calidad fisiológica de la semilla y la aplicación de herbicidas en preemergencia en soja.

Herbicides	Phytotoxicity (%)							
	7 DAE		14 DAE		21 DAE		28 DAE	
	Seed quality							
	High	Low	High	Low	High	Low	High	Low
[Sulfentrazone + diuron] 1/	5.00	5.00	5.00	5.00	0.00	0.00	0.00	0.00
Diclosulam	5.00	5.00	5.00	5.00	0.00	0.00	0.00	0.00
[Imazethapyr + flumioxazin] 1/	5.00	5.00	5.00	5.00	0.00	0.00	0.00	0.00
Control	0.00	0.00	0.00	0.00	0.00	0.00	0.00	0.00

1/ formulated mixture.
1/ mezcla formulada.

Table 4. NDVI at 7, 14, 21, 28, and 35 DAE and soybean inter-row closure at 35 and 42 DAE as a function of seed vigor and application of pre-emergence herbicides.

Tabla 4. Índice de Vegetación de Diferencia Normalizada (IVDN) a los 7, 14, 21, 28 y 35 días después de la emergencia (DAE) y cierre entre hileras de soja a los 35 y 42 DAE en función del vigor de la semilla y la aplicación de herbicidas en preemergencia.

Pre-emergence herbicides					
Seed quality	[Sulfentrazone + diuron]1/	Diclosulam	[Imazethapyr + flumioxazin]1/	Control	Average
IVDN (%) - 7 DAE					
High	24.25	23.75	24.50	26.00	24.62 a
Low	23.00	22.00	19.00	19.00	20.75 b
Average	23.62 A	22.87 A	21.75 A	22.50 A	
CV (%)			13.10		
IVDN (%) - 14 DAE					
High	38.75	43.00	39.25	46.25	41.81 a
Low	30.25	32.50	28.75	33.25	31.18 b
Average	34.50 AB	37.75 AB	34.00 B	39.75 A	
CV (%)			10.84		
IVDN (%) - 21 DAE					
High	55.75	58.75	56.25	60.25	57.75 a
Low	47.00	48.75	48.25	52.50	49.12 b
Average	51.37 A	53.75 A	52.25 A	56.37 A	
CV (%)			7.64		

1/ formulated mixture. Means followed by distinct letters, lowercase in columns and uppercase in rows, differ significantly from each other, by Tukey's test at p=0.05. Data not meeting normality y homocedasticidad were transformed into √(x+0.5).
1/ mezcla formulada indicada. Las medias seguidas de letras distintas, minúsculas en la columna y mayúsculas en la fila, difieren significativamente entre sí, según la prueba de Tukey al 5% de probabilidad. Los datos que no cumplían con el supuesto de normalidad se transformaron en √(x+0,5).

Pre-emergence herbicides					
Seed quality	**[Sulfentrazone + diuron]**[1/]	**Diclosulam**	**[Imazethapyr + flumioxazin]**[1/]	**Control**	**Average**
IVDN (%) - 35 DAE					
High	87.75	87.25	86.50	87.75	87.31 a
Low	86.00	85.25	84.25	85.50	85.25 b
Average	86.87 A	86.25 AB	85.37 B	86.62 AB	
CV (%)			0.60		
Closing between the lines (%) - 35 DAE					
High	91.25	91.25	91.25	92.50	91.56 a
Low	67.50	67.50	70.00	62.50	66.87 b
Average	79.37 A	79.37 A	80.62 A	77.50 A	
CV (%)			2.45		
Closing between the lines (%) - 42 DAE					
High	99.50	99.00	99.00	100.00	99.37 a
Low	93.75	93.75	92.50	95.00	93.75 b
Average	96.62 A	96.37 A	95.75 A	97.50 A	
CV (%)			0.09		

[1/] formulated mixture. Means followed by distinct letters, lowercase in columns and uppercase in rows, differ significantly from each other, by Tukey's test at p=0.05. Data not meeting normality y homocedasticidad were transformed into √(x+0.5).

[1/] mezcla formulada indicada. Las medias seguidas de letras distintas, minúsculas en la columna y mayúsculas en la fila, difieren significativamente entre sí, según la prueba de Tukey al 5% de probabilidad. Los datos que no cumplían con el supuesto de normalidad se transformaron en √(x+0,5).

Chlorophyll *a*, *b* and total index showed no interaction between seed physiological quality and pre-emergence herbicide application (table 5, page 8-9). Furthermore, regardless of the evaluation period (14, 28, and 35 DAE), no herbicide altered chlorophyll contents.

Nevertheless, soybean plants from seeds of higher physiological quality had higher content of chlorophyll *b* at 14 DAE, as well as chlorophyll *a* and total chlorophyll at 28 DAE (table 5, page 8-9). Since more vigorous seeds induce faster and more uniform emergence of seedlings, there is a greater need for water and nutrients in early crop development. Thus, photosynthesis occurs earlier, with greater accumulation of photoassimilates in early developmental stages, and consequent greater yield (8).

Considering agronomic traits, first pod height, plant population, pods per plant, thousand-grain weight, grain yield and relative yield showed no effects of pre-emergence herbicides or the interaction of this factor with seed quality of the seeds. However, except for pods per plant, in which there was no effect on seed quality, plants from high-quality seeds resulted in better agronomic traits than low-quality seeds (table 6, page 9-10).

Higher first pod height was observed in soybean plants originating from high-quality seeds (table 6, page 9-10), also verified by Rossi *et al*. (2017). This result is highly relevant, as soybean plants with higher pod height suffer less grain loss in mechanized harvesting, which results in higher grain yield and less infestation of volunteer plants in subsequent cultivation.

In addition to a taller pod, high-quality seeds provided, at harvest, 34,700 more soybean plants per hectare (17%) than low-quality seeds (table 6, page 9-10). Considering all treatments initiated with the same plant population, differences among treatments are only given by seed quality (3). Furthermore, higher seed quality results in more emerged seedlings and lower plant mortality, as emphasized by Rossi *et al*. (2017). Still, the null seed quality effects over pods per plant may be related to final population (table 6, page 9-10). Based on our results, low-quality seeds resulted in a smaller population, probably stimulating vegetative growth in the form of branches, inducing pod development (11).

Another benefit of using high-quality seeds is the larger thousand-grain weight (table 6, page 9-10) (3, 8). This leads to the belief that soybean plants with better photosynthetic apparatus, as observed by the higher chlorophyll levels in certain treatments, produce more photoassimilates for grain formation and filling.

Table 5. Chlorophyll *a*, *b* and total index in soybean plants at 14, 28, and 35 DAE as a function of seed vigor and pre-emergence herbicide application.

Tabla 5. Índice de clorofila *a*, *b* y total en plantas de soja a los 14, 28 y 35 días después de la emergencia (DAE) en función del vigor de la semilla y la aplicación de herbicidas en preemergencia.

Pre-emergence herbicides					
Seed quality	**[Sulfentrazone + diuron][1/]**	**Diclosulam**	**[Imazethapyr + flumioxazin][1/]**	**Control**	**Average**
Chlorophyll a index - 14 DAE					
High	24.75	23.35	25.30	26.54	24.23 a
Low	23.70	24.27	22.08	21.42	22.87 a
Average	24.23 A	23.81 A	23.69 A	22.48 A	
CV (%)			11.20		
Chlorophyll b index - 14 DAE					
High	7.76	7.53	8.18	7.49	7.74 a
Low	7.15	7.28	6.93	6.86	7.05 b
Average	7.45 A	7.40 A	7.55 A	7.17 A	
CV (%)			10.04		
Total Chlorophyll Index - 14 DAE					
High	32.51	30.87	33.48	31.03	31.97 a
Low	30.85	31.54	29.01	28.28	29.92 a
Average	31.68 A	31.21 A	31.24 A	29.65 A	
CV (%)			7.97		
Chlorophyll a index - 28 DAE					
High	29.81	31.58	32.24	33.11	31.68 a
Low	28.06	28.95	26.43	25.28	27.18 b
Average	28.93 A	30.26 A	29.33 A	29.19 A	
CV (%)			16.83		
Chlorophyll b index - 28 DAE					
High	8.19	8.30	9,01	7.75	8.31 a
Low	6.64	9.76	7.27	7.24	7.72 a
Average	7.41 A	9.03 A	8.14 A	7.50 A	
CV (%)			10.67		
Total Chlorophyll Index - 28 DAE					
High	37.10	39.87	41.24	40.86	39.99 a
Low	34.69	38.71	33.69	32.52	34.90 b
Average	36.34 A	39.29 A	37.47 A	36.69 A	
CV (%)			15.99		

[1/] formulated mixture. Means followed by distinct letters, lowercase in columns and uppercase in rows, differ significantly from each other, by Tukey's test at p=0.05. Data not meeting normality were transformed into √(x+0.5).

[1/] mezcla formulada indicada. Las medias seguidas de letras distintas, minúsculas en la columna y mayúsculas en la fila, difieren significativamente entre sí, según la prueba de Tukey al 5% de probabilidad. Los datos que no cumplían con el supuesto de normalidad se transformaron en √(x+0,5).

Pre-emergence herbicides					
Seed quality	**[Sulfentrazone + diuron][1/]**	**Diclosulam**	**[Imazethapyr + flumioxazin][1/]**	**Control**	**Average**
Chlorophyll a index - 35 DAE					
High	32.28	31.42	31.25	31.27	31.55 a
Low	32.16	32.06	31.89	33.35	32.36 a
Average	32.22 A	31.74 A	31.57 A	32.31 A	
CV (%)			3.52		
Chlorophyll b index - 35 DAE					
High	10.50	10.24	10.09	9.99	10.20 a
Low	10.52	10.70	10.08	10.52	10.45 a
Average	10.51 A	10.47 A	10.08 A	10.25 A	
CV (%)			5.60		
Total Chlorophyll Index - 35 DAE					
High	42.78	41.66	41.34	41.25	41.76 a
Low	42.67	42.76	41.96	43.86	42.81 a
Average	42.73 A	42.21 A	41.67 A	42.56 A	
CV (%)			3.89		

[1/] formulated mixture. Means followed by distinct letters, lowercase in columns and uppercase in rows, differ significantly from each other, by Tukey's test at p=0.05. Data not meeting normality were transformed into √(x+0.5).

[1/] mezcla formulada indicada. Las medias seguidas de letras distintas, minúsculas en la columna y mayúsculas en la fila, difieren significativamente entre sí, según la prueba de Tukey al 5% de probabilidad. Los datos que no cumplían con el supuesto de normalidad se transformaron en √(x+0,5).

Table 6. Height of first pod insertion, plant population, pods per plant, thousand grain weight, grain yield and relative soybean yield as a function of seed vigor and pre-emergence herbicide application.

Tabla 6. Altura de inserción de la primera vaina, población de plantas, número de vainas por planta, peso de mil granos, rendimiento de grano y rendimiento relativo de soja en función del vigor de la semilla y la aplicación de herbicidas en preemergencia.

Pre-emergence herbicides					
Seed quality	**[Sulfentrazone + diuron][1/]**	**Diclosulam**	**[Imazethapyr + flumioxazin] [1/]**	**Control**	**Average**
Height of first pod insertion (cm)					
High	16.90	16.75	17.15	16.70	16.87 a
Low	12.20	14.00	13.35	15.10	13.66 b
Average	14.55 A	15.37 A	16.12 A	15.02 A	
CV (%)			10.13		
Plant population (thousand plants ha^{-1})					
High	228.75	250.00	241.25	250.00	242.50 a
Low	203.75	211.25	210.00	206.25	207.81 b
Average	216.25 A	230.62 A	225.62 A	228.12 A	
CV (%)			4.49		

[1/] formulated mixture. Means followed by distinct letters, lowercase in columns and uppercase in rows, differ significantly from each other, by Tukey's test at p=0.05. Data not meeting normality were transformed into √(x+0.5).

[1/] mezcla formulada indicada. Las medias seguidas de letras distintas, minúsculas en la columna y mayúsculas en la fila, difieren significativamente entre sí, según la prueba de Tukey al 5% de probabilidad. Los datos que no cumplían con el supuesto de normalidad se transformaron en √(x+0,5).

Pre-emergence herbicides					
Seed quality	**[Sulfentrazone + diuron]**[1/]	**Diclosulam**	**[Imazethapyr + flumioxazin]**[1/]	**Control**	**Average**
Pods per plant					
High	49.20	48.90	51.55	50.30	49.98 a
Low	53.45	51.05	49.90	54.20	52.15 a
Average	51.32 A	49.97 A	50.72 A	52.25 A	
CV (%)			13.25		
Thousand grain weight (g)					
High	172.40	178.16	173.78	174.08	174.61 a
Low	169.31	167.42	169.74	162.73	167.30 b
Average	170.86 A	172.79 A	171.76 A	168.41 A	
CV (%)			4.78		
Grain yield (kg ha^{-1})					
High	3,989	4,217	4,003	4,081	4,072 a
Low	3,775	3,755	3,693	3,600	3,706 b
Average	3,882 A	3,986 A	3,848 A	3,840 A	
CV (%)			7,75		
Relative yield (%)					
High	97.74	103.33	98.08	100.00	99.79 a
Low	92.50	92.01	90.51	88.22	90.81 b
Average	95.12 A	97.67 A	94.30 A	94.11 A	
CV (%)			7.75		

[1/] formulated mixture. Means followed by distinct letters, lowercase in columns and uppercase in rows, differ significantly from each other, by Tukey's test at p=0.05. Data not meeting normality were transformed into √(x+0.5).

[1/] mezcla formulada indicada. Las medias seguidas de letras distintas, minúsculas en la columna y mayúsculas en la fila, difieren significativamente entre sí, según la prueba de Tukey al 5% de probabilidad. Los datos que no cumplían con el supuesto de normalidad se transformaron en √(x+0,5).

Grain yield of soybean plants from high-quality seeds was higher than in plants from low-quality seeds, regardless of pre-emergence herbicide (table 6, page 9-10). Positive effects of using better seeds are also reported (3, 8, 22, 25). In general, our analysis showed an increase of approximately 9% in grain yield for treatments using high-quality seeds than low-quality ones.

Finally, pre-emergence herbicides were selective for soybean, not affecting development or yield components, regardless of seed quality. In addition, plants from high-quality seeds have faster emergence and vegetative growth, increased plant population and thousand-grain weight.

Conclusions

The herbicides [sulfentrazone + diuron], diclosulam and [imazethapyr + flumioxazin], applied in pre-emergence, do not influence growth, plant population, yield components, or soybean grain yield, regardless of seed physiological quality in sowing.

Soybean plants from high-quality seeds provide faster emergence, taller plants, greater NDVI, inter-row cover, plant population, first pod height, thousand-grain weight and grain yield, regardless of pre-emergence herbicide.

References

1. Asami, H.; Tachibana, M.; Homma K. 2021. Chemical and cultural control of *Ipomoea hederácea* var. integriuscula in narrow-row soybean in southwestern Japan. Weed Biology and Management. 21(3): 135-145. DOI: 10.1111/wbm.12232
2. Asher, B. S.; Dotray, P. A.; Liebl, R. A.; Keeling, J. W.; Ritchie, G. D.; Udeigwe, T. K.; Reed J. D.; Keller, K. E.; Bowe, S. J.; Aldridge, R. B.; Simon, A. 2021. Vertical mobility and cotton tolerance to trifludimoxazin, a new protoporphyrinogen oxidase-inhibiting herbicide, in three West Texas soils. Weed Technology. 35(1): 144-148. DOI: 10.1017/wet.2020.95
3. Caverzan, A.; Giacomin, R.; Müller, M.; Biazus, C.; Lângaro, N. C.; Chavarria, G. 2018. How does seed vigor affect soybean yield components? Agronomy Journal. 110(4): 318-1327. DOI: 10.2134/agronj2017.11.0670
4. Cieslik, L. F.; Vidal, R. A.; Trezzi, M. M. 2014. Fomesafen toxicity to bean plants as a function of the time of application and herbicide dose. Acta Scientiarum. Agronomy. 36(3): 329-334. DOI: 10.4025/actasciagron.v36i3.17630
5. Companhia Nacional de Abastecimento (CONAB). 2025. Acompanhamento de safra brasileira: grãos, décimo primeiro levantamento, safra 2024/25. CONAB. 12(11): 85-89.
6. Dias, M. A. N.; Pinto, T. L. F.; Mondo, V. H. V.; Cicero, S. M.; Pedrini, L. G. 2011. Direct effects of soybean seed vigor on weed competition. Revista Brasileira de Sementes. 33(2): 346-351. DOI: 10.1590/S0101-31222011000200017
7. Domergue, J. B.; Abadie, C.; Limani, A.; Way, D.; Tcherkez, G. 2019. Seed quality and carbon primary metabolism. Plant, Cell & Environment. 42(10): 2776-2788. DOI: 10.1111/pce.13618
8. Ebone, L. A.; Caverzan, A.; Tagliari, A.; Chiomento, J. L. T.; Silveira, D. C.; Chavarria, G. 2020. Soybean seed vigor: uniformity and growth as key factors to improve yield. *Agronomy.* 10(4): 545. DOI: 10.3390/agronomy10040545
9. Ethridge, S.; Post, A.; Devkota, P.; Mulvaney, M.; Leon, R. 2021. Characterisation of carinata tolerance to select herbicides using field dose-response studies. Weed Technology. 35(6): 957-966. DOI: 10.1017/wet.2021.57
10. Ferreira, D. F. 2019. Sisvar: A computer analysis system to fixed effects splitplot type designs. Brazilian Journal of Biometrics. 37(4): 529-535. DOI: 10.28951/rbb.v37i4.450
11. França, E. E.; Silva, G. C.; Araújo, M. E. V.; Teixeira, I. R.; Corrêa, P. C.; Silva, A. G. 2021. Agronomic and physiological characteristics of soybean cultivars and their seeds according to plant population. Agronomía Colombiana. 39(2): 177-186. DOI: 10.15446/agron.colomb.v39n2.93019.
12. França-Neto, J. B.; Krzyzanowski, F. C.; Costa, N. P. 1998. The tetrazolium test for soybean seeds. Embrapa Soja. 71 p.
13. Gannon, T. W.; Hixson, A. C.; Keller, K. E.; Weber, J. B.; Knezevic, S. Z.; Yelverton, F. H. 2014. Soil properties influence saflufenacil phytotoxicity. Weed Science. 62(4): 657-663. DOI: 10.1614/WS-D-13-00171.1
14. Ghersa, C. M.; Holt, J. S. 1995. Using phenology prediction in weed management: a review. Weed Research. 35(6): 461-470. DOI: 10.1111/j.1365-3180.1995.tb01643.x
15. Ghirardello, G. A.; Araújo, L. S.; Bacchin, L. C.; Dotta, M. A.; Souza, R. O.; Silva, A. F. M.; Silva, G. S.; Victoria Filho, R. 2021. Selectivity index of indaziflam to sugarcane cv. IACSP95-5000 in two soil textures. Revista Facultad Nacional de Agronomía Medellín. 74(2): 9531-9539. DOI: 10.15446/rfnam.v74n2.92423
16. Henning, A. F.; Mertz, M. L.; Jacob, E. A. J.; Dorneles, M.; Ronei, G. F.; Dejalma, P. Z. 2010. Composição química e mobilização de reservas em sementes de soja de alto e baixo vigor. Bragantia. 69(3): 727-733. DOI: 10.1590/S0006-87052010000300026
17. Lima, G. C.; Silva, M. L. N.; Curil, N.; Silva, M. A.; Oliveira, A. H.; Avanzi, J. C.; Ummus, M. E. 2013. Avaliação
da cobertura vegetal pelo índice de vegetação por diferença normalizada (IVDN). Ambiente & Água. 8(2): 204-214. DOI: 10.4136/ambi-agua.959
18. Maguire, J. D. 1962. Speed of germination-aid in selection and evaluation for seedling emergence and vigor. Crop Science. 2(1): 176-177. DOI: 10.2135/cropsci1962.0011183X000200020033x
19. Meneguzzo, M. R. R.; Meneghello, G. E.; Nadal, A. P.; Xavier, F. M.; Dellagostin, S. M.; Carvalho, I. R.; Gonçalves, V. P.; Lautenchleger, F.; Lângaro, N. C. 2021. Seedling length and soybean seed vigor. Ciência Rural. 51(7): e20190495. DOI: 10.1590/0103-8478cr20190495
20. Mueller, C. T.; Boswell, B. W.; Mueller, S. S.; Steckei, L. E. 2014. Dissipation of fomesafen, saflufenacil, sulfentrazone, and flumioxazin from a Tennessee soil under field conditions. Weed Science. 62(4): 664-671. DOI: 10.1614/WS-D-13-00183.1
21. Pacanoski, Z.; Mehemeti, A. 2021. Efficacy and selectivity of pre-em herbicide on dependence of soil types and precipitation in sunflower crop. Agraarteadus: Journal of Agricultural Science. 32(1): 100-110. DOI: 10.15159/jas.21.08
22. Pino, M.; Schuch, L. O. B.; Castellanos, C. I. S.; Koch, F.; Szareski, V. J.; Pimentel, J. R.; Troyjack, C.; Carvalho, I. R.; Martins, A. B. N.; Silva, F. L.; Peter, M.; Monteiro, M. A.; Demari, G. H.; Aumonde, T. Z.; Pedó, T. 2019. Individual and population behavior of soybean plants grown in rows with different proportions of high-and low-vigor seeds. Australian Journal of Crop Science. 13(1): 151-158. DOI: 10.21475/ajcs.19.13.01.p1044

23. Procópio, S. O.; Silva, A. A.; Santos, J. B.; Araújo, E. F.; Ribeiro Jr., J. I.; Ferreira, L. R. 2002. Efeito do envelhecimento artificial de sementes sobre a tolerância do feijão ao S-metolachlor, em baixa temperatura. Revista Ceres. 49(284): 353-367. DOI: 10.7824/rbh.v2i3.362
24. Ribeiro, V. H. V.; Maia, L. G. S.; Arneson, N. J.; Oliveira, M. C.; Read, H. W.; Ané, J. M.; Santos, J. B.; Werle R. 2021. Influence of pre-emergence herbicides on soybean development, root nodulation and symbiotic nitrogen fixation. Crop Protection. 144(1): 105576. DOI: 10.1016/j.cropro.2021.105576
25. Rossi, R. F.; Cavariani, C.; França-Neto, J. B. 2017. Vigor de sementes, população de plantas e desempenho agronômico de soja. Revista de Ciências Agrárias. 60(3): 215-222. DOI: 10.4322/rca.2239
26. Rüdell, E. C.; Petrolli, I. D. S.; Santos, F. M.; Frandaloso, D.; Silva, D. R. O. 2021. Weed interference capacity on soybean yield. Revista Facultad Nacional de Agronomía Medellín. 74(2): 9541-9547. DOI: 10.15446/rfnam.v74n2.89705
27. Sanchotene, D. M.; Dornelles, S. H. B.; Bolzan, T. M.; Vos, H. M.; Escobar, O. S.; Leon, C. B.; Muller, E. N.; Shimóia, E. P. 2017. Desempenho de diferentes herbicidas pré-emergentes para controle de *Euphorbia heterophylla* na cultura da soja. Perspectiva. 41(155): 7-15.
28. Seixas, C. D. S.; Neumaier, N.; Balbinot, Jr., A. A.; Krzyzanwski, F. C.; Leite, R. M. V. B. C. 2020. Tecnologias de produção de soja: região Central do Brasil. Londrina. Embrapa Soja. 347 p.
29. Shapiro, S. S.; Wilk, M. B. 1965. An analysis of variance test for normality (complete sample). Biometrika. 52(3): 591-611.
30. Sociedade Brasileira da Ciência das Plantas Daninhas (SBCPD). 1995. Procedimentos para instalação, avaliação e análise de experimentos com herbicidas. SBCPD. 42 p.
31. Viger, P. R.; Eberlein, C. V.; Fuerst, E. P. 1991. Influence of available soil water content, temperature, and CGA-154281 on metolachlor injury to corn. Weed Science. 39(2): 227-231.

Acknowledgments

To the Research Support Foundation of the State of Goiás (FAPEG) and the Coordination for the Improvement of Higher Education Personnel (CAPES/BRASIL), for financial support to perform this project and the University of Rio Verde, for financial support to aid publication.

Epiphytic Microorganisms Associated with Banana Phyllosphere with Potential Antagonism to Black Sigatoka (*Pseudocercospora fijiensis*) in Los Ríos, Ecuador

Identificación de microorganismos epífitos asociados a la filósfera de banano con potencial antagonismo a Sigatoka Negra (*Pseudocercospora fijiensis*) en la provincia de Los Ríos, Ecuador

Solanyi Marley Tigselema Zambrano [1*], Aracelly Mabel Villalba Puga [2],
Jim Raphael Ochoa Ramos [1], Galo Efraín Lara Hidalgo [1], Diana Aracelly López [1]

Originales: *Recepción:* 21/08/2024 - *Aceptación:* 06/03/2025

ABSTRACT

Black Sigatoka (*Pseudocercospora fijiensis)* is the most important leaf spot disease of bananas worldwide, particularly affecting Cavendish banana, the most exported variety. Additionally, this pathogen has developed resistance to some effective fungicides, making its management increasingly difficult. Epiphytic microorganisms with potential antagonism to *P. fijiensis* were identified in conventional banana farms in the province of Los Ríos. Sampling areas were determined through zoning processes and selecting the cantons of Mocache, Valencia, Baba and Pueblo Viejo. Leaf tissue samples were collected from three farms per zone. Microorganisms were isolated and morphologically and molecularly characterised in nine farms in the cantons of Valencia (63 bacteria), Baba (39 bacteria), Pueblo Viejo (8 bacteria) and 8 genera of fungi including 15 species. The isolated bacteria presented macroscopic and microscopic characteristics with different shapes, elevations, edges, consistencies and pigmentations. Taxonomically, they belonged to the genera *Bacillus* and *Cocos*, 81% Gram-negative and 19% Gram-positive. The analysis conducted for sampling-site selection allowed the identification of different microbial behaviours.

Keywords
microorganisms • fungi • bacteria • *Musa* spp.

https://doi.org/10.48162/rev.39.198

1 Instituto Nacional de Investigaciones Agropecuarias. Mocache. Ecuador. C. P. 120310.
* solanyi.tigselema@iniap.gob.ec
2 Universidad de Las Américas. Facultad de Ingeniería y Ciencias Aplicadas. Quito. Ecuador. C. P. 170124.

Licenses Creative Commons
Attribution - Non Commercial - Share Alike

Resumen

Sigatoka negra es la enfermedad de la mancha foliar más importante del banano a nivel mundial. La variedad de banano Cavendish, es considerada la más común y la más exportada; sin embargo, presenta una alta susceptibilidad frente a la enfermedad. Existen fungicidas altamente efectivos para su control; sin embargo, el patógeno ha logrado generar resistencia a algunos de estos, lo que ha dificultado cada vez más su manejo. Se identificaron microorganismos epífitos con potencial antagonismo a *Pseudocercospora fijiensis* en fincas de banano convencionales de la provincia de Los Ríos. Las zonas de muestreo fueron determinadas a través de procesos de zonificación, seleccionando los cantones Mocache, Valencia, Baba y Pueblo Viejo. Se recolectó muestras de tejido foliar en tres fincas por zona. Se aislaron microorganismos y se caracterizaron morfológica y molecularmente en nueve fincas en los cantones de Valencia (63 bacterias), Baba (39 bacterias) y Pueblo Viejo (8 bacterias) y 8 géneros de hongos que incluyen 15 especies. Las bacterias aisladas presentaron características macroscópicas y microscópicas con diversas formas, elevaciones, bordes, consistencias y pigmentaciones, así como diversas taxonomías pertenecientes a los géneros *Bacillus* y Cocos, siendo 81% Gram negativas y 19% Gram positivas. El análisis realizado para la selección de los sitios de muestreo fue apropiado ya que se observó un comportamiento diferencial de los microorganismos en estas zonas.

Palabras clave
microorganismos • hongos • bacterias • *Musa* spp.

Introduction

Musaceae is a family of monocotyledonous plants that include bananas and plantains, often called giant herbs (31). These plants belong to the genus *Musa,* cultivated in tropical and subtropical regions (36).

The banana sector in Ecuador has 167,893 hectares, with a productivity of 6,684,916 tons. Los Ríos province has the highest participation in the national production of fresh fruit with 38.47% (2 571 356 t), with a contribution of 1 328 537 964.98 US dollars (45).

Investment in production and related industries (goods and services needed for banana production) and the current banana export process created jobs for more than one million households in Ecuador, benefiting around 2.5 million people in nine provinces heavily dependent on the banana industry. Compared to other non-oil sectors in the country, this sector is the backbone of economic activity, generating higher incomes and providing more employment opportunities (16).

Black Sigatoka is the most economically important leaf spot disease of *Musaceae*, affecting many plantations and resulting in forced early harvesting (27). This disease is caused by the fungus *Pseudocercospora fijiensis*, exclusive of banana foliage with sexual and asexual reproduction. It infects the plants, hindering photosynthesis and causing gradual leaf necrosis and death. Disease severity is determined by the Stover scale modified by Benavides-López (2019), Gauhl (1994) and Muimba-Kankolongo (2018).

Black Sigatoka is mainly controlled by technical management and appropriate fungicide rotation. However, given climatic variability, the disease shows different behaviours around the country. Los Ríos province is the most affected, with 74% of production losses. Twenty-two to 29 annual aerial spraying cycles are used to fight the disease, representing costs between $430 and $800 (8, 9). In addition, surgical practices like excision of mottled areas and leaf removal are carried out (9, 17).

International markets for plant protection products are dominated by synthetic pesticides (30). These chemical substances seriously affect the ecosystem and induce resistance, altering ecological equilibriums (28). Therefore, searching for alternative control strategies is relevant worldwide (24).

The search for antagonistic microorganisms for biological control of pathogens in economically important crops has aroused particular interest due to their potentialities (4, 54). Microorganisms of agricultural importance represent a key ecological strategy

towards the integrated development of practices such as nutrient, disease and pest management, reducing chemicals and improving crop yield (42). Several microorganisms showing beneficial effects on plants may constitute potential biocontrol agents (3, 41) and important actors in sustainable agriculture (51).

Biological control of Black Sigatoka has received relatively little attention due to the availability of highly effective fungicides. However, the emergence of pathogen isolates resistant to systemic fungicides and the need for cleaner production technologies have increased interest in biological control (22).

The search for effective biological products against this disease has studied different microorganisms associated with these crops (12). Therefore, this research aimed to collect, isolate and characterise microorganisms from the phyllosphere of *Musaceae.*

Materials and Methods

Study Area

This research was conducted at the Pichilingue Tropical Experimental Station (EETP) of the National Institute of Agricultural Research (INIAP) with samples obtained from conventional banana farms of Cavendish Williams cultivar in the cantons of Mocache, Valencia, Baba and Pueblo Viejo, Los Ríos province.

Field Methodology

Sampling sites were chosen by zoning with cartographic charts from the IGM (Military Geographic Institute) database. The climate micro-zonation map was generated by satellite images with ArcGIS 10.8, at a scale of 1:25 000 for geo pedological conditions considering soil pH, organic matter and surface texture, with 1:50 000 scale, considering geopedology, geomorphology, CUT (soil usage capacity) and isotherms, including climatic zones, temperature and cover use (figure 1, page 4).

Ten subsamples were collected from each farm, constituting one composite sample. In selected plants, the third and fourth leaves were identified for tissue to be obtained from the central third, both on the right and left side of the midrib. Samples were identified by recording origin and date (41).

Fungal identification from leaf tissue was conducted in Mocache, Baba and Pueblo Viejo. Bacteria were identified from leaves in Valencia, Baba and Pueblo Viejo.

Microorganism Isolation

For the isolation of bacteria, the samples obtained were processed according to Intriago Mendoza (2010). Agar culture medium was prepared in flasks, sterilised in autoclave for 30 minutes and distributed in petri dishes. Twenty-five g of leaf tissue were washed in 100 mL of sterile distilled water (SDW). Product water was used for serial dilutions up to -3. One ml of each dilution was seeded by Digralsky loop, and plates were incubated at room temperature for 5 days for growth evaluation.

In order to isolate fungi, plant tissue samples were washed with distilled water, cut into small portions of tissue (3 to 5 mm) and immersed in a 1-3% hypochlorite solution for one minute, followed by rinsing with sterile water. Tissue portions were seeded in Petri dishes with PDA (potato dextrose agar) + chloramphenicol medium and incubated at 28°C for 5 days. Isolates were purified and preserved at 5°C (20).

Morphological Characterization

After biochemical Gram staining and catalase tests, macroscopic and microscopic characterisation was carried out on the isolated microorganisms, described by their shape, colour, edges, elevation and consistency (52).

Number of Colonies

Number of colonies on the plates is expressed as CFU/ml (Colony Forming Units) according to Casas *et al.* (2017).

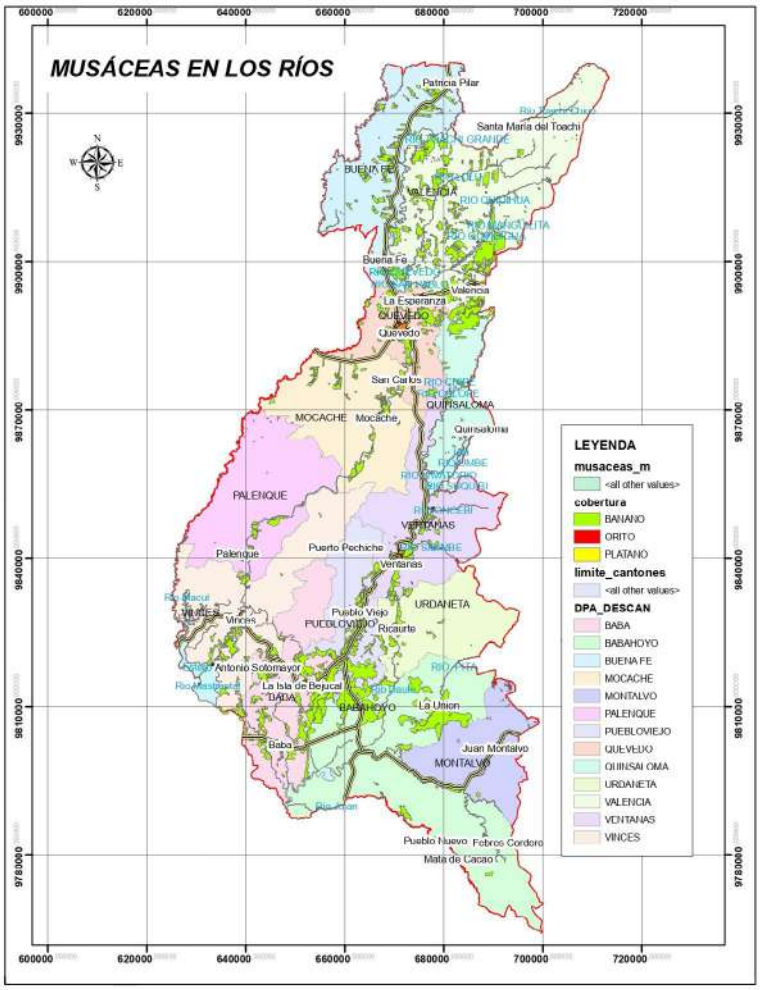


Figure 1. Climate micro-zonation map for sampling sites in the Province of Los Ríos, generated by ArcGIS 10.8 software.

Figura 1. Mapa de microzonificación climática para sitios de muestreo en la Provincia de Los Ríos, generado con el software ArcGIS 10.8.

Extraction of Fungal Genomic DNA

According to Doyle & Doyle (1987) modified by Faleiro *et al.* (2002), samples were split into two boxes per sample with 14 daysqold mycelium and triturated with liquid nitrogen. The homogenate was mixed with 800 µL extraction buffer (7% cetyltrimethylammonium bromide [CTAB], 5 M NaCl, 0.5 mM ethylenediaminetetraacetic acid [EDTA], 1 M Tris-HCl pH = 8, Polyvinylpyrrolidone (PVP-40), 1% (v/v) ß-mercaptoethanol and milliQ water). Five µL of proteinase K (concentration 20 mg/uL) was added to the homogenate and incubated at 65°C for 1 hour in a water bath. Then, it was centrifuged at 14 000 rpm for 15 minutes and the supernatant was collected into 2 mL tubes, added 55 µL of 7% CTAB and 700 µL chloroform: isoamyl alcohol (25: 1; v: v), mixed with inversion and vortexed until an emulsion was formed and centrifuged at 14 000 rpm for 16 minutes. Again, the supernatant was extracted to 2 mL tubes by adding 700 µL chloroform: isoamyl alcohol (25: 1; v: v), mixed and centrifuged. The supernatant was recovered in 1.5 mL tubes and 700 µL (2/3 of the tube) was added with ice-cold absolute ethanol (-20°C), for storage at -20°C for 1 to 2 hours. Centrifugation was performed at 14 000 rpm for 5 minutes, obtaining a white pellet and the supernatant was removed by washing the pellet 3 to 4 times with 70% ethanol at -2°C. (500 µL). Finally, the pellet was dried in a thermoblock at 55°C and DNA was resuspended in 100 µL of TE with RNAsa (concentration 20 mg/ml).

PCR Amplification of Ribosomal ITS Region

To verify the extracted DNA, amplification was performed with markers ITS1 (TCCGTAGGTGAACCTGCGG) and ITS4 (TCCTCCGCTTATTGATATATGC) and the amplification cocktail proposed by Morillo & Miño (2011). All samples were amplified on the Applied Biosystems thermal cycler in a total reaction volume of 25 µl, including 2.50 µL of 5x Green GoTaq® Flexi Buffer (Promega), 1.5µL of MgCl2 (25 mM), 0.50 µL of dNTPs (5mM), 2 µL of each primer (5 µmol), 0.50 µL of DNA polymerase (Thermo Scientific DreamTaq) (5 U/ µl), 1 µL of genomic DNA (5 ng/ µl) and 15 µL of ultrapure water. PCR included initial denaturation at 95°C for 5 min, followed by 35 cycles of denaturation at 94°C for 1 min, hybridisation at 55°C for 2 min, elongation at 72°C for 1 min and a final elongation step at 70°C for 10 min.

DNA amplicons were analysed on a 1.5% (w/v) agarose gel using Syber Safe for 30 minutes at 100V. Amplicon sizes were estimated by comparison with a TrackIt™ 1 Kb Plus DNA Ladder molecular weight marker and visualised in a photodocumenter.

Sequence Analysis

PCR products were shipped to the research laboratories of the Universidad de las Américas (UDLA), according to the university guidelines, which consisted of 10 µL of PCR product, 2 µL of each primer (ITS 1/ ITS4) (2 µM concentration) per sample and cold chain storage at 4°C or below. Sequence editing was performed using the Unipro UGENE software and the BLAST programme at the Centro Nacional de Información Biotecnológica (http://www.ncbi.nlm.nih.gov/) to obtain consensus sequences. Sequence alignment was performed by MUSCLE algorithm with MegaX software. The matrix obtained was used to assemble the phylogenetic tree based on the Maximum-Likelihood (ML) algorithm, with genetic distance calculated by the Jukes-Cantor model, Bootstrap-100 and Uniform Rates.

Results

Colony Count

Considering the three farms evaluated in each canton, in Valencia, the Bellavista farm had the highest number of colonies with $9.18x10^4$ CFU; in Baba the Soledad farm had the highest number of colonies with $3.468x10^4$ CFU and in Pueblo Viejo, Valdivia and Viviana farms had $6.12x10^3$ CFU, obtaining a total of 63 bacteria in Valencia, 39 bacteria in Baba and 8 bacteria in Pueblo Viejo (table 1).

Table 1. Bacterial colony count (CFU) per farm.
Tabla 1. Recuento de colonias bacterianas (CFU) por finca.

Estate	Colony Forming Units
Bellavista	$9.18x10^4$ CFU
El Zapote	$4.08x10^4$ CFU
Buenos Aires 2	$6.528x10^4$ CFU
San Luis	$1.224x10^4$ CFU
Carolina	$2.244x10^4$ CFU
Soledad	$3.468x10^4$ CFU
Carolina	$4.08x10^3$ CFU
Valdivia	$6.12x10^3$ CFU
Viviana	$6.12x10^3$ CFU

Strain Characterisation

Colonial morphological characterisation, microscopic morphology and biochemical tests were performed on the bacteria isolated in the province of Los Ríos (table 2, page 6).

Table 2. Characterisation of microorganisms associated with the banana phyllosphere, Los Ríos province.
Tabla 2. Caracterización de microorganismos asociados a la filósfera de banano, provincia de Los Ríos.

Cantons	Estate	Strain	Colonial morphology					Microscopic morphology	Biochemical Test
			Shape	Color	Borders	Elevation	Consistency	Gram stain	Catalase
Valencia	Bellavista	VF1C5	circular	Orange	whole	elevated	Viscous	coconuts (+)	(+)
	Bellavista	VF1C6	irregular	Yellow	wavy	elevated	Viscose	coconuts (+)	(+)
	Bellavista	VF1C9	irregular	Milky	wavy	Flat	Viscose	coconuts (+)	(+)
	Bellavista	VF1C15	irregular	Orange	wavy	Flat	Viscose	coconuts (-)	(+)
	Bellavista	VF1C16	irregular	Red	whole	Flat	Viscose	coconuts (+)	(+)
	Bellavista	VF1C17	circular	Red	whole	convex	Viscose	coconuts (-)	(+)
	Bellavista	VF1C24	irregular	Yellow	wavy	convex	Viscose	coconuts (-)	(+)
	Bellavista	VF1C29	circular	Yellow	whole	convex	Viscose	coconuts (+)	(+)
	El Zapote	VF2C3	circular	Red	wavy	convex	Viscose	coconuts (-)	(+)
	El Zapote	VF2C5	irregular	Yellow	lobed	Flat	Viscose	bacillus (-)	(+)
	El Zapote	VF2C8	circular	Orange	whole	convex	Viscose	bacillus (-)	(-)
	El Zapote	VF2C10	circular	Orange	whole	Flat	Viscose	coconuts (-)	(-)
	El Zapote	VF2C12	circular	Orange	whole	convex	Viscose	coconuts (-)	(+)
	Buenos Aires 2	VF3C13	circular	Pink	whole	convex	Viscose	coconuts (-)	(-)
	Buenos Aires 2	VF3C18	circular	White	wavy	Flat	Viscose	coconuts (-)	(+)
	Buenos Aires 2	VF3C24	circular	pink	whole	elevated	Viscose	coconuts (-)	(+)
	Buenos Aires 2	VF3C31	circular	milky	wavy	convex	Viscose	coconuts (-)	(+)
Baba	San Luis	BF1C2	circular	milky	Wavy	Flat	Viscose	bacillus (-)	(-)
	San Luis	BF1C3	irregular	white	Wavy	Flat	dry	cocobacillus (+)	(+)
	San Luis	BF1C4	circular	pink	Wavy	convex	Viscose	bacillus (-)	(+)
	San Luis	BF1C5	circular	milky	Wavy	elevated	Viscose	bacillus (-)	(+)
	San Luis	BF1C8	circular	yellow	Wavy	convex	Viscose	bacillus (-)	(+)
	Carolina	BF2C3	punctate	yellow	Wavy	Flat	Viscose	coconuts (+)	(+)
	Carolina	BF2C7	irregular	white	Wavy	Lisa	Viscose	bacillus (-)	(+)
	Carolina	BF2C8	irregular	milky	Irregular	Lisa	Viscose	bacillus (-)	(+)
	Carolina	BF2C9	circular	yellow	Lobed	Flat	Viscose	bacillus (-)	(+)
	Carolina	BF2C15	irregular	white	Irregular	Flat	Viscose	streptobacillus (-)	(+)
	Carolina	BF2C18	irregular	orange	Lobed	elevated	Viscose	bacillus (-)	(+)
	Soledad	BF3C1	circular	milky	Whole	convex	Viscose	coconuts (-)	(+)
	Soledad	BF3C2	spindle	white	Whole	Flat	Viscose	coconuts (-)	(+)
	Soledad	BF3C3	circular	white	Whole	convex	Viscose	coconuts (-)	(+)
	Soledad	BF3C5	circular	white	Whole	Flat	Viscose	coconuts (-)	(+)
	Soledad	BF3C9	irregular	milky	Lobed	Flat	Viscose	bacillus (-)	(+)
	Soledad	BF3C12	punctate	milky	Wavy	Flat	Viscose	coconuts (-)	(+)
Pueblo Viejo	Viviana	PvF1C1	circular	milky	whole	elevated	Viscose	coconuts (-)	(+)
	Viviana	PvF1C2	circular	milky	filamentous	Flat	Viscose	bacillus (-)	(+)
	Viviana	PvF1C3	circular	milky	whole	convex	Viscose	cocobacillus (-)	(+)
	Valdivia	PvF2C1	circular	milky	whole	convex	Viscose	cocobacillus (-)	(+)
	Valdivia	PvF2C2	circular	milky	whole	convex	Viscose	cocobacillus (-)	(+)
	Valdivia	PvF2C3	circular	milky	whole	convex	Viscose	cocobacillus (+)	(+)
	Valdivia	PvF2C4	circular	milky	wavy	elevated	Viscose	cocobacillus (-)	(+)
	Carolina	PvF3C1	circular	milky	lobed	Flat	Viscose	coconuts (-)	(+)

Eight fungal strains were isolated in Mocache, 5 in Baba and 13 in Pueblo Viejo. Eight PCR products were amplified from Mocache, 5 from Baba and 13 from Pueblo Viejo. Twenty-six sequences were obtained. Similarity percentages were 90-100 % with NCBI homologous sequences (table 3).

Table 3. Collection and ITS rDNA sequences of fungi isolated in the cantons of Mocache, Baba and Pueblo Viejo.

Tabla 3. Detalles de la colección y secuencias ITS del ADNr de hongos aislados en los cantones de Mocache, Baba y Pueblo Viejo.

Canton	Estate	Identity in GenBank		Identity
		Accession	Description	
Mocache	INIAP Lot 1	MN173821.1	*Colletotrichum fructicola*	100%
	INIAP Lot 1	MT982177.1	*Fusarium oxysporum*	99.41%
	INIAP Lot 1	KM519998.1	*Colletotrichum gloeosporioides*	100%
	INIAP Lot 1	KU350718.1	*Nectria haematococca*	98.66%
	INIAP Lot 2	JN649339.1	*Cymatoderma dendriticum*	98.34%
	INIAP Lot 2	MH483999.1	*Miyakei microdiplody*	99.61%
	INIAP Lot 2	MK041519.1	*Colletotrichum fructicola*	98.89%
	INIAP Lot 2	HM855208.1	*Nodulisporium sp.*	99.27%
Baba	San Luis	KY488352.1	*Cladosporium uredinicola*	99.41%
	San Luis	KT240141.1	*Cladosporium cladosporioides*	99.22%
	San Luis	MN515070.1	*Nigrospora oryzae*	98.80%
	Carolina	MW016510.1	*Fusarium subglutinans*	99.21%
	Carolina	MT645782.1	*Nigrospora osmanthi*	98.64%
Pueblo viejo	Viviana	MH864880.1	*Diatrypella vulgaris*	99.27%
	Viviana	KY488352.1	*Cladosporium uredinicola*	99.22%
	Viviana	KY488352.1	*Cladosporium uredinicola*	99.41%
	Viviana	MH864880.1	*Diatrypella vulgaris*	99.45%
	Viviana	MH270558.1	*Cladosporium tenuissimum*	99.22%
	Viviana	MN704703.1	*Cladosporium cladosporioides*	99.60%
	Viviana	MH270558.1	*Cladosporium tenuissimum*	99.42%
	Viviana	MW723859.1	*Cladosporium cladosporioides*	93.79%
	Valdivia	KY488352.1	*Cladosporium uredinicola*	98.83%
	Valdivia	KY488352.1	*Cladosporium uredinicola*	99.41%
	Valdivia	MW624421.1	*Nigrospora sphaerica*	98.84%
	Carolina	MW113408.1	*Cladosporium cladosporioides*	99.80%
	Carolina	MN959990.1	*Fusarium oxysporum*	99.21%

The identified fungi were from the genera *Fusarium* sp., *Colletotrichum* sp., *Diatrypella* sp., *Nodulisporium* sp., *Nigrospora* sp., *Microdiplodia* sp., *Cymatoderma* sp. and *Cladosporium* sp. *Fusarium* sp. is a candidate biological control agent against *Pseudocercospora fijiensis. Nodulisporium* sp. is an endophyte capable of producing insecticidal nodilosporic acids and volatile antifungal substances (Suwannarach *et al.*, 2013). *Nigrospora* sp. produce bioactive secondary metabolites with antifungal activity (23) (figure 2).

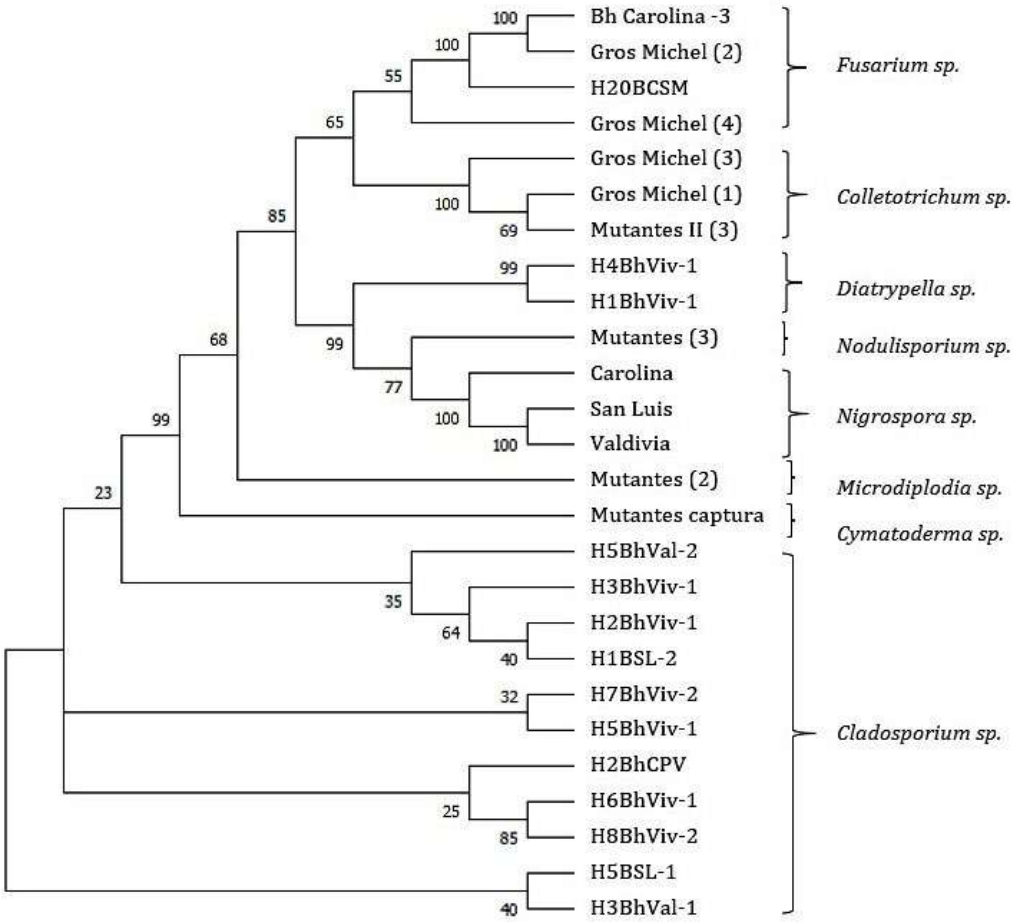


Figure 2. Phylogenetic tree of fungal isolates associated with banana phyllosphere with potential antagonism to Black Sigatoka in the cantons of Mocache, Baba and Pueblo Viejo. Phylogenetic construction by *Maximum- Likelihood* method, Jukes-Cantor model, Bootstrap-100 and Uniform Rates.

Figura 2. Árbol filogenético de aislamientos de hongos asociados a la filósfera de banano con potencial antagonismo a Sigatoka Negra en los cantones de Mocache, Baba y Pueblo Viejo. Construcción filogenética por el método Maximum-Likelihood, Jukes-Cantor model, Bootstrap-100 y Uniform Rates.

DISCUSSION

Fungal disease control mainly relies on the application of agrochemicals. However, this practice causes pathogen resistance after prolonged application, generating public concern about the effects of toxic residues on human health and the environment.

This research identified *Bacillus* bacteria. According to Cruz-Martín *et al.* (2018) *Bacillus pumilus* CCIBP-C5 decreases fungal biomass, induces phytodefense mechanisms in the plant, and may constitute a potential biological control agent against *P. fijiensis*. Based on this finding, *B. pumilus* CCIBP-C5 constitutes a guideline for further research.

Contrary to other studies, proportions of Gram-negative bacteria (81%) exceeded that of Gram-positive bacteria (19%). Previously, Ceballos *et al.* (2012) found higher proportions of Gram-positive bacteria (67%) than Gram-negative bacteria from three banana and plantain cultivars in Urabá (Northwest Colombia). Regarding the inhibitory capacity of the isolated microorganisms, the results showed that *Bacillus* bacteria have antagonistic activity against the fungus *P. fijiensis*, as seen by Villegas-Escobar *et al.* (2013) when isolating 649 strains of aerobic endospore-forming bacteria. The strain *Bacillus subtilis* showed the highest inhibition (89±1%), proving its bioactive potential against *P. fijiensis*.

After isolation, colonies showed different shapes (circular, pointed, irregular, spindle), elevations (flat, convex, smooth, raised), edges (entire, wavy, lobulated, irregular, filamentous), consistencies (viscous, dry) and pigmentations (orange, yellow, red, pink, milky, white), as reported by Alfaro (2013) when isolating and quantifying epiphytic bacteria from the banana phylloplane *Musa* AAA cv. Grande Naine.

Considering the 26 isolated fungi, 25 belonged to Ascomycota and one to Basidiomycota. Ascomycota fungi grow in subtropical conditions, as bananas (44).

Fungal molecular identification is frequently assessed with the internal transcribed spacer (ITS) region (47). The primers ITS1 and ITS4 have broad utility and presence in universal databases, with successful amplification rates of fungal lineages (53). Based on in silico analysis (49) the primer ITS1 represents 73.8% of Ascomycota and 85.6% of Basidiomycota in the SSU region, while the primer ITS4 represents 97.6% in Ascomycota and 96.9% in Basidiomycota in the LSU region. This means ITS primers allowed amplifying sequences from both Ascomycota and Basidiomycota fungi.

In a study of pathogenic taxa in wild banana (*Musa acuminata*), Brown *et al.* (1998) identified potential endophytic pathogen genera and species that may remain dormant, such as *Colletotrichum* sp. and *Nigrospora* sp. Zakaria & Aziz (2018) isolated fungi of the genus *Nigrospora* sp., *Fusarium* sp. and *Colletotrichum* sp. on bananas. Very similar results were obtained by Horra (2014) and in the present study, including *Diatrypella* sp., *Nodulisporium* sp., *Microdiplodia* sp., *Cymatoderma* sp. and *Cladosporium* sp.

Fusarium oxysporum is present among the rhizosphere microflora, and some strains cause wilting or total root rot of banana plants (19). It should be noted that all *F. oxysporum* strains are saprophytes, surviving for long periods in both soil organic matter and the rhizosphere. This possibly explains their latent presence in leaf tissue and the sampled areas. We also isolated *Nectria haematococca* (sexual morph of *F. solani*), a filamentous type of fungus. *F. solani* is part of a complex with 60 phylogenetic species (46). These two *Fusarium* sp. strains could constitute candidate biological control agents against *P. fijiensis* (2), encouraging future antagonistic tests for evaluations against black Sigatoka.

Colletotrichum sp. predominates in the tropics and subtropics with heavy rainfall and high relative humidity (43). Two species were found in this study, *C. gloeosporioides* and *C. frutícola*. The former causes banana anthracnose and leaf spot (38), while *C.* frutícola has been identified on mango plants (29). One of the main characteristics of *Colletotrichum* sp. infection in bananas is the difficulty in detecting the disease before fruit generation, given latency (37).

Diatrypaceae members like the genus *Diatrypella* are saprobes and pathogens associated with different hosts in both terrestrial and aquatic environments (14). Species of this genus are separated according to their entostrophic morphology and the number of ascospores they present (50). Fungal pathogenicity is moderate for this genus. This study firstly reports *Diatrypella vulgaris*, in banana. However, it is commonly isolated from diseased *Vitis vinifera*, causing necrotic lesions on the plant (40).

The fungal isolate *Nodulisporium* sp. produces nodilosporic acids with insecticidal properties and volatile antifungal substances used against other microorganisms through mycofumigation (48).

Fungi of *Nigrospora* sp. are host-specific phytopathogenic, endophytic and saprophytic species that produce bioactive secondary metabolites with antifungal activity (23). During isolations, *N. sphaerica* and *N. osmanthi* were isolated from the environment. *N. sphaerica* exhibits a violent spore-discharging mechanism that projects spores over long distances (57). Similarly, *Nigrospora oryzae* and *N. sphaerica* were identified from banana leaves (58). This study also firstly reports *N. osmanthi* in bananas.

Isolated fungi of the genus *Microdiplodia* sp. and *Cymatoderma* sp. have not previously been recorded in bananas. However, Pinheiro da Costa *et al.* (2021) detail the presence of *Microdiplodia* sp. with antifungal activity on Brugmansia suaveolens and *Cymatoderma* sp. as the only Basidiomycota reported in tropical rainforest (1).

Finally, the genus *Cladosporium* sp. comprises more than forty species, including pathogenic species causing leaf spot and saprophytic species acting on vegetation and soil (35). Isolated *C. cladosporioides* confirms this fungus as an endophyte isolated from foliar culture tissues of banana plants (58). In addition, *C. uredinicola*, also isolated in this study, presents small conidia formed with branched chains that facilitate its propagation over long distances (6), explaining its higher prevalence over other fungi. Another species identified, *C. tenuissimum* is an abundant saprobe in the tropics (56). Moubasher *et al.* (2016) state that the frequency of *Cladosporium* sp. isolation is moderate and peaks during winter, when humidity benefits banana development.

Conclusions

Considering the differential behavior of microorganisms and the number of strains found in the studied sites, the analysis focused on selecting sampling sites was appropriate.

The isolated microorganisms presented macroscopic and microscopic characteristics with different shapes, elevations, borders, consistencies and pigmentations. Different taxonomies belonged to the *Bacillus* and Coccus genera, 81% being Gram-negative and 19% Gram-positive.

References

1. Agudelo, M. B.; Calderón, M.; Betancourt, O.; Gallejo, Á. S. 2007. Hongos Macromycetes en dos rellictos de bosque húmedo tropical montano bajo de la vereda La Cuchilla. Marmato, Caldas. Museo de História Natural. 11: 19-31.
2. Alfaro, F. 2013. Aislamiento y cuantificación de bacterias epífitas del filoplano de banano (Musa AAA cv. Grande Naine) y selección de cepas quitinolíticas y glucanolíticas como potenciales antagonistas de *Mycosphaerella fijiensis*, agente causal de la Sigatoka negra.
3. Ayala, D.; Acevedo, C.; Enrique, B.; Aguilar, F.; Orlandoni, G. 2018. Seguimiento de la actividad PGPR de microorganismos inoculados en plantas de Sacha inchi (*Plukenetia volubilis*) bajo condiciones de vivero. Archivo digital de prácticas, Microbiología Industrial. Universidad de Santander UDES. 1-14. https://doi.org/10.13140/RG.2.2.25676.36489
4. Barrera, S.; Sarango, S.; Montenegro, S. 2019. The phyllosphere microbiome and its potential application in horticultural crops. A review. Revista Colombiana de Ciencias Hortícolas. https://revistas.uptc.edu.co/index.php/ciencias_horticolas/article/view/8405
5. Benavides-López, L. 2019. Cuantificación temprana de *Pseudocercospora fijiensis* por medio de qPCR en modelos predictivos de Sigatoka negra en plantas de banano (Musa AAA). 9-162.
6. Bensch, K.; Braun, U.; Groenewald, J. Z.; Crous, P. W. 2012. The genus Cladosporium. Studies in Mycology. 72(1): 1. https://doi.org/10.3114/SIM0003
7. Brown, K.; Hyde, K.; Guest, D. 1998. Preliminary studies on endophytic fungal communities of *Musa acuminata* species complex in Hong Kong and Australia. https://www. fungaldiversity. org/fdp/sfdp/FD_1_27-51.pdf
8. Carrión Abad, B. A. C. 2015. Análisis microbiológico del complejo orgánico activfol para determinar la efectividad en el control del hongo (*Mycosphaerella fijiensis*) causante de la Sigatoka negra en el banano.
9. Carrion Ramon, J. J. C. 2020. Monitoreo y control especial de la Sigatoka negra (*Mycosphaerella Fijiensis* M), en el cultivo de banano. UTMACH. Unidad Académica de Ciencias Agropecuarias. Machala. Ecuador. http://repositorio.utmachala.edu.ec/handle/48000/16135
10. Casas, J.; López, M.; Salinas, M.; Gisbert, J.; Giménez, E.; García, F.; Sánchez, S.; Lacalle, A.; Cortés, A.; Moyano, F. 2017. Guía para la realización de un estudio ambiental: El caso de la cuenca del río Adra (J. Casas, Ed.; Vol. 11). Universidad de Almería. 3qk3vTP
11. Ceballos, I.; Mosquera, S.; Angulo, M.; Mira, J.; Argel, L.; Uribe-Velez, D.; Romero-Tabarez, M.; Orduz-Peralta, S.; Villegas, V. 2012. Cultivable bacteria populations associated with leaves of banana and plantain plants and their antagonistic activity against *Mycosphaerella fijiensis*. Microbial Ecology. 64(3): 641-653. https://doi.org/10.1007/s00248-012-0052-8
12. Cruz-Martín, M.; Acosta-Suárez, M.; Roque, B.; Pichardo, T.; Castro, R. 2016. Diversidad de cepas bacterianas de la filosfera de Musa spp. con actividad antifúngica frente a *Mycosphaerella fijiensis* Morelet. Biotecnología Vegetal. 16(1): 53-60.

13. Cruz-Martín, M.; Alvarado, Y.; Mena, E.; Acosta, M.; Roque, B.; Pichardo, T. 2018. Cepas bacterianas con potencial para el manejo de la Sigatoka negra. Anales de la Academia de Ciencias de Cuba. 8(1). http://www.revistaccuba.sld.cu/index.php/revacc/article/view/374/373
14. Dissanayake, L. S.; Wijayawardene, N. N.; Dayarathne, M. C.; Samarakoon, M. C.; Dai, D. Q.; Hyde, K. D.; Kang, J. C. 2021. *Paraeutypella guizhouensis* gen. et sp. nov. and *Diatrypella longiasca* sp. nov. (Diatrypaceae) from China. Biodiversity Data Journal 9: e63864. https://doi.org/10.3897/BDJ.9.E63864
15. Doyle, J. J.; Doyle, J. L. 1987. A rapid DNA isolation procedure for samal quantities of fresh leaf tissue. Phytochemical Bulletin. 19: 11-15.
16. Ecuador, M. de C. E. del. 2017. Informe Sector Bananero Ecuatoriano. Ministerio de Comercio Exterior. 53(9): 1689-1699. https://doi.org/10.1017/CBO9781107415324.004
17. Etebu, E.; Young-Harry, W. 2011. Control of black Sigatoka disease: Challenges and prospects. African Journal of Agricultural Research. 6(3): 508-514. https://doi.org/10.5897/AJAR10.223
18. Faleiro, F. G.; Santos, I. S.; Bahía, R.; Santos, R. F.; Anhert, D. 2002. Otimização da extração e amplificação de DNA de *Theobroma cacao* L. visando obtenção de marcadores RAPD. 31-34.
19. Fravel, D.; Olivain, C.; Alabouvette, C. 2003. *Fusarium oxysporum* and its biocontrol. New Phytologist. 157(3): 493-502. https://doi.org/10.1046/J.1469-8137.2003.00700.X
20. García, F.; Pachacama, S.; Jarrín, D.; Iza, M. 2020. Guía andina para el diagnóstico de Fusarium Raza 4 Tropical (R4T) *Fusarium oxysporum f.sp. Cubense* (syn. *Fusarium odoratissimum*) agente causal de la marchitez por *Fusarium* en musáceas (plátanos y bananos). www.comunidadandina.org
21. Gauhl, F. 1994. Epidemiology and ecology of Black Sigatoka on plantain and banana (Musa spp.) in Costa Rica, Centro América. Ph.D. Thesis of the Systematisch Geobotanische-Institut der Georg-August-Universität Göttingen and Institut für Pflanzenpathologie und Pflanzenchutz der Georg-August-Universität Göttingen. INIBAP.
22. Guzmán, M. 2012. Control biológico y cultural de la sigatoka-negra. Tropical Plant Pathology. 37 (Suplemento). Agosto. https://doi.org/10.13140/2.1.2927.7442
23. Hao, Y.; Aluthmuhandiram, J. V. S.; Chethana, K. W. T.; Manawasinghe, I. S.; Li, X.; Liu, M.; Hyde, K. D.; Phillips, A. J. L.; Zhang, W. 2020. Nigrospora species associated with various hosts from Shandong Peninsula, China. Mycobiology. 48(3): 169-183. https://doi.org/10.1080/1229 8093.2020.1761747
24. Hernández-Montiel, L. G.; Larralde-Corona, C. P.; Vero, S.; López-Aburto, M. G.; Ochoa, J. L.; Ascencio-Valle, F. 2010. Caracterización de levaduras *Debaryomyces hansenii* para el control biológico de la podredumbre azul del limón mexicano. CYTA-Journal of Food. 8(1): 49-56. https://doi.org/10.1080/19476330903080592
25. Horra, M. L. P. 2014. Evaluación *in vitro* de la capacidad de extractos orgánicos de biodiversidad ecuatoriana para inhibir al patógeno *Mycosphaerella fijiensis* (Morelet) causante de la Sigatoka Negra en banano. http://repositorio.puce.edu.ec/bitstream/handle/22000/10936/4.42.000892.pdf?sequence=4
26. Intriago Mendoza, L. 2010. Identificación y evolución en laboratorio e invernadero de microorganismos antagonistas de Sigatoka negra *(Mycosphaerella fijiensis Morelet)* en musáceas en el Litoral Ecuatoriano. Tesis de Grado. Universidad Técnica de Manabí. Ecuador. 95 p.
27. Israeli, Y.; Lahav, E. 2016. Banana. In Encyclopedia of Applied Plant Sciences. Elsevier. 3: 363-381. https://doi.org/10.1016/B978-0-12-394807-6.00072-1
28. Izzeddin, A. N.; Medina, T. L. 2011. Efecto del control biológico por antagonistas sobre fitopatógenos en vegetales de consumo humano. Salus. 15(3): 8-18.
29. Lima, N. B.; Marcus, M. V.; Morais, M. A. D.; Barbosa, M. A. G.; Michereff, S. J.; Hyde, K. D.; Câmara, M. P. S. 2013. Five Colletotrichum species are responsible for mango anthracnose in northeastern Brazil. Fungal Diversity. 61(1): 75-88. https://doi.org/10.1007/s13225-013-0237-6
30. López, S. 2019. Bacillus un género que alberga especies que cumplen diversos roles biológicos. Infive-Conicet UNLP. 1-26.
31. Martínez, G.; Pargas, R.; Manzanilla, E. 2012. Orden Zingiberales: Las musáceas y su relación con plantas afines. Scielo. http://ve.scielo.org/scielo.php?script=sci_arttext&pid=S0002-192X2012000100014
32. Morillo, E.; Miño, G. 2011. Marcadores moleculares en biotecnología agrícola: manual de técnicas y procedimientos en INIAP. https://repositorio.iniap.gob.ec/bitstream/41000/848/4/iniapscm91.pdf
33. Moubasher, A. H.; Moharram, A. M.; Ismail, M. A.; Abdel-Hafeez, M. H. 2016. Aeromycobiota over banana plantations in Assiut Governorate and enzymatic producing potential of the most common species. Journal of Basic & Applied Mycology (Egypt). 7: 9-18.
34. Muimba-Kankolongo, A. 2018. Fruit Production. In Food crop production by smallholder farmers in Southern Africa (p. 275-312). Elsevier. https://doi.org/10.1016/B978-0-12-814383-4.00012-8

35. Nam, M. H.; Park, M. S.; Kim, H. S.; Kim, T. I.; Kim, H. G. 2015. *Cladosporium cladosporioides* and *C. tenuissimum* cause blossom blight in strawberry in Korea. Mycobiology. 43(3): 354. https://doi.org/10.5941/MYCO.2015.43.3.354
36. Novák, P.; Hřibová, E.; Neumann, P.; Koblížková, A.; Doležel, J.; Macas, J. 2014. Genome-wide analysis of repeat diversity across the family musaceae. PLoS ONE. 9(6). https://doi.org/10.1371/journal.pone.0098918
37. Nuangmek, W.; McKenzie, E. H. C.; Lumyong, S. 2008. Endophytic fungi from wild banana (*Musa acuminata* Colla) works against anthracnose disease caused by *Colletotrichum musae*. Research Journal of Microbiology. 3(5): 368-374. https://doi. org/10.3923/JM.2008.368.374
38. Photita, W.; Lumyong, S.; Lumyong, P.; Mckenzie, E. H. C.; Hyde, K. D.; Photita, W.; Lumyong, S.; Lumyong, P.; Hyde, M. E. H. C. 2004. Fungal diversity are some endophytes of *Musa acuminata* latent pathogens? Fungal Diversity. 16: 131-140.
39. Pinheiro da Costa, S.; Schuenck-Rodrigues, R.; da Silva Cardoso, V.; Valverde, S.; Vermelho, A.; Ricci-Júnior, E. 2021. Actividad antimicrobiana de hongos endofíticos aislados de *Brugmansia suaveolens* Bercht.; Presl, J. Research, Society and Development. 10(14): e113101421646. https://doi. org/10.33448/rsd-v10i14.21646
40. Pitt, W. M.; Trouillas, F. P.; Gubler, W. D.; Savocchia, S.; Sosnowski, M. R. 2013. Pathogenicity of Diatrypaceous Fungi on grapevines in Australia. Plant disease. 97(6): 749-756. https://doi.org/10.1094/PDIS-10-12-0954-RE
41. Poveda, I.; Cruz-Martín, M.; Sánchez-García, C.; Acosta-Suárez, M.; Leiva-Mora, M.; Roque, B.; Alvarado-Capó, Y. 2010. Caracterización de cepas bacterianas aisladas de la filosfera de Musa spp. con actividad antifúngica *in vitro* frente a *Mycosphaerella fijiensis*. Biotecnología Vegetal. 10(1): 57-61.
42. Ramírez, M.; Rodriguez, T.; Peniche, C.; Alfonso, L. 2010. Chitin and its derivatives as biopolymers with potential agricultural applications. Biotecnología Aplicada. 27: 270-276.
43. Riera, N. J. 2015. Caracterización molecular y de patogenicidad de *Colletotrichum* spp, en bananas var Cavendish y pruebas de antagonismo con *Trichoderma* spp., recolectadas en fincas bananeras de la región costa del Ecuador. Universidad San Francisco de Quito. 98.
44. Ruiz-Boyer, A.; Rodríguez-González, A. 2020. Preliminary list of fungi (Ascomycota and basidiomycota) and myxomycetes (myxomycota) of Isla del Coco, Puntarenas, Costa Rica. Revista de Biología Tropical. 68(S1): S33-S56. https://doi.org/10.15517/RBT.V68IS1.41165
45. SIPA. 2021. Ficha del cultivo de banano (*Musa paradisiaca* AAA). https://sipa.agricultura.gob.ec/index.php/bananos
46. Šišić, A.; Baćanović-Šišić, J.; Al-Hatmi, A. M. S.; Karlovsky, P.; Ahmed, S. A.; Maier, W.; Hoog, G. S. D.; Finckh, M. R. 2018. The 'forma specialis' issue in *Fusarium*: A case study in *Fusarium solani* f. Sp. Pisi. Scientific Reports 2018 8:1, 8(1), 1-17. https://doi.org/10.1038/s41598-018-19779-z
47. Sun, X.; Guo, L. D. 2012. Endophytic fungal diversity: Review of traditional and molecular techniques. Mycology. 3(1): 65-76. https://doi.org/10.1080/21501203.2012.656724
48. Suwannarach, N.; Kumla, J.; Bussaban, B.; Nuangmek, W.; Matsui, K.; Lumyong, S. 2013. Biofumigation with the endophytic fungus Nodulisporium spp. CMU-UPE34 to control postharvest decay of citrus fruit. Crop Protection. 45: 63-70. https://doi.org/10.1016/J.CROPRO.2012.11.015
49. Toju, H.; Tanabe, A. S.; Yamamoto, S.; Sato, H. 2012. High-Coverage ITS Primers for the DNA-Based Identification of Ascomycetes and Basidiomycetes in Environmental Samples. PLoS ONE. 7(7): 40863. https://doi.org/10.1371/JOURNAL.PONE.0040863
50. Trouillas, F. P.; Úrbez-Torres, J. R.; Gubler, W. D. 2017. Diversity of diatrypaceous fungi associated with grapevine canker diseases in California. 102(2): 319-336. https://doi.org/10.3852/08-185
51. Vázquez, J.; González, J.; Castillo, J.; Álvarez, M. 2019. Microorganismos benéficos MOBs obtenidos de plantas, como promotores en la germinación de semillas. Dominio de Las Ciencias. 5: 615-628. http://dx.doi.org/10.23857/dc.v5i1.1064 Cie
52. Velasco, R.; Tapia, R. 2014. Curso práctico de Microbiología. Universidad Autónoma Metropolitana.
53. Vilgalys, R. 2003. Taxonomic misidentification in public DNA databases. New Phytologist. 160(1): 4-5. https://doi.org/10.1046/J.1469-8137.2003.00894.X
54. Villamil Carvajal, J. E. V.; Viteri Rosero, S. E. V.; Villegas Orozco, W. L. V. 2015. Aplicación de antagonistas microbianos para el control biológico de *Moniliophthora roreri* Cif & Par en *Theobroma cacao* L. bajo condiciones de campo. Revista Facultad Nacional de Agronomía Medellín. 68(1): 7441-7450. https://doi.org/10.15446/rfnam.v68n1.47830
55. Villegas-Escobar, V.; Ceballos, I.; Mira, J. J.; Argel, L. E.; Peralta, S. O.; Romero-Tabarez, M. 2013. Fengycin C produced by *Bacillus subtilis* EA-CB0015. Journal of Natural Products. 76(4): 503-509. https://doi.org/10.1021/np300574v
56. Walker, C.; Muniz, M. F. B.; Rolim, J. M.; Martins, R. R. O.; Rosenthal, V. C.; Maciel, C. G.; Mezzomo, R.; Reiniger, L. R. S. 2016. Morphological and molecular characterization of *Cladosporium cladosporioides* species complex causing pecan tree leaf spot. Genetics and molecular research: GMR. 15(3). https://doi.org/10.4238/GMR.15038714

57. Wang, M.; Liu, F.; Crous, P. W.; Cai, L. 2017. Phylogenetic reassessment of Nigrospora: Ubiquitous endophytes, plant and human pathogens. Persoonia: Molecular Phylogeny and Evolution of Fungi. 39(December). 118-142. https://doi.org/10.3767/persoonia.2017.39.06
58. Zakaria, L.; Aziz, W. N. W. 2018. Molecular Identification of endophytic fungi from banana leaves (Musa spp.). Tropical Life Sciences Research. 29(2): 201. https://doi.org/10.21315/TLSR2018.29.2.14

Acknowledgements

The authors thank all the technical staff of the National Agricultural Research Institute, who provided their scientific contribution during the development of the research.

Monitoring of the Community of Scandent Weeds in Yerba Mate (*Ilex paraguariensis* A. St. Hil., Aquifoliaceae) Cultivated in North-Eastern Argentina

Monitoreo de la comunidad de malezas trepadoras en cultivo de yerba mate (*Ilex paraguariensis* A. St. Hil., Aquifoliaceae) en el nordeste de Argentina

Claudio Marcos Dávalos [1, 2*], Rafael Augusto Lovato Echeverría [1, 2], Laura Itatí Giménez [1], María Gabriela López [1, 2]

Originales: *Recepción:* 07/04/2025 - *Aceptación:* 29/10/2025

ABSTRACT

Perennial crops account for 10% of the world's cultivated area. In Argentina, yerba mate is grown within complex plant communities where scandent weeds are major challenges. We conducted bimonthly vegetation censuses to evaluate plant communities in yerba mate fields. These data were used to compare species presence-absence across the four seasons from 2018 to 2023. We grouped the censused species into scandent and non-scandent. The relative frequencies of the species analysed showed minor seasonal variation (chi-square = 2.0802, df = 3, p-value = 0.5559). These results indicated that frequency patterns remained stable throughout the observation period. Consequently, information on species richness and frequency may inform integrated management strategies for these challenges. Although this work focused on yerba mate, the monitoring methodology can be adapted and applied to other perennial crops of agronomic interest.

Keywords
weeds • climbing plants • perennial crops • phytosociology

https://doi.org/10.48162/rev.39.207

1 Universidad Nacional del Nordeste (UNNE). Facultad de Ciencias Agrarias. Sgto. Cabral 2131. C. P. 3400. Corrientes. Argentina.
2 Universidad Nacional del Nordeste (UNNE). Facultad de Ciencias Agrarias. Centro de Malezas. * mdavalos@agr.unne.edu.ar

Licenses Creative Commons
Attribution - Non Commercial - Share Alike

Resumen

Los cultivos perennes representan un 10% de la superficie cultivada a nivel mundial. En Argentina, la yerba mate se cultiva formando parte de una comunidad vegetal compleja y las malezas de hábito escandente están entre las principales adversidades. Con el objetivo de conocer y evaluar las comunidades vegetales asociadas a este cultivo, se realizaron censos de vegetación con una frecuencia bimestral, con esos datos se realizó la comparación de presencia-ausencia de especies en las cuatro estaciones del año desde 2018 hasta 2023. Las especies censadas fueron agrupadas en escandentes y no escandentes. Las frecuencias relativas de las formas de vida analizadas mostraron escasas variaciones en las estaciones del año (chi-cuadrado = 2,0802, df = 3, p-valor = 0,5559). Esto indica que la estructura de formas de vida fue independiente de la variación estacional a lo largo de los años de observación. Esta información acerca de riqueza específica y frecuencia de especies podría contribuir a una mejor estrategia de manejo integrado de estas adversidades. Si bien este trabajo se realizó en el cultivo de yerba mate, la metodología de monitoreo puede ser adaptada y aplicada a otros cultivos perennes de interés agronómico.

Palabras clave
arvenses • plantas trepadoras • cultivos perennes • fitosociología

Introduction

About 5,000 million hectares of land exist worldwide, of which 38% (1,900 million hectares) is used for agriculture. Only approximately 62.7 million hectares (1.25%) are cultivated with perennial crops, mainly in tropical and subtropical regions (14). Among these perennial crops, coffee (*Coffea arabica* L. and *Coffea robusta* L. Linden) stands out globally, with 11 million hectares cultivated in 75 countries. Half of this area is in the Americas, with Brazil as the leading producer, dedicating 1.7 million hectares to its cultivation (29). *Citrus* species are also important, covering 10 million hectares, with Argentina as the main producer and exporter of *Citrus limon* L., "lemon" (27). Additionally, there are approximately 5 million hectares of tea (*Camellia sinensis* (L.) Kuntze), mostly in Southeast Asia.

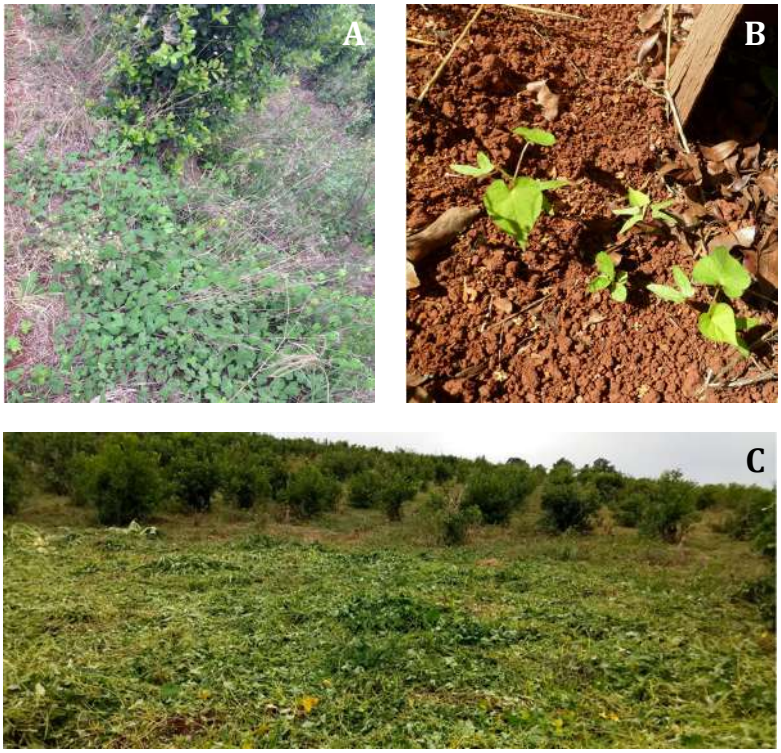
Yerba mate (*Ilex paraguariensis* A. St. Hil.) is cultivated on approximately 200,000 hectares in Argentina (7), mainly in Misiones and Corrientes (7, 15) with significant socioeconomic importance (34). According to the National Institute of Yerba Mate (INYM, 2016), 18,615 farmers produce around 750 million kilograms of green leaf. This supply supports an industry with increasing domestic and international demand (17). Farmers manually harvest 90% of the area, requiring intensive labor for much of the year (7).

Perennial crop agroecosystems generally host high biodiversity. These crops coexist year-round with various arable (spontaneous) species, mostly native, and some adventitious species (9). If this community is improperly managed, it can cause environmental and economic problems since some spontaneously growing species may become weeds for crops (2). Therefore, it is necessary to understand plant biodiversity within these perennial crop agroecosystems. This knowledge allows management strategies favoring the crop over weeds (3).

Growing land use and food demand make adopting sustainable crop practices essential. These practices should enhance production efficiency by increasing yields while conserving natural resources (30). Among these resources are plant species commonly called weeds. Although certain species exhibit weedy behavior, all play functional roles within agroecosystems (3, 31).

Knowing the floristic composition of scandent and non-scandent plants helps understand plant community functioning in perennial crops. These are commonly identified as climbing and non-climbing plants (12, 13, 28). Moreover, understanding interactions with other organisms, including arthropods, birds, and microorganisms, further improves knowledge. Consequently, this knowledge facilitates efficient and sustainable management of these environments (16). Under favorable conditions, scandent weeds can completely cover the plants within a few weeks (10, 11). Such coverage causes defoliation through

competition for light and soil nutrients (figure 1). Consequent damage can be both direct and indirect. Direct impacts include hindering weeding operations and injuring cultivated plants. Indirect effects involve altered leaf quality, the industry's main raw material, during post-harvest processes.



A- *Ipomoea grandifolia* (Dammer) O´Donell growing in crop line; B- Seedlings of *I. grandifolia* growing in spring; C- Cleaning the crop in summer, before harvest.

A- *Ipomoea grandifolia* (Dammer) O´Donell creciendo en línea del cultivo; B- Plántulas de *I. grandifolia* creciendo en primavera; C- Limpieza de cultivo en verano previo a la cosecha.

Figure 1. Scandent weeds in yerba mate crop.

Figura 1. Malezas escandentes en cultivo de yerba mate.

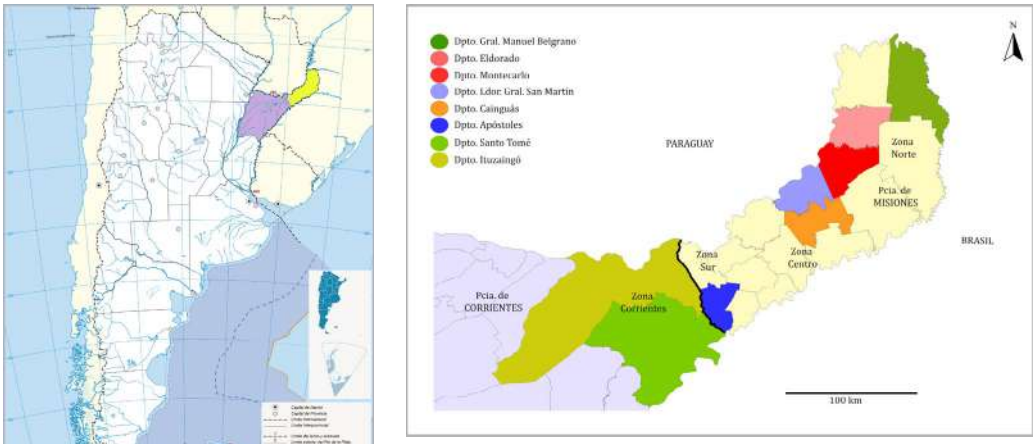
In integrated weed management, phytosociological surveys are crucial for obtaining reliable and objective data (8). Developing a weed monitoring methodology tailored to perennial crops is essential for efficiently assessing and comparing plant communities over time. This approach also helps prevent severe crop infestations and the depletion of natural resources (6). The composition of plant communities in yerba mate agroecosystems changes with the seasons (9), and plant communities can behave as weeds under certain circumstances. Nonetheless, the scandent species are present throughout the year and are the only ones considered important weeds in the crop. Certain species have medicinal uses. Examples include *Ipomoea purpurea* (L.) Roth, *Ipomoea indica* (Burm.) Merr. and *Ipomoea nil* (L.) Roth (20) or *Smilax campestris* Griseb. (22). Others, like species from the genus *Ipomoea* (19), are melliferous and serve as host plants for predatory arthropods. Certain Bignoniaceae species, including *Pyrostegia venusta* (Ker Gawl.) Miers, *Dolichandra cynanchoides* Cham. and *Dolichandra unguis-cati* (L.) L. G. Lohmann, provide materials used in crafts (3).

Understanding the importance of the scandent species in this perennial agroecosystem assists decision-making in integrated weed management. Furthermore, an adequate monitoring methodology allows efficient evaluation and comparison of plant communities over time. This approach also helps prevent severe crop infestations and loss of natural resources. Information on weed species in yerba mate cultivation is limited. Specific authors, therefore, approach the topic superficially (6) or mention a few species as competitors (12). By contrast, recent studies adopt phytosociological or integrative approaches (9, 10, 11).

This study aimed to evaluate species richness and seasonal frequency of scandent and non-scandent weed communities of yerba mate crop.

Materials and Methods

Between autumn 2018 and winter 2023, 81 censuses were conducted using the Braun-Blanquet (1950) and Mueller-Dumbois & Ellenberg (1974) phytosociological methods. Forty-four censuses were conducted during the spring-summer months of 2018, 2019, 2020, 2021, and 2023. Thirty-seven censuses were conducted during the autumn-winter months of 2018, 2021, 2022, and 2023. This schedule covered all four seasons of the year. The number of surveys per yerba mate field depended on the state of the crop at the time. Fields ranged between 2 and 6 hectares and were located across six departments in the province of Misiones and two departments in the province of Corrientes (figure 2).



Source/Fuente: IGN.

Figure 2. Geographical distribution of surveys in the north-eastern region of Argentina.

Figura 2. Distribución geográfica de los censos en la región nordeste de la República Argentina.

Fields were selected based on two criteria. First, the age of the crop, specifically those in full production with plants between 20 and 40 years old. Second, the planting framework, with the most common being traditional or modern systematized management practices for the production area (5).

Determination of the minimum sampling area: This constitutes the minimum surface area that represents the community (1, 4). In this study, a minimum area of 7 m^2 (figure 3, page 5) was determined, based on three considerations. The first consideration was the planting framework of most yerba mate fields, with 3–3.5 m between rows and 1.2-1.5 m between plants. The second consideration was the need to observe seedlings, small plants, and even propagules, which might go unnoticed in larger areas. The third consideration was the projection of the crop canopy, since plants in this area can become weeds and, in high-density populations, hinder normal crop growth (11).

Sampling Design: The minimum area was distributed using a systematized design with transects placed parallel to the plant rows (figure 4, page 5). This design was chosen for practicality and potential application to other perennial crops.

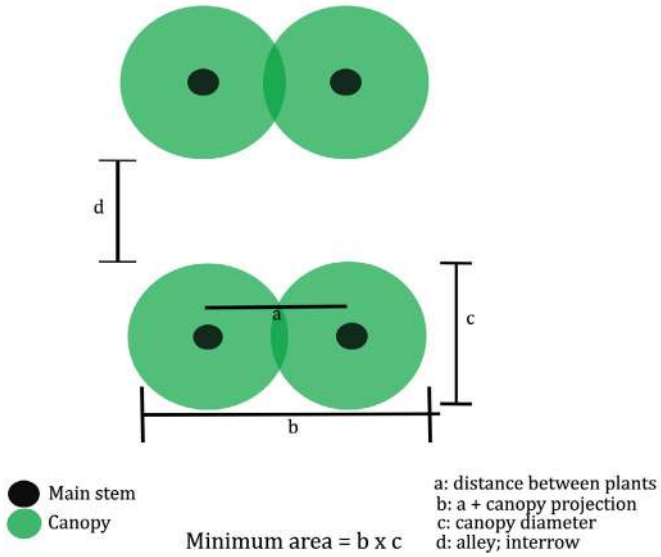
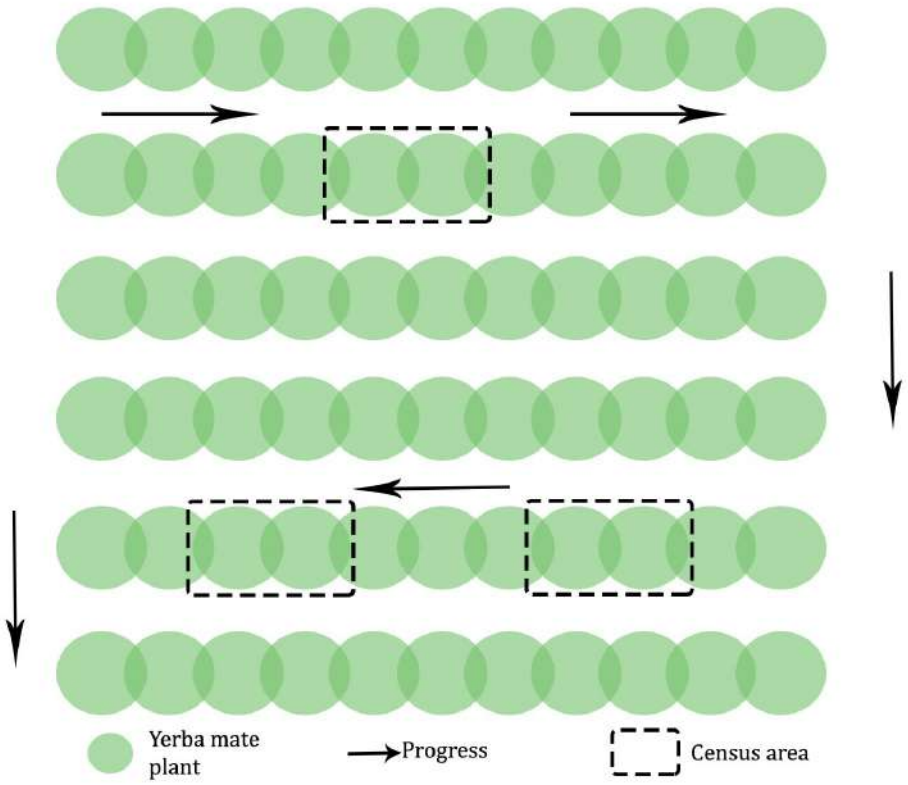


Figure 3. Determination of the minimum area for weed monitoring in perennial crops.
Figura 3. Determinación del área mínima para el monitoreo de malezas en cultivos perennes.



The arrows indicate the direction of progression, forming parallel transects.

Las flechas indican el sentido de avance formándose las transectas paralelas.

Figure 4. Distribution of the survey areas.
Figura 4. Distribución de las áreas censales.

Weed surveys: we collected plant material from species not identified in situ and took it to the Facultad de Ciencias Agrarias de la Universidad Nacional del Nordeste (FCA-UNNE) Specific taxonomic literature was used to accurately identify the species. A list of the surveyed species was compiled. For each species, presence/absence and abundance-coverage were recorded using the Braun-Blanquet scale (4). Finally, the presence/absence data were analysed and the frequency value of each species was determined.

Species richness and community composition: Species richness refers to the number of different species in an ecosystem, regardless of abundance (27). All recorded species were grouped into scandent and non-scandent species and organized by seasonal frequency in a contingency table. The four seasons were defined by summer and winter solstices and spring and autumn equinoxes, starting on 21/12, 21/6, 21/9 and 21/3, respectively. A chi-square test of independence (χ^2) was applied to determine whether the proportions of scandent and non-scandent life forms were related to the seasons. Additionally, a Pearson chi-squared analysis was conducted on the 10 species with the highest absolute and relative frequencies. This analysis included species regardless of life form and was performed to examine their seasonal patterns (23, 25).

Results and Discussion

Species Richness and Community Composition

A total of 153 species were surveyed, with 119 species (77.3%) classified as non-scandent and 34 (22.2%) as scandent (figure 5).

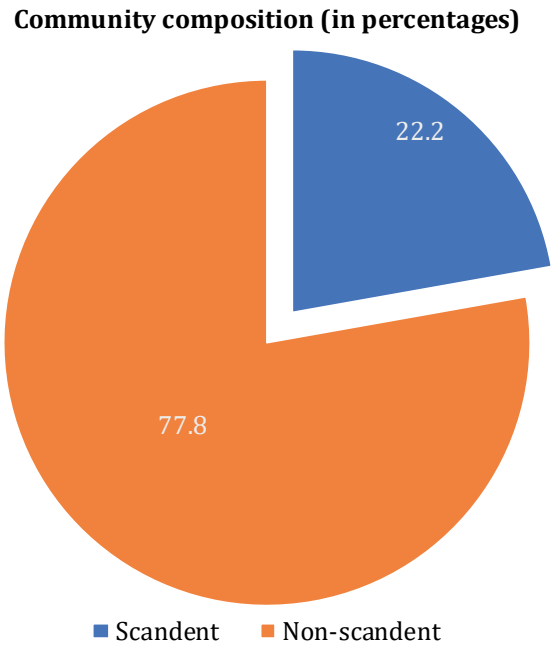


Figure 5. Community composition by scandent and non-scandent species (in percentages).

Figura 5. Composición de la comunidad por especies escandentes y no escandentes (en porcentajes).

Table 1 shows 1,705 species records obtained from 81 surveys, with 1,143 (67%) classified as non-scandent and 562 (33%) as scandent.

Table 1. Seasonal records of scandent and non-scandent species.

Tabla 1. Registros estacionales de especies escandentes y no escandentes.

	Seasons of the year			
Life Forms	Spring	Summer	Autumn	Winter
Non-scandent	487 (68.9%)	231 (65.1%)	193 (65.4%)	232 (66.7%)
Scandent	220 (31.1%)	124 (34.9%)	102 (34.6%)	116 (33.3%)
Total Records of species	1705			

Scandent and non-scandent species were organized in a contingency table displaying the frequency of life forms for each season (table 1). A chi-square (χ^2) independence test was conducted to assess whether the proportions of scandent and non-scandent species varied with the seasons.

Relative frequencies of the surveyed species (table 1) showed little variation throughout the year. This result is explained by the considered variables:

chi-square = 2.0802, df = 3, p-value = 0.5559

Notably, spring showed the highest number of individuals, while autumn had the lowest.

Absolute and Relative Frequencies of Scandent and Non-Scandent Species

In the field, certain species, such as *Ipomoea cairica* (L.) Sweet and *Scutellaria racemosa* Pers. (table 2), showed different frequencies across seasons. However, the chi-square test did not confirm this variation for scandent and non-scandent species. To verify seasonal patterns, the 10 species with the highest absolute and relative annual frequencies were selected and analyzed (table 2). Five of the six scandent species ranked at the top, highlighting their importance in the yerba mate agroecosystem throughout the year.

Table 2. Seasonal records and relative frequencies (%) of the 10 most frequent species by season of the year.

Tabla 2. Registros estacionales y frecuencias relativas (en porcentaje) de las 10 especies más frecuentes por estación del año.

Species	Sp	Su	Au	Wi	Total
Ipomoea grandifolia (Dammer) O´Donell	22 (34%)	10 (19%)	16 (25%)	14 (22%)	62
Ipomoea nil (L.) Roth	21 (35%)	12 (20%)	11 (18%)	16 (27%)	60
Ipomoea indica (Burm.) Merrill	18 (38%)	10 (21%)	8 (17%)	11 (23%)	47
Ipomoea cairica (L.) Sweet	17 (40%)	11 (26%)	11 (26%)	4 (9%)	43
Oxypetalum balansae Malme	25 (60%)	6 (14%)	4 (10%)	7 (17%)	42
Scutellaria racemose Pers.	16 (40%)	8 (20%)	9 (23%)	7 (18%)	40
Xerochrysum bracteatum (Vent.) Tzvelev	20 (54%)	4 (11%)	5 (14%)	8 (22%)	37
Cestrum parqui L´Hér	15 (43%)	5 (14%)	6 (17%)	9 (26%)	35
Maranta sobolifera L. Andersson	14 (44%)	11 (34%)	5 (16%)	2 (6%)	32
Smilax campestris Griseb.	11 (34%)	4 (16%)	5 (16%)	11 (34%)	31

S: Spring, Su: Summer, Au: Autumn, and Wi: Winter.

Sp: primavera, Su: verano, Au: otoño y Wi: invierno.

The Pearson Chi-Square test, with a value of P=205.46, was significant with a P value < 0.0001. These results suggest that the presence or absence of these species is seasonally influenced. Such observations are explained by the subtropical climate of yerba mate regions in Argentina, without dry season (5) and winter temperatures above 20°C for several weeks. Combined with precipitation during these months, this mild winter allows seed germination, seedling emergence, and sprouting of underground and vegetative organs. Blooming, fruiting, and propagule release also occur throughout the year.

The study shows that scandent species play a more significant role in the community as a life form than as contributors to floristic richness. Understanding their ecological role can help optimize resource allocation in integrated crop management. Although often considered secondary, climbing plants should receive greater attention based on these results.

Vanni *et al*. (2003) reported that scandent species contributed 20.7% to floristic richness in Iguazú National Park (PNI), while Miranda and Dummel (2016) found 18% in the Guaraní Multiple-Use Reserve (RUMG). Scandent species accounted for 22.22% in this study, higher than in natural ecosystems. Further research should determine if this difference is due to crop management. Such management may favor species preadapted to thrive as weeds, which benefit from microhabitat changes and become troublesome (22).

Swamy & Ramakrishnan (1987) report that *Mikania micrantha* rapidly spreads through disturbances, mainly forest fires, establishing seedlings or clones in newly affected areas. Dávalos *et al*. (2019) and Dávalos *et al*. (2023) report that over 90% of the accompanying species in the yerba mate agroecosystem are native. Seed banks and propagation structures facilitate their seasonal establishment. Species that adapt to the newly imposed conditions may become weeds in the crop.

In perennial crops such as coffee and sugarcane, the frequency of scandent species can vary. For example, *I. grandifolia* showed the highest relative frequency in this study. Kranz *et al.* (2009) reported this species in coffee cultivation in Paraná (Brazil) with a frequency of 21.9%. Oliveira *et al.* (2008) recorded it in sugarcane in Rio de Janeiro, with frequencies of 34.4% in autumn-winter and 15.5% in spring-summer. Despite these values, *I. grandifolia* is considered a secondary weed in coffee and sugarcane, unlike in yerba mate.

Conclusions

Scandent species are important weeds in yerba mate, representing 22% of species richness and 31.1-34.9% of the community composition in each season. Implementing a proper weed monitoring methodology, both in perennial crops generally and in yerba mate specifically, improves understanding of plant community dynamics over time. This methodology is a key tool for preventing weed infestations and evaluating the effectiveness of management strategies.

References

1. Alcaraz Ariza, F. J. 2013. El método fitosociológico. Geobotánica, Tema 11. Universidad de Murcia. España. http://creativecommons.org/licenses/by-nc/3.0/deed.es_CL
2. Altieri, M. A. 1999. Agroecología: bases científicas para una agricultura sustentable. Nordan Comunidad. 325 p.
3. Amarilla Rodríguez, S. M.; Amarilla Borja, S. C.; Insfrán Ortiz, A.; Pérez de Molas, F. 2022. Servicios ecosistémicos de provisión y culturales en el Paisaje Protegido Cerro Kavajú, Departamento de Cordillera, Paraguay. Investigación Agraria. 24(2).
4. Braun-Blanquet, J. 1950. Fitosociología. Bases para el estudio de las comunidades vegetales. Acme Agency. 444 p.
5. Bruniard, E. 1995. Geografía de los climas y de las formaciones vegetales: aportes para un modelo fitoclimático mundial. EUDENE.
6. Burtnik, O. J. 2006. Yerba mate: manual de producción. INTA-AER Santo Tomé. 52 p.
7. Capellari, P. L. 2017. Yerba mate. Reseña histórica y estadística. Producción e Industrialización en el siglo XXI. CABA: CFI. 310 p.
8. Concenço, G.; Farias, P. M. de; Quintero, N. F. A.; Schreiber, F.; Galon, L.; Tomazi, M. & Andres, A. 2017. Phytosociological Surveys in Weed Science: Old Concept, New Approach. InTech. DOI: 10.5772/intechopen.69083

9. Dávalos, C. M.; Kalitko, M.; Knott, K.; Podkowa, F.; Pawluk, L.; Rem, M. V.; López, M. G.; Vanni, R. O. 2019. Relevamiento de malezas frecuentes en el cultivo de yerba mate (*Ilex paraguariensis* A. St. Hil.) en lotes productivos de la provincia de misiones, Argentina. 1º Jornada de Divulgación Científica Producción de Yerba Mate. Misiones.
10. Dávalos, C. M.; Wilson, B. D.; Vallejos, F. E.; Alsina, A. F.; Benítez, A. E., Cardozo, A. E., López, G.; Vanni, R. O. 2023. Comunidad vegetal otoñal en un yerbal de la localidad de Andresito (Misiones). XXVIII Reunión de Comunicaciones Científicas, Técnicas y de Extensión. Corrientes.
11. Dávalos, C. M., López, M. G.; Vanni, R. O. 2025. Reconocimiento de malezas importantes en estadios juveniles en cultivos del Noreste de Argentina. Investigación Agraria. 26(2): 67-74. https://doi.org/10.18004/investig.agrar.2024.diciembre.2602807
12. De David, F.; Galon, L.; Perin, G. F.; Concenço, G.; Castamann, A.; Forte, C. T.; Rochely De David, P.; Mossin, A. J.; Andres, A.; Moisinho, I. 2018. Weed Interference in the Morphophysiological and Nutritional Characteristics of Erva-Mate (*Ilex paraguariensis*). American Journal of Plant Sciences. 9: 435-445.
13. Ellenberg, H.; Mueller-Dombois, D. A. 1967. Key to Raunkiaer plant life- forms with revised subdivisions. Berichte des Geobot Institutes der Eidg Techn Hochschule. Stift Rübel. 37: 56-73.
14. FAO. 2011. El estado de los recursos de tierras y aguas del mundo para la alimentación y la agricultura. La gestión de los sistemas en situación de riesgo. Organización de las Naciones Unidas para la Alimentación y la Agricultura. Roma y Mundi-Prensa, Madrid. https://openknowledge.fao.org/handle/20.500.14283/cb7654es
15. Giberti, G. C. 2011. La yerba mate (*Ilex paraguariensis*, Aquifoliaceae) en tempranos escritos rioplatenses de Bonpland y su real distribución geográfica en Sudamérica austral. Bonplandia. 20 (2): 203-212.
16. Gliessmann, S. R. 2002. Agroecología. Procesos ecológicos en agricultura sostenible. CATIE. 359 p.
17. Instituto Nacional de la Yerba Mate. 2016. www.inym.org.ar
18. Kranz, W. M.; Fonseca Jr., N.; Passini, T.; Brito Martins, N. 2009. Ocorrência e distribuição de plantas daninhas no Paraná. Instituto Agronómico do Paraná. Londrina.
19. Lovato Echeverría, R. A; Salgado, C.; Dávalos, M.; Royo Simonella, L.; López, M. G. 2022. Weeds of melliferous importance in crops of the Northeast Argentina Region. Revista Ciencias Agronómicas. 40 (22): 69-72. https://doi.org/10.35305/agro40.e029
20. Meira, M.; Pereira da Silva, E.; David, J. M.; David, J. P. 2012. Review of the genus Ipomoea: tradicional uses, chemistry and biological activities. Revista Brasiliera de Farmacognosia. 22(3): 682-713.
21. Miranda, D. E.; Dummel, C. 2016. Clave de identificación de especies de plantas trepadoras de la reserva de uso múltiple Guaraní (RUMG) Misiones, Argentina. Revista Forestal Yvyraretá. 23: 50-72.
22. Morais, M. I.; Pinto, M. E. A.; Araújo, S. G., Castro, A. H. F.; Duarte-Almeida, J. M.; Rosa, L. H.; Rosa, C. A.; Johan, S.; Dos Santos, L. A. R. 2014. Antioxidant and antifungal activities of *Smilax campestris* Griseb. (Smilacaceae). Natural producto Research. 28(16): 1275-1279. https://doi.org/10.1080/14786419.2014.895728
23. Mortimer, A. 2003. Manejo de malezas para países en desarrollo. Cap. 2. Estudio FAO.
24. Mueller Dumbois, D.; Ellemberg, H. 1974. Aims and methods of vegetation ecology. John Wiley & Sons, Inc.
25. Navure Team. 2023. Navure (2.7.3): A data-science-statistic oriented application for making evidence-based decisions. http://www.navure.com
26. Oliveira, A. R.; Freitas, S. P. 2008. Levantamento Fitossociológico de plantas daninhas en áreas de produção de cana-de-açúcar. Planta Daninha, Viçosa-MG. 26(1): 33-46.
27. Palacios, J. 2005. Citricultura. Tucumán. Argentina. 518 p.
28. Raunkiær, C. 1907. Planterigets livsformer, Og deres betydning for geografien. I commission hos Gyldendalske boghandel. Nordisk forlag. 132 p.
29. Sacco dos Anjos, F.; Belik, W.; Velleda Caldas, N. 2011. La caficultura en Brasil. Evolución, situación actual y nuevos retos cara al futuro. Mundo Agrario. 12(23). Recuperado de https://www.redalyc.org/articulo.oa?id=84522393005 (fecha de consulta: 7 de marzo de 2025).
30. Sánchez-Moreiras, A. M.; Vieites-Álvarez, Y; Fernández Calviño, D.; Campillo, C.; Gonzalez-de-Santos, P.; Rodríguez Silva, T.; Fedoniuk, T.; Synowiec, A.; Almeida Pinheiro de Carvalho, M. A.; Vityi, A.; Araniti, F.; Nacher, J.; Bolat, I.; Zornoza, R.; Verdeguer, M.; Shanskiy, M.; Reinhardt-Weik, H.; Johannesson, H. & Piron, L. 2024. Estrategias agroecológicas para el manejo sostenible de malas hierbas en cultivos europeos de relevancia económica (AGROSUS). Revista de Ciências Agrárias. 47(1): 107-112.
31. Sánchez-Sánchez, C.; Paz-Pellat, F.; Hernández-de la Rosa, P.; Velázquez-Rodríguez, A.; Vibrans, H.; Vargas-Hernández, J.; Valdez-Hernández, J. I.; Valdez-Lazalde, J. R. 2021. Riqueza de especies y tipos funcionales: su relación en bosques de oyamel del Monte Tláloc, Estado de México. Madera y Bosques. 27(4): e2742427. DOI: 10.21829/myb.2021.2742427
32. Swamy, P.; Ramakrishnan, P. 1987. Effect of fire on population dynamics of *Mikania micrantha* H. B. K. during early succession after slash and burn agricultura (jhum) in northeastern India. Weed Research. 27: 397-403.

33. Vanni, R. O.; López, M. G.; Dávalos, C. M. 2003. Inventario Florístico del Parque Nacional Iguazú. UNNE. Comunicaciones científicas y tecnológicas.
34. Yacovich, M. 2017. La actividad yerbatera en la provincia de Corrientes. Números para saber dónde estamos. En Yerba mate, reseña histórica y estadística, producción e industrialización en el siglo XXI.

Acknowledgments

We sincerely thank the Centro de Malezas, Facultad de Ciencias Agrarias, Universidad Nacional del Nordeste (FCA-UNNE) for their invaluable support and guidance. We also acknowledge the Instituto de Botánica del Nordeste (IBONE) and the Secretaría General de Ciencia y Técnica (SGCyT-UNNE) for financial assistance.

Finally, we are especially grateful to the farmers and their families for their warm hospitality and for welcoming us during each visit.

Mortality of the Toad Grasshopper (*Bufonacris claraziana* Saussure) Caused by *Beauveria bassiana* (Balsamo) Vullemin (Hypocreales: Clavicipitaceae) by Two Inoculation Methods under Field-Cage Conditions

Evaluación de la mortalidad causada por *Beauveria bassiana* (Balsamo) Vullemin (Hypocreales: Clavicipitaceae) contra la tucura sapo comparando dos procedimientos de inoculación en condiciones de jaulas en el campo

Yanina Mariottini [1*], Sebastián Alberto Pelizza [2], Lucas Emanuel Castelli [3], Franco Armento [4], Carlos Ernesto Lange [5, 6]

Originales: *Recepción:* 11/09/2024- *Aceptación:* 17/10/2025

ABSTRACT

Bufonacris claraziana Saussure (Orthoptera: Tristiridae) is a pest grasshopper species in Patagonia, Argentina. Outbreaks of *B. claraziana* have gained frequency in recent years. This study compared three infection methods (spraying and baits) on *B. claraziana* mortality caused by *Beauveria bassiana* under field-cage conditions in the natural habitat. The study was conducted in Cushamen, a typical outbreak area in Chubut province. Three treatments were tested: Treatment I involved spraying with a fungal suspension (1×10^8 conidia/ml), treatment II used wheat bran baits with the same suspension, and treatment III used wheat bran baits with added canola oil as a phagostimulant. Mortality rates were monitored every 24 hours for 15 days. Total mortality differed among the treatments (F: 17.58; p: 0.0007). After 15 days, mortality was 60%, 70%, and 100% for treatments I, II, and III, respectively. No mortality was observed in treatments I and II until day 5, while treatment III showed 36.7% mortality by day 5 and reached 100% by day 10. Kaplan-Meier survival curves indicated significant differences in survival among treatments, with the lowest survival in treatment III (log-rank test $p<0.05$). Wheat bran bait with canola oil (treatment III) was the most effective inoculation.

Keywords
field-cage experience • baits and spraying inoculations • *Bufonacris claraziana* • Patagonia Argentina • entomopathogenic fungus

https://doi.org/10.48162/rev.39.209

1 Universidad Nacional del Centro de la Provincia de Buenos Aires. Comisión de Investigaciones Científicas (UNICEN-CIC). Instituto Multidisciplinario sobre Ecosistemas y desarrollo sustentable. Campus Universitario Tandil. Paraje Arroyo seco S/N.
* ymariottini@ecosistemas.exa.unicen.edu.ar
2 Universidad Nacional de La Plata Facultad de Ciencias Naturales y Museo (FCNyM-UNLP). Instituto de Botánica Carlos Spegazzini. Calle 53 # 477. La Plata (1900). Argentina.
3 Grupo de Entomología Patagónica (GENTPAT), Instituto Patagónico para el Estudio de los Ecosistemas Continentales (IPEEC-CENPAT-CONICET). Bvd. Brown 2915. Puerto Madryn. Chubut. Argentina.
4 Servicio Nacional de Sanidad y Calidad Agroalimentaria (SENASA). Centro Regional Patagonia Sur. Pasaje San Juan 840, El Maitén. Chubut.
5 Universidad Nacional de La Plata (UNLP). Centro de Estudios Parasitológicos y de Vectores (CEPAVE). CCT La Plata CONICET. Boulevard 120 e/60 y 64 S/N. La Plata (1900). Argentina.
6 Comisión de Investigaciones Científicas de la Provincia de Buenos Aires (CICPBA). La Plata. Argentina.

Licenses Creative Commons
Attribution - Non Commercial - Share Alike

Resumen

Bufonacris claraziana Saussure (Orthoptera: Tristiridae) es una plaga recurrente en la Patagonia argentina. Este estudio evaluó la mortalidad causada por *Beauveria bassiana* en *B. claraizana* mediante dos métodos de infección (aspersión y cebos) bajo condiciones de semicampo en Cushamen, Chubut. Se realizaron tres tratamientos: I) Aspersión con una suspensión fúngica (1×10^8 conidios/ml), II) Cebos de salvado de trigo con la misma suspensión, y III) Cebos de salvado de trigo más aceite de canola como fagostimulante. La mortalidad se monitoreó cada 24 horas durante 15 días. La mortalidad total fue diferente entre los tratamientos y el control (F: 17,58; p: 0,0007). La mortalidad de los individuos fue del 60%, 70% y 100% para los tratamientos I, II y III, respectivamente, al final del ensayo. En los tratamientos I y II, no se observó mortalidad hasta el día 5, mientras que el III presentó un 36,7% de mortalidad en el día 5, alcanzando el 100% en el día 10. Las curvas de Kaplan-Meier mostraron diferencias significativas en la supervivencia entre los tratamientos; el tratamiento III tuvo la supervivencia más baja ($p<0,05$). Estos resultados indicarían que los cebos de salvado de trigo con aceite de canola son el método de inoculación más efectivo.

Palabras clave

experiencia en jaulas de campo • inoculación por cebos y por aspersión • *Bufonacris claraziana* • Patagonia Argentina • hongos entomopatógenos

Introduction

Tristirids (Orthoptera: Tristiridae) constitute an endemic family of South American grasshoppers with ten species distributed across the Patagonian steppe, sub-Antarctic forests, and the Puna biogeographic province in Argentina (4, 7). Among these ten species, only *Bufonacris claraziana*, commonly known as the "Toad grasshopper," is economically significant in this country and endemic to the Patagonian biogeographic province (2). This species is large (up to 36.5 mm long), robust, and wingless (6); polyphagous and univoltine, with a long obligatory embryonic diapause that extends for more than a single winter (16, 17, 19). Considered a frequent and significant pest (4), outbreaks have become more frequent in recent years, with particularly intense episodes in Chubut, Santa Cruz, and Río Negro provinces during 2016, 2019, and 2022 (18, 19). Both nymphs and adults typically undertake extensive marching migrations through the Patagonian steppe.

In contrast to global trends, the use of chemical insecticides remains the primary option for grasshopper control in our country, resulting in environmental impact and increasing concern about non-target organisms (1, 5, 11). Patagonia, rich in endemic species, has been categorized as vulnerable with maximum conservation priority (8, 23, 24). Consequently, minimized chemical applications have inspired studies on grasshopper pathogens with biocontrol potential, ranging from microsporidia to protists and fungi (26, 28, 30).

Unfortunately, *B. claraziana* is not susceptible to the microsporidium *Paranosema locustae*, a naturalized biocontrol agent causing epizootics in other harmful grasshopper species in the country (14). Entomopathogenic fungi (especially *Metarhizium anisopliae* and *Beauveria bassiana*) are the main microorganisms used to control different grasshopper species and locust pests (18, 25). To date, eleven fungal formulations are commercially available against grasshoppers and locusts worldwide (10). Recently, Mariottini *et al.* (2019) used spray inoculation with three strains of *B. bassiana*, resulting in nearly 100% mortality of adult *B. claraziana*. Later, these authors tested wheat bran bait with conidia against younger nymphs, obtaining similar mortality rates (Mariottini *et al.*, 2022).

To further evaluate the potential of *Beauveria bassiana* as a biocontrol agent against *B. claraziana*, we tested two infection procedures under field-cage conditions in natural habitat. We hypothesized that *B. bassiana* can effectively control *Bufonacris claraziana*, and under semi-field conditions, efficacy varies with the inoculation method (spray application *vs.* conidia baits).

Materials and Methods

The experiment took place in a field located in Cushamen County (42°10'23" S, 70°39'39" W), a common outbreak area of *B. claraziana* in Chubut. The area is characterized by grassy shrub steppe dominated by *Poa*, *Stipa*, *Festuca*, and *Chuquiraga avellanedae* (3, 24) and "mallines," low, wet-meadow grasslands with high forage value (21, 22). The site has short, warm summers and cold, snowy winters with average annual temperature of 8°C. Moderate to strong west winds are frequent, and average annual precipitation is 150 mm (20).

Under field-cage conditions, we evaluated nymph mortality caused by *B. bassiana* using two different infection procedures: spraying and wheat bran baits, as previously described (17, 18, 25, 27). The *B. claraziana* individuals used in the experiment were captured as young nymphs with entomological nets in early October 2022, at Cushamen. They were placed in wire-screened cages (45 x 40 x 30 cm) with no floor, allowing grasshoppers to interact with the natural soil and vegetation.

The fungal isolate used (LPSc 1227; GenBank accession number: MG012792) was obtained from the Spegazzini Institute culture collection at La Plata National University. This isolate originally came from cadavers of the South American locust *Schistocerca cancellata* (Serville) (Orthoptera: Acrididae) collected in nature near La Banda (27°44'07" S, 64°14' 36" W), Santiago del Estero Province, northwestern Argentina (28). Conidia were obtained from cultures grown on potato dextrose agar medium, incubated for 10 days at 25°C in the dark. Conidia were then harvested using disposable cell scrapers (Fisherbrand™) as described by Pelizza *et al.* (2020).

Fungal suspensions were made with conidia placed in test tubes containing 0.01% (v/v) polyoxyethylene sorbitan monolaurate (Tween 80™; Merck). Suspensions were adjusted to 1×10^8 conidia/ml using a Neubauer hemocytometer. Viability was assessed after 24 hours as described by Goettel and Inglis (1997). Germination was considered when the germ tube reached half conidium length. Each assessment was performed in triplicate with 300 conidia under each experimental condition. Three treatments were conducted with three replicates of ten individuals each. Treatment I nymphs were sprayed with a 1×10^8 conidia/ml aqueous suspension (17). In treatment II, wheat bran (200 g) was sprinkled with a 1×10^8 conidia/mL suspension. The bait was placed in the cages for the nymphs to consume, as in Mariottini *et al.* (2022). Treatment III was similar to treatment II, but with the addition of canola oil as a phagostimulant. Controls had 0.01% (v/v) Tween 80®.

Nymph mortality was recorded every 24 hours for 15 days. Dead grasshoppers with no external mycelium were surface-sterilized by sequentially dipping them in 70% ethanol (10-15 seconds), 0.5% sodium hypochlorite solution (1 minute), and sterile distilled water (1 minute, two consecutive baths) (12). They were then placed in a sterile culture chamber, consisting of a Petri dish (60 mm diameter) with a filter-paper disk periodically moistened with sterile distilled water, and incubated at 25°C in the dark. Mycosis was confirmed by microscopic examination of dead grasshoppers. Total mortality for treatments was compared using one-way ANOVA. Mortality rates at 5, 10, and 15 days were compared using the Kruskal-Wallis test and the median survival time (MST). Survival curves were calculated using Kaplan-Meier analysis. Pairwise comparisons between survival curves were performed with the Log-rank test. All analyses were conducted with Infostat (9).

Results

Mortality recorded at the end of the experiment (After 15 days) was 60%, 70%, and 100% for treatments I, II, and III, respectively. Mortality rates differed among treatments (One-Way ANOVA; F: 17.58; df:3, p: 0.0007), with control showing no mortality. Besides, significant differences in mortality percentages were observed at 5, 10, and 15 days (table 1, page 4).

Up to day 5, treatments I and II evidenced no mortality, whereas treatment III exhibited a significantly higher 36.7 ± 3.3% ($p<0.05$; table 1, page 4). By day 10, treatment III reached 100% mortality, significantly higher than treatment I ($p<0.05$). Mortality rates were not significantly different between treatment I (36.7%) and II (23.33%).

Table 1. Kruskal-Wallis test comparing treatment mortality over 5, 10, and 15 days.

Tabla 1. Prueba de Kruskal-Wallis comparando la mortalidad entre los tratamientos a los 5, 10 y 15 días.

I: Spraying, II: baits of wheat bran plus conidia, III: Baits of wheat bran with conidia plus canola oil. Different letters within each day indicate significant pairwise differences between treatments at p < 0.05.

I: Procedimiento de aspersión, II: Cebos de salvado de trigo con los conidios, III: cebos de salvado de trigo con los conidios más aceite de canola. Letras diferentes dentro de cada día indican diferencias significativas por pares entre tratamientos con p < 0,05.

Days	Kruskal-Wallis results	Treatments	Mean mortality (%)	p <0.05
5	H: 5.40, p: 0.0337	I	0	a
		II	0	a
		III	20	b
10	H: 5.60 p: 0.0357	I	23.33	a
		II	36.67	ab
		III	100	b
15	H: 5.05 p: 0.0383	I	60	a
		II	70	ab
		III	100	b

On day 15, mortality in treatment I was similar to that in treatment II ($p > 0.05$) but differed from treatment III, while treatment II and III were not significantly different from each other ($p > 0.05$). Kaplan-Meier survival curves (figure 1) further confirmed significant differences among treatments (log-rank test, $p < 0.05$) (table 2). Treatment III had the lowest survival rate (Log-rank test, $p < 0.05$).

I: Spraying procedure II: baits of wheat bran plus conidia procedure, III: Baits of wheat bran with conidia plus canola oil.

I: Procedimiento de aspersión, II: Cebos de salvado de trigo con los conidios, III: Cebos de salvado de trigo con los conidios más aceite de canola.

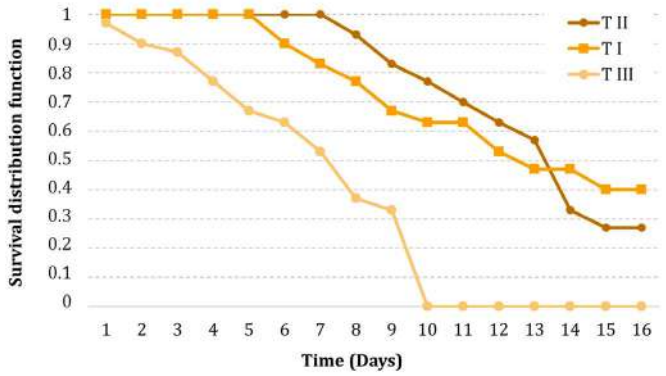


Figure 1. Kaplan-Meier survival curves of *Bufonacris claraziana* infected with *Beauveria bassiana* through different inoculation procedures.

Figura 1. Curvas de supervivencia de Kaplan-Meier de *Bufonacris claraziana* infectada con *Beauveria bassiana* a través de diferentes procedimientos de inoculación.

Table 2. X^2 test for the comparison of the Kaplan-Meier curves of each inoculation procedure.

Tabla 2. Resultados de la prueba log-rank (X^2) para la comparación de las curvas de Kaplan-Meier de cada procedimiento de inoculación.

I: Spraying procedure; II: baits of wheat bran plus conidia procedure, III: Baits of wheat bran with conidia plus canola oil.

I: Procedimiento de aspersión, II: Cebos de salvado de trigo con los conidios, III: Cebos de salvado de trigo con los conidios más aceite de canola.

Treatments	I	II	III
I	null	null	null
II	X^2: 0.083 p:0.083	null	null
III	X^2: 18.35 p:0.00001	X^2: 28.62 p:0.0000	null

Discussion

According to this study, *B. bassiana* shows potential for effective biocontrol under field conditions, similar to its performance in controlled laboratory experiments (17, 18). Field-cage effectiveness -where nymphs of *B. claraziana* were somewhat restricted in their movement and partially protected from environmental factors- suggests that *B. bassiana* could perform well in actual field scenarios. In real field conditions (*i.e.*, without cages), the use of *B. bassiana* as wheat bran baits with added canola oil seems promising. Bran baits would offer some protection from UV degradation and other environmental factors, while canola oil would act as a phagostimulant, improving bait acceptance and palatability (15, 27). In general, vegetable oils serve as carriers for control purposes, increasing both attraction to and ingestion of baits, thereby enhancing control efficacy (29, 30). In 2007, Latchininsky *et al.* (2006), reported that vegetable oils stimulated feeding in *Melanoplus sanguinipes*, one major grasshopper pest in North America. Ideally, in such a scenario, nymphs to be treated should be the youngest possible, ensuring the highest susceptibility and the shortest time lag until full mortality. Additionally, younger nymphs tend to concentrate, making it easier to control.

In recent years, large areas of Cushamen County have been affected by *B. claraziana* outbreaks. Most local ranchers are smallholders who rear sheep and goats under subsistence conditions. They manage outbreaks using chemical pesticides like pyrethroids, cypermethrin, organophosphates, dimethoate baits, or mechanical methods like barriers, trenches, and burning of grasshoppers or vegetation (17). These control methods exacerbate species extinction, alter vegetation structure, increase soil erosion, and reduce ecosystem productivity in the Patagonia steppe (21, 24).

Numerous isolates of *B. bassiana* have been developed worldwide as biocontrol agents for various agriculturally harmful insects (31). While field-cage experiments have their limitations, they provide a valuable step beyond laboratory studies (13). Given the urgent need to revise current control methods for *B. claraziana* outbreaks, we believe that isolate LPSc 1227 warrants further investigation as a potential management tool for controlling Toad grasshopper populations.

Conclusion

The isolate LPSc 1227 of *Beauveria bassiana* demonstrated high efficacy against *Bufonacris claraziana* under field-cage conditions. In our study, wheat-bran baits with canola oil were the most effective inoculation method for early nymphal stages, expanding on previous laboratory results. As discussed, larger-scale open-field trials should continue evaluating the potential of this entomopathogen as a control agent for *B. claraziana* in Patagonia.

References

1. Álvarez, M.; du Mortier, C.; Fernández Cirelli, A. 2013. Behaviour of insecticide chlorpyrifos on soils and sediments with different organic matter content from provincia de Buenos Aires, República Argentina. Water Air Soil Pollution. https://doi.org/10.1007/s11270-013-1453-0.
2. Cabrera, A. L.; Willink, A. 1973. Biogeografía de América Latina. Monogr. Ser. Biol. 13.
3. Cabrera, A. L. 1976. Regiones fitogeográficas argentinas. In: Kugler, W. F. (Ed). Enciclopedia Argentina de Agricultura y Jardinería, II. ACME. 1-85.
4. Carbonell, C. S.; Cigliano, M. M.; Lange, C. E. 2024. Acridomorph (Orthoptera) species of Argentina and Uruguay. http://163.10.203.2/ACRIDOMORPH/
5. Ceccheto, F.; Villalba, A.; Vazquez, N. D.; Ramirez, C. L.; Maggi, M. D.; Miglioranza, K. S. B. 2023. Occurrence of chlorpyrifos and organochlorine pesticides in a native bumblebee (*Bombus pauloensis*) living under different land uses in the southeastern Pampas, Argentina. Science of the total Environment. https://doi.org/10.1016/j.scitotenv.2023.167117
6. Cigliano, M. M.; Pocco, M. E.; Lange, C. E. 2014. Acridoideos (Orthoptera) de importancia agroeconómica en la República Argentina. In: Roig Juñent, S.; Claps, L.; Morrone, J. J. (Eds). Biodiversidad de Artrópodos Argentinos. Editorial INSUE-UNT. 3: 11-36.

7. Cigliano, M. M.; Lange, C. E. 2019. Toad grasshopper, *Bufonacris claraziana* (Saussure, 1884) (Orthoptera: Tristiridae). In: Lecoq, M.; Zhang, L. (Eds). Encyclopedia of pest Orthoptera of the World. China Agricultural University Publisher. 235-238.
8. Dinerstein E.; Olson, D. M.; Graham, D. J.; Webster, A. L.; Primm, S. A.; Bookbinder, M. P.; Ledec, G. 1955. A conservation assessment of the terrestrial ecoregions of Latin America and the Caribbean. World Bank.
9. Di Rienzo, J. A.; Casanoves, F.; Ballarin, M. G.; González, L.; Tablada Robledo, C. W. 2011. Grupo InfoStat, FCA, Universidad Nacional de Córdoba. Argentina. http://www.infostat.com.ar
10. Goettel, M. S.; Inglis, G. D. 1997. Hyphomycetes. In: Lacey, L. (Ed). Manual of techniques in Insect Pathology, Academic Press. 213-248.
11. Goldstein, M. I.; Lacher, T. E.; Woodbridge, B.; Bechard, M. J.; Canavelli, S. B.; Zaccagnini, M. E.; Cobb, G. P.; Scollon, E. J.; Tribolet, R.; Hooper, M. J. 1999. Monocrotophos - Induced mass mortality of Swainson's Hawks in Argentina. 1995-96. Ecotoxicology. (8): 201-214.
12. Inglis, G. D.; Enkerli, J.; Goettel, M. S. 2012. Laboratory techniques used for entomopathogenic fungi: Hypocreales. In: Lacey, L.A. (Ed). Manual of techniques in Invertebrate Pathology. Elsevier. 189-253.
13. Lacey, L. A.; Brooks, W. M. 1997. Initial handling and diagnosis of diseased insects. In: Lacey, L. A. (Ed). Manual of techniques in Insect Pathology. Academic. 1-15.
14. Lange, C. E.; Mariottini, Y.; Plischuk, S.; Cigliano, M. M. 2020. Naturalized, newly associated microsporidium continues causing epizootics and expanding its host range. Protistology. 2020: (14): 32-37. http://dx.doi.org/10.21685/1680-0826-2020-14-1-4
15. Latchininsky, A. V.; VanDyke, K. A. 2006. Grasshopper and locust control with Poisoned baits: a renaissance of the old strategy? Outlooks Pest Management. (17): 105-111.
16. Liebermann, J. 1972. The current state of the locust and grasshopper problem in Argentina. In Proceeding of the international Study Conference on Current and Future Problems of Acridiology. 191-198.
17. Mariottini, Y.; Pelizza, S. A.; Lange C. E. 2019. Susceptibility of *Bufonacris claraziana* (Orthoptera: Tristiridae) to *Beauveria bassiana* (Ascomycota: Hypocreales) under controlled conditions. Biocontrol Science and Technology. (29): 817-821. http://dx.doi.org/10.1080/09583157.2019.1597335
18. Mariottini, Y.; Lange, C. E.; Pelizza, S. A. 2022. Laboratory test of *Beauveria bassiana* (Balsamo-Crivelli) Vuillemin s.l. (Hypocreales: Clavicipitaceae) baits for the biocontrol of the Toad grasshopper pest, *Bufonacris claraziana* (Saussure) (Orthoptera: Tristiridae). Egyptian Journal of Biological Pest Control. 32:110. https://doi.org/10.1186/s41938-022- 00609-4
19. Medina, H.; Massola, M. P.; Zembo, E.; Verdejo, A.; Shicappacassi, M.; Azzaro, F.; Cienfuegos, M. S.; Sánchez, M.; Armento, F.; Mariottini, Y.; Fernández Arhex, V., Bobadilla, S.; Bobadilla, W.; Binda, S.; Napoli, S.; Camiña, D. 2020. Guía de recomendaciones para el manejo y control de la tucura sapo. SENASA. https://www.argentina.gob.ar/sites/default/files/guiade_recomendaciones_para_el_monitoreo_y_control_de_tucura_sapo.pdf
20.Mendez Casariego, H.; Bran, D. E.; Peralta, C. R.; Madariaga, M. C.; Huerta, G. J.; Villarreal, P.; Oliva, G. E.; López Raggi, F.; Santagni, A.; Easdale, M. H.; Sarmiento, A. C.; Giraudo, C. G.; Rial, P. E.; Escobar, J. M.; Marciani, S. N.; Martinez, R. S.; Elissalde, N. O. 2005. Programa Nacional de Ecorregiones. La región Patagonia: Centros Regionales Patagonia Norte y Patagonia Sur; INTA Centro Regional Patagonia Norte. EEA Bariloche. Comunicaciones Técnicas.
21. Olson, D.; Dinerstein, E. 2002. The Global 200: Priority Ecoregions for Global Conservation. Annals of Missouri Botanical Garden. 89(2): 199-224.
22. Oyarzabal, M.; Clavijo, J. R.; Oakley, L. J.; Biganzoli, F.; Tognetti, P. M.; Barberis, I.; Maturo, H. M.; Aragón, R.; Campanello, P. I.; Prado, D.; Oesterheld, M.; León, R. J. 2018. Unidades de vegetación de la Argentina; Asociación Argentina de Ecología. Ecología Austral. 28: (1-4): 40-63. https://doi.org/10.25260/EA.18.28.1.0.399
23. Paruelo, J.; Aguiar, M. 2003. Impacto humano sobre los ecosistemas. El caso de la desertificación. Ciencia Hoy. 13.
24. Paruelo, J.; Golluscio, R.; Jobbágy, E.; Canevari, M.; Aguiar, M. 2005. Situación ambiental en la estepa patagónica. In: Brown, A.; Martinez Ortiz, U.; Acerbi, M.; Corcuera, J. (Eds). La situación ambiental argentina. Buenos Aires: Fundación Vida Silvestre Argentina. 303-313.
25. Pelizza, S. A.; Mariottini, Y.; Russo, M. L.; Cabello, M. N., Lange, C. E. 2013. Survival and fecundity of *Dichroplus maculipennis* and *Ronderosia bergi* (Orthoptera: Acrididae: Melanoplinae) following infection by *Beauveria bassiana* (Ascomycota: Hypocreales) under laboratory conditions. Biocontrol Science and Technology. (23): 701-710. https://doi.org/10.1080/09583157.2013.791668
26. Pelizza, S. A.; Mariottini, Y.; Russo, L. M.; Vianna, M. F.; Scorsetti, A. C.; Lange, C. E. 2017. *Beauveria bassiana* (Ascomycota: Hypocreales) introduced as an endophyte in corn plants and its effects on consumption, reproductive capacity, and food preference of *Dichroplus maculipennis* (Orthoptera: Acrididae: Melanoplinae). Journal of Insect Science. 17(2): 53. https://doi.org/10.1093/jisesa/iex024

27. Pelizza, S. A.; Mariottini, Y.; Russo, L. M.; Vianna, F. M.; Scorsetti, A. C.; Lange, C. E. 2019. Application of *Beauveria bassiana* using diferent baits for the control of grasshopper pest *Dichroplus maculipennis* under field cage conditions. Journal of King Saudi University Science. 31(4): 1111-1115. https://doi.org/10.1016/j.jksus.2019.02.014
28. Pelizza, S. A.; Medina, H.; Ferreri, N. A.; Elíades, L. A.; Pocco, M. E.; Stenglein, S. A.; Lange, C. E.; 2020. Virulence and enzymatic activity of three new isolates of *Beauveria bassiana* (Ascomycota: Hypocreales) from the South American locust *Schistocerca cancellata* (Orthoptera: Acrididae). Journal of King Saudi University Science. (32): 44-47. https://doi.org/10.1016/j.jksus.2017.11.006
29. Pérez Panti, O.; García de la Cruz, R.; González Hernández, H.; Sánchez Soto, S.; Moscoso Ramírez, P. A.; Izquierdo Reyes, F. 2024. Bio-efficacy of entomopathogenic fungi and vegetable oils against the pink pineapple mealybug: Dysmicoccus brevipes (Cockerell). Revista de la Facultad de Ciencias Agrarias. Universidad Nacional de Cuyo. Mendoza. Argentina. 56(1): 83-93. DOI: https://doi.org/10.48162/rev.39.125
30. Sepúlveda, L.; Pietrantuono, A. L.; Buteler, M.; Fernández-Arhex, V. 2019. Effect of Vegetable Oils as Phagostimulants in Adults of *Dichroplus vittigerum* (Orthoptera: Acrididae). Journal of Economic Entomology. 112(6): 2649-2654. https://doi.org/10.1093/jee/toz190
31. Sokolova, Y. Y.; Lange, C. E.; Fuxa, J. R. 2006. Development, ultrastructure, natural occurrence, and molecular characterization of *Liebermannia patagonica* n. gen., n. sp., a microsporidium of the grasshopper *Tristira magellanica*. Journal of Invertebrate Pathology. (91): 168-182. https://doi.org/10.1016/j.jip.2006.01.003
32. Vega, F. E.; Meyling, N. V; Luangsaard, J. J.; Blackwell, M. 2012. Fungal entomopathogenes. In: Vega, F. E.; Kaya, H. K. (Eds). Insect Pathology. Elsevier. 171–220. DOI: 10.1016/ B978-0-12-384984-7.00006-3

Acknowledgments

We thank Antonio Fermín, production director of the Cushamen Locality.

Beef Quality of Braford Young Intact Males and Steers Grazing Pastures and Supplemented with Energy-Protein Sources During Growing and Fattening

Calidad de la carne de machos enteros jóvenes y novillos Braford en sistema pastoril suplementados con fuentes de energía y proteína durante el crecimiento y engorde

María José Fernández Salom [1, 2*], Natalia Verónica Taboada [1], Olegario Hernández [1, 3], Diego Bottegal [4], Sandra Luz Martinez [5], María Zimerman [4]

Originales: *Recepción:* 23/06/2024 - *Aceptación:* 03/10/2025

ABSTRACT

In this study, the quality parameters of the carcass and meat of Braford young intact males (YIM) and steers (STR) aged 17 and 20 months were evaluated and compared under Rhodes grass grazing with supplementation systems. YIM and STR (n = 60) were assigned to the grazing period and finished concentration. The carcass quality parameters studied were conformation, fat content, tissue composition, carcass weight, dressing, *longissimus thoracis* area (LTA) and subcutaneous fat thickness (SFT). Meat quality parameters such as pH, color, water holding capacity and texture were studied in the *longissimus thoracis* (LT) and *semitendinosus* (ST) muscles at two aging times, 3 and 15 days. YIM exhibited significantly higher body weight (BW), lower subcutaneous fat thickness (SFT), and larger longissimus thoracis area (LTA) postmortem compared to STR. Significant differences (p <0.05) were found between the two slaughter ages for LTA. Among texture parameters, only the elasticity of LT varied with the age of animals, and this parameter decreased as the age of animals increased (p <0.05). Results show that YIM generate a good quality product (carcasses and meat), which justifies the implementation of this new category for productive advantages, demonstrating superiority in the meat industry.

Keywords
meat quality • carcasses • young intact males • steers

https://doi.org/10.48162/rev.39.208

1 Universidad Nacional de Santiago del Estero. Facultad de Agronomía y Agroindustrias. Av. Belgrano (S) 1912. Santiago del Estero 4200. Argentina.
2 Instituto Multidisciplinario de Salud, Tecnología y Desarrollo (CONICET-UNSE). Ruta Nacional No 9 Km 1125. S/N. Villa El Zanjón. Santiago del Estero. C. P. 4206. * mjfsalom2439@gmail.com
3 Estación Experimental Agropecuaria Santiago del Estero. Instituto Nacional de Tecnología Agropecuaria (INTA). Jujuy 850. Santiago del Estero 4200. Argentina.
4 Instituto de Investigación Animal del Chaco Semiárido (IIACS). Centro de investigaciones Agropecuarias (CIAP). Insittuto Nacional de Tecnología Agropecuaria (INTA) Chañar Pozo s/n. Leales. Tucumán. C. P. 4113.
5 Universidad Nacional de Santiago del Estero. Facultad de Agronomía y Agroindustrias. Instituto de Ciencia y Tecnología de los Alimentos ICYTA.

Licenses Creative Commons
Attribution - Non Commercial - Share Alike

Resumen

En este estudio se compararon parámetros de calidad de carcasa y de carne en MEJ (machos enteros jóvenes) y novillos de la raza Braford (n = 60), a dos edades, 17 y 20 meses, invernados en sistema pastoril con suplementación. Los parámetros de calidad de la canal estudiados fueron conformación, engrasamiento, composición del tejido, peso de la canal, rendimiento, área de ojo de bife (AOB) y espesor de grasa dorsal (EGD). Se evaluaron parámetros de calidad de la carne: pH, color, capacidad de retención de agua y perfil de textura en los músculos *Longissimus thoracis* (LT) y *Semitendinosus* (ST) en dos tiempos de maduración 3 y 15 días. Los MEJ mostraron ($p \leq 0,05$) un mayor peso vivo antes del sacrificio, menor nivel de EGD y mayor AOB *postmortem* en comparación con los novillos. Se encontraron diferencias significativas ($p \leq 0,05$) entre las dos edades de faena para AOB. En lo referido a los parámetros de textura solo la elasticidad del LT varía con la edad de los animales, esta disminuye a medida que aumenta la edad del animal ($p \leq 0,05$). Los resultados muestran que el MEJ genera un producto de buena calidad para la industria cárnica y presenta ventajas productivas en sistemas pastoriles con suplementación, que evidencian su superioridad para la industria cárnica.

Palabras claves
calidad de la carne • canales • machos enteros jóvenes • novillos

Introduction

The creation of the category ¨young intact male¨ (YIM) (in Spanish *MEJ*, *macho entero joven*) in 2010 by the Ministry of Agriculture, Livestock and Fisheries (Ministerio de Agricultura, Ganadería y Pesca) (Resolution No. 4906/2010) allows including a product underexplored in the Argentine beef market. The YIM category seems to be an interesting alternative for obtaining heavy and leaner carcasses from feedlot animals, especially in countries where growth promoters are forbidden (4). The world meat market has undergone significant changes in recent years, some resulting from factors that have modified the consumption habits of the population. Forage-feeding systems could confer specific physical, chemical and sensory characteristics to meat, as well as a positive image for consumers, who associate pastoral systems with natural products (14). Numerous studies have highlighted the advantages of using intact males in terms of growth rate and feed conversion efficiency compared with steers (STR) for beef production (23, 37). To exploit these biological advantages while increasing the profitability of bull production, there is considerable interest in including a grazing period to decrease production costs (38). Feedstuff accounts for a major proportion of the total costs in most cattle production systems, and grazed grass is the cheapest feedstuff in temperate climates (17). Forage systems need to increase their beef production to achieve adequate exportable balances, which translates into greater foreign exchange income for the sector (21). A large part of the expansion of beef export in global volumes came from Argentina, Canada, the European Union, Thailand and the United States (36). The balance of exportable meat in our country results from the decrease in per capita consumption (44.3 kg/capita/year) attributed to factors such as fall in purchasing power and growth of alternative meat (poultry and pork) (7). In Argentina, one of the challenges for agricultural producers is to innovate production systems that improve the growth rate of animals, feed conversion efficiency and carcass development, both qualitatively and quantitatively (29). This concept underlies the production of YIM (with testicles), with up to two (2) permanent incisors teeth (less than 24 months of age) at the time of slaughter and intervertebral cartilages of the sacral region with incipient ossification. Age at slaughter significantly affects beef quality. Younger cattle typically produce meat with finer muscle fibers, leading to more tender cuts, whereas older animals may yield tougher meat due to increased collagen cross-linking and reduced water-holding capacity. The aging process of meat (maturation) further improves tenderness and flavor (3). Meat aged for 3 days retains much of its original structure, with minimal enzymatic breakdown of proteins. However, after 15 days of aging, natural enzymes

break down muscle fibers, improving tenderness, juiciness and flavor. Extended aging allows for the degradation of connective tissue, enhancing the overall meat quality (24). The study aimed to compare and evaluate the quality of carcass and meat of YIM and STR cattle at two slaughter ages (17 and 20 months) in a grazing system with supplementation and two aging times of beef (3 and 15 days) to define quality parameters for the meat industry.

Materials and Methods

Nutritional and animal management was carried out under controlled conditions at the Animal Research Institute of the Semi-Arid Chaco (IIACS), Leales, Tucumán, Argentina (27°11'10.60" S and 65°14'32.45" O) at 335 m a. s. l. This region is subtropical, sub-humid, with a dry season and an average annual rainfall of 880 mm between October and March. The average annual temperature is 19°C, ranging from 25°C in the warmest month to 13°C in the coldest month.

Animals and Treatments

Sixty Braford crossbred yearling males (177 kg ± 12.5 kg body weight, (BW) were divided into two groups: YIM, non-castrated (n=30) and steers (STR), surgically castrated at 9 months of age (n=30). Animals grazed on a pasture plot of 14 ha for each treatment, seeded with Rhodes grass (*Chloris gayana*, cv Fine Cut). Rearing and fattening were under grazing with supplementation, with higher levels of supplementation during fattening. Throughout the experiment, all animals were handled according to age and BW. During rearing, supplementation with corn and soybean expeller was adjusted to achieve an average daily gain (ADG) of 0.6-0.7 kg/animal/d, thus, the ration was modified throughout this period. During fattening, supplementation consisted of 3 kg of whole corn, 2 kg of ground corn and 1 kg of soybean expeller representing 1.5% of BW to achieve an ADG of 1 kg/animal/d. The body condition score (BCS) scale for bovines ranges from 1 (emaciated) to 9 (obese) and is used to evaluate fat reserves. On-farm BW was measured with an electronic scale. The *longissimus thoracis* (LT) muscle area (LTA) and subcutaneous fat thickness (SFT) between the 12^{th} and 13^{th} ribs were recorded 24 h before slaughter, using an Esaote Aquila Vet portable ultrasound scanner. At each slaughter age (17 and 20 months), eight animals from each treatment (n=16) were randomly selected from those that met the pre-established criteria, *i.e.* BCS ≥ 6 and SFT ≥ 5 mm. They were transported to the Forres Beltrán commercial slaughterhouse, Santiago del Estero, 150 km from the IIACS, after a 12 h fasting period with *ad libitum* access to drinking water.

Slaughter and Collection of Meat Samples

Animal handling and husbandry procedures followed guidelines provided by the National Agricultural Technology Institute (INTA), and slaughter procedures complied with regulations established by the National Service of Animal Health (SENASA). Animals were stunned using a captive bolt pistol. Slaughter weights (final BW) were recorded. Carcasses were weighed, classified and graded (conformation and fatness) after slaughter using the Sistema oficial argentino de Tipificación (Secretaría de Agroindustria, Ganadría y Pesca, 2018). Carcass conformation was based on visual assessment of muscle mass development. The conformation score system for Argentina varies from A (excellent) to B, C, D and E (poor). Fat cover, including external and thoracic cavity fat, ranges from 0 (none) to 4 (excessive).

Analytical Methods

Meat samples were transported under refrigeration to the central laboratories of the Instituto de Ciencia y Tecnologia de los Alimentos, Facultad de Agronomia y Agroindustrias, N Universidad Nacional de Santiago del Estero (UNSE). This guaranteed the integrity of samples for subsequent analysis under controlled conditions. Muscle samples were collected within 90 min after slaughter from the left LT muscle between the 8^{th} and 13^{th} ribs and from the complete *semitendinosus* (ST) muscle, according to the method reported by Cañeque and Sañudo (2005). Samples were stored at 12-15°C for 24 h. *The longissimus thoracis* area and SFT were measured with AUTOCAD® and a caliber, respectively. The pH was recorded

at 45 min (pH45), 3 h (pH3), 6 h (pH6) and 24 h (pH24) *postmortem* using a pH meter Van London Phoenix model 557-3512, according to methodologies described in Cañete and Sañudo (2005). Instrumental color was measured with a Minolta CR-300 colorimeter (Cielab L*, a*, b*; Ø 8 mm, Illuminant C, 2° Observer). Water-holding capacity (WHC) was determined in the LT of the 9th rib 48 h *postmortem* as expressible juice, *i.e.*, release of juice from meat during external pressing (40). Tissue composition was estimated following the method reported by Garcia Torres (2005), dissecting the 10th rib into lean, subcutaneous fat, intermuscular fat, bone and other tissues such as blood vessels, ligaments, tendons. The ageing times (3 and 15 days) for each sample were randomized within the same muscle (ribs 8-9th and 11-12th). The matured samples were vacuum-packed and refrigerated at 4°C ± 1°C in the dark and then frozen at -20°C ± 1°C until processing. After thawing in a refrigerator for 24 h, samples were cooked with a press grill Speedy G3 model 1096 (Speedy, Mar del Plata), 220 V, 50 Hz frequency and 3 kW power until reaching an internal temperature of 70°C, following the general guidelines of AMSA (1995). After cooking, steaks were allowed to rest and cool to room temperature for approximately 4 h. Cores (1.27 cm diameter) were removed parallel to the fiber orientation with a hand-held coring device. Eight cores were taken from each LT and ST steak, according to the surface area of each steak. Texture profile analysis (TPA) was performed with a TA-XT Plus model texture analyzer (Texturolab, Mexico City). The texture parameters recorded were hardness, elasticity, gumminess and chewiness.

Statistical Analysis

To evaluate the effects of category, animal age and ageing time of meat on the parameters measured, a comparison of means was carried out through analysis of variance (ANOVA) with a significance level of $\alpha = 0.05$. Statistical analyses were performed with InfoStat statistical software (14). The statistical model included the main effects of category, slaughter age, ageing time and all two-way interactions. When interactions were not significant, they were removed from the model. Results were expressed as mean ± standard deviation (SD).

Results

Carcass Quality

We analyzed the effects of castration and slaughter age on parameters related to carcass quality, such as final BW, carcass yield, LTA and SFT *antemortem* and *postmortem*, tissue composition, and classification and grading of carcasses. Table 1 (page 5), shows the results related to carcass quality. No interaction effects (Category × Age) (p>0.1) were found in any variable evaluated (annex Table 1). The YIM were heavier and showed a larger LTA than STR, which had greater SFT. There was an effect of slaughter age on LTA *postmortem* (p <0.05) and cold carcass weight; however, no effect was found on SFT *postmortem* (p > 0.1).

Classification and Grading

Regarding conformation, at 17 months of age, YIM were typified in 62.5% as C (good), 12.5 % as B (very good) and 25% as A (excellent), while STR were typified in 50% as C and 50 % as B. At 20 months, 50% of YIM were classified as B and 50% as C, while 62.5% of STR were classified as C and 37.5% as B. Regarding fatness, at 17 months of age, 100% of the carcasses of YIM were grade 1, while 75% of the carcasses of STR were grade 1 and 25% were grade 2. Regarding 20 months of age, STR obtained grade 1 in 62.5 % and grade 2 in 37.5 %, while YIM obtained grade 1 in 100 %. However, all carcasses evaluated met the conditions required for special consumption (annex Figure 1).

Tissue Composition

Table 2 (page 5), presents the results of the study on the tissue composition of the 10th rib, where the percentages of different tissue components in both category and slaughter age were determined.

Table 1. Carcass characteristics (mean ± SD) in young intact males (YIM) and steers (STR) at two slaughter ages, 17 and 20 months, in a pastoral system with supplementation.

Tabla 1. Características de la canal (media ± DE) de machos enteros jóvenes (MEJ) y novillos con dos edades de faena, 17 y 20 meses, en sistema pastoril con suplementación.

Item	YIM		STR		*p-value*		
AGE x ca	17 MTH	20 MTH	17 MTH	20 MTH	Age [1]	Category [2]	Age x Category
antemortem							
Body condition score	5.75 ± 0.46	6.38 ± 0.52	6.13 ± 0.64	6 ± 0.45	NS	NS	NS
Final BW (kg)	434.75 ± 28.09	505.25 ± 29.31	400.75 ± 31.54	455.63 ± 19.42	<0.01	<0.001	NS
SFT (mm)	0.58 ± 0.08	0.58 ± 0.05	0.78 ± 0.21	0.95 ± 0.19	NS	<0.05	NS
LTA (cm^2)	67.32 ± 6.26	67.70 ± 8.34	62.51 ± 4.78	67.48 ± 9.02	NS	<0.001	NS
postmortem							
Carcass yield (%)	56.31 ± 1.43	59.89 ± 5.51	56.51 ± 1.34	57.41 ± 3.27	NS	<0.01	NS
Cold carcass weight (kg)	245 ± 20.67	289.5 ± 11.41	226.75 ± 22.51	273.13 ± 30.19	<0.001	<0.05	NS
SFT (mm)	3.20 ± 1.38	3.27 ± 0.61	5.54 ± 2.82	10.25 ± 7.72	NS	<0.01	NS
LTA (cm^2)	75.85 ± 12.46	78.75 ± 0.01	62.62 ± 10.86	77.25 ± 9.68	<0.01	<0.01	NS

[1] effect of slaughter age, 17 or 20 months. / [2] effect of animal category, YIM or STR
NS: Non-Significant. / NS: No Significativo.
[1] efecto de la edad de faena, 17 o 20 meses de edad / [2] efecto de la categoría de animal, MEJ o novillo.

Table 2. Tissue composition of the 10th rib (mean ± SD) of young intact males (YIM) and steers (STR) at two slaughter ages, 17 and 20 months, in a pastoral system with supplementation.

Tabla 2. Composición tisular de la 10ª costilla (media ± DE) de machos enteros jóvenes (MEJ) y novillos con dos edades de faena, 17 y 20 meses, en sistema pastoril con suplementación.

Item	YIM		STR		*p-value*		
	17 MTH	20 MTH	17 MTH	20 MTH	Age [1]	Category [2]	Category x Age
Lean (g)	644.98 ± 223.80	692.58 ± 105.13	464.51 ± 94.40	508.89 ± 131.40	NS	<0.01	NS
Bone (g)	215.54 ± 44.53	200.17 ± 30.07	160.30 ± 31.18	169.92 ± 38.09	NS	<0.01	NS
Subcutaneous fat (g)	56.01 ± 17.26	64.50 ± 37.72	97.02 ± 38.09	87.47 ± 27.98	NS	<0.05	NS
Intermuscular fat (g)	97.29 ± 29.97	95.57 ± 15.92	135.26 ± 58.86	126.99 ± 54.3	NS	<0.05	NS
Others (g)	20.84 ± 10.65	12.45 ± 9.52	19.70 ± 12.87	16.59 ± 11.51	NS	NS	NS
Lean (%)	61.48 ± 5.38	73.25 ± 9.26	53.16 ± 3.93	54.96 ± 10.21	NS	<0.01	NS
Bone (%)	21.11 ± 2.23	21.19 ± 2.58	18.48 ± 2.83	18.73 ± 4.00	<0.05	<0.01	NS
Subcutaneous fat (%)	5.78 ± 2.43	6.9 ± 4.07	10.76 ± 2.78	9.81 ± 3.70	NS	<0.05	NS
Intermuscular fat (%)	9.63 ± 3.14	10.27 ± 2.29	15.25 ± 5.27	14.08 ± 5.93	NS	<0.05	NS
Others (%)	2.00 ± 0.84	1.33 ± 1.02	2.35 ± 1.66	1.79 ± 1.16	NS	<0.05	NS

[1] effect of slaughter age, 17 or 20 months. / [2] effect of animal category, YIM or STR
NS: Non-Significant. / NS: No Significativo.
[1] efecto de la edad de faena, 17 o 20 meses de edad / [2] efecto de la categoría de animal, MEJ o novillo.

YIM had a greater percentage of lean (p <0.05) and a lower percentage of subcutaneous and intermuscular fat, providing a larger amount of meat than that of castrated animals. However, between categories, bone quantity was significantly different (p <0.05). Slaughter age affected the percentage of bone (p <0.05) (annex Table 2).

Variation in muscle-to-fat ratio is important because it influences the proportion of marketable meat in cuts. YIM had a higher percentage of muscle and a lower proportion of subcutaneous and intermuscular fat, resulting in a higher muscle-to-fat ratio than that of castrated animals.

Meat Quality

Table 3 shows the physicochemical parameters (pH, color, WHC) corresponding to LT muscle in both categories and slaughter age.

Table 3. Characteristics of the meat (mean ± SD) of young intact males (YIM) and steers (STR) at two slaughter ages, 17 and 20 months, in a pastoral system with supplementation.

Tabla 3. Características de la carne (media ± DE) de machos enteros jóvenes (MEJ) y novillos con dos edades de faena, 17 y 20 meses, en sistema pastoril con suplementación.

Item	YIM		STR		*p-value*		
	17 MTH	20 MTH	17 MTH	20 MTH	Age[1]	Category[2]	Category x Age
pH 45 min	7.15 ± 0.23	6.68 ± 0.25	7.15 ± 0.16	6.67 ± 0.31	<0.01	NS	NS
pH 3 h	6.76 ± 0.30	6.04 ± 0.38	6.75 ± 0.18	6.30 ± 0.35	<0.01	NS	NS
pH 6 h	6.49 ± 0.23	5.92 ± 0.23	6.56 ± 0.13	5.99 ± 0.28	<0.01	NS	NS
pH 24 h	5.71 ± 0.21	5.85 ± 0.08	5.65 ± 0.22	5.76 ± 0.10	<0.05	NS	NS
Lightness (L*)	46.62 ± 1.54	46.93 ±1.69	45.72 ± 1.11	46.12 ± 0.87	NS	NS	NS
Redness (a*)	14.24 ± 0.86	14.91 ± 1.40	13.94 ± 0.96	15.05 ± 0.89	<0.05	NS	NS
Yellowness (b*)	2.55 ± 0.45	3.18 ± 0.74	3.33 ± 0.74	3.51 ± 0.73	NS	<0.05	NS
WHC (%)	49.25 ± 17.40	51.38 ± 13.75	54.50 ± 14.41	51.63 ± 14.5	NS	NS	NS

[1] effect of slaughter age, 17 or 20 months. / [2] effect of animal category, YIM or STR

NS: Non-Significant. / NS: No Significativo.

[1] efecto de la edad de faena, 17 o 20 meses de edad / [2] efecto de la categoría de animal, MEJ o novillo.

In this study, significant differences (p <0.05) were found for pH at 45 min, 3 h, 6 h and 24 h between the two slaughter ages, but not between animal categories (YIM and STR) (annex Figure 2). As shown in table 3, the effect of category on meat color fell in the blue-yellow coordinate b*. The meat of 20-month-old animals was redder than that of 17-month-old animals. No differences were observed due to the factors studied in the other parameters evaluated (L* and WHC) (annex Table 3).

Texture of Meat

Meat TPA corresponding to LT and ST muscles in both categories and slaughter age are presented in table 4 (page 7).

Table 4. Texture parameters (mean ± SD) in *Longissimus Thoracis* (LT) and *Semitendinosus* (ST) muscles, aged 3 and 15 days, of young intact males (YIM) and steers (STR) at two slaughter ages, 17 and 20 months, in a pastoral system with supplementation.

Tabla 4. Parámetros de textura (media ± DE) de los músculos *Longissimus thoracis* (LT) y *Semitendinosus* (ST), madurados 3 y 15 días, de machos enteros jóvenes (MEJ) y novillos con dos edades de faena, 17 y 20 meses, en sistema pastoril con suplementación.

YIM				
	17 MTH		20 MTH	
LT	**A3**	**A15**	**A3**	**A15**
Hardness (N)	45.83 ±16.22	34.48 ± 16.99	37.01 ± 12.5	30.95 ± 14.56
Elasticity	0.40 ± 0.08	0.37 ± 0.07	0.32 ± 0.07	0.32 ± 0.06
Gumminess (N)	19.18 ± 7.00	14.03 ± 7.11	17.29 ± 5,54	13.19 ± 5.77
Chewiness (N)	7.76 ± 3.37	5.59 ± 3.59	5.84 ± 2.77	4.53 ± 2.97
ST	**A3**	**A15**	**A3**	**A15**
Hardness (N)	58.31 ± 9.56	40.35 ± 8.61	56.26 ± 17.56	38.80 ± 17.61
Elasticity	0.44 ± 0.04	0.43 ± 0.04	0.40 ± 0.06	0.35 ± 0.07
Gumminess (N)	26.9 ± 5.07	19.23 ± 4.35	24.54 ± 6.8	18.35 ± 7.82
Chewiness (N)	12.02 ± 3.03	8.40 ± 2.17	10.28 ± 3.8	6.83 ± 3.83

STR				*p-value*		
17 MTH		20 MTH				
A3	**A15**	**A3**	**A15**	**Category [2]**	**Age [1]**	**Ageing [3]**
37.89 ± 14.49	26.21 ± 15.63	27.48 ± 12.4	28.82 ± 5.24	NS	NS	NS
0.39 ± 0.05	0.34 ± 0.07	0.28 ± 0.05	0.31 ± 0.03	NS	<0.05	NS
14.86 ± 5.46	14.00 ± 5.07	15.31 ± 4.37	12.71 ± 2.03	NS	NS	NS
6.03 ± 1.70	5.34 ± 0.55	4.47 ± 0.20	3.96 ± 0.84	NS	NS	NS
A3	**A15**	**A3**	**A15**	**Category**	**Age**	**Ageing**
44.05 ± 17.30	37.89 ± 18.91	58.62 ± 8.69	49.09 ± 13.18	NS	NS	<0.01
0.39 ± 0.08	0.41 ± 0.1	0.42 ± 0.04	0.43 ±0.05	NS	NS	NS
19.95 ± 6.78	19.43 ± 8.27	23.78 ± 5.84	22.33 ± 6.74	NS	NS	<0.05
8.17 ± 4.22	8.62 ± 5.34	10.13 ± 2.9	9.87 ± 3.71	NS	NS	NS

The hardness and elasticity of ST muscle showed an interaction between slaughter age and category. Significant differences (p <0.05) were found in the elasticity of LT muscle between the two ages of slaughter, but not between animal categories (YIM and STR). Meat elasticity decreased with increasing animal age. Significant differences (p <0.05) were also found in hardness and gumminess of ST muscle between ageing time of 3 and 15 days, concluding that as ageing progressed, meat became less hard and gummy.

Discussion

The effect of castration on the quality parameters of carcass and meat agrees with previous studies in terms of the advantages shown by the YIM category in the products it generates (carcass and meat), which do not generally differ from those obtained from the STR category.

Carcass weight, BW, yield, LTA, SFT

Significant differences (p <0.05) were observed in the final BW and carcass yield between YIM and STR (table 1, page 5). Our results are consistent with previous research showing that YIM produces heavier carcasses than those of steers (23, 25, 28). While carcass yield differed notably between the two categories, no variation was found in slaughter age (table 1, page 5). Galo González *et al.* (2012) reported no significant difference in the dressing percentage between intact and castrated males in feedlots (average 51.3%). However, in our pastoral system, the percentages of carcass yield ranged from 56% to 60%, consistent with previous findings (10). Additionally, YIM under two feeding systems (pasture and stabled) exhibited similar dressing percentages, while YIM produced 1% more leg yield than steers (6).

Classification and Grading

YIM showed better scores in conformation and fatness, mainly in the second slaughter (20 months). Our results agree with those reported by other authors (1, 31), where the dressing percentage of YIM was very high, and the conformation of the carcass was excellent. In the European grading system (S-EUROP), Piedmontese carcasses are positioned within the acronyms S and E, with scores equivalent to those reported in our study, *i.e.*, type A for YIM. In other studies (9, 10) involving YIM slaughtered at 21 months and fed with two different diets, animals obtained grade 1 covering fat and were classified in category "V" including young steers, steers, heifers and young cows, consistent with our findings. French *et al.* (2000) found similar values of dressing percentage and fat thickness in steers fed on pasture supplemented with concentrates and slaughtered at the same age.

Tissue Composition

The superiority of YIM carcass over that of STR in the proportion of lean tissue should be considered across different segments of the beef chain, even though YIM produce carcasses with higher cut dressing but lower fat content. The values reported for this parameter agree with those found by Cuvelier *et al.* (2006) in the YIM of Limousin, Aberdeen Angus and Belgian Blue breeds fed with concentrates. Results reported by Blanco *et al.* (2010) who worked on grass-based fattening systems and concentrates also showed similarity. Seideman *et al.* (1982) obtained results similar to those found in this study linked to the subcutaneous and intermuscular fat content of both categories. Marcondes *et al.* (2012) developed prediction equations based on the dissection of the 10th rib of Nelore and Guzerah YIM of 20-24 months of age compared with STR. Their results confirmed higher lean values and lower fat values due to sex, in agreement with the findings in our work.

Instrumental Quality of Meat

pH

The present study did not show effects of castration on pH values. However, no positive effects of the slaughter age were noted, which could be attributed to different events with different transport and handling conditions. Consistent with this study, several authors (5, 13, 33) reported similar pH values in YIM fed in a stable. On the other hand, Marti *et al.* (2010) found higher final pH values in YIM than in castrated animals, attributing this difference to the greater susceptibility of intact animals to stress and to the mounting activity of bulls. This explains why bulls have higher pH values and darker meat than steers (24). Marino *et al.* (2005) and Mounier *et al.* (2006) studied the final pH of YIM meat in the handling and waiting time before slaughter. They observed that high pH levels are associated with handling, travel duration and lairage time at the slaughter plant. In the present work, the effect of slaughter age on meat pH was observed. However, these values

were within the normal range for bovine meat. It is concluded that correcting management methods, such as composition of YIM social groups and lairage times, can help achieve normal ultimate pH values.

Color

In this study, we found effects of slaughter age on redness (a*), with meat appearing redder in older animals than in younger ones. Additionally, there was an effect of category on yellowness (b*), with lower values observed in YIM than in STR. In agreement with our study, Sanchez *et al.* (2005) cited values for parameter a* in young Nelore bulls (14.62 ± 0.66) similar to those of YIM in our study (14.24 ± 0.86). Likewise, other studies (13, 34) reported similar values for lightness (L*) and redness (a*) in beef from young bulls. The results of our study are generally consistent with those of several authors who found no differences between categories (33, 42). Yet, previous studies (11, 49) reported that STR meat was redder (a*) and lighter (L*) than YIM meat. Similarly, Picallo *et al.* (2012) reported that YIM meat was less clear (L*) and showed lower a* and b* values than STR meat. It is generally accepted that castrated animals have lighter flesh color than intact males (46) due to greater aerobic muscular activity (27).

WHC

WHC showed no effect of castration or slaughter age, in agreement with the findings of several authors (44, 49). However, Crews *et al.* (2003) observed lower WHC values for YIM than for STR. Despite this, the WHC values found in our study exceeded those reported by Sanchez *et al.* (2005) who identified values of 25.8 % to 27 % for Nelore and Rubia Gallega young bulls, respectively. Similarly, by Guerrero *et al.* (2011), who worked with Gasconne YIM under semi-intensive and extensive productive systems, reported WHC values of 23.5% and 21.4%, respectively.

Instrumental Texture of Meat

The TPA presented in table 4 (page 7), shows an effect (p <0.05) of slaughter age on the elasticity of LT muscle, but not on category. In ST muscle, an interaction category x slaughter age was observed (p <0.05) for hardness and elasticity (annex Table 4). Regarding the hardness and gumminess of ST muscle, only the effect of ageing time was found. In agreement with our study, several authors (16, 42, 44, 48) found no differences in meat tenderness between YIM and other categories, such as cows and STR. However, Steen *et al.* (2003) observed higher values of compression parameters for YIM than for STR. Relatively, few studies performed TPA in both categories, as much of the literature reports results of the resistance to cutting stress measured through Warner Bratzler shear force (WBSF) (41, 48). In cooked meat, hardness was better predicted by the TPA method than by the WB method (R^2 = 0.23, p <0.008 and R^2 = 0.09, p <0.04, respectively) (43).

Conclusions

YIM achieved higher final BW and lower SFT levels than STR under the system of this study. In terms of the meat quality parameters evaluated, YIM presented a similar quality to that of STR, positioning the YIM category as a high-quality product for the beef industry. This could potentially lead to a shift in management practices on a production scale, avoiding unnecessary animal castration (a practice questioned by Animal Welfare standards) under the premise that they produce better-quality meat. Note the significant differences in SFT, with STR showing significantly higher levels in the second age of slaughter, while in YIM, it did not vary significantly between the first and second slaughter age. Muscle color showed differences in redness (a*) between the two slaughter ages and yellowness (b*) between animal categories. Note the interaction category x slaughter age for hardness and elasticity in ST muscle. This category should be further studied under different feeding systems to determine how they influence the yield and quality of each cut, providing insights into the improvement of meat production.

Supplemmentary Material

https://drive.google.com/file/d/13I5vx-OsN14U8wXH44UCifxiNUUlLJk-/view?usp=sharing

References

1. Albertí, P.; Lahoz, F.; Tena, R.; Jaime, S.; Sañudo, C.; Olleta, J. L.; Campo, M. M.; Panea, B.; Pardos, J. J. 2001. Producción y rendimiento carnicero de siete razas bovinas españolas faenadas a distintos pesos. Informaciones Técnicas. 101: 1-16.
2. AMSA. 1995. Research guidelines for cookery, sensory evaluation and instrumental tenderness measurements of fresh meat. American Meat Science Association. Chicago. IL.
3. Bautista-Martínez, Y.; Granados-Rivera, L. D.; Jimenez-Ocampo, R.; Maldonado-Jáquez, J. A. 2024. Morphostructural composition and meat quality in local goat kids from the northeastern region of Mexico. Revista de la Facultad de Ciencias Agrarias. Universidad Nacional de Cuyo. Mendoza. Argentina. 56(1): 127-137. DOI: https://doi.org/10.48162/rev.39.129
4. Benedetto, A.; Pezzolato, M.; Biasibetti, E.; & Bozzetta, E. 2021. Omics applications in the fight against abuse of anabolic substances in cattle: challenges, perspectives and opportunities. Current Opinion in Food Science. 40: 112-120. doi: 10.1016/j.cofs.2021.03.001
5. Blanco, M.; Casasús, I.; Ripoll, G.; Panea, B.; Albertí, P.; Joy, M. 2010. Lucerne grazing compared with concentrate-feeding slightly modifies carcass and meat quality of young bulls. Meat Science. 84: 545-552. doi.org/10.1016/j.meatsci.2009.10.010
6. Brännäng, E. 1971. Studies on monozigous cattle twins XVIII. The effect of castration and age of castration on the development of single muscles, bones and special sex characters. Part II. Swedish Journal of Agricultural Research. 1: 69-78.
7. Cámara de la Industria y Comercio de Carnes y Derivados de la República Argentina (CICCRA). 2023. Informe 279b. https://ciccra.com.ar/(Date of consultation 27/09/2023).
8. Cañeque, V.; Sañudo, C. 2005. Estandarización de las metodologías para evaluar la calidad del producto (animal vivo, canal, carne y grasa) en los rumiantes. Monografías INIA. Serie Ganadera. 3: 216-225.
9. Catrileo, A. S.; Rojas, C. G. 2012. A beef production system from dairy bulls under pasture in the south of Chile. Chilean Journal of Agricultural and Animal Science. 28(1): 41-50.
10. Catrileo, A.; Morales, R.; Rojas, C.; Cancino, D. 2014. Beef production from dairy bulls under two different production systems and its effect on the fatty acid profile and beef quality. Chilean Journal of Agricultural Research. 74(3): 366–370. doi:10.4067/S0718-58392014000300017
11. Cervieri, V.; Cossu, M. E.; Castro, L. 2012. Características cualitativas del macho entero joven. Revista Argentina de Producción Animal. 32(Supl.1): 223-263.
12. Crews Jr, D. H.; Pollak, E. J.; Weaber, R. L.; Quaas, R. L.; Lipsey, R. J. 2003. Genetic parameters for carcass traits and their live animal indicators in Simmental cattle. Journal of Animal Science. 81(6): 1427-1433. doi.org/10.2527/2003.8161427x
13. Cuvelier, C.; Clinquart, A.; Hocquette, J. F.; Cabaraux, J. F.; Dusfrasne, I.; Istasse, L.; Hornick, J. L. 2006. Comparison of composition and quality traits of meat from young finishing bulls from Belgian Blue, Limousin and Aberdeen Angus breeds. Meat Science. 74: 522-531. doi.org/10.1016/j.meatsci.2006.04.032
14. Dieguez Cameroni, F.; Hornick, J. L.; Cabaraux, J. F.; Istasse, L.; Dufrasne, I. 2006. Less intensified grazing management with growing fattening bulls. Animal Research. 55: 105-120. doi: 10.1051/animres:2006007
15. Di Rienzo, J. A.; Casanoves, F.; Balzarini, M. G.; Gonzalez, L.; Tablada, M.; Robledo, C. W. InfoStat versión 2020. Centro de Transferencia InfoStat. FCA. Universidad Nacional de Córdoba. (Date of consultation 21/04/23).
16. Dransfield, E.; Martin, J. F.; Bauchart, D.; Abouelkaram, S.; Lepetit, J.; Culioli, J.; Jurie, C.; Picard, B. 2003. Meat quality and composition of three muscles from French cull cows and young bulls. Animal Science. 76(3): 387-399. doi:10.1017/S1357729800058616
17. Finneran, E.; Crosson, P.; O'Kiely, P.; Shalloo, L.; Forristal, D.; Wallace, M. 2011. Stochastic modelling of the yield and input price risk affecting home produced ruminant feed cost. Journal of Agricultural Science. 150: 123-139. doi:10.1017/S002185961100061X
18. French, P.; O'Riordan, E. G.; Monahan, F. J.; Caffrey, P. J.; Vidal, M.; Mooney, M. T.; Troy, D. J.; Moloney, A. P. 2000. Meat quality of steers finished on autumn grass, grass silage or concentrate-based diets. Meat Science. 56(2): 173-180. doi.org/10.1016/S0309-1740(00)00037-1
19. Galo González, P. A.; Paniagua Alcaraz, P. L.; Ocampos Olmedo, D. A.; Dueck, J.; González Balbuena, J. M. 2012. Desempeño productivo de bovinos macho enteros y castrados en un sistema de engorde a corral en el Departamento de Boquerón-Chaco Central. Investigación Agraria. 14(2): 101-106.
20. García-Torres, M.; Espejo, M.; López Parra, M.; Izquierdo, J. A.; Mendizábal, M., Purroy, A. 2005. Conformación, engrasamiento y sistemas de clasificación de la canal bovina. En; Estandarización de las metodologías para evaluar la calidad del producto (animal vivo, canal, carne y grasa) en los rumiantes. INIA. Serie Ganadera 3: 243-250.

21. Gregoretti, G.; Baudracco, J.; Dimundo, C.; Lazzarini, B.; Scarel, J.; Alesso, A.; Machado, C. 2024. Traditional cow-calf systems of the northern region of Santa Fe, Argentina: current situation and improvement opportunities. Revista de la Facultad de Ciencias Agrarias. Universidad Nacional de Cuyo. Mendoza. Argentina. 56(1): 106-116. DOI: https://doi.org/10.48162/rev.39.127
22. Guerrero, A.; Alberti, P.; Sañudo, C.; Campo, M. M.; Olleta, J. L.; Panea, B.; Ripoll, G.; Monge, P.; Santolaria, P. 2011. Efecto del sistema de producción previo al cebo sobre la calidad instrumental de la carne de vacuno. Asociación Interprofesional para el Desarrollo Agrario XIV Jornadas de Producción Animal, Tomo II: 661-663.
23. Jones, S. D. M.; Price, M. A.; Berg, R. T.; Hardin, R. T. 1981. The influence of dietary roughage level on efficiency of growth and muscle deposition in bulls and steers. Canadian Journal of Animal Science. 61(2): 369-374. doi.org/10.4141/cjas81-045
24. Katz, L. S. 2007. Sexual behavior of domesticated ruminants. Hormones and Behavior. 52: 56-63. doi.org/10.1016/j.yhbeh.2007.03.012
25. Knight, T. W.; Cosgrove, G. P.; Death, A. F.; Anderson, C. B. 2010. Effect of age of pre- and post-pubertal castration of bulls on growth rates and carcass quality. New Zealand Journal of Agricultural Research. 43: 585-588. doi.org/10.1080/00288233.2000.9513455
26. Koohmaraie, M., & Geesink, G. H. 2006. Contribution of postmortem muscle biochemistry to the delivery of consistent meat quality with particular focus on the calpain system. Meat science. 74(1): 34-43. doi.org/10.1016/j.meatsci.2006.04.025
27. Lawrie, R. A.; Ledward, D. A. 2006. Chemical and biochemical constitution of muscle. In R. A. Lawrie & D. A. Ledward (Eds.). Lawrie's Meat Science. Washington, DC. Woodhead Publishing. (p. 105). doi.org/10.1533/9781845691615.75
28. Maggioni, D.; Arques, J. A.; Rotta, P. P.; Perotto, D.; Ducatti, T.; Visentainer, J. V.; Prado, I. N. 2010. Animal performance and meat quality of crossbred young bulls. Livestock Science. 127: 176-182. doi.org/10.1016/j.livsci.2009.09.006
29. Maldonado-Jáquez, J. A.; Torres-Hernández, G.; Hernández-Mendo, O.; Gallegos-Sánchez, J.; Mora-Flores, J. S.; Granados-Rivera, L. D. 2025. Long-term Supplementation Affects the Production, Composition and Lactation Curve of Local Grazing Goats. Revista de la Facultad de Ciencias Agrarias. Universidad Nacional de Cuyo. Mendoza. Argentina. 57(2): 155-164. DOI: https://doi.org/10.48162/rev.39.179
30. Marcondes, M. I.; Tedeschi, L. O.; Valadares Filho, S. C.; Chizzotti, M. L. 2012. Prediction of physical and chemical body compositions of purebred and crossbred Nellore cattle using the composition of a rib section. Journal of Animal Science. 90: 1280-1290. doi: 10.2527/jas.2011-3839
31. Marino, R.; Albenzio, M.; Girolami, A.; Muscio, A.; Sevi, A.; Braghieri, A. 2006. Effect of forage to concentrate ratio on growth performance, and on carcass and meat quality of Podolian young bulls. Meat Science. 72(3): 415-424. doi.org/10.1016/j.meatsci.2005.08.007
32. Marti, S.; Velarde, A.; de la Torre, J. L.; Bach, A.; Aris, A; Serrano, A.; Manteca, X.; Devant, M. 2010. Effects of ring castration with local anesthesia and analgesia in Holstein calves at 3 months of age on welfare indicators. Journal of Animal Science. 88: 2789-2796. doi:10.2527/jas.2009-2408
33. Mohan Raj, A. B.; Moss, B, W.; Rice, D. A.; Kilpatrick, D. J.; McCaughey, W. J.; Mc Lauchlan, W. 1992. Effect of mixing male types of cattle on their meat quality and steers related parameters. Meat Science. 32: 367-386. doi.org/10.1016/0309-1740(92)90079-J
34. Moloney, A. P.; Wilson, S. S.; Siphambili, S.; Moran, L.; O'Riordan, E. G.; O'Sullivan, M.G.; Kerry, J. P.; Monahan, F. J.; McGee, M. 2022. The Colour, Composition and Eating Quality of Beef from Late-or Early-Maturing Suckler Bulls Finished at Pasture with or without Concentrate Supplementation. Animals. 12(18): 2417. doi.org/10.3390/ ani12182417
35. Mounier, L.; Dubroeucq, H.; Veissier, I.; Andanson, S. 2006. Variations in meat pH of beef bulls in relation to conditions of transfer to slaughter and previous history of the animals. Journal of Animal Science. 84: 1567-1576. doi: 10.2527/2006.8461567x
36. OCDE/FAO. 2020–2029. Perspectivas Agrícolas. Estadísticas de la OCDE sobre a JA Di. https://openknowledge.fao.org/server/api/core/bitstreams/a7323b78-3837-4081-8745-e13968511c1c/content (Date of consultation 24/3/2024).
37. O'Riordan, E. G.; O'Kiely, P. 1996. Potential of beef production systems based on grass. Irish Grassland and Animal Production Association Journal. 30: 185–217. https://www.cabidigitallibrary.org/doi/full/10.5555/19970710420
38. O'Riordan, E. G.; Crosson, P.; McGee, M. 2011. Finishing male cattle from the beef suckler herd. Irish Grassland and Animal Production Association Journal. 45: 131-146. https://www.irishgrassland.com/docs/Journal%202011.compressed.pdf
39. Picallo, A.; Cossu, M. E.; Fernández Madero, J.; Grigera Naon, J.; Schor, A.; Rozen, F.; Gambetti, P.; Lamanna, M. L.; Colombatto, D.; Von Bernard, H.; Coste, B.; Moisá, S. 2012. Beef quality young bulls *vs* castrated from the northwest Argentina productive area. 35º Congreso Argentino de Producción Animal.
40. Pla, T. M. 2005. Capacidad de retención de agua. En Cañeque, V.; Sañudo, C. (Eds.). Estandarización de las metodologías para evaluar la calidad del producto (animal vivo, canal, carne y grasa) en los rumiantes. INIA. Serie Ganadera 3: 243-250.

41. Prado, R. M.; Prado, I. N.; Marques, J. A.; Rotta, P. P.; Visentainer, J. V.; Silva, R. R.; Souza, N. E. 2009. Meat quality of the Longissimus muscle of bulls and steers (½ Nellore *vs*. ½ Simmental) finished in feedlot. Journal of Animal and Feed Science. 18: 221-230. doi.org/10.22358/jafs/66386/2009
42. Ruiz de Huidobro, F.; Miguel, E.; Onega, E.; Blazquez, B. 2003. Changes in meat quality characteristics of bovine meat during the first 6 days' postmortem. Meat Science. 65: 1439-1446. doi.org/10.1016/S0309-1740(03)00068-8
43. Ruiz de Huidobro, F.; Miguel, E.; Blazquez, M.; Onega, E. 2005. A comparison between two methods (Warner-Bratzler and texture profile analysis) for testing either raw meat or cooked meat. Meat Science. 69(3): 527-536. doi: 10.1016/j.meatsci.2004.09.008
44. Sánchez, L.; Carballo, J. A. Sanchez, B. Monserrat, L. 2005. Características de la canal y de la carne de machos procedentes de la cruza de Rubia Gallega con Nelore. Archivos de Zootecnia. 54(206-207): 485-489.
45. Secretaría de Agricultura, Ganadería y Pesca. 2018. Normas de tipificación de carnes en Argentina. https://www.argentina.gob.ar/agricultura/tipificacion.carneshttps://www.magyp.gob.ar/sitio/areas/tipificacion. (Date of consultation 03/03/2024).
46. Seideman, S. C.; Cross, H. R.; Oltjen, R. R.; Schanbacher, B. D. 1982. Utilization of the intact male for red meat production: a review. Journal of Animal Science. 55(4): 826-840. doi.org/10.2527/ jas1982.554826x
47. Steen, R. W. J.; Lavery, N. P.; Kilpatrick, D. J.; Porter, M. G. 2003. Effects of pasture and high-concentrate diets on the performance of beef cattle, carcass composition at equal growth rates, and the fatty acid composition of beef. New Zealand Journal of Agricultural Research. 46(2): 69-81. doi=10.1080/00288233.2003.9513533
48. Vásquez, R. E.; Ballesteros, H. H.; Muñoz, C. A. 2007. Factores asociados con la calidad de la carne. I Parte: la terneza de la carne bovina en 40 empresas ganaderas de la Región Caribe y el Magdalena Medio. Revista Corpoica-Ciencia y Tecnología Agropecuaria. 8(2): 60-65.
49. Zea Salgueiro, J.; Díaz Díaz, M. D.; Carballo Santaolalla, J. A. 2007. El efecto del sistema de producción y del sexo en la calidad de la carne de vacuno joven. Archivos de Zootecnia. 56(216): 817-828.

Enterococcus gallinarum CRL 1826 as a Probiotic for Ranaculture: *in vitro* Safety, Technological, and Physiological Properties

Enterococcus gallinarum CRL 1826 como probiótico para ranicultura: seguridad *in vitro*, propiedades tecnológicas y fisiológicas

María Andreína Acevedo [1], María Claudia Otero [1], María Constanza Lizárraga [2], Cesar Emmnuel Ale [1], Ricardo Javier Llanos [2], María Elena Nader-Macías [3], Sergio Pasteris [1*]

Originales: *Recepción:* 17/09/2024 - *Aceptación:* 12/12/2024

ABSTRACT

This study aimed to progress in designing a probiotic containing autochthonous *Enterococcus gallinarum* CRL 1826 for application during the life cycle of *Lithobates catesbeianus* in hatchery conditions. We assessed bacterial resistance to chemotherapeutics used in ranaculture, the presence of genes encoding virulence factors (VF) and vancomycin resistance, and bacterial survival and maintenance of beneficial properties after freeze-drying and storage. The strain exhibited resistance to antiseptics, sensitivity to most chemotherapeutics, presence of *vanC*, and absence of VF genes. It demonstrated resistance to freeze-drying and the highest survival when using skim milk+sucrose and storage at 4°C for 24 months. It also displayed bacteriocin activity against *Listeria monocytogenes*. Pre-lyophilized and lyophilized cultures grew/resisted individual gastrointestinal conditions and simulated gastrointestinal digestion, keeping bacteriocin activity and surface properties. For the first time, we demonstrated that *E. gallinarum* CRL 1826 is a safe bacterium with technological and physiological properties that would allow bullfrog gut colonization. These studies are essential for progressing towards selecting *E. gallinarum* CRL 1826 as a probiotic to prevent epizootics during bullfrog breeding and control foodborne bacteria, potentially improving growth performance of *L. catesbeianus*.

Keywords
Enterococcus gallinarum • safety characteristics • lyophilization • probiotics for aquaculture • bullfrog

https://doi.org/10.48162/rev.39.201

1 Instituto Superior de Investigaciones Biológicas (INSIBIO-CONICET). Chacabuco 461. T4000ILI. San Miguel de Tucumán. Argentina.
* sergio.pasteris@fbqf.unt.edu.ar
2 Universidad Nacional de Tucumán. Facultad de Bioquímica, Química y Farmacia. Instituto de Biología "Dr. Francisco D. Barbieri". Chacabuco 461. T4000ILI. San Miguel de Tucumán. Argentina.
3 Centro de Referencia para Lactobacilos (CERELA-CONICET). Chacabuco 145. T4000ILC. San Miguel de Tucumán. Argentina.

Licenses Creative Commons Attribution - Non Commercial - Share Alike

Resumen

En este estudio se avanzó en el diseño de un probiótico con *Enterococcus gallinarum* CRL 1826, autóctono de *Lithobates catesbeianus*, para su aplicación durante el ciclo de vida de este anfibio en criaderos. Evaluamos: resistencia bacteriana a quimioterapéuticos utilizados en ranicultura, presencia de genes que codifican para factores de virulencia (FV) y resistencia a vancomicina, y sobrevida y mantenimiento de propiedades benéficas luego de la liofilización y almacenamiento. La cepa fue resistente a antisépticos, sensible a la mayoría de los quimioterapéuticos, posee el gen *vanC* y ausencia de genes de FV. Resistió la liofilización, con la mayor sobrevida con leche descremada+sacarosa durante su almacenamiento a 4°C, 24 meses. También presentó actividad bacteriocina frente *Listeria monocytogenes*. Los cultivos pre-liofilizados y liofilizados crecieron/resistieron en las condiciones individuales y luego de la digestión gastrointestinal simulada, manteniendo la actividad bactericiona y propiedades de superficie. Por primera vez, demostramos que *E. gallinarum* CRL 1826 es una bacteria segura con propiedades tecnológicas y fisiológicas que le permitirían colonizar el intestino de rana toro. Estos estudios permiten avanzar en la selección de *E. gallinarum* CRL 1826 como probiótico para prevenir epizootias durante la cría de rana toro, controlar bacterias transmitidas por alimentos y, potencialmente, mejorar el rendimiento de crecimiento de *L. catesbeianus*.

Palabras clave

Enterococcus gallinarum • características de seguridad • liofilización • probióticos para acuicultura • rana toro

Introduction

In aquaculture, ranaculture is committed to amphibian breeding. Over recent decades, ranaculture has experienced significant growth, driven by conservation efforts (46) and commercial interests.

The American bullfrog (*Lithobates catesbeianus*) provides meat for human consumption and various by-products such as gut, liver, adipose tissue oil, and carcasses (50). Additionally, *L. catesbeianus* is reared in captivity to obtain skin for the pharmaceutical industry as a source of biologically active molecules including biogenic amines, hormones (54), anti-tumor agents, antimicrobials, and antioxidants (22, 51).

Profitability of amphibian hatcheries is linked to animal health status, as demonstrated in other aquaculture activities (17). The microbiome includes the microbiota, microbial metabolites, and genetic elements (3), exerting physiological functions for the host, including maintenance of ecological equilibrium, immunological modulation, and infectious disease prevention (18). However, in intensive breeding systems like bullfrog production, with high animal densities and consequent crowded conditions, the microbiome may undergo modifications favoring epizootics caused by pathogens or potential pathogens that usually belong to native microbiota (31, 35, 36).

The Red-Leg Syndrome (RLS) represents a major infectious disease affecting bullfrog hatcheries, resulting in high mortality and significant economic losses (11). The RLS-related pathogens include *Aeromonas hydrophila*, *Citrobacter freundii*, *Pseudomonas aeruginosa*, and *Proteus vulgaris*, entering the host via the gastrointestinal tract or skin, and affecting the animals at different ages (55). Therapeutic and preventive measures often involve using antiseptics and antibiotics (19, 52). However, these procedures can affect native microbiota and contribute to antibiotic resistance (52). Consequently, a novel alternative introduces the application of probiotics to restore the microbiome (18).

Our research group has investigated the microbial population of bullfrog hatcheries, revealing that lactic acid bacteria (LAB) and RLS-related pathogens are part of the native microbiota of animals and hatchery environments (31, 35, 36). Among LAB, *Lactococcus lactis* CRL 1584, CRL 1827, *Lactiplantibacillus plantarum* CRL 1606, and *Enterococcus gallinarum* CRL 1826 were preselected as potential probiotics for ranaculture (31, 33, 36, 37, 38).

However, *E. gallinarum* CRL 1826 emerged as a promising strain with antimicrobial activity against native RLS-related pathogens and *Listeria monocytogenes* (responsible for bullfrog meat spoilage), adhesion and colonization properties (31, 34), and *in vivo* safety when administered to bullfrog embryos (38). Nevertheless, additional studies are needed to fully validate the hypothesis that *E. gallinarum* CRL 1826 exhibits suitable properties as a probiotic for bullfrog breeding.

This study aimed to assess the *in vitro* safety profile to chemotherapeutics used in bullfrog farms, the presence of virulence factors and antibiotic-encoding genes, and the bacterial resistance and maintenance of beneficial properties after freeze-drying, storage, and exposure to gastrointestinal conditions.

Materials and Methods

Bacterial Strains and Culture Conditions

Enterococcus gallinarum CRL 1826 was isolated from healthy *L. catesbeianus* and identified by phenotypic and genotypic approaches (31). The LAB strain was grown on de Man, Rogosa & Sharpe (MRS) broth pH 6.8 (10 h at 37°C) in microaerophilia. *Pseudomonas aeruginosa* 1007 and 1047, and *C. freundii* CFb (RLS-related pathogens from ranaculture) were grown in nutritive broth pH 6.9 for 7 h, while *L. monocytogenes* Scott A was grown in BHI broth, pH 7.4 for 6 h (29, 34). All cultures were incubated at 37°C in microaerophilia. Bacterial strains were stored at -20°C in their specific growth media supplemented with 20% (v/v) glycerol.

Chemotherapeutics Resistance of Native Microorganisms from Bullfrog Hatcheries

Vancomycin resistance of *E. gallinarum* CRL 1826 was determined via the methodology proposed by "Clinical and Laboratory Standards Institute" (CLSI) (2015). The strain was grown in MRS broth (10 h at 37°C) and adjusted to an OD_{625nm} of 0.08-0.10, corresponding with 0.5 of McFarland scale (0.5% $BaSO_4$). Bacterial suspensions were seeded by spread on Müeller Hinton (MH) agar discs containing 30 µg vancomycin (Britania Laboratories, Argentina). The plates were incubated for 24 h at 37°C. Vancomycin susceptibility was determined by considering breakpoint values proposed by CLSI (2022). The MIC for vancomycin and other antibiotics (Amikacin, Ceftazidime, Ciprofloxacin, Chloramphenicol, Oxytetracycline, Penicillin), and Metronidazole (Britania Laboratories, Argentina) frequently applied in bullfrog hatcheries, was also determined via agar dilution method. Thus, antibiotic solutions were prepared to final concentrations in MH plates from 0.25 to 512 µg/mL. In each plate, 10^4 CFU/mL of the strain were inoculated and incubated at 37°C for 24 h. Susceptibility determination considered breakpoint values (8, 20, 48). Finally, we evaluated the MIC of *P. aeruginosa* strains, *C. freundii*, and *L. monocytogenes* to antiseptics (methylene blue, malachite green, benzalkonium chloride, $CuSO_4$, $KMnO_4$) commonly used in ranaculture (4). Final antiseptic concentrations in MH plates ranged from 0.25 to 16,384 µg/mL. Later, indicator strains were inoculated and incubated as previously indicated. The MIC was defined as the lowest antiseptic concentration completely inhibiting growth of the tested microorganisms.

Vancomycin Resistance and Virulence Factors Genes in *E. gallinarum* CRL 1826

For DNA isolation, cells from a 10 h culture of *E. gallinarum* on MRS broth were harvested (3,000 x *g*, 10 min, at 4°C), washed with TE buffer (10 mM Tris-HCl pH 8, 10 mM EDTA pH 8), and processed according to Pospiech and Neumann (1995). The polymerase chain reaction (PCR) technique amplified genes encoding vancomycin resistance (*vanA*, *vanB*, and *vanC*) and those for virulence factors (*agg*, *gelE*, *esp*, *efa*, and *cylA*) in *E. gallinarum* CRL 1826. Primers and PCR conditions are described in Supplementary Table S.1. The reaction mixture was prepared with DNA sample, 20 ng; PCR buffer 10X, 2.5 µL; $MgCl_2$ (1.5 mM), 1.25 µL; dNTPs (200 µM), 1 µL each; *Taq* DNA polymerase (0.1 U/mL), 0.25 µL; primer forward/f/ and primer reverse/r/ (0.5 µM), 2.5 µL each; MilliQ water to achieve 25 µL.

10X PCR buffer: 200 mM Tris-HCl pH 8.4; 500 mM KCl.

A MyCycler thermal cycler from BioRad (BioRad, Richmond, California, USA) was used for the PCR reaction.

Separation of the amplification products was performed according to Sambrook and Gething (1989). The run was carried out with 1X TAE buffer (0.04 M Tris-Acetate; 1 mM EDTA, pH 8) by applying 85 V. A 1 Kb DNA Ladder (Invitrogen, Argentina) was used as a molecular weight marker. Gels were then stained with ethidium bromide (1 µg/mL) and DNA visualized with a U.V. light transilluminator (λ=320 nm).

Viability and Bacteriocin Activity of *E. gallinarum* CRL 1826 After Freeze-Drying and Storage

The LAB strain was grown in MRS (10 h at 37°C). Cells were harvested by centrifugation (3,000 x *g*, 10 min at 4°C), washed twice with sterile distilled water, and centrifuged. The pellets were re-suspended in lyoprotectants (w/v): 10% lactose (L), 10% sucrose (S), 10% skim milk (SM), 10% whey protein concentrate (WPC; Lacprodan 35, Arla-Foods Ingredients, Argentina), 5% L + 5% S (L-S), 5% SM + 5% L (SM-L), 5% SM + 5% S (SM-S), 5% WPC + 5% L (W-L), and 5% WPC + 5% S (W-S) to obtain ~10^{11} CFU/mL. Cells were also re-suspended in neutral sterile distilled water (control). Finally, samples were frozen at -20°C for 12 h, and lyophilized according to Montel Mendoza *et al.* (2014). Dried cells were distributed in glycogelatin capsules, packed in plastic bottles with silica gel, and stored at 4 and 25°C for 24 months. The number of viable cells (CFU) before and after freeze-drying was determined by the serial dilution method and plated on MRS agar (1.5% w/v). Cell viability for each lyoprotectant was expressed as Survival Factor (SF), and calculated as follows:

$$SF=1 - (\text{Log CFU}_{before} - \text{Log CFU}_{after}) / \text{Log CFU}_{before}$$

$$CFU_{before}=\text{CFU/mL } x \text{ total culture volume (mL)}$$

$$CFU_{after}=\text{CFU/mL x [total weight pre-lyophilized sample (g) / weight lyophilized sample (g)]}$$

Cell viability during storage was expressed as Survival Factor during *t* month of Storage (SFS_t), and calculated as follows:

$$SFS_t=1 - (\text{Log CFU}_0 - \text{Log CFU}_t) / \text{Log CFU}_0$$

CFU_0=initial CFU/g x total weight of dried sample (g); CFU_t=t time CFU/g x total weight of dried sample (g).

The maintenance of bacteriocin activity of *E. gallinarum* CRL 1826 was determined after lyophilization and during storage by the plate dilution method (34). Thus, the LAB strain was inoculated in MRS broth, and incubated for 72 h at 37°C with subsequent cultures every 24 h. When cultures reached an OD~1.0 (540 nm), cell-free supernatants were obtained and stored (-20°C) until bacteriocin activity determination (33). The antimicrobial titer was defined as the reciprocal of the greatest two-fold dilution producing a clear inhibition zone of ~1 mm, expressed as arbitrary units per milliliter of culture supernatant (AU/mL). Besides, bacteriocin activity was expressed as relative activity to freeze-dryng (RA) and storage (RAS), and calculated by equations:

$$RA=1 - (AU/mL_b - AU/mL_a) / AU/mL_b$$

a=after freeze-drying; b=before freeze-drying

$$RAS_t=1 - (AU/mL_0 - AU/mL_t) / AU/mL_0$$

0=after freeze-drying; t=month of storage

Growth and Viability of *E. gallinarum* CRL 1826 at Different pH Values, Bile Salts, and Digestive Enzymes

Assays were conducted with pre-lyophilized (PL) and lyophilized (L) (5% SM + 5% S) *E. gallinarum* CRL 1826 cells. Thus, 10^6 CFU/mL were inoculated in the following media: LAPTg broth at pH 2, 3, 4, 5, 6, 6.8 (optimal bacterial growth), 7, and 8; LAPTg broth + pepsin 0.05; 0.15; 0.3, and 0.6% at pH 2; LAPTg broth + bile 0.1; 0.3; 0.5; 1; 1.5; 3; 6, and 10% at pH 8, and LAPTg broth + pancreatin: 0.01; 0.05; 0.1; 0.15, and 0.2% at pH 8. Cultures were incubated at 37°C and bacterial growth was determined by optical density ($OD_{540\ nm}$) for 24 h.

In media without OD changes, 10^9 CFU/mL were inoculated and incubated for 18 min at different pH and pepsin concentrations, 10 min with 1 to 10% bile, and 90 min with 0.3 to 0.5% bile. Subsequently, CFU/mL were determined on LAPTg agar (incubation at 37°C, 24 h, in microaerophilia) and a Survival Factor (SF) was calculated. Likewise, cells from each medium were grown as described, determining AU/mL.

Simulated Gastrointestinal Digestion Model

For these experiments, we considered the highest individual concentrations of each factor allowing high *E. gallinarum* CRL 1826 viability and bacteriocin activity, as well as gastrointestinal conditions reported for adult amphibians (47). Therefore, 10^9 CFU/mL of PL and L cultures were resuspended in PBS solution (pH 7.4) + pepsin 0.6%, and incubated for 90 min at 37°C. During this time, a gradual pH decrease (7.4 to 2) was induced using 1N HCl and samples were taken at 0, 30, 60, and 90 min (Phase 1: stages a, b, c, and d, respectively). Then, the suspensions were centrifuged and cells were resuspended in PBS solution pH 8 + 1% bile (OX-bile, FLUKA) for 10 min (Phase 2: stage e). Subsequently, cells were collected and inoculated in PBS solution pH 8 containing 0.3% bile + 0.1% pancreatin (SIGMA-ALDRICH), and samples were taken at 30, 60, and 90 min (Phase 3: f, g, and h, respectively). At each stage, SF and AU/mL were evaluated. Finally, surface properties (hydrophobicity and autoaggregation) were determined according to Niederle *et al.* (2019).

Statistical Analysis

Data processing was done using Minitab (30) and Infostat (13) softwares. Results are the average of three independent assays, evaluated by ANOVA or General Linear Models. When residuals showed a normal distribution, a post-test (at 0.05 significant levels) for multiple comparisons was performed. When assumptions were not met, nonparametric variance analysis was applied (Mood's median test).

Results

Susceptibility to Antimicrobials of *E. gallinarum* CRL 1826, RLS-Related Pathogens, and *L. monocytogenes*

Table 1 shows MIC values for chemotherapeutics frequently used in bullfrog hatcheries.

Table 1. Minimum inhibitory concentration (µg/mL) of antimicrobials frequently used in ranaculture.

Tabla 1. Concentración inhibitoria mínima (µg/mL) de antimicrobianos frecuentemente utilizados en ranicultura.

Chemotherapeutics	*E. gallinarum* CRL 1826	Breakpoint
Penicilin	≤0.25	≥16[a]
Ceftazidime	512	≥64[c]
Amikacin	8	≥256[a]
Ciprofloxacin	1	≥4[a]
Oxytetracyclin	1	≥16[b]
Chloramphenicol	4	≥32[a]
Metronidazole	>512	≥32[a]
Vancomycin	2	≥32[a]

[a] (7); [b] (20); [c] (48).

Based on breakpoint values, *E. gallinarum* CRL 1826 was sensitive to most antimicrobials except ceftazidime and metronidazole, whose MIC values were 512 and >512, respectively. Concerning vancomycin, the disc diffusion assay revealed that the LAB strain was sensitive (data not shown), and the MIC value below the breakpoint. Moreover, MIC of antiseptics for *E. gallinarum* CRL 1826, *C. freundii*, *P. aeruginosa*, and *Listeria monocytogenes* was also determined (table 2).

Table 2. MIC (µg/mL) of antiseptics frequently used in ranaculture.
Tabla 2. CIM (µg/mL) de antisépticos frecuentemente utilizados en ranicultura.

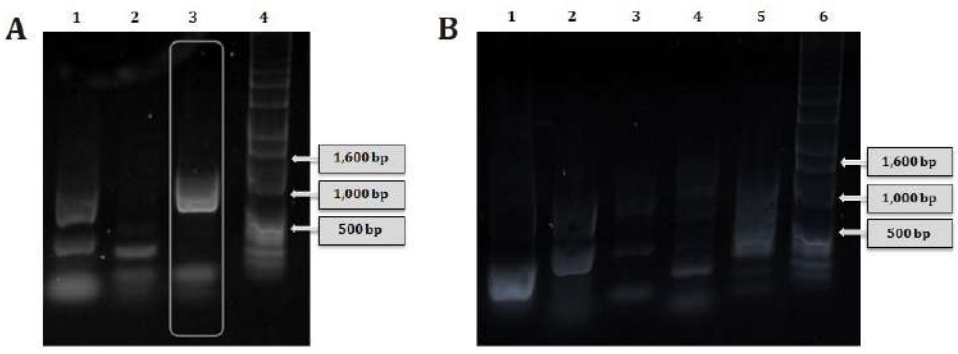
Strain	Benzalkonium chloride	Methylene blue	Malachite Green	$CuSO_4$	$KMnO_4$
E. gallinarum CRL 1826	32	4,096	4	1,024	8,192
C. freundii Cfb	>128	>16,384	>256	2,048	>16,384
P. aeruginosa 1007	>128	>16,384	>256	2,048	16,384
P. aeruginosa 1047	>128	>16,384	>256	2,048	16,384
L. monocytogenes	16	16,384	8	1,024	4,096
Dose*	2	0.25	5	0.5	1,000

* Antiseptic concentrations used in bullfrog hatcheries (4).
* Concentraciones de antisépticos utilizados en la cría de rana toro (4).

Therefore, all strains showed MIC values greater than the dose usually used in ranaculture, excepting *E. gallinarum* CRL 1826 when using malachite green. Therefore, *E. gallinarum* CRL 1826 is sensitive to antibiotics and resistant to antiseptics used in bullfrog farms.

Vancomycin Resistance and Virulence Factors Genes in *E. gallinarum* CRL 1826

The presence of *vanA*, *vanB*, and *vanC* genes was determined by PCR amplification (figure 1A). In lane 3, an approximately 800 bp band was detected and matched with the amplification product of *vanC* gene (822 bp). Concerning virulence factor genes described for *Enterococcus*, the LAB strain did not display any tested factor (figure 1B) when compared to the standard band size (Supplementary, Table S.1). Thus, our results demonstrate that *E. gallinarum* CRL 1826 is a safe LAB strain.



(A) Vancomycin resistance genes 1: amplification product *vanA* gen; 2: *vanB*; 3: *vanC*; 4: ladder 1Kb DNA marker. (B) Virulence factor genes. 1: *agg*; 2: *cylA*; 3: *gelE*; 4: *esp*; 5: *efa*; 6: ladder 1Kb DNA marker.
(A) Genes de resistencia a vancomicina 1: producto de amplificación del gen *vanA*; 2: *vanB*; 3: *vanC*; 4: marcador de peso molecular de ADN de 1 Kb. (B) Genes de factores de virulencia. 1: *agg*; 2: *cylA*; 3: *gelE*; 4: *esp*; 5: *efa*; 6: marcador de peso molecular de ADN de 1 Kb.

Figure 1. Vancomycin resistance and virulence factor genes in *E. gallinarum* CRL 1826.
Figura 1. Genes de resistencia a vancomicina y de factores de virulencia en *E. gallinarum* CRL 1826.

Effect of the Drying Medium on Survival and Bacteriocin Activity to Lyophilization of *E. gallinarum* CRL 1826

We determined the freeze-drying resistance of the LAB strain using nine lyoprotectants. The three average SF values ranged between 0.81 to 0.97 (figure 2).

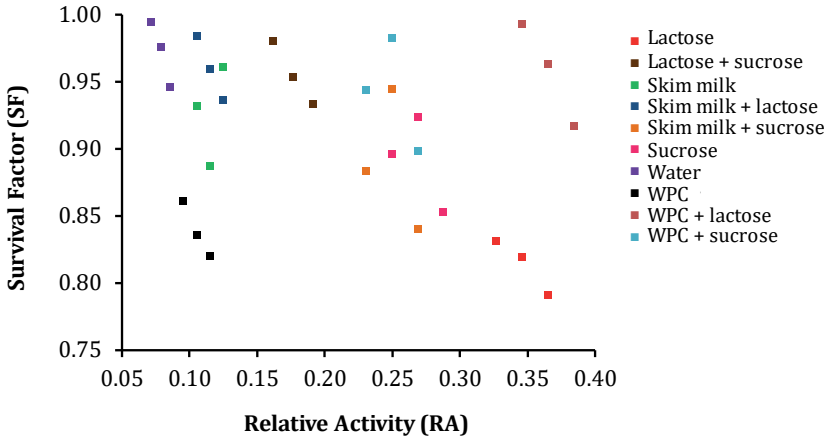


Figure 2. Viability (SF) and bacteriocin activity (RA) scatter plot of lyophilized *E. gallinarum* CRL 1826. WPC: whey protein concentrate.

Figura 2. Diagrama de dispersión de viabilidad (SF) y actividad bacteriocina (RA) de *E. gallinarum* CRL 1826 liofilizado. WPC: concentrado proteico de suero.

Optimal cell viability recuperation was detected in water, SM-L, WPC-L, L-S, WPC-S, and SM, with SF values from 0.93 to 0.97, without significant differences ($p \leq 0.05$, Fisher test). Bacteriocin production in lyophilized cultures was calculated as relative activity (RA) (table 3). Thus, the nine lyoprotectant solutions increased RA values (0.11-0.37) when compared with those obtained in water (0.08) after freeze-drying (figure 2). However, the highest RA values were detected when the LAB strain was lyophilized in L (RA=0.35) and WPC-L (RA=0.37), without significant differences ($p \leq 0.05$, Fisher test). Considering RA and SF values, the optimal freeze-drying condition was WPC-L (figure 2). However, no correlation was found between both factors (Pearson correlation coefficient: 0.08).

Table 3. Bacteriocin activity of lyophilized *E. gallinarum* CRL 1826.

Table 3. Actividad bacteriocina de *E. gallinarum* CRL 1826 liofilizado.

Lyoprotectant	Activity (AU/mL)	Relative Activity (RA)
WPC	56,320^{b}	0.11^{b}
Skim milk	61,440^{b}	0.12^{b}
Lactose	184,320^{e}	0.35^{e}
Sucrose	143,360^{d}	0.27^{d}
Skim milk + lactose	61,440^{b}	0.12^{b}
Skim milk + sucrose	133,120^{d}	0.25^{d}
Lactose + sucrose	94,320^{c}	0.18^{c}
WPC + lactose	194,560^{e}	0.37^{e}
WPC + sucrose	133,120^{d}	0.25^{d}
Water	42,240^{a}	0.08^{a}

$^{a-b}$: indicates significant differences (p>0.05); WPC: whey protein concentrate.

$^{a-b}$: indica diferencias significativas (p>0,05). WPC: concentrado proteico de suero.

Viability and Bacteriocin Activity of Lyophilized *E. gallinarum* CRL 1826 During Storage

Survival of freeze-dried cultures in different lyoprotectants during storage at 4°C was analyzed by general linear models (figure 3).

* Indicates significant differences compared to 1-month storage for each lyoprotectant (p>0.05).

WPC: whey protein concentrate.

* Indica diferencias significativas respecto del almacenamiento durante 1 mes para cada lioprotector (p>0,05).

WPC: concentrado proteico de suero.

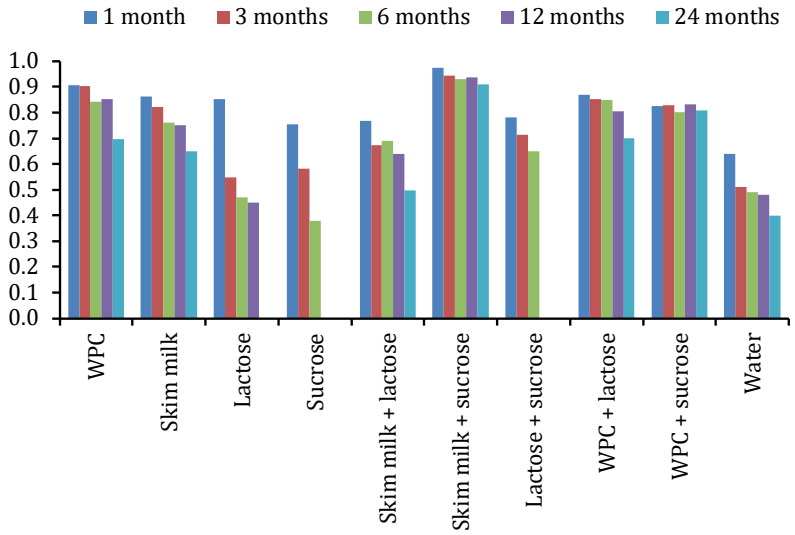


Figure 3. Viability (SF) of lyophilized *E. gallinarum* CRL 1826 during 24 months of storage at 4°C.

Figura 3. Viabilidad (SF) de *E. gallinarum* CRL 1826 liofilizado y almacenado durante 24 meses a 4°C.

Therefore, cell viability values over 0.90 during 24 months were obtained in SM-S, without significant differences up to 12 months (p≤0.05). Cell viability for lyophilized LAB strain stored at 25°C was analyzed by Mood's median test, where the general median value was 0.47 (figure 4).

WPC: whey protein concentrate.

WPC: concentrado proteico de suero.

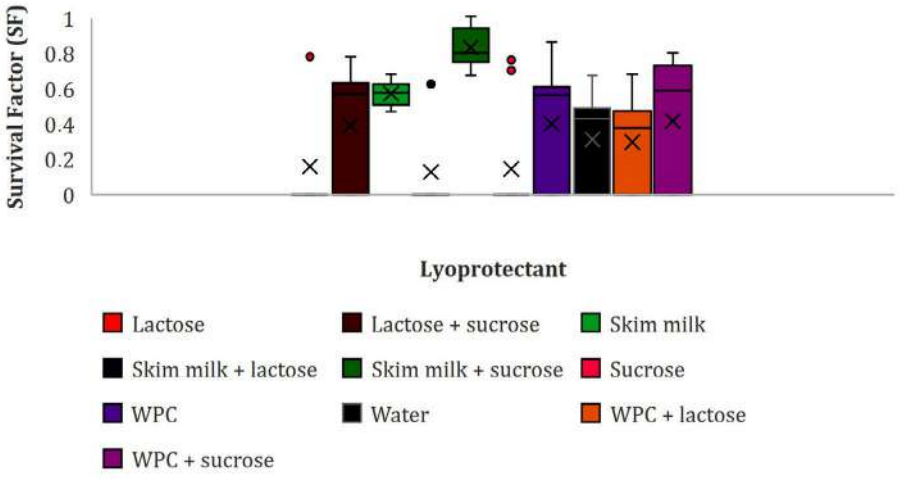


Figure 4. Viability (SF) of lyophilized *E. gallinarum* CRL 1826 during 24 months storage at 25°C.

Figura 4. Viabilidad (SF) de *E. gallinarum* CRL 1826 liofilizado y almacenado durante 24 meses a 25°C.

Thus, after 24 months, viability was greater than the median when using SM and SM-S, with mean SF values of 0.72 and 0.49, respectively. In those cultures, dried in S, L, and SM-L, cell viability was only detected at 1-month storage (figure 4, page 8). Regarding bacteriocin production (RA), a Mood's median test analyzed the freeze-dried cultures in different lyoprotectants and stored at 4 and 25°C (median: 0.14 and 0.006, respectively). Therefore, during 24 months of storage at 4°C the best RA values were obtained in WPC (figure 5), while at 25°C the greatest RA values were detected in SM and SM-S (figure 5).

(A):4°C; (B):25°C. WPC: whey protein concentrate.

(A):4°C; (B):25°C. WPC: concentrado proteico de suero.

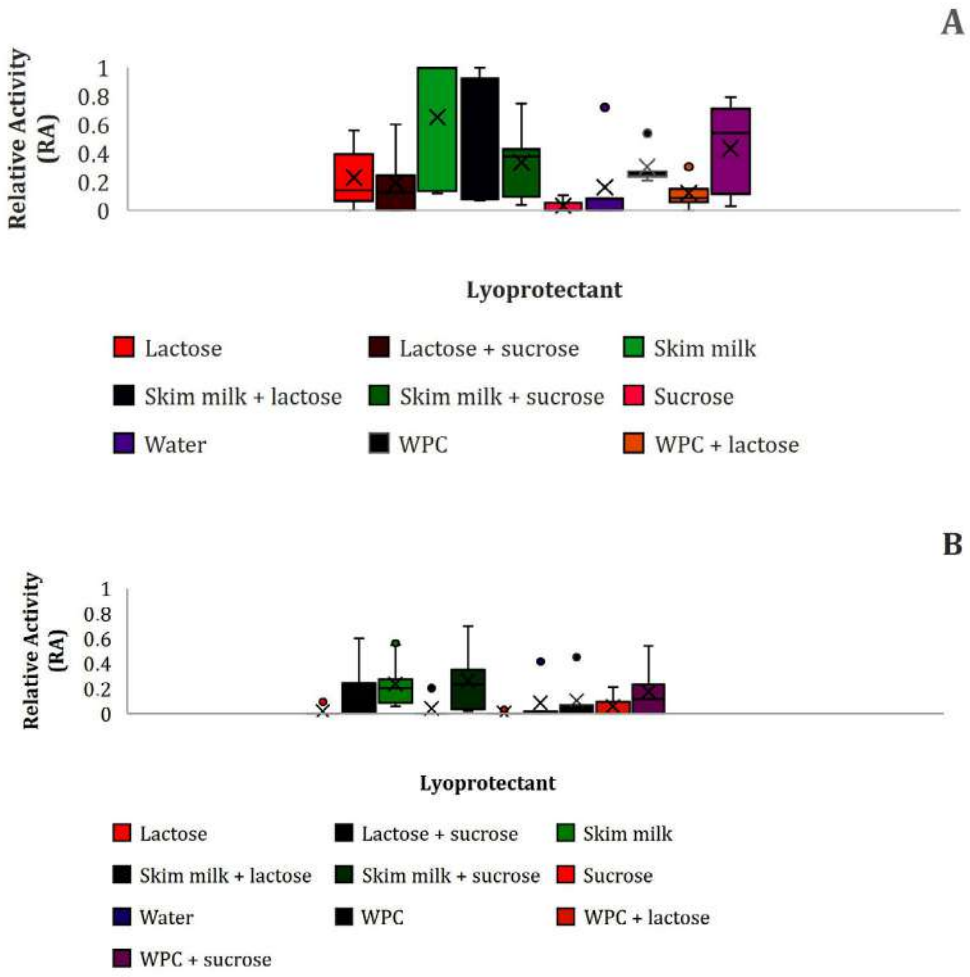


Figure 5. Bacteriocin activity (RA) of lyophilized *E. gallinarum* CRL 1826 during 24 months storage.

Figura 5. Actividad bacteriocina (RA) de *E. gallinarum* CRL 1826 liofilizado durante 24 meses de almacenamiento.

Growth/Resistance and Bacteriocin Activity of *E. gallinarum* CRL 1826 in Individual Gastrointestinal Conditions

Tests compared pre-lyophilized (PL) and lyophilized (L) bacterial cultures with the best lyophilisation matrix. Thus, PL cultures of *E. gallinarum* CRL 1826 grew ≥ 3 logarithmic units in LAPTg broth pH 5 to 8, 0.1% bile, and 0.01 to 0.2% pancreatin (table 4, page 10). In these conditions, the highest bacteriocin activities (79,600 AU/mL) were detected at pH 6.8 (control) and pH 7. Likewise, PL cultures resisted all tested conditions (SF=0.44-0.99) (table 4, page 10), except 6 and 10% bile for 10 min. Moreover, the highest bacteriocin activity (8,080 AU/mL) was determined with 1% bile for 10 min.

Table 4. Growth (Log CFU/mL), viability (SF) and bacteriocin activity (AU/mL) of pre-lyophilized (PL) and lyophilized (L) *E. gallinarum* CRL 1826 when subjected to individual gastrointestinal conditions.

Tabla 4. Crecimiento (Log CFU/mL), viabilidad (SF) y actividad bacteriocina (AU/mL) de *E. gallinarum* CRL 1826 preliofilizado (PL) y liofilizado (L) cuando se somete a condiciones gastrointestinales individuales.

	Log UFC/mL		SF		AU/mL	
Condition	**PL**	**L**	**PL**	**L**	**PL**	**L**
pH 2	NG	NG	0.96^{o}	0.6^{h}	235^{a}	1,520^{a}
pH 3	NG	NG	0.96^{o}	0.8^{lm}	7,440^{cd}	1,320^{a}
pH 4	NG	10.34^{o}	0.96^{o}	NT	4,810^{bc}	11,520^{ef}
pH 5	9.39^{a}	10.44^{q}	NT	NT	760^{a}	11,520^{ef}
pH 6	9.83^{ef}	10.99^{s}	NT	NT	1,320^{a}	14,400^{fg}
pH 6.8 (control)	9.96^{l}	11.27^{u}	NT	NT	79,600^{j}	15,900^{gh}
pH 7	10.01^{m}	11.19^{t}	NT	NT	79,600^{j}	15,900^{gh}
pH 8	10.36^{p}	10.48^{r}	NT	NT	2,280^{ab}	17,820^{h}
Pepsin 0.05%	NG	NG	0.78^{kl}	0.56^{gh}	2,520^{ab}	0^{a}
Pepsin 0.15%	NG	NG	0.76^{j-l}	0.49^{de}	1,840^{ab}	0^{a}
Pepsin 0.3%	NG	NG	0.76^{j-l}	0.45^{cd}	2,520^{ab}	0^{a}
Pepsin 0.6%	NG	NG	0.53^{e-g}	0.41^{bc}	520^{a}	0^{a}
Bile 0.1%	9.65^{b}	10.26^{n}	NT	NT	8,240^{d}	22,500^{i}
Bile 0.3%	NG	9.81e	0.96^{o}	NT	6,720^{cd}	22,500^{i}
Bile 0.5%	NG	9.82e	0.88^{n}	NT	1,680^{a}	15,900^{gh}
Bile 1%	NG	9.68c	0.54^{fg}	NT	8,080^{d}	14,400^{fg}
Bile 1.5%	NG	9.99^{m}	0.66^{i}	NT	1,140^{a}	15,900^{gh}
Bile 3%	NG	9.85^{g}	0.44^{bc}	NT	340^{a}	11,520^{ef}
Bile 6%	NG	NG	0.03^{a}	0.83^{m}	0^{a}	420^{a}
Bile 10%	NG	NG	0^{a}	0.75^{ik}	0^{a}	295^{a}
Pancreatin 0.01%	9.94^{n}	9.91^{k}	NT	NT	1,520^{a}	15,900^{gh}
Pancreatin 0.05%	9.81^{e}	9.86^{gh}	NT	NT	520^{a}	7,840^{cd}
Pancreatin 0.1%	9.95^{n}	9.72^{d}	NT	NT	2,040^{ab}	8,640^{de}
Pancreatin 0.15%	9.74^{d}	9.72^{d}	NT	NT	1,140^{a}	8,640^{de}
Pancreatin 0.2%	9.88^{ij}	9.65^{b}	NT	NT	1,020^{a}	9,280^{de}

$^{a-b}$: indicates significant differences (p>0.05); NG: not grown; NT: not tested.

$^{a-b}$: indica diferencias significativas (p>0,05); NG: sin crecimiento; NT: no testeado.

Lyophilized cultures (L) grew in a greater number of conditions. For example, LAPTg broth at pH 4, and 0.3-3% bile. Moreover, the highest bacteriocin activities (22,500 AU/mL) were detected with 0.1 and 0.3% bile (table 4). Also, L cultures resisted acid pH (2 and 3), 6 and 10% bile, and all pepsin concentrations. In these conditions, the highest bacteriocin activity (1,520 AU/mL) was determined at pH 2 for 18 min and was not detected with pepsin (table 4). Therefore, L cultures showed the greatest mean growth value (10.17 Log CFU/mL) and resistance (SF=0.83) significantly higher than for PL (8.50 Log CFU/mL and SF=0.73, respectively) (LSD Fisher, p>0.05).

Viability and Beneficial Properties of *E. gallinarum* CRL 1826 in a Simulated Gastrointestinal Digestion Model

Overall, LAB strain viability decreased during the simulated gastrointestinal digestion process. The L cultures showed higher viability values (mean SF=0.92) than PL (mean SF=0.82). Both PL and L cultures showed no significant differences in viability between stages b to d (Phase 1: pH 7.4 to 2.0 + pepsin 0.6%, 90 min). Moreover, the lowest viability values were observed at stages f to h (Phase 3: pH 8 + 0.3% bile + 0.1% pancreatin; 30, 60, and 90 min), where no significant differences were determined (p>0.05) (table 5).

Table 5. Viability (SF) and beneficial properties of pre-lyophilized (PL) and lyophilized (L) *E. gallinarum* CRL 1826 in a simulated gastrointestinal digestion model.

Tabla 5. Viabilidad (SF) y propiedades benéficas de *E. gallinarum* CRL 1826 preliofilizado (PL) y liofilizado (L) en un modelo de digestión gastrointestinal simulado.

Stages	SF		AU/mL		H (%)	
	PL	L	PL	L	PL	L
a	1.00^{f}	1.00^{f}	6^{a}	1,253^{cd}	66.87^{a-c}	81.27^{b-c}
b	0.93^{e}	1.08^{h}	33^{a}	1,333^{cd}	72.03^{a-c}	81.13^{b-c}
c	0.95^{e}	1.09^{h}	30^{a}	1,426^{cd}	67.03^{a-c}	84.03^{c}
d	0.93^{e}	1.05^{gh}	40^{a}	1,333^{cd}	52.17^{a}	60.77^{a-c}
e	0.70^{b}	0.86^{d}	0^{a}	1,920^{d}	71.20^{a-c}	79.70^{b-c}
f	0.65^{a}	0.83^{cd}	110^{ab}	920^{a-c}	78.77^{bc}	79.97^{b-c}
g	0.68^{ab}	0.84^{d}	180^{ab}	1,160^{cd}	75.37^{a-c}	75.63^{a-c}
h	0.68^{ab}	0.83^{cd}	83^{a}	853^{a-c}	76.63^{a-c}	70.70^{a-c}

Stages	AA (%)			
	1h		4h	
	PL	L	PL	L
a	23.73^{d-i}	14.37^{a-g}	48.50^{k}	24.67^{e-i}
b	19.60^{b-h}	10.73^{a-f}	37.40^{i-k}	16.40^{a-g}
c	15.70^{a-g}	12.70^{a-f}	41.37^{j-k}	18.63^{b-g}
d	12.37^{a-f}	11.30^{a-f}	34.17^{h-k}	17.03^{b-g}
e	10.33^{a-e}	15.87^{a-g}	48.57^{k}	25.30^{f-i}
f	7.83^{a}	13.30^{a-f}	24.20^{e-i}	20.07^{b-h}
g	28.00^{g-j}	10.80^{a-f}	41.80^{j-k}	18.90^{b-g}
h	19.80^{b-h}	14.40^{a-g}	36.60^{i-k}	21.40^{c-h}

Stages: a-d: gradual pH decrease of PBS solution (7.4 to 2) + pepsin 0.6%, 0, 30, 60, and 90 min; e: PBS solution pH 8 + 1% bile; f-g: PBS solution pH 8 containing 0.3% bile + 0.1% pancreatin, 30, 60, and 90 min. $^{a-b}$: indicates significant differences (p>0.05).

AU/mL: bacteriocin activity; H: hydrophobicity; AA: autoaggregation.

Etapas: a-d: disminución gradual del pH de solución PBS (7,4 a 2) + pepsina 0,6%, 0, 30, 60 y 90 min; e: solución PBS pH 8 + bilis 1%; f-g: solución PBS pH 8 conteniendo bilis 0,3% + pancreatina 0,1%, 30, 60 y 90 min. $^{a-b}$: indica diferencias significativas (p>0,05).

AU/mL: actividad bacteriocina; H: hidrofobicidad; AA: auto-agregación.

The highest bacteriocin activity (1,920 AU/mL) was observed in L cultures at stage "e" with significant differences at stages f and h (table 5). However, PL cultures presented lower activity during whole digestion, increasing slightly between stages f and h without significant differences (table 5). Concerning surface properties, hydrophobicity values did not show significant differences for PL or L cultures (table 5). The highest value was observed in L cultures (84.03%) at stage "c", remaining above 52.17% during the assay. Moreover, auto-aggregation (AA) mean values in PL cultures (28.12%) were significantly higher than those observed for L cultures (16.62%), independently of sampling stage. The AA values were always higher at 4 h (table 5). Overall, opposite stages (a and h) exhibited no significant differences in any culture. The highest value (48.57%) was observed in PL cultures at stage "e" at 4 h, while the lowest value (7.83%) was detected in PL cultures at stage "f" at 1 h (table 5).

Discussion

Designing a probiotic product involves safety considerations (resistance to chemotherapeutics and absence of virulence factors), technological aspects (lyophilization and spray drying), and physiological studies (tolerance to host conditions such as pH, digestive enzymes, and bile) (2).

In high-scale aquaculture, chemotherapeutics could lead to resistance among pathogenic bacteria (52). Therefore, probiotics represent an alternative to chemotherapeutics reducing disease outbreaks (18).

Enterococcus genus presents both beneficial and technological properties for constituting probiotic products. However, this genus is not universally considered Generally Regarded As Safe (GRAS) given virulence factors and vancomycin resistance genes (2). Evaluating sensitivity and resistance to various antimicrobials, including vancomycin, is regulated (15). Moreover, microorganisms should not contain antimicrobial resistance genes that could be horizontally transferred to members of the autochthonous microbiota or potential pathogens (37).

According to their beneficial properties, *E. gallinarum* CRL 1826 from bullfrog was selected as a probiotic candidate for ranaculture (31, 33). The LAB strain showed antibiotic sensitivity, except for ceftazidime, related to the intrinsic resistance of *Enterococcus* to cephalosporins (12). Metronidazole sensitivity explains the antagonistic activity mainly on anaerobic bacteria (29).

Nowadays, vancomycin resistance genes in *Enterococcus* are associated with three well-defined phenotypes, according resistance degrees, induction, and transfer. Likewise, only the *vanC* gene is chromosomal, constitutive, and non-transferable (6). *Enterococcus gallinarum* CRL 1826 could be accepted as a safe strain since its vancomycin sensitiveness (MIC=4-32 mg/L), and only present *vanC* gene.

Considering that *E. gallinarum* is associated with infections in aquaculture (44), and that the *esp* gene was revealed in *E. gallinarum* from ready-to-eat seafood (21), we demonstrated the absence of virulence factors genes of the CRL 1826 strain supporting their GRAS characteristics.

Concerning antiseptics, *E. gallinarum* CRL 1826, RLS-related pathogens (*C. freundii*, *P. aeruginosa*), and *L. monocytogenes* resulted to be highly resistant to doses used in bullfrog hatcheries. Thus, we could hypothesize that the bioaugmentation with this LAB strain in hatchery conditions would eliminate the pathogens and potential pathogens by competitive exclusion or antibiosis (11, 34, 38).

Technologically, freeze-drying preserves cell viability and beneficial properties during probiotic product design, storage, and transport (32). Lyoprotectants, including sugars, amino acids, and proteinaceous compounds often mitigate cellular damage during freeze-drying (32).

Cocci generally exhibit greater resistance to lyophilization compared to bacilli. This can be explained by its low surface/volume ratio, as demonstrated in *E. faecium*, *Streptococcus thermophilus*, *L. lactis* subsp. *lactis*, and *L. lactis* subsp. *cremoris* strains (24). However, the behavior towards lyophilization is related to strain characteristics, such as an *E. faecium* strain (potential probiotic isolated from oysters) with low viability recovery in skim milk (36.2%) (25), while Romyasamit *et al.* (2022) demonstrated 96% of viability recovery for the same lyoprotectant in two *E. faecium* strains with probiotic potential for functional food, medicine, and feed industries. *Enterococcus gallinarum* CRL 1826 showed 93% viability recovery in skim milk and intrinsic resistance to lyophilization (water).

Regarding bacteriocin activity maintenance, we demonstrated a diminution of relative activity after lyophilization. However, antimicrobial titer values could be suitable for RLS-related pathogens and foodborne bacteria control (33).

As relative indices to initial lyophilization stages and storage, we defined survival and bacteriocin activity parameters (SF, RA). These parameters allowed data analysis independently of the initial values of viability and bacteriocin activity. Similar criteria were applied by Vera Pingitore *et al.* (2012) who studied a bacteriocin produced by *Lactobacillus salivarius* and evaluated specific activity after lyophilization and storage. Our study demonstrated a non-correlation between bacterial viability and bacteriocin activity, indicating that factors were differently affected by freeze-drying conditions.

However, Jawan *et al.* (2022) verified a correlation between these two factors when analyzed as absolute values.

Despite lyoprotectants enhance survival during lyophilization, they may not provide protection during storage (9). Thus, the CRL 1826 strain viability decreased gradually and a total loss was observed at 25°C in L, S, and SM-L after one month of storage.

Skim milk+sucrose was the best lyoprotectant for *E. gallinarum* CRL 1826 strain during storage. In ranaculture, *L. plantarum* CRL 1606 lyophilized in SM-S showed high viability recovery at 4 and 25°C up to 18 months' storage (31). The protein matrix added to sugars increased viability recovery concerning the individual components. Using SM would represent an extra source of proteins and carbohydrates for bullfrog feeding, considering that balanced feed used in hatcheries provides 40% of proteins (fish meal, meat meal, and milk powder).

Enterococcus gallinarum CRL 1826 kept its bacteriocin activity after lyophilization in SM and SM-S during 24 months' storage at 4 and 25°C. These results are in agreement with Jawan *et al.* (2022) who demonstrated that *Lactococcus lactis* Gh1, isolated from an Iranian traditional flavor enhancer, maintained the ability to produce bacteriocin with various lyoprotectants during 2 months of storage at 4°C.

Adult bullfrog specimens have a developed gastrointestinal tract (GIT) that represents one entry route for RLS-related pathogens (35). Considering that probiotics must be applied in bullfrog hatcheries during life cycle and that these microorganisms must resist host conditions and reach the intestine for adhesion and colonization, we evaluated GIT restrictive conditions on viability and maintenance of beneficial properties of *E. gallinarum* CRL 1826. All studies were performed by considering physiological concentration ranges (47) in sequence, temperature, and time.

The pH affects growth factors transport across the cell membrane of LAB and antagonistic efficacy (14). In PL cultures of *E. gallinarum* CRL 1826 exposed for 18 min at pH 2, viability recovery was similar to initial values (SF=0.96), whereas PL cultures of *Enterococcus avium*, *E. pseudoavium*, and *E. raffinosus* (from carp) treated at pH 2.5 up to 5 h showed viability diminution around 2 log units (43).

Bacteriocins constitute an important competitive advantage for microorganisms, particularly interesting for bioinputs (40). The highest bacteriocin production by *E. gallinarum* CRL 1826 was detected at pH 6.8 and 7, and the lowest at pH 2. Bacteriocins are stable over a wide pH range, with high activity at neutral and basic pH (14). Thus, PL cultures of *Pediococcus pentosaceus* 1101, from fermented meat products, showed the highest bacteriocin activity at pH 5.5 and 7 (14).

Considering that pH/time interaction and pepsin presence could affect bacterial survival (26), we observed that pepsin diminished *E. gallinarum* CRL 1826 growth of PL and L cultures, probably given by enzymatic action since viability values were lower than those obtained at pH 2 (table 4, page 10) (LSD Fisher, $p>0.05$).

Bile significantly affects protein and DNA and participates in the emulsification of fats and cell membranes (49). Our bile concentration ranged from 0.1 to 10%. Thus, PL and L cultures of *E. gallinarum* CRL 1826 maintained viability up to 90 min in 0.5% bile. In this sense, different behaviors have been reported for PL cultures of aquaculture enterococci. Some resisted up to 3 h (40) while others perished after 4 and 24 h (5, 27) with 0.3% bile. Pereira *et al.* (2018) measured OD 630 nm, and reported that PL cultures of *L. plantarum* strains, isolated from bullfrog hatcheries, tolerated 5% bile for 24 h. Nevertheless, PL cultures of *E. gallinarum* CRL 1826 resisted 0.5% bile for 90 min, while L cultures resisted 10% bile for 10 min.

Pancreatin from porcine pancreas contains proteases, lipase, and amylase, that cleave specific molecules for their assimilation (10). This enzyme complex could affect *E. gallinarum* CRL 1826 and, consequently, its probiotic effect. However, we observed that PL and L cultures of the LAB strain grew in all concentration ranges (0.01-0.2%) tested.

When *E. gallinarum* CRL 1826 was subjected to simulated gastrointestinal digestion, we observed that L cultures over-performed (growth/resistance, bacteriocin activity, and surface properties maintenance) than PL cultures. This behavior could relate to a protective effect of the freeze-drying matrix (SM-S) that would interfere with gastrointestinal conditions as reported for a *L. rhamnosus* strain (28). Moreover, some authors postulate an adaptation mechanism of probiotics called "cross-protection", occurring when microorganisms are

pre-adapted and gain greater tolerance towards different types of stress than the original (1, 16). In our experimental conditions, lyophilization of *E. gallinarum* CRL 1826 could act as a pre-adaptation process improving bacterial survival to simulated gastrointestinal digestion.

Finally, PL and L cultures of *E. gallinarum* CRL 1826 maintained hydrophobicity and auto-aggregation when subjected to the simulated gastrointestinal digestion model that would enhance its capability of gut colonization.

Conclusion

Enterococcus gallinarum CRL 1826 exhibits promising characteristics as a probiotic for bullfrog hatcheries, offering viability and bacteriocin activity even after lyophilization and under simulated gastrointestinal conditions. These properties, combined with its safety profile, make it a potential solution for preventing RLS outbreaks and controlling foodborne bacteria, with potential benefits for bullfrog growth performance.

Supplemmentary Material

https://docs.google.com/document/d/1TiIVRmyx6FpD5iHolsoowCzZwDxggrWU/edit?usp=sharing&ouid=111310786017351827239&rtpof=true&sd=true

References

1. Anglenius, H.; Mäkivuokko, H.; Ahonen, I.; Forssten, S. D.; Wacklin, P.; Mättö, J.; Lahtinen, S.; Lehtoranta, L.; Ouwehand, A. C. 2023. *In vitro* screen of lactobacilli strains for gastrointestinal and vaginal benefits. Microorganisms. 11(2): 329. https://doi.org/10.3390/microorganisms11020329
2. Barzegar, H.; Alizadeh Behbahani, B.; Falah, F. 2021. Safety, probiotic properties, antimicrobial activity, and technological performance of *Lactobacillus* strains isolated from Iranian raw milk cheeses. Food Sci. Nutr. 9(8): 4094-4107. https://doi.org/10.1002/fsn3.2365
3. Berg, G.; Rybakova, D.; Fischer, D.; Cernava, T.; Vergès, M. C. C.; Charles, T.; Chen, X.; Cocolin, L.; Eversole, K.; Herrero Corral, G.; Kazou, M.; Kinkel, L.; Lange, L.; Lima, N.; Loy, A.; Macklin, J. A.; Maguin, E.; Mauchline, T.; McClure, R.; Mitter, B.; Ryan, M.; Sarand, I.; Smidt, H.; Schelkle, B; Roume, H.; Kiran, G. S.; Selvin, J.; Soares Correa de Souza, R.; van Overbeek, L; Singh, B. K.; Wagner, M.; Walsh, A.; Sessitsch, A.; Schloter, M. 2020. Microbiome definition re-visited: old concepts and new challenges. Microbiome. 8: 1-22. https://doi.org/10.1186/s40168- 020-00875-0
4. Bühler, M. I.; Sánchez Toranzo, G.; Zaltz, S. 2000. La ranicultura: una alternativa productiva. Top. Graph. Argentina.
5. Cai, X.; Wen, J. S.; Long, H.; Ren, W.; Zhang, X.; Huang, A. Y.; Xie, Z. Y. 2022. The probiotic effects, dose, and duration of lactic acid bacteria on disease resistance in *Litopenaeus vannamei*. Aquac. Rep. 26: 101299. https://doi.org/10.1016/j.aqrep.2022.101299
6. CDC. Vancomycin-Resistant Enterococci (VRE) and the Clinical Laboratory HAI CDC. 2020. https://www.cdc.gov/hai/settings/lab/vreclinical-laboratory.html.
7. Clinical and Laboratory Standards Institute. Methods for antimicrobial dilution and disk susceptibility testing of infrequently isolated or fastidious bacteria 3rd ed. CLSI guideline M45. 2015. Clinical and Laboratory Standards Institute. Wayne. PA. USA.
8. Clinical and Laboratory Standards Institute. Performance standards for antimicrobial susceptibility testing, 32nd ed. CLSI guideline M100. 2022. Wayne. PA. USA.
9. Crowe, J. H.; Crowe, L. M.; Carpenter, J. F.; Wistrom, C. A. 1987. Stabilization of dry phospholipid-bilayers and proteins by sugars. Biochem. J. 242(1): 1-10. https://doi.org/10.1042/bj2420001
10. Dehkordi, R. A. F.; Karimi, I.; Karimi, B.; Eshkaftaki, R. G.; Abtahi, R.; Mohammadi, H. 2023. Effect of pancreatin on acute pancreatitis resulting from L-arginine administration in mice, a morpho-histopathological and biochemical study. Braz. J. Pharm. Sci. 59: e21494. https://doi.org/10.1590/s2175-97902023e21494
11. Densmore, C. L.; Green, D. E. 2007. Diseases of amphibians. ILAR J. 48(3): 235-254. https://doi.org/10.1093/ilar.48.3.235
12. De Oliveira, D. M.; Forde, B. M.; Kidd, T. J.; Harris, P. N.; Schembri, M. A.; Beatson, S. A.; Paterson, D. L.; Walker, M. J. 2020. Antimicrobial resistance in ESKAPE pathogens. Microbiol. Rev. 33(3): e00181-19. https://doi.org/10.1128/cmr.00181-19
13. Di Rienzo, J. A.; Casanoves, F.; Balzarini, M. G.; Gonzalez, L.; Tablada, M. R. C. W.; Robledo, C. W. 2020. InfoStat versión 2020. Centro de Transferencia InfoStat, FCA, Universidad Nacional de Córdoba, Argentina. URL http://www. infostat. com. ar

14. Escobar-Sánchez, M.; Carrasco-Navarro, U.; Juárez-Castelán, C.; Lozano-Aguirre, L.; Pérez-Chabela, M. L.; Ponce-Alquicira, E. 2022. Probiotic properties and proteomic analysis of *Pediococcus pentosaceus* 1101. Foods. 12(1): 46. https://doi.org/10.3390/ foods12010046
15. European Food Safety Authority Panel on Additives and Products or Substances used in Animal Feed (FEEDAP). 2018.efsa.2018.5206
16. Fiocco, D.; Longo, A.; Arena, M. P.; Russo, P.; Spano, G.; Capozzi, V. 2020. How probiotics face food stress: They get by with a little help. Crit. Rev. Food Sci. Nutr. 60(9): 1552-1580. https:// doi.org/10.1080/10408398.2019.1580673
17. Garza, M.; Mohan, C. V.; Rahman, M.; Wieland, B.; Häsler B. 2019. The role of infectious disease impact in informing decision-making for animal health management in aquaculture systems in Bangladesh. Prev. Vet. Med. 167: 202-213. https://doi.org/10.1016/j. prevetmed.2018.03.004
18. Gloor, G. B.; Reid, G. 2016. Compositional analysis: a valid approach to analyze microbiome high-throughput sequencing data. Can. J. Microbiol. 62(8): 692-703. https://doi.org/10.1139/ cjm-2015-0821
19. Hadfield, C. A.; Whitaker, B. R. 2005. Amphibian emergency medicine and care. Seminars in avian and exotic pet medicine. 14(2): 79-89. https://doi.org/10.1053/j.saep.2005.04.003
20. Hidano, A.; Yamamoto, T.; Hayama, Y.; Muroga, N.; Kobayashi. S.; Nishida, T.; Tsutsui, T. 2015. Unraveling antimicrobial resistance genes and phenotype patterns among *Enterococcus faecalis* isolated from retail chicken products in Japan. PloS One. 10(3): e0121189. https:// doi.org/10.1371/ journal.pone.0121189
21. Igbinosa, E. O.; Beshiru, A. 2019. Antimicrobial resistance, virulence determinants, and biofilm formation of *Enterococcus* species from ready-to-eat seafood. Front. Microbiol. 10: 728. https://doi.org/ 10.3389/fmicb.2019.00728
22. Indriani, S.; Sae Leaw, T.; Benjakul, S.; Quan, T. H.; Karnjanapratum, S.; Nalinanon, S. 2022. Impact of different ultrasound-assisted processes for preparation of collagen hydrolysates from Asian bullfrog skin on characteristics and antioxidative properties. Ultrason. Sonochem. 89: 106163. https://doi.org/ 10.1016/j.ultsonch.2022.106163
23. Jawan, R.; Abbasiliasi, S.; Tan, J. S.; Kapri, M. R.; Mustafa, S.; Halim, M. 2022. Influence of type and concentration of lyoprotectants storage temperature and storage duration on cell viability and antibacterial activity of freeze-dried lactic acid bacterium *Lactococcus lactis* Gh1. Dry. Technol. 40(9): 1774-1790. https://doi.org/ 10.1080/07373937.2021.1874968
24. Kandil, S.; El Soda, M. 2015. Influence of freezing and freeze drying on intracellular enzymatic activity and autolytic properties of some lactic acid bacterial strains. Adv. Microbiol. 5: 371-382. https://doi.org/ 10.4236/aim.2015.56039
25. Kang, C. H.; Gu, T.; So, J. S. 2018. Possible probiotic lactic acid bacteria isolated from oysters (*Crassostrea gigas*). Probiotics Antimicrob. Proteins. 10(4): 728-739. https://doi.org/ 10.1007/s12602-017-9315-5
26. Ko, H. I.; Jeong, C. H.; Hong, S. W.; Eun, J. B.; Kim, T. 2022. Optimizing conditions in the acid tolerance test for potential probiotics using response surface methodology. Microb. Spectrum. 10(4): e01625-22. https://doi.org/10.1128/spectrum.01625-22
27. Maji, U. J.; Mohanty, S.; Mahapatra, A. S.; Maiti, N. K. 2016. Diversity and probiotic potentials of putative lactic acid bacteria for application in freshwater aquaculture. Turkish J. Fish Aquat. Sci. 16: 805-818. https://doi.org/10.4194/1303-2712-v16_4_07
28. Melchior, S.; Marino, M.; Innocente, N.; Calligaris, S.; Nicoli, M. C. 2020. Effect of different biopolymer-based structured systems on the survival of probiotic strains during storage and *in vitro* digestion. J. Sci. Food Agric. 100: 3902-3909. https://doi.org/10.1002/ jsfa.10432
29. Mendes, S. D. N. C.; Esteves, C. M.; Mendes, J. A. V.; Feres, M.; Figueiredo, N.; de Miranda, T. S.; Shibli, J. A.; Figueiredo, L. C. 2023. Systemic antibiotics and chlorhexidine associated with periodontal therapy: Microbiological effect on intraoral surfaces and saliva. Antibiotics. 12(5): 847. https://doi.org/ 10.3390/antibiotics12050847
30. Minitab, LLC. 2018. Statistical (versión 2018) [Software]. www.minitab.com
31. Montel Mendoza, G.; Pasteris, S. E.; Ale, C. E.; Otero, M. C.; Bühler, M. I.; Nader Macías, M. E. 2012. Cultivable microbiota of *Lithobates catesbeianus* and advances in the selection of lactic acid bacteria as biological control agents in raniculture. Res. Vet. Sci. 93: 1160-1167. https:// doi.org/ 10.1016/j.rvsc.2012.05.007
32. Montel Mendoza, G.; Pasteris, S. E.; Otero, M. C., Nader Macías, M. E. F. 2014. Survival and beneficial properties of lactic acid bacteria from raniculture subjected to freeze-drying and storage. J. Appl. Microbiol. 116: 157-166. https://doi.org/ 10.1111/jam.12359
33. Montel Mendoza, G.; Ale, C. E.; Nader Macías, M. E. F.; Pasteris, S. E. 2015. Characterization of a bacteriocin produced by *Enterococcus gallinarum* CRL 1826 isolated from captive bullfrog: evaluation of its mode of action against *Listeria monocytogenes* and Gram-negatives. J. Bioprocess Biotech. 5: 250-256. https://doi.org/ 10.4172/2155-9821.1000250
34. Niederle, M. V.; Bosch, J.; Ale, C. E.; Nader Macías, M. E.; Aristimuno Ficoseco, C.; Toledo, L. F.; Valenzuela, Sánchez, A.; Soto Azat, C.; Pasteris, S. E. 2019. Skin-associated lactic acid bacteria from North American bullfrogs as potential control agents of *Batrachochytrium dendrobatidis*. PLoS One. 14(9): e0223020. https://doi.org/ 10.1371/journal. pone.0223020

35. Pasteris, S. E.; Bühler, M. I.; Nader Macías, M. E. 2006. Microbiological and histological studies in farmed-bullfrog (*Rana catesbeiana*) displaying red-leg syndrome. Aquaculture. 251: 11-18. https://doi.org/ 10.1016/j.aquaculture.2005.05.007
36. Pasteris, S. E.; Roig Babot, G.; Otero, M. C.; Nader Macías, M. E. 2009. Beneficial properties of lactic acid bacteria isolated from a *Rana castesbeiana* hatchery. Aquac. Res. 40: 1605-1615. https://doi.org/10.1111/j.1365-2109.2009.0226.x
37. Pasteris, S. E.; Vera Pingitore, E.; Roig Babot, G.; Otero, M. C.; Bühler, M. I.; Nader Macías, M. E. 2009. Characterization of the beneficial properties of lactobacilli isolated from bullfrog (*Rana catesbeiana*) hatchery. Antonie van Leeuwenhoek. 95: 375-385. https://doi.org/10.1007/s10482-009-9329-4
38. Pasteris, S. E.; Montel Mendoza, G.; Llanos, R. J.; Pucci Alcaide, F.; Nader Macías, M. E. F. 2017. Preliminary assessment of *in vivo* safety of potentially probiotic lactic acid bacteria for American bullfrog culture. Aquac. Res. 48(5): 2157-2172. https://doi.org/ 10.1111/are.13053
39. Pereira, S. A.; Jerônimo, G. T.; Marchiori, N. C.; Oliveira, H. M.; Jesus, G. F. A.; Schmidt, E. C.; Bouzon, Z. L.; Vieira, F. N.; Martins, M. L.; Mouriño, J. L. P. 2018. Tadpoles fed supplemented diet with probiotic bacterium isolated from the intestinal tract of bullfrog *Lithobates catesbeianus*: Haematology, cell activity and electron microscopy. Microb. Pathog. 114: 255-263. https:// doi.org/10.1016/j.micpath.2017.11.033
40. Pereira, W. A.; Mendonça, C. M. N.; Urquiza, A. V.; Marteinsson, V.; LeBlanc, J. G.; Cotter, P. D.; Villalobos, E. F.; Romero, J.; Oliveira, R. P. 2022. Use of probiotic bacteria and bacteriocins as an alternative to antibiotics in aquaculture. Microorganisms. 10(9): 1705. https://doi.org/10.3390/microorganisms10091705
41. Pospiech, A.; Neumann, B. 1995. A versatile quick-prep of genomic DNA from Gram-positive bacteria. Trends Genet. 11: 217-218.
42. Romyasamit, C.; Saengsuwan, P.; Boonserm, P.; Thamjarongwong, B.; Singkhamanan, K. 2022. Optimization of cryoprotectants for freeze-dried potential probiotic *Enterococcus faecalis* and evaluation of its storage stability. Dry. Technol. 40(11): 2283-2292. https://doi.org/10.1080/07373937.2021.1931294
43. Sahoo, T. K.; Jena, P. K.; Nagar, N.; Patel, A. K.; Seshadri, S. 2015. *In vitro* evaluation of probiotic properties of lactic acid bacteria from the gut of *Labeo rohita* and *Catla catla*. Probiotics Antimicrob. Proteins. 7(2): 126-136. https://doi.org/10.1007/s12602-015-9184-8
44. Salama, S. A. E. H. 2022. Bacterial pathogens causing the blue crab (*Callinectes sapidus*) mortality at Suez Canal (El-Temsah Lake) in Ismailia Governorate. Egypt J. Aquat. Biol. Fish. 26(2): 151-168. https://doi.org/10.21608/ejabf.2022.226167
45. Sambrook, J.; Gething, M. J. 1989. Protein structure Chaperones paperones. Nature. 342(6247): 224-225.
46. Silla, A. J.; Calatayud, N. E.; Trudeau, V. L. 2021. Amphibian reproductive technologies: approaches and welfare considerations. Conserv. Physiol. 9(1): coab011. https://doi.org/10.1093/conphys/coab011
47. Stevens, E. C.; Hume, I. D. 1995. Digestion of carbohydrate, lipids and protein. In Comparative Physiology of the Vertebrate Digestive System. 152-171. Cambridge Academic Press 2nd ed.
48. Stone, G. G.; Newell, P.; Bradford, P. A. 2018. *In vitro* activity of ceftazidime-avibactam against isolates from patients in a phase 3 clinical trial for treatment of complicated intra-abdominal infections. Antimicrob. Agents. Chemother. 62(7): e02584-17. https://doi.org/10.1128/aac.02584-17
49. Szopa, K.; Szajnar, K.; Pawlos, M.; Znamirowska-Piotrowska, A. 2023. Probiotic fermented goat's and sheep's milk: effect of type and dose of collagen on survival of four strains of probiotic bacteria during simulated *in vitro* digestion conditions. Nutrients. 15(14): 3241. doi:10.3390/nu15143241
50. Teixeira, R. D.; Mello, S. C. P.; dos Santos, C. A. L. 2001. The world market for frog legs. Food and Agriculture Organization of the United Nations, GLOBEFISH. Fishery Industries Division. 68: 1-44.
51. Timmons, P. B.; Hewage, C. M. 2021. Conformation and membrane interaction studies of the potent antimicrobial and anticancer peptide palustrin-Ca. Sci. Rep. 11(1): 22468. https://doi.org/10.1038/s41598-021-01769-3
52. Tong, Q.; Cui, L. Y.; Bie, J.; Han, X. Y.; Hu, Z. F.; Wang, H. B.; Zhang, J. T. 2021. Changes in the gut microbiota diversity of brown frogs (*Rana dybowskii*) after an antibiotic bath. BMC Vet. Res. 17(1): 1-13. https://doi.org/10.1186/s12917-021-03044-z
53. Vera Pingitore, E.; Bru, E.; Nader Macías, M. E. 2012. Effect of lyophilization and storage temperature on the activity of salivaricin CRL 1328, a potential bioactive ingredient of a urogenital probiotic product. J. Gen. Appl. Microbiol. 58(2): 71-81. https://doi.org/10.2323/jgam.58.71
54. Wang, H.; Zhou, N.; Zhang, R.; Wu, Y.; Zhang, R.; Zhang, S. 2014. Identification and localization of gastrointestinal hormones in the skin of the bullfrog *Rana catesbeiana* during periods of activity and hibernation. Acta Histochem. 116(8): 1418-1426. https://doi.org/10.1016/j.acthis.2014.09.005

55. Yang, P.; Zheng, Y.; Zou, X.; Sun, Y.; Liu, Y. 2023. Comparative transcriptomic analysis of gene expression profiles in the liver and spleen of American bullfrog (*Lithobates catesbeianus*) in response to *Citrobacter freundii* infection. J. World Aquac. Soc. 55(1): 1-20. https://doi.org/10.1111/jwas.12999

Acknowledgements, Financial Support, and Full Disclosure

Financial support from Consejo de Investigaciones de la Universidad Nacional de Tucumán (PIUNT D-528) and Agencia Nacional de Promoción Científica y Tecnológica (PICT 2017-2244) are gratefully acknowledged.

The authors declare that they have no known competing financial interests or personal relationships that could have appeared to influence the work reported in this paper.

Net Protein Requirements for Maintenance and Weight gain in Male Guinea Pigs (*Cavia porcellus*) of the Peru Breed

Requerimientos de proteína neta para mantenimiento y ganancia de peso en cuyes machos (*Cavia porcellus*) de la raza Perú

William Armando Tapie Canacuan [1], Sandra Lucia Posada-Ochoa [2], Jaime Ricardo Rosero-Noguera [2]

Originales: *Recepción:* 18/08/2024 - *Aceptación:* 25/02/2025

ABSTRACT

Net protein requirements for weight gain (NP_g) and maintenance (NP_m) in meat-producing guinea pigs are not yet established. The objective of this study was to estimate the requirements for NP_m and NP_g in male guinea pigs of the Peru breed using the comparative slaughter method. Sixty guinea pigs with an initial body weight (BW) of 393 ± 55 g were distributed in five groups of 12 animals. The animals were fed a pelleted diet. At the beginning of the experiment, a reference group with a BW 385.9 ± 44.5 g was slaughtered. Two groups were fed *ad libitum*, another group received 75% of the feed provided to the *ad libitum* groups, and a fifth group was kept at the maintenance level. One of the *ad libitum*-fed groups was slaughtered when its BW reached 846.6 ± 48 g. The other animals, distributed according to their feeding level, were slaughtered when the second *ad libitum*-fed group reached 1197 ± 84 g BW. The NP_m requirement was 3.97 g/kg/$EBW^{0.75}$ (empty body weight). And the requirement was NP_g 2.5 g/kg $EBW^{0.75}$. The protein use efficiency was 0.629.

Keywords
crude protein • retained protein • digestible protein • requirement protein

https://doi.org/10.48162/rev.39.200

1 Universidad Católica de Oriente. Grupo de Investigación GIAZ. AA 008. Rionegro. Colombia. * watapiec@unal.edu.co
2 Universidad de Antioquia. Facultad de Ciencias Agrarias. Grupo de Investigación en Ciencias Agrarias-GRICA, AA 1226. Medellín-Colombia.

Licenses Creative Commons Attribution - Non Commercial - Share Alike

Resumen

Los requerimientos de proteína neta para ganancia de peso (PN_g) y mantenimiento (PN_m) en cuyes de producción de carne aún no han sido establecidos. El objetivo fue estimar los requerimientos de PN_m y PN_g en cuyes machos de la raza Perú utilizando la metodología de sacrificio comparativo. Se utilizaron 60 cuyes con un peso vivo (PV) inicial de 393 ± 55 g, distribuidos en cinco grupos de 12 animales. Los animales se alimentaron con una dieta peletizada. Al inicio del experimento, se sacrificó un grupo de referencia con un PV 385,9 ± 44,5 g. Dos de los grupos fueron alimentados *ad libitum*, mientras que a otro grupo se le proporcionó el 75% en comparación con los que tenían acceso *ad libitum*, y un quinto grupo se mantuvo en el nivel de mantenimiento. Uno de los grupos que tuvo acceso *ad libitum* fue sacrificado cuando su PV alcanzó 846,6 ± 48 g. Los demás animales, distribuidos según su nivel de alimentación, fueron sacrificados cuando el otro grupo con acceso *ad libitum* alcanzó 1197 ± 84 g PV. El requerimiento de PN_m fue 3,97 g/kg/$PCV^{0,75}$ (peso corporal vacío) y PN_g 2,5 g/kg/$PCV^{0,75}$. La eficiencia de utilización de proteína fue 0,629.

Palabras clave
proteína cruda • proteína retenida • proteína digestible • requerimiento de proteína

Introduction

The guinea pig (*Cavia porcellus*) is an herbivorous, monogastric mammal native to Peru, Ecuador, Bolivia, and Colombia, where it is primarily raised for meat production (5). In these countries, the demand for guinea pig meat has increased due to its nutritional quality, palatability, and, above all, the population's consumption habits (10). Its production has spread to countries such as Brazil, Cameroon, the Democratic Republic of Congo, Tanzania, and Mexico (3, 26, 35). Guinea pig farming has contributed to improved family diets, food security, and overall economic conditions (10).

However, guinea pig production as a food source is relatively unknown worldwide (7). Guinea pigs have been used for scientific research (27) or as pets, and some of the available reference information on husbandry and diet is based on work under laboratory conditions (18 Since meat-producing guinea pigs have higher productive yields, these recommendations are not applicable (6, 8). Thus, the information available on nutritional requirements for maintenance and weight gain of this species is limited with little or no research available (19, 27). Protein requirements can be divided into maintenance and weight gain and are the fundamental components of muscle tissue, certain hormones, and all enzymes (23). Proteins and amino acids are indispensable nutrients for guinea pig performance. If guinea pigs do not receive adequate protein, they do not achieve the growth potential characteristic of their breed (32). In addition, the protein deposition of an animal is considered the most important determinant for weight gain, due to the high water content of protein-rich tissues (33).

Usually, rations for guinea pigs are formulated with the 18% crude protein (CP) recommended by the NRC (1995) for laboratory animals. In some cases, because the rabbit is a species with digestive anatomy and physiology similar to that of guinea pigs, comparisons have been made in terms of feeding and nutrient utilization efficiency at the digestive level (34, 36). So far, no studies report nutritional requirements discriminated in maintenance requirements and weight gain in guinea pigs for meat production (32). Based on the above aspects, this study aimed to determine the protein requirements for maintenance and weight gain in male guinea pigs of the Peru breed.

Material and Methods

Animal ethics: The experiment was approved by the Ethics Committee for Animal Experimentation of the University of Antioquia (Act N°138 of 09 February 2021).

Housing and Handling of Animals

A total of 60 male guinea pigs of the Peru breed were used. All animals were given a 20-day acclimation period to adapt to handling and the experimental diet. During the entire experimental period, the animals were housed in individual metabolic cages 0.3 m long x 0.3 m wide x 0.25 m high, which were equipped with an automatic feeder and drinker The average temperature was 18°C, with a relative humidity of 80%, annual precipitation of 2304 mm, and an altitude of 2150 meters above sea level (masl). The experiment began when the animals were 35 days old and had an initial body weight (BW) of 393 ± 55 g. The animals were weighed every seven days to monitor daily weight gain (DWG) to the amount of feed to be fed.

Diet and Dietary Levels

Animal diet was balanced according to the NRC's (1995) report. Although this report suggests the inclusion of wheat (23.6%) and whole oats (25.2%); for reasons of availability, it was decided to replace them with rice and corn meal (table 1), respectively. The feed was provided in pellet form twice daily, at 7:00 and 15:00 h.

Table 1. Ingredients and percentage composition on a dry basis of the experimental diet.
Tabla 1. Ingredientes y composición porcentual en base seca de la dieta experimental.

Ingredient	Quantity %
Alfalfa hay	35.0
Soybean meal, expeller	12.0
Corn	44.3
Rice flour	3.0
Soybean oil	3.0
Dicalcium phosphate	0.5
Calcium carbonate	1.0
Salt	0.8
Mineral premixes and vitamins*	0.4
Dry matter	92.1
Crude protein	16.4
Ether extract	4.0
Ash	5.5
Neutral detergent fiber	22
Acid detergent fiber	16
Non-fiber carbohydrates[2]	50.5
Digestible energy (kcal kg^{-1}DM)	3705
Metabolizable energy (kcal kg^{-1}DM)	3520

*Minerals: cobalt 1.5; copper 6.6; manganese 39.7; zinc 19.8; iodine 1.1; iron 50; selenium 0.3 (mg kg^{-1}). Vitamins: vitamin A 6614; vitamin D3 2200 (IU kg^{-1}), vitamin E 22; vitamin K 5; thiamine 4.4; riboflavin 3.3; niacin 11; pantothenic acid 11; choline 529; pyridoxine 5; folic acid 4.8; biotin 2.2; ascorbic acid 250; methionine hydroxy analog 500(mgkg^{-1});vitaminB12 11 µg kg^{-1}. Antioxidant BHT0.1gkg^{-1};Salinomycin 20 mg kg^{-1}. Source NRC (1995). 2 CNF=100%-(Crude protein+Ether extract+Ash+Neutral detergent fiber).

*Minerales: cobalto 1,5; cobre 6,6; manganeso 39,7; zinc 19,8; yodo 1,1; hierro 50; selenio 0,3 (mg/kg). Vitaminas: vitamina A 6614; vitamina D3 2200 (UI/kg), vitamina E 22; vitamina K 5; tiamina 4,4; riboflavina 3,3; niacina 11; ácido pantoténico 11; colina 529; piridoxina 5; ácido fólico 4,8; biotina 2,2; ácido ascórbico 250; metionina hidroxi análogo 500 (mg/kg); vitamina B1211µg/kg.Antioxidante BHT 0,1 g/kg; Salinomicina 20 mg/kg. Fuente NRC (1995).

[2] CNF= 100%-(Proteína bruta+Extracto Etéreo+Cenizas+Fibra detergente neutra).

The diet was provided at three levels: *ad libitum* feeding (24 animals), where feed rejected (orts) accounted for 20% of the offered amount; restricted feeding (12 animals), with intake set at 75% of the ad libitum level; and maintenance feeding (12 animals), based on an intake of 150-160 kcal DE kg^{-1} $BW^{0.75}$, which is 30-40% higher than the 115.2 kcal DE kg^{-1} $BW^{0.75}$ reported by Matin *et al.* (1975) for laboratory guinea pigs. The DE was considered 95% of ME, following Xiccato and Trocino (2020); the EM was calculated using the diet composition values (table 1). Then, the diet energy density was estimated at 3705 kcal DE kg^{-1}. The described feeding levels are necessary to establish energy requirements, using linear regression, according to comparative slaughter method (22).

Digestibility Test

To determine the retained protein (RP) and crude protein (CP) losses associated with the digestive process, an apparent digestibility test was performed 28 days after the start of the experiment at three feeding levels (*ad libitum*, restricted, maintenance) with six animals each. The test lasted six days. Dry matter intake (DMI) was calculated as the difference between the amount of feed offered and the amount rejected by the animals. Each day, the rejected feed per animal was weighed and stored at -15°C, thus obtaining an individual composite sample for subsequent chemical analysis. Fecal dry matter production was determined by the total fecal collection procedure. Each day, in the morning and the afternoon, the feces were removed from the collection tray, stored individually, and frozen at -15°C.

Urine Collection

Simultaneously with the digestibility test, total urine collection was performed. Urine was stored in containers containing 5 ml of sulfuric acid (5% H_2SO_4) to avoid nitrogen (N) losses in the form of ammonium and was stored at -15°C. Urinary weight and volume were recorded daily. At the end of the six days, urine samples were pooled to obtain a composite sample per animal for subsequent chemical analysis.

Slaughter of Animals

The 60 guinea pigs were divided into five groups of twelve animals each and were slaughtered in three periods. The first group was slaughtered at the beginning of the experiment with a BW of 385.9 ± 44.5 g. This group was designated as the reference group, allowing for the estimation of the initial composition of the 48 animals culled later, facilitating the comparison of the final body composition with the initial composition. Twenty-eight days after the experiment began, a second group of 12 animals fed *ad libitum* with a BW of 846.6 ± 48 g was culled, marking this point as the intermediate slaughter. Finally, the remaining 36 animals, 12 per feeding level (*ad libitum*, restricted, and maintenance), were culled at 90 days, when one of the *ad libitum*-fed groups reached a BW of 1189.7 ± 105 g. Before slaughter, the animals were subjected to an 18-hour fasting, after which they were weighed to determine the shrunk body weight (SBW). For slaughter, a Dick KTBG captive bolt pistol (Friedr Dick GmbH & Co. Deizisau, Germany) was used. The procedure followed the method described by Limon *et al.* (2016). Immediately after the stunning, the jugular veins were bilaterally severed and blood was collected. Animals were depilated by exposing to water heated to 90°C for 10 seconds. Then, after weighting, gastrointestinal contents were removed. Empty body weights (EBW) were determined by the difference between the SBW and the weight of the gastrointestinal contents. Hair, blood, and body plus organs (BO) were stored separately at -15°C for later chemical analysis.

Chemical Analysis

The BO was ground in a mill model ML C012 (capacity 150kg h^{-1}, power 850W, voltage 110). In the offered and orts, feces, BO, hair, and blood were analyzed for DM (AOAC 2007; Method 39.1.02), ether extract (AOAC 2007; Method 39.1.05), CP (AOAC 2007; Method 39.1.19), ash (AOAC 2007; Method 39.1.09) and gross energy (GE) (LECO AC600 calorimetric pump, MI, USA). Only DM, CP, and GE were analyzed in the urine samples. The results for the body plus organs, hair, and blood were summed to obtain the body's chemical composition at each slaughter.

Crud Protein Balance

Each animal's CP intake (CPI) was determined by the difference between the amount of CP offered and rejected. Digestible protein intake (DPI) was obtained by comparing CPI and CP losses through feces. In the protein balance, RP was estimated by the difference between CPI and losses through urine and feces. In the comparative slaughter trial, the RP was obtained by the difference between the body RP at the time of slaughter and the beginning of the study, based on the body composition of the reference animals. Crud protein balance results were expressed in g/kg/$EBW^{0.75}$. The EBW value corresponded to the mean weight, obtained as (initial EBW + final EBW/2).

Net Protein Requirements for Weight Gain (NP_g) and Maintenance (NP_m)

The NP_g (g/kg $EBW^{0.75}$/day) corresponded to the average RP in animals fed *ad libitum* throughout the entire experimental period. From the regression parameters: $logy = a + b * logx$, where: y = $\log_{10}$ of total CP content and x = $\log_{10}$ of EBW. The net protein requirement per kg EBW was calculated by the derivative of the above equation, according to the following model (2): $y` = b * 10^{a} * x^{(b-1)}$, where: $y`$ = NP_g required to gain one kg of EBW (g/kg/EWG/day) and x = EBW (kg). The equations were constructed with the information from the 24 animals fed *ad libitum* and the 12 animals from the restricted feeding level. The NP_m requirement was estimated using linear regression equations between retained nitrogen (RN, g/kg $EBW^{0.75}$/day) in the EBW of the animals during the experimental period (y) as a function of nitrogen intake (NI, g/kg $EBW^{0.75}$/day) from the diet (x). To estimate the dietary CP requirement for maintenance (CP_m), the intersection with the X-axis was multiplied by a factor of 6.25. Endogenous and metabolic losses were estimated based on the negative intersection with the Y-axis, while the slope of the line was considered as the efficiency of nitrogen utilization from the feed (16). The digestible protein requirements for maintenance (DP_m) and digestible protein for weight gain (DP_g) were estimated by the ratio of the CP digestibility coefficient. The conversion of the EBW requirement into a BW requirement was carried out using the factor derived from the BW/EBW ratio.

Statistical Analysis

The results of the metabolism trial were analyzed using a completely randomized design through analysis of variance, considering the feeding level (maintenance, restricted, and *ad libitum*) as a fixed effect with six animals per group. Means were compared using Tukey's test, with statistical differences considered significant at $p < 0.05$. In the linear regression analyses conducted with the data obtained from the comparative slaughter trial, the significance ($p < 0.05$) of the slope and intercept in each model was verified. Data processing was performed using the R statistical package (29).

Results

Protein Balance and Body Composition

Table 2 (page 6) presents the CP balance data for the three feeding levels: maintenance, restricted, and *ad libitum*. DMI and CPI were significantly higher in animals fed ad libitum ($p < 0.05$). Protein digestibility was significantly lower in animals fed *ad libitum (*$p<0.05$). The percentage of RP estimated in the digestibility test decreased as CPI increased ($p<0.05$). CP in feces differed with feeding level ($p<0.05$). When the percentage of CPI in urine was compared to DPI and CPI, no differences were present.

Comparative Slaughter Trial

Table 3 (page 6) shows weight and body composition at slaughter for three feeding levels and a reference group of animals slaughtered at the beginning of the experiment. The average BW of the restricted-fed animals represented about 80% of the BW of the *ad libitum* animals. The EBW/BW ratio, fat, and BW increased with feeding level ($p<0.05$), while water content decreased($p<0.05$). CP and ash were stable, with values close to 20, and 5%, respectively.

Table 4 (page 7) presents the results of comparative slaughter at the different feeding levels (*ad libitum*, restricted, maintenance). DWG was proportional to feeding level. a*d libitum-fed* animals were found to have higher DWG and to be more efficient in RP at an average weight of 846.6 g, at 28 experimental days. The average RP of animals fed *ad libitum* and slaughtered at 90 days was considered the requirement NP_g (2.5 g/kg $BW^{0.75}$/day).

Table 2. Protein partitioning in *ad libitum*, restricted, and maintenance-fed guinea pigs.
Tabla 2. Partición de proteína en cuyes alimentados *ad libitum*, restringidos y de mantenimiento.

Items	Maintenance	Restricted	*ad libitum*
Experimental days	28	28	28
BW (g)	481.8^{b} ± 60	611^{a} ± 81	698^{a} ± 34
DMI (g/day)	23.19^{b} ± 2.3	37.21^{a} ± 5	42.9^{a} ± 3.5
Crude protein intake and excretion (g/d)			
CPI	3.8^{b} ± 0.3	6.09^{a} ± 0.8	6.90^{a} ± 0.6
Fecal CP	0.59^{c} ± 0.08	1.1^{b} ± 0.18	1.7^{a} ± 0.22
DPI	3.21^{b} ± 0.3	4.99^{a} ± 0.7	5.21^{a} ± 0.5
CP urine	0.04^{a} ± 0.0	0.06^{a} ± 0.01	0.09^{a} ± 0.08
RP	3.17^{b} ± 0.3	4.93^{a} ± 0.7	5.11^{a} ± 0.5
Protein utilization efficiency (%)			
DP	84.5^{a} ± 1.3	81.9^{a} ± 2.3	75.4^{b} ± 2.5
RP/CPI	83.5^{a} ± 1.3	80.9^{a} ± 2.6	74.1^{b} ± 2.1
RP/DPI	98.8^{a} ± 0.3	98.8^{a} ± 0.4	98.2^{a} ± 1.3
CP feces/CPI	15.5^{b} ± 1.4	18.1^{b} ± 2.4	24.5^{a} ± 2.6
CP urine/CPI	0.95^{a} ± 0.2	0.95^{a} ± 0.3	1.3^{a} ± 1.0
CP urine/DPI	1.1^{a} ± 0.3	1.2^{a} ± 0.4	1.7^{a} ± 1.3

BW = body weight; DMI = dry matter intake; CP = crude protein; DPI = digestible protein intake; CPI=crudeproteinintake; RP = retained protein; EBW = empty body weight; DP = digestible protein. a,b,c. Averages within the same row with different letters differ ($p < 0.05$).

PVC = peso vivo corporal; CMS = consumo de materia seca; PC = Proteína cruda; CPD = consumo de proteína digestible; CPC = Consumo de proteína cruda; PR = Proteína retenida; PCV = peso corporal vacío; PD = proteína digestible, ^{a,b,c} Promedios dentro de la misma fila con letras diferentes difieren ($p < 0,05$).

Table 3. Body composition at slaughter with three feeding levels in guinea pigs.
Tabla 3. Composición corporal al sacrificio bajo tres niveles de alimentación en cuyes.

Items	Feeding level				
	Reference group	Maintenance	Restricted	*ad libitum*	
Experimental days	-	90	90	28	90
BW (g)	385.9^{c} ± 45	495.3^{c} ± 80	949.1^{b} ± 185	846.6^{b} ± 48	1189.7^{a} ± 105
EBW (g)	317.1^{c} ± 39	410.2^{c} ± 86.7	862.5^{b} ± 198.9	784.8^{b} ± 44.8	1128.4^{a} ± 103.6
EBW/BW	0.82^{c} ± 0.04	0.82^{c} ± 0.05	0.90^{b} ± 0.04	0.92^{ab} ± 0.01	0.94^{a} ± 0.01
EBW$^{0.75}$ (kg)	0.42^{c} ± 0.04	0.51^{c} ± 0.07	0.89^{b} ± 0.15	0.83^{b} ± 0.03	1.09^{a} ± 0.07
Chemical composition of EBW (%)					
Water	71.7^{a} ± 1.5	70.7^{a} ± 1.7	65.0^{b} ± 2.3	66.0^{b} ± 0.7	59.0^{c} ± 1
Fat	1.6^{c} ± 0.2	3.5^{c} ± 1.3	10.0^{b} ± 3.4	10.2^{b} ± 0.9	16.2^{a} ± 1.3
Crud protein	20.3^{a} ± 1.5	20.3^{a} ± 1.1	20.0^{a} ± 1.1	19.8^{a} ± 1	20.8^{a} ± 1.3
Ash	5.4^{a} ± 0.7	5.2^{a} ± 0.6	5.2^{a} ± 0.5	4.9^{a} ± 0.2	5.0^{a} ± 0.8
GE (kcal/kg EBW)	1332^{c} ± 135	1404^{c} ± 154	2143^{b} ± 291	2090^{b} ± 97	2625^{a} ± 174

BW = body weight; EBW = empty body weight; $BW^{0.75}$=metabolic empty body weight; GE = gross energy, ^{a,b,c} Averages within the same row with different letters differ ($p < 0.05$).

PVC = peso vivo corporal; PCV = peso corporal vacío; $PCV^{0.75}$ = peso corporal vacío metabólico; EB = energía bruta, ^{a,b,c} Promedios dentro de la misma fila con letras diferentes difieren ($p < 0,05$).

Table 4. Daily weight gain, protein intake, and crud protein balance in guinea pigs across three feeding levels: results from a comparative slaughter study.

Tabla 4. Ganancia diaria de peso, consumo y balance de proteína cruda en cuyes bajo tres niveles de alimentación: resultados del estudio de sacrificio comparativo.

Items	Feeding level			
	Maintenance	Restricted	*ad libitum*	
BW (g)	495.3^{c} ± 80	949.1^{b} ± 185	846.6^{b} ± 48	1189.7^{a} ± 105
Experimental days	90	90	28	90
DMI (g/day)	21.7^{c} ± 3.1	37.4^{b} ± 6.4	49.6^{a} ± 2.8	48.8^{a} ± 4.1
DWG (g/day)	1.1^{d} ± 0.4	5.9^{c} ± 1.5	13.2^{a} ± 1.9	9.3^{b} ± 1.0
CPI (g/day)	3.5^{c} ± 0.5	6.1^{b} ± 1	8.0^{a} ± 0.4	7.8^{a} ± 0.6
CPI (g/kg EBW$^{0.75}$/day)	7.5^{d} ± 0.3	9.1^{c} ± 0.3	12.0^{a} ± 0.6	10.3^{b} ± 0.5
RP (g/day)	0.19^{b} ± 0.1	1.2^{c} ± 0.4	2.7^{a} ± 0.4	1.9^{b} ± 0.3
RP (g/kg EBW$^{0.75}$/day)	0.4^{d} ± 0.2	1.8^{c} ± 0.3	4.1^{a} ± 0.5	2.5^{b} ± 0.4
RP/CPI (%)	5.4^{c} ± 3.7	19.9^{b} ± 3.8	33.8^{a} ± 4.4	23.7^{b} ± 3.2
EBW$^{0.75}$ average (g)	468.6^{c} ± 59	667.5^{b} ± 96	663.5^{b} ± 25	760.7^{a} ± 37

BW = body weight; DMI = dry matter intake; EBW=empty bodyweight; DWG = daily weight gain; CPI = crude protein intake; RP = retained protein.

PVC = peso vivo corporal; CMS = consumo de materia seca; PCV = peso corporal vacío; GPD = ganancia de peso diaria; CPC = consumo de proteína cruda; PR = proteína retenida, ^{a,b,c} Promedios dentro de la misma fila con letras diferentes difieren ($p < 0,05$).

Net Protein Requirement for Weight Gain and Maintenance

Table 5 shows the equations used to estimate the NP_g requirement and the EBW. The equations exhibited a good fit with determination coefficients exceeding 0.93 (R^2).

Table 5. Equations for estimating empty body weight and net protein requirement for weightgain in guinea pigs.

Tabla 5. Ecuaciones para estimar el peso corporal vacío y el requerimiento de proteína neta para la ganancia de peso en cuyes.

Equation	R^2	Equation of NP requirements for gain (g/kg)
Log10 Protein = 2.315 ± 0.004 + 1.0681 ± 0.049*Log_{10}EBW	0.932	221* EBW$^{0.0681}$
EBW = -0.093 ± 0.023 + 1.0231 ± 0.023*BW	0.982	

EBW (kg) = empty body weight; BW (kg) = body weight; NP = net protein.

PCV (kg) = peso corporal vacío; PVC (kg) = peso vivo corporal; PN = proteína neta.

With the equation to estimate the NP_g requirement and the equation to estimate the BW (table 5). The NP_g requirements for different BW (900, 1000, 1100, and 1200 g) were expressed in different DWG (5, 10, 15, and 20 g) (table 6, page 8).

Figure 1 (page 8) shows the relationship between NI and RN, both variables expressed in g.kg^{-1} EBW$^{0.75}$ d^{-1}. The regression was constructed with animal data at the three feeding levels (*ad libitum*, restricted, and maintenance).

From the equation in figure 1 (page 8), NI was estimated when the RN was zero, corresponding to the N requirement for maintenance (1.01 g). This requirement was expressed in CP_m when multiplied by the factor 6.25 (6.32 g/kg/EBW$^{0.75}$/day). On the other hand, the regression intercept corresponded to endogenous and metabolic N losses (0.6359 g/kg EBW$^{0.75}$/day) and its slope represented the N utilization efficiency (0.629). Based on this efficiency, the NP_m requirement was determined to be 3.97 (g/kg/EBW$^{0.75}$/day). With the protein digestibility coefficient found in the digestibility test at the maintenance level (84.5 %), the DP_m was estimated at 5.34 g/kg EBW$^{0.75}$/day.

Table 6. Net protein requirements for weight gain in guinea pigs.

Tabla 6. Requerimientos de proteína neta para la ganancia de peso en cuyes.

BW(g)	EBW (g)	Protein EWG (g/kg)	Net protein requirement (g/day) at different BW gains (g)			
			5	10	15	20
900	828	217.8	1.00	2.00	3.01	4.01
1000	930	219.5	1.02	2.04	3.06	4.08
1100	1033	220.1	1.04	2.08	3.11	4.15
1200	1135	222.5	1.05	2.10	3.16	4.21

BW = body weight; EBW = empty body weight; EWG = empty body weight gain.

PVC = peso vivo corporal; PCV = peso corporal vacío; GPC = ganancia de peso corporal vacío.

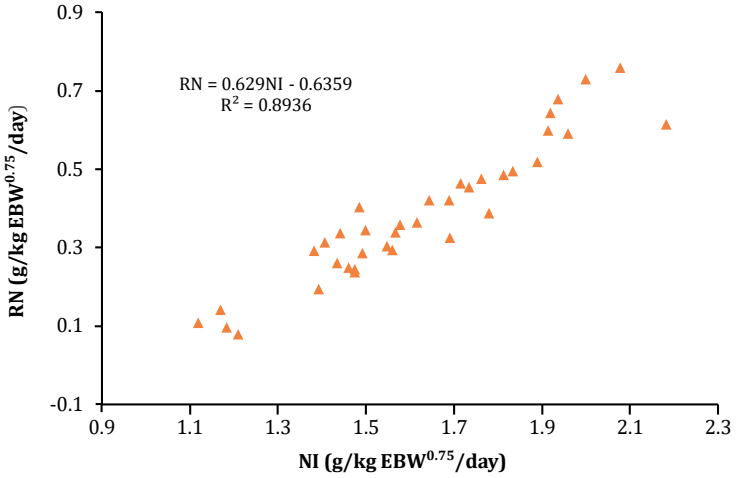


Figura 1. Relación entre el consumo de nitrógeno (CN g/kg PCV$^{0.75}$/día) y nitrógeno retenido (NR g/kg PCV$^{0.75}$/día).

Figure 1. Relationship between nitrogen intake (NI g/kg EBW$^{0.75}$/day) and nitrogen retained (RN g/kg EBW$^{0.75}$/day).

Table 7 presents the requirements of NP_m, NP_g, total NP, DP_m, DP_g, total DP, and total CP, for different BW gains (5, 10, 15, and 20 g/day) for animals of 900, 1000, 1100, and 1200 g of BW. Protein maintenance and gain increased as BW is higher and DWG increases.

Table 7. Protein requirements (g/day): net (NP), digestible (DP), and crude (CP), for maintenance ($_m$), gain ($_g$), and total for guinea pigs.

Tabla 7. Requerimientos de proteína (g/día): neta (NP), digestible (DP) y cruda (CP), para mantenimiento (m), ganancia (g) y total para cuyes.

BW, g	DWG, g/day	NP_m	NP_g	NP_{total}	$^*DP_m$	$^*DP_g$	$^*DP_{total}$	$^\dagger CP_{total}$
900	5	3.45	1.00	4.45	4.39	1.27	5.66	7.08
	10	3.45	2.00	5.45	4.39	2.55	6.94	8.67
	15	3.45	3.01	6.45	4.39	3.82	8.21	10.26
	20	3.45	4.01	7.46	4.39	5.10	9.48	11.85
1000	5	3.76	1.02	4.79	4.79	1.30	6.09	7.61
	10	3.76	2.04	5.81	4.79	2.60	7.38	9.23
	15	3.76	3.06	6.83	4.79	3.90	8.68	10.85
	20	3.76	4.08	7.85	4.79	5.19	9.98	12.48

BW = body weight; DWG = daily weight gain; * value calculated with the average protein digestibility coefficient of 80%; † value calculated with the protein utilization efficiency coefficient of 62.9%.

PVC = peso vivo corporal; GPC = ganancia de peso corporal vacío; * valor calculado con el coeficiente de digestibilidad promedio de la proteína del 80%; † valor calculado con el coeficiente de eficiencia de uso de la proteína del 62.9%.

1100	5	4.07	1.04	5.11	5.18	1.32	6.50	8.12
	10	4.07	2.08	6.15	5.18	2.64	7.82	9.77
	15	4.07	3.11	7.18	5.18	3.96	9.14	11.42
	20	4.07	4.15	8.22	5.18	5.28	10.45	13.07
1200	5	4.37	1.05	5.42	5.56	1.34	6.90	8.62
	10	4.37	2.10	6.47	5.56	2.68	8.23	10.29
	15	4.37	3.16	7.53	5.56	4.01	9.57	11.97
	20	4.37	4.21	8.58	5.56	5.35	10.91	13.64

BW = body weight; DWG = daily weight gain; * value calculated with the average protein digestibility coefficient of 80%; † value calculated with the protein utilization efficiency coefficient of 62.9%.

PVC = peso vivo corporal; GPC = ganancia de peso corporal vacío; * valor calculado con el coeficiente de digestibilidad promedio de la proteína del 80%; † valor calculado con el coeficiente de eficiencia de uso de la proteína del 62.9%.

Discussion

Protein Balance

Since CP losses in the feces increased with the feeding level ($p<0.05$) due to a higher intake, DP decreased. When comparing *ad libitum* and maintenance levels, an average variation of 9.1 percentage units in DP was observed ($p<0.05$). A lower DMI at the maintenance level may have prolonged the retention time of the feed in the gastrointestinal tract, which extends the period of exposure of the feed to digestive enzymes, thus facilitating feed absorption (17), which was finally reflected in higher protein digestibility. In general, a high protein digestibility was observed, 75.4% in *ad libitum* and 84.5% in the maintenance group. Similar findings have been recorded in the DP (77.02 to 86.56%) of wholesoybean meal in guinea pigs of the Peru breed (11). According to Chauca (1997), the guinea pig demonstrates a remarkable efficiency in the digestion of CP present in energyand protein foods compared to other monogastric species, thanks to its digestive physiology, which involves a first stage of enzymatic digestion in the stomach followed by a microbial phase in the cecum and colon. In a study with male guinea pigs, 63 feeds classified into fivecategories were evaluated (1, dry forages; 2, green forages; 3, agro-industrial and kitchen waste; 4, energy meals; 5, protein meals of animal and vegetable origin), an average DP of 73.53% was found (7). The higher digestibility observed in our study could be attributed to the quality of the feed used (table 1, page 3).

Crude protein losses in urine for guinea pigs with balanced feed intake have been estimated at 2.8 g/day (25), which value differs considerably from the value of 0.09 g/day found in this study, with a diet containing 16.4% CP (table 1, page 3). This difference can be attributed to the higher CP content in the diet (18.3 %) and higher DMI (49.49 g/day) reported by Bastianelli and Sauvant (1997). In rabbits, Lv *et al.* (2009) found that RP does not improve with increasing CP levels from 12 to 20% in the diet, which is ultimately reflected in higher CP excretion in feces and urine and low efficiency as CP supply increases. Because CP in urine and feces were lower at the maintenance level, RP (RP/CPI%) was higher, suggesting that animals use protein more efficiently under limited feeding conditions. Moon (1988) reports higher metabolic efficiency in guinea pigs under fasting conditions than other rodents.

Net Weight Gain Protein

The NP_g requirement was 2.5 g/kg $EBW^{0.75}$/day. The higher DWG of 13.2 g/day observed in the *ad libitum* animals of intermediate slaughter (846.6 g of BW), was related to the higher protein deposition (2.7 g/day) found in this same group of animals (table 4, page 7), this is due to the high content of water and protein in the tissues, which largely determines the DWG in an animal (4). This was also evidenced by the higher efficiency in the RP (33.8%) at 28 days of performance compared to the efficiency in the *ad libitum* animals at the final slaughter (23.7%). This is because as the guinea pig reaches the adult stage, it accumulates more fat than protein. According to De Figueiredo *et al.* (2020), the fat content of guinea pig meat is inversely proportional to the water and protein content. This was demonstrated by the body composition of reference animals versus *ad libitum* slaughter animals, in which fat content increased from 1.6 to 10.2 and 16.2 % as water content decreased from 71.7 to 66.0 and 59.0% for the reference animals and the two *ad libitum* groups, respectively (table 3, page 6). Similar body composition trends are reported at three months of age

(water 75%, protein 19%, and fat 2.64%) versus the body composition of guinea pigs at 18 months of age (water 72.6%, protein 19.6% and fat 5.7%) (31). NP_g requirements showed low variation, with values between 21.8 to 22.3 g/100 g for 828 to 1135 g of EBW, respectively (table 6, page 8). Studies reveal that protein in guinea pigs for meatproduction is very stable and even between the lines and age of the animal; Peru breed 19.34% (18), Inka and Andean 20.36 and 19.26% CP respectively (31). It has been shown that guinea pigs respond efficiently with rations of 20% CP and that higher levels have no beneficial effect on growth (37).

Net Maintenance Protein and Use Efficiency

Endogenous and metabolic losses of N were estimated at 0.6359 g/kg $EBW^{0.75}$. In rabbits with a BW between 2.1 to 2.8 kg and diets with a CP between 12 to 20%, an endogenous N value of 0.485 g/kg $BW^{0.75}$ has been reported (23), 23.7% higher than that found in this study. In contrast, in rabbits (New Zealand White x Californian)with a BW of 3.79 kg and a daily intake of 44.4 g DM/kg $BW^{0.75}$ from a protein-free diet, the endogenous N was 0.2539 g/kg $BW^{0.75}$ (15). Although thereare no reports on endogenous N losses in guinea pigs, the higher value found in comparison with rabbits suggests that N recycling and protein turnover may be more efficient in rabbits than in guineapigs in the conditions of this study. In guinea pigs, being smaller animals, the amount of endogenous N is related to protein turnover, which could result in higher metabolic rates and thus higher endogenous N values (30), explaining in part the higher losses compared to rabbits.

With the CP utilization efficiency of 0.629 (figure 1, page 8), an NP_m requirement of 3.97 g/kg $BW^{0.75}$ was estimated. This value was found to be lower than that reported for growing wool-type rabbits (4.87 g/kg $BW^{0.75}$) (21) and higher than the requirements in growing rabbits (NP_m 3.03 g/kg $BW^{0.75}$) (23). Despite the absence of data on NP_m requirements in guinea pigs, the physiological, digestive, and nutritional similarity between rabbits and guinea pigs (36) suggests that the data obtained here are biologically consistent. From the relationship between NI and RN, protein use efficiency values of 0.585 and 0.6781are reported for growing and finishing rabbits, respectively (23). Xiccato and Trocino (2020) reported a value of 0.56 for rabbits in general. These values agree with the 0.629 found in this study (figure 1, page 8). The efficiency observed for guinea pigs and that reported for rabbits is relatively high compared to other species such aslambs (0.29) (16) and beef cattle (0.34) (12). This could indicate that most of the amino acids absorbed from the guinea pig diet, were available for protein synthesis, rather than being used for other metabolic processes, such as gluconeogenesis (14).

On the other hand, based on the protein digestibility coefficient of 84.5% obtained with themaintenance feeding level (table 2, page 6), the amount of DP_m was determined to be 5.34 g/kg $EBW^{0.75}$. When comparing this result with the DP_m requirements for rabbits in the growingand finishing stages, which were 2.14 and 2.11 g/kg $BW^{0.75}$ respectively (23), notable differences exceeding 50% are observed. Parigi-Bini *et al.* (1992) report a DP_m requirement of 3.8 g/kg $BW^{0.75}$ for meat production rabbits, the latter value being the closest to the 5.34 found in this study, but still higher by 24%. The higher DP_m requirementsin guinea pigs can be attributed to the fact that small herbivorous mammals such as guinea pigs according to Sakaguchi (2003) have a higher energy and protein demand per unit of body mass than larger herbivorous animals such as rabbits. However, it should be noted thatthis value can be directly affected by protein digestibility.

Conclusions

The requirements of NP_m and NP_g in male guinea pigs of the Peru breed were 3.97 (g/kg $EBW^{0.75}$) and 2.5 (g/kg $EBW^{0.75}$), respectively. These values exceed some of those proposed for rabbits, but they align with the concept that small animals have higher requirements in terms of metabolic weight.

References

1. AOAC (Association of Official Analytical Chemists). 2007. 18th ed. Official methods of analysis of AOAC International. AOAC Int. Gaithersburg. MD.
2. ARC (Agricultural Research Council). 1980. The nutrient requirements of ruminant livestock: Technical review. Published on behalf of the Agricultural Research Council by the Commonwealth Agricultural Bureaux. England. Farnham Royal.
3. Ayagirwe, R. B.; Meutchieye, F.; Manjeli, Y.; Maass, B. L. 2018. Production systems, phenotypic and genetic diversity, and performance of cavy reared in sub-Saharan Africa: a review. Livestock Research for Rural Development. 30: 1-12. http://www.lrrd.org/lrrd30/6/ayagi30105.html
4. Bastianelli, D.; Sauvant, D. 1997. Modelling the mechanisms of pig growth. Livestock Production Science. 51(1-3): 97-107. https://doi.org/10.1016/S0301-6226(97)00109-7
5. Benavides, B.; Cisneros-López, H. D.; Peláez-Sánchez, R. G. 2021. Evidencia molecular de Leptospira interrogans sensu stricto en Cavia porcellus (cuyes) destinados para el consumo humano en el municipio de Pasto, Nariño. Universidad y Salud. 24(1): 55-64. https://doi.org/10.22267/rus.222401.258
6. Castro, B. J.; Chirinos, P. D.; Calderón Inga, J. 2018. Calidad nutricional del rastrojo de maca (*Lepidium peruvianum Chacón*) en cuyes. Revista de Investigaciones Veterinarias del Perú. 29(2): 410-418. http://dx.doi.org/10.15381/rivep.v29i2.13405
7. Castro, B. J.; Chirinos, P. D. 2021. Nutritional value of some raw materials for guinea pigs (*Cavia porcellus*) feeding. Translational Animal Science. 5(2): 1-11. https://doi.org/10.1093/tas/txab019
8. Castro, B. J.; Chirinos, P. D.; Quijada-Caro, E. 2022. Digestible and metabolizable energy prediction models in guinea pig feedstuffs. Journal of Applied Animal Research. 50(1): 355-362. https://doi.org/10.1080/09712119.2022.2079647
9. Chauca, L. 1997. Producción de cuyes (Cavia porcellus). Roma: Organización de las Naciones Unidas para la Agricultura y Alimentación (FAO). http://www.fao.org/docrep/w6562s/w6562s00.HTM (accessed May 2023).
10. Chauca, L. 2020. Manual de crianza de cuyes. http://repositorio.inia.gob.pe/handle/20.500.12955/1077 (accessed May 2023).
11. Chillpa. C. 2022. Energía y proteína digestibles de la harina integral de soya (*Glycine max*) en cuyes (*Cavia porcellus* L.). Tesis. Universidad Nacional de San Antonio Abad del Cusco. http://hdl.handle.net/20.500.12918/6728
12. Chizzotti, M. L.; Tedeschi, L. O.; Valadares Filho, S. C. 2008. A meta-analysis of energy and protein requirements for maintenance and growth of Nellore cattle. Journal of Animal Science. 86(7): 1588-1597. https://doi.org/10.2527/jas.2007-0309
13. De Figueiredo, L. B.; Rodrigues, R. T.; Leite, M. F.; Gois, G. C.; Araújo, D. H.; de Alencar, M. G.; Queiroz, M. A. 2020. Effect of sex on carcass yield and meat quality of guinea pig. Journal of Food Science and Technology. 57: 3024-3030. https://doi.org/10.1007/s13197-020-04335-3
14. Galvani, D. B.; Pires, A. V.; Susin, I.; Gouvêa, V. N.; Berndt, A.; Abdalla, A. L.; Tedeschi, L. O. 2018. Net protein requirements and metabolizable protein use for growing ram lambs fed diets differing in concentrate level and roughage source. Small ruminant research. 165: 79-86. https://doi.org/10.1016/j.smallrumres.2018.05.012
15. García, A.; De Bias, J.; Carabaño, R. 2004. Effect of type of diet (casein-based or protein-free) and caecotrophy on ileal endogenous nitrogen and amino acid flow in rabbits. Animal Science. 79(2): 231-240. https://doi.org/10.1017/S1357729800090093
16. Gonzaga Neto, S.; Silva Sobrinho, A. G.; Resende, K. T.; Zeola, N. M.; Silva, A. M., Marques, C. A.; Leão, A. G. 2005. Composição corporal e exigências nutricionais de proteína e energía para cordeiros Morada Nova. Revista Brasileira de Zootecnia. 2446-2456. https://doi.org/10.1590/S1516-35982005000700033
17. Hidalgo, L.; Víctor, Y.; Valerio, C.; Henry. 2020. Digestibilidad y energía digestible y metabolizable del gluten de maíz, hominy feed y subproducto de trigo en cuyes (*Cavia porcellus*). Revista de Investigaciones Veterinarias del Perú. 31(2): e17816. https://dx.doi.org/10.15381/rivep.v31i2.17816
18. Higaonna, O. R.; Muscari, G. J.; Chauca, F. L.; Astete, F. 2008. Composición química de la carne de cuy (*Cavia porcellus*). INIA. Investigaciones en cuyes, Trabajos presentados a la Asociación Peruana de Producción Animal. Lima, Perú. Universidad Agraria La Molina.
19. Keeble, E. 2023. Guinea pig nutrition: what do we know? In Practice. 45(4): 200-210. https://doi.org/10.1002/inpr.309
20. Limon. G.; Gonzales-Gustavson. E. A.; Gibson. T. J. 2016. Investigation into the humaneness of slaughter methods for guinea pigs (*Cavia porcelus*) in the Andean Region. Journal of Applied Animal Welfare Science. 19(3): 280-293. https://doi.10.1080/10888705.2016.1138116
21. Liu, S. M.; Zhang, L.; Wei, C. M.; Chang, X.; Lu, Y. X.; Peng, D. H. 1991. The maintenance requirements of protein for Angora rabbits and the efficiency of digested protein by the rabbits. Chinese Journal of Animal and Veterinary Sciences. 22: 323-326.

22. Lofgreen, G. P.; Garrett, W. N. 1968. A system for expressing net energy requirements and feed values for growing and finishing beef cattle. Journal of Animal science. 27(3): 793-806. https://doi.org/10.2527/jas1968.273793x
23. Lv, J. M.; Chen, M. L.; Qian, L. C.; Ying, H. Z.; Liu, J. X. 2009. Requirement of crude protein for maintenance in a new strain of laboratory rabbit. Animal feed science and technology. 151(3-4): 261-267. https://doi.org/10.1016/j.anifeedsci.2009.01.001
24. Matin. C. M.; Ostwald. R. 1975. Food intake and growth of guinea pigs fed a cholesterol-containing diet. The Journal of Nutrition. 105(5): 525-533. https://doi.org/10.1093/jn/105.5.525
25. Montalvo, K. R.; Navarro, M.K. 2012. Determinación de la digestibilidad, energía digestible y metabolizable de broza de arveja (*Pisum Sativum* l) y betarraga (*Beta Vulgaris*) para la formulación de raciones en la alimentación de cuyes (*Cavia Porcellus*). Tesis. Universidad Nacional del centro de Perú. http://hdl.handle.net/20.500.12894/1954
26. Moon, T. W. 1988. Adaptation, constraint, and the function of the gluconeogenic pathway. Canadian journal of zoology. 66(5): 1059-1068. https://doi.org/10.1139/z88-156
27. NRC (National Research Council). 1995. Nutrient requirements of laboratory animals: Fourth revised edition, 1995. Washington, DC: The National Academies Press. https://doi.org/10.17226/4758.
28. Parigi-Bini. R.; Xiccato. G.; Cinetto. M.; Dalle Zotte. A. 1992. Energy and protein utilization and partition in rabbit does concurrently pregnant and lactating. Animal Science. 55(1): 153-162. https://doi.org/10.1017/S0003356100037387
29. R Core Team. 2022. R: A lenguage and environment for statistical computing. R foundation for statistical computing Computing, Vienna. Austria. https://www.R-project.org/
30. Sakaguchi, E. I. 2003. Digestive strategies of small hindgut fermenters. Animal Science Journal. 74(5): 327-337. https://doi.org/10.1046/j.1344-3941.2003.00124.x
31. Sánchez-Macías, D.; Barba-Maggi, L.; Morales-delaNuez, A.; Palmay-Paredes, J. 2018. Guinea pig for meat production: A systematic review of factors affecting the production, carcass and meat quality. Meat Science. 143: 165-176. https://doi.org/10.1016/j.meatsci.2018.05.004
32. Tapie, W. A.; Posada Ochoa, S. L.; Rosero Noguera, R. 2024a. A theoretical approach to energy requirements in guinea pigs (*Cavia porcellus*). Agronomía Mesoamericana. 35:57058. https://doi.org/10.15517/am.2024.57058
33. Tapie, W. A.; Posada-Ochoa, S. L.; Rosero-Noguera, J. R.; Muñoz-Tamayo, R. 2024b. Desarrollo de un modelo dinámico mecanicista para predecir el crecimiento de cuyes (*Cavia porcellus*) machos del genotipo Perú. Revista De La Academia Colombiana De Ciencias Exactas, Físicas y Naturales. 48(189): 859-70. https://doi.org/10.18257/raccefyn.2997
34. Trejo-Sánchez, F.; Mendoza-Martínez, G. D.; Plata Perez, F. X.; Martínez-García, J. A.; Villarreal Espino-Barros, O. A. 2019. Crecimiento de cuyes (*Cavia porcellus*) con alimento para conejos y suplementación de vitamina C. Revista MVZ Córdoba. 24(3): 7286-7290. https://doi.org/10.21897/rmvz.1384
35. Vargas-Romero, J.; Losada-Custardoy, H.; Cortés-Zorrilla, J.; Alemán-López, V.; Vieyra-Durán, J.; Luna-Rodríguez, L. 2020. Propuesta gastronómica con *Cavia porcellus*. Abanico veterinario. 10: 1-12. http://dx.doi.org/10.21929/abavet2020.31
36. Vela-Román, L.; Césare-Coral, M.; Norabuena-Meza, E.; Valderrama Rojas, M.; Paitan-Anticona, E.; Airahuacho-Bautista, F.; Sotelo, A. 2024. Digestibility and estimation of digestible energy of palm kernel (*Elaeis guineensis*) cake in guinea pigs (*Cavia porcellus*). Livestock Research for Rural Development. 36. http://www.lrrd.org/lrrd36/2/3612fair.html.
37. Vignale, L. K. 2010. Evaluación de diferentes niveles de energía y proteína cruda en cuyes (*Cavia porcellus*) en crecimiento en crianza comercial. MSc. Thesis. Universidad Nacional Agraria La Molina. https://hdl.handle.net/20.500.12996/1726
38. Xiccato, G.; Trocino, A. 2020. Energy and protein metabolism and requirements. In: De Blas, C.; Wiseman. J. (Eds.). The nutrition of the rabbit, 3rd ed. CAB International. 41-57. https://www.cabi.org/bookshop/book/9781789241273/

Synergistic Action of the Essential Oils of *Elionorus muticus* and *Lippia junelliana* Against the Causative Agent of Chalkbrood in Bees (*Ascosphaera apis*)

Acción sinérgica de los aceites esenciales de *Elionorus muticus* y *Lippia junelliana* sobre el agente causal de la cría yesificada en abejas (*Ascosphaera apis*)

Maricel Vega [1*], Maria Laura Susevich [2], María Inés Troncozo [3, 4], Francisco Jose Reynaldi [5], Graciela Noemi Albo [1]

Originales: *Recepción:* 20/03/2025 - *Aceptación:* 26/09/2025

ABSTRACT

Ascosphaera apis is the fungus that causes chalkbrood in *Apis mellifera*. Traditionally, its control has relied on synthetic fungicides, which can be harmful to bees and ecosystems. An alternative treatment has explored safer alternatives, such as the antimicrobial properties of plant-based essential oils. This study evaluated the combined effect of the essential oils of *Elionorus muticus* and *Lippia junelliana on* 10 isolates of *A. apis* using a "chessboard" experimental design. Minimum inhibitory concentrations, fungal growth rates and inhibition percentages were determined. Analyses were performed with ANOVA and *post-hoc* tests. The results showed that the combination of 200 µL/L of *E. muticus* and 25 µL/L of *L. junelliana* (C5) completely inhibited fungal growth after 144 h, with MIC_{50} significantly more effective than controls. The combined use of *E. muticus* and *L. junelliana* shows synergistic activity (FICI ≤0.5) in controlling *A. apis* and achieves full inhibition of the fungus under controlled conditions. These findings suggest that essential oils may be a viable alternative for the sustainable management of bee diseases.

Keywords
biocontrol • pathogenic fungi • natural products • apiculture

https://doi.org/10.48162/rev.39.213

1 Universidad Nacional de La Plata (UNLP). Facultad de Ciencias Agrarias y Forestales. 119 y 60 y s/n. C. P. 1900. La Plata. Buenos Aires. Argentina.
* maricel.vega@agro.unlp.edu.ar
2 Universidad Nacional de La Plata (UNLP). Facultad de Ciencias Naturales y Museo. Centro de Estudios Parasitológicos y de Vectores. Bvard. 120 entre Av. 60 y 64 S/N. C. P. 1900. La Plata. Buenos Aires. Argentina.
3 Universidad Nacional de La Plata (UNLP). Facultad de Ciencias Naturales y Museo. Instituto de Botánica Carlos Spegazzini. 122 y s/n. C. P. 1900 La Plata. Buenos Aires. Argentina.
4 Consejo Nacional de Investigaciones Científicas y Técnicas (CONICET). Godoy Cruz 2290. Ciudad Autónoma de Buenos Aires 1425. Argentina.
5 Universidad Nacional de La Plata (UNLP). Facultad de Ciencias Veterinarias. Cátedra de Micología Médica. Centro de Microbiología Básica y Aplicada (CEMIBA). Calle 60 y 118 s/n. C. P. 1900. La Plata. Buenos Aires. Argentina.

Licenses Creative Commons
Attribution - Non Commercial - Share Alike

Resumen

Ascosphaera apis es el hongo que causa la cría yesificada en *Apis mellifera*. Tradicionalmente, su control ha dependido de fungicidas sintéticos, que pueden ser dañinos para las abejas y el ecosistema. Por ello, se han investigado alternativas más seguras, como los aceites esenciales de plantas, que poseen propiedades antimicrobianas. Este estudio evaluó el efecto combinado de los AEs de *Elionorus muticus* y *Lippia junelliana* sobre diez aislamientos de *A. apis*, utilizando un diseño experimental tipo "tablero de ajedrez". Se determinaron las concentraciones inhibitorias mínimas y se calcularon las tasas de crecimiento fúngico y porcentajes de inhibición mediante ANOVA y pruebas *post hoc*. Los resultados indicaron que la combinación de 200 µL/L de *E. muticus* y 25 µL/L de *L. junelliana* (C5) inhibió completamente el crecimiento del hongo tras 144 horas, con una CIM_{50} significativamente más efectiva que los controles. La combinación de aceites esenciales *E. muticus* y *L. junelliana* presenta una solución prometedora para el control de *A. apis*, con un efecto sinérgico ≥0,5; que permite una inhibición total del hongo en condiciones controladas. Estos hallazgos sugieren que los AEs podrían ser una alternativa viable para el manejo sostenible de enfermedades en abejas.

Palabras clave
biocontrol • hongo patógeno • productos naturales • apicultura

Introduction

Mycotic infections are major contributors to the decline of honey bee (*Apis mellifera* L.) populations, causing significant economic losses in apiculture (6). Among them, the entomopathogenic fungus *Ascosphaera apis* (Maasen ex Claussen) Spiltoir & Olive (1955) causes ascospherosis, or chalkbrood, characterized by dehydrated larvae that change from white to black (depending on the number of sexual reproduction structures present). The infection begins when larvae inadvertently ingest fungal spores with their food (5). Once in larval hindgut, the spores germinate, and subsequent mycelial development causes larval death (22). The fungus affects the bee brood during the pupal stage, reducing the colony's health and productivity (1). Transmission is facilitated by the accumulation of *A. apis* spores in the hive, on beekeeping tools, and in food sources such as nectar and pollen (32).

Currently, ascospherosis is considered a cosmopolitan disease (25). Chemicals are widely used to treat and control chalkbrood, but their use is allowed only in certain countries and under critical conditions. Another alternative is the use of natural products, such as essential oils (EOs) and plant extracts (25). According to some researchers, synthetic fungicides have been linked to increased bee mortality, colony contamination, and reduced beneficial fungi that ferment pollen and support bee nutrition (34). Therefore, natural and ecologically safe products provide a promising option for managing chalkbrood.

Essential Oils (EOs) have long been known to exert antimicrobial effects against pathogens in plants, animals, insects, and honey bees (21, 27). EOs are aromatic substances produced by the secondary metabolism of aromatic plants and can be extracted from leaves, flowers, fruits, seeds, sprouts, rhizomes, roots and bark (23). *Lippia junelliana* (Mold.) Tronc. (Verbenaceae) is an aromatic shrub endemic to the Prepuna and Chaqueña biogeographic regions of Argentina (18). *Elionorus muticus* (Spreng.) is a native grass widely distributed in Argentina and other South American countries (24). Vega *et al*. (2022) determined that 500 µL/L of *L. junelliana* was safe and palatable to honey bees. Albo *et al*. (2014) established the minimum inhibitory concentration (MIC_{50}) of *L. junelliana* EO capable of controlling the chalkbrood pathogen. Up to now, few studies have examined the use of *E. muticus* to control ascospherosis (2).

Mráz *et al.* (2023) suggested that one limitation of EO treatment is the substantial amount of vegetal material required to obtain enough for *in vivo* application. Combining different EOs could address this issue, allowing a reduction in the applied dose in honey bee

colonies. However, most studies have focused on the effects of individual EOs. The present study aimed to evaluate the *in vitro* effects of a combination of *E. muticus* and *L. junelliana* on the pathogenic fungus *A. apis* and to determine the fractional inhibitory concentration index (FICI) of the combinations for potential field application.

Materials and Methods

Isolation and Culture of *A. apis*

Ten *A. apis* isolates were selected for this study due to their reported entomopathogenic capacity in *A. mellifera* brood (table 1) (29). These isolates were stored at -20°C in vials containing 20% glycerol in sterile distilled water and deposited in the Animal Production Course I collection, Facultad de Ciencias Agrarias y Forestales, Universidad Nacional de La Plata (FCAyF, UNLP). For fungal inoculum, isolates of *A. apis* were cultured on Petri dishes with MY20 medium (5 g peptone, 3 g yeast extract, 3 g malt extract, 200 g glucose and 20 g agar per liter of distilled water) at 35°C for 7 days, following the methodology of Albo *et al*. (2016).

Table 1. Fungal isolates of *A. apis* and their geographical origin.
Tabla 1. Aislamientos fúngicos de *A. apis* y su origen geográfico.

Isolated #	County	Province	Country
44	General Paz	Buenos Aires	Argentina
99	La Plata	Buenos Aires	Argentina
73	Florencio Varela	Buenos Aires	Argentina
76 (Aa31)*	Punta Indio	Buenos Aires	Argentina
77 (Aa40)	Tandil	Buenos Aires	Argentina
39 (Aa41)	Unión (Justiniano Posse)	Córdoba	Argentina
75 (Aa39)	Marcos Juárez (Monte Buey)	Córdoba	Argentina
98 (Aa35)	Guatraché	La Pampa	Argentina
26	Neuquén	Neuquén	Argentina
8 (Aa8)		Valdivia (Region X)	Chile

*Isolation number assigned by Reynaldi *et al.*, 2003.

*Número de aislamiento asignado en Reynaldi *et al.*, 2003.

Essential Oils

The EOs of *E. muticus* and *L. junelliana* were provided by the Aromatics Group, Institute of Instituto Nacional de Tecnología Agropecuaria (INTA), Castelar, Buenos Aires, Argentina. The EOs were extracted from plant tissue via Clevenger hydrodistillation (IRAM Standard No. 18.729) and stored in brown glass vials at -20°C for later use. Vega *et al.* (2022) described the chemical characterization of the EOs. The main components of *L. junelliana* are cis- and trans-ocimenone, myrcenone, cis-davone, and camphor, while those of *E. muticus* are geranial, neral, geranyl acetate, linalool, and methyl heptenone.

Experimental Procedure

To assess the effect of the combination of EOs on the entomopathogenic fungus, the "chessboard" method was used (13). Initial concentrations of 200 µL/L for *E. muticus* and 400 µL/L for *L. junelliana* were selected based on preliminary trials (unpublished data). The experimental design, shown in figure 1 (page 4), included five decreasing concentrations in a geometric series. Dilutions of the EOs were prepared using 2.5% v/v ethanol at 70°C as a diluent, which was then added to the melted MY20 liquid medium (45°C) and poured into Petri dishes to create each combination. Approximately 20 ml of medium was poured

into glass Petri dishes (9 cm x 1.5 cm). Mycelium discs (7 mm diameter) from each fungal isolate were placed on the medium surface with the different EO/diluent combinations in duplicate. As a control, we inoculated each strain in MY20 medium. All plates were incubated at 35°C, 12% CO_2, 65% relative humidity, and in darkness for 144 h. The fungal growth diameter (mm) was measured with a caliper every 24 h.

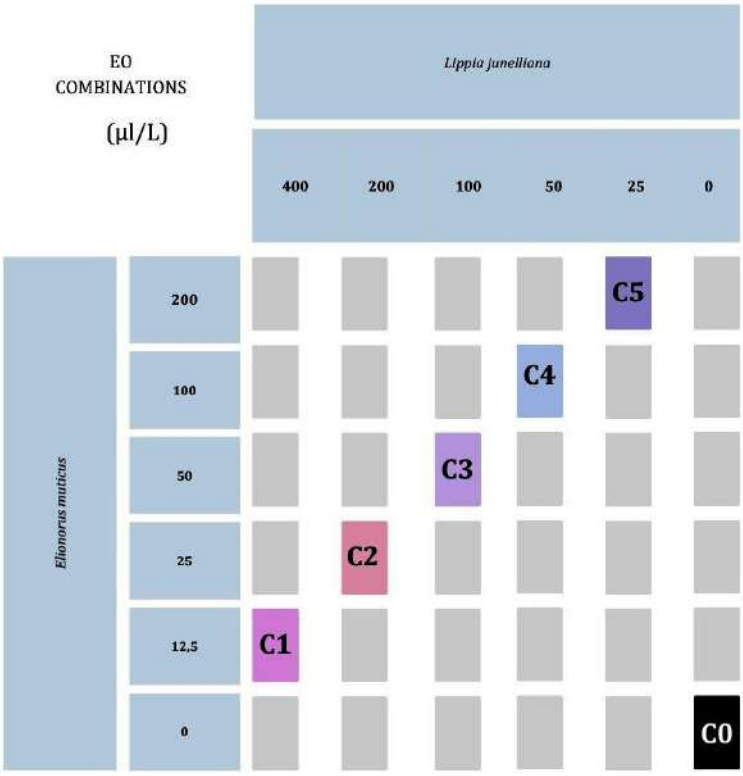


Figure 1. Chessboard. The matrix was structured with rows representing *E. muticus* concentrations and columns representing *L. junelliana* concentrations. Each box at the row-column intersection represents a combination of *E. muticus* and *L. junelliana.*

Figura 1. Tablero de ajedrez. La matriz se estructuró utilizando filas (Concentraciones de *E. muticus*) y columnas (Concentraciones de *L. junelliana*), en la cual cada casilla (intersección de fila y columna) representa una combinación de *E. muticus* y *L. junelliana.*

Growth Parameters

Based on the data obtained, the absolute growth was calculated for each culture time, and growth curves were constructed. The exponential growth rate per hour (GR; mm/h) was determined using the following equation 1:

$$\mathbf{TC = \sum (DC_C - DC_T)/DC_C \times 100\%} \quad (1)$$

DC_C corresponds to the control growth diameter and DC_T to the treatment growth diameter.

$$\mathbf{TC = C24h + C48h + C72h + C144h/4} \quad (2)$$

$$\mathbf{C24h = total\ mycelium\ length - 7} \quad (3)$$

$$\textbf{C48h = (total mycelium length - 7) - C24h} \quad (4)$$

$$\textbf{C72h = (total mycelium length - 7) - C48h} \quad (5)$$

$$\textbf{C144 h = (total mycelium length - 7) - C72h} \quad (6)$$

ANOVA followed by Tukey's post-hoc test (p = 0.05) was used to determine differences among the GRs for each treatment.

Descriptive statistics were calculated for the final fungal growth diameter at the end of the experiment (144 h). ANOVA followed by Holm-Sidak's test was used to determine differences between the control and EOs combinations. Then, Tukey's post-hoc test ($p \leq 0.05$) was used to determine differences among EO combinations, excluding the control.

Percent Growth Inhibition

The percentage of growth inhibition (GI) was calculated according to Chen *et al*. (2019) using the following formula (Eq. 7):

$$\textbf{IC (\%)} = (DC_C - DC_T)/DC_C \times 100\% \quad (7)$$

Where DC_C is the control growth diameter and DC_T is the treatment growth diameter.

A bifactorial ANOVA followed by Tukey's *post hoc* test ($p \leq 0.05$) was conducted to assess differences among EO combinations and culture times on growth inhibition percentage. Before statistical analysis, percentage data were transformed using arcsine $\sqrt{p}$.

Minimum Inhibitory Concentration (MIC_{50})

To assess the efficacy of the combination of EOs against the entomopathogenic fungus, the number of inhibited strains relative to the control was calculated (10). The MIC_{50} was determined at the time points of the linear growth phase (72 and 144 h). It was defined as the lowest EO concentration causing 50% or more inhibition compared to the control (4).

Fractional Inhibitory Concentration Index (FICI)

The FICI value was calculated from the results obtained for MIC_{50} using the following equations (36):

$$\textbf{FICi = FICa + FICb} \quad (8)$$

$$\textbf{FICa = A/MICa} \quad (9)$$

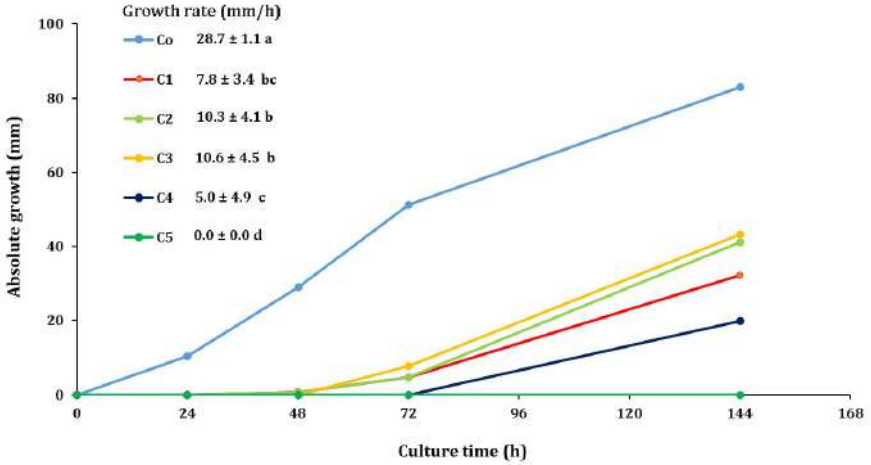
$$\textbf{FICb = B/MICb} \quad (10)$$

A, MIC of EO A in combination; MIC_a, MIC of EO A alone; B, MIC of EO B in combination; MIC_b, MIC of EO B alone.

FICI values were interpreted according to Amassmoud *et al.* (2023) as follows: synergism ($FICI \leq 0.5$), additive ($0.5 < FICI \leq 1.0$), neutral ($1 < FICI \leq 4.0$), or antagonism ($FICI > 4.0$).

Results

Figure 2 (page 6), shows the growth curves and rates of *A. apis* for the EO combinations and control. All EO combinations inhibited fungal growth during the logarithmic phase. *A. apis* required more than 72 h to overcome the fungistatic effect produced by C4 (100 µL/L *E. muticus* and 50 µL/L *L. junelliana*). Fungal growth was not observed when exposed to C5 (200 µL/L *E. muticus* and 25 µL/L *L. junelliana*) after 144 h of culture. All EO combinations showed growth rates below 50% compared to the control ($F: 102.29$; $p < 0.001$).



Different letters in the growth rate values indicate significant differences among treatments (Tukey's test, $p < 0.05$).

Letras distintas en los valores de tasa de crecimiento indican diferencias significativas entre los tratamientos (Test de Tukey, $p < 0,05$).

Figure 2. Growth curves and rates of *A. apis*.

Figura 2. Curvas y tasas de crecimiento de *A. apis*.

Table 2, shows descriptive and parametric analyses of *A. apis* growth at the final time point (144 h) after exposure to the EO combinations. ANOVA revealed significant differences among treatments (F: 136.08; $p < 0.0001$), with each EO combination differing from the control with a highly significant p value ($p \leq 0.001$, Holm-Sidak's test). Growth was strongly affected by combination C5, followed by C4 (Tukey's test, $p < 0.05$).

Table 2. Descriptive statistics and *post-hoc* parametric analysis of EO combinations on *A. apis* growth diameter (mm) at 144 h of culture.

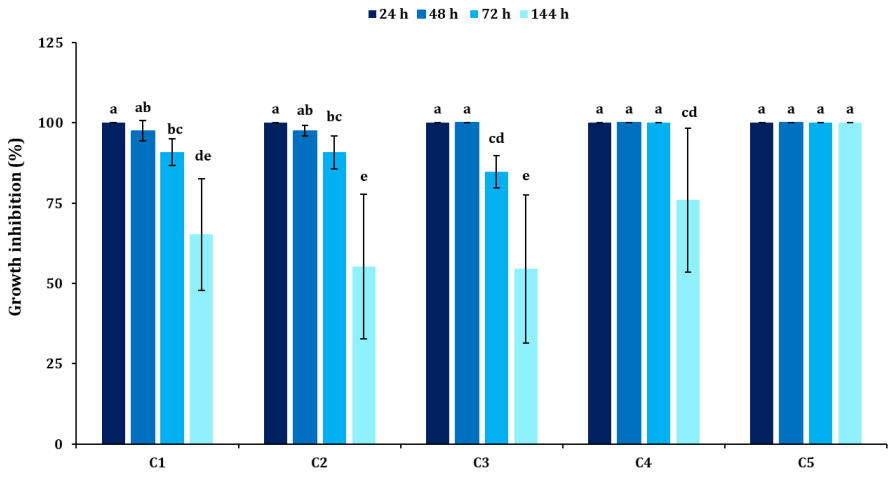
Tabla 2. Estadística descriptiva y análisis paramétrico *post-hoc* de la combinación de los AEs sobre el diámetro de crecimiento (mm) de *A. apis* a las 144 h de cultivo.

Treatment	Co	C1	C2	C3	C4	C5
Minimum	26.0	0.0	0.0	0.0	0.0	0.0
Maximum	30.0	13.0	18.5	18.3	14.0	0.0
Average	28.0	7.8	10.3	10.6	6.3	0.0
Deviation	1.1	3.9	4.1	4.9	4.5	0.0
Holm-Sidak's test [a]		<0.0001	<0.0001	<0.0001	<0.0001	<0.0001
Tukey's test [b]		ab	a	a	b	c

a p value obtained. b Different letters indicate significant differences among treatments ($p < 0.05$).

a, valor de p obtenido. b, Letras distintas indican diferencias significativas entre los tratamientos ($p < 0,05$).

The relative growth inhibition of *A. apis* showed significant differences (F: 9.01; $p < 0.001$), depending on the EO combination and culture time (figure 3, page 7). All EO combinations and culture times inhibited 50% of fungal growth; however, C5 was the only one that achieved 100% inhibition at all time points.



Different letters indicate significant differences among treatments ($p < 0.05$).

Letras distintas indican diferencias significativas entre los tratamientos ($p < 0,05$).

Figure 3. Growth inhibition (%) of *A. apis* the EO combinations.

Figura 3. Inhibición porcentual del crecimiento de *A. apis* en las diferentes combinaciones de los Aceites esenciales.

The relative growth inhibition of *A. apis* strains at each culture time is shown in table 3. The percentage of affected strains (< 50%) decreased as culture time increased for combinations C1, C2, C3, and C4, while C5 maintained inhibition of 50% or more at all time points. Based on the MIC_{50} values, the FICI was calculated. The FICI for C5 was 0.5, indicating that the combination of both EOs exerted a synergistic effect that led to the total inhibition of *A. apis* strains.

$$FICA = 200/400 = 0.5$$
$$FICB = 25/3200 = 0.007$$
$$FICi = 0.5 + 0.0 = 0.5$$

Table 3. Relative percentage inhibition of *A. apis* strains at different culture times.

Tabla 3. Porcentaje relativo de inhibición del número de cepas de *A. apis* en los distintos tiempos de cultivo.

Time (H)	C1	C2	C3	C4	C5
24	100	100	100	100	100
48	40	20	100	100	100
72	0	0	0	100	100
144	0	0	0	40	100

Discussion

Essential oils have well-known antimicrobial properties and are used to treat infections caused by several pathogens (5). Previous studies (briefly described below) have examined *Lippia junelliana* and *Elionurus muticus* separately against pests and pathogens, but never in combination. This study investigated the inhibitory effects of combining *L. junelliana* and *E. muticus* against *A. apis*.

The EO of *L. junelliana* is mainly composed of myrcenone and cis-davanone (33). Comelli *et al*. (2023) reported strong insecticidal activity against *Oryzaephilus mercator* (L.) (Nitidulidae), with LC_{50} values of 7.02–7.17 µL/L and LC_{100} values of 10.00-20.00 µL/L. El Youssfi *et al*. (2024) demonstrated that this EO exhibits virucidal activity against the hemorrhagic yellow fever virus (Junín virus), with a MIC_{50} (VC_{50}) of 20 ppm. Regarding its antifungal activity, *in vitro* tests showed that *L. junelliana* effectively controlled molds and yeast, including *Candida krusei, C. albicans*, and *Aspergillus spp.* of the section *fumigati* (13). Regarding pests and pathogens in beekeeping, Dellacasa *et al*. (2003) found that *L. junelliana* repelled the mite *Varroa destructor* at 1.9 µL per bee. The inhibitory effect of this EO against *A. apis* was studied alone but never in combination (15).

The *E. muticus* essential oil used in this study was mainly composed of approximately 50% α-citral (geranial) and 25% β-citral (neral) (33). *In vivo* tests demonstrated its fumigant activity against the agricultural pest *Tetranychus urticae* C.L. Koch (Acari) at low concentrations (0.03-1 µL/L) (17). Regarding its bactericidal activity, *E. muticus was* effective against *Escherichia coli, coagulase-negative Staphylococcus, S. aureus, S. pseudintermedius, S. uberis, P. aeruginosa,* and *Bacillus cereus*, with MIC values ranging from 1 to 150 mg/mL (8). Fungicidal activity was observed against *Candida albicans* (9), *C. krusei*, and *C. neoformans* Vuillemin (20), with MIC values of 0.5-5 µg/mL. Fungistatic activity was reported against *C. parapsilosis* and *C. utilis* (28).

Davis and Ward (2003) determined that the minimum fungicidal concentration against *A. apis* was 250 ppm for *C. citratus*, *Eucalyptus citriodora*, and *Leptospermum petersonii* oils, all rich in citral. Similarly, the essential oil of *Litsea cubeba* (Lour.) Pers (Lauraceae) showed fungicidal activity against *A. Apis* at 50 µg/mL using the agar diffusion method (5, 26). Dellacasa *et al.* (2003) reported that 800 ppm of *Tagetes minuta*, which shares components with *L. junelliana*, was required to control *Ascosphaera apis in vitro*. In our study, the combination of *E. muticus* (200 µL/L) and *L. junelliana* (25 µL/L), referred to as C5, produced a FICI of 0.5, showing the most effective control of *A. apis* through synergistic action. This effect likely resulted from the complementary interaction of the oils' active components, yielding greater antifungal efficacy than either oil used alone. This finding aligns with recent research showing that synergistic essential oil combinations can fully inhibit various fungal pathogens (35). According to previous studies, citral, a major component of the *E. muticus* EO used here, effectively inhibited both dematiaceous fungi and the hyaline fungus causing chalkbrood (7, 29). Our combination of *L. junelliana* and *E. muticus* reduced the required *L. junelliana* amount by at least 75% compared to the 800 ppm reported by Dellacasa *et al.* (2003) for *Tagetes minuta*, which contains similar major components.

It is important to highlight the time-dependent effects of the essential oil combinations on *A. apis*. Combination C4 (100 µL/L of *E. muticus* and 50 µL/L of *L. junelliana*) showed a fungistatic effect, requiring more than 72 h for the fungus to recover. However, it did not fully inhibit fungal growth. Analysis of relative inhibition percentages and their temporal variation revealed significant differences in the efficacy of the essential oil combinations. Combinations C1, C2, C3, and C4 showed reduced effects over time, whereas C5 consistently maintained inhibition above 50% throughout the study. Sustained complete inhibition is desirable for controlling fungal pathogens, providing more effective and long-lasting protection (20). The synergistic effect and temporal stability observed make C5 a promising candidate for controlling *Ascosphaera apis*.

Conclusions

Our results showed that combining *L. junelliana* (25 µL/L) and *E. muticus* (200 µL/L) synergistically inhibited *A. apis* growth. This combination outperformed the inhibitory efficacy of each oil alone and reduced the required amount of *L. junelliana* by at least 75% compared to previously reported values, lowering the costs of potential health management. Although our results provide valuable information on *in vitro* control dosages, further studies on the toxicity of the tested compounds in larval, pupal, and adult honey bees are needed to successfully apply this knowledge in field conditions.

References

1. Albo, G. N.; Reynaldi, F. J.; Elder, H.; Juárez, M. A.; Córdoba, S. B. 2014. Control *in vitro* de *Ascosphaera apis* con *Schinus molle* y *Lippia junelliana*. Efectos tóxicos potenciales en abeja melífera. XI Congreso Latinoamericano de Apicultura FILAPI.
2. Albo, G. N.; Altamirano, R.; Henning, C.; Della Vedova, R.; Córdoba, S. B. 2015. Inhibición *in vitro* de *Ascosphaera apis* con aceites esenciales de gramíneas nativas e introducidas. III Congreso Argentino de Microbiología Agrícola y Ambiental. Ciudad Autónoma de Buenos Aires. Argentina.
3. Albo, G., Reynaldi, F., Córdoba, S., & Malbrán, C. 2016. Evaluación de la actividad inhibitoria, in vivo e *in vitro*, del aceite esencial de *Cymbopogon citratus* y cinco diluyentes sobre cultivos de *Ascosphaera apis*. Analecta veterinaria. 36: 5-11.
4. Amassmoud, O.; Abbad, I.; Iriti, M.; Hassani, L.; Mezrioui, N.; Abbad, A. 2023. Antibacterial activity of essential oils combinations based on *Thymus broussonnetii*, and their synergism with some antibiotics. Current Microbiology. 80(12): 398.
5. Ansari, M. J.; Al-Ghamdi, A.; Usmani, S.; Khan, K. A.; Alqarni, A. S.; Kaur, M.; Al-Waili, N. 2017. *In vitro* evaluation of the effects of some plant essential oils on *Ascosphaera apis*, the causative agent of Chalkbrood disease. Saudi Journal of Biological Sciences. 24(5): 1001-1006. https://doi.org/10.1016/j.sjbs.2016.04.016
6. Aziz, M. A.; Alam, S. 2024. Diseases of Honeybee (*Apis mellifera*). In Melittology-New Advances. IntechOpen.
7. Capetti, F.; Tacchini, M.; Marengo, A.; Cagliero, C.; Bicchi, C.; Rubiolo, P.; Sgorbini, B. 2021. Citral-containing essential oils as potential tyrosinase inhibitors: A bio-guided fractionation approach. Plants. 10(5): 969.
8. Celaya, L. S.; Le Vraux, M. A.; Heit, C. I.; Viturro, C. I.; Martina, P. F. 2023. Phytochemical and Biological Profile of Essential Oils of *Elionurus muticus* (Spreng.) Growing in Northeastern Argentina. Chemistry & Biodiversity. 20(6), e202201105. https://doi.org/10.1002/cbdv.202201105
9. Chagonda, L. S.; Fungirayi, B. 2016. Antifungal activity of the essential oil of *Elionurus muticus* (Spreng) Kunth from Zimbabwe against *Candida albicans*, C. krusei and *Cryptococcus neoformans*. J Multidiscip Eng Sci Technol. 3: 5331-5335.
10. Chen, C. J.; Li, Q. Q.; Ma, Y. N.; Wang, W.; Cheng, Y. X.; Xu, F. R.; Dong, X. 2019. Antifungal effect of essential oils from five kinds of Rutaceae plants-avoiding pesticide residue and resistance. Chemistry & Biodiversity. 16(4): e1800688.
11. Clinical and Laboratory Standards Institute (CLSI). 2008. Reference method for broth dilution antifungal susceptibility testing of filamentous fungi. Approved Standard CLSI. Doc. M 38-A2. 2° Ed. Wayne.
12. Comelli, N. C.; Diez, P. A.; Rodríguez, M. R.; Denett, G. O.; López, T. E.; Bracamonte, D. M.; Ortiz, E. V.; Sampietro, D. A.; Duchowicz, P. R. 2023. Excito-repellent and Pesticide-Likeness Properties of Essential Oils on *Carpophilus dimidiatus* (Fabricius) (Nitidulidae) and *Oryzaephilus mercator* (L.) (Silvanidae). Journal of Chemical Information and Modeling. https://doi.org/10.1021/acs.jcim.3c01198
13. Córdoba, S.; Vivot, W.; Szusz, W.; Albo, G. 2019. Antifungal Activity of Essential Oils Against Candida Species Isolated from Clinical Samples. Mycopathologia. 184(5): 615-623. https://doi.org/10.1007/s11046-019-00364-5
14. Davis, C.; Ward, W. 2003. Control of chalkbrood disease with natural products: a report for the RIRDC. Publication N° 03/107. Kingston. ACT. AU. p. 1-23.
15. Dellacasa, A. D.; Bailac, P. N.; Ponzi, M. I.; Ruffinengo, S. R.; Eguaras, M. J. 2003. *In vitro* activity of essential oils from San Luis-Argentina against *Ascosphaera apis*. Journal of Essential Oil Research. 15(4): 282-285.
16. El Youssfi, C.; Dadou, S.; Loukili, E. H.; El Hammoudani, Y.; Soujaa, H.; Rejdali, M.; Zerrouk Mohammed, H.; Mourabit, N.; Aarab, S. 2024. Biological activities of essential oils: A mini-review. BIO Web of Conferences, 109, 01031. EDP Sciences.
17. Hauschild, R.; Ott, A.; da Silva, M. A. S. 2020. Ação fumigante de óleos essenciais de *Baccharis dracunculifolia* e *Elionurus muticus* contra o Ácaro rajado (*Tetranychus urticae*, Koch 1836) em morangueiro. Cadernos de Agroecologia. 15(2).
18. Juárez, M. A.; Elechosa, M. A.; Molina, A. M.; Viturro, C. I.; Molina, A. C.; Heit, C. I. 2007. Estudio del aceite esencial de *Lippia junelliana* (Mold) Tronc. Obtenido de colectas en Tucumán, Argentina. Boletín Latinoamericano y del Caribe de Plantas Medicinales y Aromáticas. 6(5): 254-255.
19. Krutmuang, P.; Rajula, J.; Pittarate, S.; Chatima, C.; Thungrabeab, M.; Mekchay, S.; Senthil-Nathan, S. 2022. The inhibitory action of plant extracts on the mycelial growth of *Ascosphaera apis*, the causative agent of chalkbrood disease in Honey bee. Toxicology Reports. 9: 713-719.
20. Lameck, S.; Chagonda, L.; Fungirayi, B. 2016. Antifungal Activity of the Essential Oil of *Elionurus muticus* (Spreng) Kunth from Zimbabwe against *Candida albicans*, *C. krusei* and *Cryptococcus neoformans*. Journal of Multidisciplinary Engineering Science and Technology. 3: 2458-9403.
21. Lazăr, R. N.; Pătruică, S. 2020. Use of Essential Oils in Bees. Scientific Papers Animal Science and Biotechnologies. 53(1): 74-74.

22. Lopes, L. Q. S.; Quatrin, P. M.; De Souza, M. E.; De Almeida Vaucher, R.; Vianna Santos, R. C. 2015. Fungal infections in honey bees. Fungal Genomics. Biol. 5: 1-4.
23. Mohamed, A. A.; Alotaibi, B. M. 2023. Essential oils of some medicinal plants and their biological activities: a mini review. Journal of Umm Al-Qura University for Applied Sciences. 9(1): 40-49.
24. Moreno, E. M.; Almirón, N. E. A.; Peichoto, M. C.; Solís Neffa, V. G. 2018. Variabilidad genética en poblaciones de *Elionurus muticus* (Poaceae) de Corrientes, Argentina, a partir de marcadores moleculares de ADN nuclear y cloroplástico. Boletín de La Sociedad Argentina de Botánica. 53(2): 1-10. https://www.scielo.org.ar/scielo.php?script=sci_abstract&pid=S1851-37220180002000012&lng=es&nrm=iso&tlng=en
25. Mráz, P.; Žabka, M.; Hoštičková, I.; Kopecký, M.; Bohatá, A.; Tomčala, A.; Hýbl, M. 2023. Effect of selected botanical compounds on *Ascosphaera apis* and *Apis mellifera*. Industrial Crops and Products. 197: 116649. https://doi.org/10.1016/j.indcrop.2023.116649
26. Nardoni, S.; D'Ascenzi, C.; Rocchigiani, G.; Papini, R.; Pistelli, L.; Formato, G.; Najar, B.; Mancianti, F. 2017. Stonebrood and chalkbrood in *Apis mellifera* causing fungi: *In vitro* sensitivity to some essential oils. Natural Product Research. 32: 1-6. https://doi.org/10.1080/14786419.2017.1306703
27. Pérez Panti, O.; García de la Cruz, R.; González Hernández, H.; Sánchez Soto, S.; Moscoso Ramírez, P. A.; Izquierdo Reyes, F. 2024. Bio-efficacy of entomopathogenic fungi and vegetable oils against the pink pineapple mealybug: *Dysmicoccus brevipes* (Cockerell). Revista de la Facultad de Ciencias Agrarias. Universidad Nacional de Cuyo. Mendoza. Argentina. 56(1): 83-93. DOI: https://doi.org/10.48162/rev.39.125
28. Puppin, D. de G. P. B. 2018. Ação antifúngica e toxicidade do óleo essencial de *Elionurus muticus* (capim-limão brasileiro). http://repositorio.unicamp.br/jspui/handle/REPOSIP/333555
29. Pusceddu, M.; Floris, I.; Mangia, N. P.; Angioni, A.; Satta, A. 2021. *In vitro* activity of several essential oils extracted from aromatic plants against *Ascosphaera apis*. Veterinary sciences. 8(5): 80.
30. Reynaldi, F. J.; López, A. C.; Albo, G. N.; Alippi, A. M. 2003. Differentiation of *Ascosphaera apis* isolates by rep-PCR fingerprinting and determination of chalkbrood incidence in Argentinean honey samples. Journal of Apicultural Research. 42(4): 68-76.
31. Spiltoir, C. F.; Olive, L. S. 1955. A reclassification of the genus Pericystis Betts. Mycologia. 47(2): 238-244.
32. Tapia-González, J. M.; Alcazar-Oceguera, G.; Macías-Macías, J. O.; Contreras-Escareño, F.; Tapia- Rivera, J. C.; Petukhova, T.; Guzmán-Novoa, E. 2020. Ascosferosis en abejas melíferas y su relación con factores ambientales en Jalisco, México. Revista mexicana de ciencias pecuarias. 11(2): 468-478.
33. Vega, M.; Reynaldi, F. J.; Altamirano, R.; Marcos, D.; Juárez, M. A. 2022. Preliminary report on the toxicity of *Lippia junelliana* (Lamiales: Verbenaceae) and *Elionorus muticus* (Poales: Poaceae) on *Apis mellifera* (Hymenoptera: Apidae). Revista de la Sociedad Entomológica Argentina. 81(1).
34. Yoder, J. A.; Jajack, A. J.; Rosselot, A. E.; Smith, T. J.; Yerke, M. C.; Sammataro, D. 2013. Fungicide contamination reduces beneficial fungi in bee bread based on an area-wide field study in honey bee, *Apis mellifera*, colonies. Journal of Toxicology and Environmental Health. Part A. 76(10): 587-600. https://doi.org/10.1080/15287394.2013.798846
35. Yuan, X.; Cao, D.; Xiang, Y.; Jiang, X.; Liu, J.; Bi, K.; Dong, X.; Wu, T.; Zhang, Y. 2024. Antifungal activity of essential oils and their potential synergistic effect with amphotericin B. Scientific Reports. 14(1): 31125. https://doi.org/10.1038/s41598-024-82380-0
36. Zeng, Z. Y.; Li, Q. Q.; Huo, Y. Y.; Chen, C. J.; Duan, S. S.; Xu, F. R.; Cheng Y. X.; Dong, X. 2021. Inhibitory effects of essential oils from Asteraceae plant against pathogenic fungi of *Panax notoginseng*. Journal of Applied Microbiology. 130(2): 592-603.

Transition Management and Dairy Cow Performance: Insights from Dairy Farms in Argentina

Manejo de la Transición y Desempeño de las Vacas Lecheras: Perspectivas de Establecimientos en Argentina

María Paula Turiello [1, 2, 3*], Claudina Vissio [1, 4]

Originales: *Recepción:* 15/03/2025- *Aceptación:* 08/09/2025

ABSTRACT

This study aims to describe nutritional strategies, management practices, and health events in transitioning cows on 28 commercial dairy farms in Argentina, selected based on their association with graduate students. During 2022, we surveyed herd management, feeding, health events, and milk yield, based on local research and validated recommendations. Most cows were housed in dry lots, with 97% of farms having far-off and close-up groups, but only half had a fresh group. The average dry period was 59±11.4 days. The mortality and culling rate were 1.2% and 1.4%, respectively. The herd incidence rates were 1.8% for milk fever, 0.3% for clinical mastitis, 2.7% for metritis, and 1.4% for retained placenta. All farms used anionic diets and monitored urinary pH, with corn silage included in all diets, and soybean meal/expeller as the main protein source. Lactating cows produced an average of 33.8±10.43 kg of milk on the first test day and 38.2±10.05 kg at peak. Primiparous cows produced 75% of the milk of mature cows. Bulk tank milk averaged 3.9±0.19% fat and 3.5±0.07% CP. This report highlights strengths and areas for improvement in Argentina's dairy transition programs.

Keywords
dry cow • prefresh • dairy cow performance • health and nutrition

https://doi.org/10.48162/rev.39.199

1 Universidad Nacional de Río Cuarto (UNRC). Facultad de Agronomía y Veterinaria (FAV). Ruta 36 km 601. Río Cuarto. C. P. 5800. Córdoba. Argentina.
* mpturiello@ayv.unrc.edu.ar
2 Universidad Nacional de Villa María (UNVM). Instituto Académico Pedagógico de Ciencias Sociales (IAPCBA). Arturo Jauretche 1555. Villa María. C. P. 5248. Córdoba. Argentina.
3 Instituto de Formación e Investigación en Nutrición Animal (IFINA). Zona rural. Las Higueras. C. P. 5805. Córdoba. Argentina.
4 Universidad Nacional de Río Cuarto (UNRC) Instituto para el Desarrollo Agroindustrial y de la Salud CONICET. Ruta 36 km 601. Río Cuarto. Córdoba. ARCP 5800. Argentina.

Licenses Creative Commons
Attribution - Non Commercial - Share Alike

Resumen

El objetivo del estudio fue describir estrategias nutricionales y de manejo, eventos de salud y producción de vacas en transición en 28 establecimientos argentinos seleccionados por su vinculación con estudiantes de posgrado. Durante el año 2022 se relevaron aspectos de manejo, alimentación, salud y producción, según recomendaciones validadas y estudios locales. La mayoría de las vacas se alojaban en dry-lots y 97% tenían rodeos de seca y preparto, pero solo la mitad tenía rodeo de vacas frescas. La duración del período seco fue de 59±11,4 días. La mortalidad y descarte fueron del 1,2% y 1,4%, respectivamente. Las incidencia de hipocalcemia, mastitis, metritis y placenta retenida fueron 1,8%, 0,3%, 2,7% y 1,4%, respectivamente. Los establecimientos utilizaban sales aniónicas y monitoreaban pH urinario preparto; incluían silaje de maíz, y harina o expeller de soja como fuente proteica. La producción promedió 33,8±10,43 kg/vaca/día al primer control lechero y alcanzó un pico promedio de 38,2±10,05 kg/vaca/d. Las vacas primíparas produjeron el 75% de las vacas adultas. La leche de tanque presentó 3,9±0,19% de grasa y 3,5±0,07% de proteína. Este informe resalta los puntos fuertes y áreas de mejora en los programas de transición lechera en Argentina.

Palabras clave
vaca seca • preparto • performance de vaca lechera • salud y nutrición

Introduction

The transition period in dairy cows spans from the last 3 weeks prepartum to the first 3 weeks postpartum (10). This critical phase has been emphasized as pivotal in the lactation cycle by Drackley (1999), primarily due to its influence on health disorders, production outcomes, and subsequent profitability. This latter author highlights several essential aspects, including nutritional strategies to support dry matter intake and metabolic adaptation, environmental comfort to reduce stress, monitoring of body condition to avoid excessive reserve mobilization, and timely detection of clinical and subclinical health issues.

Recent literature has highlighted various aspects of transition cow management in commercial settings. Heuwieser *et al.* (2010) surveyed German farmers on fresh cow management practices, while Espadamala *et al.* (2016) examined methods for identifying postpartum health disorders in California dairy farms. Both studies underscored the challenge of implementing specific and objective observation systems in fresh groups to enhance transition cow care. More recently, Kerwin *et al.* (2022) investigated the management and herd characteristics of the transition period in freestall dairy herds in the northeastern United States. Their findings highlighted the industry's adherence to prevailing recommendations from both academia and practical experience.

Effective management and nutrition during the transition period aim to reduce metabolic disorders, enhance milk yields, lower culling rates, and improve reproductive performance throughout lactation (8). However, while numerous dietary and management recommendations exist, their implementation varies based on practical considerations (2). Furthermore, Kerwin *et al.* (2023) noted that not all recommendations are equally adopted, often due to financial constraints or insufficient research support. Understanding the influence of nutritional and management factors on commercial dairy farms can shed light on how these elements contribute to transition cow success across diverse farm practices (15).

This study aims to describe nutritional and management strategies, as well as the productive performance and health events of transitioning cows in commercial dairy farms in Argentina. By identifying areas for improvement within these transition programs, this research seeks to enhance overall herd health and productivity. In Argentina, there is limited available information on the nutritional and management strategies applied during the transition period, making this type of research essential for designing evidence-based interventions to improve animal performance and farm profitability during this critical stage.

As has been highlighted for cow-calf systems, the systematic characterization of management practices and the identification of areas for improvement are key steps to increase efficiency and profitability in livestock production (10).

Materials and Methods

Study Design

A cohort of graduate students specializing in bovine nutrition at the National University of Villa Maria facilitated the selection of 28 dairy farms across the provinces of Cordoba (19%), Santa Fe (50%), and Buenos Aires (31%), Argentina. These farms primarily housed Holstein cows, averaging 470 milking cows each, with herd sizes ranging from 180 to 1,200.

Farm visits conducted in August involved interviews with farm owners or managers, supplemented by observational assessments. The survey was developed based on nutritional and management recommendations from the literature, expert opinions, and insights gleaned from local studies (27, 29). It encompassed risk factors affecting milk yield and health during the transition period, drawing on recent research (1, 6, 7). Data collection focused on health events during the first 21 days in milk (DIM) and milk yield and quality metrics from cows calved between April and May 2022 due to operational and logistical limitations. Body condition scores in dry-off, close-up and fresh (< 30 DIM) cows and ketonemia in fresh cows (3-14 DIM) were evaluated in a stratified sample of cows based on group size: 20% of the cows in groups with more than 60 cows, 12 cows in groups with 12 to 60 cows, or all cows in smaller groups where the number was insufficient.

All animals involved in this investigation were cared for in accordance with the International Guiding Principles for Biomedical Research Involving Animals (CIOMS-ICLAS, 2012).

Survey Structure

The survey comprehensively addressed four main areas:

Herd Management: This section focused on dry cow and fresh cow programs, including criteria for grouping, frequency of management interventions, facilities, and cow comfort. Consultants also assessed the duration of the dry period for cows calved between April and May 2022. Body condition scores (BCS) were evaluated using a 1 to 5 scale (31) at different stages of the transition period.

Feeds and Feeding Management: Information regarding feed formulations for far-off, close-up, and fresh cow diets was collected. The survey also gathered data on feed sample frequency, feed bunk management practices, intake estimations, and monitoring of urinary pH when formulating acidogenic diets in pre-fresh stages.

Health Events: Defined health events included milk fever, retained placenta, mastitis, and metritis as they are among the most common and impactful health disorders during the transition period (2). Diagnosis criteria were standardized, with milk fever diagnosed based on symptoms and response to treatment, retained placenta noted if not expelled within 12 hours postpartum, mastitis identified through mammary gland inflammation or milk changes, and metritis detected via abnormal vaginal discharge and clinical signs. Blood samples from the coccygeal vessels assessed ketonemia, with hyperketonemia defined as blood BHB concentrations ≥1.2 mmol/L, measured by the consultant the day of the visit using handheld devices following manufacturer guidelines (23).

Milk Yield and Quality: Data on milk yield during startup (10 to 30 days in milk, DIM) and peak lactation (75 to 105 DIM) were obtained from individual cow records. Bulk tank milk quality parameters, including fat and protein content, somatic cell count (SCC), and colony-forming units (CFU), as reported primarily by industry standards, were documented.

Data Analysis

Descriptive statistics were employed to characterize general management practices during the transition period across the surveyed farms. Incidence rates of health events during early lactation were calculated as the proportion of new cases relative to the total number of calvings in April and May. Dietary composition, feeding management practices, and milk yield and quality traits were analyzed using positional and dispersion statistics to identify trends and variations across the surveyed farms.

Results and Discussion

A total of 28 dairy farms across the provinces of Cordoba, Santa Fe, and Buenos Aires, Argentina, were selected for the study based on the availability and willingness of farmers to participate. The study encompassed all cows calved in these farms during April and May 2022, totaling 3,267 animals (1,223 multiparous and 2,044 primiparous cows). The median of calvings per farm was 32 for multiparous cows (range: 10 to 120) and 64 for primiparous cows (range: 12 to 204).

Herd Management

Most cows (85.7% groups) in the study were housed in dry-lots, the remaining groups were grazing. Ninety-seven percent of the farms had separate far-off and close-up groups. Yet, only half of them had fresh group, in line with observations reported by Heuwieser *et al.* (2010). Nearly all herds (27 out of 28) segregated far-off cows from close-up dry cows, with regrouping occurring at varying frequencies: monthly (1 farm), bi-weekly (13 farms), and weekly (13 farms). This two-group strategy during the dry period is commonly associated with nutritional management practices, particularly the use of anionic diets in the close-up group. While regrouping can affect feeding behavior and intake, studies indicate minimal impact under favorable conditions of feed access and resting areas (4, 26). Primiparous cows were housed together with multiparous cows in most herds (n = 22) for more than 20 days; only 6 herds separated primiparous from multiparous cows in the close-up period.

Regarding facilities, most farms allocated far-off and close-up dry cows in dry-lots (21 and 26 farms, respectively), with the remainder on pasture. Dry-lots generally provided adequate space without significant cost implications. They were in good condition, with a low depth of mud and good access to feed bunks and waterers, although it is highly dependent on rain events. Thirty-six percent of the farms did not provide shade to their far-off cows, whereas 93% of the close-up groups ensured shade provision. As demonstrated by Laporta *et al.* (2020), heat abatement provision to dry cows is important to prevent milk losses in the subsequent lactation and in the progeny.

A common practice is to have fresh cow groups to identify sick cows (9), considering that 30% to 50% of dairy cows affected by metabolic and infectious diseases are detected around parturition (18). The intensive monitoring of fresh cows to detect disorders at an early stage and to treat the cows if necessary is an important factor in promoting good performance of the cow during future lactation (28). In this context, accounting with fresh cow groups and daily management protocols can optimize fresh cow management efficiency.

Concerning consultancy, most herds (n = 27/28) were assessed by feed company consultants, and some by private consultants (n = 20/28) on weekly visits. Farmers prefer to act in response to information provided to their contexts. Referents may vary for each producer, but veterinarians often influence farmers' decision-making about infectious disease prevention (24).

The average length of the last dry period for multiparous cows was 59 days (SD = 11.4). This duration aligns closely with recommendations from previous studies advocating a 60-day dry period, aimed at optimizing milk production income and minimizing metabolic disorders (12). However, recent research suggests potential benefits in shortening or even customizing dry period strategies to balance milk yield and metabolic health (3, 16). In this study, although intentions behind these shorter periods were not explicitly confirmed, 20% of the farms implemented shorter dry periods, averaging 50 days or less.

Evaluations of BCS across far-off, close-up, and fresh cows revealed average scores of 3.2 (SD = 0.38), 3.6 (SD = 0.32), and 3.6 (SD = 0.37), respectively. While far-off cows exhibited similar average BCS as reported in previous studies (14), 25% of them scored 3.5 or higher, potentially impacting metabolic health outcomes (5). More on, close-up cows were evidently fatter than far-off cows. Although controlled energy diets were meant to be fed to the latter (see nutrient composition in *Feeds and feeding management* section), maybe the net energy for lactation (NE_L) content should be even lower (1.4 Mcal/kg) (2). According to these authors, a greater decrease in BCS after calving is expected in these cows, increasing metabolic disorders and impairing reproductive performance. Probably, shortening the dry period to 45 d could improve energy balance in the transition period.

Feeds and Feeding Management

Considering the initial 28 farms, diet composition data were successfully gathered for far-off dry cows from 22 farms, close-up cows from 26 farms, and fresh or lactating cows from 27 farms. However, some farms were excluded due to missing data, particularly those using pasture diets exclusively.

Far-off cow diets, excluding those on pasture, generally contained lower dry matter (DM), crude protein (CP), starch, and ether extract (EE) compared to close-up and fresh/lactating cow diets (table 1). This difference primarily stems from higher forage inclusion in far-off diets, with most being total mixed rations (TMRs) featuring corn silage. In contrast, a subset of farms utilized pasture-based diets for far-off cows, resulting in lower DM content. Close-up diets maintained similar NE_L levels to far-off diets but included higher starch and EE content, often supplemented with high-fiber ingredients such as wheat straw to mitigate health disorders during the fresh period. Notably, far-off diets exhibited higher NE_L than those reported by Kerwin *et al.* (2023), potentially contributing to an increased BCS during this period. Excessive energy consumption is known to accumulate in adipose tissue, increasing the risk of metabolic issues (2). Regarding dietary cation-anion difference (DCAD), all close-up diets included anionic salts as a strategy to reduce the incidence of hypocalcemia, an important practice supported by regular urinary pH measurements in these farms. In fresh/lactating diets, carbohydrate balances were maintained to achieve 15-28% of fNDF, 15-19% CP and 20-32% starch levels across diets. In these diets, DCAD values were generally positive, with a few farms achieving values greater than 350 mEq/kg, which is recommended to enhance dry matter intake and fat-corrected milk (20).

Table 1. Nutrient composition means (SD) of far-off, close-up and fresh or lactating groups in dairy farms in Argentina.

Tabla 1. Composición nutricional promedio (DE) de vacas secas, preparto y frescas o en lactancia en establecimientos lecheros de Argentina.

Group, n	DM, %	CP, %	NE_L, Mcal/kg	NDFom, %	fNDF, %
Far-off, 22*	38.1 (11.8)	13.3 (1.7)	1.49 (0.11)	43.3 (5.6)	41.4 (6.7)
Close-up, 26	46.7 (6.6)	14.6 (2.0)	1.49 (0.09)	43.0 (4.5)	36.0 (6.1)
Fresh/Lactating, 30	47.4 (6.2)	17.1 (1.2)	1.69 (0.09)	30.3 (2.9)	20.0 (3.8)

Group, n	Starch, %	Fat, %	Ash, %	DCAD, mEq/kg
Far-off, 22*	12.9 (4.3)	2.7 (0.4)	8.3 (1.6)	285.5 (65.2)
Close-up, 26	16.9 (2.8)	3.1 (0.7)	8.9 (1.4)	-150.6 (85.7)
Fresh/Lactating, 30	25.8 (2.6)	4.2 (0.9)	7.0 (1.2)	249.5 (83.1)

*Far-off groups fed only pasture were not included.

DM= dry matter; CP= crude protein; NE_L= net energy for lactation; NDFom= neutral detergent fiber, organic matter-based; fNDF= forage NDF; DCAD= dietary cation-anion difference.

*No se incluyeron los rodeos de vacas secas en pastoreo.

DM= materia seca; CP= proteína cruda; NE_L= energía neta de lactancia; NDFom= fibra detergente neutro base materia orgánica; fFDN=FDN de forraje; DCAD= diferencia catiónica-aniónica dietaria.

All farms fed different diets during the dry period (far-off and close-up diets). Table 2 (page 6) summarizes the ingredient compositions for far-off, close-up and lactating cow diets.

Every farm included corn silage in at least one of their diets. Concentrates predominantly comprised corn and soybean meal, aligning closely with nutrient compositions reported by Kerwin *et al.* (2022) from dairy herds in the northeastern United States.

Far-off and close-up cow diets were typically delivered once daily, with most farms (93%) monitoring feed bunk refusals in close-up groups but less in far-off (74%). Most fresh/lactating cows were fed twice daily, with daily monitoring of feed bunks. Sampling and analysis practices for forages and concentrates varied significantly across farms. Forages were sampled and analyzed only when a new bag or ingredient was used on most farms. Wet concentrates were not sampled and analyzed in most farms (64%), although wet forages were sampled and analyzed every 3 months (24%) or when a new ingredient was used or a new bag opened (62%). Dry concentrates were not sampled in one-third of the

cases, and hays were sampled when a new lot came to the farm or every 3 months in 2 thirds of the farms. Sampling schedules often fall short of optimal frequencies recommended for small and large herds (30).

Table 2. Ingredient composition means (SD) of far-off, close-up and fresh or lactating groups in dairy farms in Argentina.

Tabla 2. Inclusión promedio (DE) de ingredientes de dietas de vacas secas, preparto y frescas o en lactancia en establecimientos lecheros de Argentina.

Ingredient	Dry-off Diet		Close-up Diet		Lactating Diet	
	Number of groups	Inclusion mean and SD, %	Number of groups	Inclusion mean and SD, %	Number of groups	Inclusion mean and SD, %
Corn silage	20	44.5 (16.2)	27	48.8 (8)	30	30.4 (7)
Wheat straw	6	28.9 (11.7)	20	20.7 (8)	-	-
Soybean meal	7	5.8 (2.9)	19	12.8 (5.5)	23	15.1 (4.3)
Corn grain	6	8.8 (4.0)	10	6.3 (2.0)	25	21.2 (5.6)
Alfalfa hay/silage	20	44.0 (16.5)	-	-	30	17.7 (10.6)
Cottonseed whole	-	-	-	-	14	8.4 (2)
Soybean hulls	2	11.9 (0.0)	-	-	11	6.2 (2.4)

Health Events

Data on milk fever, clinical mastitis, metritis, retained placenta, culling, and death events were recorded across 2,957 cows that calved during April and May 2022 (table 3).

Table 3. Incidence of health events during the first 21 days in milk at cow- and herd-level in dairy farms in Argentina.

Tabla 3. Incidencia de eventos de salud durante los primeros 21 días en lactancia a nivel de vaca y de rodeo en establecimientos lecheros de Argentina.

Health events	At cow level (n = 2,957)		At herd level (n = 24)
	Primiparous cows (n = 1,116)	Multiparous cows (n = 1,841)	
	n (%)	n (%)	Median, % (range)
Milk fever	0 (0)	65 (3.5)	1.8 (0-5.6)
Clinical mastitis	7 (0.6)	39 (2.1)	0.3 (0-6.5)
Metritis	54 (4.8)	72 (3.9)	2.7 (0-11.1)
Retained placenta	18 (1.6)	45 (2.4)	1.4 (0-20)
Culled	6 (0.5)	30 (1.6)	1.2 (0-5.1)
Death	6 (0.5)	33 (1.8)	1.4 (0-4.6)

In our study, we observed lower herd incidences and reduced variability in specific health events such as milk fever, metritis, culling, and death compared to recent data published by Kerwin *et al.* (2022). Our data fall below the achievable prevalence levels determined by Caixeta and Omontese (2021), which could be attributed to the selection process of these farms. Additionally, at the cow level, our data indicate higher incidences compared to those reported by Masia *et al.* (2022) and Ruprechter *et al.* (2018) in farms located in Argentina and Brazil. In the case of Masia *et al.* (2022), the database was provided by DairyComp - Clientes Ciale Alta, whose farms are generally considered well-managed or at least benefit from professional advice. Ruprechter *et al.* (2018) included data from only one farm. On the other hand, our data suggest significantly lower incidences of mastitis and retained placenta compared to the findings in other studies, which could indicate underreporting of these events, although this could also be the case in those other studies.

Blood sample results from 310 analyzed cows showed that 28 had hyperketonemia, representing a 9% overall incidence, with the majority being multiparous cows (n = 24). At the herd level, we found a median incidence of 8% (range: 0 - 30%). Similarly, Kerwin *et al.* (2022) reported that nearly half of the farms in their study had less than 15% of cows with values >1.2 mmol/L of BHB.

Our study, similar to surveys of German farmers (13) and farms in California (9), included assessments of fresh cows. However, both studies noted that the evaluation of fresh cows primarily relied on nonspecific observations, suggesting potential benefits from implementing more objective practices to identify health disorders.

Milk Yield and Quality

We recorded milk yield at start-up (10 to 30 DIM) and peak (75 to 105 DIM) from 2,064 and 2,084 cows, respectively, that calved during April and May 2022 (table 4).

Table 4. Milk yield at start-up and peak average (SD) for cows calved during April and May 2022 in dairy farms in Argentina.

Tabla 4. Promedio (DE) de producción de leche al inicio y al pico en vacas paridas durante abril y mayo de 2022 en establecimientos lecheros de Argentina.

Lactation number	Start-up milk yield		Peak milk yield	
	n	Average, kg	n	Average, kg
1	776	28.0 (7.3)	808	34.3 (8.1)
2	559	37.2 (9.6)	540	39.8 (9.7)
≥3	729	37.5 (11.1)	736	41.4 (10.8)
Overall	2064	33.8 (10.4)	2084	38.2 (10.1)

Our results show that primiparous cows produced 75% of the milk yield of mature cows (≥3 lactations) at the beginning of lactation. This proportion is slightly higher than the 71.3% reported by Kerwin *et al.* (2023), although absolute milk yield in our study was 1.5 kg lower. A greater disparity is evident in milk yield among mature cows, with almost a 4 kg difference, though standard deviations are similar. This highlights a clear opportunity to increase individual milk yield, particularly among primiparous cows.

In comparison to the national average milk yield in 2022, which was 24 kg/cow/day (21), these farms generally exhibit higher milk yields. Similarly, mean fat and crude protein content (3.9% and 3.5%, respectively) on these farms were greater than national average values (3.7% ± 0.18 and 3.4% ± 0.07 for fat and crude protein in milk, respectively) according to OCLA (2023), but lower than those reported by Kerwin *et al.* (2023) from farms in northeastern United States. While most industries in our country pay based on volume, some farms trade directly with factories, presenting different challenges in terms of milk composition.

The study has some limitations that warrant consideration. Firstly, dairy farms were chosen based on their receipt of professional consultancy from graduate students specialized in nutrition, indicating a likelihood of better-than-average management practice. Additionally, the herds surveyed had more cows per farm than the national average of 158 cows per farm (22), which may result in management practices and performance indicators that differ from those observed in smaller-scale operations. Secondly, measurements and records were gathered over a short period, which may not fully capture seasonal variations that could influence study outcomes. Thirdly, health event records relied on reports from farm personnel, potentially leading to variability in data accuracy and completeness. These limitations underscore the need for cautious interpretation of the findings, particularly regarding the generalizability and temporal applicability of the results. However, this study provides valuable insights into transition cow management practices, feeding regimes, health outcomes, and milk production characteristics across a sample of dairy farms in Argentina. Overall, while the studied farms generally exhibited good management practices, opportunities exist to enhance feeding management, health monitoring protocols, and data recording practices. Future research could explore the economic implications of implementing more intensive health monitoring and feeding strategies, focusing on milk yield and composition.

Conclusions

This study contributes valuable data on transition cow management and performance metrics in Argentine dairy farms, highlighting areas of strength and opportunities for refinement to support sustainable dairy production practices.

On the positive side, a key strength observed across the farms was the routine separation of far-off and close-up dry cows, which enables targeted nutritional and health management strategies during this critical period. Notably, the implementation of negative DCAD diets in close-up groups reflects a proactive approach to preventing hypocalcemia. Frequent bunk monitoring during the transition period also suggests a high level of attention to feed access and intake, which likely contributes to the low incidence of metabolic disorders, culling, and mortality recorded in these systems. In addition, milk composition data revealed higher-than-average solids content compared to national data, indicating effective nutritional strategies and potential for improved milk quality and value.

However, the study also identified several opportunities for refinement. One important area is the grouping strategy in the prepartum phase: primiparous and multiparous cows are often housed together, which may negatively affect younger animals due to social stress and competition. Additionally, the lack of shade for dry cows in some farms may compromise animal comfort, health and productivity, especially in warmer seasons. A second key issue is the length of the dry period, which in several cases exceeded 50 days. This extended duration, in combination with increased energy density in prepartum diets, was associated with undesirable increases in body condition, highlighting the need for more precise energy balance management during the transition. Moreover, the frequency of forage and wet feed sampling was often lower than recommended, limiting the accuracy of ration formulation and monitoring. On the production side, individual milk yield, particularly among primiparous cows, and milk solids content were identified as areas with potential for further improvement, suggesting that refinements in feeding, grouping, or overall cow comfort could yield better performance outcomes.

In summary, while transition cow management in the surveyed Argentine dairy farms shows solid foundational practices, the study underlines the importance of continued attention to grouping strategies, environmental aspects, feed monitoring, and precision nutrition to optimize both animal welfare and productive efficiency during this critical period of the lactation cycle.

References

1. Caixeta, L. S.; Omontese, B. O. 2021. Monitoring and improving the metabolic health of dairy cows during the transition period. Animals 11: 1-17. https://doi.org/10.3390/ani11020352
2. Cardoso, F. C.; Kalscheur, K. F.; Drackley, J. K. 2020. Symposium review: Nutrition strategies for improved health, production, and fertility during the transition period. J. Dairy Sci. 103:5684-5693. https://doi.org/10.3168/jds.2019-17271
3. Cermakova, J.; Kudrna, V.; Simeckova, M.; Vyborna, A.; Dolezal, P.; Illek, J. 2014. Comparison of shortened and conventional dry period management strategies. J. Dairy Sci. 97: 5623-5636. https://doi.org/10.3168/jds.2013-7499
4. Chebel, R. C.; Silva, P. R. B.; Endres, M. I.; Ballou, M. A.; Luchterhand, K. L. 2016. Social stressors and their effects on immunity and health of periparturient dairy cows. J. Dairy Sci. 99: 3217-3228. https://doi.org/10.3168/jds.2015-10369
5. Contreras, L. L.; Ryan, C. M.; Overton, T. R. 2004. Effects of dry cow grouping strategy and prepartum body condition score on performance and health of transition dairy cows. J. Dairy Sci. 87: 517-523. https://doi.org/10.3168/jds.S0022-0302(04)73191-4
6. Couto Serrenho, R.; Church, C.; McGee, D.; Duffield, T. F. 2022. Environment, nutrition, and management practices for far-off, close-up, and fresh cows on Canadian dairy farms-A retrospective descriptive study. J. Dairy Sci. 105: 1797-1814. https://doi.org/10.3168/jds.2021-20919
7. Daros, R. R.; Weary, D. M.; von Keyserlingk, M. A. G. 2022. Invited review: Risk factors for transition period disease in intensive grazing and housed dairy cattle. J. Dairy Sci. 105: 4734-4748. https://doi.org/10.3168/jds.2021-20649
8. Drackley, J. K. 1999. ADSA foundation scholar award: Biology of dairy cows during the transition period: The final frontier? J. Dairy Sci. 82: 2259-2273. https://doi.org/10.3168/jds.s0022-0302(99)75474-3
9. Espadamala, A.; Pallarés, P.; Lago, A.; Silva-del-Río, N. 2016. Fresh-cow handling practices and methods for identification of health disorders on 45 dairy farms in California. J. Dairy Sci. 99: 9319-9333. https://doi.org/10.3168/jds.2016-11178
10. Gregoretti, G.; Baudracco, J.; Dimundo, C.; Lazzarini, B.; Scarel, J.; Alesso, A.; Machado, C. 2024. Traditional cow-calf systems of the northern region of Santa Fe, Argentina: current situation and improvement opportunities. Revista de la Facultad de Ciencias Agrarias. Universidad Nacional de Cuyo. Mendoza. Argentina. 56(1): 106-116. DOI: https://doi.org/10.48162/rev.39.127
11. Grummer, R. R. 1995. Impact of changes in organic nutrient metabolism on feeding the transition dairy cow. J. Anim. Sci. 73(9): 2820-2933. https://doi.org/10.2527/1995.7392820x
12. Grummer, R. R.; Rastani, R. R. 2004. Why reevaluate dry period length? J. Dairy Sci. 87: E77-E85. https://doi.org/10.3168/jds.S0022-0302(04)70063-6
13. Heuwieser, W.; Iwersen, M.; Gossellin, J.; Drillich, M. 2010. Short communication: Survey of fresh cow management practices of dairy cattle on small and large commercial farms. J. Dairy Sci. 93: 1065-1068. https://doi.org/10.3168/jds.2009-2783
14. Kerwin, A. L.; Burhans, W. S.; Mann, S.; Tetreault, M.; Nydam, D. V.; Overton, T. R. 2022. Transition cow nutrition and management strategies of dairy herds in the northeastern United States: Part I-Herd description and performance characteristics. J. Dairy Sci. 105: 5327-5348. https://doi.org/10.3168/jds.2021-20862
15. Kerwin, A. L.; Burhans, W. S.; Nydam, D. V.; Overton, T. R. 2023. Transition cow nutrition and management strategies of dairy herds in the northeastern United States: Part III-Associations of management and dietary factors with analytes, health, milk yield, and reproduction. J. Dairy Sci. 106: 1246-1266. https://doi.org/10.3168/jds.2022-21876
16. Kok, A.; van Hoeij, R. J.; Kemp, B.; van Knegsel, A. T. M. 2021. Evaluation of customized dry-period strategies in dairy cows. J. Dairy Sci. 104: 1887-1899. https://doi.org/10.3168/ jds.2020-18719
17. Laporta, J.; Ferreira, F. C.; Ouellet, V.; Dado-Senn, B.; Almeida, A. K.; De Vries, A.; Dahl, G. E. 2020. Late-gestation heat stress impairs daughter and granddaughter lifetime performance. J. Dairy Sci. 103: 7555-7568. https://doi.org/10.3168/jds.2020-18154
18. Leblanc, S. 2010. Monitoring metabolic health of dairy cattle in the transition period introduction-metabolic challenges in peripartum dairy cows and their associations with reproduction. J. Reprod. Dev. 56: 29-35.
19. Masia, F.; Molina, G.; Vissio, C.; Balzarini, M.; de la Sota, R. L.; Piccardi, M. 2022. Quantifying the negative impact of clinical diseases on productive and reproductive performance of dairy cows in central Argentina. Livest. Sci. 259: 104894. https://doi.org/10.1016/j.livsci.2022.104894
20. NASEM (National Academies of Sciences, Engineering, and Medicine). 2021. Nutrient Requirements of Dairy Cattle. 8th rev. ed. Washington, DC: National Academies Press.
21. OCLA (Observatorio de la Cadena Láctea Argentina). Informe Anual de la Cadena Láctea Argentina 2022. Buenos Aires. Argentina.
22. OCLA (Observatorio de la Cadena Láctea Argentina). Informe Anual de la Cadena Láctea Argentina 2023. Buenos Aires, Argentina.

23. Oetzel, G.; McGuirkl, S. 2010. Fact Sheet - Cowside Blood BHBA Testing with a Hand-Held "Ketometer." University of Wisconsin-Madison. School of Veterinary Medicine 1-4.
24. Ritter, C.; Jansen, J.; Roche, S.; Kelton, D. F.; Adams, C. L.; Orsel, K.; Erskine, R. J.; Benedictus, G.; Lam, T. J. G. M.; Barkema, H. W. 2017. Invited review: Determinants of farmers' adoption of management-based strategies for infectious disease prevention and control. J. Dairy Sci. 100: 3329-3347. https://doi.org/10.3168/jds.2016-11977
25. Ruprechter, G.; Adrien, M. de L.; Larriestra, A.; Meotti, O.; Batista, C.; Meikle, A.; Noro, M. 2018. Metabolic predictors of peri-partum diseases and their association with parity in dairy cows. Res. Vet. Sci. 118: 191-198. https://doi.org/10.1016/j.rvsc.2018.02.005
26. Schirmann, K.; Chapinal, N.; Weary, D. M.; Heuwieser, W.; von Keyserlingk, M. A. G. 2011. Short-term effects of regrouping on behavior of prepartum dairy cows. J. Dairy Sci. 94: 2312-2319. https://doi.org/10.3168/jds.2010-3639
27. Schuenemann, G. M.; Piñeiro, J. M.; Turiello, P. 2016. Association between management practices and reproductive performance of lactating dairy cows. Page 600 in Proc. 2016 JAM.
28. Silva, M. A.; Veronese, A.; Belli, A.; Madureira, E. H.; Galvão, K. N.; Chebel, R. C. 2021. Effects of adding an automated monitoring device to the health screening of postpartum Holstein cows on survival and productive and reproductive performances. J. Dairy. Sci. 104: 3439-3457. https://doi.org/10.3168/jds.2020-18562
29. Turiello, P.; Piñeiro, J. M.; Schuenemann, G. M. 2016. Association between management practices and dairy herd performance. Page 600 in Proc. 2016 JAM.
30. Weiss, W. P.; St-Pierre, N. R. 2009. Impact and Management of Variability in Feed and Diet Composition. Pages 83-96 in Proc. 18th Annual Tri-State Dairy Nutrition Conference.
31. Wildman, E. E.; Jones, G. M.; Wagner, P. E.; Boman, R. L.; Troutt, H. F.; Lesch, T. N. 1982. A Dairy Cow Body Condition Scoring System and Its Relationship to Selected Production Characteristics. J. Dairy Sci. 65: 495-501. https://doi.org/10.3168/jds.S0022-0302(82)82223-6

Acknowledgements

The authors gratefully acknowledge the contributions of consultants Rodrigo Cuello Antón, Mauro Gorgerino, José Prai, Guillermo Ciepielak, Nicolás Hajduczyk, and Leonardo Bussi for their dedicated work in conducting the farm audits.

Longevity of Purebred and Triple-Cross Dairy Cows in Entre Rios, Argentina

Longevidad de vacas lecheras razas puras y triples cruzas en un establecimiento de Entre Ríos, Argentina

Roberto Cheij [1, 2*], María Gabriela Molina [3], María Laura Fischman [4], Walter Mancuso [5], Pablo Roberto Marini [1, 2]

Originales: *Recepción:* 28/11/2024 - *Aceptación:* 22/10/2025

ABSTRACT

This study evaluated animal longevity according to age at first calving of pure and triple-cross dairy cows in an establishment in Entre Ríos, Argentina. Retrospective data from 1.498 dairy cows between 2012 and 2021 were analyzed, belonging to a commercial establishment in the center-west of Entre Ríos province, Argentina. Analyzed cows were those discarded (due to sale or death) and with records of their entire productive life. They belonged to five different racial groups, pure Holstein (H), pure Jersey (J) and triple crosses, resulting from the insemination of Holstein x Jersey (F1) cross cows with semen from bulls of the Brown Swiss (P), Guernsey (G) and Montbeliarde (M) breeds, respectively. The cows were grouped into three levels (CAT), according to age at first calving. These categories were: CAT1: < 24 months; CAT2: 24 ≤ CAT2 ≤ 30 months and CAT3: > 30 months. Significant differences were found in survival curves of the productive life variable ($p=0.0001$) at 50% survival probability. Jersey cows had the lowest longevity (60.4 months) and showed significant differences with Guernsey (72.7 months), Holstein (65.8 months) and Montbeliarde (70 months). Brown Swiss cows (86 months) had the highest longevity compared to the rest (CAT was not considered). In CAT1, Brown Swiss showed significant differences from the rest ($p<0.05$). In CAT2, Brown Swiss showed significant differences ($p<0.05$), as J when compared with Guernsey. In CAT3, only Brown Swiss showed significant differences ($p<0.05$) compared to Guernsey, Jersey and Montbeliarde. Triple-cross Brown Swiss dairy cows had greater longevity. Those having their first calving at a later age showed higher longevity, both in comparison with other genotypes and among the Brown Swiss cows.

Keywords
dairy cow • adaptation • welfare • fertility • grazing system

https://doi.org/10.48162/rev.39.211

1 Universidad Nacional del Chaco Austral. Carrera de Ing. Zootecnista. Comandante Fernández 755. (C. P. 3700). Presidencia Roque Sáenz Peña. Argentina.
2 Facultad de Ciencias Veterinarias (FCV). Universidad Nacional de Rosario (UNR). Doctorando en Ciencias Veterinarias. Ovidio Lagos y Ruta 33. (C. P. 2170). Casilda. Argentina. * roberto_cheij_2000@hotmail.com
3 Universidad Nacional de Córdoba. Facultad de Ciencias Agropecuarias. Juan Filloy s/n. (C. P. 5000). Córdoba. Argentina.
4 Universidad de Buenos Aires. Facultad de Ciencias Veterinarias. INITRA. Chorroarín 280. (C. P. 1427). Ciudad Autónoma de Buenos Aires. Argentina.
5 INTA EEA Paraná. Ruta 11 Km 12,5 (CP 3100). Paraná. Argentina.

Licenses Creative Commons
Attribution - Non Commercial - Share Alike

Resumen

En este trabajo se evaluó la longevidad animal según la edad al primer parto de vacas lecheras puras y triple cruza en un establecimiento de Entre Ríos, Argentina. Se analizaron datos retrospectivos de 1.498 vacas lecheras entre los años 2012 y 2021, pertenecientes a un establecimiento comercial ubicado en el centro-oeste de la provincia de Entre Ríos, Argentina. Las vacas analizadas fueron aquellas descartadas (por venta o muerte) en el establecimiento, vacas con registro de toda su vida productiva. Pertenecían a cinco grupos raciales diferentes, Holstein puras (H), Jersey puras (J) y triple cruzas, resultantes de la inseminación de vacas cruzas Holstein x Jersey (F1) con semen de toros de las razas Pardo Suizo (P), Guernsey (G) y Montbeliarde (M), respectivamente. Las vacas se agruparon en tres niveles (CAT), según la edad al primer parto. Estas categorías fueron: CAT1: < 24 meses; CAT2: 24 ≤ CAT2 ≤ 30 meses y CAT3: > 30 meses. Se encontraron diferencias significativas entre las curvas de supervivencia de la variable vida productiva (p=0,0001) al 50% de probabilidad de supervivencia. Las vacas Jersey presentaron la menor longevidad (60,4 meses) y mostraron diferencias significativas con Guernsey (72,7 meses), Holstein (65,8 meses) y Montbeliarde (70 meses). Las vacas Pardo Suizo (86 meses) presentaron la mayor longevidad respecto del resto (no se consideró CAT). En CAT1, Pardo Suizo presentó diferencias significativas respecto del resto (p<0,05). En CAT2, Pardo Suizo mostró diferencias significativas (p<0,05), al igual que J al compararse con Guernsey. En CAT3, solo Pardo Suizo presentó diferencias significativas (p<0,05) respecto de Guernsey, Jersey y Montbeliarde. Las vacas lecheras triple cruza Pardo Suizo presentaron mayor longevidad. Aquellas que tuvieron su primer parto a una edad más tardía mostraron una mayor longevidad, tanto en comparación con otros genotipos como entre las vacas Pardo Suizo.

Palabras clave
vaca • adaptación • bienestar • fertilidad • sistema de pastoreo

Introduction

Recently, dairy cow longevity has gained increasing relevance, primarily due to the consequences of high levels of individual production (3, 33), low fertility (9, 22) and environmental (2, 15, 16) and economic factors (10, 15) associated with a shorter than expected lifespan.

Culling dairy cows in early production stages, before reaching biological maturity, is considered unsustainable (14, 25, 35). The concept of longevity has been linked to animal welfare (31).

Without human intervention, a dairy cow is biologically capable of living up to 20 years. However, average time spent in the herd currently ranges from 4.5 to 5.5 years, or between 2.5 and 3.5 lactations (11). Marini and Di Masso (2019) compared purebred cows and cows with breeding records living together in the same establishment. They found the productive lifespan (measured as the number of births) was 3 (1-8) and 3 (1-10), respectively, with no significant survival difference between groups.

Today, dairy farmers seek to capitalize on the favorable traits of "alternative" dairy breeds to mitigate the negative effects associated with inbreeding and leverage heterosis benefits (30, 32). Many studies have demonstrated increased fertility and survival rates when using crossbred cows compared to purebred Holstein or Holstein-Friesian cows, in pasture-based and high-input confinement systems (5, 27, 34). Economic analyses also indicate improved profitability in these systems, due to lower replacement costs and higher herd productivity (19, 28).

Reducing age at first calving seems to enhance productive lifespan and increase milk production per cow over their lifetime (12). Copas Medina *et al.* (2022) and Cañete *et al.* (2025) concluded that Holstein and Brown Swiss cows that calved earlier remained productive longer on the farm and produced more milk over their lifetime.

Information on longevity of dairy cows in grazing systems and its evolution over time is scarce in Argentina. Therefore, the objective of this study was to evaluate longevity of purebred and triple-cross dairy cows based on age at first calving in a farm in Entre Ríos, Argentina.

Materials and Methods

Retrospective data from 1498 dairy cows were analyzed from 2012 to 2021, from a commercial dairy farm located center-west of Entre Ríos (32°00' South y 59°34' West), Argentina.

Dairy Herd

The farm has 2,400 cows managed in 5 similar milking units. Average milk yield is 8,800 liters per lactation (24 liters/cow/day), with an average composition of 3.90% fat and 3.70% protein. The production system was grazing with supplementation, consisting of an average diet with 45% pastures for direct consumption, 20% preserved forage (hay and silage) and 35% concentrates. The diet varies according to availability, based on climatic conditions or feed prices. The pastures used for direct grazing during the evaluation period consisted of polyphytic meadows based on alfalfa (*Medicago sativa L.*), mixed with fescue (*Lolium arundinaceum* Schreb. Darbysh), white clover (*Trifolium repens L.*) and native barley (*Bromus catharticus* Vahl). Also, monophytic winter greens of oats (*Avena sativa L.*) and annual ryegrass (*Lolium multiflorum L.*), depending on the season and availability of standing forage. Additionally, they were provided with preserved forage, including corn silage (*Zea mays L.*), hay from pastures, and concentrates. The concentrates were formulated onsite using grains, by-products from agro-industry and mineral salts, according to the needs of balanced diets and/or forage supply for milking cows. Table 1 shows average dry matter supply per milking cow and seasonal dietary composition.

Table 1. Seasonal average (kg/cow and day) and percentage composition of ration offered (% on DM).

Tabla 1. Promedio estacional (kg/vaca y día) y composición porcentual de la ración ofrecida (% sobre MS).

Food	% Offered by season of year			
	Spring	Summer	Autumn	Winter
Alfalfa-based polyphytic pastures	39%	39%	23%	19%
Winter green fodder	9%	0%	12%	17%
Corn silage, whole plant	22%	29%	29%	30%
Pasture hays	2%	1%	3%	2%
Concentrated mix*	28%	31%	33%	32%
TOTAL (kg DM/cow and day)	23.0	22.1	24.3	23.5

References: * Mix contained variable percentages of corn and/or sorghum grain, soybean expeller, wheat and/or rice bran and mineral salts, depending on availability and season.

Referencias: * Mezcla con porcentajes variables, según disponibilidad y estación, de: grano de maíz y/o sorgo, expeler de soja, afrechillo de trigo y/o arroz y sales minerales.

Database

The analyzed cows were those culled (due to sale or death) from the establishment, specifically those with complete productive records belonging to five racial groups (RG), pure Holstein (H) cows (n=72), pure Jersey (J) (n=38) and triple cross cows, resulting from the insemination of Holstein x Jersey (F1) with semen from Brown Swiss (P) (n=436), Guernsey (G)(n=396) and Montbeliarde (M) (n=556) bulls. The cows were grouped into three levels (CAT) according to age at first calving. These categories were CAT1: < 24 months; CAT2: 24 ≤ CAT2 ≤ 30 months and CAT3: > 30 months. The following data were recorded for each cow: Date of birth (DB); Date of calving (DCP); Date of culling or death (FDM); Longevity (L) in days (FN - FDM); Number of calvings (NP); Age at first calving (AFC) in days (DC - CP); Culling (C). A cow was considered culled when it died or was sold for different reasons.

Records containing incomplete or missing data were excluded from the analysis. Table 2 (page 4), shows the final number of animals analyzed, classified by category and racial group.

Table 2. Number of animals analyzed per category of age at first calving (CAT) and racial group (RG), after removing incomplete records.

Tabla 2. Número de animales analizados por categoría de edad al primer parto (CAT) y grupo racial (GR), después de eliminar los registros incompletos.

CAT \ RG	G	H	J	M	P	Sum
1	222	32	7	238	276	775
2	162	32	23	268	135	620
3	12	8	8	50	25	103
Sum	396	72	38	556	436	1498

Statistical Analysis

Longevity of purebred and triple-cross dairy cows was evaluated by *Age at First Calving*. Two survival models were used, each with a particular purpose and focus.

Overall Survival Model: In the first analysis, a Kaplan-Meier survival model assessed longevity of the different GRs, not considering age at first calving as a stratifying factor. This model allowed comparing GRs' survival curves throughout their productive life.

Survival Model Stratified by Age at First Calving (AFC): A stratified survival model used CAT-adjusted log-rank test. This approach was chosen to control potential heterogeneity caused by age at first birth. Stratification by AFC allowed a precise assessment of survival differences between RG, considering variability introduced by AFC.

Using these two approaches was based on the first model, on the need to identify overall differences in longevity between breeds and crosses, providing a general performance overview of the different RG throughout their productive life. Considering the stratified model, the effect of age at first calving on longevity was isolated, providing a more detailed understanding of how these variables influence survival, allowing specific conclusions in the context of age at first calving.

Both analyses were carried out using the statistical software R (2023). The survival library was used to fit the models and estimate survival curves. In both survival models, the event of interest was the cow leaving the herd (due to culling by death or sale), and the analyzed time was longevity, measured in days from calving until culling date (sale or death). The general survival model (Kaplan-Meier) involved survival curves generated by the survfit function from the survival package in R. Differences between survival curves were evaluated using the Long-rank test, implemented via the survfit function from the same package, considering racial group (RG) as the sole predictor factor. The survival model stratified by age at first calving (AFC) reutilized the survfit function, including the argument strata = CAT (category of age at first calving), controlling heterogeneity introduced by age and accurately evaluating differences in survival among breed groups within each stratum. Age at first calving (CAT) was categorized into three levels (CAT1: <24 months; CAT2: between 24 and 30 months; CAT3: >30 months). This stratified model assessed survival differences among breed groups adjusted by the defined AFC categories.

Results

Figure 1 (page 5), shows the Kaplan-Meier survival curves of purebred H, J cows, and triple-crossbreds, P, G and M cows, not accounting for age effects. Significant differences were found between the survival curves of the productive lifespan variable (p=0.0001) at 50% probability of survival. J cows had the shortest longevity (60.4 months), showing significant differences with G (72.7), H (65.8) and M (70 months). The P cows (86 months) presented the longest longevity, 86 months.

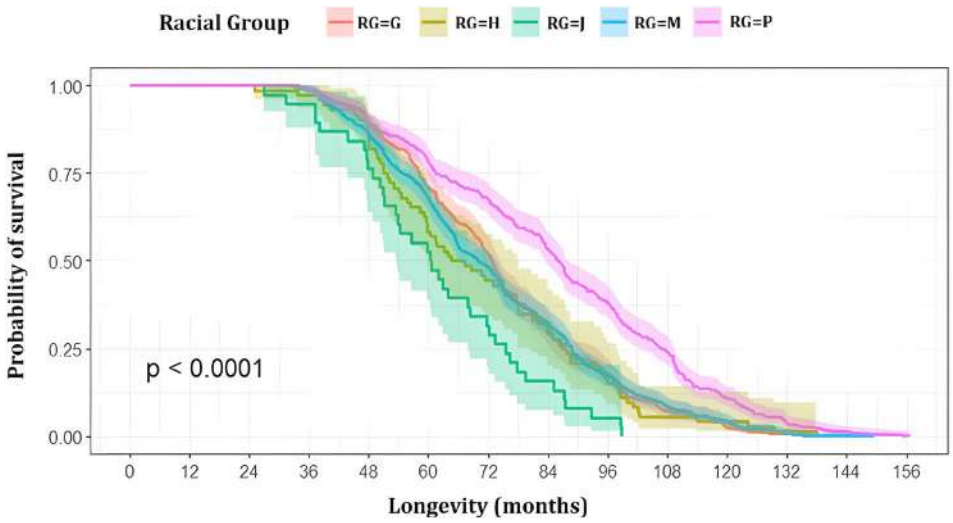


Figure 1. Survival analysis for longevity of purebred and crossbred dairy cows.

Figura 1. Análisis de supervivencia para la longevidad de vacas lecheras puras y cruzas.

Table 3 shows culling risk for each analyzed genotype, with differences in survival patterns. Considering 60 months of age as a comparison point, 71% of individuals in RG G, 58.3% in RG H, 52.6% in RG J, 68% in RG M and 78% in RG P reached this threshold, confirming survival trends observed in figure 1.

Table 3. Proportion of cows under culling risk.

Tabla 3. Proporción de vacas en riesgo de ser descartada.

Groups	Percentage of cows													
G	100	100	100	99	89	71	52	31	18	7	3	1	0	0
H	100	100	100	97	82	58	44	29	15	6	4	1	0	0
J	100	100	100	95	76	53	32	16	5	0	0	0	0	0
M	100	100	100	99	87	68	48	33	17	9	4	1	0	0
P	100	100	100	99	90	78	68	53	37	24	11	4	1	0
Months	**0**	**12**	**24**	**36**	**48**	**60**	**72**	**84**	**96**	**108**	**120**	**132**	**144**	**156**

Note: Holstein (H), Jersey (J) and triple crosses, resulting from the insemination of Holstein x Jersey (F1) cross cows with semen from bulls of the Brown Swiss (P), Guernsey (G) and Montbeliarde (M) breeds.

Nota: Holstein (H), Jersey (J) y triples cruzas, resultantes de la inseminación de vacas cruza Holstein x Jersey (F1) con semen de toros de las razas Pardo Suizo (P), Guernsey (G) y Montbeliarde (M).

In the AFC Stratified Model, the chi-square statistic was 90.7 (with 4 degrees of freedom, p<2e-16). This result indicates significant differences in survival among the evaluated groups when considering age at first birth. Pairwise comparisons within each category are detailed in table 4 (page 6).

Table 4. Median months of life by age category at first calving.
Tabla 4. Medianas de los meses de vida por categoría de edad al primer parto.

	G	H	J	M	P
CAT1	72.6 [a]	63.4 [a]	79.4 [a]	72.3 [a]	85.6 [b]
CAT2	73.1 [a]	69.6 [a,b]	60.5 [b,c]	67.0 [a,b]	85.9 [d]
CAT3	62.5 [a]	80.8 [a,c]	54.0 [a,b]	71.1[a,b]	96.7 [c, d]

In CAT1, RG P shows significant differences compared to the other groups ($p<0.05$). In CAT2, P shows significant differences ($p<0.05$) against any other group. In CAT3, only P has significant differences ($p<0.05$) with G, J and M (figure 2).

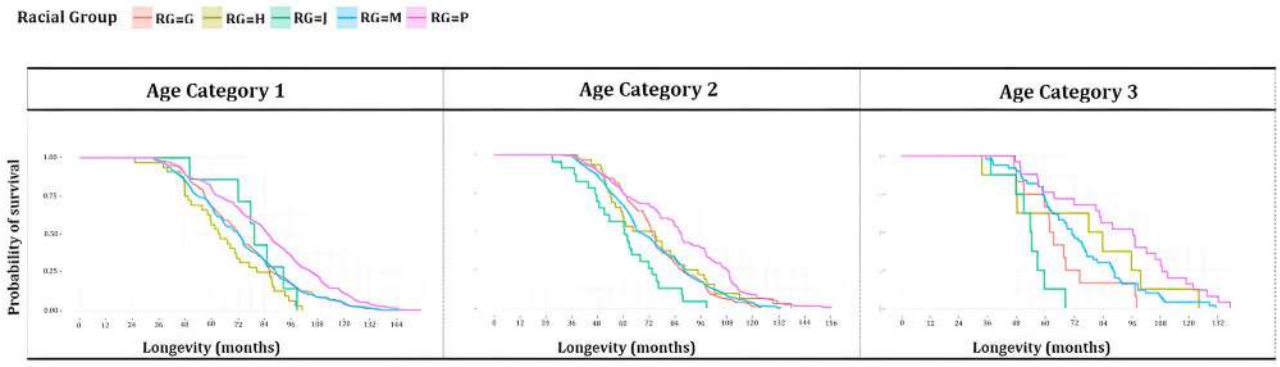


Figure 2. Survival probability according to age at first calving and RG.
Figura 2. Probabilidad de supervivencia según edad al primer parto y GR.

Discussion

In recent decades, dairy cows have achieved significant advancements in individual milk production (within a limited number of breeds). However, this progress has been accompanied by considerable drawbacks, including a loss of genetic diversity and a decline in health, resilience, robustness, welfare and longevity (4). Moreover, Piccardi *et al.* (2014) and Pipino *et al*. (2023) reported that Swedish Red x Holstein crossbred cows were superior in longevity compared to pure Holstein cows, with higher survival rates across successive lactations.

In dairy systems under grazing with supplementation, Frana-Bisang *et al*. (2023) found no significant differences in survival curves for the productive life variable analyzed for purebred Holstein (HO) cows, and HO x Jersey (F1), F1 x Montbeliarde (M) and M x Holstein (XB) crosses. However, although no differences were found in the productive life variable, when survival to subsequent births was analyzed, all crosses exhibited greater persistence in the second and third calvings compared to pure HO cows. An earlier study in the same establishment examined purebred, crossbred and triple-crossbred cows (23). Studying Holstein, Holstein x Jersey, (Holstein x Jersey) x Brown Swiss and (Holstein x Jersey) x Guernsey genotypes, these authors found survival curves with 50% probability that individuals from all genotypes would reach the end of their first lactation before 1100 days of age for the event of completion of the first lactation. Furthermore, there was a 90% probability of Brown Swiss cows finishing their first lactation before 1.200 days of age, while Guernsey, Holstein x Jersey and Holstein cows required an additional 150 days to achieve the same probability. Differences between survival curves for the different genotypes were statistically significant.

Likewise, our results show that crossbred cows have a longer lifespan than the studied purebred. In turn, among the crossbred cows, P cows had the longest lifespan (figure 1, page 5). This aligns with Andersen (2008), who indicated that Brown Swiss showed comparative advantages in longevity, especially in adverse ecosystems for Holstein. Dairy farms employing this type of crossbreeding could achieve a herd structure with older cows producing more milk, butterfat, and protein, with a lower replacement rate. Consequently, the crossbred studied would improve survival expectancy in grazing-based production systems, particularly when supplemented strategically with bulk and concentrated feeds (table 1, page 3). Previous studies by Kargo *et al.* (2012) and Buckley *et al.* (2014) demonstrated that crossbred cows exhibited higher fertility and survival rates compared to pure Holstein cows, using a variety of modern breeds in high-input (confined production) and low-cost (grazing-based) systems.

Hazel *et al*. (2017) suggested that using only two breeds for crossbreeding does not fully exploit heterosis, and rotational crossbreeding involving three breeds better enhances reproductive aspects. Similarly, considering longevity, crossbreeding among three breeds would have the same weight, showing that triple crosses are longer-lived (figure 1, page 5).

This study also examined whether age at first calving influences final life expectancy, a topic not extensively discussed. In this sense, P cows showed the greatest longevity regardless of age at first calving. However, P cows with the oldest age at first calving had the greatest longevity (compared to the other genotypes) and higher values in median life months, compared to the P of CAT1 and CAT2 (table 2, page 4). However, Copas Medina *et al.* (2022) showed that, in tropical systems, pure Holstein and Brown Swiss cows that gave birth at an early age (<36 months) lived longer, remained productive for a longer period within the system and had higher overall milk production throughout their lives. Similarly, Casanova *et al*. (2011) found that cows calving for the first time at an older age (40 months) had a 23% higher risk of being culled than those calving at 30 months. Marini and Di Masso (2019), comparing purebred cows and cows with breeding records, in the same establishment, could not find an association between age at first calving and calving number. However, a significant association was observed in those with breeding records, indicating that the older the age at first calving, the lower the total number of calvings.

Mean longevity of Brown Swiss cows first calving at a younger age (<2.5 years) was shorter than that of cows calving for the first time at an older age. However, as for Holstein cows, Brown Swiss cows calving at a younger age had more days in production and more lifetime milk production than those calving later (9).

Few studies have analyzed the association between age at first calving and longevity; therefore, the impact of reduced age at first calving on long-term performance remains unclear (21). Haworth *et al*. (2008) reported that cows between 24 and 29 months at first calving had greater longevity and productivity than those calving at 30 months or older. This finding aligns with a retrospective study on Holstein herds that calve younger (24-25 months), demonstrating better survival rates and higher productivity (8).

Based on these findings, crossbreeding would be a relevant alternative to counteract the current challenge of low longevity of dairy cows in herds corresponding to these regions (11). To effectively overcome this issue, comprehensive measures are needed.

Conclusions

This study confirms that crossbred dairy cows, especially triple P crossbreds, have greater longevity compared to the studied purebred. This finding suggests that dairy farms implementing crossbreeding, like for P cows, could benefit from a herd structure with older cows. This could lead to increased total production of milk, butterfat, and protein throughout their productive lifespan, while reducing replacement needs in the herd.

Age at first calving constitutes a significant factor influencing cow longevity. Although P-crossed cows showed general greater longevity, we observed that those first calving at a later age showed greater longevity, compared to other genotypes and among themselves. These results support the idea that an adequate age at first calving can benefit longevity throughout cow life.

Applying global and stratified survival models allowed effective evaluation of the genetic and management factors on dairy cows longevity. This suggests that a selection strategy considering age at first calving and genotype could optimize longevity and productivity in grazing dairy production systems, leading to long-term economic and productive benefits.

Considering the study used information from commercial herds in grazing production systems with supplementation, rather than from experimental herds, our results hold importance for the Humid Pampas – Argentina, and other temperate climates worldwide.

References

1. Andersen, H. 2008. Alternativas genéticas para la ganadería lechera intensiva. Manual de ganadería lechera. Capítulo 1.3. http://handresen.perulactea.com/manual-de-ganaderia-lechera/
2. Bergea, H.; Roth, A.; Emanuelson, U.; Agenas, S. 2016. Farmer awareness of cow longevity and implications for decision-making at farm level. Acta Agriculturae Scandinavica, Section A - Animal Science. 66(1): 25-34. DOI: https://doi.org/10.1080/09064702.2016.1196726
3. Bobadilla, P. E.; López-Villalobos, N.; Sotelo, F.; Damián, J. P. 2024. Dairy cow longevity is affected by dam parity and age. Dairy. 5(4): 590-597. DOI: https://doi.org/10.3390/dairy5040044
4. Brito, L. F.; Bedere, N.; Douhard, F.; Oliveira, H. R.; Arnal, M.; Peñagaricano, F.; Schinckel, A. P.; Baes, C. F.; Miglior, F. 2021. Review: Genetic selection of high-yielding dairy cattle toward sustainable farming systems in a rapidly changing world. Animal. The international journal of animal biosciences. 15(1). DOI: https://doi.org/10.1016/j.animal.2021.100292
5. Buckley, F.; Lopez-Villalobos, N.; Heins, J. B. 2014. Crossbreeding: Implications for dairy cow fertility and survival. Animal. 8(1): 122-133. DOI: https://doi.org/10.1017/S1751731114000901
6. Casanova, D; Schneider, M. P.; Andere, C. I.; Rodriguez, E. M.; Rubio, N. E.; Juliarena, M.; Diaz, C.; Carabaño, M. J. 2011. Análisis de la longevidad funcional de la raza Holando Argentino. Revista Taurus, Buenos Aires. 13(51): 21-29
7. Cañete, V.; Lazzarini, B.; Alesso, A.; Baudracco, J.; Marini, P. R. 2025. Milk Production, Age at First Calving, and Calving-to-Conception Interval in Holstein, Brown Swiss, and Holstein x Brown Swiss Cows. Revista de la Facultad de Ciencias Agrarias. Universidad Nacional de Cuyo. Mendoza. Argentina. 57(2): 148-154.. DOI: https://doi.org/10.48162/rev.39.178
8. Cooke, J. S.; Cheng, Z.; Bourne, N. E.; Wathes, D. C. 2013. Association between growth rates, age at first calving and subsequent fertility, milk production and survival in Holstein-Friesian heifers. Open Journal of Animal Sciences. 3(1): 1-12. DOI: https://doi.org/10.4236/ojas.2013.31001
9. Copas Medina, K. A.; Valladares Rodas, M.; Baeza Rodríguez, J. J.; Magaña Monforte, J. G.; Segura Correa, J. C. 2022. Effect of early age at first calving on longevity, number of days in production and lifetime milk yield of Holstein and Brown Swiss dairy cows in Honduras. Revista Mexicana de Ciencias Pecuarias. 13(1): 163-174. DOI: https://doi.org/10.22319/rmcp.v13i1.5444
10. Dallago, G. M.; Wade, K. M.; Cue, R. I.; McClure, J. T.; Lacroix, R.; Pellerin, D.; Vasseur, E. 2021. Keeping dairy cows for longer: A critical literature review on dairy cow longevity in high milk-producing countries. Animals. 11(10). DOI: https://doi.org/10.3390/ ani11030808
11. De Vries, A.; Marcondes, M. I. 2020. Review: Overview of factors affecting productive lifespan of dairy cows. Animal. 14(1): 155-164. DOI: https://doi.org/10.1017/S1751731119003264
12. Eastham, N. T.; Caots, A.; Cripps, P.; Richardson, H.; Smith, R.; Oikonomou, G. 2018. Association between age at first calving and subsequent lactation performance in UK Holstein and Holstein-Friesian dairy cows. PloS ONE. 13(6): eo197764. DOI: https://doi.org/10.1371/journal.pone.0197764
13. Frana Bisang, E.; Quercia, E.; Pipino, D.; Piccardi, M.; Marini, P. R. 2023. Vida productiva, supervivencia, descartes y muertes de vacas en diferentes cruzamientos de razas lecheras en un sistema a pastoreo. Revista Veterinaria, Facultad de Ciencias Veterinarias-UNNE. 34(2): 76-80. DOI: https://doi.org/10.30972/vet.3427047
14. Gambonini, A. P.; Hadrich, J. C.; Roberts, A. R. 2022. Estimation and analysis of cow-level cumulative lifetime break-even on financial resiliency. Journal of Dairy Science. 105(1): 4653-4668. DOI: https://doi.org/10.3168/jds.2021-20644
15. Grandl, F.; Furger, M.; Kreuzer, M.; Zehetmeier, M. 2019. Impact of longevity on greenhouse gas emissions and profitability of individual dairy cows analysed with different system boundaries. Animal. 13(1): 198-208. DOI: https://doi.org/10.1017/S175173111800112X
16. Gregoretti, G.; Baudracco, J.; Dimundo, C.; Lazzarini, B.; Scarel, J.; Alesso, A.; Machado, C. 2024. Traditional cow-calf systems of the northern region of Santa Fe, Argentina: current situation and improvement opportunities. Revista de la Facultad de Ciencias Agrarias. Universidad Nacional de Cuyo. Mendoza. Argentina. 56(1): 106-116. DOI: https://doi.org/10.48162/rev.39.127
17. Haworth, G. M.; Tranter, W. P.; Chuck, J. N.; Cheng, Z.; Wathes, D. C. 2008. Relationships between age at first calving and first lactation milk yield, and lifetime productivity and longevity in dairy cows. Veterinary Record. 162(20): 643-647. DOI: https://doi.org/10.1136/vr.162.20.643

18. Hazel, A. R.; Heins, B. J.; Hansen, L. B. 2017. Fertility, survival, and conformation of Montbeliarde x Holstein and Viking Red x Holstein crossbred cows compared with pure Holstein cows during first lactation in 8 commercial dairy herds. Journal of Dairy Science. 100(11): 9447-9458. DOI: https://doi.org/10.3168/jds.2017-12824
19. Hazel, A. R.; Heins, B. J.; Hansen, L. B. 2020. Herd life, lifetime production, and profitability of Viking Red-sired and Montbeliarde-sired crossbred cows compared with their Holstein herdmates. Journal of Dairy Science. 104(3): 3261-3277. DOI: https://doi.org/10.3168/jds.2020-19137
20. Kargo, M.; Madsen, P.; Norberg, E. 2012. Short communication: Is crossbreeding only beneficial in herds with low management level? Journal of Dairy Science. 95(2): 925-928. DOI: https://doi.org/10.3168/jds.2011-4707
21. Kusaka, H.; Yamazaki, T.; Sakaguchi, M. 2023. Association of age at first calving with longevity, milk yield, and fertility up to the third lactation in a herd of Holstein dairy cows in Japan. Journal of Reproduction and Development. 69(6): 291-297. DOI: https://doi.org/10.1262/jrd.2023-012
22. López Parra, J. C.; Marini, P. R.; Macagno, A. J.; Bó, G. A. 2024. Effect of three different fixed-time AI protocols on follicular dynamics and pregnancy rates in suckled, dual-purpose cows in the Ecuadorian Amazon. Revista de la Facultad de Ciencias Agrarias. Universidad Nacional de Cuyo. Mendoza. Argentina. 56(1): 138-148. DOI: https://doi.org/10.48162/rev.39.130
23. Mancuso, W. A.; Barbona, I.; Marini, P. R. 2015. Survival curves to evaluate age of end of lactation in dairy cows from different genotypes. Asian Journal of Agriculture and Food Sciences. 3(5): 514-521. https://ajouronline.com/index.php/AJAFS/article/view/3043
24. Marini, P. R.; Di Masso, R. J. 2019. Edad al primer parto e indicadores de eficiencia en vacas lecheras con diferente potencialidad productividad en sistemas a pastoreo. La Granja: Revista de Ciencias de la Vida. 29(1): 84-96. DOI: http://doi.org/10.53588/alpa.320502
25. Marini, P. R. 2024. Crossbreeding: a device to improve the longevity of dairy cows. Archivos Latinoamericanos de Producción Animal. V Congreso Internacional de Producción Animal Especializada en Bovinos. 32(1): 9-18. DOI: http://doi.org/10.17163/lgr.n29.2019.07
26. Piccardi, M.; Pipino, D.; Bó, G. A.; Balzarini, M. 2014. Productive and reproductive performance of first lactation pure-bred Holstein versus Swedish red & white x Holstein in central Argentina. Livestock Science. 165(1): 37-41. DOI: http://doi.org/10.1016/j.livsci.2014.04.025
27. Pipino, D.; Piccardi, M.; Lopez-Villalobos, N.; Hickson, R. E.; Vázquez, M. I. 2023. Fertility and survival of Swedish Red and White x Holstein crossbred cows and purebred Holstein cows. Journal of Dairy Science. 106(4): 2475-2486. DOI: https://doi.org/10.3168/jds.2022-22403
28. Pipino, D.; Lopez-Villalobos, N.; Hickson, R.; Cabrera, V.; Balzarini, M.; Piccardi, M. 2024. Profitability of Swedish Red and White × Holstein crossbred cows compared with purebred Holstein cows. J. Dairy Sci. 108: 1602-1614. https://doi.org/10.3168/jds.2024-25260
29. R Core Team. 2023. R: A Language and Environment for Statistical Computing. R Foundation for Statistical Computing, Vienna, Austria. https://www.R-project.org/
30. Rinell, E.; Heringstad, B. 2018. The effects of crossbreeding with Norwegian Red dairy cattle on common postpartum diseases, fertility and body condition score. Animal. 12(12): 2619-2626. DOI: https://doi.org/10.1017/S175173111800037X
31. Rocklinsberg, H.; Gamborg, C.; Gjerris, M.; Rydhmer, L.; Tjarnstrom, E.; Wallenbeck, A. 2016. Understanding Swedish dairy farmers' view on breeding goals - ethical aspects of longevity. Food futures: ethics, science and culture. DOI: https://doi.org/10.3920/978-90-8686-834-6_7
32. Sørensen, M. K.; Norberg, E.; Pedersen, J.; Christensen, L. G. 2008. Crossbreeding in dairy cattle: a Danish perspective. Journal of Dairy Science. 91(11): 4116-4128. DOI: https://doi.org/10.3168/jds.2008-1273
33. Turiello, M. P.; Vissio, C. 2026. Transition management and dairy cow performance: insights from dairy farms in Argentina. Revista de la Facultad de Ciencias Agrarias. Universidad Nacional de Cuyo. Mendoza. Argentina. 58(1): e8540. DOI: https://doi.org/10.48162/rev.39.199
34. Vance, E. R.; Ferris, C. P.; Elliott, C. T.; McGettrick, S. A.; Kilpatrick, D. J. 2012. Food intake, milk production performance, and tissue changes of Holstein-Friesian and Jersey x Holstein-Friesian dairy cows within a medium-input grazing system and a high input total confinement system. Journal of Dairy Science. 95(3): 1527-1544. DOI: https://doi.org/10.3168/jds.2011-4410
35. Vredenberg, I.; Han, R.; Mourits, M.; Hogeveen, H.; Steeneveld, W. 2021. An empirical analysis on the longevity of dairy cows in relation to economic herd performance. Frontiers in Veterinary Science. 8. DOI: https://doi.org/10.3389/fvets.2021.646672

Author Contributions

CR, PRM, WM: Conceptualization, Writing - review & editing; CR, PRM, MMG, Supervision, Methodology, Writing; MMG: Data curation, PRM, MW, FML: Writing, review & editing.

Conflicts of Interest

The authors declare no conflicts of interest.

Declaration of Funding and Acknowledgments

The authors would like to thank Brandi, Santiago and the members of the El Caraguatá S.A. establishment who made this work possible.
To the Secretariat of Research, Science and Technology of the National University of Chaco Austral for financing the PhD student Roberto Cheij, through a postgraduate scholarship (SICyT-UNCAUS).

A Data Availability Statement

The data that supports this study will be shared upon reasonable request to the corresponding author.

Valorization of Regional Crude Glycerol. Culture Media Optimization for Batch Docosahexaenoic Acid (DHA) Production with *Aurantiochytrium* sp.

Valorización de glicerol crudo regional. Optimización de medios de cultivo para la producción batch de ácido docosahexaenoico (DHA) con *Aurantiochytrium* sp.

Esteban Andrés Sanchez [1*], Debora Laura Manuale [1], Pablo Antonio Torresi [1], Vanina Elizabet Marquez [2], Francisco Collombati [3], Alejandro José Beccaria [2], Juan Carlos Yori [1]

Originales: *Recepción:* 10/04/2024 - *Aceptación:* 05/04/2025

ABSTRACT

Docosahexaenoic acid (DHA) has many benefits for human health. Commercial DHA sources derive from marine fish but present several production challenges. *Aurantiochytrium* sp., an abundant marine microalga, becomes an alternative for DHA production. Crude glycerol produced by small-scale biodiesel refineries is a regional, available, and inexpensive waste that can be converted into value-added compounds. This study investigated crude glycerol as a potential carbon source for DHA-rich oil production using an aerobically isolated *Aurantiochytrium* sp. in batch shake flasks. We also optimized the culture medium formulation by varying carbon and nitrogen sources, thereby reducing medium costs while maximizing DHA production. A larger initial *Aurantiochytrium* sp. inoculum improved cell concentration and medium carbon depletion, increasing DHA productivity (P_{DHA}). Increasing culture time showed no differences in *Aurantiochytrium* sp. growth parameters, but reduced DHA production. The absence of yeast extract in the culture media resulted in faster substrate metabolism by *Aurantiochytrium* sp. and increased DHA production. Crude glycerol yielded the highest P_{DHA} (15.35 mg L^{-1} h^{-1}) at 120 h. Crude glycerol can be used as a cheaper carbon source in media formulation with *Aurantiochytrium* sp. cultures for DHA production.

Keywords
crude glycerol • *Aurantiochytrium* sp. • DHA • inoculum • culture medium

https://doi.org/10.48162/rev.39.202

1 Universidad Nacional del Litoral (UNL). Facultad de Ingeniería Química (FIQ). Programa de Valorización, Desarrollo y Escalado de Procesos Agroindustriales (PROVADE). Ruta Nacional 168 Km 0 (S3000). Santa Fe. Argentina. * esanchez@fiq.unl.edu.ar
2 Universidad Nacional del Litoral (UNL). Facultad de Bioquímica y Ciencias Biológicas (FBCB). Laboratorio de Fermentaciones. Ruta Nacional 168 Km 0 (S3000). Santa Fe. Argentina.
3 Universidad Nacional del Litoral (UNL). Ruta Nacional 168 Km 0 (S3000). Santa Fe. Argentina.

Licenses Creative Commons
Attribution - Non Commercial - Share Alike

Resumen

El ácido docosahexaenoico (DHA) posee muchos beneficios para la salud humana. Las fuentes comerciales de DHA se obtienen de peces marinos, pero presenta desventajas. *Aurantiochytrium* sp., una microalga marina abundante, surge como alternativa para la producción de DHA, solucionando los problemas de obtener DHA a partir de peces marinos. El glicerol crudo producido por pequeñas refinerías de biodiesel es un descarte regional, disponible y barato, capaz de ser transformado en compuestos de valor agregado. El objetivo de este trabajo fue investigar la potencial utilización de glicerol crudo regional como fuente de carbono para producir aceite rico en DHA, utilizando la cepa aeróbica aislada *Aurantiochytrium* sp. en matraces batch agitados; y optimizar la formulación de medios de cultivo, variando las fuentes de carbono y nitrógeno, para reducir costos y maximizar la producción de DHA. Los tamaños de inóculo iniciales más grandes de *Aurantiochytrium* sp mejoran la concentración celular y agotan la fuente de carbono, mejorando la productividad a DHA (P_{DHA}). El aumento del tiempo de cultivo no mostró diferencias en los parámetros de crecimiento de *Aurantiochytrium* sp., pero disminuyó la producción de DHA. La ausencia de extracto de levadura en los medios de cultivo produjo una metabolización más rápida del sustrato por *Aurantiochytrium* sp., mejorando la producción de DHA. Con glicerol crudo se alcanzó la mejor P_{DHA} (15,35 mg L^{-1} h^{-1}) a 120 h. El glicerol crudo se puede utilizar como fuente de carbono barata en la formulación de medios en cultivos con *Aurantiochytrium* sp. para producir DHA.

Palabras clave

glicerol crudo • *Aurantiochytrium* sp. • DHA • inóculo • medio de cultivo

Introduction

Polyunsaturated fatty acids (PUFA), particularly omega-3 (ω-3), play an important role in physiological functions (13). Docosahexaenoic acid (DHA, C22:6 ω-3) and eicosapentaenoic acid (EPA, C20:5 ω-3) have vasodilatory and anti-inflammatory capacity, prevent atherosclerosis and hypertension, reduce risk factors for thrombosis, arthritis, and Alzheimer's disease, and increase development of the central nervous system and retinal tissue, improving visual acuity and cognitive capacity in children (5, 33). DHA is commonly presented in pharmaceuticals (nutraceutical and functional products), medicine (Alzheimer's and cerebrovascular drugs), and food (soft drinks, dairy, and infant products) (12, 33).

Commercial sources of ω-3 DHA are obtained from marine fish and shellfish using a well-known technology that produces 600,000 tonnes annually (21). However, the process faces overfishing, strong seasonal dependence, low DHA yield (< 50% w/w), high levels of marine pollutants (dioxins, methylmercury, polychlorinated biphenyls, metals), fish odor, and low DHA stability (17). Given these problems and the constant demand for high-quality ω-3 DHA, new strategies like microalgae cultures become promising alternatives (6).

Microalgae cultures for DHA production offer high purity and good organoleptic properties, use renewable waste, are toxins-free, and have low fermentation costs (23). Heterotrophic strains of the Thraustochytriaceae family (*Aurantiochytrium*, *Schizochytrium,* and *Thraustochytrium*) have significant growth rates compared to photoautotrophic microalgal cultivation, producing more than 50% of their dry cell weight as lipids, with ω-3 DHA reaching 50% of total fatty acids in some species (8, 20). *Aurantiochytrium* sp., an aerobic thraustochytrid abundant in marine environments, has been an alternative source of ω-3 DHA. This microalga can grow readily on various carbon sources and has high P_{DHA}, replacing traditional marine fish oil production (20, 37).

Efforts regarding *Aurantiochytrium* sp. have focused on optimizing culture conditions and media (C, N, and micronutrients) to increase DHA production, mainly because costs highly depend on C sources (26, 28). Carbon concentration affects the synthesis of organic molecules and energy availability, while nitrogen concentration affects amino acids and nucleic acid synthesis (10). A traditional C source for fermentative DHA synthesis is glucose,

but in microalgal heterotrophic fermentation, glucose represents almost 80% of media cost (24, 37). The use of regional, highly available, and low-cost medium components with high C and/or N content instead of glucose economizes fermentation processes and provide energy for cell maintenance and biosynthesis (32).

In central Argentina, many companies produce large quantities of agro-industrial waste. The biodiesel industry produces crude glycerol (10% w/w) as a by-product. World biodiesel production will reach 40 million tonnes in 2025, producing 6.3 million tonnes of crude glycerol, and the market is estimated to grow to 3,670 million USD by 2030 (1, 16, 34). In biodiesel refineries, small-scale purification is not economically viable and the by-product is sold at low cost, depending on its quality level. This calls for a sustainable and economic process for converting crude glycerol into value-added compounds. Thus, crude glycerol could constitute a cheaper carbon source in microalgae cultures for ω-3 DHA production.

This study investigated two main points: i) the use of crude glycerol, without any purification treatment, as substrate for ω-3 DHA-rich oil production using a locally isolated oleaginous *Aurantiochytrium* sp. strain in batch cultures; and ii) the optimization of culture medium formulation, varying carbon and nitrogen sources, reducing costs and increasing ω-3 DHA-rich oil yield (P_{DHA}).

Materials and Methods

Materials

Crude glycerol (CG) was obtained as biodiesel by-product from Bolzán (Argentina). Pure anhydrous glycerol (AG), monohydrated glucose (MG) and methanol, ethanol, and isopropanol for extractive techniques were purchased from Cicarelli (Argentina). Peptone and yeast extract were purchased from Britania (Argentina). Salts for media preparation, KOH and *n*-hexane for fatty acid extraction, and Na_2SO_4 for total fatty acid determination were purchased from Research AG (Argentina). Fatty acid methyl ester (FAME) analytical standards were obtained from Merck (Argentina).

Isolation and Identification of Microorganisms

Aurantiochytrium sp. was obtained from seawater samples from the Argentinean coast and isolated in our laboratory. *Aurantiochytrium* sp. was isolated using the streak plate technique in Petri dishes (2). The culture medium was a synthetic AS100 (35) modified with 0.2 M NaCl (31), and supplemented with peptone (10 g L^{-1}), yeast extract (10 g L^{-1}), and monohydrated pure glucose (35 g L^{-1}), designed as PMG* medium. After adjusting pH to 7.00 and adding 1% agar, the medium was autoclaved at 115°C for 20 min. Cool but still liquid PMG* agar medium was distributed in sterile Petri dishes. Approximately 0.1 mL of the sample to be isolated was placed in these Petri dishes and spread with a sterilized bacteriological loop. Petri dishes were incubated at 28 ± 2°C for 3 to 4 days. Isolated colonies were then selected and transferred to another Petri dish until pure microalgae were obtained. Tubes containing 5 mL of liquid PMG* medium were prepared and autoclaved at 115°C for 20 min. Isolated microalgae were incubated at 28 ± 2°C for 2 to 3 days obtaining a higher-density culture for working stocks preparation. At all isolation stages, possible contamination with other microorganisms was detected by observing the microalgae under a 40X light microscope. The strain was stored in 25% (v/v) glycerol at -80 °C and cell viability was checked monthly.

Genomic DNA extraction was performed using the Easy Pure Plant Genomic DNA Kit (Transgene Biotech, China) identifying the microalgae at a molecular level. Polymerase chain reaction (PCR) was performed using a universal primer set (ITS Fo: 5' TCCGTAGGTGAACCTGCGG 3', ITS Rev: 5' TCCTCCGCTTATTGATATGC 3') to amplify the internal transcriber spacer (ITS) region at the ribosomal locus, including the 5.8S rRNA gene. The resulting PCR product was sequenced and the nucleotide sequence was analyzed with NCBI Basic Local Alignment Search Tool (BLAST). The sequence analysis showed 100% identity with the 5.8S rRNA gene of *Aurantiochytrium* sp. strain CCAP_4062/3 (MF766428.1). It also had a high percentage of identity (~98%) with *Aurantiochytrium limacinum* IMB188 (KP899823.1). Considering these results, the isolated organism would belong to the genus *Aurantiochytrium,* closely related to *A. limacinum*.

Batch Shake Flask Cultures

Aliquots of 1.5 mL of cells preserved in 25% (v/v) glycerol were used to inoculate 125 mL shake flasks containing 15 mL PMG* medium and placed on a heated orbital shaker at 150 rpm and 28 ± 2°C for 48 h. Four fermentation media were used for screening assays in batch shake flasks. Table 1 shows substrate carbon composition for media preparation, comparing useful carbon used per L of culture medium. We prepared PMG* medium and three other media identically formulated to PMG* but without yeast extract. The first was supplemented with 35 g L^{-1} of pure monohydrate glucose (PMG medium), the second replaced glucose with 35 g L^{-1} pure anhydrous glycerol (PAG medium), and the third replaced glucose with 42.5 g L^{-1} biorefinery crude glycerol (BCG medium) achieving identical amounts of available carbon in each medium. Media pH was adjusted to 7.00 before autoclaving at 115°C for 20 min. Ten mL of 10% (v/v) inoculum medium were transferred to 250 mL shake flasks containing 90 mL medium and placed in a heated orbital shaker at 150 rpm and 28 ± 2°C for 120 and 240 h assays.

Table 1. Substrate carbon composition used in modified artificial seawater medium for cultures of *Aurantiochytrium* sp.

Tabla 1. Composición de carbón de los sustratos utilizados en el medio agua de mar artificial modificado para cultivos de *Aurantiochytrium* sp.

Substrate	% G	% W	% A	% MONG	% M	gC L^{-1}
MG	99.5	---	0.5	---	---	13.99
AG	99.5	---	0.4	0.1	---	13.69
CG	81.7	11.5	4.2	2.5	0.1	13.74

% G: % glucose or glycerol; % W: % water; % A: % ash; % MONG: % matter organic non-glycerol; % M: % methanol; gC L^{-1}: g of useful carbon per L of culture medium.

% G: % glucosa o glicerol; % W: % agua; % A: % cenizas; % MONG: % materia orgánica no glicerol; % M: % metanol; gC L^{-1}: g de carbono útil por L de medio de cultivo.

Cell Disruption and Extraction of Algal Lipids

Once cultures finished, a 40 mL aliquot was transferred to a glass beaker with 10 mL of distilled water. Cells were homogenized and lysed using an ultrasonic cell disruptor for 1.2 kW and 20 kHz (Bald Design, Argentina) at 25°C for 30 s. Then, 50 mL of pure *n*-hexane was added to the lysed cells, maintaining a 5:1 (v/v) ratio with respect to distilled water. The mixture was vigorously shaken with a magnetic stirrer for 10 min. Finally, the organic phase was transferred to a 250 mL balloon and total lipids were extracted by vacuum distillation at 55°C.

Analytical Procedures

Biomass, Glucose and Glycerol Determinations

Culture samples (1 mL) were periodically taken and centrifuged at 9000 g and 25°C for 10 min. The supernatant was stored at -20°C. Biomass concentration was determined by cell counting using a Neubauer chamber (Boeco, Germany). Glucose and glycerol concentrations were identified with Glycemia and TG colorimetric kits (Wiener Lab, Argentina), in a UV spectrophotometer at 505 nm.

Dry Cell Weight and Total Fatty Acids

Culture samples (50 mL) were centrifuged at 3000 g and 25°C for 15 min. The supernatant was discarded and the biomass was washed twice with distilled water. Biomass was transferred to Petri dishes with filter paper (previously tared), oven-dried at 70°C for 12 h, and weighed until constant weight, obtaining dry cell mass. The filter paper (with dry biomass) was then removed from the Petri dishes and placed in a 50 mL Falcon tube for saponifiable lipid determination. The Falcon tube was filled with 5 mL of 30% w/v KOH and 5 mL of 96% v/v ethanol, and incubated in a thermostatic bath at 70°C for 16 h. The biomass-KOH-ethanol mixture was cooled to room temperature. Then 10 mL of *n*-hexane was added, the tube was vortexed for 1 min and the contents were centrifuged at 6000 rpm for 5 min, discarding the organic phase. This step was done twice.

The washed aqueous phase was incubated in an ice bath. Concentrated HCl was added until a pH of 1. Next, 10 mL of n-hexane was added, the tube was stirred vigorously for 1 min and the contents were centrifuged at 6000 rpm for 5 min to recover the organic phase. This step was also done twice. The two organic fractions (10 mL each) were transferred to a glass beaker (previously tared), oven-dried at 80 °C for 12 h, and weighed to constant weight. Saponifiable lipids obtained were compared with a calibration curve using crescent concentrations of standard fatty acid vs. the saponifiable fraction obtained by the described technique, obtaining total fatty acid (TFA) mass for each culture.

Fatty Acids Composition

Total lipids extraction employed a mixture of *n*-hexane:isopropanol (3:2) and 6% w/v Na_2SO_4 at room temperature (36). Extracted lipids were dried under a N_2 stream at 40°C. FAME was prepared following a cold method using *n*-hexane and KOH 2N in methanol (3). The obtained FAME fraction was quantified with a gas chromatograph GC-2014 (Shimadzu) equipped with a capillary column CP-Sil 88, 100 m x 0.25 mm ID (Varian) and a flame ionization detector (FID), using operating conditions as previously described (22).

Fatty acids were identified by comparing retention times of each peak and quantified from peak areas obtained from chromatograms with a FAME standard, using nonadecanoic acid methyl ester (19:0 ME) as internal standard (4, 11, 22).

DHA Quality

The nutritional quality and sensory properties of DHA-rich oil are highly dependent on the efficiency of the extraction method used (29). Peroxide value (PV, AOCS Official Method Cd 8b-90), representing the amount of peroxide (meq of active oxygen per kg of lipids) in a sample was determined as follows. Hydroperoxides (dissolved in acetic acid and chloroform) reacted with iodide ions from KI to form iodine, and PV was determined by titration of the liberated iodine with a known concentration of Na2S2O3 solution, using starch as an indicator (27). Acid value (AV, AOCS Official Method Da 14-48), *i.e.* free fatty acids (% oleic acid) in a sample was determined by titration technique determining the mg of KOH (0.1 N, in ethanolic solution) required to neutralize free FA per g of sample, dissolved in a mixture of ethyl ether:ethanol, employing phenolphthalein as an indicator (14). Elemental analysis for metal identification (Pb, Cd, Hg, As, Ni, Cu, Fe, Cr, and Co) was performed using an Optima 2100 DV inductively coupled plasma optical emission spectrometer (ICP-OES) (Perkin Elmer) with a CCD detector. Limit values were extracted from the results published by the European Union report (9).

Kinetic and Stoichiometric Parameters

Specific growth rate (μ, h^{-1}), substrate consumption rate (S_R, mg L^{-1} h^{-1}), DHA productivity (P_{DHA}, mg L^{-1} h^{-1}) and yield ($Y_{X/S}$, g g^{-1}) were calculated from experimental culture data obtained from dry cell weight (DCW, g L^{-1}), total fatty acid concentration (C_{TFA}, g L^{-1}), ω-3 PUFA concentration (C_{PUFA}, g L^{-1}) and DHA concentration (C_{DHA}, g L^{-1}).

Results and Discussion

Influence of Inoculum Size on Culture Parameters

To understand the influence of the initial inoculum size added to the media on main culture parameters, tests were developed in 250 mL batch shake flasks with 100 mL PMG* medium at 150 rpm and 28 ± 2°C for 120 h. Figure 1 (page 6), shows the initial inoculum concentration of *Aurantiochytrium* sp. in relation to final cell concentration (f_{DCW}), $S_{R,}$ and P_{DHA}. Increasing the initial inoculum size lowered final *Aurantiochytrium* sp. concentration only for the first inoculum size (0.5% v/v), but did not significantly increase the last three inoculum sizes (2.5, 5.0 and 10.0% v/v), which showed similar DCW levels. As *Aurantiochytrium* sp. metabolism produces a maximum cell concentration after 5 culture days, this was not much affected when the inoculum size added was between 2.5 and 10.0% v/v of fresh culture medium. Larger inoculum sizes could be tested but increasing inoculum sizes would not be economically viable in a scale-up process. As expected, S_R slightly increased with increasing inoculum size given a greater number of *Aurantiochytrium* sp.

cells growing in the same volume of initial culture medium. Only the two largest initial inoculum sizes (5.0 and 10.0% v/v) practically exhausted the medium substrate. The P_{DHA} markedly increased with increasing inoculum size, due to higher S_R obtained by a greater amount of *Aurantiochytrium* sp. cells available in culture. P_{DHA} was 2.85 and 6.84 mg L^{-1} h^{-1} at inoculum size of 0.5 and 10.0% v/v fresh culture medium, respectively.

Dashed lines show linear adjustment for each parameter. Tests were conducted in triplicate.

Las líneas discontinuas muestran el ajuste lineal para cada parámetro. Los ensayos fueron realizados por triplicado.

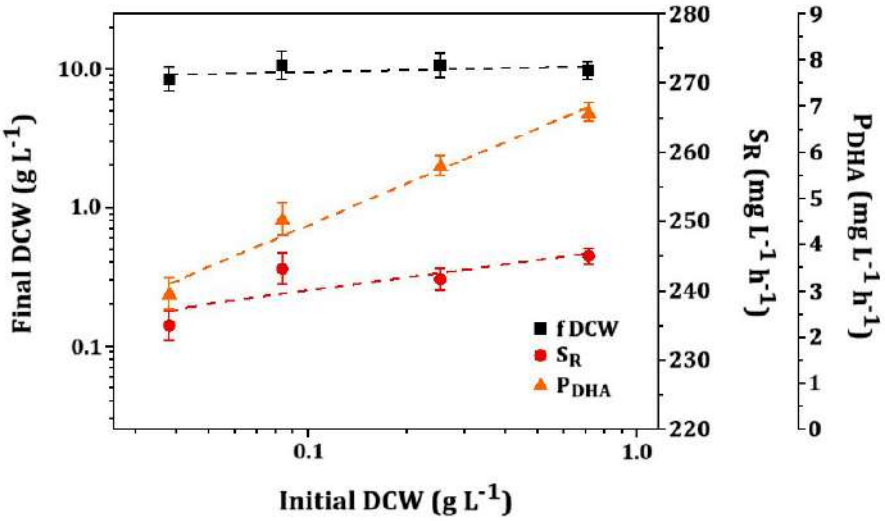


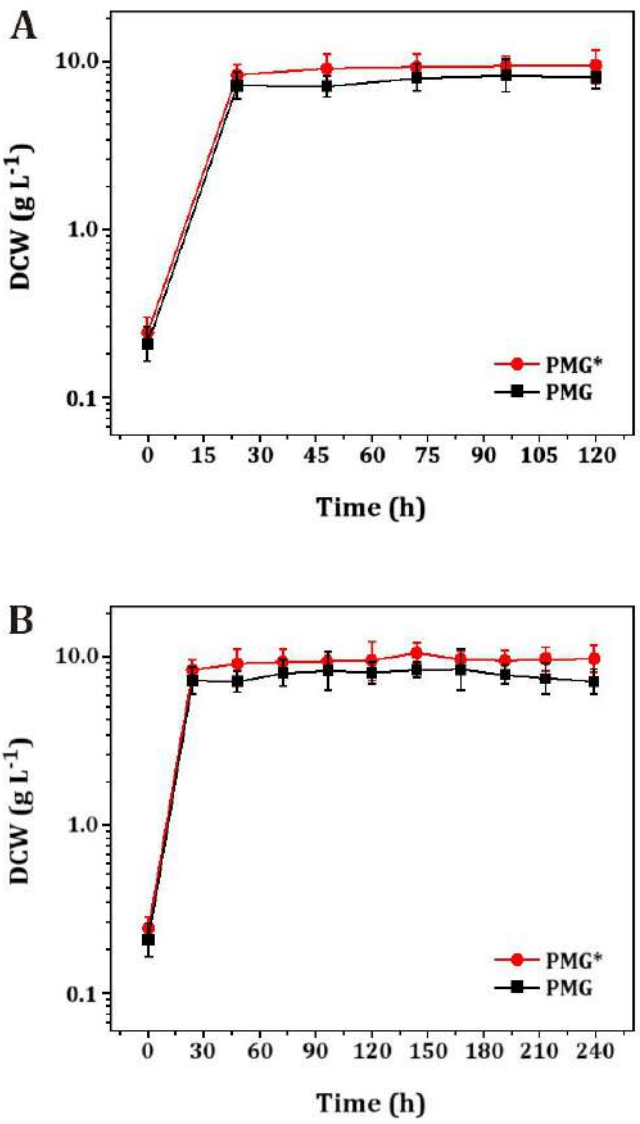
Figure 1. Final dry cell concentration (fDCW), S_R, and P_{DHA} vs. initial dry cell concentration (iDCW) for *Aurantiochytrium* sp. in 250 mL batch shake flasks with 100 mL PMG* medium, tested at 150 rpm and 28 ± 2 °C for 120 h.

Figura 1. Concentración celular final en base seca (fDCW), S_R y P_{DHA} vs. Concentración celular inicial en base seca (iDCW) para *Aurantiochytrium* sp. en matraces batch agitados de 250 mL con 100 mL de medio PMG*, testeados a 150 rpm y 28 ± 2 °C durante 120 h.

Previous results with *A. limacinum* SR21 demonstrate that inoculum preparation is fundamental for DHA production, with inoculum size having a significant effect on biomass production. High lipid accumulation was obtained with 10.0% v/v inoculum size, with higher P_{DHA} and DHA production (11 g L^{-1}) in a shorter time (30). In addition, the greatest increase occurred when inoculum size changed from 0.5 to 2.5% v/v of fresh culture medium, obtaining 60% more P_{DHA}. When inoculum size was doubled, from 2.5 to 5.0% v/v, and then from 5.0 to 10.0% v/v, 25% increase in P_{DHA} was achieved in both cases. Increasing initial inoculum size to 10.0% v/v had a direct effect on P_{DHA} and S_R, as a greater number of *Aurantiochytrium* sp. cells metabolize high amounts of substrate at the same medium volume and culture time.

Influence of Yeast Extract and Test Time on Culture Parameters

The development of *Aurantiochytrium* sp. cultures in 250 mL batch shake flasks at two final culture times was analyzed using PMG* and PMG media. Figure 2 (page 7), shows cell concentration curves at 120 h (figure 2A, page 7) were slightly higher for PMG* than for PMG medium, but showed similar behavior. An increase in culture time until 240 h (figure 2B, page 7) displayed the same behavior as for 120 h, with no major difference in DCW, and remaining constant during the stationary phase.



Tests were conducted in duplicate.

Los ensayos fueron realizados por duplicado.

Figure 2. Cell concentration curves of *Aurantiochytrium* sp. cultures in 250 mL batch shake flasks with 100 mL PMG* and PMG, tested at 150 rpm and 28 ± 2 °C for: A) 120 h and B) 240 h culture times.

Figura 2. Curvas de concentración celular de cultivos *Aurantiochytrium* sp. en matraces batch agitados de 250 mL con 100 mL de medios PMG* y PMG, ensayados a 150 rpm y 28 ± 2 °C durante: A) 120 h y B) 240 h de cultivo.

Table 2 (page 8), exhibits the main parameters obtained during fermentation of *Aurantiochytrium* sp. with 100 mL medium in batch shake flasks at 120 to 240 h culture times. The μ parameter was practically similar for all tests, but DCW decreased by 12.3 and 18.1% in PMG* and PMG media respectively, between 120 and 240 h culture time. Cultures with yeast extract did not deplete the supplied glucose, consuming 82.5 and 83.5% of added glucose at 120 and 240 h, respectively. PMG cultures also showed higher S_R than PMG* cultures. With PMG medium, consumed glucose reached 98.1% of the total added substrate at 120 h, and was practically consumed (99.7%) at 240 h. A preliminary screening revealed that adding 3.0% w/v glucose concentration from 2 to 10% w/v showed optimal culture parameters for *Aurantiochytrium* sp. cultures (18). In our tests, adding 35 g L^{-1} glucose (3.5% w/v) as initial substrate was appropriate.

Table 2. Culture parameters obtained during *Aurantiochytrium* sp. tests in 250 mL batch shake flasks with 100 mL PMG* and PMG, tested at 150 rpm and 28 ± 2 °C for two culture times.

Tabla 2. Parámetros de cultivo obtenidos durante los ensayos con *Aurantiochytrium* sp. en matraces batch agitados de 250 mL con 100 mL de medios PMG* y PMG, testeados a 150 rpm y 28 ± 2 °C a dos tiempos de cultivo.

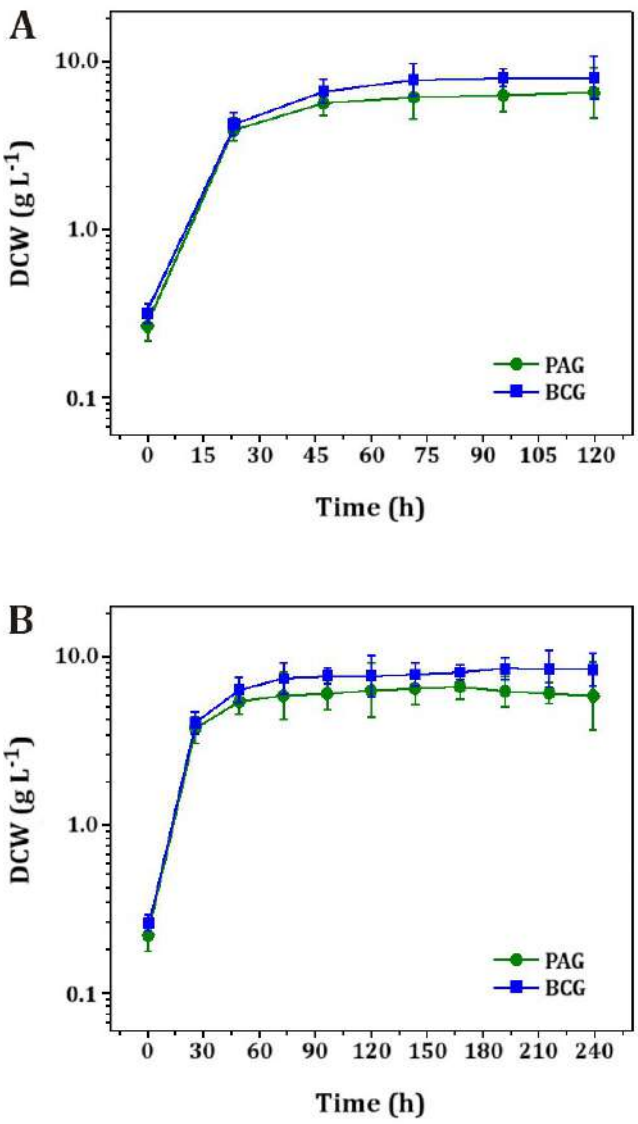
Parameter	120 h		240 h	
	PMG*	PMG	PMG*	PMG
μ (h^{-1})	0.72	0.72	0.69	0.70
DCW ($g\ L^{-1}$)	11.01	10.42	9.66	8.37
S_R ($mg\ L^{-1}\ h^{-1}$)	243.83	290.75	120.41	141.60
C_{TFA} ($g\ L^{-1}$)	1.55	5.47	0.32	2.55
C_{PUFA} ($g\ L^{-1}$)	1.17	4.21	0.24	1.96
C_{DHA} ($g\ L^{-1}$)	0.71	2.65	0.15	1.22
P_{DHA} ($mg\ L^{-1}\ h^{-1}$)	6.04	21.80	0.63	5.07
$Y_{X/S}$ ($g\ g^{-1}$)	0.38	0.30	0.33	0.20

Eliminating yeast extract (an expensive ingredient) in culture media causes *Aurantiochytrium* sp. to metabolize glucose 1.2 times faster. These results agree with a previous study where optimal culture conditions were achieved only with peptone as N source in culture media, and cell concentration and DHA yield were significantly increased (7). Another work replaced yeast extract with discarded orange peel extract and nitrates ($NaNO_3$, NH_4Cl, urea) for a more economical culture formulation in microalgae DHA production (25). Finally, when culture time was increased to 240 h, S_R was reduced by half for both evaluated cultures. Interestingly, absent yeast extract increased C_{DHA} by 3.6 times at 120 h and 8.1 times at 240 h. However, at longer culture time, C_{PUFA} and C_{DHA} were less than half than at 120 h for both cultures tested.

Decreased P_{DHA} was also observed when culture time increased from 120 to 240 h, resulting in 6.04 and 0.63 mg L^{-1} h^{-1} for PMG* medium, and 21.80 and 5.07 mg L^{-1} h^{-1} for PMG medium. This suggests that increasing culture time to 240 h was not appropriate, in agreement with previous results (7). Although DCW remains at the same level in all cultures, *Aurantiochytrium* sp. metabolism changes by decreasing lipid synthesis while some reserve substances are used for cell maintenance. Therefore, no yeast extract was added to media for the next tests.

Influence of Glycerol Quality and Assay Time on Culture Parameters

Pure and crude glycerol was used as a carbon source in *Aurantiochytrium* sp. cultures to evaluate the differences between glycerol qualities, analyzing crude glycerol as an economical and accessible substrate from regional small-scale biodiesel refineries. Figure 3 (page 9), shows cell concentration curves of *Aurantiochytrium* sp. cultures at 120 and 240 h in 250 mL batch shake flasks with 100 mL PAG and BCG media, without yeast extract addition. The best performance was observed with BCG medium compared to PAG medium at 120 h (figure 3A, page 9), becoming more evident at 240 h (figure 3B, page 9). Cell concentration curves obtained with glycerol cultures and PMG medium showed similar behaviors but were slightly higher with PMG. Table 3 (page 10) shows the main parameters obtained in *Aurantiochytrium* sp. cultures at 120 and 240 h with PAG and BCG media in batch shake flasks. The μ parameters are practically similar for all tests, with values close to those reported with PMG medium, demonstrating that glycerol was an adequate substrate for *Aurantiochytrium* sp. Concerning DCW, BCG showed the best performance at both culture times, and lower values were observed at 240 h culture, with a decrease of 10 and 24% for PAG and BCG, respectively.



Tests were conducted in duplicate.

Los ensayos fueron realizados por duplicado.

Figure 3. Cell concentration curves of *Aurantiochytrium* sp. cultures in 250 mL batch shake flasks with 100 mL PAG and BCG media, tested at 150 rpm and 28 ± 2 °C for: A) 120 h and B) 240 h culture times.

Figura 3. Curvas de concentración celular de cultivos *Aurantiochytrium* sp. en matraces batch agitados de 250 mL con 100 mL de medios PAG y BCG, testeados a 150 rpm y 28 ± 2 °C durante: A) 120 h y B) 240 h de cultivo.

Table 3. Culture parameters obtained during *Aurantiochytrium* sp. tests in 250 mL batch shake flasks with 100 mL PAG and BCG, tested at 150 rpm and 28 ± 2 °C for two culture times.

Tabla 3. Parámetros de cultivo obtenidos durante los ensayos con *Aurantiochytrium* sp. en matraces batch agitados de 250 mL con 100 mL de medios PAG y BCG, testeados a 150 rpm y 28 ± 2 °C a dos tiempos de cultivo.

Parameter	120 h		240 h	
	PAG	BCG	PAG	BCG
μ (h^{-1})	0.70	0.73	0.74	0.74
DCW ($g\ L^{-1}$)	9.72	10.60	6.51	8.08
S_R ($mg\ L^{-1}\ h^{-1}$)	351.67	350.42	150.84	169.93
C_{TFA} ($g\ L^{-1}$)	3.25	3.86	0.61	0.63
C_{PUFA} ($g\ L^{-1}$)	2.49	2.96	0.47	0.48
C_{DHA} ($g\ L^{-1}$)	1.55	1.84	0.29	0.30
P_{DHA} ($mg\ L^{-1}\ h^{-1}$)	12.89	15.35	1.21	1.25
$Y_{X/S}$ ($g\ g^{-1}$)	0.23	0.25	0.12	0.12

PAG and BCG cultures have a high S_R but decreased by 43% for PAG and 54% for BCG at 240 h. The S_R values in cultures with glycerol are higher than with glucose. Adequate C_{TFA} and C_{PUFA} were obtained at 120 h but strongly decreased when the culture was extended to 240 h. Higher C_{DHA} (1.84 g L^{-1}) was reached with BCG medium at 120 h, whereas with PAG C_{DHA} was 1.55 g L^{-1}, a value 16% lower than with BCG medium. The best P_{DHA} (15.35 mg L^{-1} h^{-1}) was produced with BCG medium at 120 h, slightly lower than the value obtained with PMG (21.80 mg L^{-1} h^{-1}) at 120 h. The use of glycerol or monosaccharides (fructose, glucose, mannose) in culture media resulted in higher concentrations of DCW and DHA than with disaccharides (maltose, lactose, sucrose) and polysaccharides (starch) (7). At 240 h, C_{DHA} decreased between 5 and 6 times with respect to 120 h. This result suggests that longer culture times cause *Aurantiochytrium* sp. to consume lipid reserves given lower carbon availability in batch culture. Lipids are accumulated as carbon and energy sources in the first culture stage, maybe after the faster cell growth (*i.e.*, culture time higher than 15 h). Some authors reported that glucose promotes rapid cell growth and lipid synthesis in early fermentation stages and glycerol produces late DHA accumulation with *A. limacinum* SR21 (15). Times over 240 h were not tested, as no clear improvement in culture parameters could be demonstrated with *Aurantiochytrium* sp.

These results are key since no prior (and more expensive) purification step, and no conditioning treatment was necessary before using crude glycerol as substrate in culture media. The good performance reached with BCG medium was explained by glucose being a C-6 compound, and glycerol a C-3 compound, easier to incorporate and assimilate by *Aurantiochytrium* sp. Increasing C_{TFA} and C_{DHA} induced by glycerol in *Aurantiochytrium* sp. cultures could be explained by the up-regulation of two important metabolites, oxalic acid (intermediate in citric acid cycle) and myo-inositol (growth promoter) (18). The cumulative effect of these metabolites produces an up-regulation of the citric acid cycle directly affecting cell metabolism, together with the pentose phosphate pathway, which generates reducing power, causing dynamic changes at a molecular level in enzymatic activities (18, 19).

Lipid Composition and Quality

Fatty acid production by *Aurantiochytrium* sp. cultures was analyzed with different substrates in a modified artificial seawater medium, prepared from a mixture of salts and nutrients in water. Figure 4 (page 11) shows these strategies concerning total fatty acid production expressed as DHA, DPA (docosapentaenoic acid), EPA, and other fatty acid concentrations. The most efficient culture for C_{DHA} was PMG medium, with a maximum C_{DHA} of 2.65 g L^{-1} and C_{TFA} of 5.47 g L^{-1} (table 2, page 8). C_{DHA} increased 3.7 times in PMG compared to PMG* medium, while P_{DHA} is about 3.5 times higher, indicating that absent yeast

extract greatly favors cellular machinery for lipid production, allowing C_{TFA} to increase. It should be noted that the DPA concentration (healthy ω-3 PUFA) also increases in the PMG culture and represents almost half of the total amount of DHA obtained. The highest C_{DHA} for glycerol cultures was obtained with BCG, reaching 1.84 g L^{-1}, and C_{TFA} of 3.86 g L^{-1}. In this medium, DPA concentration was more than half of the total amount of DHA obtained, and the P_{DHA} reached a maximum of 15.35 g L^{-1} h^{-1}, superior to PAG medium. In all tests, EPA concentration (another healthy ω-3 PUFA) is negligible, reaching a maximum value of 0.10 g L^{-1} with PMG medium.

Numbers on bars represent P_{DHA} (mg L^{-1} h^{-1}) for each culture strategy. Assays were run in duplicate.

Los números sobre las barras representan la P_{DHA} (mg L^{-1} h^{-1}) para cada estrategia de cultivo. Los ensayos fueron realizados por duplicado.

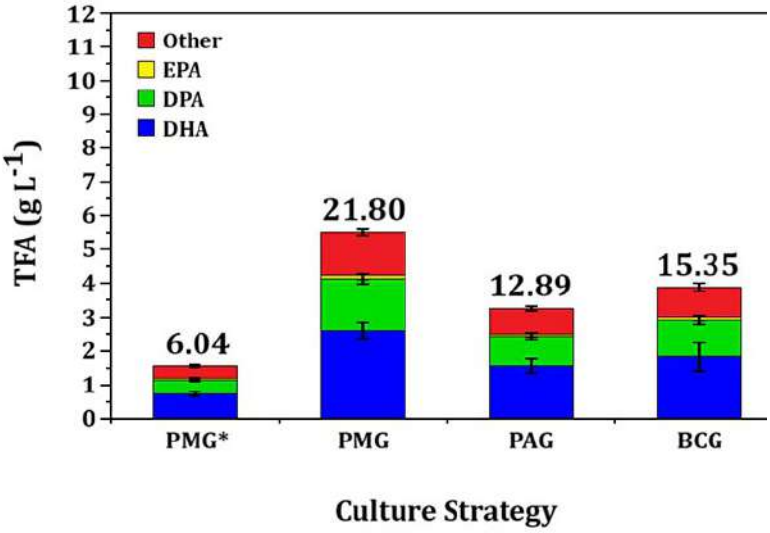


Figure 4. C_{TFA}, as concentration of DHA, DPA, EPA, and other fatty acids, obtained in *Aurantiochytrium* sp. cultures in 250 mL batch shake flasks with 100 mL media, tested at 150 rpm and 28 ± 2 °C for 120 h culture time.

Figura 4. Concentración de ácidos grasos totales (C_{TFA}), expresada como concentración de DHA, DPA, EPA y otros ácidos grasos, obtenidos en cultivos *Aurantiochytrium* sp. en matraces batch agitados de 250 mL con 100 mL de medio de cultivo, testeados a 150 rpm y 28 ± 2 °C durante 120 h de cultivo.

The obtained DHA-rich oil constitutes a safe product for human and animal food formulation. However, it requires certain quality parameters to be a stable product. After extraction from the obtained TFA, DHA quality parameters were obtained by titrimetric assays and metal identification. For PV and AV assays, DHA products comply with the limit (< 1.20 meq O_2 kg^{-1}, and < 0.10 meq KOH g^{-1}, respectively) set by the European Union standards for algal oils (9). Since the main difference between ω-3 DHA obtained from microalgae and marine fish was the presence of heavy metals, ICP-OES analysis of DHA products obtained from *Aurantiochytrium* sp. cultures showed that metal contents (Pb < 0.001, Cd < 0.020, Hg < 0.015, As < 0.030, Ni < 0.135, Cu < 0.090, Fe < 0.505, Cr < 0.060, Co < 0.135, expressed in ppm) were below the maximum levels established by the European Union legislation (9). This ω-3 DHA-rich oil obtained from microalgae was safer and had greater competitiveness and commercial advantage than marine fish DHA.

Our results demonstrated that crude glycerol is an adequate, cheap, and available substrate resource for producing ω-3 DHA-rich oil employing the microalgae *Aurantiochytrium* sp. in batch cultures. Applying simple culture strategies allowed increasing C_{TFA}, $C_{PUFA,}$ and C_{DHA} production in batch shake flasks, reducing culture costs by eliminating useless components and employing a cheaper and widely available regional waste, presenting identical substrate consumption and product yield rates as those using purified sugars. Our next challenge is to develop future assays for ω-3 DHA-rich oil production in bioreactor systems at 10X or 100X

scale factor. These experiences will allow the implementation an integrated process also able to evaluate other valuable wastes from regional agro-industries minimizing effluent production in a circular economy system.

Conclusions

Crude glycerol has great potential as substrate for ω-3 DHA-rich oil production using a locally isolated strain of *Aurantiochytrium* sp. in batch cultures. The largest initial inoculum (10.0% v/v) of *Aurantiochytrium* sp. improved DCW, practically exhausted glucose substrate, and enhanced P_{DHA}. Absent yeast extract in culture media enabled faster glucose metabolism in *Aurantiochytrium* sp. favoring lipid production and improving C_{TFA} and C_{DHA}. Longer culture times showed no differences in μ and DCW but decreased S_R and C_{DHA} due to *Aurantiochytrium* sp. consumed lipid reserves for cell maintenance. Better DCW performance was observed with BCG medium, with μ values similar to those reported with PMG medium. For glycerol cultures, the best C_{DHA} and P_{DHA} (1.84 g L^{-1} and 15.35 mg L^{-1} h^{-1}, respectively) were reached with BCG at 120 h, and S_R was higher than in glucose cultures. Quality assays showed ω-3 DHA-rich oil product is safer for human and animal food formulation. This study confirms that crude glycerol, without prior and expensive purification steps or conditioning treatment, constitutes a cheap and highly available carbon source for media formulation in *Aurantiochytrium* sp. cultures for ω-3 DHA-rich oil production. The next experiences for ω-3 DHA-rich oil production will focus on evaluating other wastes from regional agro-industries and developing scale-up assays in bioreactor systems.

References

1. Attarbachi, T.; Kingsley, M. D.; Spallina, V. 2023. New trends on crude glycerol purification: A review. Fuel 340: 127485. DOI: 10.1016/j.fuel.2023.127485
2. Band Schmidt, C. J. 2007. Aislamiento, purificación y mantenimiento de cepas de microalgas. In: Arredondo-Vega, B. O.; Voltolina, D. (Eds.), Métodos y herramientas analíticas en la evaluación de la biomasa microalgal. La Paz (Mexico), Centro de Investigaciones Biológicas del Noroeste. p. 1-11.
3. Bannon, C. D.; Breen, G. J.; Craske, J. D.; Hai, N. G.; Harper, N. L.; O'Rourke, K. L. 1982. Analysis of fatty acid methyl esters with high accuracy and reliability. III. Literature review of and investigations into the development of rapid procedures for the methoxide-catalysed methanolysis of fats and oils, J. Chromatogr. 247(1): 71-89. DOI: 10.1016/S0021-9673(00)84857-8
4. Bautista-Martínez, Y.; Granados-Rivera, L. D.; Jimenez-Ocampo, R.; Maldonado-Jáquez, J. A. 2024. Morphostructural composition and meat quality in local goat kids from the northeastern region of Mexico. Revista de la Facultad de Ciencias Agrarias. Universidad Nacional de Cuyo. Mendoza. Argentina. 56(1): 127-137. DOI: https://doi.org/10.48162/rev.39.129
5. Campoy, C.; Escolano-Margarit, M.; Anjos, T.; Szajewska, H.; Uauy, R. 2012. Omega-3 fatty acids on child growth, visual acuity neurodevelopment. Br. J. Nutr. 107: S85-106. DOI: 10.1017/S0007114512001493
6. Chauton, M. S.; Reitan, K. I.; Norsker, N. H.; Tveteras, R.; Kleivdal, H. T. 2015. A techno-economic analysis of industrial production of marine microalgae as a source of EPA and DHA-rich raw material for aquafeed: research challenges and possibilities. Aquaculture. 436: 95-103. DOI: 10.1016/j.aquaculture.2014.10.038
7. Chen, X.; Sen, B.; Zhang, S.; Bai, M.; He, Y.; Wang, G. 2021. Chemical and physical culture conditions significantly influence the cell mass and docosahexaenoic acid content of *Aurantiochytrium limacinum* strain PKU#SW8. Mar. Drugs. 19(12): 671. DOI: 10.3390/md19120671
8. Du, F.; Wang, Y. Z.; Xu, Y. S.; Shi, T. Q.; Liu, W. Z.; Sun, X. M.; Huang, H. 2021. Biotechnological production of lipid from thraustochytrids. Biotechnol. Adv. 48(8): 107725. DOI: 10.1016/j.biotechadv.2021.107725
9. EFSA Panel on Nutrition. Novel Foods and Food Allergens. 2020. Safety of *Schizochytrium* sp. oil as a novel food pursuant to regulation EU 2015/2283. EFSA J 18(10): e06242. DOI: 10.2903/j.efsa.2020.6242
10. Furlan, V.; Maus, V.; Batista, I.; Bandarra, N. 2017. Production of docosahexaenoic acid by *Aurantiochytrium* sp. ATCC PRA-276. Braz. J. Microbiol. 48(2): 359-365. DOI: 10.1016/j.bjm.2017.01.001

11. González-Martinez, A.; Angón, E.; González, M. A.; Rodríguez Tobar, J. M.; Barba Capote, C.; García Martínez, A. R. 2021. Effect of rearing system and sex on the composition and fatty acid profile of *Andinoacara rivulatus* meat from Ecuador. Revista de la Facultad de Ciencias Agrarias. Universidad Nacional de Cuyo. Mendoza. Argentina. 53(2): 232-242. DOI: https://doi.org/10.48162/rev.39.056
12. Hermida, L. G.; Gallardo, G. 2015. Food applications of microencapsulated omega-3 oils. In: Sagis L.M.C. (Ed.), Microencapsulation and microspheres for food applications. Academic Press. p. 271-299. DOI: 10.1016/B978-0-12-800350-3.00018-2
13. Janssen, C. I.; Kiliaan, A. J. 2014. Long-chain polyunsaturated fatty acids (LC-PUFA) from genesis to senescence: the influence of LC-PUFA on neural development, aging, and neurodegeneration, Prog. Lipid Res. 53: 1-17. DOI: 10.1016/j.plipres.2013.10.002
14. Kamal Eldin, A. 2010. Methods to determine the extent of lipid oxidation in foods. In: Decker, E.; Elias, R.; McClements, D. (Eds.). Oxidation in foods and beverages and antioxidant applications. Understanding mechanisms of oxidation and antioxidant activity. Sawston (UK), Woodhead Publishing. p. 181-195.
15. Li, J.; Liu, R.; Chang, G.; Li, X.; Chang, M.; Liu, Y.; Jin, Q.; Wang, X. 2015. A strategy for the highly efficient production of docosahexaenoic acid by *Aurantiochytrium limacinum* SR21 using glucose and glycerol as the mixed carbon sources. Biores. Technol. 177: 51-57. DOI: 10.1016/j.biortech.2014.11.046
16. Liu, Y.; Zhong, B.; Lawal, A. 2022. Recovery and utilization of crude glycerol, a biodiesel byproduct. RSC Adv. 12: 27997-28008. DOI: 10.1039/D2RA05090K
17. Lu, Q.; Li, H.; Xiao, Y.; Liu, H. 2021. A state-of-the-art review on the synthetic mechanisms, production technologies, and practical application of polyunsaturated fatty acids from microalgae. Algal Res. 55: 102281. DOI: 10.1016/j.algal.2021.102281
18. Mariam, I.; Kareya, M. S.; Nesamma, A. A.; Jutur, P. P. 2021. Delineating metabolomic changes in native isolate *Aurantiochytrium* for production of docosahexaenoic acid in presence of varying carbon substrates. Algal Res. 55: 102285. DOI: 10.1016/j.algal.2021.102285
19. Martínez-Reyes, I.; Chandel, N. S. 2020. Mitochondrial TCA cycle metabolites control physiology and disease. Nat. Commun. 11(1): 102. DOI: 10.1038/s41467-019-13668-3
20. Martins, D.; Custódio, L.; Barreira, L.; Pereira, H.; Ben-Hamadou, R.; Varela, J.; Abu-Salah, K. 2013. Alternative sources of n-3 long-chain polyunsaturated fatty acids in marine microalgae. Marine Drugs. 11(7): 2259-2281. DOI: 10.3390/md11072259
21. Nazir, Y.; Halima, H.; Al-Shorgani, N. K. N.; Manikan, V.; Hamid, A. A.; Song, Y. 2020. Efficient conversion of extracts from low-cost, rejected fruits for high-valued docosahexaenoic acid production by *Aurantiochytrium* sp. SW1. Algal Res. 50(5528): 101977. DOI: 10.1016/j.algal.2020.101977
22. Negro, E.; González, M. A.; Bernal, C. A.; Williner, M. R. 2016. Saturated and trans fatty acids content in unpackaged traditional bakery products in Santa Fe city, Argentina: nutrition labeling relevance. Int. J. Food Sciences Nutr. 68(5): 546-552. DOI: 10.1080/09637486.2016.1268100
23. Ochsenreitheri, K.; Gluck, C.; Stressler, T.; Fischer, L.; Syldatk, C. 2016. Production strategies and applications of microbial single cell oils. Front. Microbiol. 7: 1539. DOI: 10.3389/ fmicb.2016.01539
24. Oliver, L.; Dietrich, T.; Marañón, I.; Villarán, M.; Barrio, R. 2020. Producing Omega-3 polyunsaturated fatty acids: A review of sustainable sources and future trends for the EPA and DHA market. Resources 9(12): 148. DOI: 10.3390/resources9120148
25. Park, W. K.; Moon, M.; Shin, S. E.; Cho, J. M.; Suh, W. I.; Chang, Y. K.; Lee, B. 2018. Economical DHA (Docosahexaenoic acid) production from *Aurantiochytrium* sp. KRS101 using orange peel extract and low cost nitrogen sources. Algal Res. 29: 71-79. DOI: 10.1016/j.algal.2017.11.017
26. Patel, A.; Rova, U.; Christakopoulos, P.; Matsakas, L. 2020. Mining of squalene as a value-added byproduct from DHA producing marine thraustochytrid cultivated on food waste hydrolysate, Sci. Total Environ. 736: 139691. DOI: 10.1016/j.scitotenv.2020.139691
27. Patterson, H. B. W. 2011. Quality and control. In: List, G.R.; King, J.W. (Eds.). Hydrogenation of fats and oils. Theory and practice. AOCS Press. p 329-350.
28. Pleissner, D.; Lam, W. C.; Sun, Z.; Lin, C. S. 2018. Food waste as nutrient source in heterotrophic microalgae cultivation. Bioresour. Technol. 137: 139-146. DOI: 10.1016/j.biortech.2013.03.088
29. Plua Montiel, J.; Neira Mosquera, J. A.; Sanchez Llaguno, S. N.; Aldas Morejon, J. P.; Revilla Escobar, K. Y.; Caicedo-Álvarez, E. (en prensa). Comparison of fatty acid profiles of sacha inchi oil (*Plukenetia huayllabambana*), sesame oil (*Sesamum indicum*), and peanut oil (*Arachis hypogaea*) using two extraction methods for food purposes. Revista de la Facultad de Ciencias Agrarias. Universidad Nacional de Cuyo. Mendoza. Argentina.
30. Rosa, S.; Soria, M.; Vélez, C.; Galvano, M. 2010. Improvement of a two-stage fermentation process for docosahexaenoic acid production by *Aurantiochytrium limacinum* SR21 apply statistical experimental designs and data analysis, Biores. Technol. 101(7): 2367-2374. DOI: 10.1016/j.biortech.2009.11.056
31. Santos Jesus, S.; Maciel Filho, R. 2010. Modeling growth of microalgae *Dunaliella salina* under different nutritional conditions. Am. J. Biochem. Biotechnol. 6(4): 279-283. DOI: 10.3844/ajbbsp.2010.279.283

32. Sartori, M.; García, D.; Grossi Vanacore, M. F.; Fessia, A.; Nesci, A. (en prensa). Biofungicide formulation based on *Bacillus velezensis* EM-A8 for control of maize foliar diseases. Revista de la Facultad de Ciencias Agrarias. Universidad Nacional de Cuyo. Mendoza. Argentina.
33. Siriwardhana, N.; Kalupahana, N. S.; Moustaid-Moussa, N. 2012. Health benefits of n-3 polyunsaturated fatty acids: eicosapentaenoic acid and docosahexaenoic acid. Adv. Food Nutr. Res. 65: 211-222. DOI: 10.1016/B978-0-12-416003-3.00013-5
34. Verified Market Research. 2023. Global glycerin market size. Report ID 17400. 202 p. www.verifiedmarketresearch.com/product/glycerin-market. Accessed December 2023.
35. Vonshak, A. 1986. Laboratory techniques for the cultivation of microalgae. In: Richmond, A. (Ed.), Handbook of microalgal mass culture. CRC Press. p. 117-145.
36. Wolff, R. L. 1995. Content and distribution of trans-18:1 acids in ruminant milk and meat fats. Their importance in European diets and their effect on human milk. J. Am. Oil Chem. Soc. 72(1): 259-272. DOI: 10.1007/BF02541081
37. Yu, X. J.; Liu, J. H.; Sun, J.; Zheng, J. Y.; Zhang, Y. J.; Wang, Z. 2016. Docosahexaenoic acid production from the acidic hydrolysate of Jerusalem artichoke by an efficient sugar-utilizing Aurantiochytrium sp. YLH70. Ind. Crops Prod. 83: 372-378. DOI: 10.1016/j.indcrop.2016.01.013

Acknowledgements

The authors thank CONICET (Consejo Nacional de Investigaciones Científicas y Técnicas) and FIQ-UNL (Facultad Ingeniería Química, Universidad Nacional del Litoral) for financial support.

Optimization of Antioxidant Extraction from *Mutisia friesiana*, Native Plant of the Quebrada and Puna Regions of Argentina

Optimización de la extracción de antioxidantes de *Mutisia friesiana*, una planta nativa de las regiones de Quebrada y Puna de Argentina

Mónica Daniela Godoy [1, 2*], Norma Beatriz Farfán [2], Diego Cristos [3], Gabriela Grigioni [3]

Originales: *Recepción:* 04/04/2025 - *Aceptación:* 23/10/2025

ABSTRACT

The study determined the optimal conditions for extracting antioxidant phenols from *Mutisia friesiana* (*Asteraceae*) using ultrasound-assisted extraction. We evaluated extraction time, ethanol concentration, and solid/solvent ratio, applying a Box-Behnken experimental design. Response variables were total phenolic content (TPC), DPPH free radical scavenging activity (EC50), and ferric reducing antioxidant power (FRAP). All extraction variables were optimized by the response surface methodology. The optimal conditions resulted in 15 minutes of extraction, 65% ethanol, and a solid/solvent ratio of 5 g/100 mL. Under these conditions, TPC, EC50, and FRAP values were 54.24 mg GAE/g dw, 31.40 µg/mL, and 965.32 µmol EFe(II)/g dw, respectively. Extract HPLC–MS analysis under optimal conditions identified four phenolic compounds, previously reported for their antioxidant properties. This study provides valuable insights into optimal extraction parameters of bioactive compounds from *M. friesiana,* positioning the species as a promising natural antioxidants source for the food industry, particularly meat products.

Keywords
Mutisia friesiana • antioxidants • phenolic compounds • ultrasound-assisted extraction • response surface methodology

https://doi.org/10.48162/rev.39.203

1 Consejo Nacional de Investigaciones Científicas y Técnicas (CONICET). Godoy Cruz 2290. C. P. C1425FQB. CABA. Buenos Aires. Argentina.
2 Universidad Nacional de Jujuy. Facultad de Ingeniería. Ítalo Palanca 10. C. P. 4600. San Salvador de Jujuy. Jujuy. Argentina. * danielagodoy@outlook.com
3 Instituto de Tecnología de Alimentos. Instituto de Ciencia y Tecnología de Sistemas Alimentarios Sustentables. INTA CONICET. Nicolás Repetto y de los Reseros s/n. C. P. 1686. Hurlingham. Buenos Aires. Argentina.

Licenses Creative Commons
Attribution - Non Commercial - Share Alike

Resumen

El estudio determinó las condiciones óptimas para la extracción de fenoles antioxidantes de *Mutisia friesiana* (*Asteraceae*) mediante extracción asistida por ultrasonido. Se evaluaron el tiempo de extracción, la concentración de etanol y la relación sólido/disolvente, utilizando un diseño experimental Box-Behnken. Las variables de respuesta fueron el contenido fenólico total (TPC), la actividad de eliminación de radicales libres DPPH (EC50) y el poder antioxidante férrico reductor (FRAP). Todas las variables de extracción se optimizaron mediante metodología de superficie de respuesta. Las condiciones óptimas correspondieron a 15 minutos de extracción, etanol al 65% y una relación sólido/disolvente de 5 g/100 mL. Bajo estas condiciones, los valores de TPC, EC50 y FRAP fueron 54,24 mg GAE/g ps, 31,40 µg/mL y 965,32 µmol EFe(II)/g ps, respectivamente. El análisis por HPLC-MS del extracto obtenido en condiciones óptimas identificó cuatro compuestos fenólicos previamente reportados por sus propiedades antioxidantes. Este estudio proporciona información valiosa sobre los parámetros óptimos de extracción de compuestos bioactivos de *M. friesiana*, posicionando a la especie como una fuente natural prometedora de antioxidantes para la industria alimentaria, en particular para productos cárnicos.

Palabras clave

Mutisia friesiana • antioxidantes • compuestos fenólicos • extracción asistida por ultrasonido • metodología de superficie de respuesta

Introduction

The genus *Mutisia (Asteraceae,* subfamily *Mutisioideae,* tribe *Mutisieae)* comprises between 59 and 63 species, found exclusively in South America. Species within this genus are distributed along the Andes, from northern Colombia to southern Argentina (6, 7, 14, 21, 27). Previous studies have investigated several *Mutisia* species, including *M. acuminata, M. orbignyana, M. venusta, M. lanata, M. cochabambensis,* and *M. ledifolia,* collected from Peru, Chile, and Bolivia. Studies on their phytochemical composition identified secondary metabolites such as flavonoids, hydroxycinnamic acids, and chlorogenic acid derivatives (8, 10, 11, 13, 17, 18, 20, 31). In addition, antioxidants (10, 18) and antibacterial activities (9) linked to phenolic compounds have been reported.

Mutisia friesiana is a perennial shrub native to southern Bolivia and northwestern Argentina, growing at 3500-4000 m above sea level. In northern Argentina, especially in the Quebrada and Puna regions, its leaves are used to prepare medicinal infusions consumed to treat respiratory diseases and stomach pains (1, 24, 38). Locally, the plant is known as "romerillo" and is obtained from local markets or through direct collection. Although *M. friesiana* is well known and widely used, research on this species remains limited. A search in PubMed, Google Scholar, SciELO, and Latindex using the keywords "Mutisia friesiana" retrieved several works by Viturro *et al.* (1999, 2000, 2001, 2003, 2004, 2005). Viturro *et al.* (2001, 2003, 2004, 2005) elucidated furanones, methylphenones, 5-methylcoumarins, 5-methylcoumaranones, and a chromone derivative from *M. friesiana* extracts. Several of these compounds showed antifungal and bactericidal activity. Viturro *et al.* (2000) identified 127 volatile compounds in its essential oil. Viturro *et al.* (1999) reported antioxidant activity in methanolic extracts of aerial parts using a DPPH discoloration assay. Additionally, bioassay-guided isolation revealed the presence of caffeic acid derivatives and flavonoids.

Based on this literature review, a clear research gap exists regarding the antioxidant potential of *M. friesiana*. This gap motivated a detailed investigation into the bioactive properties of its extracts, driven by the current interest in natural antioxidants. Antioxidants from natural sources have gained increasing interest due to their diverse applications. Over the past decade, research has focused on their safety, beneficial properties, and potential use in food and pharmaceutical industries (25, 30). The Quebrada and Puna regions host plant species with largely unexplored antioxidant potential. Studying these native plants supports sustainable resource use and offers economic opportunities for local communities.

This study aimed to optimize ultrasound-assisted extraction (UAE) conditions for antioxidant phenols from *M. friesiana*. Extraction time, solvent concentration, and solid/solvent ratio were optimized by response surface methodology (RSM). Finally, phenolic compounds in the optimized extract were identified and quantified using HPLC-MS.

Materials and Methods

Plant Material

The *M. friesiana* samples were collected in March in Cianzo, Jujuy, Argentina (latitude: -23.1768, longitude: -65.1668, altitude: 3539 m above sea level). A voucher specimen was deposited at the PRONOA-UNJu herbarium (Facultad de Ingeniería, Universidad Nacional de Jujuy), identified as HN° 21-19. The plant material (aerial parts) was oven-dried at 30°C until constant weight and then ground (Peabody PE-MC9100 mill) to a fine powder. The powder was sieved, and a 250-150 µm particle fraction was separated.

Extraction

Samples were extracted by UAE with ethanol as solvent. Each sample and solvent were placed in an Erlenmeyer flask and sonicated in an ultrasound bath (Cole-Parmer 8890 Instrument, USA). Ethanol concentration, solid/solvent ratio, and sonication time were set according to the experimental design. Extraction was performed at 20°C, 80 W power, and 47 kHz frequency. The extracts were filtered to remove plant debris. The filtrate was centrifuged (20 min at 2500 rpm), and the supernatant was filtered using filter paper (Schleicher & Schuell N°0859). Extracts were stored at 4°C and protected from light until analysis.

Total Phenolic Content (TPC)

TPC was determined using the Folin-Ciocalteu method (32) with minor modifications. Each microtube contained 100 µL of extract (0.5-0.0625 mg/mL) and 200 µL of Folin-Ciocalteu reagent (10%). After 3 min, 800 µL of sodium carbonate solution (7.4%) was added, and the mixture was vortexed for 30 seconds. After 60 min in the dark at room temperature, absorbance was measured at 760 nm (Epoch spectrophotometer, BioTeK), against a blank prepared using 100 µL of solvent. The analysis was performed in triplicate. TPC values were expressed as mg gallic acid equivalents per gram of *M. friesiana* dry weight (mg GAE/g dw), using a gallic acid standard curve.

Antioxidant Activity

DPPH (2,2-diphenyl-1-picrylhydrazyl) free radical scavenging activity was evaluated following Brand-Williams *et al.* (1995), with slight modifications. Serial dilutions were prepared from each extract. Then, 25 µL of each dilution and 200 µL of methanolic DPPH solution (absorbance 1.0 at 515 nm) were added to microplate wells. The mixture was kept in the dark for 30 min, and absorbance was measured at 515 nm (Microplate Spectrophotometer Epoch, BioTeK). Antioxidant activity was expressed as the Effective Concentration 50 (EC50, µg/mL), which represents the extract concentration required to reduce DPPH absorbance by 50%. The analysis was performed in triplicate.

For FRAP (ferric reducing antioxidant power), the method of Benzie & Strain (1996) was used. Each microtube contained 30 µL of extract, 90 µL of water, and 900 µL of FRAP reagent. After 30 min at 37°C, absorbance was recorded at 595 nm (Microplate Spectrophotometer Epoch, BioTeK). The FRAP reagent was prepared by mixing acetate buffer (pH 3.6), 2,4,6-tripyridyl-s-triazine (10 mM in 40 mM hydrochloric acid), and ferric chloride hexahydrate (20 mM) in a 10:1:1 ratio. The analysis was performed in triplicate. Results were expressed as µmol Fe(II) equivalents per gram of *M. friesiana* dry weight (µmol EFe(II)/g dw) using a ferrous sulfate heptahydrate standard curve.

Analysis of Phenolic Compounds

Chromatographic analysis was performed on the extract obtained under optimal conditions using ultra-high performance liquid chromatography (UPLC) (Waters Acquity system) with a single quadrupole mass detector. Separation was

achieved using an XBridge BEH C18 column (2.5 µm, 2.1x150 mm) maintained at 45°C. Mobile phases were 0.1% acetic acid in water (eluent A) and 0.1% acetic acid in methanol (eluent B), at 0.2 mL/min flow. The injection volume was 10 µL. The gradient was: (95:5)-(95:5) 0-2 min, (95:5)-(80:20) 2-5 min, (80:20)-(20:80) 5-10 min, (20:80)-(0:100) 10-11 min, (0:100)-(0:100) 11-13 min, (0:100)-(95:5) 13-14 min, (95:5) 14-20 min. Quantification was performed in selected ion monitoring mode, under positive ESI ionization. Identification was based on retention time and the abundance of the confirmation ion (C ion) relative to that of the quantification ion (Q ion).

Experimental Design and Statistical Analysis

A Box-Behnken design was used in a single block with five central points (Design-Expert 11 software). Table 1 shows independent variables and their levels. Maximum and minimum limits were defined from preliminary trials. The response variables included TPC, DPPH, and FRAP.

Table 1. Independent variables and their coded and uncoded levels.
Tabla 1. Variables independientes y sus niveles codificados y no codificados.

Independent variables	Coded level		
	-1	0	+1
A- Extraction time (min)	10	20	30
B- Ethanol concentration (% v/v)	60	75	90
C- Solid/solvent ratio (g/100 mL)	5	7.5	10

Experimental data were fitted using equation 1, where y represents the predicted response. Regression coefficients (β_0, β_i, β_{ii}, and β_{ij}) corresponded to central, linear, quadratic, and interaction terms. n was the number of independent variables, and x_i and x_j were coded values (-1 to 1). Analysis of variance (ANOVA) was performed at 95% confidence to test model significance and fit.

$$y = \beta_0 + \sum_{i=1}^{n} \beta_i x_i + \sum_{i=1}^{n} \beta_{ii} x_i^2 + \sum_{i=1}^{n-1} \sum_{j=i+1}^{n} \beta_{ij} x_i x_j \quad (1)$$

To optimize extraction, RSM was applied. Validation was performed under the predicted optimal conditions. Experimental and predicted values were compared, and error rates calculated using equation 2. A Pearson correlation analysis was performed between DPPH-TPC and FRAP-TPC responses.

Error rate (%) = 100 * (Experimental value - Predicted value)/Experimental value (2)

Results and Discussion

Fitting Models

Table 2 (page 5), shows the Box-Behnken experimental design and the values obtained for each response variable.

Table 2. Box-Behnken design for the independent variables and corresponding response values for each extraction.

Tabla 2. Diseño experimental Box-Behnken para las variables independientes y valores de respuesta correspondientes a cada extracción.

N°	Independent variables			Response variables		
	Extraction time (min)	Ethanol concentration (% v/v)	Solid/solvent ratio (g/100 mL)	TPC	DPPH	FRAP
1	10	60	7.5	53.03 ± 2.14	34.18 ± 0.14	848.98 ± 2.78
2	30	60	7.5	50.12 ± 6.72	31.19 ± 0.13	801.23 ± 3.23
3	10	90	7.5	35.27 ± 3.82	43.90 ± 0.32	605.45 ± 2.55
4	30	90	7.5	29.59 ± 1.88	48.02 ± 0.15	542.33 ± 2.76
5	10	75	5	39.37 ± 3.13	34.15 ± 0.03	982.13 ± 4.96
6	30	75	5	49.40 ± 1.92	31.70 ± 0.16	845.57 ± 4.31
7	10	75	10	50.36 ± 3.02	35.74 ± 0.15	876.25 ± 4.07
8	30	75	10	45.95 ± 1.25	36.44 ± 0.19	969.08 ± 2.84
9	20	60	5	60.65 ± 5.62	30.45 ± 0.15	917.42 ± 11.96
10	20	90	5	32.54 ± 3.40	43.50 ± 0.08	477.83 ± 2.94
11	20	60	10	50.73 ± 6.57	29.03 ± 0.13	739.82 ± 2.26
12	20	90	10	30.01 ± 1.72	48.85 ± 0.14	630.04 ± 1.00
13	20	75	7.5	45.09 ± 1.22	36.06 ± 0.04	868.30 ± 4.31
14	20	75	7.5	47.55 ± 4.76	35.03 ± 0.31	899.69 ± 2.84
15	20	75	7.5	53.37 ± 0.66	34.17 ± 0.29	901.13 ± 1.45
16	20	75	7.5	46.10 ± 5.28	33.69 ± 0.12	933.66 ± 1.46
17	20	75	7.5	52.70 ± 7.93	33.16 ± 0.25	~~1022.18 ± 2.17~~

Values are expressed as mean (n=3) ± standard deviation. TPC: total phenolic content (mg GAE/g dw), DPPH: effective concentration 50 (µg/mL), FRAP: ferric reducing antioxidant power (µmol EFe(II)/g dw).

Los valores corresponden a la media (n=3) ± desviación estándar. TPC: contenido fenólico total (mg GAE/g ps), DPPH: concentración efectiva 50 (µg/mL), FRAP: poder antioxidante reductor férrico (µmol EFe(II)/g ps).

The relationship between independent and response variables was fitted using a reduced second-order polynomial model. Non-significant terms ($p > 0.05$) not involved in significant interactions were excluded. Reduced models for TPC, DPPH, and FRAP are presented in equations 3, 4, and 5, respectively. Regression coefficients correspond to coded independent variables (A: extraction time; B: ethanol concentration; C: solid/solvent ratio).

$$\mathbf{TPC\ (mg\ GAE/g\ dw) = 47.76 - 10.89\ B - 5.02\ B^2} \quad (3)$$

$$\mathbf{DPPH\ (\mu g/mL) = 34.16 - 0.08\ A + 7.43\ B + 1.28\ C + 1.78\ A*B + 1.69\ B*C + 4.18\ B^2} \quad (4)$$

$$\mathbf{FRAP\ (\mu mol\ EFe(II)/g\ dw) = 909.48 - 19.32\ A - 131.48\ B - 0.97\ C + 57.35\ A*C + 82.45\ B*C - 214.09\ B^2} \quad (5)$$

Analysis of variance confirmed that all models were significant ($p < 0.0001$) with non-significant lack of fit (p-values: TPC = 0.4518, DPPH = 0.3260, FRAP = 0.8196). Coefficients R^2 (TPC = 0.8147, DPPH = 0.9681, FRAP = 0.9891) and adjusted R^2 values (TPC = 0.7883, DPPH = 0.9489, FRAP = 0.9818) indicated a strong fit between experimental and predicted data. Predicted R^2 values (TPC=0.7295, DPPH=0.8541, FRAP=0.9678) differed by less than 0.2 from adjusted R^2, confirming model reliability (26).

Influence of Independent Variables on TPC

Based on the model (equation 3, page 5), the linear and quadratic effects of ethanol concentration (B and B^2) significantly influenced TPC. TPC increased as ethanol concentration decreased from 90% to 60%, reaching the highest value at 60% (figures 1a and 1b). In contrast, TPC remained stable despite variations in extraction time and solid/solvent ratio. No significant interaction was observed between these two variables (figure 1c).

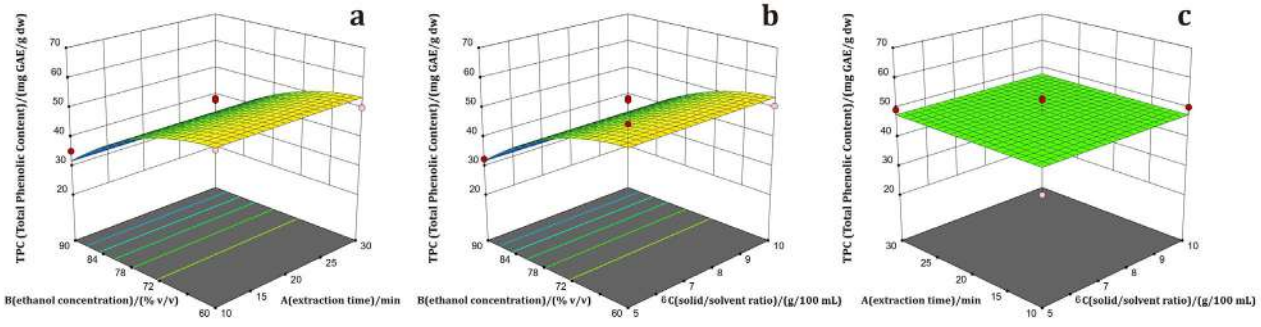


Figure 1. Response surface plots of a) ethanol concentration *vs.* extraction time, b) ethanol concentration *vs.* solid/solvent ratio, and c) extraction time *vs.* solid/solvent ratio on TPC of *Mutisia friesiana* extracts.

Figura 1. Gráficos de superficie de respuesta de a) concentración de etanol *vs.* tiempo de extracción, b) concentración de etanol *vs.* relación sólido/disolvente y c) tiempo de extracción *vs.* relación sólido/disolvente sobre TPC de los extractos de *Mutisia friesiana*.

The solvent plays a crucial role in extracting secondary metabolites from plant matrices (4, 15, 36). In this study, a 60% ethanol concentration enhanced the extraction of polar antioxidant phenols. This suggests that phenolic compounds in *M. friesiana* have a polarity compatible with 60% aqueous ethanol. Aqueous ethanol also promotes plant tissue hydration, facilitates solvent penetration, and improves mass transfer through diffusion (19). Similar findings were reported by Fang *et al.* (2014) for the UAE of phenolic compounds from *Eclipta prostrata (Asteraceae)*. TPC increased significantly when ethanol concentration rose from 30% to 50% but decreased when ethanol concentration increased from 55% to 80%. A comparable pattern was observed for *Achillea kellalensis* (*Asteraceae*), where TPC increased up to 43% ethanol before declining (44). Differences in optimal ethanol concentration may result from variations in plant matrix composition and specific phenolic profiles.

Influence of Independent Variables on Antioxidant Activity

Ethanol concentration (B), solid/solvent ratio (C), and the interactions A*B, B*C, and B^2 significantly affected DPPH activity (equation 4, page 5). EC50 decreased as ethanol concentration declined from 90 to 60% (figure 2a, page 7). At 60% ethanol, an extraction time of 30 min improved free radical scavenging activity by 9% compared to 10 min. Figure 2b (page 7), shows greater antioxidant activity at lower ethanol concentrations and solid/solvent ratios. No significant interaction was observed between extraction time (A) and solid/solvent ratio (C) (figure 2c, page 7). EC50 is inversely related to antioxidant capacity, meaning lower EC50 values indicate stronger antioxidant activity.

Extraction time (A), ethanol concentration (B), and the interactions A*C and B*C significantly influenced FRAP (equation 5, page 5). FRAP was highest with 60% ethanol and 10 min of extraction (figure 3a, page 7), and increased at a solid/solvent ratio of 5 g/100 mL (figure 3b, page 7). In contrast, longer extraction times and higher solid/solvent ratios decreased FRAP values (figure 3c, page 7).

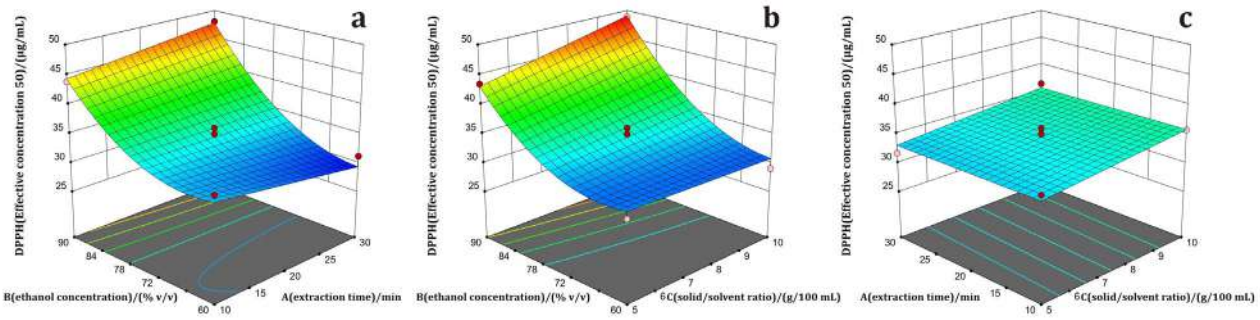


Figure 2. Responses surface plots of a) ethanol concentration *vs.* extraction time, b) ethanol concentration *vs.* solid/solvent ratio, and c) extraction time *vs.* solid/solvent ratio on DPPH of *Mutisia friesiana* extracts.

Figura 2. Gráficos de superficie de respuesta de a) concentración de etanol *vs.* tiempo de extracción, b) concentración de etanol *vs.* relación sólido/disolvente y c) tiempo de extracción *vs.* relación sólido/disolvente, sobre DPPH de los extractos de *Mutisia friesiana*.

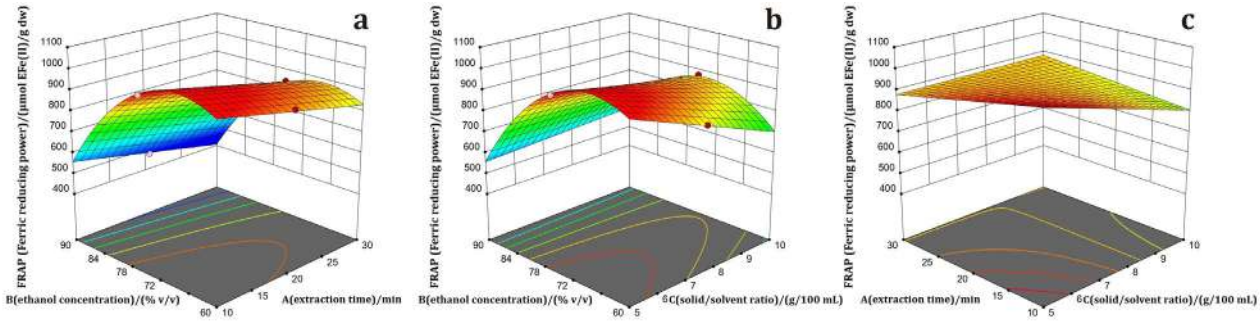


Figure 3. Responses surface plots of a) ethanol concentration *vs.* extraction time, b) ethanol concentration *vs.* solid/solvent ratio, and c) extraction time *vs.* solid/solvent ratio, on FRAP of *Mutisia friesiana* extracts.

Figura 3. Gráficos de superficie de respuesta de a) concentración de etanol *vs.* tiempo de extracción, b) concentración de etanol *vs.* relación sólido/disolvente y c) tiempo de extracción *vs.* relación sólido/disolvente, sobre FRAP de los extractos de *Mutisia friesiana*.

The extraction process is based on mass-transfer principles, where concentration gradients between the solid and solvent act as the driving force (37). Reducing the solid/solvent ratio increases this gradient, improving diffusivity and solute dissolution (22). Consequently, the extraction efficiency of antioxidant phenols is enhanced. However, extended extraction times may cause phenolic degradation due to prolonged cavitation (19).

Ethanol concentration was the main factor influencing antioxidant activity. This likely reflects the higher affinity of antioxidant phenols for the polarity of aqueous ethanol. The higher TPC obtained at 60% ethanol agrees with the stronger antioxidant activity of the extract. Sobhani *et al.* (2022) found similar trends for *Echinacea purpurea* hydroalcoholic extracts. Antioxidant activity correlated strongly with total phenolic content. Phenolic compounds can transfer electrons and/or hydrogen atoms to neutralize free radicals, thereby exerting antioxidant action (28). Pearson correlation analysis showed a significant correlation ($p < 0.001$) between antioxidant activity and phenolic content in *M. friesiana* extracts. Correlation coefficients for DPPH-TPC and FRAP-TPC were -0.89 and 0.83, respectively. Comparable correlations were reported for ethanolic extracts of Sudanese medicinal plants (15) and Andean plant extracts (10).

Optimization

Extraction conditions were optimized to maximize TPC and FRAP and minimize DPPH values. Based on response surface analysis (Design-Expert 11 software), the optimal combination of parameters was 15 min of extraction, 65% ethanol, and a solid/solvent ratio of 5 g/100 mL. Model validation was performed under these predicted optimal conditions. Experimental results agreed with predicted values, with error rates between 1.40 and 3.20% (table 3). These values are consistent with optimization studies of *Berberis asiatica* methanolic extracts (2) and *Centaurea* sp. leaves (4). The results confirmed the models accurately described the extraction process and can reliably predict and optimize the extraction of antioxidant phenols from *M. friesiana*.

Table 3. Experimental and predicted values of response variables under optimal extraction conditions.

Tabla 3. Datos experimentales y valores predichos de las variables de respuesta bajo condiciones de extracción óptimas.

	Response variables		
	TPC	**DPPH**	**FRAP**
Predicted value	52.79	31.84	996.25
Experimental value	54.24 ± 3.17	31.40 ± 1.18	965.32 ± 4.64
Error rate (%)	2.67	-1.40	-3.20

Values are expressed as mean (n=3) ± standard deviation. TPC: total phenolic content (mg GAE/g dw), DPPH: effective concentration 50 (µg/mL), FRAP: ferric reducing antioxidant power (µmol EFe(II)/g dw).

Los valores corresponden a la media (n=3) ± desviación estándar. TPC: contenido fenólico total (mg GAE/g ps), DPPH: concentración efectiva 50 (µg/mL), FRAP: poder antioxidante reductor férrico (µmol EFe(II)/g ps).

Analysis of Phenolic Compounds in the Optimized Extract

Eleven phenolic compounds were selected for targeted analysis in the optimized extract, as they had been previously reported in species of the same genus (table 4, page 9) (8, 17, 38). Four phenolic compounds were identified in the *M. friesiana* extract (table 4, page 9): 3-*O*-caffeoylquinic acid, 5-*O*-caffeoylquinic acid, caffeic acid, and arbutin, of which only two were quantified. For comparison, table 4 (page 9), lists values reported by other authors. Catalano *et al.* (1995) and Daily *et al.* (1988) reported higher arbutin contents in *M. acuminata* extracts than those found in *M. friesiana.* Similarly, Viturro *et al.* (1999) and Fernández-Galleguillos *et al.* (2023) confirmed the presence of 3-*O*-caffeoylquinic acid, 5-*O*-caffeoylquinic acid, and caffeic acid in *M. friesiana* extracts. According to previous studies, 3-*O*-caffeoylquinic acid, 5-*O*-caffeoylquinic acid, caffeic acid, and arbutin exhibit high antioxidant activity (12, 34, 35).

Total phenolic content in the optimized *M. friesiana* extract was comparable to the *M. acuminata* extract (59.4 mg GAE/ g dw) (10). However, the concentration of quantified antioxidant phenols in the *M. friesiana* extract was lower than previously reported (table 4, page 9). Only four of the eleven target compounds were detected. These differences may result from the extraction method and the solvent used, which directly influence extract composition. Palmieri *et al.* (2020) reported variations in the chemical profiles of *Cannabis sativa*, *Thymus vulgaris*, and *Coriandrum sativum* depending on the extraction method. Likewise, Llorent-Martínez *et al.* (2020) observed compositional changes in *Cirsium yildizianum* extracts when modifying the extraction solvent and technique. Therefore, the *M. friesiana* extract obtained in this study may contain additional antioxidant phenols beyond those previously reported. Further chemical characterization should fully define its phenolic profile.

Table 4. Phenolic compounds identified in the optimized *Mutisia friesiana* extract by HPLC-MS analysis.

Tabla 4. Compuestos fenólicos identificados en el extracto optimizado de *Mutisia friesiana* por HPLC-MS.

Compounds	Current study (ng/g of extract)	Reference 38 (mg/g of extract)	Reference 17 (mg/g of extract)	Reference 8 (mg/g of extract)
3-*O*-caffeoylquinic acid	Detectable	0.75	90.03 ± 0.46	
5-*O*-caffeoylquinic acid	Detectable	0.35	5.92 ± 0.01	
1,5-dicaffeoylquinic acid	ND		9.86 ± 0.02	
3,5-dicaffeoylquinic acid	ND		8.51 ± 0.01	
Caffeic acid	0.10 ± 0.03	Detectable	2.74 ± 0.01	
Quercetin	ND		1.89 ± 0.19	Detectable
Quercetin-3-*O*-rutinoside	ND	0.60	2.49 ± 0.08	
Quercetin-3-*O*-glucoside	ND		1.05 ± 0.06	
Quercetin-3-*O*-glucuronide	ND		17.80 ± 0.20	Detectable
Arbutin	0.04 ± 0.01			166.67
Isorhamnetin-3-*O*-rutinoside	ND	0.50	1.21 ± 0.00	

Values are expressed as mean (n=3) ± standard deviation. LC: 0.02 ng/g. ND: not detectable.

Los valores corresponden a la media (n=3) ± desviación estándar. LC: 0.02 ng/g. ND: no detectable.

Conclusions

An extract with antioxidant activity was successfully obtained from *M. friesiana*. Ultrasound-assisted extraction parameters (extraction time, ethanol concentration, and solid/solvent ratio) were optimized to enhance the recovery of antioxidant phenols. The highest phenolic yield and antioxidant activity were achieved using 15 minutes of extraction, 65% ethanol, and a solid/solvent ratio of 5 g/100 mL. Under these conditions, total phenolic content reached 54.24 mg GAE/g dw, and antioxidant activity values were 31.40 µg/mL (DPPH) and 965.32 µmol EFe(II)/g dw (FRAP). HPLC-MS analysis identified four phenolic compounds, all previously reported for their antioxidant properties. These findings highlight the potential of *M. friesiana* as a promising natural source of antioxidants. The extract may have multiple applications in the food industry, particularly to prevent oxidative damage during storage. However, further studies are needed to assess its safety, stability, and functional effectiveness. Research on this native species could also benefit local communities by promoting the sustainable use of traditional plant resources. Moreover, the development and commercialization of products derived from *M. friesiana* could support local economies in northern Argentina.

References

1. Barboza, G. E.; Cantero, J. J.; Núñez, C.; Pacciaroni, A.; Ariza Espinar, L. 2009. Medicinal plants: A general review and a phytochemical and ethnopharmacological screening of the native Argentine Flora. Kurtziana. 34(1-2): 7-365.
2. Belwal, T.; Dhyani, P.; Bhatt, I. D.; Rawal, R. S.; Pande, V. 2016. Optimization extraction conditions for improving phenolic content and antioxidant activity in *Berberis asiatica* fruits using response surface methodology (RSM). Food Chemistry. 207: 115-124. https://doi.org/10.1016/j.foodchem.2016.03.081
3. Benzie, I. F.; Strain, J. J. 1996. The ferric reducing ability of plasma (FRAP) as a measure of antioxidant power: the FRAP assay. Analytical Biochemistry. 239(1): 70-76. https://doi.org/10.1006/abio.1996.0292

4. Bouafia, M.; Colak, N.; Ayaz, F. A.; Benarfa, A.; Harrat, M.; Gourine, N.; Yousfi, M. 2021 The optimization of ultrasonic-assisted extraction of *Centaurea* sp. antioxidative phenolic compounds using response surface methodology. Journal of Applied Research on Medicinal and Aromatic Plants. 25:100330. https://doi.org/10.1016/j.jarmap.2021.100330
5. Brand-Williams, W.; Cuvelier, M. E.; Berset, C. L. W. T. 1995. Use of a free radical method to evaluate antioxidant activity. LWT-Food Science and Technology. 28(1): 25-30. https://doi.org/10.1016/S0023-6438(95)80008-5
6. Bremer, K. 1994. Asteraceae. Cladistics and classification. Timber Press.
7. Cabrera, A. L. 1965. Revisión del género *Mutisia (Compositae)*. Opera Lilloana 13. San Miguel de Tucumán. Fundación Miguel Lillo.
8. Catalano, S.; Cioni, P. L.; Flamini, G.; De Feo, V.; Morelli, I. 1995. Chemical investigation of the aerial parts of *Mutisia acuminata*. International Journal of Pharmacognosy. 33(1): 73-74. https://doi.org/10.3109/13880209509088152
9. Catalano, S.; Cioni, P. L.; Panizzi, L.; Morelli, I. 1998. Antimicrobial activity of extracts of *Mutisia acuminata* var. acuminata. Journal of Ethnopharmacology. 59(3): 207-209. https://doi. org/10.1016/S0378-8741(97)00113-X
10. Chirinos, R.; Pedreschi, R.; Rogez, H.; Larondelle, Y.; Campos, D. 2013. Phenolic compound contents and antioxidant activity in plants with nutritional and/or medicinal properties from the Peruvian Andean region. Industrial Crops and Products. 47: 145-152. https://doi.org/10.1016/j.indcrop.2013.02.025
11. Chui Tinco, G. 2021. Estudio fitoquímico preliminar de cinco especies vegetales del altiplano sur y determinación de componentes mayoritarios de la especie vegetal *Lampaya castellani* Moldenke. Tesis de grado en Licenciatura en Ciencias Químicas. Facultad de Ciencias Puras y Naturales. Universidad Mayor de San Andrés. La Paz. Bolivia.
12. Cizmarova, B.; Hubkova, B.; Bolerazska, B.; Marekova, M.; Birkova, A. 2020. Caffeic acid: A brief overview of its presence, metabolism, and bioactivity. Bioactive Compounds in Health and Disease. 3(4): 74-81. https://doi.org/10.31989/bchd.v3i4.692
13. Daily, A.; Seligmann, O.; Nonnenmacher, G.; Fessler, B.; Wong, S. M.; Wagner, H. 1988. New chromone, coumarin, and coumestan derivatives from *Mutisia acuminata* var. hirsuta. Planta Medica. 54(1): 50-52. https://doi.org/10.1055/s-2006-962334
14. Del Vitto, L. A.; Petenatti, E. M. 2009. Asteráceas de importancia económica y ambiental: Primera parte. Sinopsis morfológica y taxonómica, importancia ecológica y plantas de interés industrial. Multequina. 18(2): 87-115.
15. Dirar, A. I.; Alsaadi, D. H. M.; Wada, M.; Mohamed, M. A.; Watanabe, T.; Devkota, H. P. 2019. Effects of extraction solvents on total phenolic and flavonoid contents and biological activities of extracts from Sudanese medicinal plants. South African Journal of Botany. 120: 261-267. https://doi.org/10.1016/j.sajb.2018.07.003
16. Fang, X.; Wang, J.; Wang, Y.; Li, X.; Zhou, H.; Zhu, L. 2014 Optimization of ultrasonic-assisted extraction of wedelolactone and antioxidant polyphenols from *Eclipta prostrate* L using response surface methodology. Separation and Purification Technology. 138: 55-64. https://doi.org/10.1016/j.seppur.2014.10.007
17. Fernández-Galleguillos, C.; Jiménez-Aspee, F.; Mieres-Castro, D.; Rodríguez-Núñez, Y. A.; Gutiérrez, M.; Guzmán, L.; Echeverría, J.; Sandoval-Yañez, C.; Forero-Doria, O. 2023. Phenolic Profile and Cholinesterase Inhibitory Properties of Three Chilean Altiplano Plants: *Clinopodium gilliesii* (Benth.) Kuntze [Lamiaceae], *Mutisia acuminata* Ruiz & Pav. var. hirsuta (Meyen) Cabrera, and *Tagetes multiflora* (Kunth) [Asteraceae]. Plants. 12(4): 819. https://doi.org/10.3390/plants12040819
18. Flores, Y.; Rodrigo, G.; Mollinedo, P.; Akesson, B.; Sterner, O.; Almanza, G. R. 2009. A 5-methylcoumarin glucoside and a coumestan derivative from *Mutisia orbignyana*. Revista Boliviana Química. 26(1): 21-26.
19. Ghitescu, R. E.; Volf, I.; Carausu, C.; Bühlmann, A. M.; Gilca, I. A.; Popa, V. I. 2015. Optimization of ultrasound-assisted extraction of polyphenols from spruce wood bark. Ultrasonics Sonochemistry. 22: 535-541. https://doi.org/10.1016/j.ultsonch.2014.07.013
20. Juárez, B. E.; Mendiondo, M. E. 2003. Flavonoids from *Mutisia acuminata*. Pharmaceutical Biology. 41(4): 291-292. https://doi.org/10.1076/phbi.41.4.291.15669
21. Katinas, L.; Pruski, J.; Sancho, G.; Tellería, M. C. 2008. The subfamily *Mutisioideae (Asteraceae)*. The Botanical Review. 74(4): 469-716. https://doi.org/10.1007/s12229-008-9016-6
22. Kumar, K.; Srivastav, S.; Sharanagat, V. S. 2021. Ultrasound assisted extraction (UAE) of bioactive compounds from fruit and vegetable processing by-products: A review. Ultrasonics Sonochemistry. 70:105325. https://doi.org/10.1016/j.ultsonch.2020.105325
23. Llorent-Martínez, E. J.; Zengin, G.; Sinan, K. I.; Polat, R.; Canlı, D.; Picot-Allain, M. C. N.; Mahomoodally, M. F. 2020. Impact of different extraction solvents and techniques on the biological activities of *Cirsium yildizianum* (Asteraceae: Cynareae). Industrial Crops and Products. 144:112033. https://doi.org/10.1016/j.indcrop.2019.112033
24. Lopez, V. L.; Cellini, J. M. 2022. Plantas medicinales asociadas a bosques de *Polylepis tarapacana* del altiplano jujeño: Riqueza y cobertura en gradientes geográficos, topográficos y de estructura forestal. Ecología Austral. 32(3): 894-907. https://doi.org/10.25260/EA.22.32.3.0.1905

25. Lourenço, S. C.; Moldão-Martins, M.; Alves, V. D. 2019. Antioxidants of natural plant origins: From sources to food industry applications. Molecules. 24(22): 4132. https://doi.org/10.3390/molecules24224132
26. Montgomery, D. C. 2004. 2° ed. Métodos de superficies de respuesta y otros enfoques para la optimización de procesos. In John Wiley & Sons (Ed.). Diseño y análisis de experimentos. Limusa. 427-510.
27. Moreira-Muñoz, A.; Scherson, R. A.; Luebert, F.; Román, M. J.; Monge, M.; Diazgranados, M.; Silva, H. 2020. Biogeography, phylogenetic relationships and morphological analyses of the South American genus *Mutisia* Lf (Asteraceae) shows early connections of two disjunct biodiversity hotspots. Organisms Diversity & Evolution. 20: 639-656. https://doi. org/10.1007/s13127-020-00454-z
28. Olszowy, M. 2019. What is responsible for antioxidant properties of polyphenolic compounds from plants? Plant Physiology and Biochemistry. 144: 135-143. https://doi.org/10.1016/j.plaphy.2019.09.039
29. Palmieri, S.; Pellegrini, M.; Ricci, A.; Compagnone, D.; Lo Sterzo, C. 2020. Chemical composition and antioxidant activity of thyme, hemp and coriander extracts: A comparison study of maceration, Soxhlet, UAE and RSLDE techniques. Foods. 9(9): 1221. https://doi.org/10.3390/foods9091221
30. Pham, D. C.; Nguyen, H. C.; Nguyen, T. H. L.; Ho, H. L.; Trinh, T. K.; Riyaphan, J.; Weng, C. F. 2020. Optimization of ultrasound-assisted extraction of flavonoids from *Celastrus hindsii* leaves using response surface methodology and evaluation of their antioxidant and antitumor activities. BioMed Research International. 2020(1): 3497107. https://doi.org/10.1155/2020/3497107
31. Pillco Paulo, D. 2023. Perfil de componentes fenólicos mediante cromatografía líquida y espectrometría de masas de alta resolución en tándem, MS/MS, de cinco especies del género *Mutisia.* Tesis de grado en Química. Facultad de Ciencias Químicas, Físicas y Matemáticas. Universidad Nacional de San Antonio Abad del Cusco. http:// hdl.handle.net/20.500.12918/7286
32. Singleton, V. L.; Rossi, J. A. 1965. Colorimetry of total phenolics with phosphomolybdic-phosphotungstic acid reagents. American Journal of Enology and Viticulture. 16(3): 144-158. https://doi. org/10.5344/ajev.1965.16.3.144
33. Sobhani, A.; Noormohammadi, N.; Moradi, K.; Ebrahimi, M.; Khanahmadi, M. 2022. Optimization of heat and ultrasound assisted extraction of bioactive compounds from *Echinacea purpurea* using response surface methodology. Journal of Applied Research on Medicinal and Aromatic Plants. 31:100399. https://doi.org/10.1016/j.jarmap.2022.100399
34. Sova, M. 2012. Antioxidant and antimicrobial activities of cinnamic acid derivatives. Mini-Reviews in Medicinal Chemistry. 12(8): 749-767. https://doi.org/10.2174/138955712801264792
35. Sova, M.; Saso, L. 2020. Natural sources, pharmacokinetics, biological activities and health benefits of hydroxycinnamic acids and their metabolites. Nutrients. 12(8): 2190. https://doi.org/10.3390/nu12082190
36. Tirado-Kulieva, V. A.; Oblitas, J.; León-Roque, N.; Castro, W. 2026. Physicochemical Properties, Bioactive Compounds, and Antioxidant Activity of Andean Fruits: Optimization of Extraction by Response Surface Methodology. Revista de la Facultad de Ciencias Agrarias. Universidad Nacional de Cuyo. Mendoza. Argentina. 58(1): e9133.
37. Villamil-Galindo, E.; Piagentini, A. 2024. Green solvents for the recovery of phenolic compounds from strawberry (*Fragaria x ananassa* Duch) and apple (*Malus domestica*) agro-industrial bio-wastes. Revista de la Facultad de Ciencias Agrarias. Universidad Nacional de Cuyo. Mendoza. Argentina. 56(1): 149-160. DOI: https://doi.org/10.48162/rev.39.131
38. Viturro, C. I.; Molina, A.; Schmeda-Hirschmann, G. 1999. Free radical scavengers from *Mutisia friesiana (Asteraceae)* and *Sanicula graveolens (Apiaceae)*. Phytotherapy Research. 13(5): 422-424. https://doi.org/10.1002/(SICI)1099-1573(199908/09)13:5%3C422::AID-PTR462%3E3.0.CO;2-M
39. Viturro, C. I.; de la Fuente, J. 2000. Chemical study of the essential oil of Mutisia friesiana. Molecules. 5(3): 568-570. https://doi.org/10.3390/50300568
40. Viturro, C. I.; Maier, M. S.; Stortz, C. A.; de la Fuente, J. R. 2001. Antifungal diastereomeric furanones from *Mutisia friesiana*: structural determination and conformational analysis. Tetrahedron: Asymmetry. 12(7): 991-998. https://doi.org/10.1016/S0957-4166(01)00163-X
41. Viturro, C. I.; de la Fuente, J. R.; Maier, M. S. 2003. Antifungal methylphenone derivatives and 5-methylcoumarins from *Mutisia friesiana*. Zeitschrift für Naturforschung C. 58(7-8): 533-540. https://doi.org/10.1515/znc-2003-7-815
42. Viturro, C. I.; de la Fuente, J. R.; Maier, M. S. 2004. 5-Methylcoumaranones from *Mutisia friesiana* and their bioactivity. Journal of Natural Products. 67(5): 778-782. https://doi.org/10.1021/ np0304058
43. Viturro, C. I.; de la Fuente, J. R.; Maier, M. S. 2005. One new prenylated furanone and other non-polar constituents from *Mutisia friesiana*. Zeitschrift für Naturforschung B. 60(5): 585-589. https://doi.org/10.1515/znb-2005-0519
44. Yancheshmeh, B. S.; Panahi, Y.; Allahdad, Z.; Abdolshahi, A.; Zamani, Z. 2022. Optimization of ultrasound-assisted extraction of bioactive compounds from Achillea kellalensis using response surface methodology. Journal of Applied Research on Medicinal and Aromatic Plants. 28:100355. https://doi.org/10.1016/j.jarmap.2021.100355

Physicochemical Properties, Bioactive Compounds, and Antioxidant Activity of Andean Fruits: Optimization of Extraction by Response Surface Methodology

Propiedades fisicoquímicas, compuestos bioactivos y actividad antioxidante de frutas andinas: optimización de la extracción mediante metodología de superficie de respuesta

Vicente Amirpasha Tirado-Kulieva [1*], Jimy Oblitas [2], Noemí León-Roque [3], Wilson Castro [4]

Originales: *Recepción:* 25/07/2025 - *Aceptación:* 18/10/2025

ABSTRACT

Native fruits from the Peruvian Andes, such as *ushpa* (*Vaccinium floribundum* Kunth) and *sachon* (*Hesperomeles obtusifolia* (Pers.) Lindl.), grow in high-altitude environments that favor the accumulation of bioactive compounds. However, limited characterization has restricted their sustainable utilization. This study analyzed the physicochemical properties, total phenolic content (TPC), total flavonoid content (TFC), total anthocyanin content (TAC), vitamin C (VC), and antioxidant activity (AA) of both fruits. It also evaluated the effects of solvent type (ethanol and methanol) and concentration (70% and 80%), and extraction time (60, 90, and 120 minutes) on extraction efficiency using response surface methodology. Both fruits exhibited higher levels of bioactive compounds and antioxidant activity compared to other berry species. Optimal conditions for *ushpa* (64.86% methanol, 139.68 minutes) and for *sachon* (64.86% ethanol, 90 minutes) yielded TPC = 3,587 and 948 mg GAE/100 g, TFC = 1,821 and 701 mg CE/100 g, TAC = 252 and 8 mg C3G/100 g, and AA = 563 and 501 µmol TE/g, respectively. These findings support further research and potential valorization of these native fruits.

Keywords
andean berries • paramo • polyphenols • vitamin C • antioxidant activity • RSM

https://doi.org/10.48162/rev.39.204

1 Asociación para la Ciencia e Innovación Agraria para la Red Norte - AgroRed Norte. Piura 20009. Perú. * vamir0803@gmail.com
2 Universidad Privada del Norte. Facultad de Ingeniería. Cajamarca 06002. Cajamarca. Perú.
3 Universidad Nacional Pedro Ruiz Gallo. Facultad de Ingeniería Química e Industrias Alimentarias. Lambayeque 14013. Lambayeque. Perú.
4 Universidad Nacional de Frontera. Facultad de Ingeniería de Industrias Alimentarias y Biotecnología. Sullana 20103. Piura. Perú.

Licenses Creative Commons
Attribution - Non Commercial - Share Alike

Resumen

Los frutos nativos de los Andes peruanos, como *ushpa* (*Vaccinium floribundum* Kunth) y *sachon* (*Hesperomeles obtusifolia* (Pers.) Lindl.), crecen en ambientes de altura que favorecen la acumulación de compuestos bioactivos. Sin embargo, la caracterización limitada ha restringido su uso sostenible. Este estudio evaluó las propiedades fisicoquímicas, contenido total de fenoles (TPC), contenido total de flavonoides (TFC), contenido total de antocianinas (TAC), vitamina C (VC) y actividad antioxidante (AA) de ambos frutos. Asimismo, se analizó el efecto del tipo (etanol y metanol) y concentración (70% y 80%) de solvente y tiempo de extracción (60, 90 y 120 minutos) mediante metodología de superficie de respuesta. Ambas frutas presentaron niveles superiores de compuestos bioactivos y actividad antioxidante en comparación con otras especies de bayas. Las condiciones óptimas para *ushpa* (64,86% de metanol, 139,68 minutos) y *sachon* (64,86% de etanol, 90 minutos) generaron valores de TPC = 3 587 mg y 948 GAE/100 g, TFC = 1 821 y 701 mg CE/100 g, TAC = 252 y 8 mg C3G/100 g, y AA = 563 y 501 µmol TE/g, respectivamente. Estos resultados respaldan futuras investigaciones y posible valorización de estos frutos nativos.

Palabras clave
bayas andinas • páramo • polifenoles • vitamina C • actividad antioxidante • RSM

Introduction

Peru, a globally recognized megadiverse country, is home to more than 780 edible plant species, including 525 native fruits (MIDAGRI, 2022). Within its diverse ecosystems, the Andean *paramo,* a high-mountain ecosystem located between 3,500 and 4,200 meters above sea level, stands out for its rich plant biodiversity and extreme climatic conditions. These conditions have favored the development of native fruit species with unique sensory and functional properties that remain largely unexplored (Torres-Guevara *et al.*, 2020).

Compared with countries such as Ecuador (Guevara-Terán *et al.*, 2022), Brazil (Rigolon *et al.*, 2020), Chile (Oyarzún *et al.*, 2020), Cameroon (Bayang *et al.*, 2021), and China (Liu *et al.*, 2022), where native fruits have been extensively characterized, studies in the Peruvian Andes remain scarce. For example, Torres-Guevara *et al.* (2023) identified 39 native fruit species in northern Peru, most of which are still unknown in commercial markets. Berries were predominant among them, widely recognized for their richness in vitamin C and phenolic compounds that confer strong antioxidant activity (Bezerra *et al.*, 2024).

Two native berries from the Andean paramo, *ushpa* (*Vaccinium floribundum Kunth*) and *sachon* (*Hesperomeles obtusifolia (Pers.) Lindl.*), have long been consumed by local communities for both nutritional and medicinal purposes. Despite their ethnobotanical relevance, scientific studies on these species are scarce and mostly limited to preliminary assessments of their phytochemical composition (Torres-Guevara *et al.*, 2020).

In this context, the present study provides a comprehensive analysis of the physicochemical traits (soluble solids and pH), total phenolic content (TPC), total flavonoid content (TFC), total anthocyanin content (TAC), vitamin C (VC), and antioxidant activity (AA) of *V. floribundum* and *H. obtusifolia* from the Peruvian Andean *paramo*. Recognizing that efficient extraction processes depend on multiple interrelated variables, this study applies multivariate optimization to identify the best extraction conditions.

We hypothesize that both species exhibit high levels of bioactive compounds and antioxidant activity, and that extraction parameters significantly influence their recovery. These findings provide insights into the bioactive potential of these native species and support future research and valorization.

Materials and Methods

Chemicals and Reagents

All chemicals used in this study were of analytical grade or higher. Gallic acid, the Folin-Ciocalteu reagent, and quercetin standard were purchased from Millipore-Sigma (Steinheim, Germany). HPLC-grade methanol, along with analytical-grade or higher ethanol and methanol were sourced from Supelco (Bellefonte, PA, USA). The ascorbic acid standard was obtained from Merck (Darmstadt, Germany). 6-Hydroxy-2,5,7,8 -tetramethylchroman-2-carboxylic acid (Trolox) was acquired from Sigma-Aldrich (Steinheim, Germany).

Sample Collection

In April 2023, 1 kg of mature fruits of both *sachon* (*H. obtusifolia*) and *ushpa* (*V. floribundum*) were collected from the *paramo* ecosystem in the locality of Totora, Pacaipampa district, Ayabaca province, Piura region, Peru, at an elevation of 3,000-3,700 meters above sea level. The characteristics of this ecosystem, along with the distribution of these species and other relevant information, are described in Torres-Guevara *et al.* (2023). Species identification was based on previous studies by botanist Fidel A. Torres-Guevara. These species (figure 1) were selected because, although they are not commonly commercialized, they are widely used by local communities for nutritional and medicinal purposes.

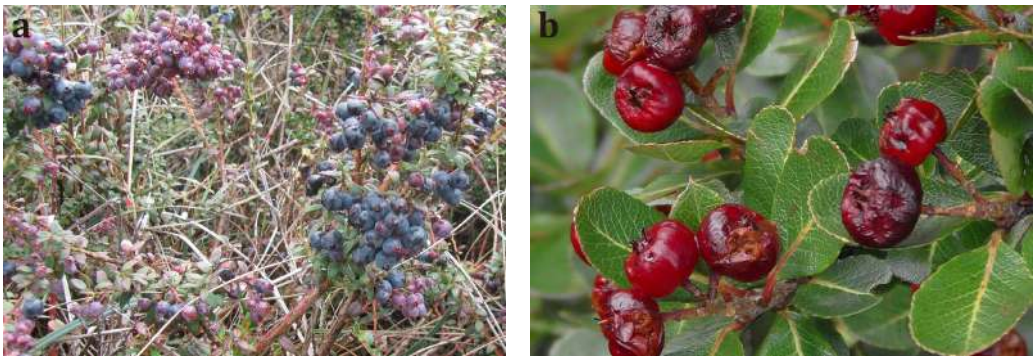


Figure 1. Fruit-bearing shrubs of (a) *V. floribundum* Kunth and (b) *H. obtusifolia* (Pers.) Lindl.

Figura 1. Frutales de (a) *V. floribundum* Kunth y (b) *H. obtusifolia* (Pers.) Lindl.

Physicochemical Analyses

Fruits were washed, dried, and homogenized. Juice was filtered and analyzed for pH (pHep-HI98107, HANNA Instruments, Italy) and total soluble solids (°Brix) using a HI96801 digital refractometer (HANNA Instruments, Italy). Analyses were conducted in quintuplicate at room temperature. Color parameters (L*, a*, b*) were measured in the CIELab* color space using a FRU WR-10QC colorimeter (Shenzhen Wave Optoelectronics Technology Ltd., China), with measurements taken at five random points on each sample's surface.

Extraction and Chemical Analysis

Samples were freeze-dried (BK-FD10PT, Biobase, China), ground (IKA M20 universal mill, Germany), and sieved using a Ro-Tap RX29-16 shaker (WS Tyler, USA). Particle fractions between 150 and 300 µm were collected, packaged, and stored at -20°C in a refrigerated incubator (FOC 215I, Velp Scientifica, Italy).

Extract Preparation

Extracts were prepared by maceration with agitation, adapting the method from a previous study (León-Roque *et al.*, 2023). The evaluated factors were: solvent type (ethanol or methanol), solvent concentration (70% or 80%), and extraction time

(60, 90, or 120 minutes). Briefly, 0.5 g of sample was mixed with 10 mL of solvent and extracted at room temperature using a vortex mixer (Labnet International, USA). Extracts were centrifuged (5000×g, 15 minutes, 4°C) in a Bio RS-24 multi-rotator (Boeco, Germany), and the supernatants were stored at -20°C in 2 mL amber tubes. Before chromatographic analysis, extracts were filtered through 0.45 µm PTFE syringe filters.

Phenolic Compounds

TPC was determined using the Folin–Ciocalteu method adapted from Magalhães *et al.* (2010). Absorbance was measured in triplicate at 765 nm using a Genesys 30 UV-Vis spectrophotometer (Thermo Scientific, USA), and results were expressed as mg gallic acid equivalents (mg GAE) per 100 g of dry basis (d.b.).

TFC was measured by the aluminum chloride colorimetric assay described by Abderrahim *et al.* (2015). Absorbance was recorded in triplicate at 415 nm, and results were expressed as mg catechin equivalents (mg CE) per 100 g d.b.

TAC was quantified using the pH differential method described by Giusti & Wrolstad (2001). Absorbance was recorded at the visible maximum wavelength (λ_vis-max) and at 700 nm. Analyses were performed in triplicate, and results were expressed as mg cyanidin-3-glucoside equivalents (C3G) per 100 g d.b.

Vitamin C

VC concentration was determined in triplicate by HPLC-DAD (Shimadzu LCMS-2020) using ascorbic acid as the standard. A stock solution of 500 ppm was prepared, and calibration was constructed from 0-250 ppm. Chromatographic detection was performed at 254 nm using a Shim-pack GIST C18 (5 µm, 150 × 4.6 mm) column at a flow rate of 0.5 mL/min and an injection volume of 10 µL. The column temperature was maintained at 30°C, and the mobile phase consisted of a methanol-water (80/20 v/v, solvent B) for 10 minutes. Extracts were filtered through 0.45 µm syringe filters into 2 mL vials, which were then placed in the autosampler. Results were expressed as mg VC per liter d.b., and data were processed using LabSolutions software.

In Vitro Antioxidant Activity

AA was determined in triplicate using the ABTS radical cation assay described by Re *et al.* (1999), and results were expressed as µmol Trolox equivalents (TE) per gram d.b.

Experimental Design

The effects of solvent type, solvent concentration, and extraction time on TPC, TFC, TAC, and AA were evaluated using response surface methodology (RSM), with 12 randomized runs and 36 total experiments. Data were fitted to a second-order polynomial equation, and analysis of variance (ANOVA) was applied to assess the significance of individual factors and their interactions. Regression coefficients were used to establish the direction of the effects, where positive values reflected increases in the response, while negative values indicated decreases. A Pareto chart of standardized effects illustrated the magnitude and importance of each factor.

Since maximizing one response variable may compromise another, global optimization was conducted using a multiple-response strategy based on the desirability function. This approach converts each response into a standardized scale (0-1), where 1 represents the optimal condition.

Vitamin C content was excluded from the optimization process, as it was not detected in most methanol-based extractions of both *ushpa* and *sachon*.

Data Analysis

Physicochemical differences between *ushpa* and *sachon* were assessed using Student's t-test ($\alpha = 0.05$). The effects of extraction treatments were analyzed via ANOVA ($\alpha = 0.05$) followed by Tukey's test for multiple comparisons. Statistical analyses were conducted with Minitab 18.0 (Minitab Inc., USA), while optimization analyses were performed using Statistica 12 (Stat Soft Inc., USA) ($\alpha = 0.05$).

Results and Discussion

Physicochemical Characteristics

The physicochemical analysis of *ushpa* and *sachon* fruits revealed significant differences ($p < 0.05$) in color parameters (figure 2(a-c), page 6), with higher values in *sachon* (L*: 46.44 ± 0.21, a*: 2.18 ± 0.55, b*: 1.03 ± 0.21) compared to *ushpa* (L*: 45.88 ± 0.47, a*: -2.38 ± 0.20, b*: 0.50 ± 0.17).

Lower L* values have been reported in other berries, such as 18.6 in *Rubus ulmifolius*, 20.0 in *Aristotelia chilensis* (Mattson *et al.*, 2022), 31.1 in *Rubus* sp., 27.2 in *Vaccinium* sp. (Rigolon *et al.*, 2020), and 25.7 in *Vaccinium myrtillus* L. (Vega *et al.*, 2023). The L* value tends to decrease during fruit ripening, leading to a darker appearance, although high L* values have also been recorded in ripe fruits such as *Fragaria vesca* L. (56.7) and *Prunus avium* L. (62.9) (Vega *et al.*, 2023).

Regarding total soluble solids (°Brix) content (figure 2(d), page 6), no significant differences were observed between *ushpa* (12.90 ± 3.13) and *sachon* (13.14 ± 3.08) ($p > 0.05$). Both fruits showed values comparable to other berries, such as *Vitis vinifera* L. (16.9) and *Rubus idaeus* (7.0-11.0) (Frías-Moreno *et al.*, 2021; Gomes *et al.*, 2021). These values indicate a sweetness level similar to that of widely commercial fruits, suggesting good potential for direct consumption or industrial processing.

Several authors have noted that °Brix content can vary depending on cultivar, climate, ripening stage, and agronomic practices (King *et al.*, 2021). Saad *et al.* (2022) reported values ranging from 3.8 to 8.2 in *Fragaria × ananassa*, depending on the maturity stage. Seki *et al.* (2024) found values of 8.1 and 10.0 in red and white *Fragaria* sp., respectively. Cuesta-Riaño *et al.* (2022) reported values of 5.7 and 7.8 in *Rubus glaucus* Benth and *Rubus adenotrichos*, respectively. Aliman *et al.* (2020) documented high variability in °Brix among *Vaccinium myrtillus* L. cultivars depending on the harvest year.

With respect to pH (figure 2(e), page 6), both *ushpa* and *sachon* exhibited values close to 3.1, with no significant differences between them ($p > 0.05$). This similarity is attributed to shared environmental factors in the paramo ecosystem that influence acidity. For example, environmental conditions have been shown to affect the quality, including the acidity, of both cultivated and wild apples collected from different locations in China (Li *et al.*, 2021). Other berries exhibit a range of pH values: 3.6 in grapes, 2.9-3.1 in *Rubus idaeus* (Frías-Moreno *et al.*, 2021), 3.09-3.5 in different *Aronia mitschurinii* harvests (King *et al.*, 2021), 3.1 in *Rubus glaucus* Benth and 3.2 in *Rubus adenotrichos* (Cuesta-Riaño *et al.*, 2022), and 3.2-3.6 in *Vaccinium myrtillus* L. (Aliman *et al.*, 2020).

Chemical Analysis and Antioxidant Activity

Table 1 (page 7), presents the results for *ushpa* and *sachon* extracts, which confirmed our hypothesis of their high levels of TPC, TFC, TAC, VC, and AA, highlighting their strong bioactive potential. Comparative values for other berries are provided in Table S1.

TPC, TFC and TAC

Ushpa displayed higher TPC (3,004.62 mg GAE/100 g d.b. vs. 772.15 mg GAE/100 g d.b.) and TFC (1,661.10 mg CE/100 g d.b. vs. 564.08 mg CE/100 g d.b.), exceeding levels found in other berries, including *Vaccinium corymbosum* L. (Aliman *et al.*, 2020) and *Vaccinium myrtillus* L. (Vega *et al.*, 2023). A study on *Vaccinium floribundum* in Ecuador reported much lower TPC (Monge-Sevilla *et al.*, 2024), highlighting the high regional variability in phenolic content. While *sachon* exhibited considerable TPC and TFC levels, they were lower than those reported for *Aronia mitschurinii* (King *et al.*, 2021), *Aristotelia chilensis* (Mattson *et al.*, 2022), and *Sorbus aucuparia* L. (Orsavová *et al.*, 2023).

Ushpa (240.50 mg C3G/100 g d.b.) also had significantly higher TAC than *sachon* (4.46 mg C3G/100 g d.b.), consistent with the dark blue pigmentation of *ushpa*. TAC values in *ushpa* surpassed those reported for *Rubus ulmifolius* (Mattson *et al.*, 2022), *Rubus idaeus* (Frías-Moreno *et al.*, 2021), *Sorbus aucuparia* L. (Orsavová *et al.*, 2023), and *Vitis vinifera* L. (Gomes *et al.*, 2021).

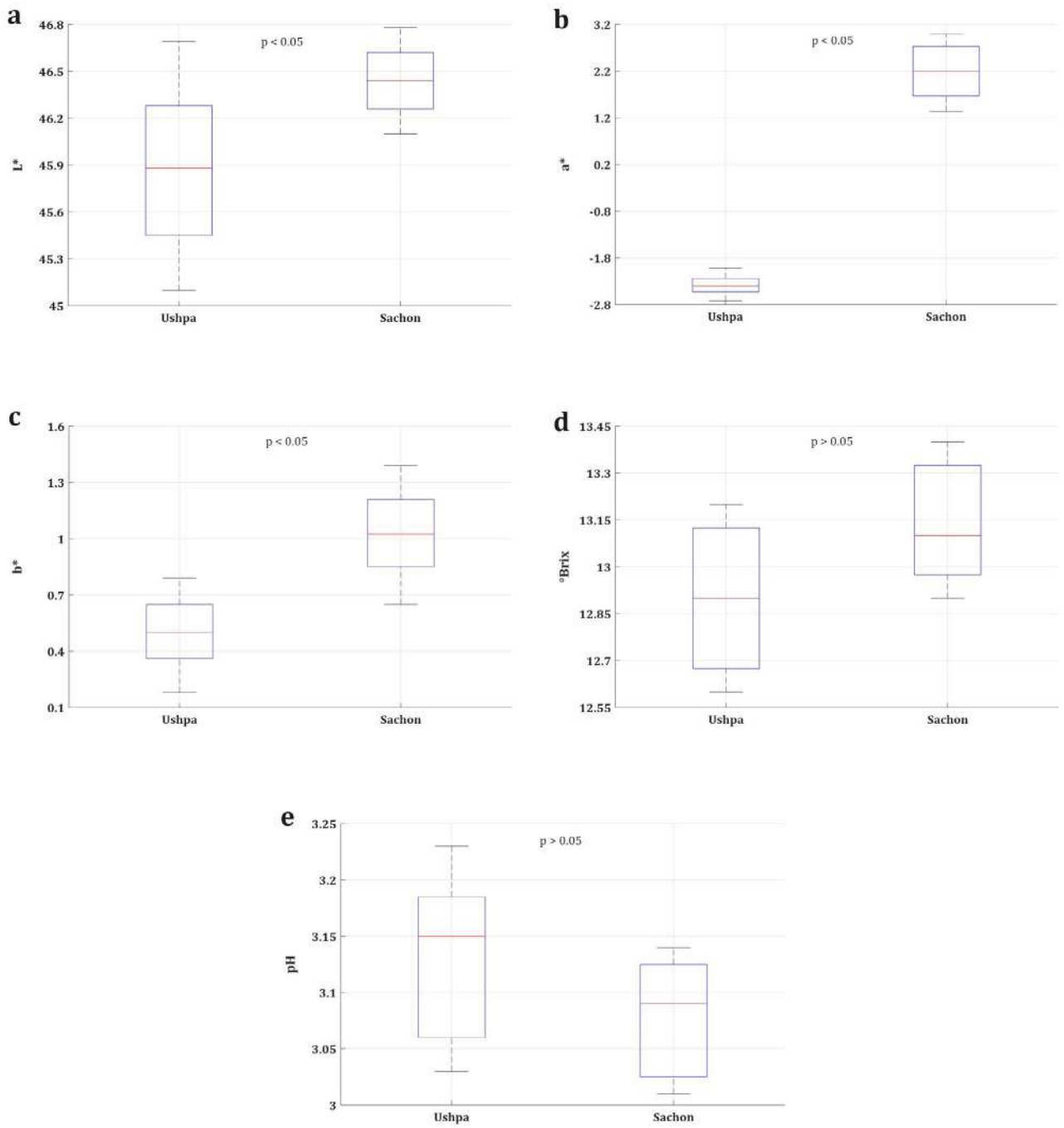


Figure 2. Values of (a) L*, (b) a*, (c) b*, (d) °Brix, and (e) pH in *ushpa* and *sachon*.

Figura 2. Valores de (a) L*, (b) a*, (c) b*, (d) °Brix, y (e) pH en *ushpa* y *sachon*.

Differences in metabolite content can be attributed to factors such as climate, altitude, and ripening stage (Aliman *et al.*, 2020; Guevara-Terán *et al.*, 2022). Studies on *Vaccinium floribundum* have shown that fruits harvested at higher elevations exhibit greater phenolic content due to increased solar exposure (Guevara-Terán *et al.*, 2022).

Table 1. TPC, TFC, TAC, VC, and AA of *ushpa* and *sachon* extracts.
Tabla 1. TPC, TFC, TAC, VC, and AA de extractos de *ushpa* y *sachon*.

Treatment	TPC (mg GAE/100 g d.b.)		TFC (mg CE/100 g d.b.)	
	Ushpa	*Sachon*	*Ushpa*	*Sachon*
70% methanol for 60 minutes	2,438.99 ± 16.93^{g}	782.98 ± 2.01^{d}	1,647.31 ± 38.43^{cdef}	492.22 ± 0.39^{g}
70% ethanol for 60 minutes	3,075.57 ± 78.40^{bcd}	926.48 ± 23.14^{a}	1,713.55 ± 9.78^{bc}	663.86 ± 10.38^{a}
80% methanol for 60 minutes	2,933.87 ± 85.95^{de}	812.61 ± 8.94^{bcd}	1,683.52 ± 27.67^{bcd}	499.93 ± 3.55^{fg}
80% ethanol for 60 minutes	2,981.49 ± 21.78^{cde}	848.03 ± 5.33^{b}	1,567.34 ± 31.62^{fg}	579.67 ± 8.42^{d}
70% methanol for 90 minutes	3,224.85 ± 54.50^{b}	597.11 ± 10.21^{h}	1,662.93 ± 38.46^{bcde}	511.54 ± 3.28^{f}
70% ethanol for 90 minutes	3,148.19 ± 49.30^{bc}	738.84 ± 7.60^{e}	1,742.83 ± 51.33^{b}	630.71 ± 0.60^{b}
80% methanol for 90 minutes	3,042.08 ± 22.12^{cd}	759.96 ± 1.02^{cd}	1,652.63 ± 25.93^{efg}	565.18 ± 2.23^{f}
80% ethanol for 90 minutes	2,894.93 ± 136.95^{de}	795.18 ± 19.19^{d}	1,614.83 ± 11.38^{defg}	614.26 ± 2.52^{c}
70% methanol for 120 minutes	2,705.57 ± 32.24^{f}	832.93 ± 10.59^{bc}	1,686.13 ± 30.51^{bcd}	544.43 ± 5.70^{e}
70% ethanol for 120 minutes	3,122.61 ± 26.33^{bc}	781.23 ± 9.61^{d}	1,642.56 ± 10.65^{cdef}	649.11 ± 7.29^{a}
80% methanol for 120 minutes	3,650.03 ± 63.52^{a}	648.37 ± 18.56^{g}	1,829.97 ± 2.44^{a}	452.93 ± 6.37^{h}
80% ethanol for 120 minutes	2,846.72 ± 44.33^{ef}	697.60 ± 13.08^{f}	1,545.44 ± 11.13^{g}	616.74 ± 4.52^{bc}

Treatment	VC (mg /L d.b.)		TAC (mg C3G/100 g d.b.)		AA (µmol TE/g d.b.)	
	Ushpa	*Sachon*	*Ushpa*	*Sachon*	*Ushpa*	*Sachon*
70% methanol for 60 minutes	475.31 ± 5.92^{b}	93.70 ± 4.90^{g}	255.38 ± 0.08^{a}	6.50 ± 0.15^{b}	470.79 ± 0.45^{d}	445.26 ± 0.45^{bc}
70% ethanol for 60 minutes	n.d.^{c}	n.d.^{h}	234.32 ± 0.13^{g}	6.50 ± 0.31^{b}	465.06 ± 1.56^{d}	423.90 ± 3.69^{d}
80% methanol for 60 minutes	525.20 ± 1.58^{b}	121.68 ± 0.81^{g}	239.66 ± 0.13^{e}	2.23 ± 0.08^{g}	504.92 ± 1.35^{b}	399.67 ± 1.19^{e}
80% ethanol for 60 minutes	n.d.^{c}	n.d.^{h}	241.22 ± 0.15^{d}	4.45 ± 0.08^{cd}	400.71 ± 0.45^{g}	284.77 ± 1.19^{i}
70% methanol for 90 minutes	477.88 ± 0.57^{b}	97.82 ± 1.42^{g}	240.11 ± 0.20^{e}	1.96 ± 0.15^{g}	374.92 ± 7.83^{h}	398.36 ± 1.19^{ef}
70% ethanol for 90 minutes	n.d.^{c}	n.d.^{h}	237.61 ± 0.41^{f}	4.41 ± 0.00^{d}	478.87 ± 0.45^{c}	360.33 ± 2.34^{h}
80% methanol for 90 minutes	412.46 ± 0.52^{b}	248.52 ± 22.06^{b}	239.61 ± 0.54^{b}	4.57 ± 0.00^{c}	449.73 ± 2.07^{f}	416.69 ± 1.19^{h}
80% ethanol for 90 minutes	n.d.^{c}	198.01 ± 0.32^{d}	243.09 ± 0.43^{c}	4.68 ± 0.13^{cd}	326.19 ± 2.74^{i}	382.99 ± 0.78^{g}
70% methanol for 120 minutes	470.16 ± 11.77^{b}	176.37 ± 8.42^{e}	237.70 ± 0.20^{f}	3.34 ± 0.13^{ef}	499.97 ± 0.90^{b}	476 ± 0.00^{a}
70% ethanol for 120 minutes	n.d.^{c}	377.02 ± 1.51^{a}	241.13 ± 0.13^{d}	7.66 ± 0.08^{a}	463.50 ± 1.35^{de}	388.20 ± 10.38^{fg}
80% methanol for 120 minutes	1,065.81 ± 134.94^{a}	241.90 ± 2.05^{c}	231.65 ± 0.27^{h}	3.70 ± 0.08^{e}	528.11 ± 0.45^{a}	435.10 ± 5.20^{c}
80% ethanol for 120 minutes	419.32 ± 0.31^{b}	188.37 ± 0.38^{de}	239.93 ± 0.13^{e}	3.25 ± 0.08^{f}	456.2 ± 2.51^{e}	452.56 ± 1.56^{b}

Results are presented as mean ± standard deviation. Different letters within each column indicate statistically significant differences between treatments ($p < 0.05$). Significant differences ($p < 0.05$) in TPC, TFC, TAC, VC, and AA were observed between ushpa and sachon. n.d. = not detected.

Los resultados se presentan como media ± desviación estándar. Letras diferentes dentro de cada columna indican diferencias estadísticamente significativas entre tratamientos ($p < 0,05$). Se observaron diferencias significativas ($p < 0,05$) en TPC, TFC, TAC, VC y AA entre ushpa y sachon. n.d. = no detectado.

Similarly, plant genetics also plays a key role in metabolite biosynthesis and antioxidant activity. For instance, Lebedev *et al.* (2022) reported a strong positive correlation (r = 0.8) between the genetic diversity of *Rubus idaeus* L. and its TPC, TFC, and TAC. However, another study found no correlation between TPC, TFC, TAC, and AA in *Vaccinium macrocarpon* Aiton and its genetic profile (Debnath & An, 2019). This discrepancy may be due to the use of non-specific genetic markers (Lebedev *et al.*, 2022), or to the complex interaction between environmental conditions and genetics, as observed in VC content of *Fragaria × ananassa* Duchesne (Ali & Serçe, 2022).

Vitamin C

Ushpa had significantly higher VC content than *sachon* (568.92 *vs.* 200.48 mg/L d.b.). This difference may be due to bioactive compounds in *sachon* being more strongly bound within its solid matrix, requiring more intensive extraction methods (Cuesta-Riaño *et al.*, 2022; Mattson *et al.*, 2022).

VC levels in *ushpa* were higher than those in *Vaccinium floribundum* and *Rubus glabratus* Kunth (Monge-Sevilla *et al.*, 2024), but lower than those in *Sorbus aucuparia* L. and *Rubus idaeus* (Frías-Moreno *et al.*, 2021; Orsavová *et al.*, 2023). VC content is influenced by genotype and environmental factors such as altitude and sunlight (Bayang *et al.*, 2021). In *Vaccinium floribundum*, VC content increased with elevation (Guevara-Terán *et al.*, 2022).

Antioxidant Activity (AA)

AA measured with ABTS was significantly higher in *ushpa* than in *sachon* (449.47 *vs.* 401.03 µmol TE/g d.b.), consistent with findings in other fruit species, such as *Opuntia ficus-indica*, *Myrica rubra*, *Vaccinium floribundum*, and *Rubus glabratus* (El Mannoubi, 2021; Liu *et al.*, 2022; Monge-Sevilla *et al.*, 2024).

However, although *ushpa* exhibited greater AA, the difference with *sachon* was smaller than expected, possibly due to the presence of other antioxidant compounds not measured in this study, such as tannins (Varo *et al.*, 2021). For example, in *Vaccinium corymbosum* L., the cultivar Jewel contained more resveratrol but had lower AA than Windsor, while Millenia had the highest VC yet lower AA than both (Varo *et al.*, 2021).

AA levels, like TPC and TFC, are influenced by altitude, solar exposure, and fruit variety, with higher AA reported in *Vaccinium floribundum* harvested at greater elevations (Guevara-Terán *et al.*, 2022).

It is also important to note that AA results can vary depending on the assay (table 1, page 7). For instance, Vega *et al.* (2023) reported that using the DPPH method, *Vaccinium myrtillus* L. showed the highest AA, followed by *Fragaria vesca* L. and *Prunus avium* L. However, when the FRAP assay was used, the ranking partially reversed, with strawberries showing the highest AA, followed by blueberries and cherries.

Effect of Extraction Conditions

Certain extraction parameters had a significant impact on the outcomes, consistent with our hypothesis. However, as detailed below, the magnitude and direction of these effects varied depending on the fruit species and the metabolite or response assessed.

Influence of Solvent Type and Concentration

The solvent type significantly impacted the extraction of bioactive compounds (Figure S1 and Figure S2), with methanol showing greater efficacy in extracting TFC and maximizing AA in *ushpa*, while in *sachon*, methanol had a negative effect on TPC and TFC but a positive effect on TAC and AA ($p < 0.05$). This variability is likely due to the relative polarity of solvents, with methanol being slightly more polar than ethanol, which favors the extraction of polar compounds such as anthocyanins but may hinder the extraction of non-polar compounds (More & Arya, 2021).

Previous studies also highlight these trends. In *Opuntia ficus-indica*, 80% ethanol outperformed methanol in the extraction of polyphenols (El Mannoubi, 2021). However, in *Băbească neagră* peels, ethanol also enhanced TAC extraction (Serea *et al.*, 2023), whereas for TFC, ethanol was more efficient in the peel of *Opuntia ficus-indica*, while methanol was superior in the pulp (El Mannoubi, 2021). These results underscore that solvent effectiveness also depends on the fruit part and the specific class of metabolites.

Solvent concentration also showed significant effects ($p < 0.05$). In *ushpa*, it positively affected TFC, while in *sachon*, it positively influenced TFC, TAC, and AA. Moreover, in *ushpa*, the interaction between solvent type (ethanol) and concentration was significant for both TPC and TFC.

More diluted mixtures allow for greater solvent penetration into the plant matrix, thereby promoting phenolic release. However, high ethanol concentrations reduce polarity, hindering polar compound extraction. This relationship is not linear; for example, Serea *et al.* (2023) reported that 50% ethanol was optimal for TAC in *Băbească neagră* peels, whereas 85% was optimal for TPC.

Interestingly, pure methanol also enhanced TPC, TFC, and AA, as observed in seeds of *Carica papaya* L. (Robles-Apodaca *et al.*, 2024), *Passiflora edulis*, and *Nephelium lappaceum* L. (Sai-Ut *et al.*, 2023). The addition of water increases polyphenol ionization, promoting their solubilization. For instance, in *Vaccinium floribundum*, 20% ethanol improved TAC extraction compared to 60% (Pérez *et al.*, 2021). In *Sambucus nigra* L., 45% ethanol was suitable for TPC extraction (Pascariu *et al.*, 2024).

Influence of Extraction Time

Extraction time had variable effects depending on the species and the bioactive compound evaluated. In *ushpa*, longer extraction times positively affected TAC and AA, while in *sachon*, extraction time had both linear and quadratic effects on AA. However, prolonged extraction tended to negatively impact TPC, particularly in *ushpa*, and both species exhibited a decline in TPC over extended extraction periods. This suggests that while longer extraction may improve yields, it can also lead to compound degradation due to exposure to oxygen, light, or heat.

The nature of this response also depends on the interaction between time and solvent. For example, in *ushpa*, extraction with methanol at short times was particularly favorable for TAC, whereas prolonged methanol use reduced both TPC and TFC. These results align with findings in *Carica papaya* L. seeds, where methanol exhibited a non-linear behavior depending on both time and concentration. At longer extraction times, the highest TFC yields were obtained when using either pure water (0% methanol) or absolute methanol (100%) as the extraction solvent (Robles-Apodaca *et al.*, 2024).

The literature reports similarly variable results. In *Passiflora edulis* and *Nephelium lappaceum* L., time had no effect on TPC at a fixed ethanol concentration (Sai-Ut *et al.*, 2023). However, in *Băbească neagră* peels, a short extraction (25 minutes) with 85% ethanol reduced TAC and AA, while a longer duration (≥44 minutes) and 64% ethanol improved AA (Serea *et al.*, 2023). Similarly, in *Malpighia emarginata* DC. residues, TAC extraction was more efficient with low ethanol concentrations but progressively declined with extended extraction times (Cerino *et al.*, 2023).

Global Desirability Optimization

Given the varied effects of extraction conditions on bioactive compounds, global desirability optimization was applied (Figure S3). For *ushpa*, the optimal conditions determined were 64.86% methanol and an extraction time of 139.68 minutes, resulting in estimated values of TPC = 3,586.8 mg GAE/100 g d.b., TFC = 1,820.8 mg CE/100 g d.b., TAC = 251.87 mg C3G/100 g d.b., and AA = 562.76 µmol TE/g d.b. In contrast, *sachon* exhibited optimal conditions with 64.86% ethanol and 90 minutes of extraction, achieving TPC of 948.37 mg GAE/100 g d.b., TFC of 701.06 mg CE/100 g d.b., TAC of 7.84 mg C3G/100 g d.b., and AA of 500.71 µmol TE/g d.b.

Previous studies have reported equally variable optimal conditions. For instance, in *Băbească neagră* grape peels, using 85% ethanol for 52.14 minutes yielded TPC and TAC values ranging from 24.67 to 43.97 mg/g and 1.71 to 2.74 mg C3G/g, respectively (Serea *et al.*, 2023). In passion fruit and rambutan seeds, maximum TPC and AA were achieved with 67% and 54% ethanol, respectively, after 186 and 221 minutes (Sai-Ut *et al.*, 2023). In *Carica papaya* L. seeds, extraction with 100% methanol for 6 hours resulted in 6.17 mg GAE/g (TPC) and 52.75 mg QE/g (TFC) (Robles-Apodaca *et al.*, 2024). In *Malpighia emarginata* DC. residues, TAC of 2.54 mg/g was reached with 12% ethanol and 25 minutes of extraction (Cerino *et al.*, 2023).

Conclusions and Future Directions

This study provides the first systematic characterization of the physicochemical, chemical, and antioxidant properties of two native Andean fruits from northern Peru: *ushpa* and *sachon*. Both species showed physicochemical parameters (color, °Brix, and pH) comparable to commercial berries, and remarkably high TPC, TFC, TAC, and AA values, often surpassing those of widely consumed fruits. These traits likely reflect their adaptation to harsh, high-altitude environments with intense solar radiation, which promotes the accumulation of secondary bioactive metabolites.

The study of extraction conditions revealed significant, species-specific effects on each attribute. This complexity led to the use of a multivariate optimization approach based on global desirability, which identified specific extraction conditions for maximizing bioactive compound recovery and antioxidant activity.

These findings not only provide academic insights but also highlight the potential of *ushpa* and *sachon* as sources of functional ingredients for the food, nutraceutical, and cosmetic industries. However, the limited scientific knowledge about native species in Peru, particularly regarding their chemical composition and functionality, remains a barrier to their integration into the agri-food chain. Future research should include proximate composition and detailed phytochemical profiling through chromatographic techniques to identify and quantify individual metabolites. Additionally, while the in vitro antioxidant tests used here offer an initial assessment, future studies should incorporate cellular, animal, or clinical models to better evaluate their real-world functionality.

Supplemmentary Material

https://docs.google.com/document/d/19J7wvCNfUOnINnw7pwlwWhhTfAJae_Dw/edit?usp=sharing&ouid=111310786017351827239&rtpof=true&sd=true

References

Abderrahim, F., Huanatico, E., Segura, R., Arribas, S., Gonzalez, M. C., & Condezo-Hoyos, L. (2015). Physical features, phenolic compounds, betalains and total antioxidant capacity of coloured quinoa seeds (*Chenopodium quinoa* Willd.) from Peruvian Altiplano. *Food Chemistry*, *183*, 83-90. https://doi.org/10.1016/j.foodchem.2015.03.029

Ali, M. N., & Serçe, S. (2022). Vitamin C and fruit quality consensus in breeding elite European strawberry under multiple interactions of environment. *Molecular Biology Reports*, *49*(12), 11573-11586. https://doi.org/10.1007/s11033-022-07849-5

Aliman, J., Michalak, I., Bušatlić, E., Aliman, L., Kulina, M., Radović, M., & Hasanbegović, J. (2020). Study of the physicochemical properties of highbush blueberry and wild bilberry fruit in central Bosnia. *Turkish Journal of Agriculture and Forestry*, *44*(2), 156-168. https://doi.org/10.3906/tar-1902-36

Bayang, J. P., Laya, A., Kolla, M. C., & Koubala, B. B. (2021). Variation of physical properties, nutritional value and bioactive nutrients in dry and fresh wild edible fruits of twenty-three species from Far North region of Cameroon. *Journal of Agriculture and Food Research*, *4*, 100146. https://doi.org/10.1016/j.jafr.2021.100146

Bezerra, M., Ribeiro, M., Cosme, F., & Nunes, F. M. (2024). Overview of the distinctive characteristics of strawberry, raspberry, and blueberry in berries, berry wines, and berry spirits. *Comprehensive Reviews in Food Science and Food Safety*, *23*, e13354. https://doi.org/10.1111/1541-4337.13354

Cerino, M. C., Pinela, J., Caleja, C., Saux, C., Pereira, E., & Barros, L. (2023). Dynamic Maceration of Acerola (*Malpighia emarginata* DC.) Fruit Waste: An Optimization Study to Recover Anthocyanins. *Agronomy*, *13*, 2202. https://doi.org/10.3390/agronomy13092202

Cuesta-Riaño, C. S., Castro-Guascaa, M. P., & Tarazona-Díaz, M. P. (2022). Anthocyanin Extract from Blackberry Used as an Indicator of Hydrogen Potential. *International Journal of Fruit Science*, *22*(1), 224–234. https://doi.org/10.1080/15538362.2022.2037036

Debnath, S. C., & An, D. (2019). Antioxidant properties and structured biodiversity in a diverse set of wild cranberry clones. *Heliyon*, *5*(4), e01493. https://doi.org/10.1016/j.heliyon.2019.e01493

El Mannoubi, I. (2021). Effect of extraction solvent on phenolic composition, antioxidant and antibacterial activities of skin and pulp of Tunisian red and yellow–orange Opuntia Ficus Indica fruits. *Journal of Food Measurement and Characterization*, *15*(1), 643-651. https://doi.org/10.1007/s11694-020-00673-0

Frías-Moreno, M. N., Parra-Quezada, R. Á., Ruíz-Carrizales, J., González-Aguilar, G. A., Sepulveda, D., Molina-Corral, F. J., Jacobo-Cuellar, J. L., & Olivas, G. I. (2021). Quality, bioactive compounds and antioxidant capacity of raspberries cultivated in northern Mexico. *International Journal of Food Properties*, *24*(1), 603–614. https://doi.org/10.1080/10942912.2021.1908352

Giusti, M. M., & Wrolstad, R. E. (2001). Characterization and Measurement of Anthocyanins by UV-Visible Spectroscopy. *Current Protocols in Food Analytical Chemistry*, *0*, F1.2.1-F1.2.13. https://doi.org/https://doi.org/10.1002/0471142913.faf0102s00

Gomes, V., Rendall, R., Reis, M. S., Mendes-Ferreira, A., & Melo-Pinto, P. (2021). Determination of sugar, ph, and anthocyanin contents in port wine grape berries through hyperspectral imaging: An extensive comparison of linear and non-linear predictive methods. *Applied Sciences*, *11*, 10319. https://doi.org/10.3390/app112110319

Guevara-Terán, M., Padilla-Arias, K., Beltrán-Novoa, A., González-Paramás, A. M., Giampieri, F., Battino, M., Vásquez-Castillo, W., Fernandez-Soto, P., Tejera, E., & Alvarez-Suarez, J. M. (2022). Influence of Altitudes and Development Stages on the Chemical Composition, Antioxidant, and Antimicrobial Capacity of the Wild Andean Blueberry (*Vaccinium floribundum* Kunth). *Molecules*, *27*, 7525. https://doi.org/10.3390/molecules27217525

King, E. S., Cho, J., Li, H., Jiang, X., Madler, A. K., Weishair, M. K., Glenn, S., Brand, M. H., Xu, C., & Bolling, B. W. (2021). Time of harvest affects United States-grown Aronia mitschurinii berry polyphenols, °Brix, and acidity. *Journal of Agriculture and Food Research*, *6*, 100248. https://doi.org/10.1016/j.jafr.2021.100248

Lebedev, V. G., Lebedeva, T. N., Vidyagina, E. O., Sorokopudov, V. N., Popova, A. A., & Shestibratov, K. A. (2022). Relationship between Phenolic Compounds and Antioxidant Activity in Berries and Leaves of Raspberry Genotypes and Their Genotyping by SSR Markers. *Antioxidants*, *11*, 1961. https://doi.org/10.3390/antiox11101961

León-Roque, N., Romero Guzmán, B. M., Oblitas-Cruz, J. F., & Hidalgo-Chávez, D. W. (2023). Optimization of total polyphenol extraction and flavonoid screening by mass spectrometry in mango (*Mangifera indica* L.) waste from Peru. *Food Science and Technology*, *43*(e105322). https://doi.org/10.1590/fst.105322

Li, Y., Sun, H., Li, J., Qin, S., Yang, W., Ma, X., Qiao, X., & Yang, B. (2021). Effects of genetic background and altitude on sugars, malic acid and ascorbic acid in fruits of wild and cultivated apples (Malus sp.). *Foods*, *10*, 2950. https://doi.org/10.3390/foods10122950

Liu, Z., Zhang, J., Lu, S., Tang, W., Zhou, Y., & Quek, S. Y. (2022). Effects of different drying methods on phenolic components and *in vitro* hypoglycemic activities of pulp extracts from two Chinese bayberry *(Myrica rubra* Sieb. et Zucc.) cultivars. *Food Science and Human Wellness*, *11*(2), 366–373. https://doi.org/10.1016/j.fshw.2021.11.014

Magalhães, L. M., Santos, F., Segundo, M. A., Reis, S., & Lima, J. L. F. C. (2010). Rapid microplate high-throughput methodology for assessment of Folin-Ciocalteu reducing capacity. *Talanta*, *83*(2), 441-447. https://doi.org/10.1016/j.talanta.2010.09.042

Mattson, M. G., Sozzi, A., Corfield, R., Gagneten, M., Franceschinis, L., Schebor, C., & Salvatori, D. (2022). Colorant and antioxidant properties of freeze-dried extracts from wild berries: use of ultrasound-assisted extraction method and drivers of liking of colored yogurts. *Journal of Food Science and Technology*, *59*(3), 944–955. https://doi.org/10.1007/s13197-021-05096-3

MIDAGRI. (2022). *Situación actual de las frutas y verduras en el Perú: Producción, exportación e importación*. https://repositorio.midagri.gob.pe/handle/20.500.13036/1227

Monge-Sevilla, R. D., Fernández, L., Espinoza-Montero, P. J., Méndez-Durazno, C., Cisneros-Pérez, P. A., Romero-Estévez, D., Bolaños-Méndez, D., Alvarez-Paguay, J., & Jadán, M. (2024). Chemical composition and antioxidant properties of native Ecuadorian fruits: *Rubus glabratus* Kunth, *Vaccinium floribundum* Kunth, and *Opuntia soederstromiana*. *Heliyon*, *10*, e30593. https://doi.org/10.1016/j.heliyon.2024.e30593

More, P. R., & Arya, S. S. (2021). Intensification of bio-actives extraction from pomegranate peel using pulsed ultrasound: Effect of factors, correlation, optimization and antioxidant bioactivities. *Ultrasonics Sonochemistry*, *72*, 105423. https://doi.org/10.1016/j.ultsonch.2020.105423

Orsavová, J., Juríková, T., Bednaříková, R., & Mlček, J. (2023). Total Phenolic and Total Flavonoid Content, Individual Phenolic Compounds and Antioxidant Activity in Sweet Rowanberry Cultivars. *Antioxidants*, *12*, 913. https://doi.org/10.3390/antiox12040913

Oyarzún, P., Cornejo, P., Gómez-Alonso, S., & Ruiz, A. (2020). Influence of Profiles and Concentrations of Phenolic Compounds in the Coloration and Antioxidant Properties of *Gaultheria poeppigii* Fruits from Southern Chile. *Plant Foods for Human Nutrition*, *75*(4), 532-539. https://doi.org/10.1007/s11130-020-00843-x

Pascariu, O. E., Dias, L. G., & Israel-Roming, F. (2024). Optimization of Extraction Method of Bioactive Compounds from Elderberries (*Sambucus nigra* L.) and Testing Extract Stability. *Horticulturae*, *10*(7). https://doi.org/10.3390/horticulturae10070743

Pérez, B., Endara, A., Garrido, J., & Ramírez-Cárdenas, L. (2021). Extraction of anthocyanins from mortiño (*Vaccinium floribundum*) and determination of their antioxidant capacity. *Revista Facultad Nacional de Agronomia Medellin*, *74*(1), 9453–9460. https://doi.org/10.15446/rfnam.v74n1.89089

Re, R., Nicoletta, P., Anna, P., Ananth, P., Min, Y., & Catherine, R.-E. (1999). Antioxidant activity applying an improved ABTS radical cation decolorization assay. *Free Radical Biology and Medicine*, *26*(9-10), 1231-1237.

Rigolon, T. C. B., de Barros, F. A. R., Vieira, É. N. R., & Stringheta, P. C. (2020). Prediction of total phenolics, anthocyanins and antioxidant capacity of blackberry (Rubus sp.), blueberry (Vaccinium sp.) and jaboticaba (*Plinia cauliflora* (Mart.) Kausel) skin using colorimetric parameters. *Food Science and Technology*, *40*, 620–625. https://doi.org/10.1590/fst.34219

Robles-Apodaca, S. M., González-Vega, R. I., Ruíz-Cruz, S., Estrada-Alvarado, M. I., Cira-Chávez, L. A., Márquez-Ríos, E., Del-Toro-Sánchez, C. L., Ornelas-Paz, J. de J., Suárez-Jiménez, G. M., & Ocaño-Higuera, V. M. (2024). Optimization of Extraction Process for Improving Polyphenols and Antioxidant Activity from Papaya Seeds (*Carica papaya* L.) Using Response Surface Methodology. *Processes*, *12*(2729). https://doi.org/10.3390/pr12122729

Saad, A. G., Azam, M. M., & Amer, B. M. A. (2022). Quality Analysis Prediction and Discriminating Strawberry Maturity with a Hand-held Vis–NIR Spectrometer. *Food Analytical Methods*, *15*(3), 689–699. https://doi.org/10.1007/s12161-021-02166-2

Sai-Ut, S., Kingwascharapong, P., Mazumder, M. A. R., & Rawdkuen, S. (2023). Optimization of extraction of phenolic compounds and antioxidants from passion fruit and rambutan seeds using response surface methodology. *Journal of Agriculture and Food Research*, *14*(100888). https://doi.org/10.1016/j.jafr.2023.100888

Seki, H., Murakami, H., Ma, T., Tsuchikawa, S., & Inagaki, T. (2024). Evaluating Soluble Solids in White Strawberries: A Comparative Analysis of Vis-NIR and NIR Spectroscopy. *Foods*, *13*(2274). https://doi.org/10.3390/foods13142274

Serea, D., Constantin, O. E., Horincar, G., Stănciuc, N., Aprodu, I., Bahrim, G. E., & Râpeanu, G. (2023). Optimization of Extraction Parameters of Anthocyanin Compounds and Antioxidant Properties from Red Grape (*Băbească neagră*) Peels. *Inventions*, *8*(59). https://doi.org/10.3390/inventions8020059

Torres-Guevara, F. A., Yupanqui, M. L. G., & Suárez-Rebaza, L. A. (2020). Sustancias bioactivas y actividad antioxidante de frutales nativos de páramos y bosques de neblina del norte peruano. *Revista Peruana de Medicina Integrativa*, *5*(4), 129–134. https://doi.org/10.26722/rpmi.2020.54.185

Torres-Guevara, F. A., Ganoza-Yupanqui, M. L., Mantilla-Rodriguez, E., Suárez-Rebaza, L. A., & Bussmann, R. W. (2023). Ethnobotany of fruit species native to paramos and cloud forests of Northern Peru. *Ethnobotany Research and Applications*, *25*(10). https://doi.org/10.32859/era.25.10.1-15

Varo, M. Á., Martín-Gómez, J., Mérida, J., & Serratosa, M. P. (2021). Bioactive compounds and antioxidant activity of highbush blueberry (Vaccinium corymbosum) grown in southern Spain. *European Food Research and Technology*, *247*(5), 1199–1208. https://doi.org/10.1007/s00217-021-03701-5

Vega, E. N., García-Herrera, P., Ciudad-Mulero, M., Dias, M. I., Matallana-González, M. C., Cámara, M., Tardío, J., Molina, M., Pinela, J., C. S. P. Pires, T., Barros, L., Fernández-Ruiz, V., & Morales, P. (2023). Wild sweet cherry, strawberry and bilberry as underestimated sources of natural colorants and bioactive compounds with functional properties. F*ood Chemistry, 414*(135669). https://doi.org/10.1016/j.foodchem.2023.135669

Acknowledgments

The authors thank Fidel A. Torres Guevara and David Gálvez Paucar for providing the *ushpa* and *sachon* illustrations, and Luis Juarez Calderón and Juan Garrido Arismendis for their support in the physicochemical analyses.

Funding

This work was funded by the National Council of Science, Technology, and Technological Innovation (CONCYTEC) and the National Program for Scientific Research and Advanced Studies (PROCIENCIA) under the "E041-2024-03 Basic Research Projects" competition, through contract PE501089307-2024. The project titled "Ciencia detrás del conocimiento nativo: Perfil bioactivo y actividad antioxidante con enfoque quimiométrico, y análisis filogenético de frutales nativos de páramo y bosques nublados de Piura en el contexto de cambio climático y seguridad alimentaria" was supported through this funding.

Ethics Declarations

The authors declare no conflict of interest. All experiments were conducted in strict compliance with regulations for genetic resources established by the local authority, the National Forest and Wildlife Service (SERFOR).